

HOSASH

(HYDROLOGY OF SOUTH AFRICAN SOILS AND HILLSLOPES)

Report to the
WATER RESEARCH COMMISSION

by

Research team:

PAL le Roux*, M Hensley*, SA Lorentz, JJ van Tol***, GM van Zijl*, BT Kuenene*,
D Bouwer*, CS Freese**, M Tinnefeld* & CC Jacobs***

**Department of Soil-, Crop- and Climate Sciences, University of the Free State*

*** Centre for Water Resources Research, University of KwaZulu-Natal, Scottsville*

**** University of Fort Hare*

WRC Report No. 2021/1/15

ISBN 978-1-4312-0594-3

May 2015

Obtainable from

Water Research Commission

Private Bag X03

GEZINA, 0031

orders@wrc.org.za or download from www.wrc.org.za

Eight appendices appear on the enclosed CD.

DISCLAIMER

This report has been reviewed by the Water Research Commission (WRC) and approved for publication. Approval does not signify that the contents necessarily reflect the views and policies of the WRC nor does mention of trade names or commercial products constitute endorsement or recommendation for use.

TRIBUTE

The Research Team would like to pay tribute to Malcolm Hensley for successfully mentoring another WRC project. Malcom did amongst others, water-related research supported by the WRC over more than 30 years. His research covered the Soil-Plant-Atmosphere Continuum, Infield Rain-water Harvesting (IRWH), Digital Soil Mapping (DSM) and Hydropedology as the Hydrology of South African Soils and Hillslopes (HOSASH).

Malcolm's drive in research namely to feed Africa has established itself in IRWH, DSM and HOSASH as products that is not only sound research but are already applied in industry.

Malcolm was not only a mentor for the researchers, he also mentored their personal development. He saw every achievement and completed project as a foundation for greater things.

He finally retired from official commitments at 83 years of age. We admire him.

ACKNOWLEDGEMENTS

The research team thank the members of the steering committee for their time invested, criticism, advice and leadership during the execution of this project.

Reference group:

| | | |
|------------------------|---|-----------------------------------------------|
| Mr. W. Nomquphu | : | Water Research Commission (Chairman) |
| Mr. M. Smart | : | DWA |
| Mr. F Fourie | : | DWA |
| Dr. W.P. de Clerq | : | University of Stellenbosch |
| Dr. D.P. Turner | : | ARC – ISCW |
| Dr. J.H. van der Waals | : | Terra Soil Science |
| Mr. P.W. van Deventer | : | University of North West |
| Mr. B. Grove | : | University of the Free State |

The research team wishes to thank the following persons and institutions:

The Water Research Commission for the trust it put in the research team by awarding this contract.

The management and administration of the University of the Free State, University of KwaZulu-Natal and University of Fort Hare without whose contribution, in terms of infrastructure and maintenance, this research would not have been possible.

PG Bison for making the Weatherley catchment available for research.

SANPARKS for making the Southern Granite Super Site available for research.

Institute for Soil, Climate and Water for making Land Type Data available for research.

Nancy Nortje for administration and logistics of the project.

EXECUTIVE SUMMARY

Project Aim

The project aimed to develop a hydrologically based classification system of SA soils and hillslopes. The hydrology of SA soils and hillslopes (HOSASH) aims to assist in hydrological modelling especially in ungauged basins. The project further aimed to develop techniques suitable for studying the hydrology of SA soils and hillslopes. This includes an improved understanding of soil water regime, permeability and near saturation water flow in all directions; distribution and role of characteristic hillslopes of South Africa and the possible impact of a hydrological classification of soils and hillslopes on hydrological modelling. The project aimed to develop, test and calibrate HOSASH in a variety of environments in SA with the best available hydropedological, climate, geohydrological and hillslope data. The aim includes the application Digital Soil Mapping that can help predict the response of the hillslopes of a catchment. The project aimed to transform Land Type data (based on soil distribution patterns in hillslopes) and available soil data at all scales of soil survey (from intensive to reconnaissance) into hydropedological data that can be useful for ecohydrology, hydrology and especially for hydrological prediction in ungauged basins.

Results

Hydropedology contributes to hydrology in improving conceptual hydrological response models for South African hillslopes and improved parameters for: the hydrological components of soils, namely individual soil properties; soil horizons as combinations of soil properties; soil types as combinations of soil horizons; and soil distribution patterns, as topographical combinations of soil types. Soil morphology, applied in soil classification, is now an established indicator of flowpaths and storage mechanisms of water in hillslopes. Hydrological soil properties of a variety of soil horizons and soil types were quantified paving the way to populate the national soil data base (Land Type data base) with hydrological data linked to soil horizons, soil types and soil distribution patterns.

The project has demonstrated that in cooperation with process hydrology we have, for any catchment in South Africa, generated the knowledge, skills and tools to:

- Improve conceptual hydrological response models for hillslopes using soil properties, soil horizons, soil types and the distribution of these in hillslopes as indicators and controls of flowpaths and storage mechanisms in the vadose zone;
- Identify the most important hydrological hillslopes of small catchments (large scale) by hydropedological soil surveys;
- Identify the most important hydrological hillslopes of large catchments (small scale) using Land Type Survey data;
- Measure what happens in a hydrological hillslope, including the upper and intermediate vadose zone, during rainfall events of different intensities;
- To simulate, using virtual experimentation based on a scientifically sound mechanistic flow model applying realistic soil parameters, a reasonably reliable representation of what actually happens in a hillslope during a rainfall event;
- Use these results on a continuous basis, implementing PTF's (pedotransfer functions), STFs (soil transfer functions) and HiTF's (hillslope transfer functions), and together with the improved South African soil classification system, to improve the understanding and modelling of HOSASH;

- Close the gap between experimentation and modelling by improved application of soil data, including hydropedological classification of soils and hillslopes on all scales;
- Develop modular/characteristic hydrological response models for soil components at all scales, namely horizons, soil types, hillslopes and Land Types suitable for prediction of one, two and three dimensional hydrological responses in soil bodies and hillslopes.

Equipping the team to reach this level of skills required that several barriers had to be challenged. Pedology, the science of understanding the different types of soils, creates the possibility to predict their responses to different treatments. It started in natural science but food security driven by World Wars I and II and the Cold War, focussed pedology on crop production. Awareness of global health and water shortage broadened the application to serve hydrology. Pedology benefits hydrological modelling, especially in ungauged catchments, and it will also contribute to mitigating the impact of economic development on hydrological responses and ecohydrology.

As morphological soil properties react slowly to a changing environment, the current validity of their relationship with hydrology has been questioned. The first breakthrough was that ancient, easily observable morphological soil properties used to classify soils, are well correlated with the long-term average duration of drainable water in soils. This laid the foundation for the hydrological classification of soil horizons and types. Soil chemical reactions and the associated soil chemical properties, precede soil morphological changes, are therefore hydrologically more sensitive parameters indicating more specific hydrological responses. A good correlation between soil morphology and soil chemical properties has been confirmed. The response of soil horizons, soil types and soil distribution patterns has been strengthened using natural isotope studies and hydrometry as current indicators of soil and hillslope hydrological responses.

Quantification of the contribution of soil horizons and soil types to the recession curve of the hydrograph narrowed the gap between soil data and hydrological models. On large scale the distribution of soils can therefore be classified hydrologically and used to develop conceptual hydrological response units for catchments. On small scale Land Types can be disaggregated to hydrological hillslopes as hydrological response units. Integrated soil data were used in much more detail, both as indicator and controller of hydrological response of hillslopes, to predict hydrological response using a model.

Several publications were generated in the run of this project. These include 8 papers.

Articles:

VAN TOL, J.J., LE ROUX, P.A.L. & HENSLEY, M., 2011. Soil indicators of hillslope hydrology. In: B.O Gungor & O. Mayis (eds), Principles-Application and Assessments in Soil Science. Intech, Turkey.

VAN TOL, J.J., LE ROUX, P.A.L. & HENSLEY, M., 2012. Pedotransfer function to determine the water conducting macroporosity in South African soils. Water Science and Technology, 65.3 550-557.

VAN TOL, J.J., LE ROUX, P.A.L. & HENSLEY, M., 2012. Pedological criteria for estimating the importance of subsurface lateral flow in E-horizons of South African soils. Water SA 39, 47-56.

VAN TOL J.J., P.A.L. LE ROUX, S.A. LORENTZ AND M. HENSLEY, 2013. Hydropedological Classification of South African Hillslopes. Vadose Zone Journal. 12 (4).

KUENENE, B.T., VAN HUYSSTEEN, C.W. & LE ROUX, P.A.L., 2013. Selected soil properties as indicators of soil water regime in the Cathedral Peak VI catchment of KwaZulu-Natal, South Africa. *S. Afr. J. Plant & Soil*. 30: 1, 1-6

VAN ZIJL, G.M., LE ROUX, P.A.L. TURNER, D.P., 2013. Disaggregation of land types Ea34 and Ca11 by terrain analysis, expert knowledge and GIS methods. *S. Afr. J. Plant & Soil*, 30(3), 123-129.

VAN ZIJL, G.M., LE ROUX, P.A.L., 2014. Creating a hydrological soil map for the Stevenson Hamilton Supersite, Kruger National Park. *Water SA* 40 (2), 331-336.

CHIMUNGU, J.G., HENSLEY, M., VAN RENSBURG, L.D. & LE ROUX, P.A.L., In press. Laboratory characterization of the water retention characteristics of the diagnostic horizons of a Bainsvlei form soil. *S. Afr. J. Plant & Soil*. (In press)

CAPACITY BUILDING INCLUDES 14 DEGREES:

Baccalaureus Honours degrees (7) by Darren Bouwer, Kobus Coetzee, Riaan Van der Merwe, Babalwa Mtshawu, Sandy Mufamadi, Martin Tinnefeld, Christina Jacobs.

Masters in Science degrees (4) by Bataung Kuenene, Darren Bouwer, Babalwa Mtshawu, Carl Freese (supported).

Philosophy Doctor degrees (3) by Johan van Tol, Bataung Kuenene, George van Zijl.

TABLE OF CONTENTS

| | |
|-------------------|----------------------------------------------------------------------------------|
| ACKNOWLEDGEMENTS | iv |
| EXECUTIVE SUMMARY | v |
| TABLE OF CONTENTS | ix |
| LIST OF TABLES | xiii |
| LIST OF FIGURES | xvii |
| INTRODUCTION | xxii |
| Chapter 1 | CLASSIFICATION OF SOUTH AFRICAN HILLSLOPE HYDROLOGY |
| 1 | 1 |
| 1.1 | Introduction 1 |
| 1.2 | Methodology 3 |
| 1.2.1 | Study areas..... 3 |
| 1.2.2 | Hydrological soil types 4 |
| 1.2.3 | Framework of the classification system 5 |
| 1.3 | Results and Discussion 6 |
| 1.3.1 | Hydrological hillslope classes..... 7 |
| 1.4 | Applications..... 35 |
| 1.4.1 | Distributed modelling 35 |
| 1.4.2 | Land use change impact 37 |
| 1.4.3 | Water quality 38 |
| 1.5 | Conclusion 38 |
| 1.6 | References..... 39 |
| Chapter 2 | HYDROPEDOLOGICAL RESPONSES OF SELECTED HILLSLOPES |
| 2 | 43 |
| 2.1 | Hillslope Descriptions..... 43 |
| 2.1.1 | Monitoring setup 43 |
| 2.1.2 | Hillslope 1 (LC 01-LC 07)..... 44 |
| 2.1.3 | Hillslope 2 (LC 08-LC10) 49 |
| 2.1.4 | Hillslope 3 (UC 01-UC 03)..... 55 |
| 2.1.5 | Hillslope 4 (UC3/4-UC 08) 60 |
| 2.2 | Conclusion 64 |
| 2.2.1 | Hillslope and Catchment scale δO^{18} Hydrograph Separation 66 |
| 2.3 | In-situ measurements of Weatherley 69 |
| 2.3.1 | Introduction 69 |
| 2.3.2 | Study area and methodology..... 71 |
| 2.3.3 | RESULTS AND DISCUSSION 79 |
| 2.3.4 | Conclusions 90 |
| 2.4 | in-situ measurements of TWO Streams 91 |
| 2.4.1 | Introduction 91 |
| 2.4.2 | Methodology..... 93 |
| 2.4.3 | Results and discussion 95 |
| 2.4.4 | Conclusion..... 109 |
| 2.5 | in-situ measurements of CATHEDRAL PEAK 6..... 110 |
| 2.6 | Results and discussion..... 112 |
| 2.6.1 | Soil distribution on the main hillslope 112 |
| 2.6.2 | Measurements providing evidence for the conceptual hydrological models 114 |
| 2.6.3 | Conceptual hydro pedological hillslope models 119 |
| 2.7 | Conclusion 121 |
| 2.8 | Reference 122 |

| | | |
|-----------|-----------------------------------------------------------------------------------------------------------------------------------------------------------|-----|
| Chapter 3 | FROM LAND TYPES TO HYDROLOGICAL HILLSLOPES | 125 |
| 3.1 | Introduction | 125 |
| 3.2 | Case Studies | 126 |
| 3.2.1 | Case study 1: A theoretical approach to disaggregating a land type inventory into conceptual hydrological flow models and soil maps | 126 |
| 3.2.2 | Case study 2: Using a soil map to create a hydrological response unit map..... | 137 |
| 3.2.3 | Case study 3: Creating a hydrological response unit map from scratch by combining Digital soil mapping and hillslope delineation | 146 |
| 3.3 | Application of hydropedological insights in hydrological modelling of the Stevenson Hamilton Research Supersite, Kruger National Park, South Africa | 155 |
| 3.3.1 | Introduction | 155 |
| 3.3.2 | The ACRU hydrological model | 156 |
| 3.3.3 | Methodology..... | 157 |
| 3.3.4 | Model parameterisation and configuration | 158 |
| 3.3.5 | Results and discussion | 164 |
| 3.3.6 | Conclusions | 171 |
| 3.3.7 | Acknowledgements | 171 |
| 3.4 | Conclusions | 171 |
| 3.5 | References..... | 172 |
| Chapter 4 | VIRTUAL EXPERIMENTATION | 175 |
| 4.1 | INTRODUCTION | 175 |
| 4.2 | METHODOLOGY | 177 |
| 4.2.1 | Virtual hillslope setup | 177 |
| 4.2.2 | Virtual simulations | 178 |
| 4.2.3 | IUH's and fitting ADF's | 179 |
| 4.3 | RESULTS..... | 179 |
| 4.3.1 | Multiple regressions | 179 |
| 4.4 | REFERENCES | 180 |
| Chapter 5 | HYDROLOGICAL MODELLING USING HYDROPEDOLOGICAL DATA | 182 |
| 5.1 | ABSTRACT | 182 |
| 5.2 | INTRODUCTION | 182 |
| 5.2.1 | The hydrological modelling problem | 182 |
| 5.2.2 | Study objectives..... | 183 |
| 5.3 | ACRU HYDROLOGICAL MODEL | 183 |
| 5.3.1 | Soil parameters in <i>ACRU</i> | 183 |
| 5.3.2 | Intermediate zone (<i>ACRU-Int</i>) | 186 |
| 5.4 | METHODOLOGY | 186 |
| 5.4.1 | Study area | 186 |
| 5.4.2 | Model configuration | 186 |
| 5.4.3 | Model parameterization..... | 188 |
| 5.4.4 | Simulation period, climatic inputs and comparison data | 190 |
| 5.5 | RESULTS..... | 190 |
| 5.5.1 | Streamflow..... | 190 |
| 5.5.2 | Soil water contents | 195 |
| 5.5.3 | Lateral flow from INT zone | 204 |
| 5.6 | DISCUSSION | 206 |
| 5.7 | CONCLUSIONS | 208 |
| 5.8 | REFERENCES | 209 |

| | | |
|-----------|----------------------------------------------------------------------------------------------------------------------------------------------------------------------------|-----|
| Chapter 6 | HYDROPEDOLOGICAL STUDY TECHNIQUES (A) | 211 |
| 6.1 | The hydrological Response of diagnostic horizons and Profiles | 211 |
| 6.1.1 | All data plus comparisons of horizons | 211 |
| 6.2 | References..... | 226 |
| 6.3 | Hydropedological classification of South African soil forms..... | 228 |
| 6.3.1 | Hydrology of soil types | 228 |
| 6.3.2 | Introduction | 234 |
| 6.3.3 | Factors controlling groundwater recharge | 235 |
| 6.3.4 | Interaction in vadose zone..... | 241 |
| 6.3.5 | Soil distribution pattern as a window to soil/rock/soil interaction in hillslopes | 243 |
| 6.3.6 | Conclusion..... | 244 |
| 6.4 | References:..... | 245 |
| 6.5 | Elucidating the relationship between recent (soil chemical and hydrological) soil properties and ancient (morphological) soil properties and hillslope hydropedology | 247 |
| 6.5.1 | INTRODUCTION | 247 |
| 6.5.2 | METHODOLOGY | 248 |
| 6.5.3 | RESULTS AND DISCUSSIONS..... | 250 |
| 6.6 | CONCLUSIONS | 267 |
| 6.7 | REFERENCES | 268 |
| Chapter 7 | HYDROPEDOLOGICAL STUDY TECHNIQUES | 270 |
| 7.1 | In-situ continuous measurements of theta in hillslope soils and conclusions w.r.t. appropriate instrumentation..... | 270 |
| 7.1.1 | Introduction | 270 |
| 7.1.2 | DFM Capacitance probes | 272 |
| 7.1.3 | The installation and calibration of DFM probes in the Two Streams catchment ... | 273 |
| 7.1.4 | DFM measurements in the Weatherley catchment | 279 |
| 7.1.5 | Conclusions | 282 |
| 7.2 | References..... | 285 |
| 7.3 | Field measurements of K_s and K_h low tensions – macroporosity | 286 |
| 7.3.1 | Introduction | 286 |
| 7.3.2 | Methodology..... | 288 |
| 7.3.3 | Results and discussions..... | 292 |
| 7.3.4 | Conclusions | 305 |
| 7.4 | References..... | 307 |
| 7.5 | Water retention curves to provide van Genuchten Parameters and K_h curves needed by hydrologists | 310 |
| 7.5.1 | Methodology..... | 310 |
| 7.5.2 | Results and discussion | 314 |
| 7.5.3 | Conclusion..... | 326 |
| 7.6 | References..... | 326 |
| 7.7 | Introduction to the use of isotopes..... | 328 |
| 7.7.1 | Fractionation..... | 329 |
| 7.7.2 | Isotopes of rainfall | 330 |
| Chapter 8 | CONCLUSIONS, NEEDS AND SUGGESTIONS FOR FUTURE STUDIES | 333 |
| 8.1 | Needs..... | 333 |
| 8.2 | The clarification, simplification and classification of hydrological units..... | 333 |
| 8.3 | Spatial application: maps | 334 |

| | | |
|-----|----------------------------------------------------------|-----|
| 8.4 | Pedo-logic..... | 335 |
| 8.5 | From experiments to models | 336 |
| 8.6 | Future needs and possibilities..... | 338 |
| 8.7 | Transfer functions for hydrological response units | 339 |
| 8.8 | References..... | 339 |

APPENDICES 1-8 appear on the enclosed CD

LIST OF TABLES

| | |
|------------------------------------------------------------------------------------------------------------------------------------------------------------------------------------------------------------------------------------------------------------------------------------------------------------------|-----|
| TABLE 1 BRIEF DESCRIPTION OF THE STUDIED HILLSLOPE; LEVEL OF INVESTIGATIVE DETAIL, GEOLOGY AND APPROXIMATE ARIDITY INDEX (AI)..... | 4 |
| TABLE 2 HYDROLOGICAL SOIL TYPES OF THE STUDIED HILLSLOPES..... | 5 |
| TABLE 3 WEATHERLEY, HILLSLOPE 1, ΔO^{18} ISOTOPE DATA 3-13 MARCH 2010 | 47 |
| TABLE 4 WEATHERLEY, HILLSLOPE 2, ΔO^{18} ISOTOPE DATA 3-13 MARCH 2010 | 54 |
| TABLE 5 WEATHERLEY, HILLSLOPE 3, ΔO^{18} ISOTOPE DATA 3-13 MARCH 2010 | 58 |
| TABLE 6 WEATHERLEY, HILLSLOPE 4, ΔO^{18} ISOTOPE DATA 3-13 MARCH 2010 | 63 |
| TABLE 7 HYDRUS 1-D DESCRIPTIONS USED FOR SIMULATION OF WATER FLOW AT TB4..... | 79 |
| TABLE 8 SELECTED SOIL PROPERTIES AT DIFFERENT PROFILES AT TB, CHEMICAL PROPERTIES MEASURED WITH MIR | 80 |
| TABLE 9 VERTICAL AND LATERAL HYDRAULIC CONDUCTIVITIES ($MM\ H^{-1}$) FOR DIFFERENT SITES AND HORIZONS | 83 |
| TABLE 10 K_s VALUES DETERMINED BELOW THE WATER TABLE WITH SLUG TESTS..... | 84 |
| TABLE 11 VAN GENUCHTEN PARAMETERS OF DIFFERENT HORIZONS AT TB..... | 84 |
| TABLE 12 VOLUMES (ℓ) MEASURED AT DIFFERENT DEPTHS AT PROFILE TRENCH EXPERIMENT | 86 |
| TABLE 13 VOLUMES (ℓ) MEASURED IN PIPES SLOTTED AT VARIOUS DEPTHS | 86 |
| TABLE 14 TEN MEASUREMENTS AT DIFFERENT TIMES OF TOTAL SOIL WATER CONTENTS (MM) IN THE SOLUM (0-2.1 M; UPPER VADOSE ZONE); AND THE SAPROLITE (2.55-4.65 M; INTERMEDIATE VADOSE ZONE), AT HILLSLOPE AND VALLEY BOTTOM LOCATIONS IN A TERRESTRIAL A ZONE AREA (FIGURE 103) CLOSE TO THE TWO STREAMS CATCHMENT | 97 |
| TABLE 15 CALCULATING ΣET (EQUATION 2.6) FOR THE CATCHMENT DURING THE 203 PERIOD 6/9/2004 TO 28/3/2005 | 98 |
| TABLE 16 STREAMFLOW – RAINFALL RATIOS FOR THE YEARS 2001-2008 FOR THE RESEARCH CATCHMENT | 101 |
| TABLE 17 FIVE SELECTED RAINFALL EVENTS AND INTENSITIES DURING THE DECEMBER 2004 RAIN PERIOD | 102 |
| TABLE 18 ANTECEDENT SOIL WATER IN THE A HORIZON AND TOTAL RAINFALL AND STREAMFLOW DURING RAINFALL EVENTS IN FIGURE 83..... | 107 |
| TABLE 19 ANNUAL CLIMATIC DATA MEASURED FOR 4 YEARS IN THE CP6 CATCHMENT BY EVERSON <i>ET AL.</i> (1998)..... | 111 |
| TABLE 20 DESCRIPTION OF SIX PHASES OF THE HYDROGRAPH SHOWN IN FIGURE 116, AND HYPOTHESIS REGARDING THE MAIN FLOW PROCESSES AND SOURCES OF WATER..... | 116 |
| TABLE 21 DECREASES IN WATER TABLE LEVELS AT 3 BOREHOLES, AND ESTIMATED AMOUNT OF WATER SUPPLIED TO LOW FLOW OUT OF THE CATCHMENT DURING THE PERIOD 11/05/95-30/09/95 | 119 |
| TABLE 22 : AREAS OF MAPPING UNITS OBTAINED BY THE METHODOLOGY AS WELL AS FROM THE LAND TYPE INVENTORY . | 135 |
| TABLE 23 SOIL FORMS COMPRISING EACH MAP UNIT | 141 |
| TABLE 24 AN ERROR MATRIX OF MAP 4 | 144 |
| TABLE 25 CONVERSION OF SOIL ASSOCIATIONS TO SOIL HYDROLOGICAL RESPONSE UNITS..... | 144 |
| TABLE 26 AREAS COVERED BY THE DIFFERENT CONCEPTUAL HYDROLOGICAL RESPONSES | 146 |
| TABLE 27 DESCRIPTIONS OF THE SOIL MAP UNITS..... | 150 |
| TABLE 28 SOIL DISTRIBUTION RULES FOR THE HYDROLOGICAL SOIL MAP UNITS | 152 |
| TABLE 29 AN ACCURACY MATRIX OF THE SOIL MAP | 153 |
| TABLE 30 AVERAGE MONTHLY CLIMATIC PARAMETERS FOR THE SHRS (SCHULZE <i>ET AL.</i> , 2007) | 159 |
| TABLE 31 MODEL PARAMETERS OF DIFFERENT SOIL TYPES AND CATCHMENT ORDERS FOR MODEL RUNS | 162 |
| TABLE 32 SIMULATED AGAINST OBSERVED DAILY FLOW EFFICIENCY MEASUREMENTS (R2: COEFFICIENT OF DETERMINATION; NS: NASH-SUTCLIFFE; MSE: MEAN SQUARE ERROR) | 165 |
| TABLE 33 PEARSON’S PRODUCT MOMENT CORRELATION COEFFICIENT BETWEEN MEASURED WATER TENSION (INVERSE LOG TRANSFORMED – MM) AND SIMULATED WATER CONTENTS ($MM\ MM^{-1}$) | 171 |
| TABLE 34 RANGES OF PARAMETER VALUES USED IN VIRTUAL SIMULATIONS | 178 |
| TABLE 35 FIRST ORDER CONTROLS, AND OPTIMIZED D_p AND T VALUES FOR THE 23 IUH’S..... | 180 |
| TABLE 36 SOME ATTRIBUTES OF DIFFERENT LAND SEGMENTS USED IN TO CALCULATE MODEL PARAMETERS | 189 |
| TABLE 37 SOIL PARAMETERS USED SIMULATING THE WEATHERLEY CATCHMENT..... | 190 |
| TABLE 38 ORIGIN OF PUBLISHED AND UN-PUBLISHED DATA USED IN DISCUSSION. LOCATION FROM WHERE DATA IS OBTAINED, AND WHERE IN THE DISCUSSION IT IS APPLIED, IS SUPPLIED | 213 |

| | |
|-----------------------------------------------------------------------------------------------------------------------------------------------------------------------------------------------------------------------------------------------------------------------------------------------|-----|
| TABLE 39 CONCEPTUAL HYDROLOGICAL FUNCTIONALITY OF DIAGNOSTIC HORIZONS: FLOW RATE, FLOW DIRECTION, STORAGE AND SOURCE HORIZONS | 216 |
| TABLE 40 EFFECT OF PERMEABILITY OF THE UNDERLYING ROCK IN WEATHERLY, CONTRIBUTING ON THE MORPHOLOGICAL AND HYDROLOGICAL PROPERTIES OF HORIZONS IN SEQUENCE OF A SOIL FORM (BEEH, 2003) ... | 218 |
| TABLE 41 SATURATED HYDRAULIC CONDUCTIVITY OF PEDOCUTANIC B HORIZON (SUB-ANGULAR BLOCKY) WITH STATISTICAL VALUES (STANDARD DEVIATION (SD)) IN MM H^{-1} | 219 |
| TABLE 42 SATURATED HYDRAULIC CONDUCTIVITY OF PRISMACUTANIC B HORIZONS WITH STATISTICAL ANALYSIS. VALUES (STANDARD DEVIATION (SD)) IN MM H^{-1} | 220 |
| TABLE 43 SELECTED RED-APEDAL B HORIZONS SUBJECT TO STATISTICAL ANALYSIS TO INDICATE MEAN AND STANDARD DEVIATION..... | 222 |
| TABLE 44 REAL SOILS WITH STATISTICALLY IDEALIZED SATURATED HYDRAULIC CONDUCTIVITY RATES INDICATING STORAGE CAPACITY DUE TO UNDERLYING REDUCED SATURATED HYDRAULIC CONDUCTIVITY | 222 |
| TABLE 45 TWO SOIL FORMS DIVIDED INTO DIAGNOSTIC HORIZONS WITH THEIR MEDIAN/STANDARD DEVIATION HYDRAULIC CONDUCTIVITY VALUES (MM H^{-1}) INDICATING THE EFFECT OF UNDERLYING HORIZONS ON THE ABOVE LYING "SOURCE HORIZON" | 223 |
| TABLE 46 $\text{ADS} > 0.7$ OF DIAGNOSTIC HORIZONS IN BLOEMDAL, KATSPRUIT AND KROONSTAD | 255 |
| TABLE 47 OBSERVATIONS ON THE CREST AND UPPER MIDSLOPE REPRESENTED BY BLOEMDAL PROFILE | 255 |
| TABLE 48 OBSERVATIONS ON THE FOOTSLOPE REPRESENTED BY KATSPRUIT PROFILE | 260 |
| TABLE 49 OBSERVATIONS ON THE TOESLOPE REPRESENTED BY THE KROONSTAD PROFILE..... | 265 |
| TABLE 50 RESULTS OF COMBINED DFM-NWM CALIBRATION PROCEDURE IN AN INANDA SOIL. THE WETTING PROCEDURE USED IS SHOWN IN FIGURE 210 | 277 |
| TABLE 51 CALIBRATION CURVES FOR DFM 15291 SENSORS | 279 |
| TABLE 52 DFM PROBE READINGS AND MEASURED WATER CONTENTS AT PROFILE TB4 | 282 |
| TABLE 53 CALIBRATION CURVES FOR DFM SENSORS AT TB4 | 282 |
| TABLE 54 DESCRIPTION OF THE QUANTITATIVE SOIL PROPERTIES USED IN THE DEVELOPMENT OF THE PTF'S | 291 |
| TABLE 55 DESCRIPTION OF QUALITATIVE SOIL OBSERVATIONS USED FOR DEVELOPMENT OF PTF'S..... | 292 |
| TABLE 56 DESCRIPTION OF THE MODEL VARIABLES AND THEIR ASSOCIATED VALUES | 293 |
| TABLE 57 SOIL HYDRAULIC CONDUCTIVITY (K), TOTAL EFFECTIVE POROSITY (θ_m), AND PERCENTAGE CONTRIBUTION OF MACROPORES TO K_s (ϕ) | 299 |
| TABLE 58 STREAMFLOW AND RAINFALL VOLUMES DURING THE PERIOD 31/12/04 AND 6/1/05..... | 301 |
| TABLE 59 SOIL WATER CONTENT DATA DURING CALIBRATION PROCEDURE OF A DFM PROBE INSTALLED DURING 2011 IN THE SAME INANDA SOIL PROFILE DISCUSSED IN THE PREVIOUS SECTION..... | 304 |
| TABLE 60 SELECTED MORPHOLOGICAL DESCRIPTION, TEXTURE AND CHEMICAL PROPERTIES OF THE DIAGNOSTIC HORIZONS IN THE TWO STREAMS CATCHMENT..... | 313 |
| TABLE 61 VAN GENUCHTEN PARAMETERS AND CORRELATION COEFFICIENTS (R^2) OBTAINED FROM ANALYZING MEASURED $\theta(h)$ AND $K(h)$ DATA FOR DIAGNOSTIC HORIZONS USING THE RETC PROGRAM. MEASURED K_s , K_h (30, 80 , AND 150 MM TENSIONS) AND BULK DENSITY FOR EACH HORIZON ARE SHOWN | 318 |

LIST OF FIGURES

| | |
|---------------------------------------------------------------------------------------------------------------------------------------------------------------------|----|
| FIGURE 1 GEOGRAPHICAL DISTRIBUTION OF STUDIED HILLSLOPES. | 3 |
| FIGURE 2 EXAMPLE OF HOW HILLSLOPE CLASSES ARE PRESENTED AND DISCUSSED. | 6 |
| FIGURE 3 PERCEPTUAL FLOW MODELS OF HILLSLOPE CLASS 1 (A1, A2 & A3) AND ANTICIPATED HILLSLOPE HYDROGRAPH (B) | 7 |
| FIGURE 4 SOIL DISTRIBUTION PATTERN OF THE CATHEDRAL PEAK IV HILLSLOPE 1 | 8 |
| FIGURE 5 SOIL DISTRIBUTION PATTERN OF THE CATHEDRAL PEAK IV 2 HILLSLOPE. | 9 |
| FIGURE 6 SOIL DISTRIBUTION PATTERN OF THE LOERIESFONTEIN 2 HILLSLOPE | 10 |
| FIGURE 7 SOIL DISTRIBUTION PATTERN OF THE SKUKUZA 2 HILLSLOPE | 10 |
| FIGURE 8 SOIL DISTRIBUTION PATTERN OF THE NEW CASTLE 1 HILLSLOPE | 11 |
| FIGURE 9 SOIL DISTRIBUTION PATTERN OF THE NEW CASTLE 3 HILLSLOPE | 11 |
| FIGURE 10 SOIL DISTRIBUTION PATTERN OF THE PAN AFRICAN PARLIAMENT SITE HILLSLOPE. | 12 |
| FIGURE 11 SOIL DISTRIBUTION PATTERN OF THE BLOEMFONTEIN 2&3 HILLSLOPE..... | 12 |
| FIGURE 12 SOIL DISTRIBUTION PATTERN OF THE MOKOLO 1&2 HILLSLOPE | 13 |
| FIGURE 13 SOIL DISTRIBUTION PATTERN OF THE MOKOLO HILLSLOPE 3 | 13 |
| FIGURE 14 SOIL DISTRIBUTION PATTERN OF THE THABA NCHU 2 HILLSLOPE..... | 13 |
| FIGURE 15 PERCEPTUAL FLOW MODELS OF HILLSLOPE CLASS 2 (A1 & A2) AND ANTICIPATED HILLSLOPE HYDROGRAPH (B)..... | 14 |
| FIGURE 16 SOIL DISTRIBUTION PATTERN OF THE BEDFORD B3 HILLSLOPE..... | 15 |
| FIGURE 17 SOIL DISTRIBUTION PATTERN OF THE BEDFORD B4&B5 HILLSLOPE | 16 |
| FIGURE 18 SOIL DISTRIBUTION PATTERN OF THE BEDFORD B4&B5 HILLSLOPE | 16 |
| FIGURE 19 PERCEPTUAL FLOW MODELS OF HILLSLOPE CLASS 3 (A1, A2 & A3) AND ANTICIPATED HILLSLOPE HYDROGRAPH (B) | 17 |
| FIGURE 20 SOIL DISTRIBUTION PATTERN OF THE LETABA HILLSLOPES 1, 3 & 4 | 18 |
| FIGURE 21 SOIL DISTRIBUTION PATTERN OF THE LETABA 2 HILLSLOPE..... | 18 |
| FIGURE 22 SOIL DISTRIBUTION PATTERN OF THE SCHMITSDRIFT 1 HILLSLOPE | 18 |
| FIGURE 23 SOIL DISTRIBUTION PATTERN OF THE SCHMITSDRIFT 2 HILLSLOPE | 19 |
| FIGURE 24 SOIL DISTRIBUTION PATTERN OF THE NOORD KAAP 1 HILLSLOPE | 19 |
| FIGURE 25 SOIL DISTRIBUTION PATTERN OF THE NOORD KAAP 2 HILLSLOPE | 20 |
| FIGURE 26 SOIL DISTRIBUTION PATTERN OF THE MOKOLO 4&5 HILLSLOPE | 20 |
| FIGURE 27 SOIL DISTRIBUTION PATTERN OF THE BLOEMFONTEIN 4 HILLSLOPE | 20 |
| FIGURE 28 PERCEPTUAL FLOW MODELS OF HILLSLOPE CLASS 4 (A1, A2 & A3) AND ANTICIPATED HILLSLOPE HYDROGRAPH (B) | 21 |
| FIGURE 29 SOIL DISTRIBUTION PATTERN OF THE BAVIAANS KLOOF 1 HILLSLOPE | 22 |
| FIGURE 30 SOIL DISTRIBUTION PATTERN OF THE BAVIAANS KLOOF 2 HILLSLOPE | 22 |
| FIGURE 31 SOIL DISTRIBUTION PATTERN OF THE NEW CASTLE 2 HILLSLOPE | 23 |
| FIGURE 32 SOIL DISTRIBUTION PATTERN OF THE TAYLORS HALL HILLSLOPE..... | 23 |
| FIGURE 33 SOIL DISTRIBUTION PATTERN OF THE TWO STREAMS CATCHMENT N HILLSLOPE..... | 24 |
| FIGURE 34 SOIL DISTRIBUTION PATTERN OF THE HOGSBACK 1 HILLSLOPE | 25 |
| FIGURE 35 SOIL DISTRIBUTION PATTERN OF THE HOGSBACK 2 HILLSLOPE | 25 |
| FIGURE 36 SOIL DISTRIBUTION PATTERN OF THE RIVERDALE HILLSLOPE..... | 26 |
| FIGURE 37 SOIL DISTRIBUTION PATTERN OF THE WEATHERLEY 1 HILLSLOPE..... | 27 |
| FIGURE 38 SOIL DISTRIBUTION PATTERN OF THE WEATHERLEY 2 HILLSLOPE..... | 27 |
| FIGURE 39 SOIL DISTRIBUTION PATTERN OF THE WEATHERLEY 3 HILLSLOPE..... | 27 |
| FIGURE 40 SOIL DISTRIBUTION PATTERN OF THE BLOEMFONTEIN 1 HILLSLOPE | 28 |
| FIGURE 41 PERCEPTUAL FLOW MODEL OF HILLSLOPE CLASS 5 (A) AND ANTICIPATED HILLSLOPE HYDROGRAPH (B) | 28 |
| FIGURE 42 SOIL DISTRIBUTION PATTERN OF THE SKUKUZA 3 HILLSLOPE | 29 |
| FIGURE 43 SOIL DISTRIBUTION PATTERN OF THE SKUKUZA 4 HILLSLOPE | 29 |
| FIGURE 44 SOIL DISTRIBUTION PATTERN OF THE FORT HARE 2 HILLSLOPE | 30 |
| FIGURE 45 SOIL DISTRIBUTION PATTERN OF THE BLOEMFONTEIN 5 HILLSLOPE | 30 |
| FIGURE 46 SOIL DISTRIBUTION PATTERN OF THE THABA NCHU 1 HILLSLOPE..... | 30 |
| FIGURE 47 PERCEPTUAL FLOW MODELS OF HILLSLOPE CLASS 6 (A1 & A2) AND ANTICIPATED HILLSLOPE HYDROGRAPH (B)..... | 31 |
| FIGURE 48 SOIL DISTRIBUTION PATTERN OF THE CRAGIEBURN HILLSLOPE | 31 |
| FIGURE 49 SOIL DISTRIBUTION PATTERN OF THE CRAGIEBURN 3 HILLSLOPE | 32 |
| FIGURE 50 SOIL DISTRIBUTION PATTERN OF THE CRAIGIEBURN 2 HILLSLOPE | 32 |
| FIGURE 51 SOIL DISTRIBUTION PATTERN OF THE WEATHERLEY 4 HILLSLOPE..... | 33 |
| FIGURE 52 CONCEPTUAL HYDROLOGICAL BEHAVIOUR OF THE SELECTED HILLSLOPE BASED ON SOIL INTERPRETATIONS. VARIOUS PROCESSES ARE INDICATED BY THE NUMBERED ARROWS..... | 33 |
| FIGURE 53 SOIL DISTRIBUTION PATTERN OF THE WEATHERLY 5 HILLSLOPE | 35 |

| | |
|----------------------------------------------------------------------------------------------------------------------------------------------------------------------------------------------------------------------------------------------------------------------------------------------------------------------------------------------|----|
| FIGURE 54 SCHEMATIC OF THE MODEL PROFILE WITH THE INTERMEDIATE LAYER BASE UNSATURATED (LEFT) AND SATURATED (RIGHT) WHEN PERCOLATION AND LATERAL FLOWS ARE INDUCED (AFTER LORENTZ <i>ET AL.</i> , 2007) | 36 |
| FIGURE 55 FLOW ROUTING BASED ON HYDROPEDEOLOGICAL INTERPRETATION OF SOILS (VAN TOL <i>ET AL.</i> , 2011) | 37 |
| FIGURE 56 SIMULATED AND OBSERVED STREAMFLOW IN THE WEATHERLEY CATCHMENT DURING 2000, (LE ROUX <i>ET AL.</i> , 2011) ... | 37 |
| FIGURE 57 WEATHERLEY SITUATION, GEOLOGY AND MONITORED HILLSLOPES 1-4..... | 43 |
| FIGURE 58 WEATHERLEY, HILLSLOPE 1, ILLUSTRATIVE DESCRIPTION AND CONCEPTUAL FLOW PATHS..... | 44 |
| FIGURE 59 WEATHERLEY, HILLSLOPE 1, PRE-EVENT WATER TABLE DRAINAGE AND ΔO^{18} | 46 |
| FIGURE 60 WEATHERLEY, HILLSLOPE 1, LC 06 AND LC 07 LONG TERM PIEZOMETER DEPTH OBSERVATIONS..... | 47 |
| FIGURE 61 WEATHERLEY, HILLSLOPE 1, MARCH 2010 ΔO^{18} AND $\Delta 2H$ ISOTOPES. | 48 |
| FIGURE 62 WEATHERLEY, HILLSLOPE 1, PRE EVENT (LEFT) AND POST EVENT (RIGHT) WATER TABLE DRAINAGE AND ΔO^{18} ISOTOPES.. | 49 |
| FIGURE 63 WEATHERLEY, HILLSLOPE 2, ILLUSTRATIVE DESCRIPTION AND CONCEPTUAL FLOW PATHS..... | 50 |
| FIGURE 64 WEATHERLEY, HILLSLOPE 2, MARCH 2010 ΔO^{18} AND $\Delta 2H$ ISOTOPES | 51 |
| FIGURE 65 WEATHERLEY, HILLSLOPE 2, MARCH 2010 ΔO^{18} PIEZOMETER ISOTOPE VALUES | 52 |
| FIGURE 66 WEATHERLEY, HILLSLOPE 2, PRE-EVENT WATER TABLE DRAINAGE AND ΔO^{18} | 53 |
| FIGURE 67 WEATHERLEY, HILLSLOPE 2, POST-EVENT (LEFT) AND POST EVENT (RIGHT) WATER TABLE DRAINAGE AND ΔO^{18} | 55 |
| FIGURE 68 WEATHERLEY, HILLSLOPE 3, PIEZOMETER UC 01 DEPTH OF SOIL WATER ABOVE THE BEDROCK. | 55 |
| FIGURE 69 WEATHERLEY, HILLSLOPE 3, ILLUSTRATIVE DESCRIPTION AND CONCEPTUAL FLOW PATHS..... | 56 |
| FIGURE 70 WEATHERLEY, HILLSLOPE 3, PRE-EVENT WATER TABLE DRAINAGE AND ΔO^{18} | 57 |
| FIGURE 71 WEATHERLEY, HILLSLOPE 3, MARCH 2010 ΔO^{18} PIEZOMETER VALUES | 58 |
| FIGURE 72 WEATHERLEY, HILLSLOPE 3, MARCH 2010 ΔO^{18} AND $\Delta 2H$ ISOTOPE VALUES. | 59 |
| FIGURE 73 WEATHERLEY, HILLSLOPE 3, PRE EVENT (LEFT) AND POST EVENT (RIGHT) WATER TABLE DRAINAGE AND ΔO^{18} VALUES | 59 |
| FIGURE 74 WEATHERLEY, HILLSLOPE 4, ILLUSTRATIVE DESCRIPTION AND CONCEPTUAL FLOW PATHS..... | 61 |
| FIGURE 75 WEATHERLEY, HILLSLOPE 4, PRE-EVENT WATER TABLE DRAINAGE AND ΔO^{18} ISOTOPE VALUES | 62 |
| FIGURE 76 WEATHERLEY, HILLSLOPE 4, POST-EVENT WATER TABLE DRAINAGE AND ΔO^{18} ISOTOPE VALUES | 63 |
| FIGURE 77 WEATHERLEY, HILLSLOPE 4, MARCH 2010 ΔO^{18} ISOTOPE VALUES | 64 |
| FIGURE 78 WEATHERLEY, HILLSLOPE 4, MARCH 2010 ΔO^{18} AND $\Delta 2H$ ISOTOPE VALUES..... | 64 |
| FIGURE 79 WEATHERLEY ΔO^{18} ISOTOPES OF RAINFALL STREAMFLOW AND RIPARIAN PIEZOMETERS | 65 |
| FIGURE 80 HILLSLOPE 1, HILLSLOPE NEST LC04 EVENT AND PRE EVENT CONTRIBUTIONS..... | 66 |
| FIGURE 81 HILLSLOPE 3, HILLSLOPE NEST UC01 EVENT AND PRE EVENT CONTRIBUTIONS..... | 67 |
| FIGURE 82 HILLSLOPE 4, HILLSLOPE NEST UC07 EVENT AND PRE EVENT CONTRIBUTIONS..... | 67 |
| FIGURE 83 HILLSLOPE 1, RIPARIAN NEST 13, EVENT AND PRE EVENT CONTRIBUTIONS..... | 68 |
| FIGURE 84 HILLSLOPE 2, RIPARIAN NEST 11, EVENT AND PRE EVENT CONTRIBUTIONS..... | 68 |
| FIGURE 85 HILLSLOPE 3, RIPARIAN NEST 2A, EVENT AND PRE EVENT CONTRIBUTIONS. | 69 |
| FIGURE 86 HILLSLOPE 4, RIPARIAN NEST UC 3/4, EVENT AND PRE EVENT CONTRIBUTIONS..... | 69 |
| FIGURE 87: A) INSTRUMENTATION OF THE WEATHERLEY CATCHMENT (LORENTZ <i>ET AL.</i> , 2004), B) HILLSLOPE 1-4 WITH LOCATION OF TIPPING BUCKET EXPERIMENT AND C) TIPPING BUCKET (HILLSLOPE OUTFLOW) EXPERIMENT AT THE FOOTSLOPE OF HILLSLOPE 1-4. TB1-TB10 IN C) IS PERFORATED PIPE NESTS. DFM PROBES WERE INSTALLED AT TB1-4, TB7 AND TB9 | 72 |
| FIGURE 88 TWO DIMENSIONAL (2-D) REPRESENTATION OF TRANSECT TB4-TB1 (SEE FIGURE 87C FOR LOCATION) | 73 |
| FIGURE 89 : PROPOSED METHOD TO DETERMINE LATERAL HYDRAULIC CONDUCTIVITIES IN THE FIELD: A) THE PVC RING BEING FORCED INTO A SPECIFIC HORIZON BY MEANS OF A HYDRAULIC JACK; B) THE SETUP FOR DOUBLE RING K MEASUREMENTS WITH THE CORE NOW ORIENTATED VERTICALLY; C) THE SETUP FOR LATERAL K(h) MEASUREMENTS BY TENSION INFILTRMETER..... | 74 |
| FIGURE 90 TRENCH EXPERIMENT AT LC2..... | 76 |
| FIGURE 91 SLOTTED PIPES INSTALLED TO MEASURE FLOW FROM SPECIFIC HORIZONS | 77 |
| FIGURE 92 TIPPING BUCKET MEASURING OUTFLOW FROM A SELECTED PORTION OF HILLSLOPE IMMEDIATELY BELOW THE INVESTIGATED SITES TB1 TO TB4 SHOWN IN FIGURE 87C AND IN THE CROSS SECTION IN FIGURE 88. | 78 |
| FIGURE 93 INTERPOLATION OF SELECTED SOIL PROPERTIES OF THE CROSS SECTION TB1-TB4 | 81 |
| FIGURE 94 WATER RETENTION CURVES OF DIFFERENT HORIZONS AT TB | 85 |
| FIGURE 95 HYDRAULIC CONDUCTIVITY AT DIFFERENT WATER CONTENTS FOR HORIZONS AT TB..... | 85 |
| FIGURE 96 PRESENCE OF SATURATED WATER AT TB2 (A), TB3 (B) AND TB4 (C) AS MEASURED WITH DFM PROBES..... | 87 |
| FIGURE 97 RAINFALL (MM) VS. OUTFLOW ($MM\ H^{-1}$) MEASURED AT THE HILLSLOPE OUTFLOW EXPERIMENT..... | 89 |
| FIGURE 98 MEASURED OUTFLOW RATE ($MM\ H^{-1}$) AND WATER TABLE DEPTH FROM THE SURFACE AT TB2 | 89 |
| FIGURE 99 SIMULATED VS. MEASURED WATER CONTENTS OF THE OT HORIZON AT TB4, TOGETHER WITH THE DAILY AVERAGE RAINFALL | 90 |
| FIGURE 100 DETAILED SOIL MAP OF THE TWO STREAMS CATCHMENT WITH LOCATION OF WATERMARK SENSORS A) AND NEUTRON WATER METER ACCESS TUBE IN THE A ZONE REGION..... | 94 |

| | |
|------------------------------------------------------------------------------------------------------------------------------------------------------------------------------------------------------------------------------------------------------------------------------------------------------------------------------------------------------------------------------------------------------------------------------------------------------------------------------------------------------------------------------------------------------------------------------------|-----|
| FIGURE 101 STREAMFLOW VS RAINFALL DURING A WET PERIOD 5/11/2004-31/1/2005 | 96 |
| FIGURE 102 DAILY RAINFALL FROM 22/12/2004-31/1/2005 AND DEGREE OF SATURATION (S) OBTAINED FROM MEAN DAILY MEASUREMENTS BY WATERMARK SENSORS LOCATED AT DEPTHS OF 400, 800, 1200 AND 2000 MM (A, B, C, AND D, RESPECTIVELY), AT THE THREE PROFILES IN DOWNSLOPE ORDER, UPPER INANDA, MIDDLE INANDA, MAGWA, MARKED ON FIGURE 100..... | 97 |
| FIGURE 103 STREAMFLOW AND RAINFALL FOR THE RELATIVELY RAINFREE 100 DAY HYDROGRAPH RECESSION PERIOD, 29/03/2005-06/07/2005 IMMEDIATELY FOLLOWING THE 203 DAY HIGH RAINFALL PERIOD (DATA FROM EVERSON <i>ET AL.</i> , 2006) | 99 |
| FIGURE 104 HOURLY RAINFALL FROM 22/12/2004-31/1/2005 AND DEGREE OF SATURATION (S) OBTAINED FROM MEAN HOURLY MEASUREMENTS BY WATERMARK SENSORS LOCATED AT DEPTHS OF 400, 800, AND 1200 MM IN THE INANDA SOIL (DATA FROM EVERSON <i>ET AL.</i> , 2006) | 103 |
| FIGURE 105 RAINFALL AND STREAMFLOW INTENSITIES DURING RAINFALL EVENT 1 (A) AND 2 (B) | 104 |
| FIGURE 106 RAINFALL AND STREAMFLOW INTENSITIES DURING RAINFALL EVENT 1 (A) AND 2 (B) | 105 |
| FIGURE 107 RAINFALL AND STREAMFLOW INTENSITIES DURING RAINFALL EVENT 1 (A) AND 2 (B) | 106 |
| FIGURE 108 GENERAL LINEAR RELATIONSHIP BETWEEN RUNOFF AND THE PRE-EVENT SOIL MOISTURE CONTENT. THE GOOD R^2 IS ACHIEVED WHEN EVENT 5 (CROSSED EVENT) IS EXCLUDED | 107 |
| FIGURE 109 CONCEPTUAL FLOWPATHS IN THE MAIN HILLSLOPE OF THE TWO STREAMS CATCHMENT..... | 109 |
| FIGURE 110 SOIL MAP OF THE CATHEDRAL PEAK VI CATCHMENT (KUENENE, 2008). THREE NEUTRON WATER METER ACCESS TUBE SITES FOR SOIL WATER MONITORING, AND THREE BOREHOLES, FOR DEEP GROUNDWATER MONITORING ARE SHOWN. CH 1200 = CHAMPAGNE FORM, R = ROCK, IA = INANDA FORM, KP = KRANSKOP FORM, MA = MAGWA FORM, NO = NOMANCI FORM | 111 |
| FIGURE 111 A PHOTO OF AN INANDA SOIL PROFILE SHOWING UNDIAGNOSTIC YELLOW BROWN APEDAL B HORIZON UNDERNEATH THE RED APEDAL B HORIZON | 113 |
| FIGURE 112 SOIL WATER CONTENTS (S) AT DIFFERENT DEPTHS AT THE NWM MEASURING SITES MARKED ON FIGURE 110 (A) INANDA (SITE 1); (B) MAGWA (SITE 2) ABOUT 60 M FROM A DEEP DOWNSLOPE CHANNEL; (C) MAGWA (SITE 3) CLOSE TO A DEEP DOWNSLOPE CHANNEL; MEASUREMENT ARE FOR THE PERIOD MARCH 1990 TO NOVEMBER 1993 WITH ASSOCIATED RAINFALL (BASIC DATA FROM EVERSON <i>ET AL.</i> 1998) | 117 |
| FIGURE 113 (A) RAINFALL AND STREAMFLOW FROM 1990/91 TO 1994/95 FOR THE CATHEDRAL PEAK VI CATCHMENT; (B) AND THE IMPORTANT ALMOST RAINFREE PERIOD OF 24/03/91 TO 07/10/91 PORTION OF THE HYDROGRAPH, TOGETHER WITH THE AVERAGE FLOW RATES PER DAY DURING SIX PHASES (MARKED P1 TO P6) (KUENENE <i>ET AL.</i> , 2011) | 118 |
| FIGURE 114 CONCEPTUAL FLOWPATHS IN THE MAIN HILLSLOPE OF THE CATHEDRAL PEAK VI CATCHMENT | 120 |
| FIGURE 115 CONCEPTUAL FLOWPATHS FOR THE SHORT HILLSLOPE OF CATHEDRAL PEAK VI CATCHMENT | 121 |
| FIGURE 116 USING MORPHOLOGY TO EXTRAPOLATE SOIL MEASUREMENTS TO CATCHMENTS | 126 |
| FIGURE 117 THE STUDY SITE, SHOWING THE EXTENT OF THE Dc32 AND Db12 LAND TYPES..... | 127 |
| FIGURE 118 HILLSLOPES OF THE STUDY SITE..... | 130 |
| FIGURE 119 AREAS WHERE THE DIFFERENT POSSIBLE CATENAS ARE EXPECTED TO OCCUR | 131 |
| FIGURE 120 CONCEPTUAL HYDROLOGICAL FLOW MODEL FOR THE MS – VA – ALLUVIUM CATENA..... | 132 |
| FIGURE 121 CONCEPTUAL HYDROLOGICAL FLOW MODEL FOR THE MS – Sd/Hu – ALLUVIUM CATENA | 132 |
| FIGURE 122 CONCEPTUAL HYDROLOGICAL FLOW MODEL FOR THE MS – Ss – ALLUVIUM CATENA..... | 132 |
| FIGURE 123 THE TERRAIN MORPHOLOGICAL UNITS FOR THE STUDY SITE | 133 |
| FIGURE 124 THE SOIL MAP OF THE STUDY SITE | 134 |
| FIGURE 125 SOIL MAP UNIT AREAS AGAINST AREAS OBTAINED FROM THE LAND TYPE INVENTORY. A POINT REPRESENTING ALL THE MAPPING UNITS WHICH REPRESENTS SHORTLANDS, HUTTON AND VALSRIVIER SOIL FORMS WAS INCLUDED. THE BLACK LINE IS THE 1:1 LINE | 135 |
| FIGURE 126 THE MADADENI STUDY SITE, SHOWING THE EXTENT OF THE Ca 11 AND Ea 34 LAND TYPES..... | 138 |
| FIGURE 127 TERRAIN SKETCHES OF LAND TYPES Ca11 (FIG. 127A) AND Ea34 (FIG. 127B) (LAND TYPE SURVEY STAFF, 1986) .. | 138 |
| FIGURE 128 THE GEOLOGY OF LAND TYPES Ca11 AND Ea34 (GEOLOGICAL SURVEY, 1988) (FIGURE 128A) AND THE REVISED LITHOLOGY MAP (FIGURE 128B) | 140 |
| FIGURE 129 OBSERVATION POINTS ON A GOOGLE EARTH IMAGE | 140 |
| FIGURE 130 THE FOUR MAPS CREATED IN THE PROJECT, SHOWING THEIR ACCURACIES. THE DESCRIPTIONS FOR THE SOIL MAP UNITS OF MAPS 1 AND 2 (FIGURE 130A AND FIGURE 130B) ARE AS FOLLOWS: RED CLAYS: SHORTLANDS (Sd), HUTTON (Hu); DARK CLAYS: ARCADIA (Ar), RENSBURG (Rg), BONHEIM (Bo), MILKWOOD (Mw), WILLOWBROOK (Wo); SHALLOW SOILS: MISPAH (Ms), GLENROSA (Gs); WET SOILS: KATSPRUIT (Ka), KROONSTAD (Kd), DUNDEE (Du), PLINTHIC SOILS: AVALON (Av), WESTLEIGH (We), LONGLANDS (Lo), GLENCOE (Gc), WASBANK (Wa), DRESDEN (Dr); INTERMEDIATE SOILS: VALSRIVIER (Va), SEPANE (Se) | 143 |

| | |
|--------------------------------------------------------------------------------------------------------------------------------------------------------------------------------------------------------------------------------------------------------------------------------------------------|-----|
| FIGURE 131 THE CONCEPTUAL HYDROLOGICAL FLOW MODELS FOR THE FOUR HYDROLOGICALLY DIFFERENT HILLSLOPES. INTERFLOW-RESPONSIVE (A), RECHARGE-RESPONSIVE (B), RECHARGE-INTERFLOW-RESPONSIVE (C), RESPONSIVE-RECHARGE-INTERFLOW-RESPONSIVE (D)..... | 145 |
| FIGURE 132 A MAP SHOWING THE EXTENT OF EACH HYDROLOGICAL RESPONSE MODEL | 145 |
| FIGURE 133 THE STEVENSON HAMILTON RESEARCH SUPERSITE | 148 |
| FIGURE 134 SOIL OBSERVATION POSITIONS..... | 149 |
| FIGURE 135 THE HYDROLOGICAL SOIL MAP..... | 153 |
| FIGURE 136 CONCEPTUAL HYDROLOGICAL SOIL RESPONSE UNIT MAP..... | 154 |
| FIGURE 137 LOCATION OF SHRS IN SOUTH AFRICA (A), THE LOCATION OF THE STUDY AREA WITHIN SHRS (B) AND THE EXPERIMENTAL LAYOUT AND CATCHMENT ORDERS WITHIN THE STUDY AREA..... | 157 |
| FIGURE 138 RAINFALL (MM) AND DAILY MINIMUM AND MAXIMUM TEMPERATURES RECORDED DURING THE EVALUATION PERIOD | 159 |
| FIGURE 139 HYDROLOGICAL SOIL TYPES, AND REPRESENTATIVE HILLSLOPES OF THE STUDY AREA. MAIN STREAM CHANNEL AND CATCHMENT ORDERS ARE DEMARCATED IN BLUE AND RED RESPECTIVELY. THE THREE PROFILES USED FOR EVALUATION PURPOSES ARE MARKED SGR1_R, SGR2_R AND SGR3_R | 160 |
| FIGURE 140 CONCEPTUAL HYDROLOGICAL RESPONSES OF THE DOMINANT RESPONSE OF THE HILLSLOPES IN THE STUDY AREA..... | 163 |
| FIGURE 141 MODEL CONFIGURATION (ACRU2000 AND ACRU-INT); NUMBERS IN SHADED BLOCKS REFERS TO LAND SEGMENT NUMBER, WITH NUMBERS IN BRACKETS AT THE RIGHT OF THE LAND SEGMENTS AS THE AREA (IN HA). THE KEY IN FIGURE 140 WERE USED TO INDICATE THE HYDROLOGICAL SOIL TYPE OF EACH LAND SEGMENT..... | 164 |
| FIGURE 142 DAILY OBSERVED AND SIMULATED STREAMFLOW FOR THE THREE LEVELS OF DETAIL FROM 1ST ORDER CATCHMENT AS WELL AS CUMULATIVE FLOW DURING THE EVALUATION PERIOD | 166 |
| FIGURE 143 DAILY OBSERVED AND SIMULATED STREAMFLOW FOR THE THREE LEVELS OF DETAIL FROM 2ND ORDER CATCHMENT AS WELL AS CUMULATIVE FLOW DURING THE EVALUATION PERIOD | 167 |
| FIGURE 144 DAILY OBSERVED AND SIMULATED STREAMFLOW FOR THE THREE LEVELS OF DETAIL FROM 3RD ORDER CATCHMENT AS WELL AS CUMULATIVE FLOW DURING THE EVALUATION PERIOD | 168 |
| FIGURE 145 SIMULATED AND OBSERVED DAILY STREAMFLOW AND RAINFALL DURING THE LARGE RAIN EVENT OF 19 AND 20 JANUARY 2013 | 169 |
| FIGURE 146 MEASURED VS. SIMULATED WATER REGIMES FOR DIFFERENT PROFILES, HORIZONS AND SOIL INFORMATION LEVELS.... | 170 |
| FIGURE 147 SETUP OF VIRTUAL HILLSLOPE IN HYDRUS-2D | 178 |
| FIGURE 148 WATER CONTENTS (%) FOR THREE HORIZONS WITH DIFFERENT RESP VALUES SIMULATED OVER 6 YEARS WITH ACRU-INT | 185 |
| FIGURE 149 DIFFERENT LAND SEGMENTS WITH THEIR REPRESENTING SOIL PROFILES IN THE WEATHERLEY CATCHMENT..... | 187 |
| FIGURE 150 FLOW ROUTING FOR THE SIMULATION, MAGNITUDE OF ARROWS GIVE INDICATION OF DOMINANT FLOW DIRECTION IN VARIOUS LAND SEGMENTS..... | 188 |
| FIGURE 151 SIMULATED VS. MEASURED FLOW DURING THE SELECTED SIMULATION PERIOD..... | 191 |
| FIGURE 152 SIMULATED VS. MEASURED DAILY STREAMFLOW FLOW PLOTTED AGAINST DAILY RAINFALL FOR THE SIMULATION PERIOD | 192 |
| FIGURE 153 LOG OF SIMULATED VS. MEASURED FLOW OVER SELECTED SIMULATION PERIOD | 193 |
| FIGURE 154 SIMULATED VS. MEASURED STREAMFLOWS DURING A WET PERIOD..... | 193 |
| FIGURE 155 SIMULATED VS. MEASURED STREAMFLOWS DURING A DRY PERIOD | 194 |
| FIGURE 156 COMPARISON BETWEEN THE CONTRIBUTION OF LAND SEGMENTS 4 & 7 TO TOTAL STREAMFLOW | 195 |
| FIGURE 157 CUMULATIVE FLOWS FROM LAND SEGMENTS 4 & 7 DURING SIMULATION PERIOD | 195 |
| FIGURE 158 RAINFALL AND SIMULATED VS. MEASURED WATER CONTENTS OF A, B AND C-HORIZONS OF LAND SEGMENT 1, REPRESENTED BY P202, A PINEDENE SOIL | 196 |
| FIGURE 159 RAINFALL AND SIMULATED VS. MEASURED WATER CONTENTS OF A, B AND C-HORIZONS OF LAND SEGMENT 2, REPRESENTED BY P204, A LONGLANDS SOIL | 197 |
| FIGURE 160 RAINFALL AND SIMULATED VS. MEASURED WATER CONTENTS OF A, B AND C-HORIZONS OF LAND SEGMENT 3, REPRESENTED BY P212, A TUKULU SOIL | 199 |
| FIGURE 161 RAINFALL AND SIMULATED VS. MEASURED WATER CONTENTS OF A, B AND C-HORIZONS OF LAND SEGMENT 4, REPRESENTED BY P206, A KROONSTAD SOIL..... | 200 |
| FIGURE 162 RAINFALL AND SIMULATED VS. MEASURED WATER CONTENTS OF A, B AND C-HORIZONS OF LAND SEGMENT 5, REPRESENTED BY P210, A BLOEMDAL SOIL | 201 |
| FIGURE 163 RAINFALL AND SIMULATED VS. MEASURED WATER CONTENTS OF A, B AND C-HORIZONS OF LAND SEGMENT 6, REPRESENTED BY P209, A KATSPRUIT SOIL..... | 202 |
| FIGURE 164 RAINFALL AND SIMULATED VS. MEASURED WATER CONTENTS OF A, B AND C-HORIZONS OF LAND SEGMENT 7, REPRESENTED BY P208, A KROONSTAD SOIL..... | 203 |

| | |
|---------------------------------------------------------------------------------------------------------------------------------------------------------------------------------------------------------------------------------------------------------------------------------------------------------|-----|
| FIGURE 165 RAINFALL AND SIMULATED LATERAL FLOWS (MM. DAY ⁻¹) FOR LAND SEGMENT 1-4 (TOP) AND 5-7 (BOTTOM)..... | 205 |
| FIGURE 166 THE CONCEPT OF WATER FLOWING THROUGH A SOIL BY GRAVITY, WITH AND WITHOUT SLOPE, WITH AND WITHOUT TEXTURAL AND STRUCTURAL IMPEDING LAYERS (INFILTRATION RATES ARE IDEALIZED) (SCHEMATIC REPRESENTATION OF FLOW PRINCIPLES DERIVED FROM SCHULZE, 1995 AND TICEHURST <i>ET AL.</i> , 2007)..... | 215 |
| FIGURE 167 HYDRAULIC CONDUCTIVITY OF PEDOCUTANIC B HORIZON (SUB-ANGULAR BLOCKY) OVER TIME..... | 219 |
| FIGURE 168 HYDRAULIC CONDUCTIVITY OF PRISMACUTANIC B HORIZON OVER TIME | 220 |
| FIGURE 169 SATURATED HYDRAULIC CONDUCTIVITIES OF TWO DIFFERING PARENT MATERIAL RED APEDAL B HORIZONS. | 221 |
| FIGURE 170 STORAGE CORRELATION TO AID IN HYDROLOGICAL GROUPING OF DIAGNOSTIC HORIZONS ACCORDING TO TABLE 39. .. | 224 |
| FIGURE 171 RAINFALL AND MATRIC PRESSURE HEAD OF THREE ORTHIC A HORIZONS OVER 6 MONTHS IN THE WEATHERLEY CATCHMENT (VAN TOL <i>ET AL.</i> , 2012, PRESENTED WITH PERMISSION OF THE AUTHORS) (BEEH, 2003) | 225 |
| FIGURE 172 VARIATION OF SATURATED HYDRAULIC CONDUCTIVITY OF ORTHIC A HORIZONS | 225 |
| FIGURE 173 MEAN ADS>0.7 (%) VALUES IN A TYPICAL RECHARGE SOIL: P221, HUTTON 2100 (WRB – ORTHIDISTRICT CAMBISOL), WEATHERLEY (AFTER VAN HUYSSTEEN <i>ET AL.</i> , 2005) | 229 |
| FIGURE 174 DEGREE OF SATURATION VS. RAINFALL OVER 6 YEARS OF A RECHARGE SOIL: P221, HUTTON 2100 (WRB – ORTHIDISTRICT CAMBISOL) IN THE WEATHERLEY CATCHMENT (AFTER VAN HUYSSTEEN <i>ET AL.</i> , 2005) | 230 |
| FIGURE 175 MEAN ADS>0.7 (%) VALUES IN A TYPICAL INTERFLOW SOIL: P225, LONGLANDS 1000 (WRB – FERRIC-ENDOEUTRIC ALBELUVISOL) IN THE WEATHERLEY CATCHMENT (VAN HUYSSTEEN <i>ET AL.</i> , 2005)..... | 231 |
| FIGURE 176 DEGREE OF SATURATION VS. RAINFALL OVER 6 YEARS OF AN INTERFLOW SOIL: P225, LONGLANDS 1000 (WRB – FERRIC-ENDOEUTRIC ALBELUVISOL) IN THE WEATHERLEY CATCHMENT (AFTER VAN HUYSSTEEN <i>ET AL.</i> , 2005) | 232 |
| FIGURE 177 VOLUME OF OVERLAND FLOW MEASURED AT FIVE RUNOFF PLOTS VS. TOPSOIL MATRIC POTENTIAL IN THE WEATHERLEY CATCHMENT..... | 233 |
| FIGURE 178 MEAN ADS>0.7 (%) VALUES IN A TYPICAL RESPONSIVE SOIL: P235, KATSPRUIT 1000, (WRB – HYPERDISTRICT GLEYSOL) IN THE WEATHERLEY (VAN HUYSSTEEN <i>ET AL.</i> , 2005) | 233 |
| FIGURE 179 DEGREE OF SATURATION VS. RAINFALL OVER 6 YEARS OF A RESPONSIVE SOIL: P235, KATSPRUIT 1000, (WRB – HYPERDISTRICT GLEYSOL) IN THE WEATHERLEY CATCHMENT (AFTER VAN HUYSSTEEN <i>ET AL.</i> , 2005) | 233 |
| FIGURE 180 ALTERNATING LAYERS OF SANDSTONE AND MUDSTONE CONTROLLING GROUNDWATER RECHARGE AND ITS FLOWPATHS | 236 |
| FIGURE 181 BASALT WITH PIPE AMYGDALES SHOWING ITS LACK IN FRACTURES RESULTING IN THE HAMPERING OF WATER FLOW.... | 237 |
| FIGURE 182 DOLERITE WITH ITS COMPLEX FRACTURE SYSTEM WHICH MAY OR MAY NOT ALLOW WATER FLOW | 237 |
| FIGURE 183 ARIDITY INDEX FOR SOUTH AFRICA (ZOMER <i>ET AL.</i> , 2008)..... | 239 |
| FIGURE 184 PROCESSES REGULATING WATER FLOW | 239 |
| FIGURE 185 INTERACTIONS BETWEEN THE FACTORS OF VADOZONE HYDROLOGY | 241 |
| FIGURE 186 LAND TYPE DATA FOR INGULA IN THE FREE STATE (KUENENE & LE ROUX, 2011)..... | 243 |
| FIGURE 187 LAND TYPE INVENTORY FOR INGULA AREA (KUENENE & LE ROUX, 2011)..... | 244 |
| FIGURE 188 CONCEPTUAL HILLSLOPE HYDROLOGICAL BEHAVIOR OF INGULA SOILSCAPE. (KUENENE & LE ROUX, 2011) | 245 |
| FIGURE 189 A) WEATHERLEY CATCHMENT TOPOGRAPHY AND POSITION OF SOILSCAPE B) SOIL TYPES INCLUDED IN THE SOILSCAPE AND AUGER OBSERVATIONS | 249 |
| FIGURE 190 CLAY CONTENT, PHOTOGRAPH AND PROFILE DESCRIPTION OF THE BLOEMDAL SOIL (VAN HUYSSTEEN <i>ET AL.</i> , 2005). P, T AND N REFER TO PIEZOMETER, TENSIO-METER AND NEUTRON WATER METER POSITIONS, RESPECTIVELY. REDOX MORPHOLOGY TYPICAL OF AQUIC CONDITIONS WAS NOT PHOTOGRAPHED | 251 |
| FIGURE 191 CALCIUM, MG, PH AND BASE SATURATION OF THE BLOEMDAL..... | 251 |
| FIGURE 192 FE AND MN DISTRIBUTION IN THE BLOEMDAL | 252 |
| FIGURE 193 RAINFALL AND MATRIC PRESSURE MEASURED IN THE BLOEMDAL (P210) SOIL DURING MARCH 2001..... | 253 |
| FIGURE 194 CLAY CONTENT, PHOTOGRAPH AND PROFILE DESCRIPTION OF THE KATSPRUIT SOIL (VAN HUYSSTEEN <i>ET AL.</i> , 2005). P, T AND N REFER TO PIEZOMETER, TENSIO-METER AND NEUTRON WATER METER POSITIONS, RESPECTIVELY | 257 |
| FIGURE 195 CALCIUM, MG, PH AND BASE SATURATION OF THE KATSPRUIT | 258 |
| FIGURE 196 FE AND MN DISTRIBUTION IN THE KATSPRUIT | 259 |
| FIGURE 197 RAINFALL AND MATRIC PRESSURE MEASURED IN THE KATSPRUIT (P209) SOIL DURING MARCH 2001 | 259 |
| FIGURE 198 CLAY CONTENT, PHOTOGRAPH AND PROFILE DESCRIPTION OF THE KROONSTADSOIL (VAN HUYSSTEEN <i>ET AL.</i> , 2005). P, T AND N REFER TO PIEZOMETER, TENSIO-METER AND NEUTRON WATER METER POSITIONS, RESPECTIVELY | 261 |
| FIGURE 199 CALCIUM, MG, PH AND BASE SATURATION OF THE KROONSTAD | 262 |
| FIGURE 200 FE AND MN DISTRIBUTION IN THE KROONSTAD | 263 |
| FIGURE 201 RAINFALL AND MATRIC PRESSURE MEASURED IN THE KROONSTAD(P208) SOIL DURING MARCH 2001..... | 264 |
| FIGURE 202 CONCEPTUAL HYDROLOGICAL RESPONSE MODEL OF SOILSCAPE BASED ON MORPHOLOGY | 266 |
| FIGURE 203 BASE SATURATION DISTRIBUTION AND POSITION OF REPRESENTATIVE PROFILES IN THE SOILSCAPE..... | 267 |

| | |
|--------------------------------------------------------------------------------------------------------------------------------------------------------------------------------------------------------------------------------------------------------------------------------------------------------------------------------------------------------------------------------------------------------------|-----|
| FIGURE 204 STANDARD VERSION OF 800 MM DFM CAPACITANCE PROBE WITH 6 SENSORS..... | 272 |
| FIGURE 205 MODIFIED VERSION OF DFM PROBE FOR DEEP MEASUREMENTS OF SOIL WATER CONTENTS | 273 |
| FIGURE 206 LOCATION OF DFM PROBES IN THE TWO STREAMS CATCHMENT..... | 274 |
| FIGURE 207 THE PROCEDURE USED TO SATURATE THE SOIL AROUND A DFM PROBE N. 15291 IN AN INANDA SOIL AT LAT. S. 29°12.47'; LONG. E 30°39.125' TO OBTAIN CALIBRATION READINGS BETWEEN FSAT AND DUL. A SIMILAR WETTING AND MEASURING PROCEDURE WAS USED FOR A NEARBY NWM ACCESS TUBE (CALIBRATION RESULTS IN TABLE 50)..... | 276 |
| FIGURE 208 CALIBRATION CURVE FOR NWM CALIBRATION AT 30 CM (A); AND DFM PROBE 15291 CALIBRATION CURVE AT 30 CM. THE NEUTRON WATER METER CALIBRATION EQUATION FOR THE B HORIZON IS $Y=0.009X-0.151$ PROVIDING FOR THE RESULTS PROVIDED IN TABLE 50 | 278 |
| FIGURE 209 A) INSTRUMENTATION OF THE WEATHERLEY CATCHMENT (LORENTZ <i>ET AL.</i> , 2004), B) HILLSLOPE 1-4 WITH LOCATION OF TIPPING BUCKET EXPERIMENT AND C) TIPPING BUCKET (HILLSLOPE OUTFLOW) EXPERIMENT AT THE FOOTSLOPE OF HILLSLOPE 1-4. TB1-TB10 IN C) ARE PERFORATED PIPE NESTS. DFM PROBES WERE INSTALLED AT TB1-4, TB7 AND TB9 | 279 |
| FIGURE 210 DFM PROBE SETUP AT LC2 (MARCH-SEPTEMBER 2010) | 280 |
| FIGURE 211 A SCHEMATIC DIAGRAM OF A PROCEDURE TO CALIBRATE DFM PROBES USING A NWM..... | 283 |
| FIGURE 212 MODAL PROFILE LOCATIONS ON THE THREE DIFFERENT SOILSCAPES OF THE TWO STREAMS CATCHMENT | 288 |
| FIGURE 213 PREDICTED VS. MEASURED WCM USING MODEL 2. TEST 1 & 2 REPRESENTS THE DOUBLE-CROSS VALIDATION PREDICTION RESULTS WHEREAS 'COMPLETE' REPRESENTS THE ORIGINAL DATASET AND MODEL EQUATION FROM TABLE 56 | 294 |
| FIGURE 214 PREDICTED VS. MEASURED WCM USING MODEL 3. TEST 1 & 2 REPRESENTS THE DOUBLE-CROSS VALIDATION PREDICTION RESULTS WHEREAS 'COMPLETE' REPRESENT THE ORIGINAL DATASET AND MODEL EQUATION FROM TABLE 56 | 295 |
| FIGURE 215 SOIL HYDRAULIC CONDUCTIVITY VS TENSION RELATIONSHIP IN DIAGNOSTIC HORIZONS OF (A) KRANSKOP, (B) INANDA, (C) MAGWA PROFILES LOCATED ON THE NORTH FACING HILLSLOPE, AND (D) KATSPRUIT PROFILE IN THE VALLEY BOTTOM | 296 |
| FIGURE 216 SOIL HYDRAULIC CONDUCTIVITY VS. TENSION RELATIONSHIP IN DIAGNOSTIC HORIZONS OF (A) OAKLEAF, (B) CLOVELLY PROFILES LOCATED ON THE SOUTH FACING HILLSLOPE AND (C) GRIFFIN AND (D) OAKLEAF PROFILE LOCATED ON THE EAST FACING HILLSLOPE..... | 296 |
| FIGURE 217 Θ_m (cm^2/m^2 OF SOIL SURFACE) WITH WCM PTF VS. MEASURED Θ_m IN THE A HORIZONS OF THE SOILS IN THE TWO STREAM'S CATCHMENT | 298 |
| FIGURE 218 HYDROGRAPH RESPONSE DURING THE 72 MM EVENT ON THE 03 JANUARY 2005 (DATA FROM EVERSON <i>ET AL.</i> , 2006) | 300 |
| FIGURE 219 A RECORD OF SOIL WATER CONTENT MEASURED BY WATER SENSOR, AT 40 CM DEPTH IN THE INANDA SOIL ON THE NORTH FACING HILLSLOPE DURING THE 72 MM RAINFALL EVENT ON 3/1/05 (ADAPTED FROM EVERSON <i>ET AL.</i> , 2006) (A); MEASUREMENTS AT 2.4 HOUR INTERVALS (B). | 302 |
| FIGURE 220 A RECORD OF THE SOIL WATER CONTENT AT 80 CM DEPTH OF THE INANDA SOIL OF FIGURE 219 DURING THE 72 MM RAINFALL EVENT ON 3/1/05 (ADAPTED FROM EVERSON <i>ET AL.</i> , 2006) | 303 |
| FIGURE 221 A RECORD OF THE DRAINING OF THE SATURATED A HORIZON INANDA SOIL DURING A DFM PROBE CALIBRATION PROCEDURE DURING 2011 | 304 |
| FIGURE 222 INANDA SOIL PROFILE (A), WITH EVIDENCE OF SOIL MIXED WITH ASH PARTICLES ON THE SURFACE AND TRANSLOCATED ASH PARTICLES DOWN THE CRACKS OF THE PROFILE AND (B) SURFACE EVIDENCE OF WATER REPELLENCY | 306 |
| FIGURE 223 PHOTOS ILLUSTRATING (A) UNDISTURBED CORE SAMPLES, (B) THE LABORATORY VACUUM/SATURATION CHAMBER AND HANGING WATER COLUMN SETUP FOR DETERMINING WATER RETENTION CURVES | 311 |
| FIGURE 224 THE WATER RETENTION CURVES OF INVESTIGATED (A) KRANSKOP, (B) INANDA, AND (C) MAGWA SOIL PROFILES ON THE NORTH FACING HILLSLOPE OF THE CATCHMENT. MEAN VALUES MEASURED SAMPLES ARE SHOWN AS POINTS. RETC-FITTED VAN GENUCHTEN-MUALEM (VGM) CURVES ARE DISPLAYED AS SOLID LINES. AH = HUMIC A, RE = RED APEDAL B, YE = YELLOW BROWN APEDAL B, ON = UNSPECIFIED MATERIAL WITH SIGNS OF WETNESS | 315 |
| FIGURE 225 THE WATER RETENTION CURVES OF INVESTIGATED (A) KATSPRUIT, AND (B) OAKLEAF SOIL PROFILES. MEAN VALUES MEASURED SAMPLES ARE SHOWN AS POINTS. RETC-FITTED VAN GENUCHTEN-MUALEM (VGM) CURVES ARE DISPLAYED AS SOLID LINES. OT = ORTHIC A, GH = G HORIZON, NE = NEOCUTANIC B HORIZON..... | 316 |
| FIGURE 226 THE WATER RETENTION CURVES OF INVESTIGATED (A) CLOVELLY, (B) GRIFFIN AND (C) OAKLEAF PROFILES ON THE SOUTH AND EAST FACING HILLSLOPE. MEAN VALUES MEASURED SAMPLES ARE SHOWN AS POINTS. RETC-FITTED VAN GENUCHTEN-MUALEM (VGM) CURVES ARE DISPLAYED AS SOLID LINES. OT = ORTHIC A, RE = RED APEDAL B, YE = YELLOW BROWN APEDAL B, NE = NEOCUTANIC B HORIZON. | 317 |
| FIGURE 227 HYDRAULIC CONDUCTIVITY VS DEGREE OF SATURATION FOR DIFFERENT SOIL PROFILE (A), KRANSKOP (B), INANDA (C), MAGWA AND (D), KATSPRUIT SOIL PROFILES. FOR CONVENIENCE REGARDING SCALE, THE VERY HIGH K_s VALUES FOR THE B HORIZONS OF SOME PROFILES ARE NOT SHOWN. THESE K - S RELATIONSHIPS ARE BASED ON $K(\theta)$ CURVES PREDICTED USING THE VGM HYDRAULIC MODEL. | 320 |

| | |
|-----------------------------------------------------------------------------------------------------------------------------------------------------------------------------------------------------------------------------------------------------------------------------------------------------------------------------------------------------------------------------------------------------------------------------------------------------------------------------|-----|
| FIGURE 228 HYDRAULIC CONDUCTIVITY VS DEGREE OF SATURATION FOR DIFFERENT SOIL PROFILE (A), OAKLEAF (B), CLOVELLY (C), GRIFFIN AND (D), OAKLEAF SOIL PROFILES. FOR CONVENIENCE REGARDING SCALE, THE VERY HIGH K _s VALUES FOR THE B HORIZONS OF SOME PROFILES ARE NOT SHOWN. THESE K-S RELATIONSHIPS ARE BASED ON K(θ) CURVES PREDICTED USING THE VGM HYDRAULIC MODEL. | 321 |
| FIGURE 229 UNSATURATED HYDRAULIC CONDUCTIVITY (K _h) CURVES FOR THE INANDA (A), KRANSKOP (B), MAGWA (C) AND KATSPRUIT SOIL PROFILES | 323 |
| FIGURE 230 UNSATURATED HYDRAULIC CONDUCTIVITY (K _h) CURVES FOR THE OAKLEAF (A), CLOVELLY (B), GRIFFIN (C) AND OAKLEAF SOIL PROFILES..... | 324 |
| FIGURE 231 COMPARISONS BETWEEN K _h CURVES OBTAINED IN THREE DIFFERENT WAYS, I.E. USING OBSERVED TENSION INFILTRMETER (TI-OBS) K _h DATA ONLY; USING THE VGM HYDRAULIC MODEL WITH RETENTION DATA ONLY; AND VGM MODEL FITTED TO TENSION INFILTRMETER DATA (VGM-TI). THE RESULTS ARE FOR THE A HORIZONS OF THE FOLLOWING SOILS: (A) KRANSKOP; (B) INANDA, AND (C) MAGWA. | 325 |
| FIGURE 232 COMPARISONS BETWEEN K _h CURVES OBTAINED IN THREE DIFFERENT WAYS, I.E. USING OBSERVED TENSION INFILTRMETER (TI-OBS) K _h DATA ONLY; USING THE VGM HYDRAULIC MODEL WITH RETENTION DATA ONLY; AND VGM MODEL FITTED TO TENSION INFILTRMETER DATA (VGM-TI). THE RESULTS ARE FOR THE A HORIZONS OF THE FOLLOWING SOILS: (A) OAKLEAF, (B) CLOVELLY, BOTH ON THE SOUTHERN HILLSLOPE; AND (C) GRIFFIN AND (D) OAKLEAF BOTH ON THE EASTERN SLOPE..... | 326 |
| FIGURE 233 STABLE ISOTOPE PROFILE OF A SATURATED SOIL (AFTER KENDALL AND McDONNELL, 2003)..... | 330 |
| FIGURE 234 SOIL WATER ISOTOPIC COMPOSITION AT VARYING SOIL DEPTHS, MUNICH GERMANY (LEIBUNBGUT AND MALOSZEWSKI, 2009) | 330 |
| FIGURE 235 CONCEPTUAL ISOTOPE COMPOSITIONS OF RAINFALL AND RUNOFF | 331 |

INTRODUCTION

Soil is a product of, and therefore integrates the influences of parent material, topography, vegetation/land use, and climate and can therefore act as a first order control on the partitioning of hydrological flowpaths, residence time distributions and water storage (Park, McSweeney & Lowery, 2001 and Soulsby *et al.* 2006). Soils differ in these responses and therefore, because hillslopes have different soil distribution patterns, their hydrological response differs. Hydrologists agree that the spatial variation of soil properties significantly influences hydrological processes but they lack the skill to gather and interpret soil information (Lilly, Boorman & Hollis, 1998 and Chirico, Medina & Romano, 2006). This includes vertical (horizonisation) and lateral (catenal) variation.

The relationship between soil and hydrology is interactive. Water is the active agent in soil genesis, acting on parent material to generate soil properties serving as unique signatures of the hydrology of soils and hillslopes. Some soil properties control the hydrological responses of soils and hillslopes, while others do not have any direct effect and serve as indicators of flowpaths, flow direction and storage mechanisms. This is an extremely important role of soil, because soils cover hillslopes and the behaviour of water in hillslopes is not easily measureable. Soils, however serve as a window to subsurface hydrological response in the vadose zone.

This interactive relationship serves as a basis for a new interdisciplinary research field, hypopedology, which promotes “...synergistic integration of pedology with hydrology to enhance the holistic study of soil-water interactions and landscape-soil-hydrology relationships across space and time, aiming to understand pedologic controls on hydrologic processes and properties, and hydrologic impacts on soil formation, variability, and functions” (Lin *et al.*, 2008). This field aims to bridge gaps between pedology, soil physics, hydrology, geohydrology and geomorphology and also between micro- and macroscopic scales of soil-water and saprolite-water interactions. Issues covered by hypopedology include: i) hydrology, including hillslope hydrology as a factor controlling soil formation and its relation to soil properties, ii) soil and the role of the intermediate vadose zone (IVZ) as essential components of the hydrological cycle and filters of water, iii) soil and IVZ morphological features as signatures of soil and hillslope hydrology and iv) landscape-soil-water relationships across scales.

The downslope spatial distribution of soil properties, exhibits a common form of organization and symmetry. This typical distribution of soils in the landscape has first been referred to as a catena by Milne (1936), but modified a few years later by Bushnell (1942) to replace the catena with toposequence. This concept of the association of soil properties with topography relates more to hydrological processes than to relief and is captured in the terms pedosequence, hydrosequence or hillslope (Flügel, 1997; Sivapalan, 2003a and Weiler *et al.*, 2004).

The hillslope is the smallest hydrologically unit and generally accepted as a fundamental landscape unit in hydrological studies (Weiler *et al.*, 2004 and Lin *et al.*, 2006). The interaction between topography, soils, climate and vegetation results in patterns or laws which contain valuable information on the way they function (Sivapalan, 2003a). The hillslope is therefore an important building block for understanding and simulating hydrological processes (Tromp-van Meerveld & Weiler, 2008). How catchments respond is

determined by the particular mix of different hillslopes (shapes and sizes) in the particular catchment (Sivapalan, 2003b). It is therefore not surprising that the hillslope forms the backbone for a number of hydrological models. Variation in the hydrological response of soil types (Le Roux *et al.*, 2011) and the distribution of soils in hillslopes, combined with variation in geological properties and short and long-term variation in climate, results in a mixed response that tends to average out the differences in the hydropedology of soils and hillslopes.

One of the major outcomes of the IAHS decade on 'Predictions in Ungauged Basins' (Sivapalan 2003a and Sivapalan *et al.*, 2003) is the need for a catchment classification system. This led to a special issue in *Hydrology and Earth System Services* (HESS) on catchment classification and PUB (Castellarin *et al.*, 2011) in which leading hydrologists, environmentalists and (fortunately) soil scientists reveal their ideas on how to classify catchments.

It seems that classification should be a logical build-up of properties resulting in a unique entity. For example; in soil taxonomy, distinct properties in different layers results in the classification of different horizons, and their vertical sequence, into a classifiable soil form. It would seem logical that since the hydrological response of a catchment is determined by the response of individual hillslopes, the hillslopes should first be classified before classification of catchments will be possible. This important step is missing in the current ideas of catchment classification. Also, somewhat disappointing, in the special issue of HESS are proposals to classify catchments based on measured hydrological "signatures" such as runoff ratio, slope of flow duration curves, baseflow index, etc. This seems to be directly opposed to the ideas of PUB (Sawicz *et al.*, 2011).

The vision of HOSASH is very much in line with the aims of PUB and should be used as a basis for classification of catchments. The overall aim of the project was described as follows in 2009:

– "*The project aims to develop a hydrologically based classification system of SA soils and hillslopes. The hydrology of SA soils and hillslopes (HOSASH) aims to assist in hydrological modelling especially in ungauged basins.*"

We can now add that the aim includes and emphasizes distinguishing hydrologically between different soils and hillslopes. This variation naturally tends to generalize with decreasing scale and large catchments as the variety averages out. HOSASH see this as of contradictory nature with river flow which hydrologically cumulative and change accordingly with decrease in scale and increase in catchment size.

This principle makes the HOSASH principle equally important on site specific impact of urbanisation and mining activities as the impact can only be evaluated using soil and hillslope specific hydrology.

As project studies progressed it became apparent that this vision had been wisely formulated; a conclusion that has remained valid throughout. Emphasis in focus has resulted from increased awareness of the fact that although hydropedology serves the study of 'ungauged basins', it is not on these as whole entities. Our contribution needs to be the result of efforts to elucidate the functioning and classification of different kinds of hillslopes. Improved understanding in this regard should also be of value in connection with the influence of land use changes on the hydrology of hillslopes. This information is also needed by catchment management agencies that will inevitably play an ever increasing role in promoting efficient water resources management in South Africa.

The importance of the influence of the IVZ on hillslope hydrology has become increasingly apparent during the course of the project. The systematic change in properties of the IVZ down slope and with the rainfall gradient, implies that it has potential to add to the knowledge gained from soil as a window to subsoil hydrological response in different geologies and climates. There is a great need for characterization of the IVZ in terms of hydrological properties inferred from soil and geological surveys, and measured conductivities in selected geologies.

The dominance of particle size distribution in controlling saturated flow in disturbed soil is surpassed by the role of biopores in undisturbed soil. The relationship of biopores with bio-activity and organic carbon accumulation is expressed in the pedotransfer function. The impact of water repellancy on the effectivity of water conducting macroporosity has been quantified. It emphasises the value of measuring flux at saturation and near saturation in different soils and management systems.

Stable isotopes of oxygen and deuterium sampled in rainfall, saturated soil water, seepage and stream flow indicate that horizons can be grouped into hydrological units, indicating their different hydrological functionality, and therefore that this study can assist in understanding hillslope hydrology. Hydrological functionality of each horizon individually allows for rates, direction and storage to be assigned. Unlike HOST, real soils are being dealt with, allowing for numerous scenarios to be conceptually presented.

Needs show that extrapolation of data is more important than generating data. Land types can serve as relatively uniform areas to which hydrological data of the vadose zone can be extrapolated. Land type data involves a soil survey done for South Africa providing data on soil properties. Soil's properties and soil distribution are related to geology, climate and topography and therefore interactively control hillslope hydrology, determining flowpaths and storage mechanisms in the upper and lower vadose zones, and groundwater recharge. As fracture patterns, layering and bedding planes are typical of specific kinds of lithology, the flowpaths and soil/fractured rock interaction are also typical and related to the soil properties and soil distribution patterns. These are also related to the topography and vegetation. Climate has a dominant influence on the type of weathering and therefore also on soil properties and soil distribution patterns. Since all these factors are included in demarcating land types, it should therefore be possible to use them effectively for delineation of areas of relatively homogeneous recharge and interflow.

It has become increasingly apparent that since soil morphology is an ancient but stable indicator of soil water regime, flowpaths and storage mechanisms, there is great value of using soil types based on soil morphology to design conceptual hydrological response models for hillslopes. Validity in this connection can be confirmed by chemical soil properties and hydrometry snapshots of current conditions serving as indicators of the recent behaviour of the soil water regime.

Several new techniques were developed. Quantification of potential flow by measuring hydraulic conductivity at saturation and near saturation produced valuable results that questioned the application of vertical flow parameters for predicting lateral flow. A trench experiment confirmed near surface macropore quick flow and the use of slotted pipes offer promising results.

The potential flow in a recharge soil/saprolite/deep interflow soil/responsive soil flowpath, predicted from soil profile morphology, was quantified by measuring hydraulic properties. This was supported by deep continuous measurements indicating that ET excess water

rapidly flowed through deep recharge soils on the hillslopes to become stored in the saprolite, and then flowed laterally to exit into the stream via deep interflow soils in the toe slope and responsive soils in the valley bottom.

The distribution of hydrological soil types spread over South Africa made it possible to classify hillslopes hydrologically. Six classes with different hydrological responses are defined. Detail quantitative characterisation of some of these hillslopes produced good results and combined with the potential to extrapolate the hydrological hillslopes to larger areas by disaggregation of land types and digital soil mapping, makes on-site application of the results for application of the impact of land-use change possible on all scales, and takes these results a step closer to large scale incorporation in hydrological modelling.

References

- BUSHNELL, T.M., 1942. Some aspects of the soil catena concept. *Soil Sci. Soc. Am. Proc.* **7**, 466-476.
- CASTELLARIN, A., CLAPS P., TROCH, P.A., WAGENER, T., & WOODS, R., 2013. Catchment classification and PUB. Hydrology and Earth System Sciences. EGU Journals, Copernicus publications.
- CHIRICO, G.B., MEDINA, H., ROMANO, N., 2006. Uncertainty in predicting soil hydraulic properties at the hillslope scale with indirect methods. *Journal of hydrology* 334 (3), 405-422.
- FLÜGEL, W. A., 1997. Combining GIS with regional hydrological modelling using hydrological response units (HRU's): An application from Germany. *Math. Comput. Simulat.* 43, 297-304.
- MANNA, P., BASILE, A., BONFANTE, A., DE MASCELLIS, R., & TERRIBILE, F., 2009. Comparative Land Evaluation approaches: An itinerary from FAO framework to simulation modelling, *Geoderma*, 150, 367-378.
- LE ROUX, P. A. L., VAN TOL, J. J., KUENENE, B. T., HENSLEY, M., LORENTZ, S. A., EVERSON, C. S., VAN HUYSSTEEN, C. W., KAPANGAZIWIRI, E., RIDDEL, E. D and FREESE, C., 2011. Hydropedological interpretations of the soils of selected catchments with the aim of improving the efficiency of hydrological models. Report no. K5/1748. Water Research Commission, Pretoria.
- LIN, H. S., KOGELMAN, W., WALKER, C. & BRUNS, M. A., 2006. Soil moisture patterns in a forested catchment: A hydropedological perspective. *Geoderma* 131, 345-368.
- LIN, H. S., BOUMA, J., OWENS, P. & VERPRASKAS, M., 2008. Hydropedology: Fundamental issues and practical applications. *Catena* 73, 151-152.
- LILLY, A., BOORMAN, D.B. & HOLLIS, J.M., 1998. The development of a hydrological classification of UK soils and the inherent scale changes. *Nutr. Cycl. Agroecosys.*, 50, 299-302.
- MILNE, G., 1936. A provisional Soil Map of East Africa. East African Agriculture Research Station, Amani Memoirs, Tangayika Territory
- PARK, S.J., MCSWEENEY, K., & LOWERY, B. (2001) Identification of the spatial distribution of soils using a process-based terrain characterisation. *Geoderm.* **103** 249-272.

- SAWICZ, K., WAGENER, T., SIVAPALAN, M., TROCH, P.A. & CARRILLO, G., 2011. Catchment classification: empirical analysis of hydrologic similarity based on catchment function in the eastern USA. *Hydrol. Earth Syst. Sci.*, 15, 2895-2911.
- SAWICZ, K., WAGENER, T., SIVAPALAN, M., TROCH, P.A. & CARRILLO, G., 2011. Catchment classification: empirical analysis of hydrologic similarity based on catchment function in the eastern USA. *Hydrol. Earth Syst. Sci.*, 15, 2895-2911.
- SOULSBY, C., TETZLFF, D., RODGERS, P., DUNN, S. & WALDRON, S., 2006. Runoff processes, stream water residence times and controlling landscape characteristics in a mesoscale catchment: An initial evaluation. *J. Hydrol.*, 325, 197-221.
- SIVAPALAN, M. 2003a. Prediction in ungauged basins: a grand challenge for theoretical hydrology. *Hydrol. Process.*, 17, 3163-3170.
- SIVAPALAN, M., 2003b. Process complexity at hillslope scale, process simplicity at the watershed scale: is there a connection? *Hydrol. Process.*, 17, 1037-1041.
- SIVAPALAN, M., TAKEUCHI, K., FRANKS, S.W., GUPTA, V.K., KARAMBIRI, H., LAKSHMI, V., LIANG, X., MCDONNELL, J.J., MENDIONDO, E. M., O'CONNELL, P.E., OKI, T., POMEROY, J.W., SCHERTZER, D., UHLENBROOK, S., & ZEHE, E., 2003. IAHS decade on prediction in ungauged basins (PUB), 2003-2012: Shaping an exciting future for the hydrological sciences. *Hydrol. Sci. J.*, 48, 857-880.
- TROMP-VAN MEERVELD, H.J. & WEILER, M., 2008. Hillslope dynamics modelled with increasing complexity. *J. Hydrol.* 361, 24-40.
- WEILER, M. & MCDONNELL, J., 2004. Virtual experiments: a new approach for improving process conceptualization in hillslope hydrology. *J. Hydrol.* 285, 3-18.

SECTION 1: HILLSLOPE HYDROLOGY

Chapter 1 CLASSIFICATION OF SOUTH AFRICAN HILLSLOPE HYDROLOGY

1.1 INTRODUCTION

The need for a globally agreed-upon catchment classification system has received a great deal of attention in the last decade (McDonnell & Woods, 2004; Wagener *et al.*, 2007; Wagener *et al.*, 2008; Bouma *et al.*, 2011; Sawicz *et al.*, 2011, etc.), largely motivated by the challenges of hydrological predictions in ungauged basins (PUB) and uncertainty of the growing awareness of the impact of climate change and land-use change on hydrology and of environmental pollution. Indeed classification of central entities of interest is essential in many scientific disciplines. A catchment, being a landscape element that integrates all aspects of the hydrological cycle, is considered to be the central entity in hydrological studies (Wagener *et al.*, 2007). However, Sawicz *et al.* (2011) maintains that although the catchment provides a sensible unit for classification, it is not necessarily the only unit/scale driving dominant hydrological processes. To be functional as a classification system of a spatial element of nature it must have easily identifiable taxons and the criteria defining it must be visible (easily detectable) or correlated with one, or a combination, of detectable elements of nature to facilitate mapping of space with a unique response.

The hillslope is generally accepted as a fundamental landscape unit (Weiler & McDonnell, 2004 and Lin *et al.*, 2006). It exhibits a common form of organisation and symmetry needed to construct a classification system. Functional classification units can be grouped on a higher level for improving communication of general information and divided on several lower levels for reduced variation and improved application. The interaction between topography, soils, climate and vegetation results in patterns or laws which contain valuable information on the way they function (Sivapalan, 2003a). These elements play a significant role in controlling hydrology and their relationships with water distribution are valuable for serving as indicators of hydrological response (Le Roux *et al.*, 2011; Van Tol *et al.*, 2010a & b; Kuenene *et al.*, 2011). The hillslope is therefore an important building block for understanding and simulating hydrological processes (Tromp-van Meerveld & Weiler, 2008). The hydrological response of catchments is determined by the combined hydrological response of hillslopes in the particular catchment (Sivapalan, 2003b).

Similar to catchment classification there is no general consensus on methods to characterize and classify hillslopes (Weiler & McDonnell 2004; McDonnell *et al.*, 2007 and Tromp-van Meerveld & Weiler, 2008). Some researchers argue that every hillslope is unique (Beven, 2001). Experiments in the past focused on documentation of the unconventional behaviour of new hillslopes instead of the systematic examination of first order controls of hillslope hydrological behaviour, without intercomparisons to obtain common process behaviours (Weiler *et al.*, 2004). The transference of these studies is limited. McDonnell *et al.*, (2007)

therefore argued that any mapping and characterization should be driven by the desire to generalize and extrapolate from one place to another over multiple scales using an interdisciplinary approach, without relying on calibration “...but rather a systematic learning from observed data and an increased understanding and search for new hydrologic theories through embracing new organizing principles behind watershed behaviour that are derived from our sister disciplines”.

Soils integrate the influences of parent material, topography, vegetation/land use, and climate and act as a first order control on the partitioning of hydrological flow paths, residence time distributions and water storage (Park *et al.*, 2001 and Soulsby *et al.* 2006). Soils science is therefore clearly one of the ‘sister disciplines’ that should be considered in any hydrologic classification system (Bouma *et al.*, 2011). The influence of soil on hydrological processes is due to the ability of soil to transmit, store and react with water (Park *et al.*, 2001). These influences are primarily controlled by the physical and hydraulic properties of soils. Hydrologists agree that the spatial variation of soil properties significantly influence hydrological processes but they lack the skill to gather and interpret soil information at the scale required for hydrological response estimation (Lilly *et al.*, 1998). The relationship between soil and hydrology is interactive. Water is a primary agent in soil genesis, resulting in the formation of soil properties containing unique signatures of the way they formed (Ticehurst *et al.*, 2007; Van Tol *et al.*, 2010a & b).

Almost every hydrological process of interest to hydrologists (for example evapotranspiration, infiltration and subsurface flow) is difficult to observe and measure, because these processes are dynamic in nature with strong temporal variation (Sivapalan, 2003a). The dominant hydrological processes are invisible. Spatial and temporal variation requires long-term measurements to develop an understanding of the patterns of response. On the other hand, soil properties are in the short term not dynamic in nature and their spatial variation is not random (Webster, 2000). The spatial distribution of soil properties, exhibit a common form of organization and symmetry including vertical horizonation typical of soils and lateral topographic related distribution of soils in a hillslope. This typical distribution of soils in the landscape has first been referred to as a catena by Milne (1936), but modified later by Bushnell (1942) to replace the catena concept with the toposequence. This concept of the association of soil properties with topography and hydrological processes is also captured in the terms pedosequence or hydrosequence in relation to hillslopes (Flügel, 1997; Sivapalan, 2003a and Weiler & MacDonnell 2004). The correct interpretation of spatially varying soil properties associated with the interactive relationship between soil and hydrology can serve as indicators of the dominant hydrological processes (Ticehurst *et al.*, 2007 and Van Tol, 2010a & b), and improve the understanding of hillslope hydrology (Lin *et al.*, 2006). Some soil properties play an interactive role with hydrology while others, e.g. colour, do not control hydrology but serve as indicators of soil water regime (Van Huyssteen *et al.*, 2005; Van Tol *et al.*, 2010a & b; Kuenene *et al.*, 2011).

The hydrological behaviour of hillslopes is seen as a first step to classify them. The hypothesis is that soil properties controlling current (and future) hydrology, and soil properties indicative of ancient hydrological behaviour genetically related to the interactive relationship between soil and water, are scientifically sound and can serve as criteria to define functional units for hydrological hillslopes. The control of hillslope hydrology by parent material, both lithology and weathering patterns, and climate, is framed in and therefore effectively represented by the distribution of soils in the landscape. The classification is largely based on qualitative interpretations of the hydrological behaviour of

different hillslopes based on spatial distribution of hydrologically important soil properties, grouped in horizons of profiles. The entire hillslope is considered a hydrological response unit (HRU).

1.2 METHODOLOGY

1.2.1 Study areas

A total of 52 hillslopes were surveyed in this study. The hillslopes cover a range of geographical, geological and climate regions in South Africa (Figure 1 and Table 1). The level of investigative detail varied considerably between the different hillslopes (Table 1). Some hillslopes form part of research catchments (e.g. Weatherley, Cathedral Peak VI and Two Streams) with detailed pedological and soil physical measurements and long term hydrometric data available whereas other hillslopes (e.g. Schmitsdrift and Bloemfontein) were surveyed morphologically with varied soil physical support measurements. Although the hillslopes in research catchments were integral to theory development and improved understanding of the interactive relationship between soil and hydrology (see *inter alia* Riddell *et al.*, 2010; van Tol *et al.*, 2010a & b; van Tol *et al.*, 2011; Kuenene *et al.*, 2012), the classification of hillslopes in this study was based solely on results of hydropedological surveys of the hillslopes.



Figure 1 Geographical distribution of studied hillslopes.

However, all the hillslopes were surveyed with a hydropedological survey technique presented in Le Roux *et al.* (2011). This technique involves the identification of representative hillslopes in a study area, augering observations along transect/s perpendicular to the slope, detailed descriptions, identification of horizons, taxonomic classification of the soil profiles and recording of all soil features related to hydrology. The

soil information gathered during the survey phase was interpreted and related to associate hydrological responses.

Table 1 Brief description of the studied hillslope; level of investigative detail, geology and approximate aridity index (AI)

| Catchment | Hillslope | Pedology | Soil | | Geology | AI |
|----------------|-----------|----------|---------|--------------|--------------------|------|
| | | | physics | Hydrometrics | | |
| Craigieburn | 3 | ✓ | ✓ | ✓ | Granite | 0.28 |
| Letaba | 4 | ✓ | ✓ | ✓ | Granite | 0.2 |
| Skukuza | 4 | ✓ | ✓ | ✓ | Granite | 0.25 |
| Mokolo | 5 | ✓ | X | x | Aeolian | 0.2 |
| New Castle | 3 | ✓ | X | x | Sandstone/dolerite | 0.35 |
| Two Streams | 3 | ✓ | ✓ | ✓ | Sandstone | 0.4 |
| Taylor's Halt | 1 | ✓ | ✓ | x | Sandstone | 0.45 |
| Noord Kaap | 2 | ✓ | ✓ | x | Aeolian | <0.1 |
| Thaba Nchu | 2 | ✓ | X | x | Sandstone/mudstone | 0.28 |
| Schmitsdrift | 2 | ✓ | X | x | Alluvium | 0.15 |
| Bloemfontein | 5 | ✓ | X | x | Shales/dolerite | 0.25 |
| Cathedral Peak | 2 | ✓ | ✓ | ✓ | Basalt | >0.6 |
| Weatherley | 5 | ✓ | ✓ | ✓ | Mudstone/dolerite | 0.5 |
| Loeriesfontein | 2 | ✓ | X | x | Shales | 0.1 |
| Hogsback | 2 | ✓ | X | x | Shales/dolerite | >0.6 |
| Fort Hare | 2 | ✓ | ✓ | x | Shales | 0.26 |
| Bedford | 2 | ✓ | ✓ | ✓ | Shales | 0.2 |
| Riversdale | 1 | ✓ | X | x | Sandstone | 0.5 |
| Baviaanskloof | 2 | ✓ | X | x | Conglomerate | 0.2 |
| PAP | 1 | ✓ | X | x | Granite | 0.3 |






1.2.2 Hydrological soil types

Hydropedological classification transforms pedogenetic knowledge of geochemical and hydrological relationships, embedded in soil properties, to hydrological information that is useful for classifying soils. Soils with the same pedogenetic classification might have significantly different hydrological functions. On the other hand, soils classified into different pedogenetic classes might have similar hydrological functions (Bouma *et al.*, 2011). Pedogenetically classified soils were successfully regrouped into hydrological functional units based on their hydrological responses (van Tol *et al.* 2011; Kuenene *et al.* 2011). This classification is similar to the Hydrology Of Soil Types (HOST) classification system of the UK (Boorman *et al.*, 1995). In HOST soils are divided into 29 classes based on their expected hydrological responses. In a catchment or area of interest each soil class is expected to have a unique influence on the hydrology, the HOST classes are therefore HRU's. Pedological differences are credited with a high value even if the hydrological responses are expected to be similar.

Soil types are not randomly distributed and therefore hydrological soil types typically occupy specific positions in the hillslope and by implication can play more of a releasing or receiving role related to hillslope position, altering its role in hillslope hydrology. By implication pedogenetically different soils may be grouped in the same hydrological functional class. The hillslope can therefore be used as an HRU, and the division of soils into different hydrological response classes as building blocks of the spatial systematic variation

in a hillslope. Six different hydrological classes have been assigned to the soils in the study of hillslopes. A brief description of the properties of these soils is presented in Table 2. These soils could be subdivided further, but further subdivision at this level is seen as inappropriate for the hydrological classification of hillslopes.

Table 2 Hydrological soil types of the studied hillslopes

| Hydrological soil type | Description | Symbol |
|--------------------------|----------------------------------------------------------------------------------------------------------------------------------------------------------------------------------------------------------------------------------------------------------------------------------------------------------------------------------------------------------|---------------------------------------------------------------------------------------|
| Recharge | Soils without any morphological indication of saturation. Vertical flow through and out of the profile into the underlying bedrock is the dominant flow direction. These soils can either be shallow on fractured rock with limited contribution to evapotranspiration or deep freely drained soils with significant contribution to evapotranspiration. |  |
| Interflow (A/B) | Duplex soils where the textural discontinuity facilitates build up of water in the topsoil. Duration of drainable water depends on rate of ET, position in the hillslope (lateral addition/release) and slope (discharge in a predominantly lateral direction) |  |
| Interflow (soil/bedrock) | Soils overlying relatively impermeable bedrock. Hydromorphic properties signify temporal build of water on the soil/bedrock interface and slow discharge in a predominantly lateral direction. |  |
| Responsive (shallow) | Shallow soils overlying relatively impermeable bedrock. Limited storage capacity results in the generation of overland flow after rain events. |  |
| Responsive (saturated) | Soils with morphological evidence of long periods of saturation. These soils are close to saturation during rainy seasons and promote the generation of overland flow due to saturation excess. |  |

1.2.3 Framework of the classification system

The classification system proposed is based on intercomparisons of the perceptual hydrological behaviour of hillslopes. Flowpaths of water through the hillslope and into the stream is the fundamental aspect considered in the intercomparisons. Due to the complexity of the hydrological system and strong time dependencies of hydrological processes, only the hydrological response during the peak rainy season was considered in this study, i.e. not the wetting-up and drying out phases typical of seasonal climates.

The classification further strongly relies on Jenny's algorithm of the factors of soil formation (Jenny, 1941), where soil properties are the result of the impact of parent material, climate, topography, organisms and time. The latter are therefore not considered in the classification as their influence is revealed in the soil properties and their spatial distribution for example steep slopes (topography) with high intensity rain storms (climate), low vegetative growth (organisms) and impermeable bedrock (geology) will favour erosion and eventually (time) result in shallow soils. For this reason the hydrological soil types in the hillslopes are presented as 2-dimensional bars without inclination or differences in slope

length. Arrows indicate dominant flowpaths in the hillslope (Figure 2) and a hydrograph indicates the anticipated impact of the hillslope's hydrology on stream flow (Figure 3). The length of the bars is relative to the fraction occupied by a hydrological soil type in a specific hillslope. A.

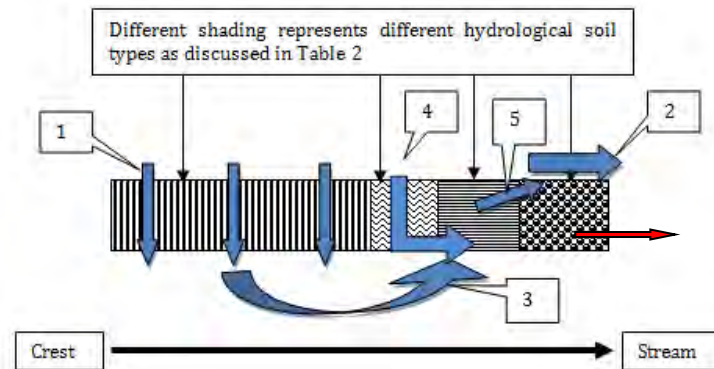


Figure 2 Example of how hillslope classes are presented and discussed.

The hillslope classes are presented as 2-dimensional shaded block diagrams where the different shades refers to the hydrological soil types (Table 2). The left hand side of the block diagram represents the crest with the stream at the right hand side. The numbered arrows in Figure 2 refer to dominant hydrological pathways; arrow 1 refers to vertical flow through and out of the soil profile into fractured rocks or other material with higher permeability, arrow 2 refers to overland flow, arrow 3 refers to fractured rock to the soil return flow, arrow 4 represent infiltration and lateral flow on the soil/bedrock interface and arrow 5 represents shallow lateral flow which eventually returns to the surface to contribute to overland flow. The magnitude of the different arrows gives some indication of the dominance of the various pathways.

The perceptual schematic representations of the 52 hillslopes were compared with one another. Four aspects were considered in the intercomparisons: 1) occurrence of different hydrological soil response types in a hillslope; 2) the sequence in which different hydrological soil types occur in a hillslope; 3) the fraction of the hillslope covered by different hydrological soil types and most importantly, 4) how water will reach the stream, as expressed by the hydrograph. Based on these aspects the 52 hillslopes were grouped into classes with similar anticipated hydrological responses.

The conceptual hydrographs accompanying different hillslope classes are representations of the hydrological responses of the specific hillslopes during typical rain events and are only provided to improve the conceptual understanding through graphical representation. No attempt was made to accommodate climate, antecedent moisture conditions, land use, etc.

1.3 RESULTS AND DISCUSSION

The 52 hillslopes and their classes are presented in Figure 3. Hillslopes from the same geographical area may fall into different hillslope classes (for example Weatherley 1-5 and Mokolo 1-5). Hillslopes occurring on different geological formations with different climates may however fall into the same hillslope class (Figure 3).

1.3.1 Hydrological hillslope classes

Figure 3 Class 1 – Interflow (soil/bedrock interface)

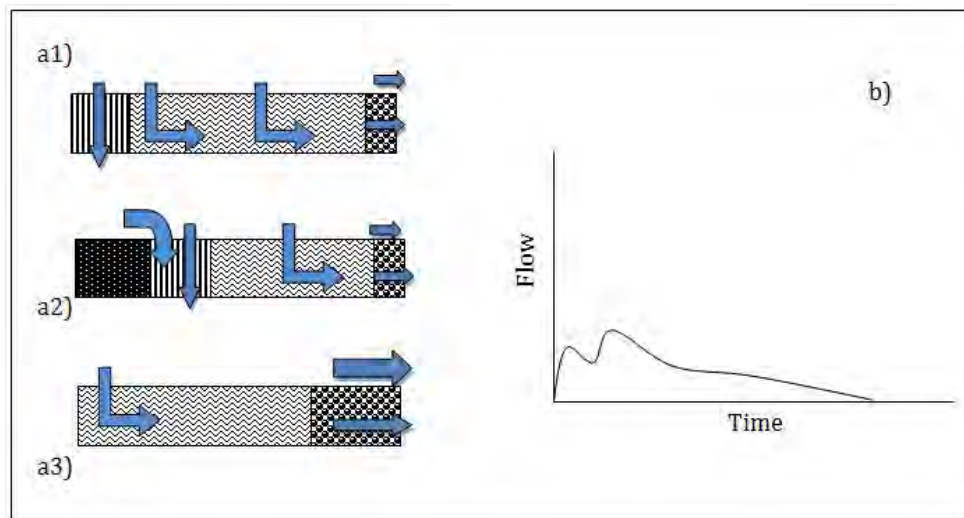


Figure 3 Perceptual flow models of hillslope class 1 (a1, a2 & a3) and anticipated hillslope hydrograph (b)

This class has the full range of recharge, interflow and responsive soils. Soil/bedrock interflow is more common but soil interflow often follows down slope. The soil/bedrock interflow soils may constitute a narrow portion of the hillslope.

In this class it is important that bedrock properties largely control redistribution of water in the hillslope. Bedrock permeability controls soil-to-bedrock flow. Bedrock layering, controlling variation in permeability, controls bedrock-to-soil return flow. The resistance of layers to weathering influence the topography. Topography supports the soil-to-surface return flow. In the valley bottom an impermeable rock layer controls the formation of a wetland and responsive soils. Upslope the bedrock is permeable and ET-excess water leaves the soil and fills up the pore space in the fractured rock. The storativity of the bedrock and depth to an impermeable layer control return flow to the subsoil. The flowpath is large and long enough to leave signatures of additional water, i.e. increased chemical weathering and reduced or redox morphology. Colluvial action could have contributed to deep weathered saprolite. This class has been identified in semi-arid and sub-humid climates.

During the wetter parts of the rainy season responsive character expands upslope including the soil interflow zone. This type of hillslope accommodates a large variation in residence times. The hydrograph typically has peak, shoulder and base flow elements. A second peak is possible where the soil, compared to surface, contribution to stream flow is delayed.

Modal hillslope of Class 1 – Cathedral Peak IV hillslope 1

The hillslopes are found in the 67.7 ha CP6 catchment (latitudes 28°30'S and 30°30'S and longitudes 28°30'E and 29°30'E) located in land type Ac265 (Land type survey staff, 2002), characterised by soils of the Clovelly, Mispah, Glenrosa, Magwa, Hutton, Kranskop, Inanda,

Nomanci and Champagne forms formed from basalt parent material. The elevation of the catchment ranges from 1 860 m at the weir to 2 070 m at the highest point. The catchment is characterised by cool temperatures, high rainfall with average aridity index of 1.8. These climatic conditions promote vigorous growth of *Themeda triandra* grassland species which dominates the catchment. Because of high rainfall, the soils are highly weathered and, promoted by low temperatures, are high in organic matter content. They are well drained and acid. The major part of the catchment consists of steeply sloping midslopes with an average slope of 19%, grading to about 8% towards the marsh at the outlet. It is dissected by a number of deep downslope channels which converge midway in the catchment before the outlet. It is considered that these channels play an important role in the hydrology of the catchment. Their depth of approximately 1 m below the surrounding soil surface shows that they have eroded to this depth in this erosion resistant soil over the centuries by conveying large volumes of water. Flowing water was observed in these channels at the end of the dry season in July and September, indicating considerable lateral water flow in the catchment.

Soil distribution pattern is presented in Figure 4. The main hillslope, located down the middle and down each of the side slopes of the catchment, between the deep downslope channels, varies in length between about 1000 and 500 m long and is represented by the following sequence of soils: Nomanci (summit and upper slopes), Inanda, with some patches of Magwa and Kranskop soils (from midslopes to lowerslopes), Magwa (footslopes), near the marsh, and Champagne in the marsh. The Nomanci soil has a thin (200 mm), dark, loamy humic A over weathering basalt bedrock. The solum is underlain by lithocutanic B which is soft basalt saprolite that still bears the original rock structure. At some parts the A horizon rests directly on the hard bedrock, resulting in some high level seeps which gave rise to Magwa soil at these seep areas. Nomanci soil form is well drained with moderately rapid infiltration rate and rapid permeability through the lithocutanic B or the cracked bedrock.

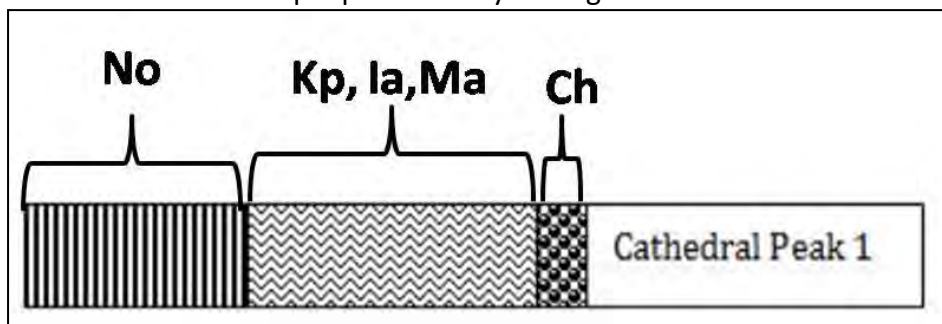


Figure 4 Soil distribution pattern of the Cathedral Peak IV hillslope 1

Nomanci are therefore predominantly recharge soils. On the mid to lower slopes, infiltrated water in the soil matrix of deep Inanda, Magwa and Kranskop soils flows vertically to recharge the deep saprolite and raise soil water content to above the drained upper limit, thereby promoting lateral flow either into nearby deep downslope channels on the short hillslope or into the wetland on the long hillslope. The soil water content measurements in the deep horizon of midslope soils were shown to be consistently > 0.78 of saturation (Kuenene, 2008). This water regime is also reflected by mottling morphology, and the formation of the non-diagnostic yellow brown apedal B horizon below the red apedal B horizon in the Inanda soil. Overland flow can be expected on the Champagne in the marsh area as saturated excess.

Morphological Hillslopes of Class 1

Cathedral Peak IV hillslope 2

The soils on this very short hillslope (approximately 40 m in length) are similar to those on the main hillslope, except that Nomanci is absent here (Figure 5). Drainage is into the deep downslope channels via lateral deep interflow. Deep Inanda soil predominates, followed by Magwa with a defined convex slope, adjacent to the deep downslope channels. The Inanda soil has a large soil water storage capacity that releases water continuously during and after the rain season that flows via the Magwa C horizon into the deep downslope channels dissecting the catchment.

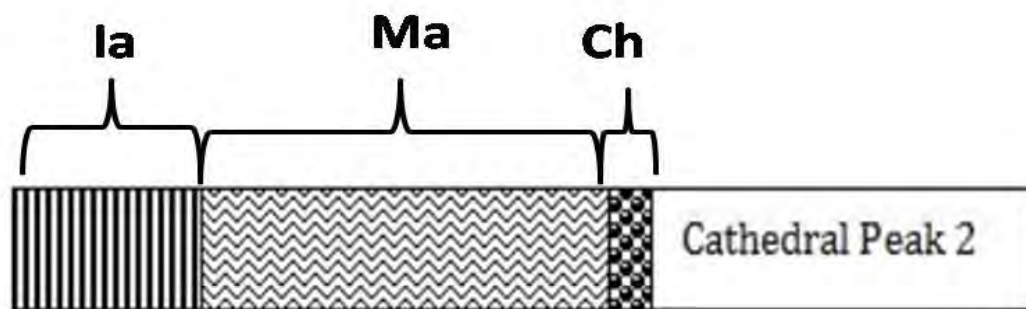


Figure 5 Soil distribution pattern of the Cathedral Peak IV 2 hillslope.

Loeriesfontein hillslope 2

The soil distribution is characterised by a distinct redistribution of salts. At the crest a combination of carbonate deposits in the subsoil occur namely Brandvlei, with soft carbonate horizon, and Coega, with a hard pan carbonate horizon (Figure 6). On terrain morphological unit 3 the Swartland soil form is enriched with gypsum in the pedocutanic B horizon with redox morphology in the saprolite. On terrain morphological unit 5 the Mispah soil in the pan has sodium chlorite precipitated on the surface of the Glenrosa soils.

The climate is arid with aridity index of about 0.10 and the underlying rock is Karoo shale. The topography is undulating with a gentle convex-convex crest changing smoothly into a straight midslope, a short concave footslope and straight, level valley bottom pan.

The lateral sequential distribution of salts is an indication of sufficient leaching in the pedon to remove the salts from the topsoils of terrestrial soils. The underlying shales limit vertical recharge of the fractured rock and water logging of the subsoil results in soil/rock interface flow. A columnar distribution of salts with different solubility products is the result. Typical of arid climates is the sporadic saturation of soils during once in a decade rain event. During dry years the soil wets up with rain events and contributes little to stream flow. During excessively wet years these hillslopes probably doesn't contribute to groundwater recharge. The morphological and chemical characteristics of the soil distribution are valuable as it indicates a recent rather than ancient flowpath activity. Climate change may influence the distribution of salts but not the dominant flow path, direction and rate of flow in the hillslope.

The distribution of salts is an indication of the role pedon and hillslope hydrology plays in the distribution of chemicals, including nutrients, in the natural ecosystem.

Due to extreme variation in rainfall, hydrometry and soil water content measurements may not contribute to the understanding of pedon and hillslope hydrology and intensive two dimensional data of soil morphology and chemistry will upgrade the conceptual hydrological response model. Distribution of salts in the matrix and pores may indicate the impact of average events on flowpaths in the soils and reveal dominance of preference or matrix flow.

Cg, Br, Sw

Ms



Figure 6 Soil distribution pattern of the Loeriesfontein 2 hillslope

Skukuza hillslope 2

The soil distribution pattern of the Skukuza hillslope 2 (Figure 7) suggests that overland flow will be generated on the shallow Mispah soils (Ms) of the upper slopes. Below the Ms, freely drained soils of the Oakleaf (Oa) form dominate, followed by Pinedene soils on the TMU 4 position. There is therefore an increase in wetness downslope. Although it is debateable whether the Prieska soils in the valley bottom of this hillslope will be saturated for long periods, it will still generate overland flow during the peak rainy season.

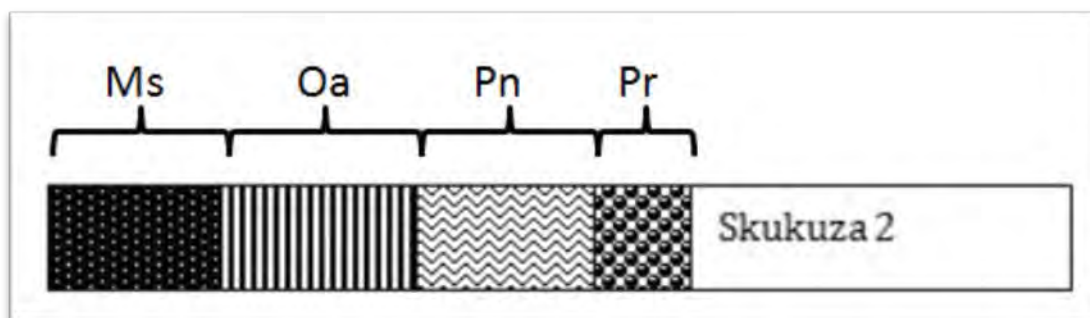


Figure 7 Soil distribution pattern of the Skukuza 2 hillslope

New Castle hillslope 1

This New Castle 1 hillslope is characterized by soils with plinthic horizons on the crests and midslopes, i.e. Avalon (Av) and Westleigh (We). A wetland with Katspruit (Ka) is found in the valley bottom (Figure 8). Thus it is a hillslope with interflow in the crest and midslope and then a saturation excess responsive soil in the valley bottom.

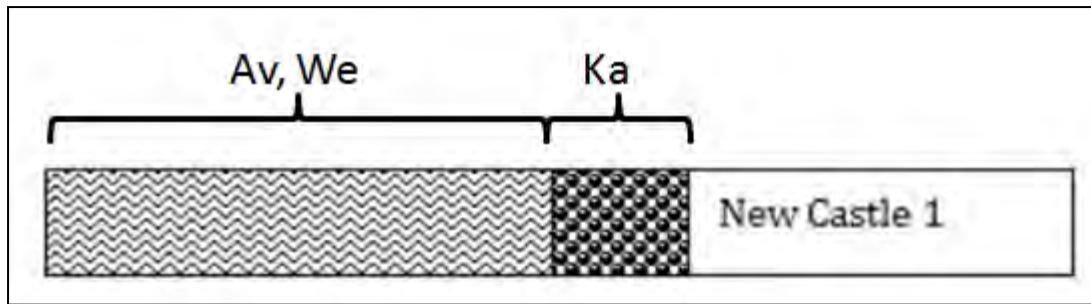


Figure 8 Soil distribution pattern of the New Castle 1 hillslope

New Castle hillslope 3

In this hillslope red clays (Hu) and shallow Mispah (Ms) soils on dolerite overlie the crests, meaning that water here will recharge the fractured rock (Figure 9). On the midslopes, interflow soils occur (soils with plinthic horizons such as Avalon and Westleigh). Thus there is a fractured rock flow path from the crest and a soil flow path from the midslope. Both these flow paths feed the wetland in the valley bottom position, where wetland soils occur (Katspruit).

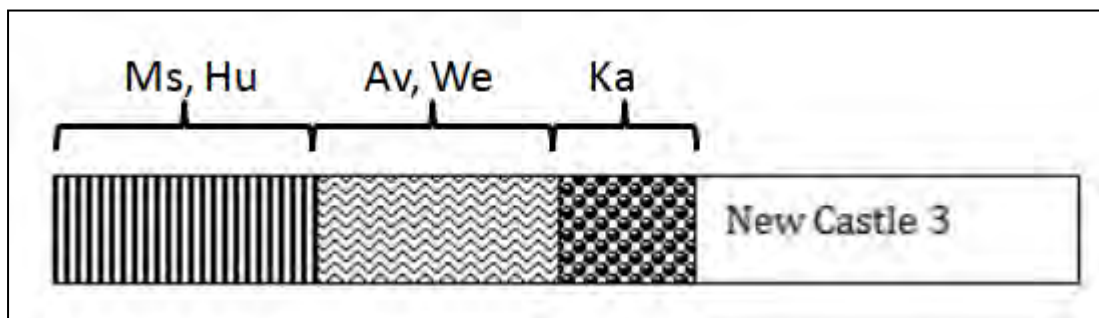


Figure 9 Soil distribution pattern of the New Castle 3 hillslope

Pan African Parliament (PAP) hillslope

Indications are that the shallow coarse textured Glenrosa soils on the crests quickly recharges and release water to the saprolite and occasional fissures of the fractured rock (Figure 10). In high rainfall regions like Pretoriuskop, Kruger National Park, the recharge soils can be deep and of the Hutton soil form. The flow paths are the same and the conceptual hydrological response model the same although the soil reservoir is bigger, the rainfall higher and the recharge of the saprolite and fractured rock more. Wetlands may be more distinct. Draining water follows shallow flowpaths in the saprolite and lower down slope it return to the subsoil as a fluctuating water table forming plinthic horizons (both soft and hard plinthic B horizons) often under redox E horizons. Increased soil interflow rises to the topsoil and the soil surface resulting in Kroonstad and Katspruit soils.

This sequence of shallow interflow and responsive soils repeats itself down slope. The distribution is controlled by larger fissures returning water to the soil pushing the water table to the surface forming horizontal strips of wetlands.

Large areas of the midslope may be classified as wetlands and areas above these wetlands is the conduits of flowpaths feeding the wetlands. Trenches of a meter to two meters may

impact radical on the hydrology of the hillslope. This is visible next to some roads where flow paths are disturbed and soil water return to the surface.

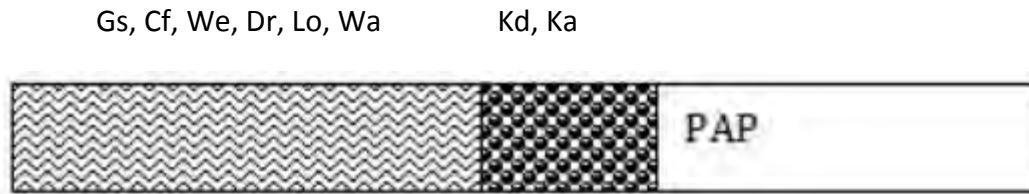


Figure 10 Soil distribution pattern of the Pan African Parliament site hillslope.

Bloemfontein hillslope 2&3

The two hillslopes studied on the farm Brandkop outside Bloemfontein was dominated by clayey Sepane and Bonheim soils on the midslope (Figure 11). The Sepane soils, with signs of wetness at the soil bedrock interface suggest that the underlying parent material is relatively impermeable and slow lateral drainage is expected on this interface. A dolerite ridge with shallow Mispah soils was observed on the TMU 1 positions; implying that recharge will dominate on this position. Arcadia soils, with smectite clays dominate the valley bottom. Although the vertic A horizon of the Arcadia soils can serve as preferential flowpaths during the dry season, these cracks are expected to close due to swelling during the rainy season. The high clay contents in the vertic A horizons are associated with low conductivities and overland flow (infiltration excess) is expected to be dominant in this landscape position.

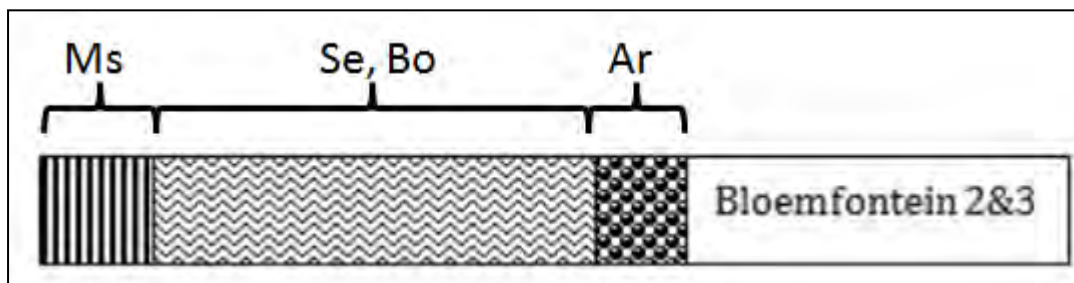


Figure 11 Soil distribution pattern of the Bloemfontein 2&3 hillslope

Mokolo hillslope 1 & 2

Mokolo hillslope 1 is dominated by plinthic soils with rock outcrops and shallow Mispah soils on the ridges (Figure 12). Soils of the Avalon and Glencoe forms dominate the mid and footslopes. In the Avalon soils, both top and sub-soils are sandy (< 5% clay), with depths ranging from 200-2 500 mm. The formation of plinthite suggests that the IVZ is impermeable. Although the sandy texture will most likely facilitate fast infiltration, recharge of groundwater levels is limited due to the impermeability of the IVZ. Water drains laterally towards the stream channel and this hillslope is expected to contribute to baseflow.

Mokolo hillslope 2 is very similar to Mokolo hillslope 1. The area covered by plinthic soils is slightly greater in Mokolo 2 and these soils are generally deeper than the plinthic soils of Mokolo 1.

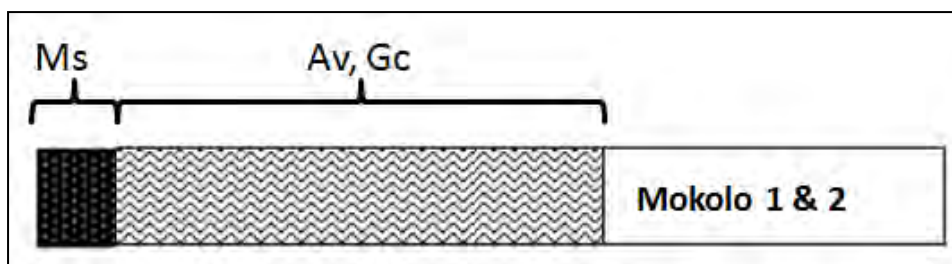


Figure 12 Soil distribution pattern of the Mokolo 1&2 hillslope

Mokolo hillslope 3

The soil distribution pattern in Mokolo hillslope 3 is very similar to Mokolo hillslope 1 and 2, the plinthic soils covers however a smaller area in hillslope 3 compared to that of Mokolo 1 and 2 (Figure 13). The dominance of Glenrosa soils in on the upper ridges suggest that recharge can occur on these positions.

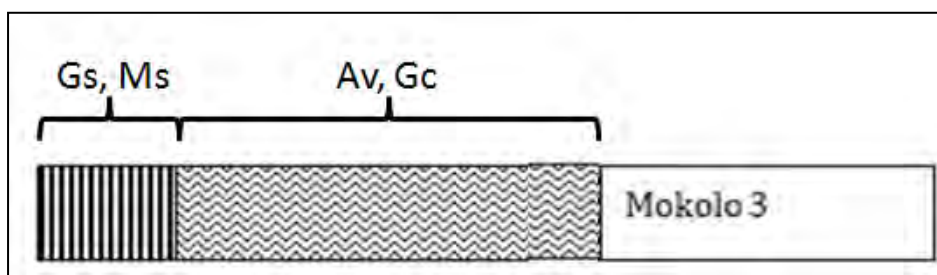


Figure 13 Soil distribution pattern of the Mokolo hillslope 3

Thaba Nchu hillslope 2

The climate is dry semi-arid and the parent material upper Beaufort mudstones. During high rainfall years water recharges the Swartland soils and ET-excess water drain to the saprolite and underlying fractured rock on the crests (Figure 14). On the midslope a prominent redox morphology in the saprolite indicate a fluctuating water table. At the upper footslope Klapmuts soils occur. The redox E horizon indicates a water table that rises to the surface and thin bands of Katspruit wetlands follow.

Sw

Sw (mottled saprolite), Km

Ka



Figure 14 Soil distribution pattern of the Thaba Nchu 2 hillslope

Class 2 – Shallow responsive

Figure 15 represents the perceptual hydrological flowpaths and anticipated hydrograph response of hillslope class 2. This hillslope is dominated by shallow responsive soils. A sharp

transition to impermeable rock controls the hydrological response in this hillslope class. During the rainy season the small water holding capacity fills up and overland flow by saturation excess occurs. This class has been identified in arid and semi-arid climates. A clear distinction between pedogenesis and hydrology is important in this hydrological class. Pedogenetically it is important that precipitates of lime, gypsum and salt are distributed downslope in drier climates. In wetter climates surface horizons are bleached. Variation in this class is limited to the presence of small areas of other hydrological soil types related to alluvium/colluvium and variation in the permeability of the parent rock. Deeper alluvial/colluvial soils next to the stream (Figure 15-a2) may have a small impact on the hydrology. The impermeability of the underlying rock promotes slow and limited discharge to the stream on the soil/bedrock interface, because it competes with ET extraction of soil water. High peak flow is typical in this class due to the prominence of overland flow and streams flow for short periods after rain events (Figure 15-b). Base flow is absent, and where present, it is expected to be low and related to groundwater aquifers. Groundwater recharge is localised to fractures in the underlying rock (Hughes & Sami, 1993).

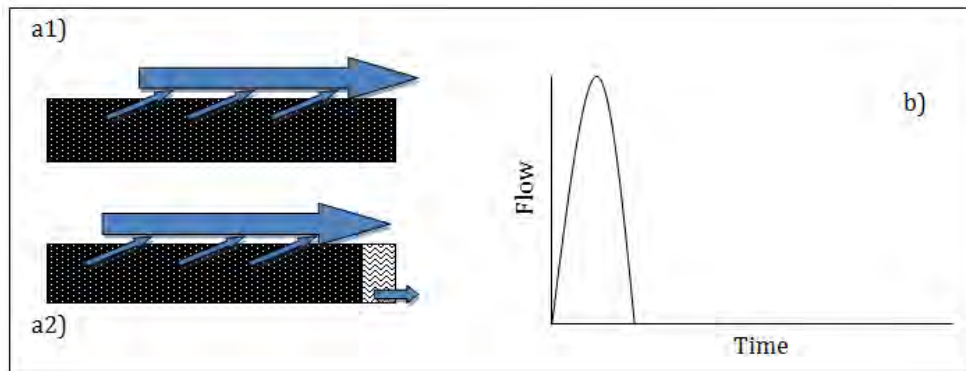


Figure 15 Perceptual flow models of hillslope class 2 (a1 & a2) and anticipated hillslope hydrograph (b)

Modal hillslope of class 2 – Bedford 3 hillslope

Bedford 3 represents hillslopes in B3, a sub catchment of the greater Bedford catchment. This hillslope in the Eastern Cape Province has a mean annual rainfall of 460 mm and is underlain by horizontally bedded sandstone and shales of the Middleton formation. The study area and methodologies followed are described in more detail in van Tol *et al.* (2010). Soils on the summit were dominated by Glenrosa soil forms, on upper backslope (TMU3) positions Cartref soils dominates (Figure 16). Shallow Mispah soils are predominant in the lower backslope and footslope positions and cover more than 60% of these hillslopes. The valley bottom is occupied by very deep alluvial deposits which were classified as Augrabies soils.

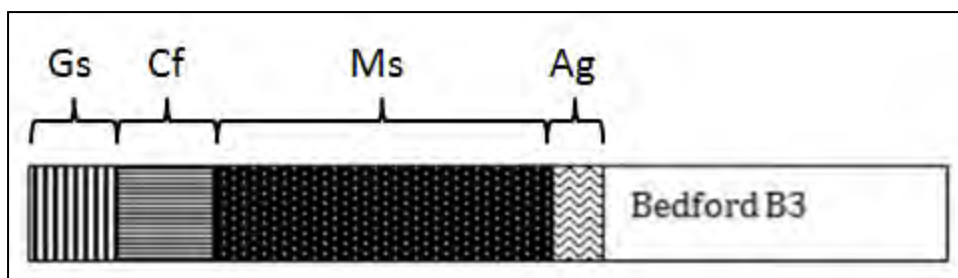


Figure 16 Soil distribution pattern of the Bedford B3 hillslope

The A horizons in the majority of the Glenrosa soils of the summit was not bleached, this implies that the bedrock is permeable enough to ensure that the surface soils are not saturated for long periods. As opposed to the relatively permeable bedrock of the summit, the E horizon of Cartref soils of the upper backslope suggests that the lithocutanic B horizons facilitate perching of soil water and lateral drainage at the A/B horizon interface, i.e. the B horizon is relatively impermeable. The majority of this hillslopes are covered by Mispah soils, predominantly with bleached A horizons, suggesting that the underlying shales are impermeable. The small storage capacity (95 mm) of the Mispah soils implies that relatively large rain events will cause saturation of the soils and facilitate the generation of overland flow resulting in high peak flows (van Tol *et al.*, 2010). The deep Augrabies soils observed in the valley bottom diffuse the quick response of the stream somewhat. These soils typically have a storage capacity of 700 mm (van Tol *et al.*, 2010), and can store hillslope water draining down the slopes as overland flow. The accumulation of calcium carbonates in these soils suggests that water is stored long enough that the carbonates can precipitate as the water is evapotranspired.

The physical and hydrological characteristics of the Bedford catchments were studied by Hughes and Sami (1997). Unfortunately a lot of the hydrometric measurements were lost due to IT failure. Validation of our morphological interpretations of hillslope hydrology were therefore largely based on personal communication with Prof. Dennis Hughes as well as flow duration curves simulated with the Pitman hydrological model as presented in Le Roux *et al.*, 2011. As Prof. Hughes work in the Bedford catchments for several years, his views on the hydrological functioning of the catchment was vital. He agreed with our interpretations of the hillslope hydrology of Bedford B3, i.e. that overland flow is the dominant hydrological process, recharge of regional groundwater levels occur rapidly in localised positions on the summit and that the valley bottom store a great volume of water which is extracted by plant roots as evapotranspiration.

Morphological hillslopes of class 2

Bedford 4&5 hillslope

Mispah soils dominate entire hillslopes in sub-catchments B4&5 of the greater Bedford catchment. These shallow soils (<300 mm) overlies slowly permeable shales (van Tol *et al.*, 2010). Due to the limited storage capacity for water in the solum these soils will tend to saturate quickly after rain events and promote the generation of overland flow. The occurrence of bleached A-horizons supports the theory of saturation and the relative impermeability of the underlying material (Figure 17).

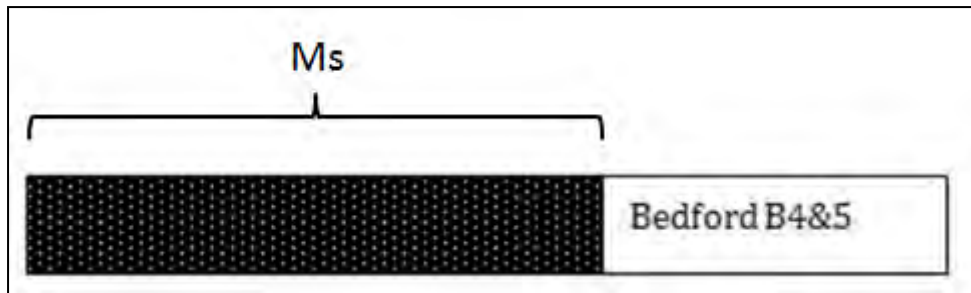


Figure 17 Soil distribution pattern of the Bedford B4&B5 hillslope

Fort Hare 1 hillslope

In this hillslope approximately 3 km North East of the University of Fort Hare's Alice campus, shallow Mispah soils dominates the upper slopes followed by shallow Westleigh soils in the narrow valley bottom (Figure 18). For reasons similar to that as discussed in the modal profile of this class (i.e. B3) overland flow will dominate during typical rainstorms resulting in a flashy streamflow response.

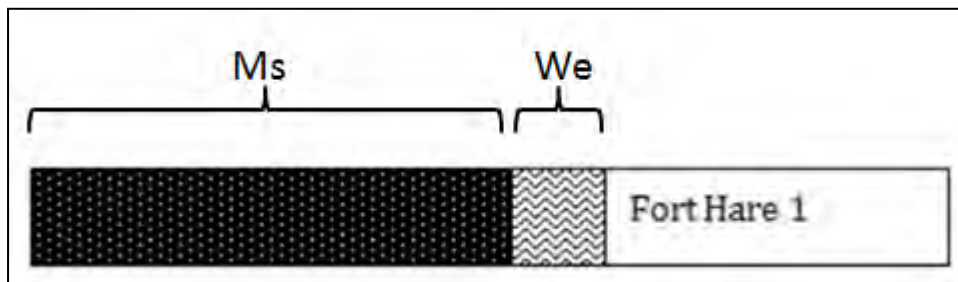


Figure 18 Soil distribution pattern of the Fort Hare 1 hillslope

Class 3 – Recharge to groundwater (not connected)

Hillslopes where recharge is dominant are represented in Figure 19. These hillslopes are dominated by high chroma soils with redoximorphic properties limited to the valley bottom, indicating that the underlying bedrock is permeable. On these hillslopes the infiltration and vertical redistribution rate is generally higher than the precipitation rate, thereby promoting sustained oxidized soil chemistry. Interflow and responsive soils are scarce. This class is commonly associated with sand deposits (aeolian deposits, coastal plains and quartzitic sandstones) and karst landscapes amongst others.

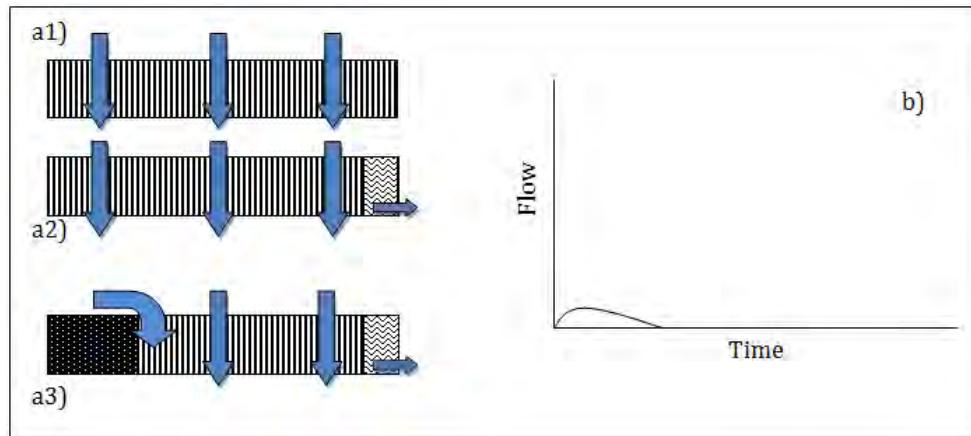


Figure 19 Perceptual flow models of hillslope class 3 (a1, a2 & a3) and anticipated hillslope hydrograph (b)

Although vertical flow through and out of the profile is the dominant flow direction, lateral flow can occur (even in vertical isotropic soil with regards to hydraulic conductivity), resulting in redoximorphic signatures in soils next to the stream (Figure 19-a2 & -a3). When shallow responsive soils occur above the recharge soils (Figure 19-a3), overland flow generated on the upper portions will not directly contribute to streamflow but rather infiltrate the recharge soils.

The direct contribution of this hillslope class to streamflow will be minimal (Figure 19-b). Groundwater recharge is high and groundwater levels are typically not connected to the stream (losing stream) and a net loss of water to deeper aquifers is anticipated. By implication the groundwater distribution pattern may not be hillslope or catchment related.

Modal hillslope of class 3 – Letaba hillslopes

The soil distribution patterns of the hillslope studied in the Letaba region are very similar. Freely drained Hutton (Hu) and/or Clovelly soils dominate the upper regions of these slopes (Figure 20 & Figure 21), with a narrow valley bottom with Dundee soils. In the Letaba hillslope 2, shallow Mispah (Ms) soils were observed on the TMU 1 positions. These soils might generate overland flow. It is however hypothesised that the generated overland flow will re-infiltrate and the freely drained soils. The absence of signs of saturation indicates either 1) evapotranspiration exceeds precipitation to such an extent that periodic saturation does not occur or 2) recharge of groundwater levels, not connected to the vadose zone in lower lying areas, is dominant.

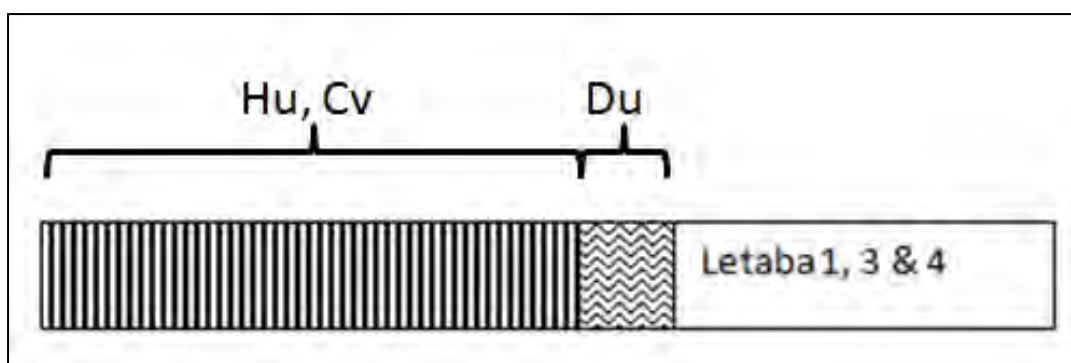


Figure 20 Soil distribution pattern of the Letaba hillslopes 1, 3 & 4

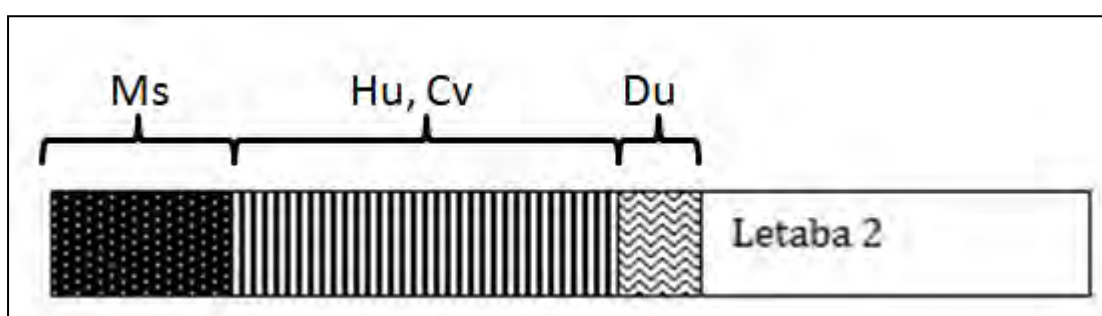


Figure 21 Soil distribution pattern of the Letaba 2 hillslope

Morphological hillslopes of class 3

Schmitsdrift hillslopes

The two Schmitsdrift hillslopes have very similar soil distribution patterns (Figure 22 and Figure 23). It might be slightly misleading to call these virtually flat areas 'hillslopes'. As previously mentioned, the idea of the hillslope classification system is to categorise the contribution of different slopes to streamflow. It is doubtful that these slopes contribute to streamflow at all. Even if the neocarbonates and soft carbonates of the Addo (Ad) soil can be seen as interflow soils, the absence of any significant slope will limit lateral flow in these soils. In the Schmitsdrift hillslope 2, a narrow portion of Dundee soils were observed in the dry riverbed (Figure 23). Valsrivier (Va) and Oakleaf (Oa) soils were also observed on these 'slopes' (Figure 22 and Figure 23).



Figure 22 Soil distribution pattern of the Schmitsdrift 1 hillslope

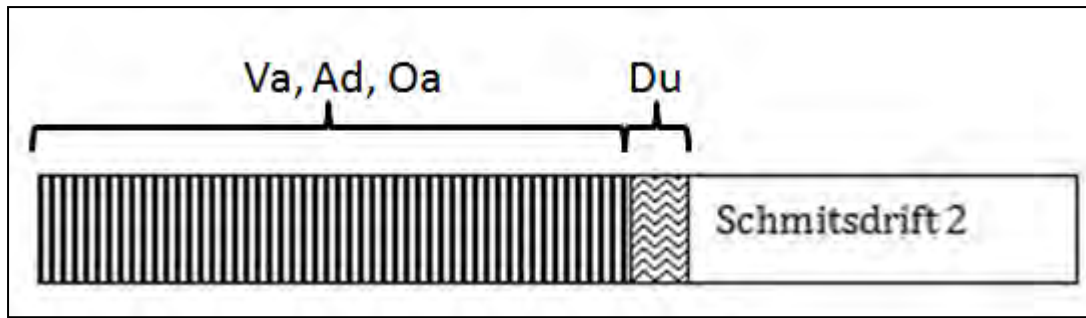


Figure 23 Soil distribution pattern of the Schmitsdrift 2 hillslope

Noord Kaap 1 hillslope

The soils on the summit are Mispah and shallow Hutton soil form (400-800 mm). The depth of the Hutton soils increase with depth (2 m +) on the backslope and this trend continues as the hillslope reaches footslope (Figure 24). Calcium carbonate was found in some of the profiles at the footslope. The underlying geology on the crest is dolerite and most probably Eccra mudstone on the footslope.

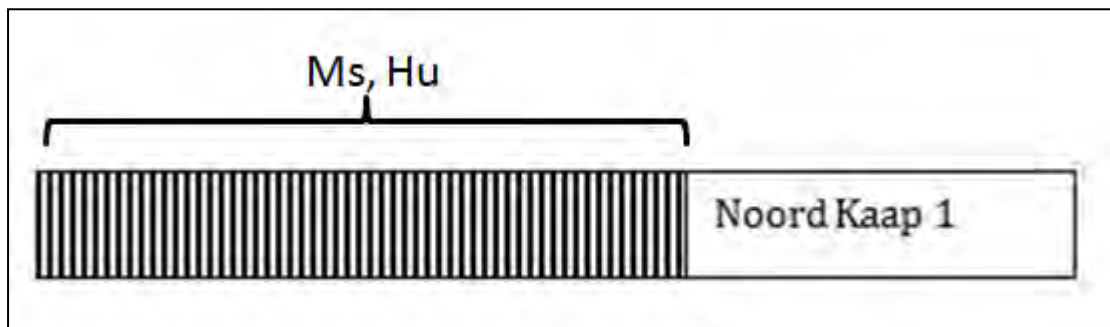


Figure 24 Soil distribution pattern of the Noord Kaap 1 hillslope

Noord Kaap 2 hillslope

The soils on the summit are Mispah and shallow Hutton soil form (400-800 mm). The depth of the Hutton soils increase with depth (2 m +) on the backslope (Figure 25). At the footslope the colour of the soil changes from a red to yellow-brown, and therefore a change to Clovelly soil form. There are erosion gullies at this position in the hillslope. The underlying geology on the crest is dolerite and most probably Eccra mudstone on the footslope.

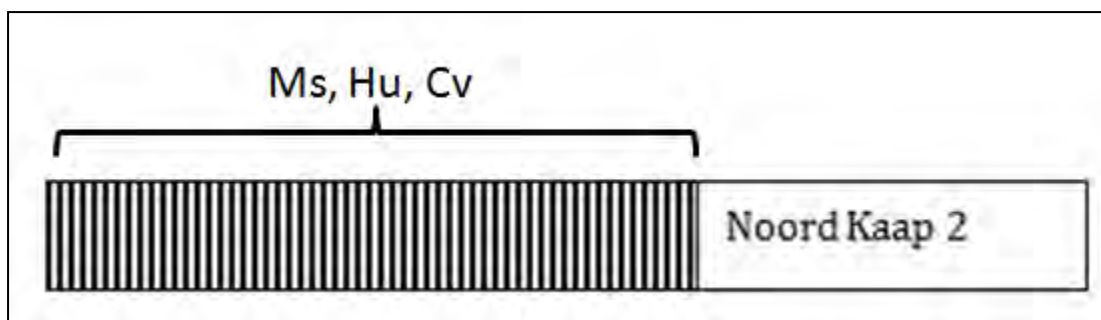


Figure 25 Soil distribution pattern of the Noord Kaap 2 hillslope

Mokolo 4 and Mokolo 5 hillslopes

The soil distribution pattern in Mokolo 4 & 5 hillslopes is predominantly deep recharge soils (Figure 26). These soils are very deep (5 m +). The Hutton soils on the ridges are an indication of recharge character. The Clovelly soils between the ridges (dunes) are an indication of slightly wetter water regimes. Hutton soils of medium sand (Hillslope 4) and coarse sand (Hillslope 5) occur as dunes. Hardpan carbonate layers occur occasionally in these soils. Recharge is the dominant hydrological process in these hillslopes. Carbonate deposits indicate however, limited leaching due to the low rainfall of this area.

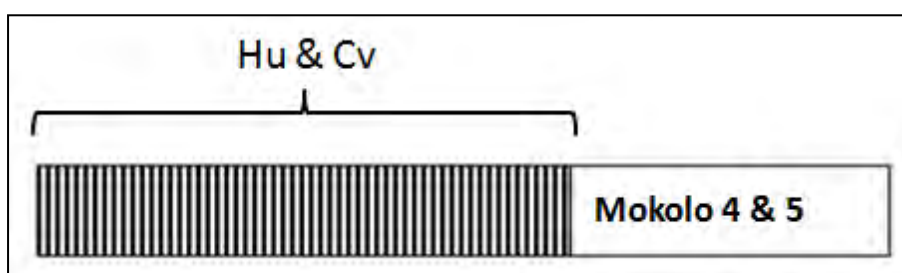


Figure 26 Soil distribution pattern of the Mokolo 4&5 hillslope

Bloemfontein 4 hillslope

In the Bloemfontein 4 hillslope, shallow Glenrosa and Mispah soils dominate the upper and midslope positions (Figure 27). These soils are likely to facilitate recharge of groundwater levels with limited lateral contributions to the stream. Colluvial deposits in the valley bottom resulted in the formation of slightly deeper Sepane soils with indications of saturation at the soil/bedrock interface.

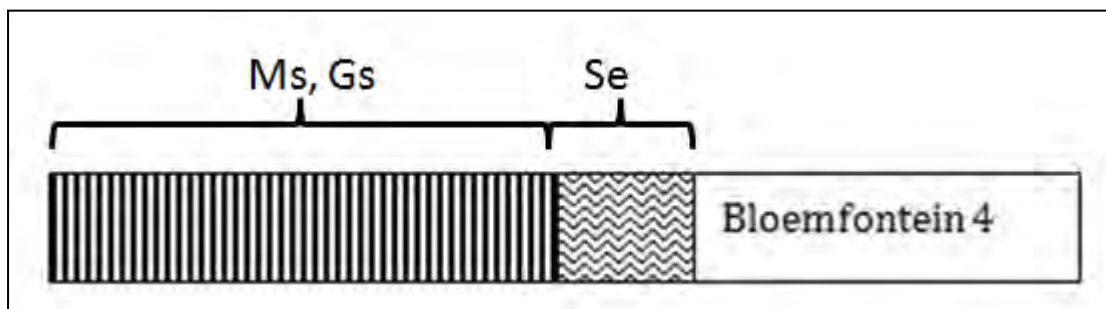


Figure 27 Soil distribution pattern of the Bloemfontein 4 hillslope

Class 4 – Recharge to wetland

This hillslope class is dominated by recharge soils and stable wetlands with indications of long periods of saturation (Figure 28). Water exiting the soil in the recharge areas, flows through fractured bedrock and feeds the soils next to the stream, resulting in waterlogged conditions. Since the soils next to the stream are saturated, additional precipitation can't infiltrate and saturation excess overland flow will be generated. Mountainous fractured rocky areas with peat wetlands are typical. The recharge area may have coarse, shallow soils of high permeability. For the formation of peat wetlands the ratio of recharge to wetland area is related to climate (Marneweck *et al.*, 2001).

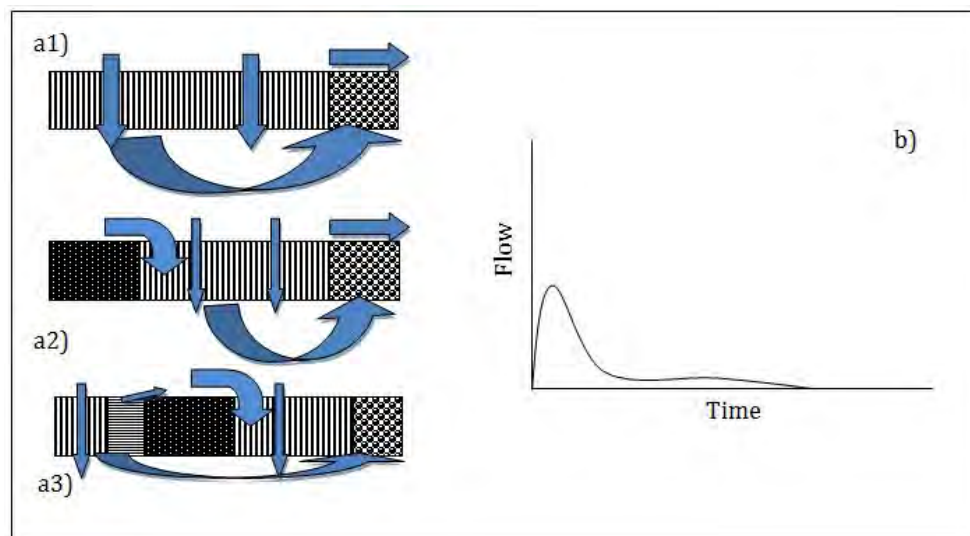


Figure 28 Perceptual flow models of hillslope class 4 (a1, a2 & a3) and anticipated hillslope hydrograph (b)

The presence of shallow responsive and interflow (A/B interface) soils above the 'recharge zone' does not affect the dominant character of the hillslope and can contribute to the recharge of the wetland (Figure 28-a2 & -a3). Peak flows associated with the overland flow generated on responsive soils can be expected with some lateral contribution from the wetland soils (Figure 28-b). A stable base flow component is characteristic of the hillslope hydrology of this class.

Morphological hillslopes of class 4

Baviaans Kloof 1 hillslope

The first hillslope in the Baviaans kloof nature reserve observed (Baviaans Kloof 1) is covered by Glenrosa (Gs) soils, with varying depths, on the steep TMU 3 positions (Figure 29). The perennial Baviaans River meanders through the valley bottom with Dundee soils (Du). It is hypothesized that the Gs soils are permeable and facilitate recharge of groundwater stores as well as the river.

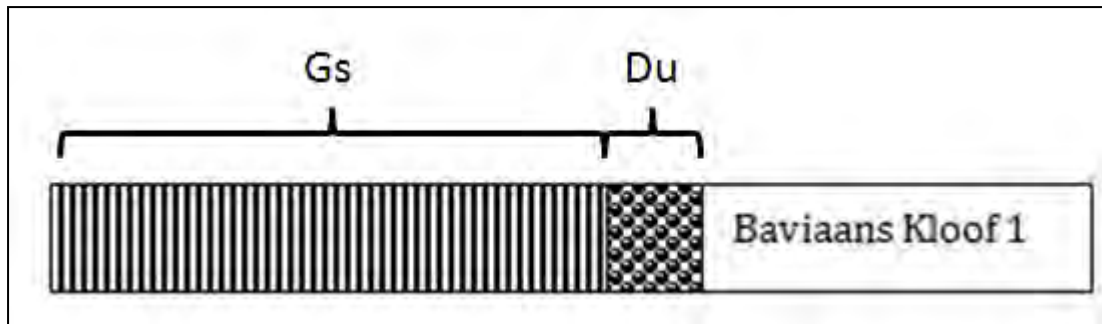


Figure 29 Soil distribution pattern of the Baviaans Kloof 1 hillslope

Baviaans Kloof 2 hillslope

Baviaans Kloof 2 hillslope has similar topography to that of Baviaans Kloof 1. Great portions of the upper midslope are however covered by rock outcrops (R) and shallow Mispah soils (Ms) (Figure 30). Hydrologically these shallow soils will promote overland flow generation before the surface water infiltrates the soil at lower midslope positions. The valley bottom is covered by Dundee (Du) soils which will probably result in the generation of overland flow, due to saturation excess, during the peak rainy season.

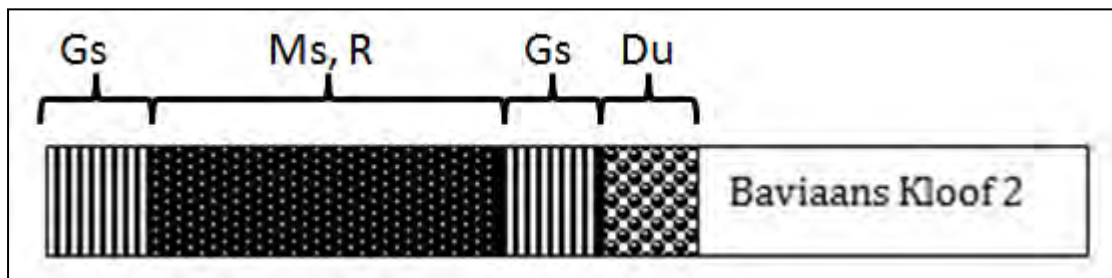


Figure 30 Soil distribution pattern of the Baviaans Kloof 2 hillslope

Newcastle 2 hillslope

The New Castle 2 hillslope has soils where the fractured rock in Mispah (Ms) and below Shortlands (Sd) soils serves as recharged conduits in the crest and midslope positions (Figure 31). A wetland with Katspruit (Ka) soils dominates the valley bottom. Thus the water which recharges the fractured rock on the crest and midslope feeds the wetland through the fractured rock flow path.

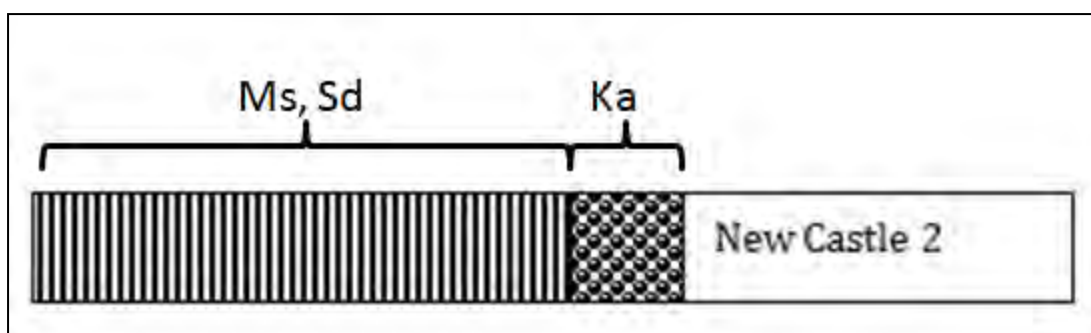


Figure 31 Soil distribution pattern of the New Castle 2 hillslope

Modal hillslope of class 4 – Taylors Halt hillslope

The Taylors Halt hillslope was surveyed as part of a WRC project focusing pollution from on-site dry sanitation systems (WRC project K5/2115). Freely drained Hutton and Clovelly soils cover the upper parts of this hillslope, i.e. TMU 1 and TMU 3 positions (Figure 32). At the break of slope (TMU4), unspecified material with signs of wetness below the yellow brown apedal B horizons was observed, i.e. Pinedene (Pn) soils. In the valley bottom, gleyzation dominates resulting in the formation of a G horizon in the Katspruit soils (Ka). Hydrologically water exiting the Hu and Cv soils appears not to recharge deeper groundwater aquifers, but rather drain downslope below the root and vadose zone, until it returns to the vadose in the foot and toeslope. This results in long periods of saturation and associated morphology (grey colours) in the lower lying areas.

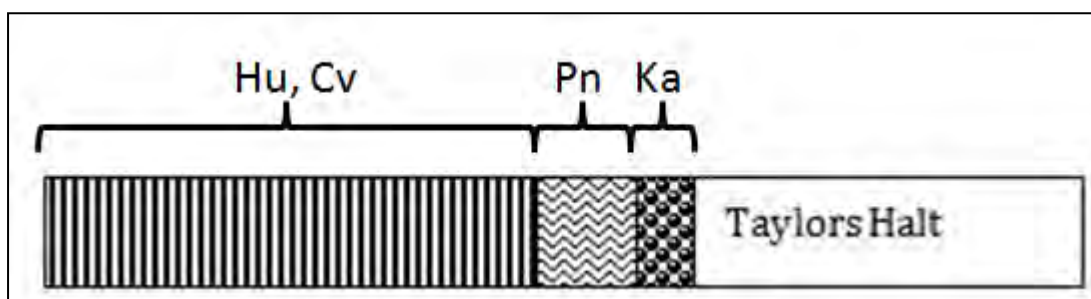


Figure 32 Soil distribution pattern of the Taylors Halt hillslope

Two Streams N hillslope

The hillslope being described here is the modal hillslope of the Two Streams catchment located at 30.76°S and 29.19°E in the KwaZulu-Natal midlands at Land Type Bb 105. The mean annual rainfall, aridity index and temperature are 945 mm, 1.1, and 17°C, respectively. The parent material of the soils is sandstone of the Natal Group, which is well weathered to depths around 4 to 5 meters. The soil pattern distribution is shown in Figure 33, and has an average slope of 16%. The soils are deep (mostly around 2 m) and rapidly permeable. On the major part of the hillslope (Kranskop and Inanda), the soils are deep, highly leached and acid as a result of strong weathering, and have high permeability. This leads to the conclusion that these upslope soils are true recharge soils and water is expected to leave the profile

rapidly in a vertical direction. The footslope soil (Magwa) was characterised by mottling in the subsoil, an indication of less permeability which will favour interflow.

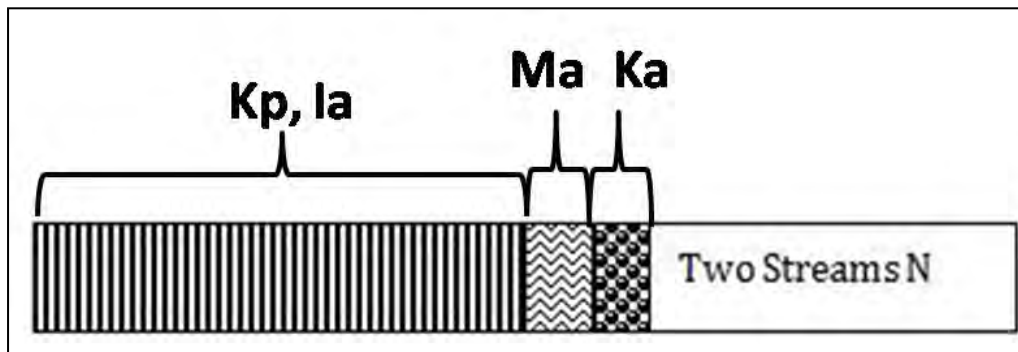


Figure 33 Soil distribution pattern of the Two Streams catchment N hillslope

Katspruit is the valley bottom soil. The bulk density in the A horizons is low owing to the relatively high content of organic carbon (> 1.8%). The porosities are also high as a result of high organic carbon content. Organic matter sediments carried in suspension from further upstream have been deposited in the streambed to create a thick orthic A horizon of the Katspruit in the valley bottom. Ks values are very high on the slopes. The Inanda soil has a thick, dark, loamy humic A over red apedal B horizon on soft sandstone saprolite. Kranskop also has a thick dark loamy humic A over a yellow brown apedal B over a red apedal B on soft sandstone saprolite. The yellow brown apedal B in the Kranskop soil has formed at the interface of humus-rich A and B horizon. This yellowing is the transformation of hematite to goethite in response to the influence of higher levels of organic matter promoting the dissolution of hematite through reduction/complexation, and then favouring the formation of goethite during subsequent precipitation by blocking crystallization from its amorphous hydroxide (ferrihydrite) precursor (Shwertmann and Taylor, 1989). The B horizons have lost bases through leaching, and show gains of clay and minerals through illuviation. Dominant drainage is vertical and soil water is expected to exit the bottom of the profile as mottling in the B2 and the saprolite was not evident. This morphology indicates a dominant vertical flowpath which is hypothesised as the major flowpath of soil water, recharging the deep weathered saprolite storage. Magwa soil form in the footslope has a thick clay loam humic A over yellow brown apedal B, over unspecified material with signs of wetness. The mottles in the unspecified material with signs of wetness horizon indicate periodic saturation as a result of a fluctuating water table. The water in the deep weathered saprolite is expected to flow laterally through the unspecified material with signs of wetness horizon of Magwa before exiting into the stream via the G horizon of the Katspruit. Katspruit has a thick humus rich orthic A horizon overlying a G horizon. Water moving laterally in the deep weathered saprolite storage cause prolonged conditions of saturation and the gleyed horizon of Katspruit soils in the valley bottom. Since they remain close to saturation for most of the year, the runoff response from this soil is very rapid after the start of a storm, and also ends relatively abruptly. This soil serves as a buffer by absorbing the lateral drainage water from the deep saprolite storage, and retaining it for a considerable time, while releasing it relatively slowly but continuously to the stream.

Hogsback hillslopes

Two opposing hillslopes in the Hogsback region were studied as part of an investigation of the impact of stream channel incision on hydromorphology of soils (Omar, van Tol & Le Roux, 2014). Hogsback 1 (Figure 34) is a short wetland with Hutton soils on the upper slopes and a relatively large wetland with Katspruit (Ka), Kroonstad (Kd) and Champagne (Ch) soils. The wetland is recharged through the Hu soils as well as from the opposing hillslope, i.e. Hogsback 2 (Figure 35). The latter is a much longer slope with its origin at Gaika's Kop, the highest peak in the Hogsback region.

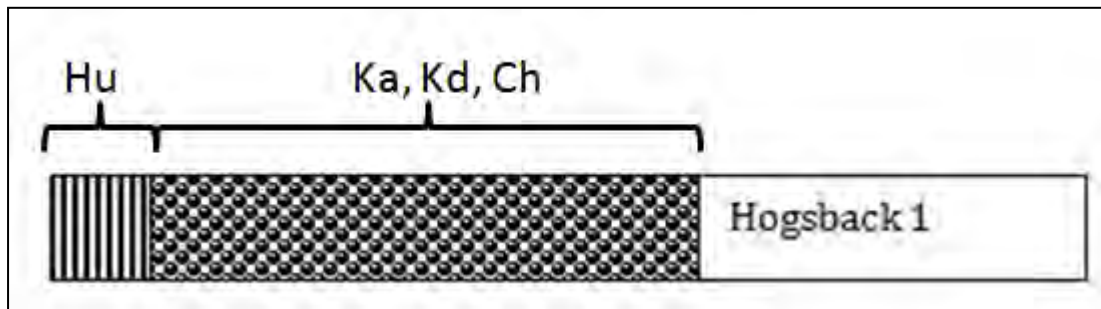


Figure 34 Soil distribution pattern of the Hogsback 1 hillslope

Glenrosa (Gs) soils dominate the steep upper slopes followed by freely drained Hu soils when the slope flattens out (Figure 35). The soils of the wetland are the same as that of Hogsback hillslope 1. Again the upper recharge soils of the upper slopes are responsible for a constant feed of water to the wetland. Parts of this wetland are complete saturated continuously, with constant water tables at the surface (Omar *et al.*, 2014).

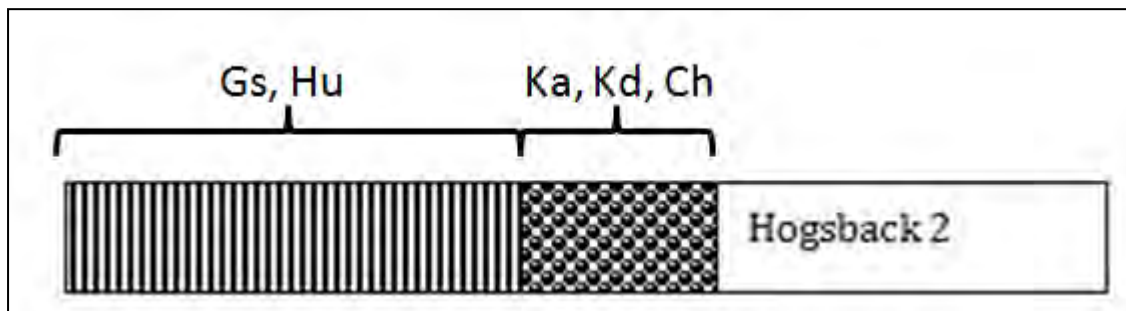


Figure 35 Soil distribution pattern of the Hogsback 2 hillslope

Riversdale hillslope

This hillslope is characterized by a Mispah (Ms) – Hutton (Hu)/Shortlands (Sd) – Alluvium/Peatland (Du) catena (Figure 36). The Mispah soils are regarded as recharge into the fractured rock, due to the folding of the Cape Sandstone Mountains. This water then returns to the surface at the bottom of the hillslope to feed the wetland. In the midslope, the freely drained Hu and Sd soils will promote recharge. The wetland is a saturated flow responsive area. Rain and overland flow that comes here will continue to flow on the

surface, whereas the water which entered the fractured rock from the recharge area will feed the wetland over a long period of time.

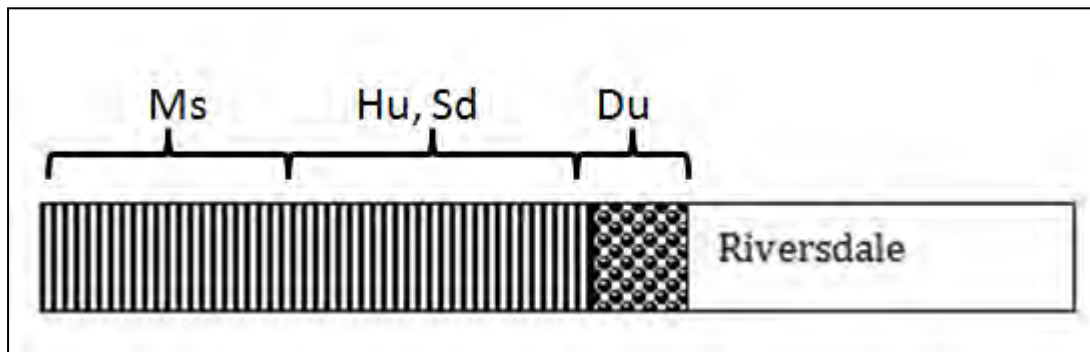


Figure 36 Soil distribution pattern of the Riverdale hillslope

Weatherley 1 hillslope

Shallow Glenrosa soils dominate the upper parts of the Weatherley 1 hillslopes (Figure 37). Below a prominent Molteno shelf a small area with freely drained Oakleaf soils were observed. The lower part of this hillslope is however dominated by wet Katspruit soils. The long duration of saturation in the Katspruit soils (van Huyssteen *et al.*, 2005) is maintained by a constant feed of water to from the recharge soils (Gs and Oa). It is expected that overland flow will be generated on the Katspruit soils due to saturation excess.

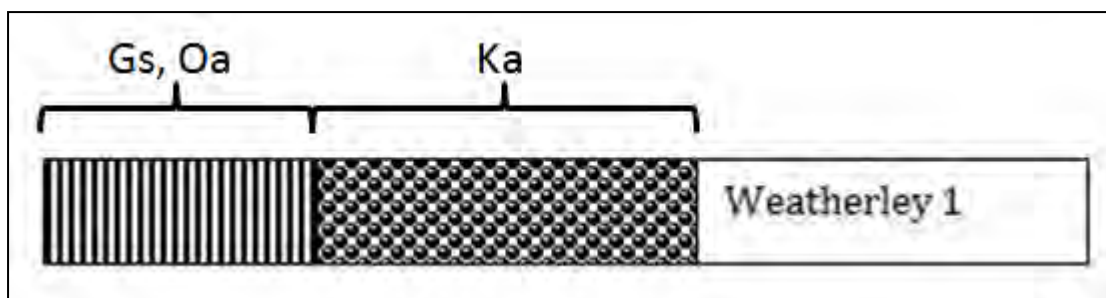


Figure 37 Soil distribution pattern of the Weatherley 1 hillslope

Weatherley 2 hillslope

The second hillslope in the Weatherley catchment is also dominated by Glenrosa and Oakleaf soils in the upper part of the slope (Figure 38). Below these recharge soils; soils with indications of saturation at the soil/bedrock interface were observed, i.e. Pinedene and Sepane soils. The valley bottom is dominated by wet Katspruit soils. The Katspruit soils are fed from both lateral contributions from the interflow soils (Pn and Se) as well as from the recharge soils through a rising water table.

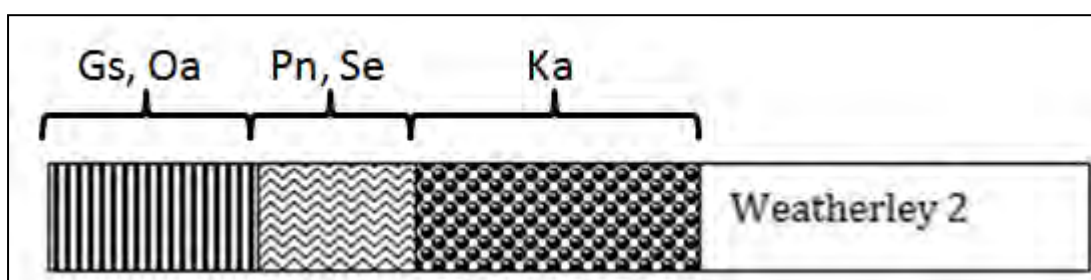


Figure 38 Soil distribution pattern of the Weatherley 2 hillslope.

Weatherley 3 hillslope

The third hillslope in the Weatherley catchment are situated in the north-western side of the catchment (Figure 39). A dolerite dyke resulted in the formation of freely drained Hutton soils, with limited presence of Clovelly soils in relatively wetter conditions. The conceptual hydrological response of this hillslope is very similar to that of Weatherley 2, with exception that recharge through the Hu and Cv soils will most likely occur at a faster rate.

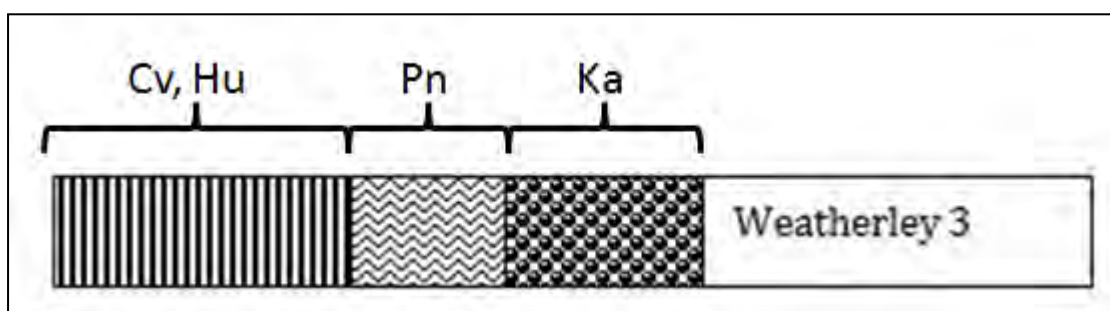


Figure 39 Soil distribution pattern of the Weatherley 3 hillslope

Bloemfontein 1 hillslope

The difference between Bloemfontein 1 and Bloemfontein 2&3 hillslopes is the relative areas covered by Glenrosa recharge soils (Figure 40). In the Bloemfontein 1 hillslope, the area covered by these recharge soils is approximately 50% of the upper parts of the slope. It is expected that these soils contribute to the wet Rensburg soils in the valley bottom through returnflow from the fractured rock.

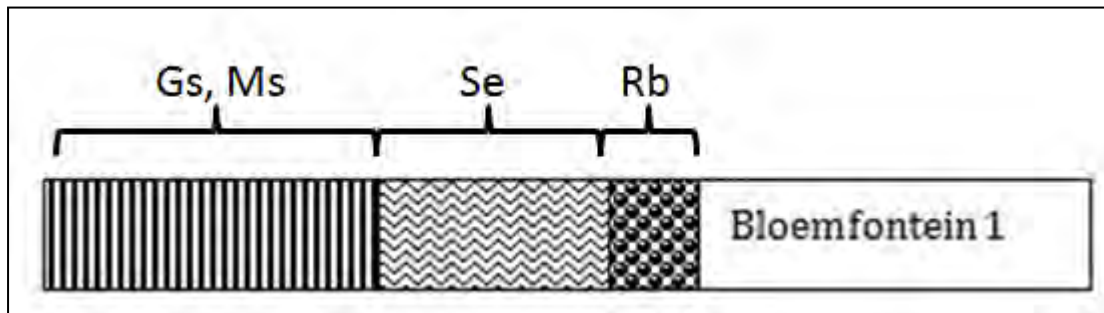


Figure 40 Soil distribution pattern of the Bloemfontein 1 hillslope

Class 5 – Recharge to midslope

The hydrology of this hillslope class is controlled by permeable fractured rock near the surface and impermeable layers deeper in the rock forcing fractured rock return flow in the midslope. It is dominated by recharge soils in the upper regions with indications of saturation on the soil/bedrock interface in lower midslope and footslope positions (Figure 41). As with hillslope class 4 the recharge soils typically feed lower lying soils via a bedrock flowpath. Lateral flow on the soil bedrock interface is the dominant contributor to streamflow. As interflow is generally considered to be fairly slow this hillslope class will have a delayed and prolonged hydrograph response (Figure 41-b). Wetlands typically form in the lower part of the interflow zone during high rainfall years. This phenomenon is periodic.

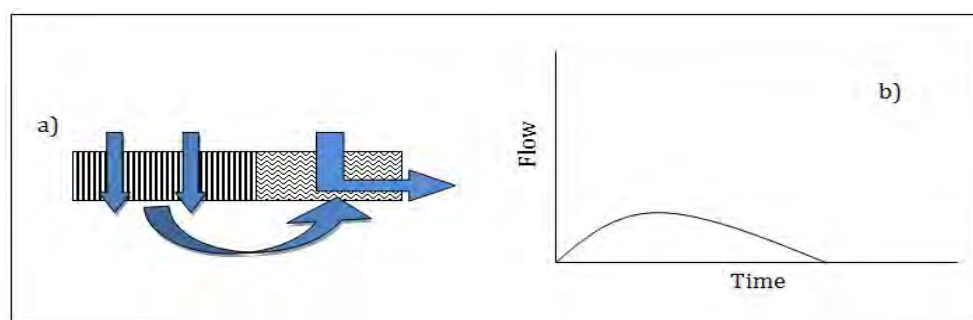


Figure 41 Perceptual flow model of hillslope class 5 (a) and anticipated hillslope hydrograph (b)

Modal profile of class 5 hillslopes- Skukuza hillslopes 3

In the Skukuza 3 hillslope Clovelly soils dominate the upper slopes, an increase in wetness as well as lime accumulations were observed in the form of signs of wetness in the Pinedene and the neocarbonate horizon in the Augrabies soil forms (Figure 42). Recharge occurs

through the Clovelly soils, this water exiting the solum are however expected to return to the solum via a return flowpath through the fractured rock aquifer.

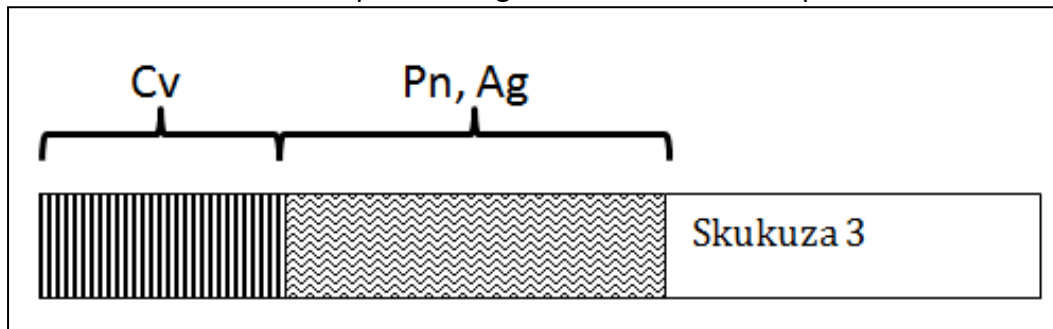


Figure 42 Soil distribution pattern of the Skukuza 3 hillslope

Morphological hillslopes of class 5

Skukuza 4 hillslope

The Skukuza 4 hillslope is dominated by shallow recharge soils (Figure 43). The Mispah soils in this hillslope overlie fractured rock and are therefore different than those of the Bedford catchment, i.e. shallow responsive. Lime accumulations in the lower parts of this slope indicate an increase in wetness, supposedly due to return flow as discussed above.

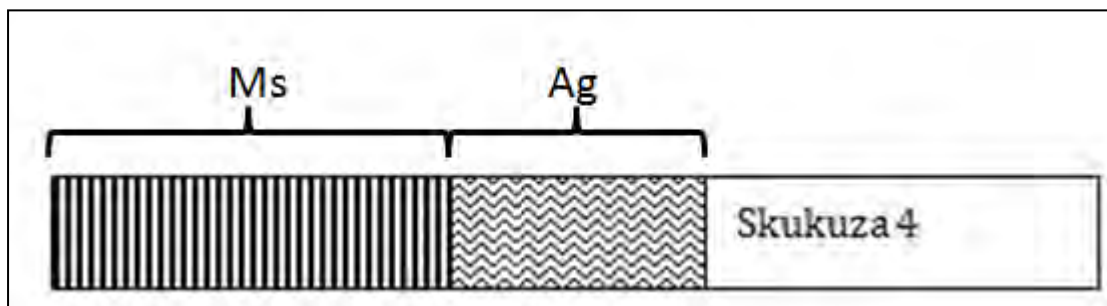


Figure 43 Soil distribution pattern of the Skukuza 4 hillslope

Fort Hare 2

A hillslope on the Fort Hare experimental farm, consist of Swartland soils in the upper regions with Sepane soils in the mid and footslope positions (Figure 44). The increase in wetness is indicative that the recharge areas (Sw) are feeding the sub-soil of the Sepane soils.

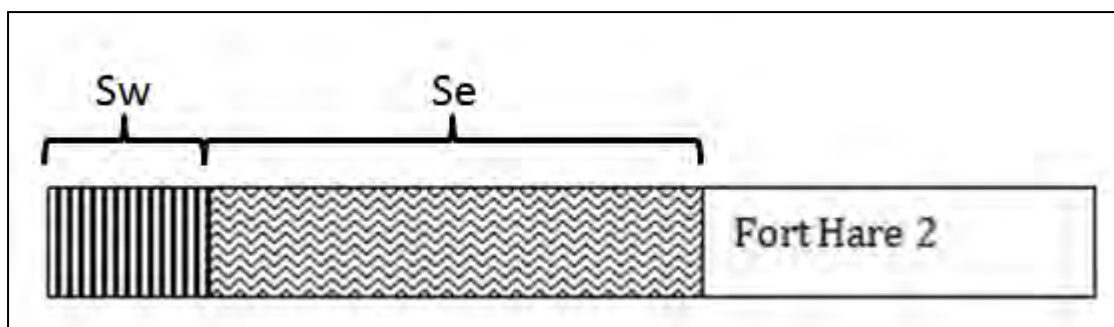


Figure 44 Soil distribution pattern of the Fort Hare 2 hillslope

Bloemfontein 5 hillslope

In the Bloemfontein 5 hillslope, freely drained Swartland and Oakleaf soils dominate the upper part of this slope (Figure 45). A definite increase in wetness is indicated by the signs of wetness at the soil/bedrock interface in the Sepane and Tukulu soil forms.

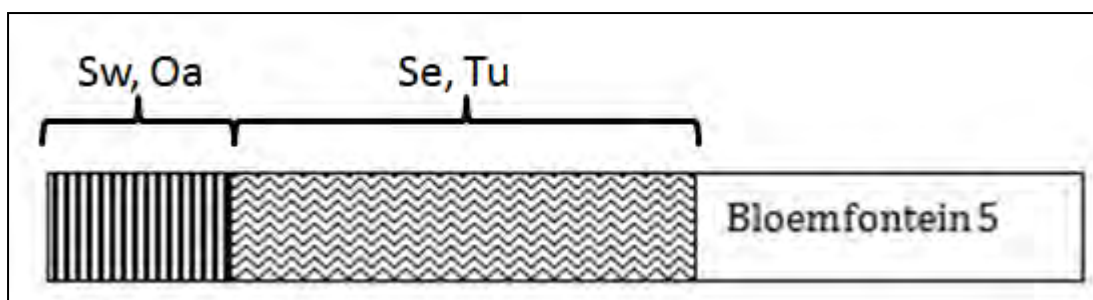


Figure 45 Soil distribution pattern of the Bloemfontein 5 hillslope

Thaba Nchu 1 hillslope

The Thaba Nchu 1 hillslope has very similar anticipated hydrological response as that of Bloemfontein 5 and Fort Hare 1 (Figure 46). Recharge soils dominate the upper slopes and soils with indications of saturation at the soil/bedrock interface are found in midslope and footslope positions (i.e. Sepane soils).

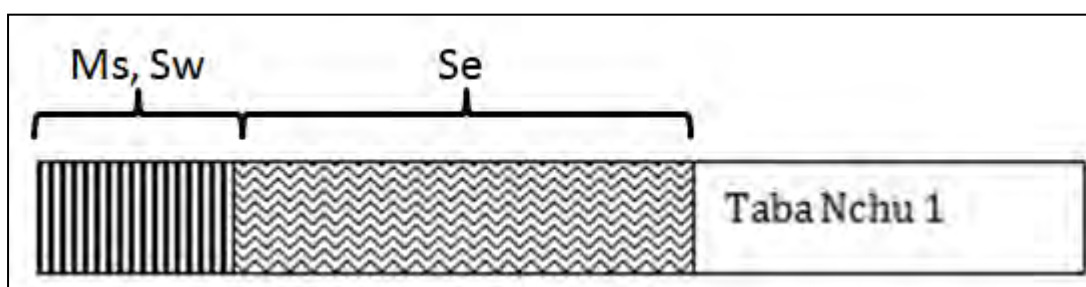


Figure 46 Soil distribution pattern of the Thaba Nchu 1 hillslope

Class 6 – Quick interflow

This hillslope class is marked by the presence of soils with indications of lateral flow at the A/B horizon interface (Figure 47-a1 & -a2). Lateral flow is typically generated by textural

discontinuities upslope and downslope due to saturation in the B horizon. This flow may result in a second peak in the hydrograph (Figure 47-b). Indications are that the hydrology of the duplex soils is controlled by the soil body according to the illuviation model. Rainwater infiltrates and drains vertically at a high rate in the A horizon, and is then retarded by the clay horizon, and saturation and interflow results. The rate of interflow on the A/B interface mainly depends on the slope (Van Tol *et al.*, 2013). Hillslope contribution of water (fractured rock soil return flow) plays a role in the subsoil of footslope soils creating two flowpaths in the soil body (Jennings *et al.*, 2008). Base flow largely depends on recharge of the fractured rock as leakage from the perched soil water table is probably negligible.

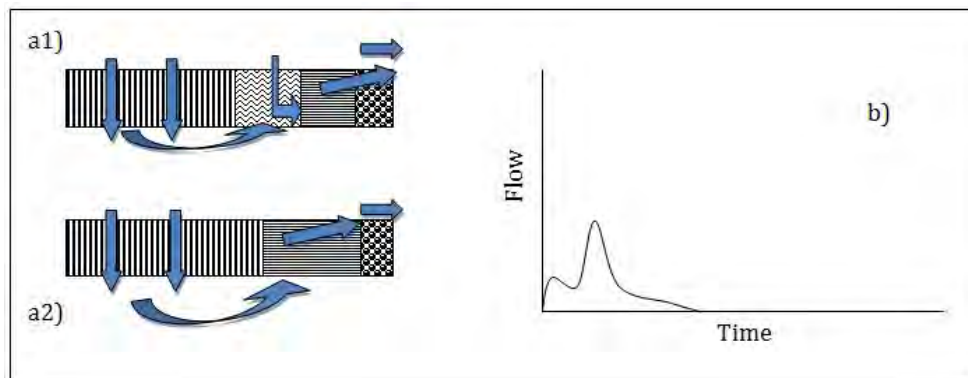


Figure 47 Perceptual flow models of hillslope class 6 (a1 & a2) and anticipated hillslope hydrograph (b)

Morphological hillslopes of class 6

Craigieburn 1&3 hillslopes

In the first and third hillslopes of the Craigieburn catchment Mispah and chemically weathered Glenrosa soils dominate the upper regions of the hillslope 1 and Mispah and Oakleaf soils dominate the upper parts of hillslope 3, i.e. recharge soils (Figures 48 & 49). At the break of slope (upper TMU 4 positions) the Glenrosa soils show indications of saturation at the soil bedrock interface, most likely due to returnflow from the fractured rock. Kroonstad soils, with indications of lateral flow at the A/B horizon interface (E horizon) releases water to the relatively wet Dundee and Katspruit soils, where saturation excess will be dominant.

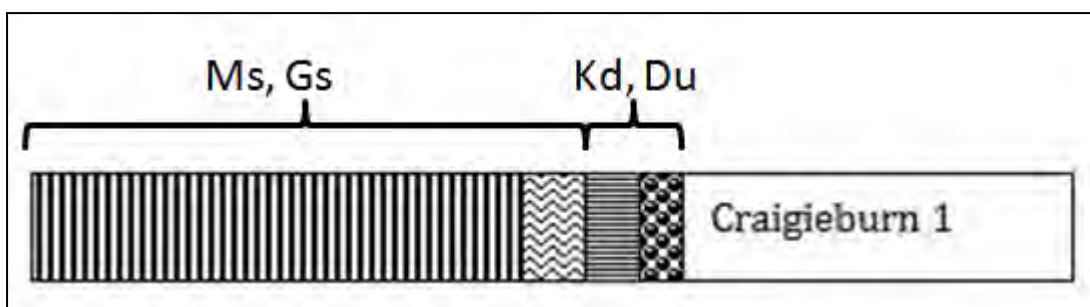


Figure 48 Soil distribution pattern of the Craigieburn hillslope

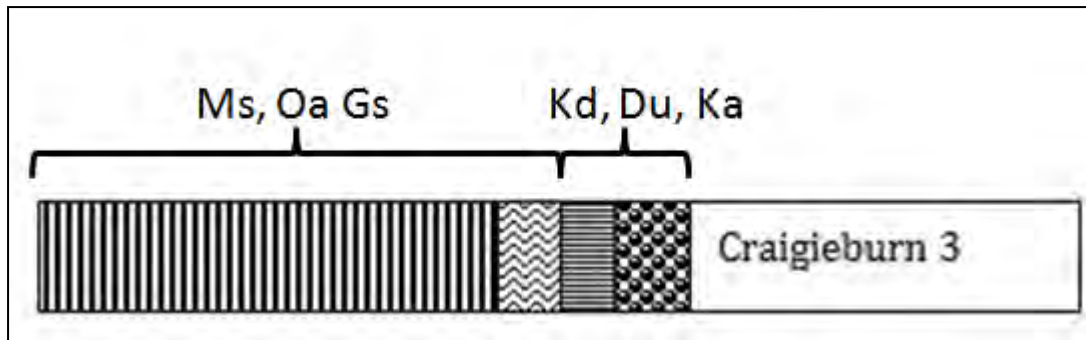


Figure 49 Soil distribution pattern of the Craigieburn 3 hillslope

Craigieburn 2 hillslope

Craigieburn 2 lies on the southern side of the catchment. In this hillslope deep freely drained Oakleaf soils were observed on TMU 4 positions of the hillslope (Figure 50). With exception of the absence of signs of wetness at the soil/bedrock interface of the TMU 4 position this hillslope will have the same conceptual hydrological response as that of Craigieburn 1 and 3.

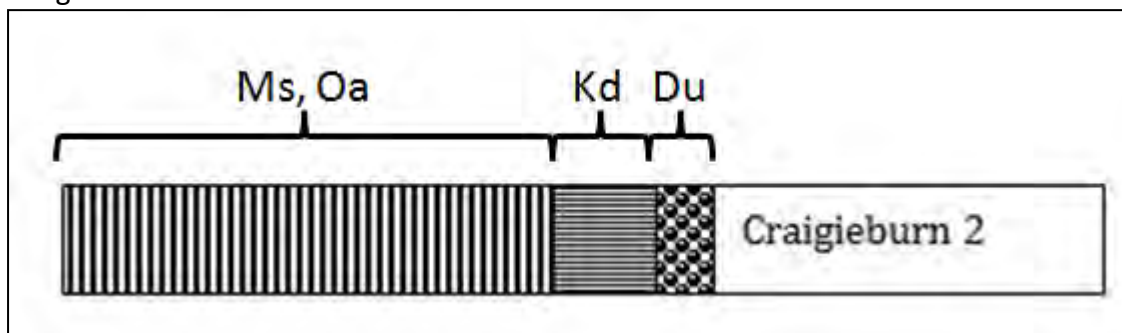


Figure 50 Soil distribution pattern of the Craigieburn 2 hillslope

Modal hillslope of class 6- Weatherley 4

The dominant soil forms in the Weatherley 4 hillslope are presented in Figure 51. A more detailed conceptual model is presented in (van Tol *et al.*, 2010) Flowpaths and storage mechanisms are indicated by numbered arrows in Figure 52 (for example 1a refers to arrow number 1a in Figure 52). A discussion of these processes follows in what can be considered as a hydropedological hypothesis of the hillslope hydrology of the Uc.

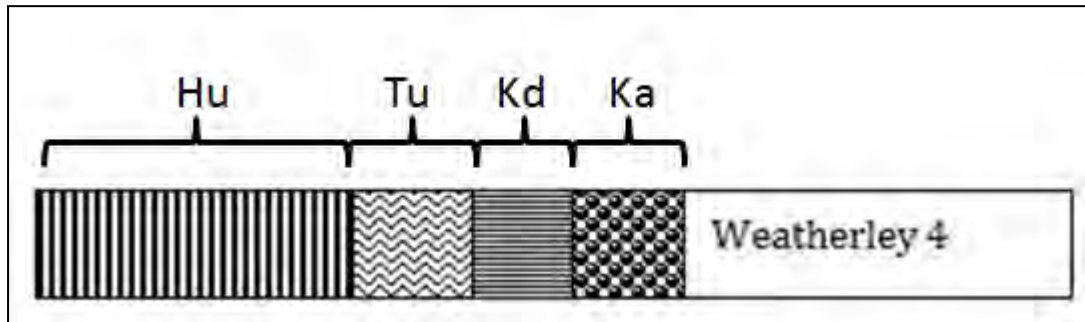


Figure 51 Soil distribution pattern of the Weatherley 4 hillslope

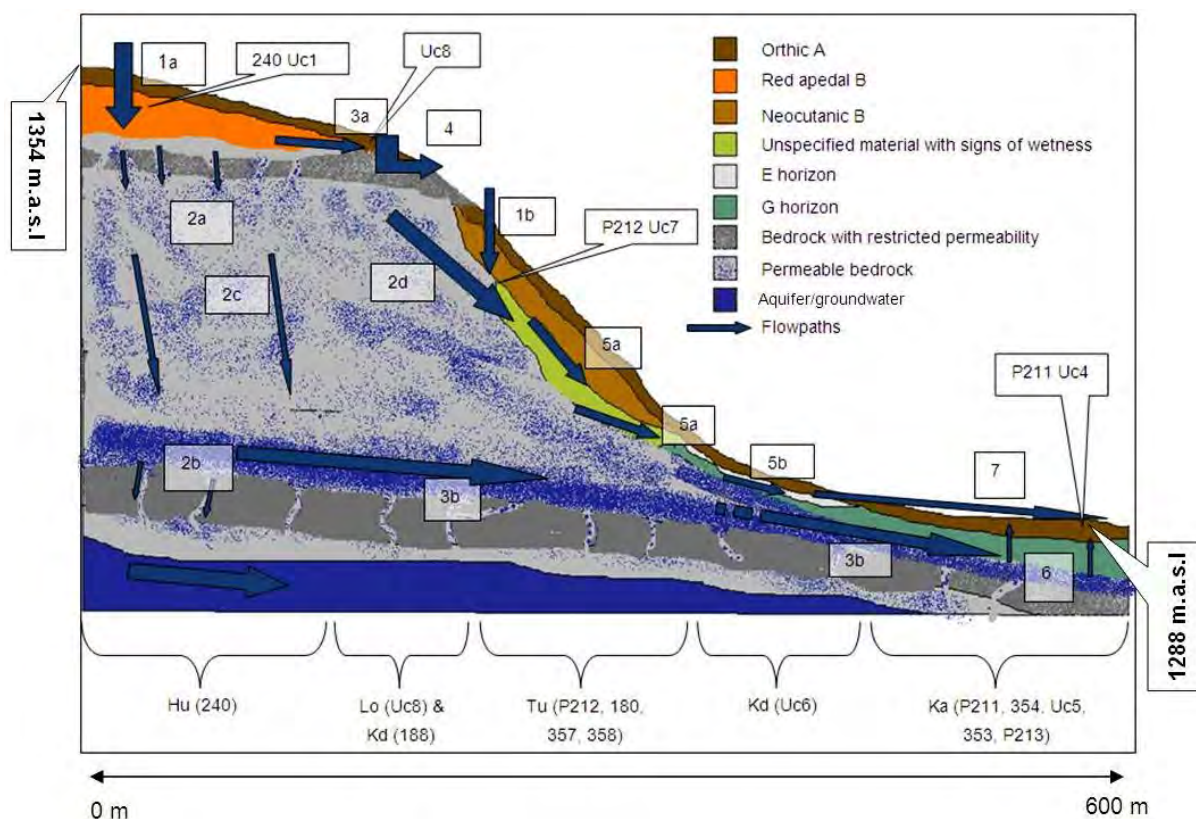


Figure 52 Conceptual hydrological behaviour of the selected hillslope based on soil interpretations. Various processes are indicated by the numbered arrows

When it rains infiltration dominates in the upper regions of this hillslope (1a). Gentle slopes as well as dense vegetation impede overland flow and facilitate infiltration. Absence of any signs of wetness in the Hu2100 soil of the upslope indicates that vertical drainage through the profile is dominant. The texture is non-luvic and the clay content is therefore relatively uniform with depth. No, or very little, lateral flow is expected to occur at the A/B horizon interface. These are considered to be true recharge soils since no signs of wetness were recorded in 240 up to a depth of 1500 mm, indicating that water does not perch in the pedon within this depth. Water draining through 240 therefore either infiltrates the

subsurface layers (2a) or flows at the soil/bedrock interface (3a), which was not reached with auger observations down to 2400 mm.

Any water which does infiltrate the fractured rock would then either flow vertically and recharge regional aquifers (2b) or, when it encounters a layer with restricted permeability (aquitar), it would flow laterally (3b) and recharge perennial hillslope groundwater downslope.

The presence of interflow soils (Lo1000 and Kd2000 soil forms) located where the rock bedding plain surfaces near Uc8 (Figure 52) is an indication that the bedding plane (Molteno shelf) has restricted permeability promoting considerable flow at the soil/bedrock interface (3a). The greater part of the water draining through the Hu soil of the upper slope is therefore expected to flow laterally at the soil/bedrock interface.

Return flow (ex-filtration) to the soil surface (4) is expected as water flowing at the soil/bedrock interface reaches the protruding Molteno shelf. The amount of water exceeds the storage capacity of the soil and returns to the surface contributing to overland flow. It is expected that the overland flow has a short duration as the water will re-infiltrate when it reaches the Tu soils below the rock outcrop (1b).

Subsurface lateral flow (5a) in the form of flow at the soil/bedrock interface is indicated by the *on* horizon present in the deep subsoil of the Tu soil of the midslope. This soil body is situated on the Molteno Formation. Groundwater responsible for the redoximorphic features of the *on* horizon is evidently supplied from the recharge soils (Hu2100) as return flow from the bedrock (2d). This return flowpath is expected to result in a fairly constant supply of water during the wet seasons to the *on* horizon, reflecting its association with perennial groundwater.

The *gs* horizon in the Kd1000 form (Uc6) of the lower slopes is an indication of the lateral flow of groundwater dominating at the A/B horizon interface (5b). Ka1000 and Kd1000 soils cover the entire TMU 4 & 5 positions of this hillslope. The gleyed conditions (P211, 354, Uc5, 353 and P213; Ka1000; Table 1 and Figure 1) are indications that these profiles are saturated for long periods. The *gh* horizons have a low hydraulic conductivity that impedes infiltration. Precipitation does not infiltrate into these soils due to the saturated state of the *gh* horizon. The water maintaining saturation in these lower areas must therefore have another origin. It is believed that there is another layer with restricted permeability present in the hillslope (Figure 52). This layer deflects water which has infiltrated through the recharge soils (Hu2100) of the upperslope towards the lower lying areas (3b), resulting in the presence of a perennial aquifer. These very wet Ka1000 soils respond rapidly to precipitation providing overland flow to the stream, the process described as saturation excess overland flow (7). Near surface macropore flow might also play a significant role in this area, as water from the *gh* horizon push up into the more porous *ot* horizon and flow laterally. The *ot* horizons of the Ka 1000 soils in the lower slope have Fe and Mn mottling, confirming periodic saturated conditions.

Since the *gh* horizons Ka and Kd soils in the lower footslope and toeslope positions (Figure 52) are saturated for long periods, the dominant flow direction within the pedon is upwards (6). Evapotranspiration will presumably extract more water from the soil than can infiltrate.

Weatherley 5 hillslope

The Weatherley 5 hillslope has a similar conceptual hydrological response model as the modal hillslope in this class, i.e. Weatherley 4 (Figure 53). The only difference is the absence of the prominent Molteno shelf in Weatherley 5.

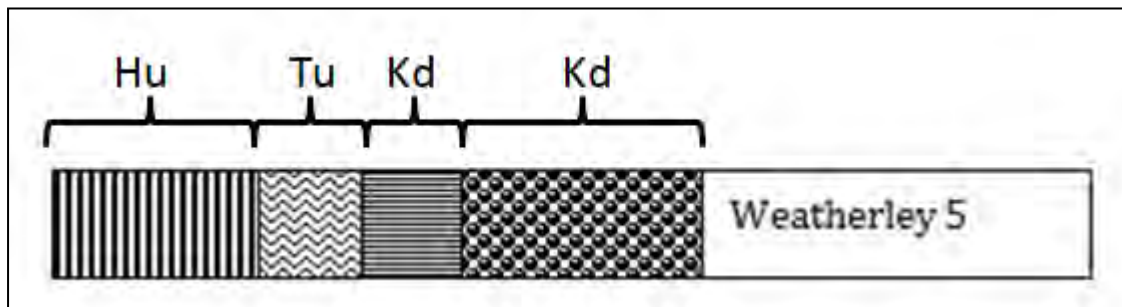


Figure 53 Soil distribution pattern of the Weatherley 5 hillslope

1.4 APPLICATIONS

1.4.1 Distributed modelling

When soil characteristics are lumped in catchment scale modelling, results may, at best, reflect an averaged catchment wide soil water balance. Even when mapped soil properties are disaggregated into hydrological response units (HRU) and used in distributed modelling, inaccuracies remain, often through neglect of topographical controls and storage mechanisms (Dunn & Lilly, 2001; Rodgers *et al.*, 2005). Indeed, Dunn & Lilly, 2001 advise that it is the way in which soils are distributed in a catchment, that is important in deriving catchment scale model parameters. It seems reasonable, therefore, that the information inherent in hydropedologically derived hillslope classes would yield valuable catchment modelling capabilities.

Differences in hydrological controls of hillslope classes are reflected in the large variability of soil and hillslope contributions to stream flow. Typically, throughflow from soils and hillslopes has travel times of months to a few years and groundwater sources may have travel times ranging between 5 and 20 years (Hoeg *et al.*, 2000; Uhlenbrook *et al.*, 2002; Asano, *et al.*, 2002; Lorentz *et al.*, 2003; Rodgers *et al.*, 2005; McGuire *et al.*, 2005; McGuire & McDonnell, 2006), although catchment response times may be considerably shorter. Nevertheless, distinctly different catchment responses have been directly related to different hillslope processes (Uhlenbrook *et al.*, 2008; Graeff *et al.*, 2009; Bachmair *et al.*, 2011).

In some hydrological models, the lack of knowledge of how these hillslope and groundwater mechanisms yield water has required the use of simplified transfer functions, which simulate the systematic release of a temporarily stored volume. The partitioning of precipitation into this runoff volume and the infiltrated water volume is driven by the antecedent soil moisture deficit, mostly through SCS techniques (ACRU, Schulze, 1995; ATHYS, Harader *et al.*, 2012) or a power function (HBV, Bergström, 1995; Uhlenbrook *et al.*, 2004). These concepts also require knowledge of rainfall intensity/soil infiltration rate

relationships. Release of the stored runoff volume, and the evapotranspiration and redistribution of the infiltrated volume, then proceed in the model. This separation of the less known surface and subsurface runoff yield processes and the better known and well-studied soil water-plant-atmosphere processes has already been defined as first order (hillslope controlled) and second order (near surface controlled) water (Uhlenbrook *et al.*, 2008). Hydropedological hillslopes could be effectively applied to yield the control parameters for both the detailed near surface processes as well as for the runoff response mechanisms.

Maximum use of the hydropedological sequence descriptions and characteristics, will be realized where model developments preserve the detail of soil water-plant-atmosphere interactions, and also capture the dominant storage and delivery mechanisms of the contributing hillslopes.

A modified version of the *ACRU* agrohydrological model (Schulze, 1995), *ACRU-Int*, is used to demonstrate the value of the hydropedological sequences derived for the catchment. Two modifications to the model are directed at providing a physical basis to the delivery of the stored runoff volume. In the first modification, an intermediate layer is introduced to the existing 2-layer structure in order to simulate the threshold responses of the interflow profile type. In this intermediate layer, the water is assumed to be distributed close to an equilibrium state so that a critical volume can be defined at which positive soil water pressures are induced at the soil/bedrock interface (Figure 54). This critical volume is easily derived from the water retention characteristics of the intermediate layer. Additional input to this layer triggers lateral discharge and percolation into the fractured bedrock.

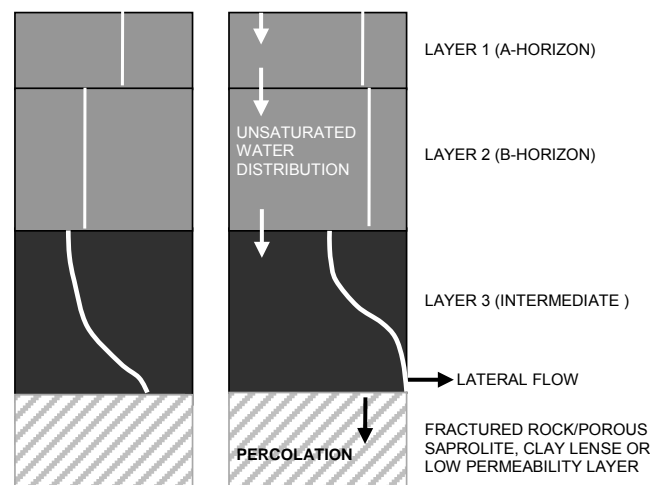


Figure 54 Schematic of the model profile with the intermediate layer base unsaturated (left) and saturated (right) when percolation and lateral flows are induced (after Lorentz *et al.*, 2007)

The second modification allows for the linking of sequential land segments to mimic the hydropedological hillslope (Figure 55). Inherent in the model structure is the ability to define *a-priori* links between any upslope layer with any downslope layer. The transfer functions linking these layers can take the form of linear, exponential or advection-dispersion equations.

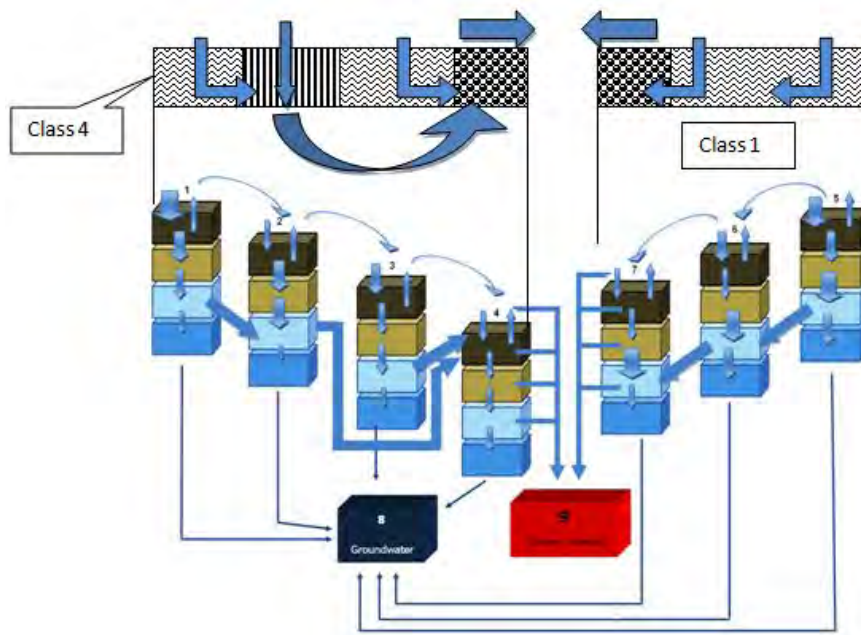


Figure 55 Flow routing based on hydropedological interpretation of soils (Van Tol *et al.*, 2011)

Application of the model in the Weatherley research catchment is based on the hydropedology of hillslope 1-4 (Lorentz *et al.*, 2008; Wenninger *et al.*, 2008). Simulated and observed streamflow values of the highly responsive catchment are in acceptable agreement ($R^2 = 0.74$) (Figure 56). However, the value of using the hydropedological descriptions is realised in the successfully simulated distribution of subsurface water.

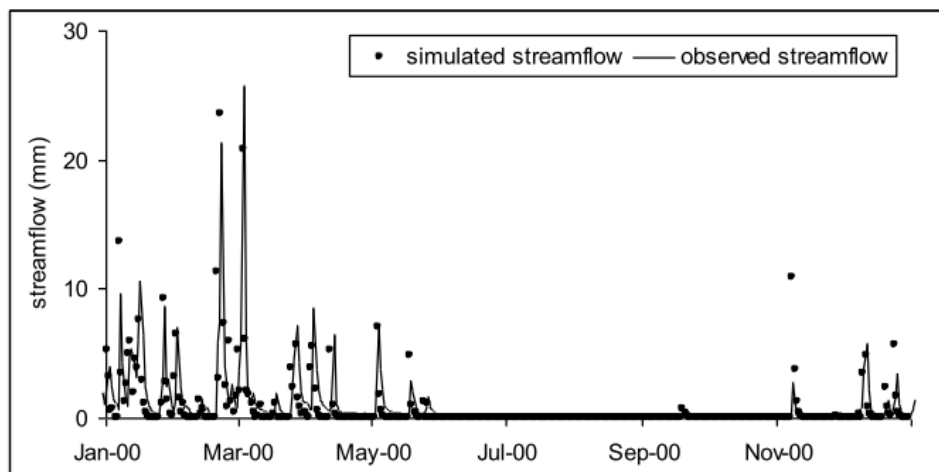


Figure 56 Simulated and observed streamflow in the Weatherley catchment during 2000, (le Roux *et al.*, 2011)

1.4.2 Land use change impact

Hydropedological sequence descriptions would contribute to effective land management. The hydropedological descriptions in the Weatherley catchment were used to demarcate

afforestation boundaries, not only in toe slope wetlands, but also at accumulation zones in the hillslopes. Also, the hydropedology of hillslopes in the Kruger National Park (Skukuza 1-4 and Letaba 1-4) is suitable for and will be applied to improved ecosystem management, where water distribution is critical to vegetation and animal interactions.

1.4.3 Water quality

Hydropedology mapping and associated water distribution dynamics could also be used directly to locate suitable development sites during land-use change (afforestation, housing development, on-site sanitation) and in assessing subsurface solute transport for limiting and remediation of pollution. The Taylor's Halt hillslope hydropedology has been used to determine the propensity for near surface, lateral flows to intercept pit latrine contents in a rural development. In addition, the Wartburg hydropedology descriptions have been used to estimate near surface discharge of nutrients in sugar cane fields.

1.5 CONCLUSION

The application of pedology in environmental science is overdue. Pedology can be researched to serve hydrology to the benefit of both (Bouma *et al.*, 2011). The most valuable information is data and symptoms of the soil-fractured rock interaction.

Firstly hydrological classification of hillslopes addresses the core of hydrological modelling, namely the conceptual hydrological response model, and therefore an important element of reliable hydrological predictions, especially in ungauged basins. The signatures of the long-term impact of water on soils, both directly by climate and modified by hydrology, is useful for defining flowpaths and residence times in soils and hillslopes. Secondly the hydrology of soil types and hillslopes has an extrapolation function. The need for improved extrapolation of data (soil physics and hydrometry) collected from micro scale (compared to the volume of soil bodies and hillslopes) to catchments, puts pedology in a position to contribute to quantification of the hydrological characteristics of soil horizons, profiles and soil bodies distributed in hillslopes. This is putting pressure on the functional classification of soils. Increased quantification of pedogenetic relationships (soil properties and processes of soil formation) and hydrological processes will enhance the classification of soils, hydrological soil types and hydrological hillslopes. Application of hillslope hydrological classification will improve the selection and enhance the extrapolation of hydrological and soil physical observations on soil survey transects. It will improve modelling and extrapolation efficiency needed badly in ungauged catchments. Thirdly the composition and distribution of hydrological hillslope classes can therefore serve as a basis for classification of catchments. This research niche encourages new approaches to the quantification of soil hydrology in the hillslope, including the assessment of lateral flow (Van Tol *et al.* 2013); subsoil/saprolite interface permeability (Theron *et al.*, 2010); flow and return flow of water through the subsoil/saprolite interface and residence time.

Hydropedology requires the quantification of soil hydrological characteristics. The hydropedological system can be compared to a biological system, with a set of hydrological properties (chromosomes) constructing soil horizons (DNA) of hydrological soil types

(individuals) arranged in hillslopes (communities) and combined in catchments (ethnic groups).

The application of hydrogeology in modelling, using sequential hillslope segments, has been demonstrated for a small research catchment (Weatherley). At larger scales the net response of the entire hillslope would be invaluable in catchment modelling, if typical hillslope responses can be defined and mapped. This will require establishing realistic response functions to each of the typical hillslope classes, which, if successful, would allow for streamflow simulation in ungauged catchments, while preserving contributing hillslope's storage and delivery dynamics.

This classification is a first approximation and will be refined as soils and hillslopes are studied. An improved understanding of the hydrology of soils (control mechanisms of flowpaths in soils, e.g. A/B interflow, subsoil interflow, water conducting macroporosity, near surface macropore interflow, biopores, structural pores, etc.) and hydrogeology (interactive soil/fractured rock/hillslope processes) and signatures of these processes will contribute to the goal. These relationships make the term "soilscape" an inviting substitute for the term "hillslope".

1.6 REFERENCES

- ASANO, Y., UCHIDA, T. & OHTE, N., 2002. Residence times and flow paths of water in steep unchannelled catchments, Tanakami, Japan. *J. Hydrol.*, 261, 173-192.
- BACHMAIR, S., WEILER, M. & TROCH, P.A. 2011. Intercomparing hillslope hydrological dynamics: Spatio-temporal variability and vegetation cover effects. *Water Resour. Res.*, 48, W05537, doi:10.1029/2011WR011196.
- BERGSTROM, S., 1995. The HBV model. In: V.P. Singh (Ed.), *Computer Models of Watershed Hydrology*. Water Resources Publications, Highlands Ranch, CO.
- BOORMAN, D.B., HOLLIS, J.M., & LILLY, A., 1995. Hydrology of soil types: a hydrologically based classification of the soils of the United Kingdom. IH Report No. 126. Institute of Hydrology, Oxfordshire, UK.
- BOUMA, J., DROOGERS, P., SONNEVELD, M.P.W., RITSEMA, C.J., HUNINK, J.E., IMMERZEEL, W.W. & KAUFMAN, S., 2011. Hydrogeological insights when considering catchment classification. *Hydrol. Earth Syst. Sci.*, 15, 1909-1919.
- DUNN, SM. & LILLY, A. 2001. Investigating the relationship between a soils classification and the spatial parameters of a conceptual catchment-scale hydrological model. *J. Hydrol.*, 252, 157-173.
- FLÜGEL, W. A., 1997. Combining GIS with regional hydrological modelling using hydrological response units (HRU's): An application from Germany. *Math. Comput. Simulat.* 43, 297-304.
- GRAEFF, T., ZEHE, E., REUSSER, D., LÜCK, E., SCHRÖDER, S., WENK, W., JOHN, H. & BRONSTERT, A., 2009. Process identification through rejection of model structures in a mid-mountainous rural catchment: observations of rainfall-runoff response, geophysical conditions and model inter-comparison. *Hydrol. Process.*, 23, 702-718.
- HARADER, EB., RICCI, S., PIACENTINI, A., BORRELL ESTUPINA, V., COUSTAU, M., BOUVIER, C. & THUAL, O., 2012. Hydrological data assimilation using the Kalman filter algorithm for the correction of rainfall forcing: case study of the Lez catchment in southern France. *SIMHYDRO 2012 – New Trends in Simulation, Hydroinformatics & 3D Modelling*. 12-14 September, Nice, France.

- HOEG, S. UHLENBROOK, S. & LEIBUNDGUT, CH. 2000. Hydrograph separation in a mountainous catchment combining hydrochemical and isotopic tracers. *Hydrol. Process.*, 14, 1199-1216.
- HUGHES, D.A. & SAMI, K., 1993. The Bedford Catchments. An introduction to their physical and hydrological characteristics. Report No.235/2/93. Water Research Commission, Pretoria.
- JENNINGS, K., LE ROUX P.A.L., VAN HUYSSTEEN C. W., HENSLEY M. and ZERE, TB, 2008. Redox behaviour in a soil of the Kroonstad form in the Weatherley catchment, Eastern Cape Province. *S. Afr. Plant Soil*, 25 (4) 204-213.
- JENNY, H., 1941. Factors of Soil Formation: A System of Quantitative Pedology. McGraw-Hill, New York, N.Y.
- KUENENE, B.T., VAN HUYSSTEEN, C.W., LE ROUX, P.A.L., HENSLEY, M. & EVERSON, C.S., 2011. Facilitating interpretation of Cathedral Peak VI catchment hydrograph using soil drainage curves. *South African Journal of Geology*, 114, 525-534.
- LE ROUX, P.A.L., VAN TOL, J.J., KUNENE, B.T., HENSLEY, M., LORENTZ, S.A., VAN HUYSSTEEN, C.W., HUGHES, D.A., EVISON, E., VAN RENSBURG, L.D. & KAPANGAZIWIRI, E., 2011. Hydropedological interpretation of the soils of selected catchments with the aim of improving efficiency of hydrological models: WRC Project K5/1748. Water Research Commission, Pretoria, South Africa.
- LILLY, A., BOORMAN, D.B. & HOLLIS, J.M., 1998. The development of a hydrological classification of UK soils and the inherent scale changes. *Nutr. Cycl. Agroecosys.*, 50, 299-302.
- LIN, H. S., KOGELMAN, W., WALKER, C. & BRUNS, M. A., 2006. Soil moisture patterns in a forested catchment: A hydropedological perspective. *Geoderma* 131, 345-368.
- LORENTZ S.A., KOLLONGEI J., SNYMAN N., BERRY S.R., JACKSON W., NGALEKA K., PRETORIUS J.J., CLARK D. & THORNTON-DIBB S., 2012. Modelling Nutrient and Sediment Dynamics at the Catchment Scale. WRC Report No. 1516/3/12, Water Research Commission, Pretoria.
- LORENTZ, S.A., BURSEY, K., IDOWU, O., PRETORIUS, J. & NGALEKA, K. 2008. Definition and upscaling of key hydrological processes for application in models. WRC Report 1320/1/08. Water Research Commission, Pretoria, South Africa.
- MARNEWECK, G.C., GRUNDLING P-L. & MULLER J.L. 2001. Defining and classification of peat wetland eco-regions in South Africa. Report to the ARC-ISCW for DLRM, Department of Agriculture, Pretoria, South Africa.
- MCDONNELL, J. J., SIVAPALAN, M., VACHÉ, k., DUNN, S., GRANT, G., HAGGERTY, R., HINZ, C., HOOPER, R., KIRCHNER, J., RODERICK, M. L., SELKER, J. & WEILER, M., 2007. Moving beyond heterogeneity and process complexity: A new vision for watershed hydrology. *Water Resour. Res.*, 43, 1-6.
- MCDONNELL, J.J. & WOODS, R., 2004. On the need for catchment classification. *J. Hydrol.*, 29, 2-3.
- MCGUIRE, K. & MCDONNELL, J.J. 2006. A review and evaluation of catchment transit time modeling. *J. Hydrol.*, 220, 543-563.
- MCGUIRE, K., MCDONNELL, J.J., WEILER, M., KENDALL, C., MCGLYNN, B.L., WELKER, J.M. & SIEBERT, J., 2005. The role of topography on catchment residence time. *Water Resour. Res.*, 41, W05002, doi:10.1029/2004WR003657.

- OMAR, M.Y., LE ROUX, P.A.L. & VAN TOL, J.J. Interactions between stream channel incision, soil water levels and soil morphology in a wetland in the Hogsback area, South Africa. **Accepted in:** *S. Afr. J. Plant & Soil*.
- PARK, S.J., MCSWEENEY, K. & LOWERY, B., 2001. Identification of the spatial distribution of soils using a process-based terrain characterization. *Geoderma*, 103, 249-272.
- RIDDELL E.S, LORENTZ S.A. & KOTZE D.C., 2010. A geophysical analysis of hydro-geomorphic controls within a headwater wetland in a granitic landscape, through ERI and IP. *Hydrol. Earth Syst. Sci.*, 14 1697- 1713.
- RODGERS, P., SOULSBY, C., WALDRON, S. & TETZLAFF, D., 2005. Using stable isotope tracers to identify hydrological flow paths, residence time and landscape controls in a mesoscale catchment. *Hydrol. Earth Syst. Sci. Discuss.*, 2, 1-35.
- SAWICZ, K., WAGENER, T., SIVAPALAN, M., TROCH, P.A. & CARRILLO, G., 2011. Catchment classification: empirical analysis of hydrologic similarity based on catchment function in the eastern USA. *Hydrol. Earth Syst. Sci.*, 15, 2895-2911.
- SCHULZE, R.E., 1995. Hydrology and Agrohydrology: A Text to Accompany the ACRU 3.00 Agrohydrology Modelling System. Water Research Commission, Pretoria, RSA, Report TT69/95.
- SIVAPALAN, M. 2003a. Prediction in ungauged basins: a grand challenge for theoretical hydrology. *Hydrol. Process.*, 17, 3163-3170.
- SIVAPALAN, M., 2003b. Process complexity at hillslope scale, process simplicity at the watershed scale: is there a connection? *Hydrol. Process.*, 17, 1037-1041.
- SIVAPALAN, M., TAKEUCHI, K., FRANKS, S.W., GUPTA, V.K., KARAMBIRI, H., LAKSHMI, V., LIANG, X., MCDONNELL, J.J., MENDIONDO, E. M., O'CONNELL, P.E., OKI, T., POMEROY, J.W., SCHERTZER, D., UHLENBROOK, S., & ZEHE, E., 2003. IAHS decade on prediction in ungauged basins (PUB), 2003-2012: Shaping an exciting future for the hydrological sciences. *Hydrol. Sci. J.*, 48, 857-880.
- SOULSBY, C., TETZLAFF, D., RODGERS, P., DUNN, S. & WALDRON, S., 2006. Runoff processes, stream water residence times and controlling landscape characteristics in a mesoscale catchment: An initial evaluation. *J. Hydrol.*, 325, 197-221.
- THERON, E., LE ROUX, P.A.L., HENSLEY, M. & VAN RENSBURG, L.D., 2010. Evaluation of the aardvark constant head soil permeameter to predict saturated hydraulic conductivity. Sustainable irrigation management, technologies and policies III. Eds. C.A. Brebbia, A.M. Marinov, H. Bjornlund. Wit Press. Ashurst Lodge, Southampton.
- TICEHURST, J.L., CRESSWELL, H.P., MCKENZIE, N.J. & CLOVER, M.R., 2007. Interpreting soil and topographic properties to conceptualise hillslope hydrology. *Geoderma*, 137, 279-292.
- TROMP-VAN MEERVELD, I. & WEILER, M., 2008. Hillslope dynamics modelled with increasing complexity. *J. Hydrol.*, 361, 24-40.
- UHLENBROOK, S. FREY, M. LEIBUNDGUT, C. & MALOSZEWSKI, P. 2002. Hydrograph separations in a mesoscale mountainous basin at event and seasonal timescales. *Wat. Resour. Res.*, 38(6), 1-14.
- UHLENBROOK, S., DIDSZUN, J. & WENNINGER, J. 2008. Source areas and mixing of runoff components at the hillslope scale—a multi-technical approach. *Hydrol. Sci. J.*, 53(4), 741-753.
- UHLENBROOK, S., ROSER, S. & TILCH, N. 2004. Hydrological process representation at the meso-scale: the potential of a distributed, conceptual catchment model. *J. Hydrol.*, 291, 278-296.

- VAN HUYSSTEEN, C.W., HENSLEY, M. & LE ROUX, P.A.L., 2005. The relationship between soil water regime and soil profile morphology in the Weatherly catchment, a forestation area in the North Eastern Cape. Report to the WRC on project Nr. K8/1 317, WRC, Pretoria.
- VAN TOL, J.J., LE ROUX, P.A.L., LORENTZ, S.A., HENSLEY, M., 2013. Hydropedological classification of South African hillslopes. *Vadoze Zone Journal*. doi:10.2136/vzj2013.01.0007.
- VAN TOL, J.J., HENSLEY, M. & LE ROUX, P.A.L., 2013. Pedological criteria for estimating the importance of subsurface lateral flow in E-horizons of South African soils. *Water SA*, 31, 47-56.
- VAN TOL, J.J., LE ROUX, P.A.L., HENSLEY, M. & LORENTZ, S.A., 2010a. Soil as indicator of hillslope hydrological behaviour in the Weatherley Catchment, Eastern Cape, South Africa. *Water SA*. 36, 513-520.
- VAN TOL, J.J., LE ROUX, P.A.L. & HENSLEY, M., 2010b. Soil properties as indicators of hillslope hydrology in the Bedford catchments. *S. Afr. J. Plant & Soil* 27, 242-251.
- VAN TOL, J.J., LE ROUX, P.A.L. & HENSLEY, M., 2011. Soil indicators of hillslope hydrology. In: B.O Gungor (eds), *Principles-Application and Assessments in Soil Science*. Intech, Turkey.
- WAGENER T., SIVAPALAN M., TROCH P. & WOODS R., 2007. Catchment classification and hydrologic similarity. *Geography Compass*, 1, 901-931.
- WAGENER, T., SIVAPALAN, M. & MCGLYNN, B.L., 2008. Catchment classification and services – Towards a new paradigm for catchment hydrology driven by societal needs, in: *Encyclopedia of Hydrological Sciences*, edited by Anderson, M.G. John Wiley & Sons Ltd.
- WEBSTER, R. 2000. Is soil variation random? *Geoderma*, 97, 149-163.
- WEILER, M. & MCDONNELL, J., 2004. Virtual experiments: a new approach for improving process conceptualization in hillslope hydrology. *J. Hydrol.*, 285, 3-18.
- WENNINGER, J., UHLENBROOK, S., LORENTZ, S.A. & LEIBUNDGUT, C. 2008. Identification of runoff generation processes using combined hydrometric, tracer and geophysical methods in a headwater catchment in South Africa. *Hydrol. Sci. J.*, 53(1), 65-80.

Chapter 2 **HYDROPEDOLOGICAL RESPONSES OF SELECTED HILLSLOPES**

2.1 HILLSLOPE DESCRIPTIONS

2.1.1 Monitoring setup

Hillslope descriptions and characterizations were developed for four separate hillslope transects within the Weatherley research catchment. The hillslopes descriptions were derived using isotope data from rainfall, soil water, deep ground water, surface seepage and streamflow. Rainfall was measured and sampled at nest LC 1. Soil water was collected from a network of piezometers along the hillslope transects drilled to bedrock. Five deep boreholes were dipped and sampled. Streamflow is gauged at two points, an upper weir draining hillslopes 3 and 4, and a lower weir draining the upper weir as well as hillslopes 1 and 2. The lower weir was gauged and sampled with a combination of a Campbell 2000 logger and an ISCO automated sampler.

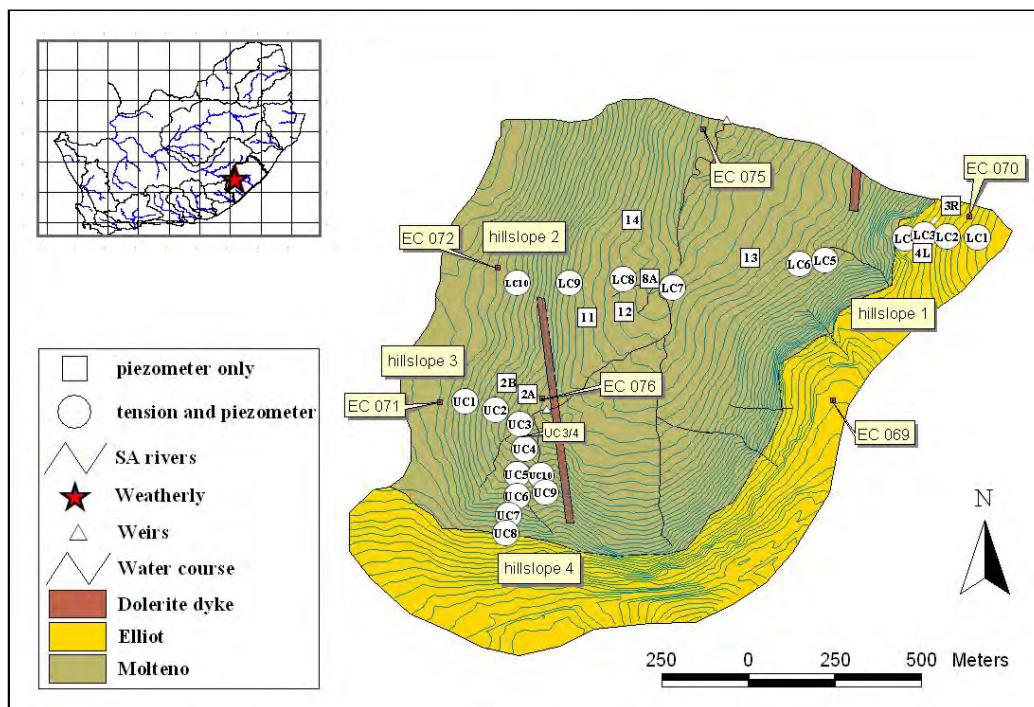


Figure 57 Weatherly situation, Geology and monitored hillslopes 1-4

To understand the role of each of these hillslopes in the generation of streamflow, a detailed isotope based description identifying dominant hillslope processes will be carried out. The Hydropedological soil classification of the Weatherley catchment is used as a basis to confirm the presence of hydrological processes using temporal isotopic trends. These hillslope descriptions will define a conceptual description to aid that derived through the observation of dominant pedological markers. For the purposes of the hillslope descriptions the detailed sampling period from 03/03/2010 to 13/03/2010, including a 30 mm event late

on 12/03/2010, will be used to distinguish different dominant pre and post event processes across 4 different intensively monitored hillslopes as illustrated in Figure 57.

2.1.2 Hillslope 1 (LC 01 – LC 07)

Hillslope 1 extends from nests LC 01 to LC 07 and is dominated by recharge soils at the crest, interflow soils on the midslope and an extensive area of riparian soils at the foot of the slope adjacent to the stream. It is expected that the riparian soils adjacent to the stream will ultimately control the drainage of this hillslope to the stream.

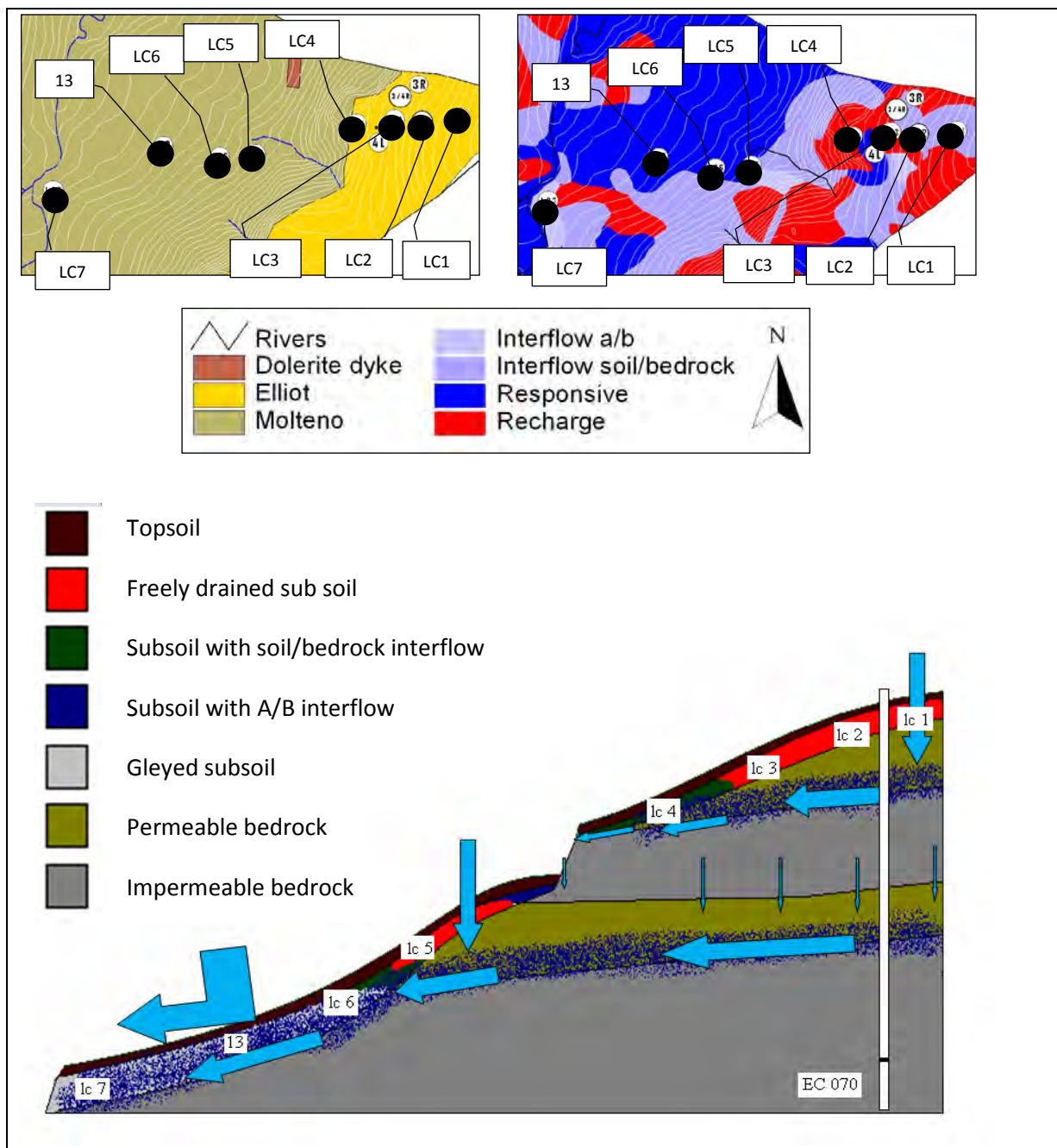


Figure 58 Weatherley, Hillslope 1, Illustrative description and conceptual flow paths

Pre-event

The pre event observation period shows upslope water tables at LC 4 draining slowly. Further down the slope at the interface between interflow and responsive soils the free water level in piezometer LC 6 remains constant during the drainage period 2012/03/03 to 2010/03/11. The most marked drainage during the recession period occurs in piezometers LC 7 and 13 situated adjacent to the stream in the responsive soils. This indicates that the responsive soils adjacent to the stream are draining to the stream. Yet the fact that the water table remains stable at LC 6 indicates that upslope soil water is draining to interflow responsive soils interface. The extent of the drainage of LC 6 in comparison to LC 7 is shown in Figure 60, where the water table is shown to be highly variable at LC 7 in respect of LC 6. Isotope values suggest this is the case. While the other piezometers show slowly depleting isotope values, indicating the presence of older hillslope water, isotope values at LC 6 remain stable varying from -3.77 to -3.16, Figure 61 and Table 3.

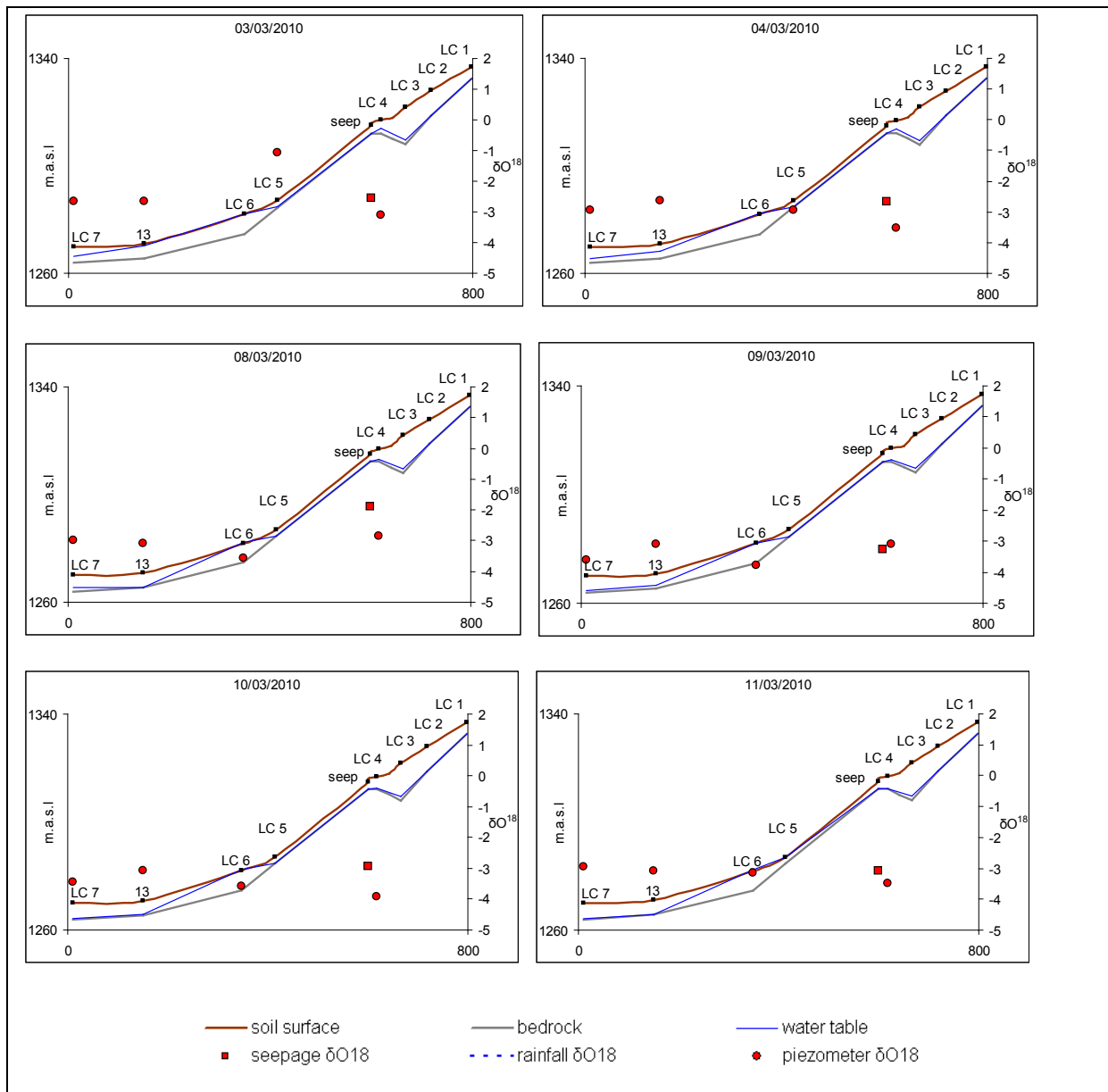


Figure 59 Weatherley, Hillslope 1, pre-event water table drainage and δO^{18}

Table 3 Weatherley, Hillslope 1, δO^{18} isotope data 3-13 March 2010

| Hillslope 1 (LC 01-LC 07) | | | | | | | |
|---------------------------|--------|--------|--------|--------|--------|--------|--------|
| location | 03-Mar | 04-Mar | 08-Mar | 09-Mar | 10-Mar | 11-Mar | 13-Mar |
| lc07 | -2.64 | -2.95 | -3.00 | -3.59 | -3.43 | -2.94 | -2.32 |
| Piezo 13 | -2.65 | -2.62 | -3.09 | -3.09 | -3.07 | -3.07 | -2.19 |
| lc06 | | | -3.58 | -3.77 | -3.60 | -3.16 | -2.502 |
| lc05 | -1.06 | -2.94 | | | | | -2.014 |
| rock o/c | -2.56 | -2.68 | -1.89 | -3.26 | -2.93 | -3.07 | -2.431 |
| lc04 | -3.12 | -3.53 | -2.83 | -3.10 | -3.92 | -3.47 | -3.27 |
| lc03 | | | | | | | |
| lc02 | | | | | | | |
| lc01 | | | | | | | |
| std dev | 0.78 | 0.36 | 0.55 | 0.23 | 0.44 | 0.23 | 0.44 |

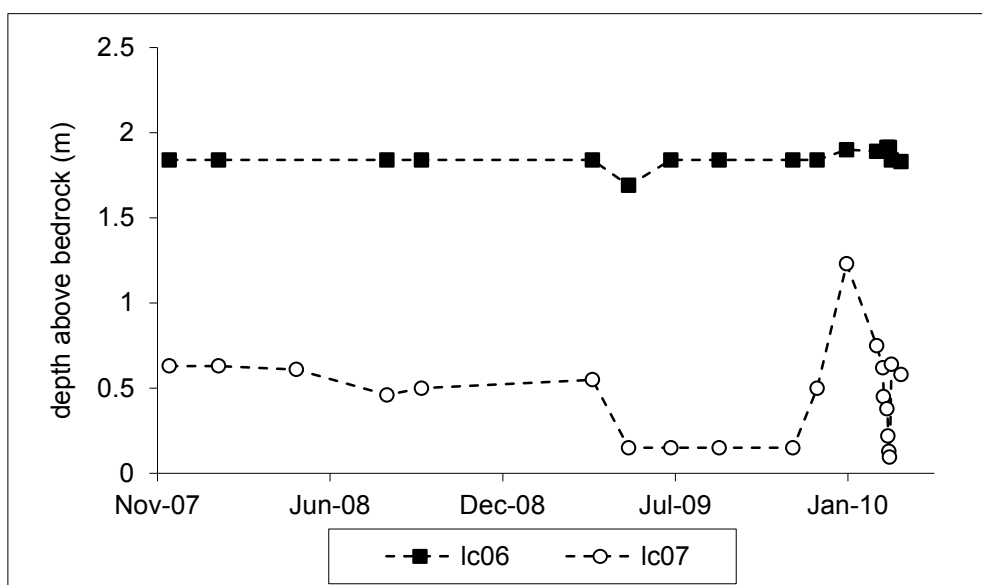


Figure 60 Weatherley, Hillslope 1, LC 06 and LC 07 long term piezometer depth observations

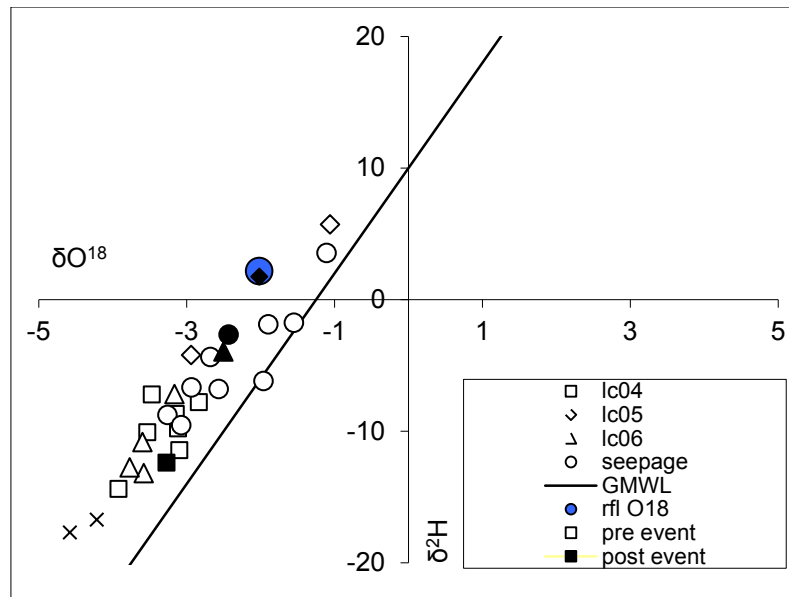


Figure 61 Weatherley, Hillslope 1, March 2010 δO^{18} and $\delta^2 H$ isotopes.

Post-event

Post event responses indicate that the responsive soils are rapidly recharged by a combination of direct precipitation and surface runoff from the interflow soils. The post event isotope values at piezometer 13 and LC 7 drop from -2.94 to -2.19 and -3.07 to -2.32 respectively, and the lumped rainfall value is -2.02, showing the combination of both pre event and event water. Upslope water tables at LC 4 show little response to the rainfall event, isotope values do not change significantly after the event indicating the dominance of older hillslope soil water at these positions.

Hillslope 1 has two distinct zone if hydrological interaction. Upslope responses are dominated by slow vertical infiltration which perpetuates well mixed attenuated time series of isotope data. These soils are expected to drain to the interflow responsive soils interface and sustain water table levels while responsive soils closer to the stream are responsible for runoff generation.

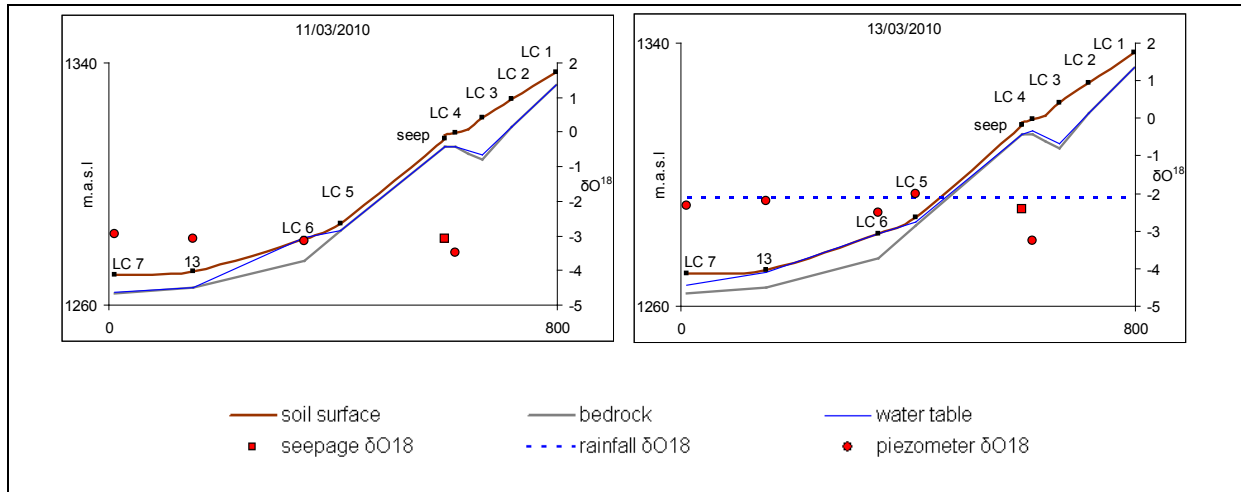


Figure 62 Weatherley, Hillslope 1, pre event (left) and post event (right) water table drainage and δO^{18} isotopes

2.1.3 Hillslope 2 (LC 08-LC10)

Hillslope 2 extends from nest LC 8 to nest LC 10, which is along the same transect, across the river from hillslope 1. Hydopedological soil type distributions across hillslope two are erratic, with no defined soil types at certain hillslope positions. Upslope areas are dominated by a combination of recharge and interflow soils. The midslope and downslope areas of hillslope 2 are relatively indistinguishable compared to hillslope 1, where a mixture of interflow and responsive soils is found. The erratic nature of the soil distributions across this hillslope is expected to be as a result of the intrusive dolerite dyke which intersects the hillslope between nests LC 9 and LC 10.

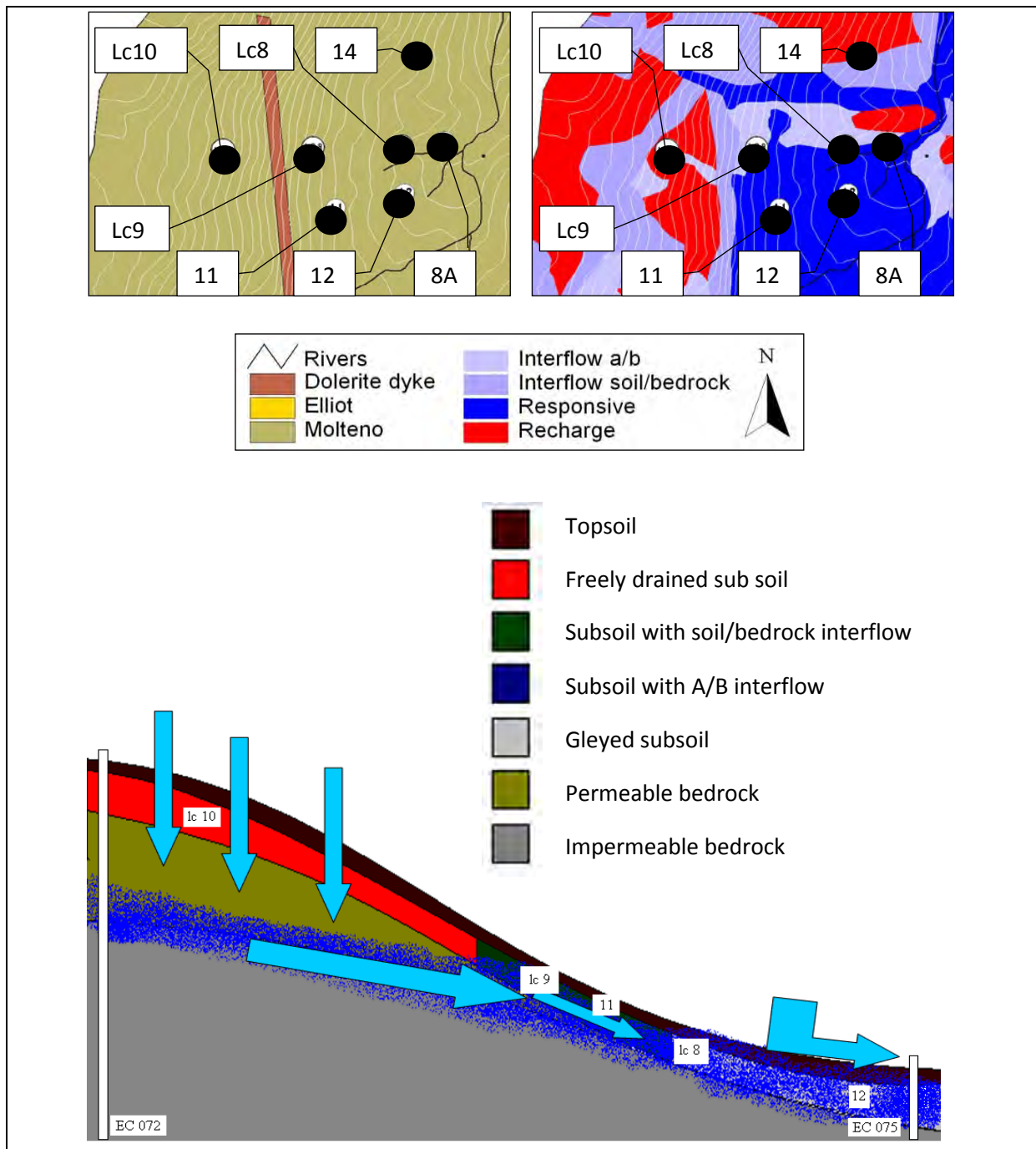


Figure 63 Weatherley, Hillslope 2, Illustrative description and conceptual flow paths

Pre-event

Upslope mid slope soil water tables remain low for the duration of the recession period 2010/03/03 to 2010/03/11. This is replicated by the isotope time series values, which vary from -3.807 to -2.254 during the recession period. The most considerable drop in water table is observed in the responder soils adjacent to the stream, where the water table drops by almost 50 percent in piezometers at nests 12, 8A and LC 8, Figure 65. As is the case with hillslope 1, these responsive soils are assumed to drain to the stream. The isotope values of the responsive soils area similar to those of the upslope piezometers, Table 4,

Figure 66. This indicates a continuous subsurface connection from the upslope to the responsive soils. The attenuated nature of the time series δO^{18} values is evidence of high levels of mixing, and thus a prevalence of old hillslope soil water feeding the responsive soils.

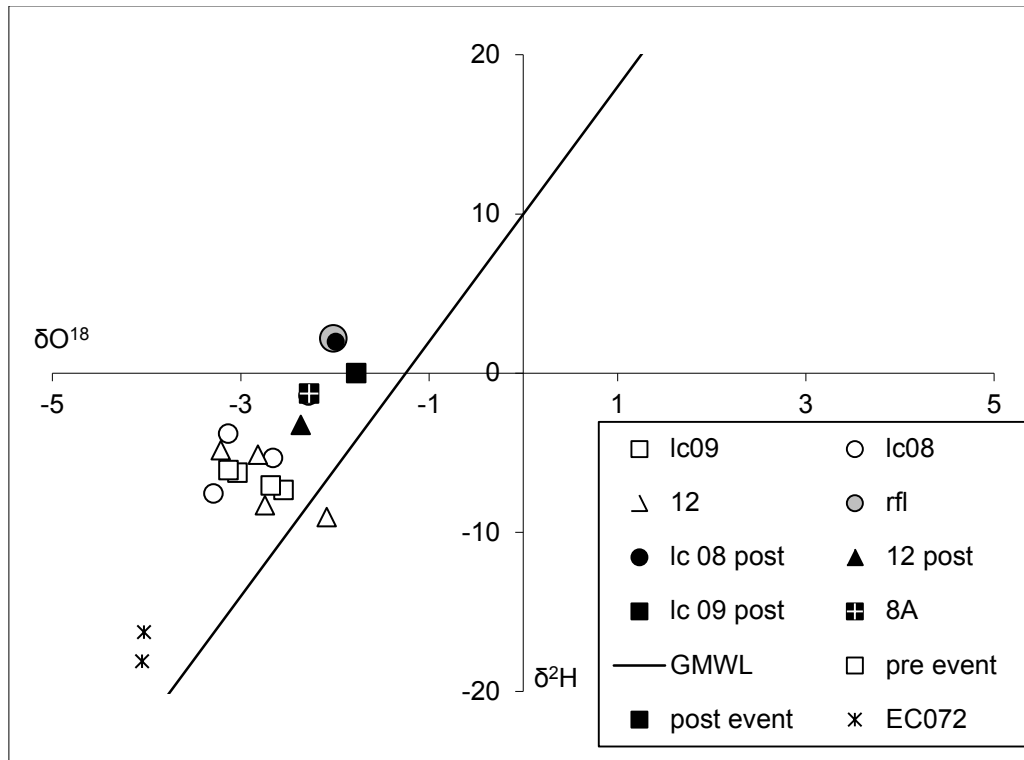


Figure 64 Weatherley, Hillslope 2, March 2010 δO^{18} and $\delta^2\text{H}$ isotopes

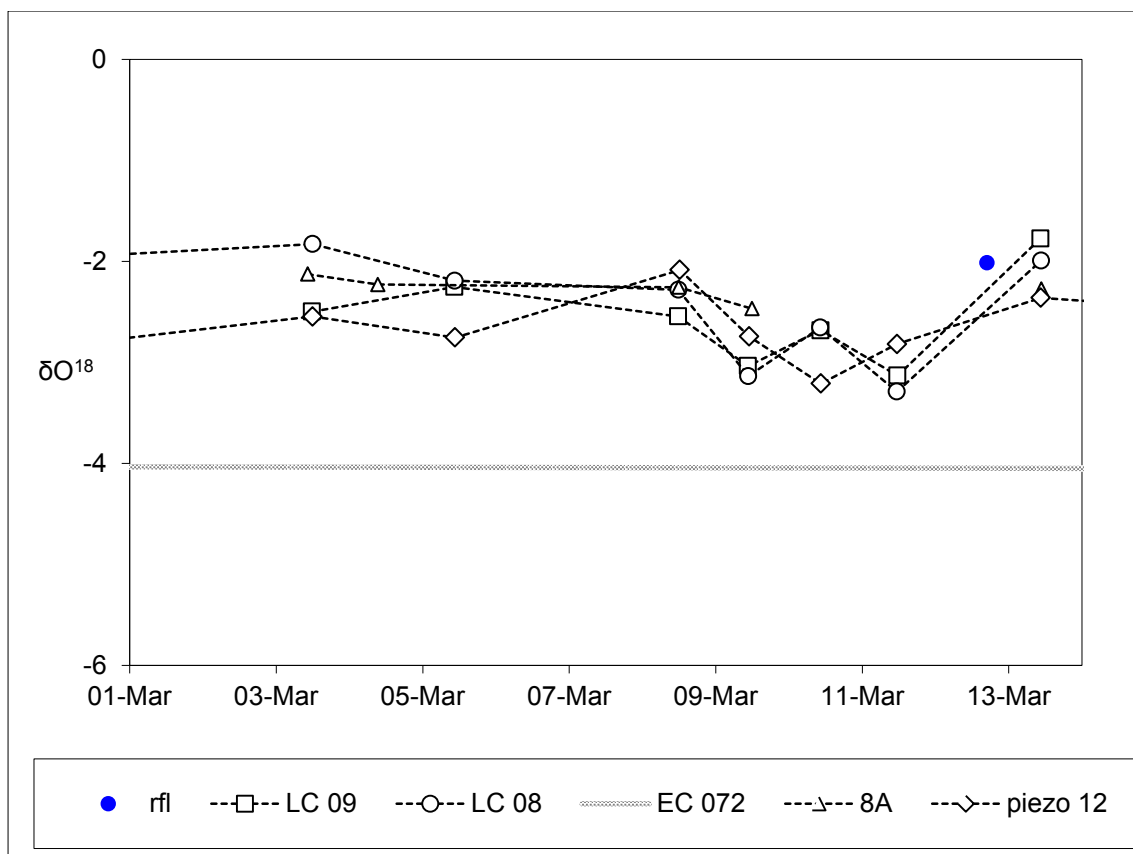


Figure 65 Weatherley, Hillslope 2, March 2010 δO^{18} piezometer isotope values

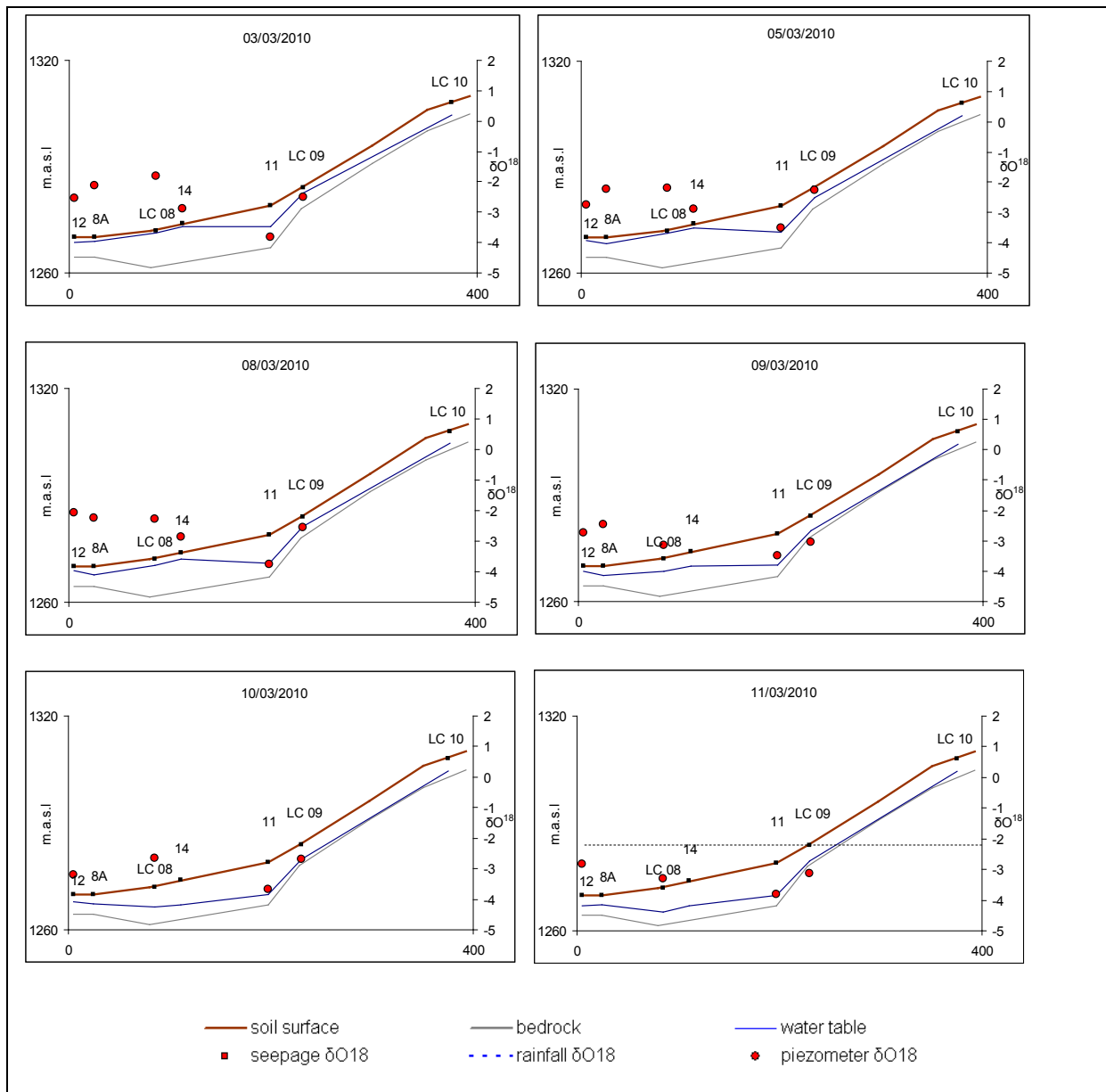


Figure 66 Weatherley, Hillslope 2, pre-event water table drainage and δO^{18}

Table 4 Weatherley, Hillslope 2, δO^{18} isotope data 3-13 March 2010

| | Hillslope 2 (LC 11 – Piezometer 8A) | | | | | | |
|----------|-------------------------------------|--------|--------|--------|--------|--------|--------|
| location | 03-Mar | 05-Mar | 08-Mar | 09-Mar | 10-Mar | 11-Mar | 13-Mar |
| Piezo 12 | -2.546 | -2.754 | -2.085 | -2.743 | -3.21 | -2.818 | -2.361 |
| Piezo 8A | -2.126 | -2.229 | -2.256 | -2.469 | | | -2.274 |
| lc08 | -1.828 | -2.191 | -2.281 | -3.135 | -2.656 | -3.29 | -1.992 |
| Piezo 14 | -2.895 | -2.874 | -2.853 | | | | -3.086 |
| Piezo 11 | -3.807 | -3.509 | -3.748 | -3.489 | -3.672 | -3.797 | -1.992 |
| lc09 | -2.497 | -2.254 | -2.544 | -3.035 | -2.683 | -3.131 | -1.773 |
| lc10 | | | | | | | |
| std dev | 0.69 | 0.52 | 0.61 | 0.39 | 0.48 | 0.41 | 0.46 |

6.2.2 Post-event

Post event responses show that responsive soils are rapidly recharged by event waters. A comparison of water table levels pre and post event, Figure 67, shows the water table rising to within a few centimetres of the soil surface. The isotopic composition of the piezometers samples indicates that this water is event derived, as δO^{18} values rise from a range of -3.797 to -2.818 to a range of -2.361 to -1.773, after a lumped rainfall input δO^{18} of -2.02. The constant lack of an observed water table at nest LC 10 both pre and post event indicates the increased hydraulic conductivity of upslope recharge soils.

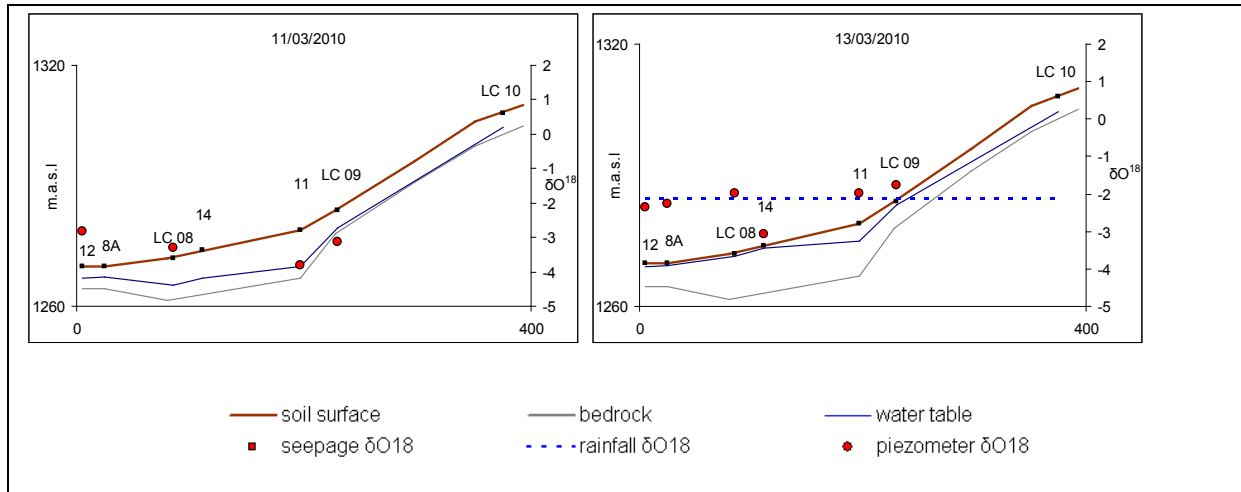


Figure 67 Weatherley, Hillslope 2, post-event (left) and post event (right) water table drainage and δO^{18}

Pre and post event responses show that no water table develops at the upslope positions; hence, vertical recharge of event waters dominates. The attenuated nature of the pre event δO^{18} values at the responsive soil piezometer sites suggests deep hillslopes water sustaining the water table in the responsive soils during the pre-event recession period.

2.1.4 Hillslope 3 (UC 01-UC 03)

Hillslope 3 lies in the north eastern corner of the Weatherley catchment, underlain by predominantly interflow soils, Figure 69, the hillslope transect extends from nest 2A adjacent to the stream, through nest UC 01 near the crest. The dominance of interflow soils along the transect indicates a sudden change in vertical permeability of the soils. This is further indicated by the presence of sustained water tables in these hillslope soils showed in Figure 68.

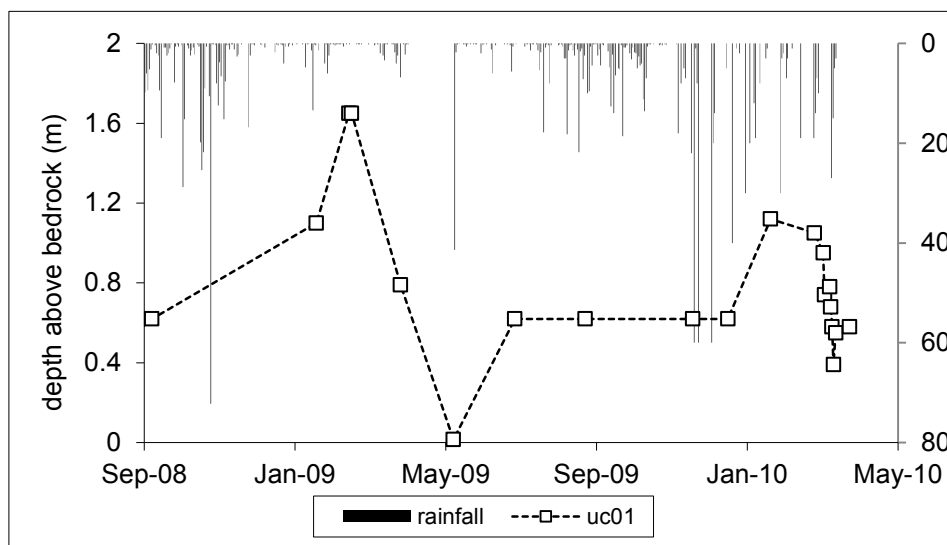


Figure 68 Weatherley, Hillslope 3, Piezometer UC 01 depth of soil water above the bedrock.

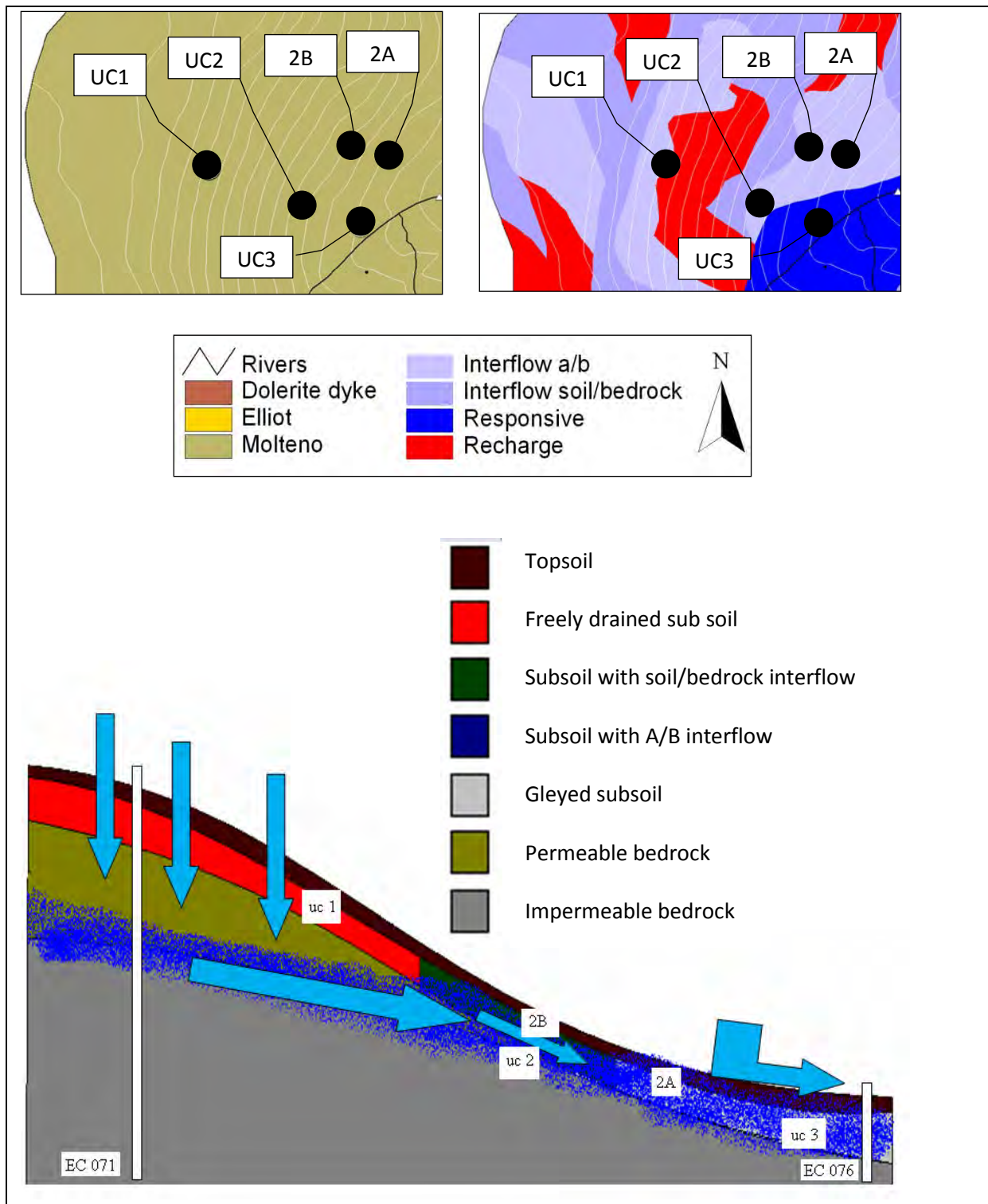


Figure 69 Weatherley, Hillslope 3, Illustrative description and conceptual flow paths

3.1.1 Pre-event

Pre event isotope signatures remain stable during the recession period Figure 71 and Figure 72. This indicates the presence of a continuous water body along the length of the hillslope transect. The absence of an observable free water table at nest 2B is evidence that the lateral response at this part of the hillslope occurs within or beneath the bedrock. The

sustained levels in the riparian soils immediately below nest 2B ,at nest 2A, is further indication of this.

Figure 71 shows the time series values of the piezometers intersecting the values of deep ground water. This is a sign that the soils along the hillslope 3 transect contribute to the regional ground water, showing an element of vertical infiltration within the predominantly interflow soils.

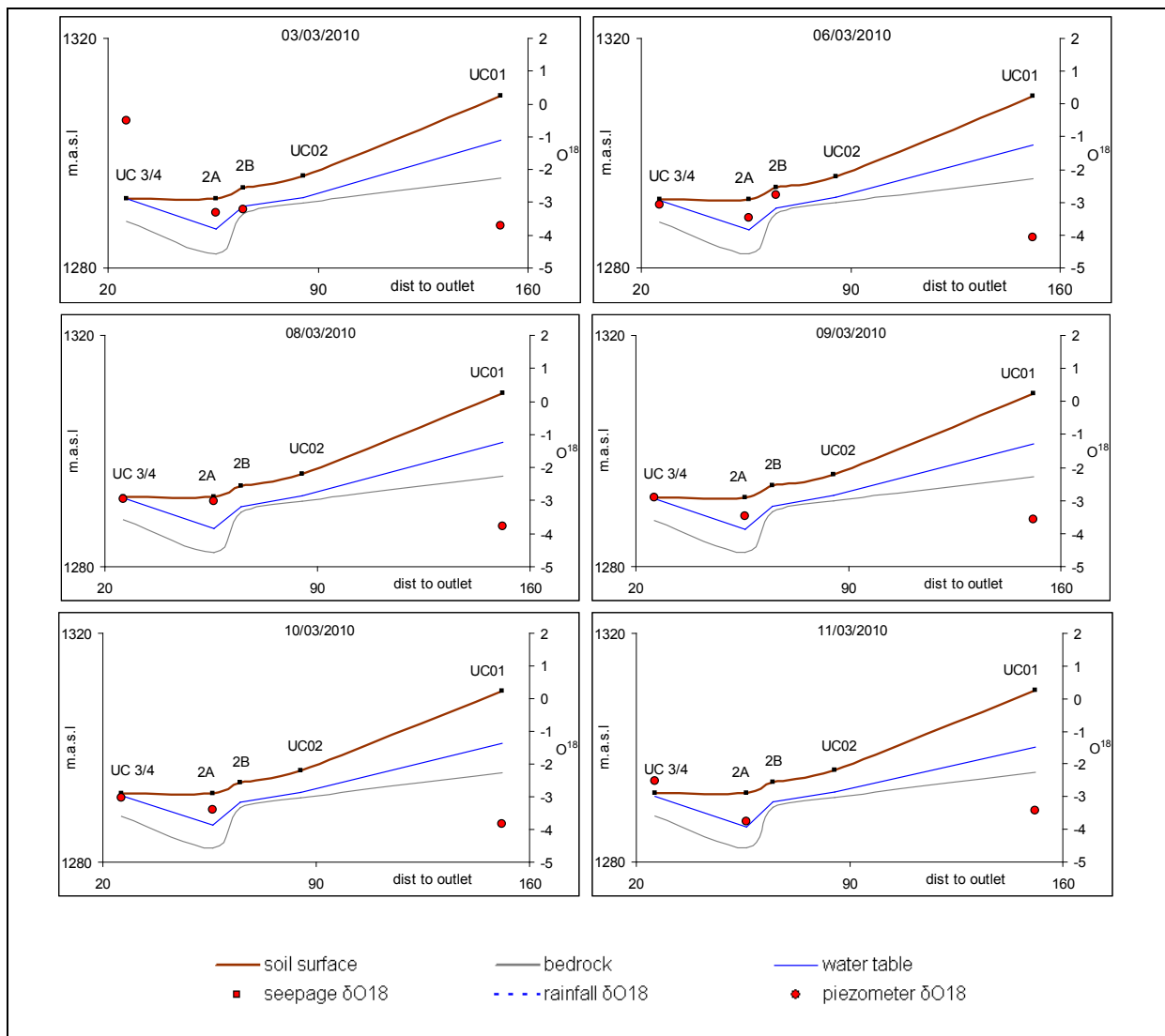


Figure 70 Weatherley, Hillslope 3, pre-event water table drainage and δO^{18}

Table 5 Weatherley, Hillslope 3, δO^{18} isotope data 3-13 March 2010

| Hillslope 3 (UC 01 – Zero tension lysimeter UC 3/4) | | | | | | | |
|-----------------------------------------------------|--------|--------|--------|--------|--------|--------|--------|
| location | 03-Mar | 06-Mar | 08-Mar | 09-Mar | 10-Mar | 11-Mar | 13-Mar |
| uc3/4 | -0.50 | -3.09 | -2.97 | -2.90 | -3.04 | -2.52 | -2.72 |
| Piezo 2A | -3.31 | -3.48 | -3.03 | -3.48 | -3.40 | -3.78 | -3.51 |
| Piezo 2B | -3.21 | -2.79 | | | | | -3.20 |
| uc02 | | | | | | | |
| uc01 | -3.70 | -4.06 | -3.78 | -3.56 | -3.84 | -3.42 | -3.43 |
| std dev | 1.47 | 0.55 | 0.45 | 0.36 | 0.40 | 0.65 | 0.36 |

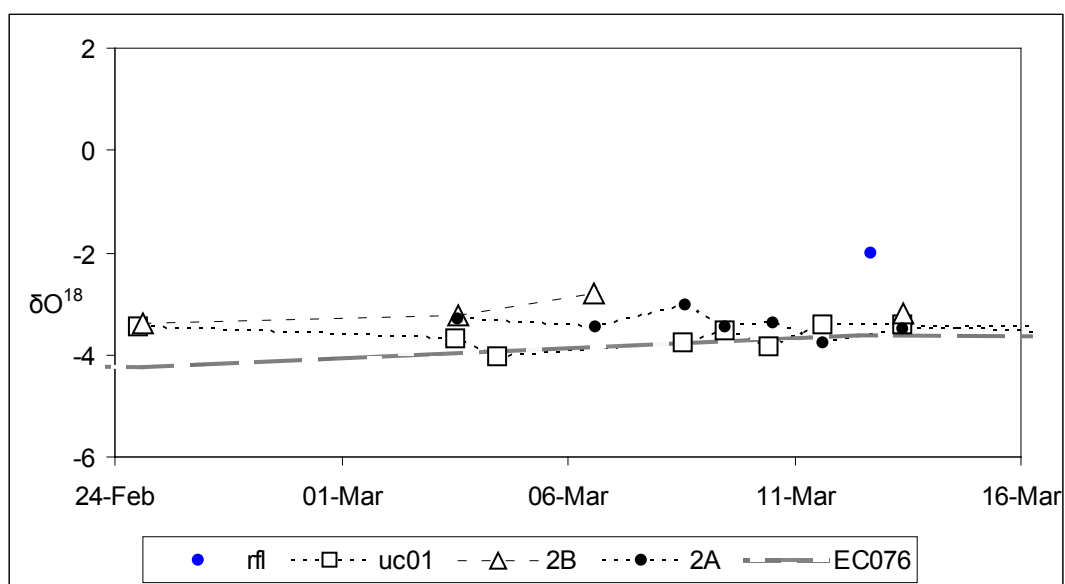


Figure 71 Weatherley, Hillslope 3, March 2010 δO^{18} piezometer values

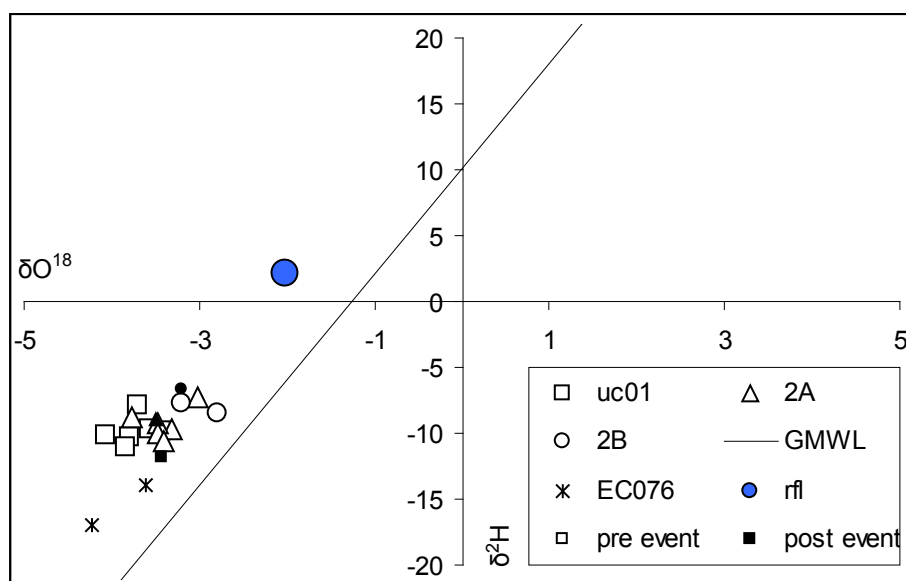


Figure 72 Weatherley, Hillslope 3, March 2010 δO^{18} and $\delta^2 H$ isotope values.

Post event

Hillslope 3 post event isotope responses show almost no change from pre event, with the exception of the observation of perched soil water in piezometer 2B. Post event δO^{18} values along the lower part of the transect (2A=-3.51, 2B=-3.20, UC01=-3.43) remain well below that of rainfall (-2.02) (Figure 72, Table 5).

This means that event derived water has little or no impact on the hillslope response, Figure 73. Overland flow generation can also be discounted as there was no surface runoff data captured in the USLE runoff plots, therefore the effective rainfall must remain in the upper soil horizons for some time as it slowly accumulates on a layer of decreased permeability, moving it horizontally toward the stream.

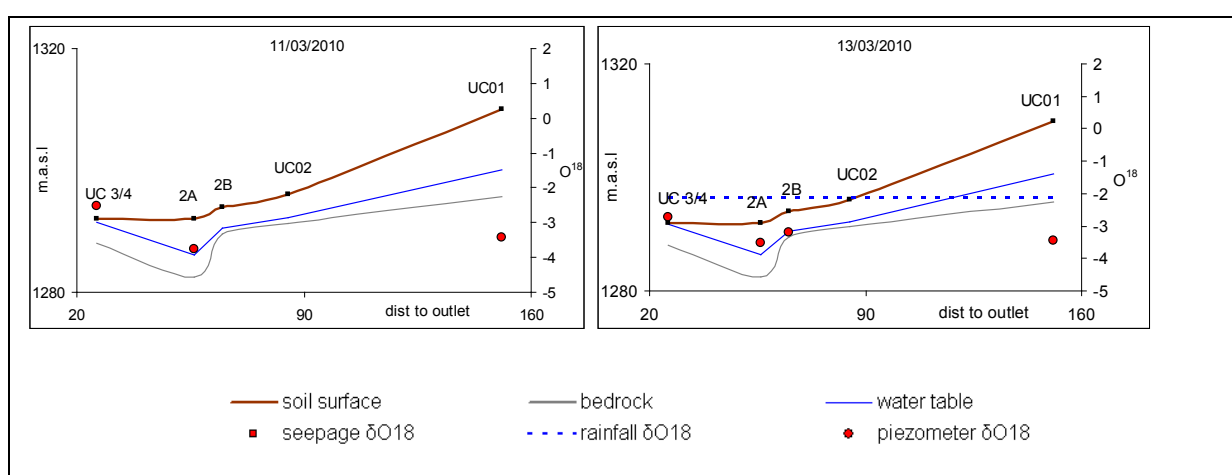


Figure 73 Weatherley, Hillslope 3, pre event (left) and post event (right) water table drainage and δO^{18} values

Hillslope 3 appears to have substantially lower event derived responses than hillslopes 1 and 2. While the presence of older pre event hillslope water is sufficient to dampen the isotope signature of event water, the stream values still show higher event derived contributions, Figure 79. However, as the recession period extends it is expected that this will change and hillslope be able to store water for longer periods that will sustain streamflow.

2.1.5 Hillslope 4 (UC3/4-UC 08)

Hillslope 4 is situated in the southern extremities of the catchment and feeds the source of the stream draining Weatherley. The hillslope transect extends from nest UC ¾ in the responsive soils through nest UC08 in the recharge soils near the crest. Soils are made up largely of responsive and recharge soil types, Figure 74. Results are expected to show that recharge in the upslope area feeds the water table in the responsive soils, similar to hillslope 1. In contrast to the other hillslopes, hillslope 4 has very deep midslope soils, near nest LC07. The effect of the soil depth causes these soils to be classified as recharge soils even though they occur on a slope of 20%. These soils are expected to store hillslope water for long periods causing a depletion and attenuation of isotope values.

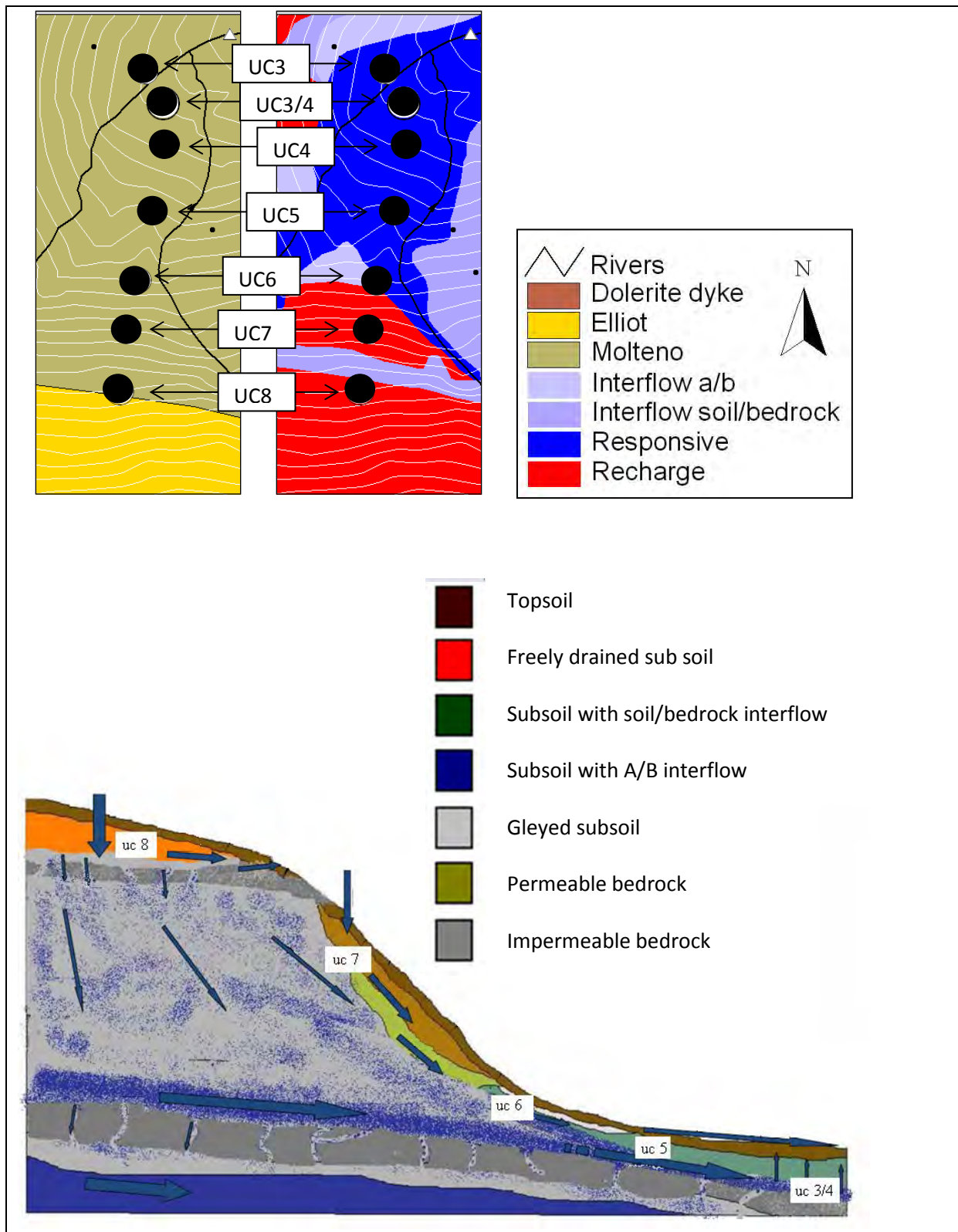


Figure 74 Weatherley, Hillslope 4, Illustrative description and conceptual flow paths

Pre-event

Pre event water table levels remain constant at nearly all nests excluding UC06 which drains by over 50% during the recession period, Figure 75. The fact that downslope water table levels at nests UC3/4 and UC5 indicates that water leaving the hillslope soils drained by UC06 are feeding soils in the responsive soils near UC3/4 and UC05, Figure 75. This is further supported by δO^{18} isotope values at these nests which range from -2.52 to -3.62 during the recession period.

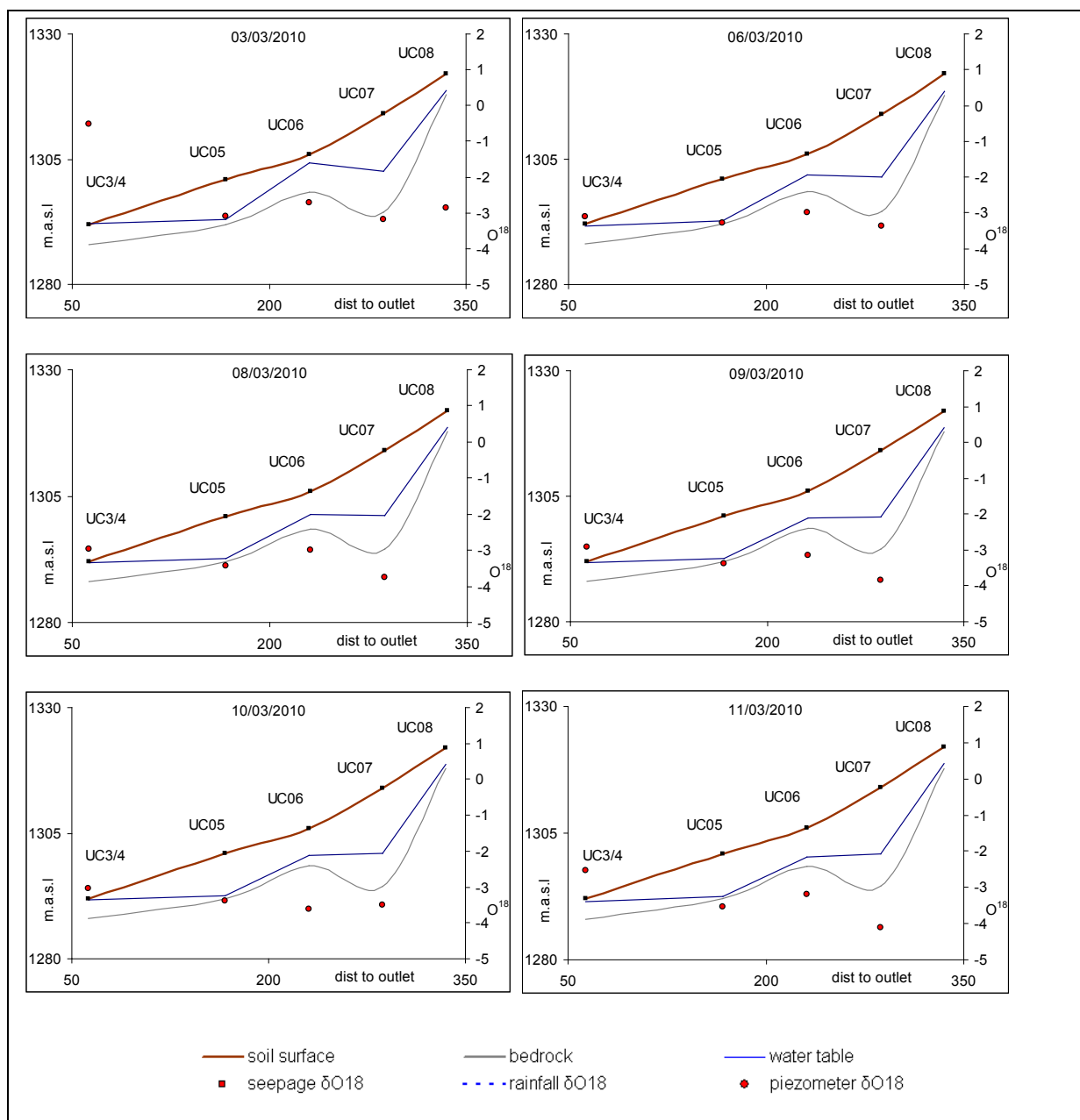


Figure 75 Weatherley, Hillslope 4, pre-event water table drainage and δO^{18} isotope values

Table 6 Weatherley, Hillslope 4, δO^{18} isotope data 3-13 March 2010

| | Hillslope 4 (UC 08 – Piezometer UC 3/4) | | | | | | |
|----------|-----------------------------------------|--------|--------|--------|--------|--------|--------|
| location | 03-Mar | 06-Mar | 08-Mar | 09-Mar | 10-Mar | 11-Mar | 13-Mar |
| uc3/4 | -0.50 | -3.09 | -2.97 | -2.90 | -3.04 | -2.52 | -2.72 |
| uc05 | -3.10 | -3.29 | -3.42 | -3.37 | -3.37 | -3.55 | -2.85 |
| uc06 | -2.71 | -2.99 | -3.00 | -3.14 | -3.62 | -3.20 | -1.81 |
| uc07 | -3.18 | -3.38 | -3.75 | -3.84 | -3.50 | -4.10 | -3.59 |
| uc08 | -2.86 | | | | | | -3.07 |
| std dev | 1.12 | 0.18 | 0.37 | 0.40 | 0.25 | 0.66 | 0.65 |

Post-event

Water table and isotope responses remain relatively constant compared to pre-event, (Figure 76, Figure 77 and Figure 78). This is with the exception of Nest UC06 which shows a sudden rise in water table and δO^{18} isotope value. The change in δO^{18} isotope value from -3.20 to -1.81 (Figure 78 and Table 6) indicates that the soils near UC06 are recharged by event derived water from upslope positions. Again no overland flow was observed on the steep midslopes of hillslope 4, indicating that the event water may have moved laterally downslope in the shallow parts of the soil horizon. Nest UC06 represent an accumulation point, much like nest LC 06 on hillslope 1, which stores event water, releasing it slowly to the responsive soils during the recession period.

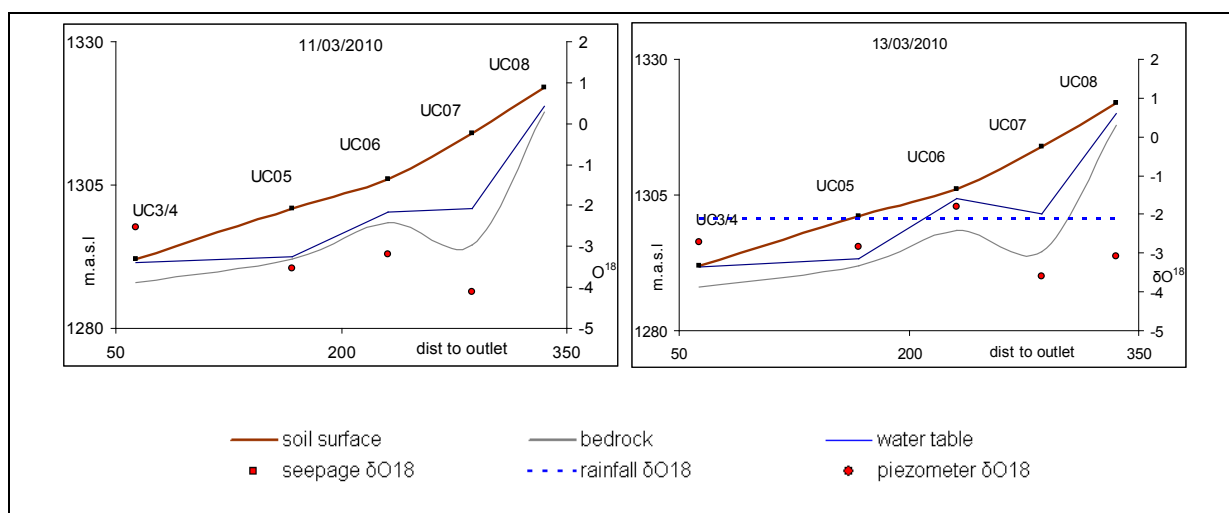


Figure 76 Weatherley, Hillslope 4, post-event water table drainage and δO^{18} isotope values

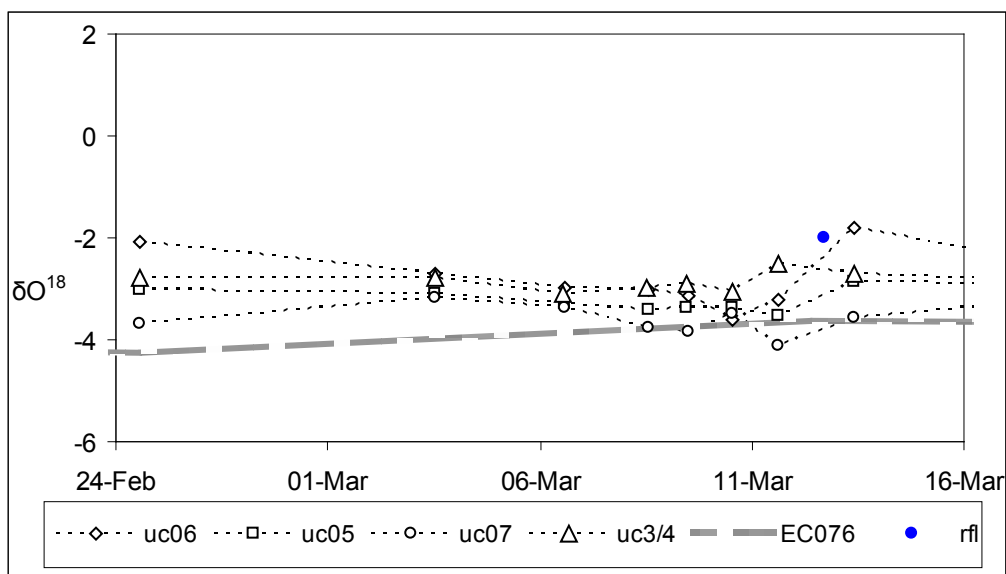


Figure 77 Weatherley, Hillslope 4, March 2010 δO^{18} isotope values

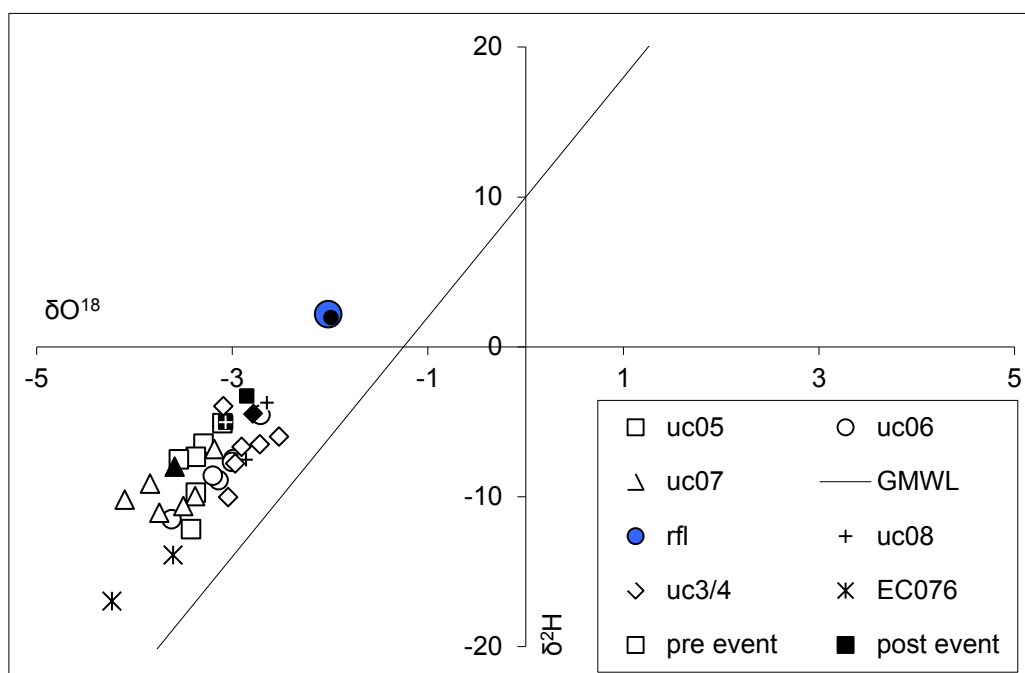


Figure 78 Weatherley, Hillslope 4, March 2010 δO^{18} and $\delta^2\text{H}$ isotope values

2.2 CONCLUSION

Streamflow is comprised of a range of different responses occurring over different spatial and temporal scales. The manner in which soils are distributed over a hillslope transect will dictate how they store and release water. Due to the topography of the Weatherley catchment all waters draining to the stream must pass through the responsive soils adjacent to the stream. This allows us to make some unique assumptions and conclusions about the hillslopes that feed shallow ground water to the responsive soils.

All of the study hillslopes show the presence of a water table on the soil bedrock interface. These water tables are shown to be fed by combinations of event and pre event water during event and drainage periods.

While all four hillslope show distinctive and unique patterns, they do express similarity at a broader scale. Both the lower catchment hillslopes 1 and 2 show a high event derived contribution in respect of the pre event δO^{18} isotope values. Upper catchment hillslopes 3 and 4 show very little or no change in δO^{18} isotope values from pre event to post event. Thus, the upper catchment and lower catchment will dominate streamflow periods at different times. The faster draining responsive soil of the lower catchment will provide the rapid streamflow response during and immediately after the event, through the generation of overland flow. The slower draining responsive soils of the upper catchment store water for longer periods, releasing it slowly to sustain stream levels during the recession period.

The hydrogeological and hydrometric descriptions of the Weatherley hillslopes allow for the development of an illustrative framework of mechanisms of hillslope water recharge, storage and drainage. This forms the first step in the modelling of these hillslopes and the eventual catchment scale simulation of Weatherley. The descriptions of the hillslopes allow for the subsurface calibration of different sources and pathways of the hillslope response to the responsive riparian soils, forming the basis of the subsurface routines in the ACUR Intermediate zone model.

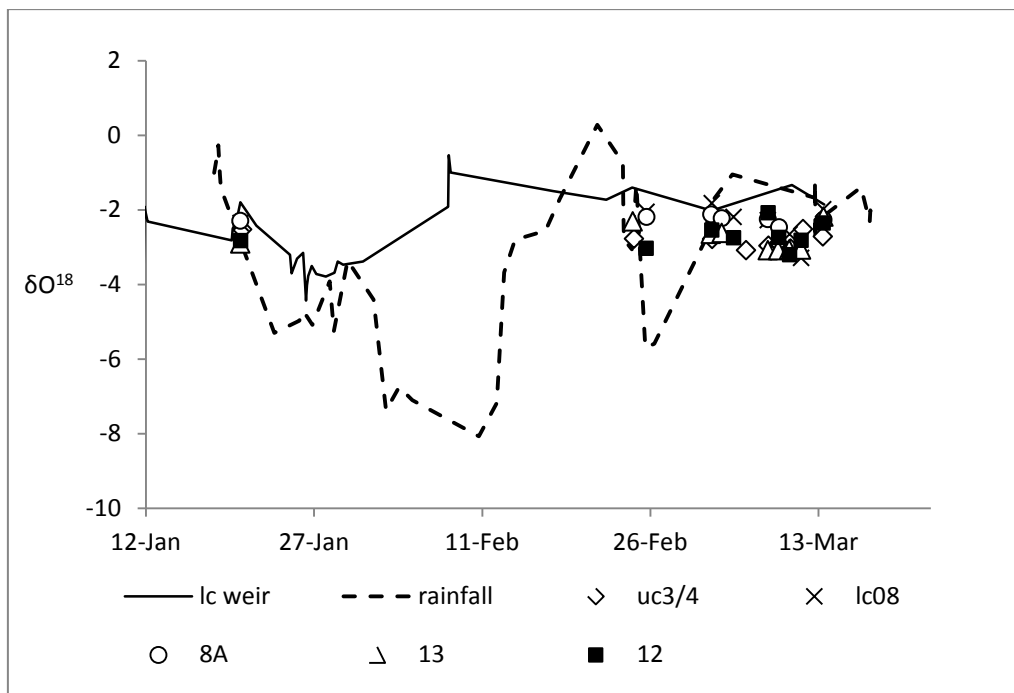


Figure 79 Weatherley δO^{18} isotopes of rainfall streamflow and riparian piezometers

2.2.1 Hillslope and Catchment scale δO^{18} Hydrograph Separation

δO^{18} hydrograph separations were carried out at two different scales. The 2 component hydrograph separation is applied firstly at individual piezometer sites along the different hillslope transects to assess the hillslope drainage characteristics. Secondly, at the catchment scale to determine which hillslopes dominate the streamflow response

Figure 79 Hillslope scale hydrograph separations

Hydrograph separations were carried out on a daily time step for the period 2010/03/03 to 2010/03/13 for each of the piezometers along the four hillslope transects with an observable water table. The results are plotted in terms of percentages of the old and new water, where old water (Q_p) is the soil water isotope value sampled in the piezometer one time step prior to the event or new water input (Q_n). The main event considered in this study was a 30 mm event on 2010/03/12. The period 2010/03/04 to 2010/03/11 will be considered the pre event drainage, while observations made on 2010/03/13 will be considered post event recharge.

Site located on the upper slopes of hillslope transects showed similar results. Pre event soil water was dominated by pre event water during both pre and post event, Figure 80, Figure 81 and Figure 82). This agrees with the hillslope descriptions where old water is found to dominate upslope positions.

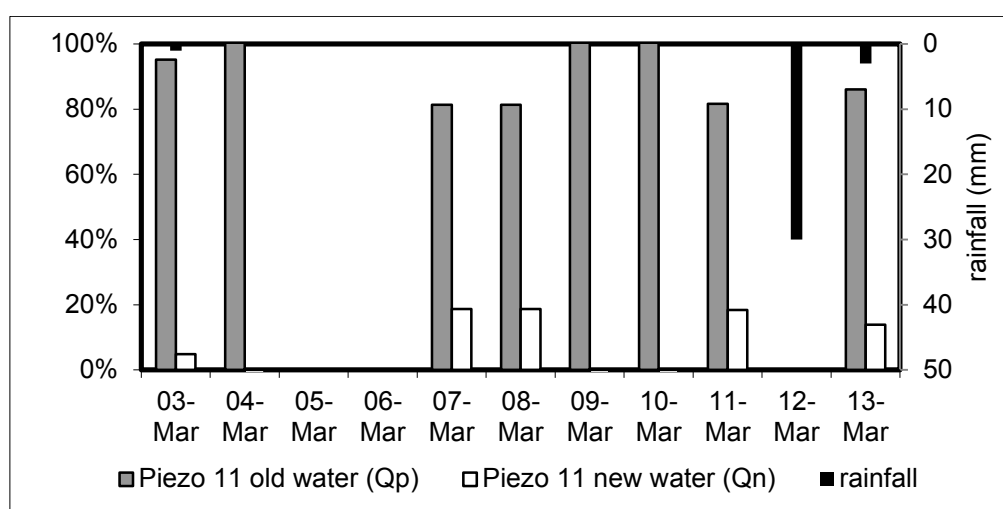


Figure 80 Hillslope 1, hillslope nest LC04 event and pre event contributions

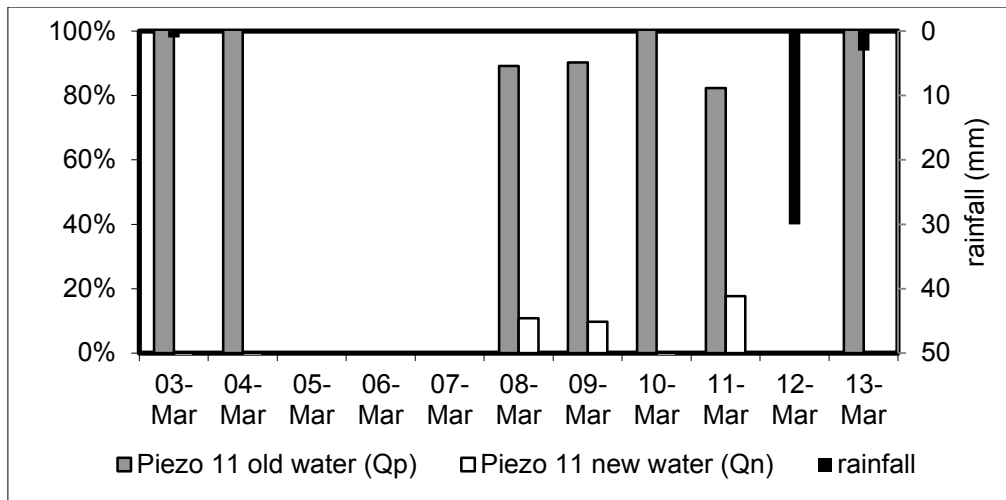


Figure 81 Hillslope 3, hillslope nest UC01 event and pre event contributions

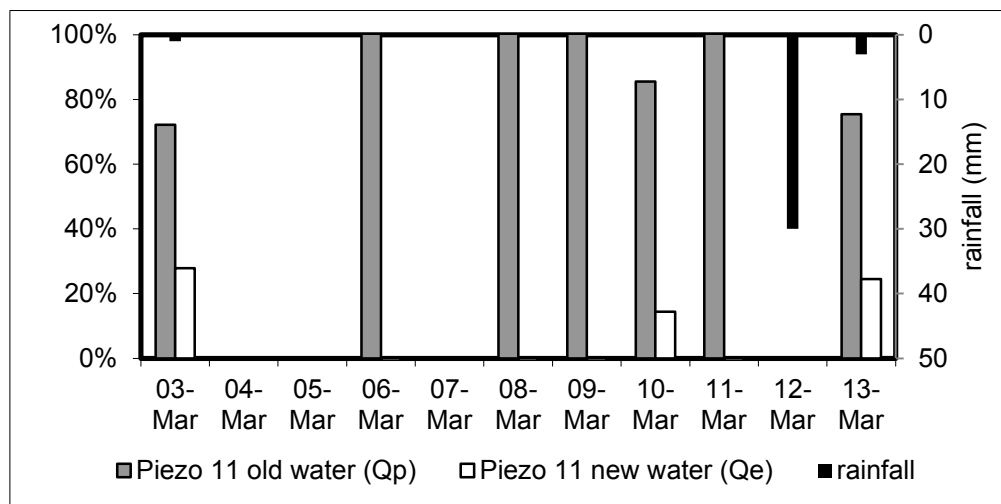


Figure 82 Hillslope 4, hillslope nest UC07 event and pre event contributions

The downslope responsive soils hydrograph separations also agreed strongly with the hillslope descriptions. Hillslopes 1 and 2, in the lower catchment, showed high levels of pre event water (80-100%) while post event results showed a complete shift to 80-100% event derived water. This indicates a rapid event based recharge of the riparian soils on hillslopes 1 and 2 by lateral hillslope drainage on the soil surface or at shallow depths within the soil profile. In stark contrast Hillslopes 3 and 4, show a muted response to the 2010/03/12 event with event contributions not exceeding 20%, Figure 83, Figure 84, Figure 85, and Figure 86. This indicates the presence of recharge conditions across the upper recharge and lower responsive soils of the upper catchment hillslopes. the presence of small contribution of event water is observed on hillslopes 3 and 4 but not on hillslopes 1 and 2, indicates that event water does eventually reach the soil bed rock interface, yet it has longer transit time compared to lower catchment hillslopes 1 and 2.

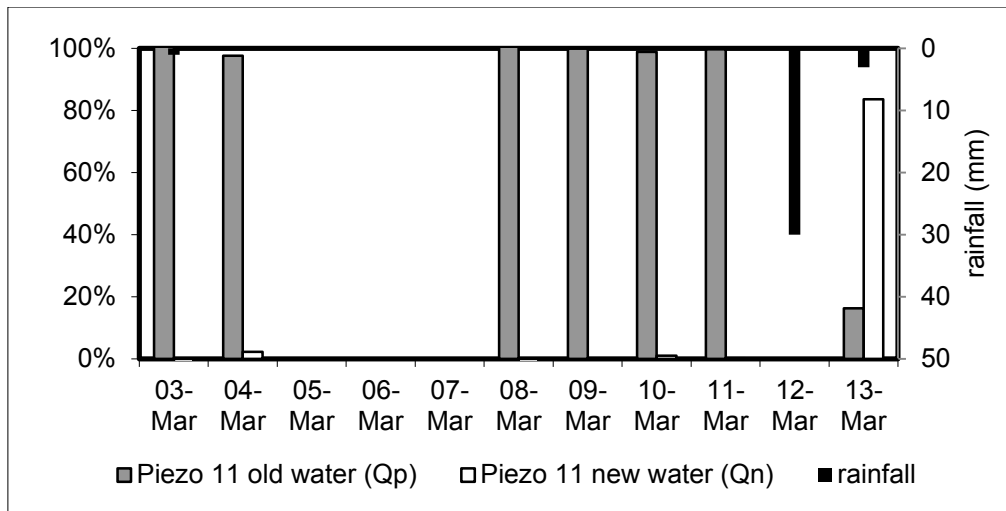


Figure 83 Hillslope 1, riparian nest 13, event and pre event contributions

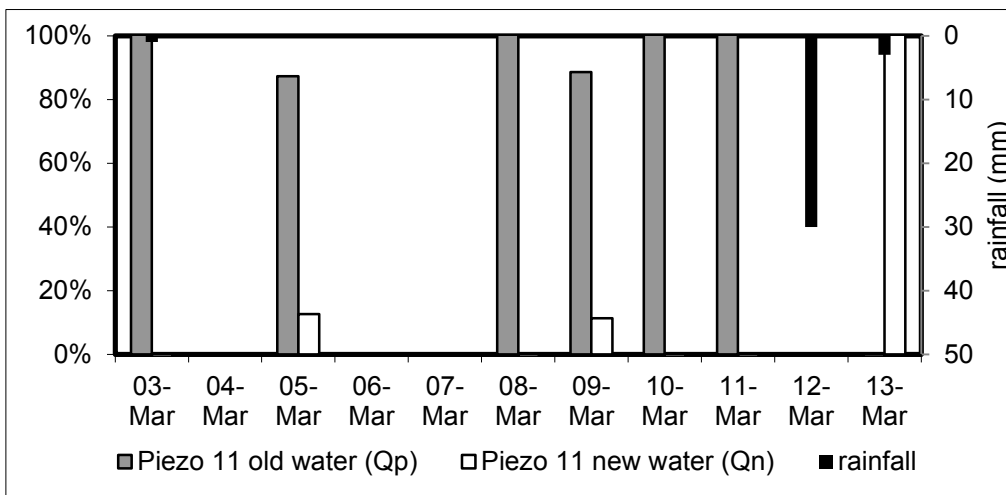


Figure 84 Hillslope 2, riparian nest 11, event and pre event contributions

While the hydrograph separations are derived from the same data used for the hillslope descriptions, they quantitatively characterize the hillslope descriptions. The dominance of pre event water at upslope positions is also shown by the attenuated isotope signal detailed in the hillslope descriptions. The high event based contributions observed in the hillslope 1 and 2 responsive soils are also shown in the descriptions where piezometer and isotope values are similar.

All four study hillslope show a subsurface hydrological connection between the upslope soils and the responsive soils adjacent to the stream. This could be attributed to the geology underlying the hillslope soils, as the sedimentary nature of the parent material results in the formation of horizontally stratified soils. However these connections occur at different soil depths. Hillslopes 1 and 2 in the lower catchment appear to have event driven connections in the shallower soils horizons. In the upper catchment Hillslopes 3 and 4, the subsurface connection occurs deeper in the soil profile on or near the soil bedrock interface. The response observed in the upper catchment is delayed compared to that of the lower catchment hillslopes.

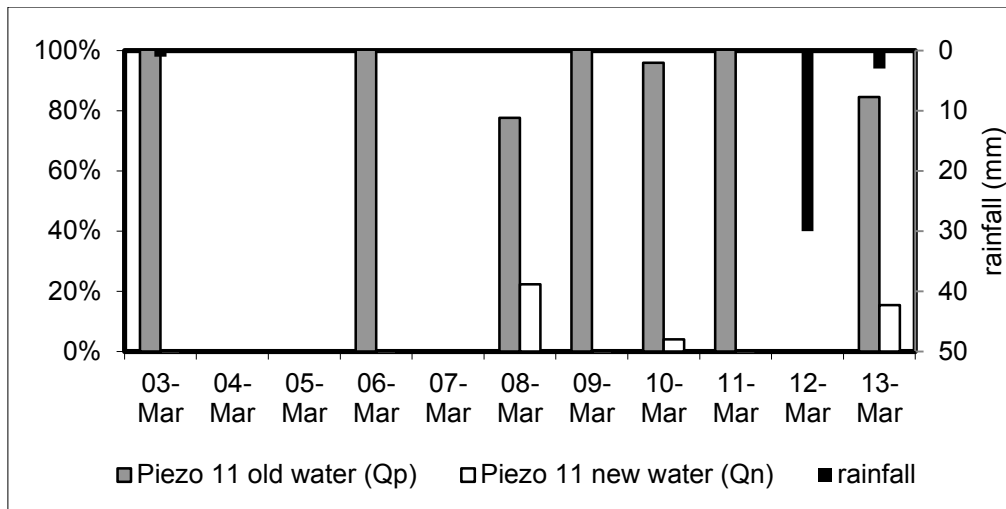


Figure 85 Hillslope 3, riparian nest 2A, event and pre event contributions.

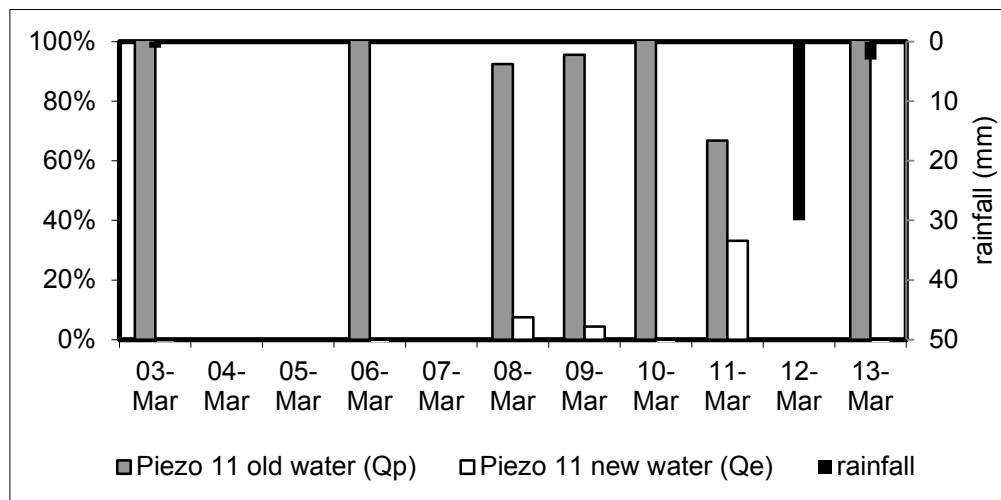


Figure 86 Hillslope 4, riparian nest UC 3/4, event and pre event contributions

2.3 IN-SITU MEASUREMENTS OF WEATHERLEY

2.3.1 Introduction

Hillslopes are fundamental landscape units (Lin *et al.*, 2006), and are important for understanding and simulating catchment hydrological processes (Tromp van Meerveld & Weiler, 2008). How catchments respond is determined by the particular mixture and dominant hydrological behaviour from individual hillslopes in the catchment (Sivapalan, 2003). Their hydrological behaviour determines how precipitation reaches the stream, i.e. residence times, flow paths and storage mechanisms (Uhlenbrook, Wenninger & Lorentz, 2005). Hillslopes, and consequently hillslope hydrological processes, are however loaded with complexity and heterogeneity with strong temporal and spatial variation in the observed processes (Sivapalan, 2003) leading to the conclusion that every hillslope is unique (Beven, 2001). Experimentalists focus therefore on the examination and documentation of

unconventional behaviour of new hillslopes under different environmental conditions, without intercomparisons, resulting in *just another* documented hillslope, with diminutive extrapolation value (Weiler & McDonnell, 2004).

Focussing on first order controls with the aim of intercomparisons between hillslopes should be the focus of any hillslope hydrological study (McDonnell *et al.*, 2007). The first order controls in hillslope hydrology are defined as “*the main and essential process constraints on water and solute flux*”. Ultimately the goal of hillslope hydrological investigations should be to ‘clarify’ and ‘simplify’ in order to ‘classify’ the hydrological responses of hillslopes (Weiler *et al.*, 2004). If this can be done, it will definitely enhance the contribution of hillslope hydrology to the challenge of ‘Predictions in Ungauged Basins’ (PUB, Sivapalan, 2003).

Soils integrate the influences of parent material, topography, vegetation/land use, and climate and can therefore act as a first order control in the partitioning of hydrological flow paths, residence time distributions and water storage (Park, McSweeney & Lowery, 2001 and Soulsby *et al.* 2006). Conversely, water plays a primary role in the genesis of most soil properties. This interactive relationship between soil and hydrology can be exploited to predict the hydrological behaviour of hillslopes on a qualitative/conceptual basis (Ticehurst *et al.*, 2007, Van Tol *et al.*, 2010a and Van Tol *et al.*, 2010b). The correct interpretation of soil properties, and their vertical and horizontal distribution, is useful for determining the first order controls in hillslope hydrology for example: soils prone to crusting or soils with indications of prolonged saturation in the topsoil will favour the generation of overland flow, and consequently peak flow, whereas deep permeable soils with little anisotropy in terms of the hydraulic conductivity will favour deep drainage and recharge of groundwater levels. The conceptual behaviour, especially in terms of the preferred flowpaths, of a hillslope can also be employed to representing the downslope allocation, or cascading, of water in distributed models (Riddell, 2010).

Converting the qualitative conceptual behaviours into quantitative descriptions of the hydrological processes with the aim of parameterising models, while still imitating the physical processes, is however a thorny task. Ideally quantifications should be based on a number of physical measurements of surface and subsurface flows, water table fluctuations, connectivity of the various water bodies and the residence flow time of water through the landscape (Park & Van de Giesen, 2004 and Ticehurst *et al.*, 2007). Keeping in mind that the main focus is on first order controls and intercomparisons in order to classify hillslopes with the aim of serving PUB’s, measurements of hydrological processes should be limited to first order processes, with the aim of comparison with other hillslopes, focussing on similarities rather than differences. Measurements should include a variety of physical and chemical techniques in order to derive a holistic understanding of the system (McDonnell, 2003). From a hydrogeological viewpoint, measurements should be collected to enable extrapolation of the quantitative behaviour of soil distribution patterns, both vertically and horizontally downslope, to areas with similar distribution patterns.

This chapter reports on experiments and the instrumentation of sections of a hillslope in the Weatherley research catchment. Preliminary results of the hydrological behaviour of this hillslope are presented.

2.3.2 Study area and methodology

The Weatherley catchment

The Weatherly research catchment is partially forested, 1.57km² site, situated in the northern part of the Eastern Cape, within lower altitudes of the 300km² Mooi river quaternary catchment (Department of Water Affairs No. T35C). The altitude of the Weatherly catchment ranges between 1254 and 1352 m.a.s.l., with geology dominated by Elliot and Molteno flatbed sedimentary formations interrupted by intrusive dolerite dykes. The eastern upslope areas are underlain by the Elliot sandstone formation. Molteno mudstone occupies the remainder of the mid slopes and wetland areas (De Decker, 1981). Both these sedimentary formations are relatively impermeable to water when compared to the conditions arising from the intrusion of the dolerite dykes into the sandstone and mudstone terraces. There are two dolerite dykes within Weatherly, the eastern dyke controlling the hydrological response of the midslope area, while the western dyke intersects different slope positions across 2 opposite hillslopes, thus controlling the response from the upper catchment area.

The mean annual precipitation (MAP) is approximately 1000 mm year⁻¹ (Van Huyssteen *et al.*, 2005) with a mean annual potential evaporation (MAE) of 1488 mm (BEEH, 2003). The winters are cold, with mean minimum temperatures of 4 °C. Frost and snowfall is common in the higher lying surrounding areas during the winter. The summers are warm with a mean maximum temperature of 25 °C (Roberts *et al.*, 1996). The natural land cover consists of Highland Sourveld grasslands with a basal cover of 50-75% on the hillslopes. *Eucalyptus nitens*, *Pinuselliottii* and *Pinuspatula* trees were planted on selected areas during 2002. Wetland conditions exist throughout the catchment along the stream with a width of 100 to 400 m. The widest areas of this wetland are associated with seepage lines from contributing hillslopes (Lorentz *et al.*, 2007). For more detail on the description and instrumentation of the Weatherly research catchment refer to Lorentz *et al.* (2007) and Uhlenbrook *et al.* (2005).

A hillslope in the upper eastern segment of the catchment was selected for this study (Figure 87). This hillslope ends abruptly at an altitude of about 1319 m.a.s.l. (Figure 87a) where a rock shelf of Molteno sandstone occurs. This rock layer underlying the hillslope is evidently almost impermeable and therefore seriously impairs vertical drainage of evapotranspiration excess water from the hillslope (termed LC1-LC4 in Figure 87a), thereby promoting considerable internal lateral flow which exits at collection points on the Molteno shelf in an almost continuous low flow during the rainy season. This hillslope includes four tensiometer/piezometer nests, four neutron probe access tubes close to the tensiometer/piezometer nests, and an Electrical Resistivity Imaging (ERI) survey from LC1-LC4 in Figure 87a. New instrumentation was done at nr. 2 (LC2) in Figure 87b as well as at the location marked TB in Figure 87 b, which are presented in more detail in Figure 87c. A two dimensional (2-D) cross section of TB4 to TB1 is presented in Figure 88. The instruments and instrumentation are discussed in detail in the following sections.

Soil information and measurements of soil chemical properties

Soil information

The soil profile at LC2 (2 in Figure 87b) was classified as a Pinedene 1100 soil form (Soil Classification Working Group, 1991) equivalent to a Gleyic-Orthidistic Cambisol (WRB, 2006). The profile consists of an orthic A horizon (*ot*) from 0-400 mm, overlying a yellow brown apedal B horizon (*ye*) from 400-800 mm, overlying a horizon with evidence of long periods of saturation (*on*) 800-2400+ mm. For detailed description of profile LC2 see Van Huyssteen *et al.* (2005).

The dominant soil form in the TB area is Kroonstad 2000 (Soil Classification Working Group, 1991) equivalent to a Gleyic-Albic Planosol (WRB, 2006). The profile consists of an *ot* horizon with variable depth overlying a thick E horizon (*gs*). Below the *gs* is a relatively clay rich G-horizon (*gh*) with bedrock at its base.

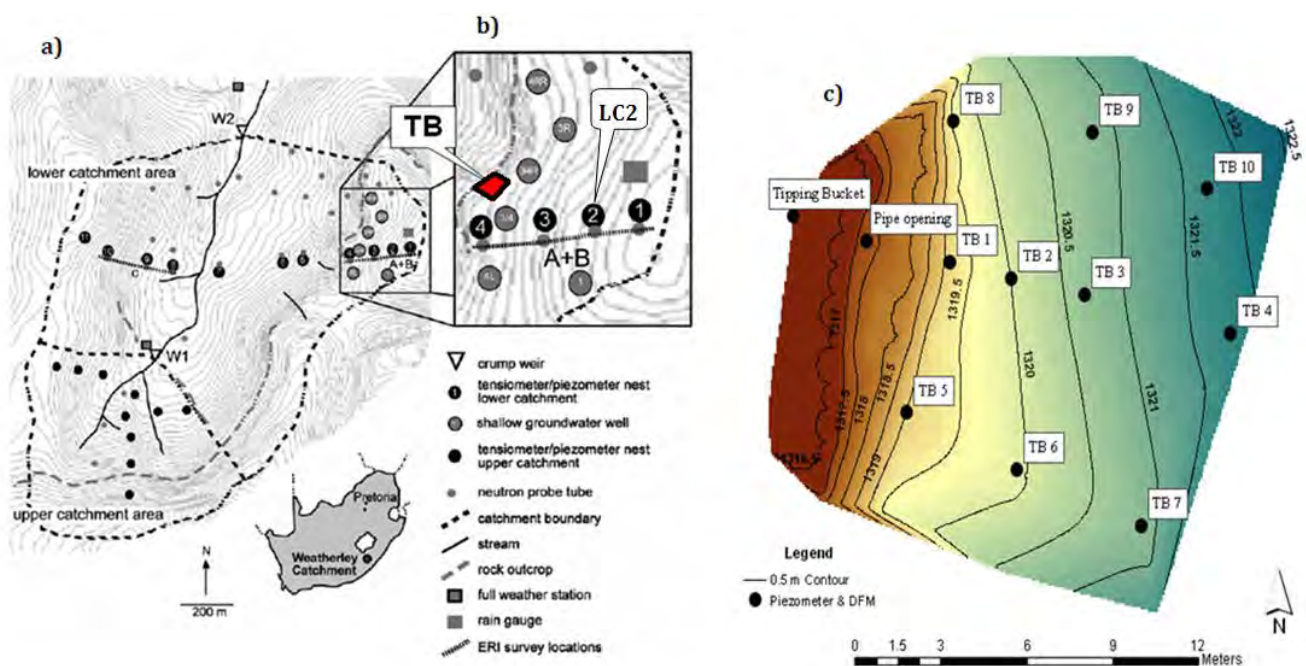


Figure 87: a) Instrumentation of the Weatherley catchment (Lorentz *et al.*, 2004), b) hillslope 1-4 with location of tipping bucket experiment and c) tipping bucket (hillslope outflow) experiment at the footslope of hillslope 1-4. TB1-TB10 in c) is perforated pipe nests. DFM probes were installed at TB1-4, TB7 and TB9

TB7 and TB9 were classified as Pinedene 1100 soil form (Soil Classification Working Group, 1991) equivalent to a Gleyic-Orthidistic Cambisol (WRB, 2006). The thick *gs* horizon is also present in these profiles but is overlain by a *ye* horizon.

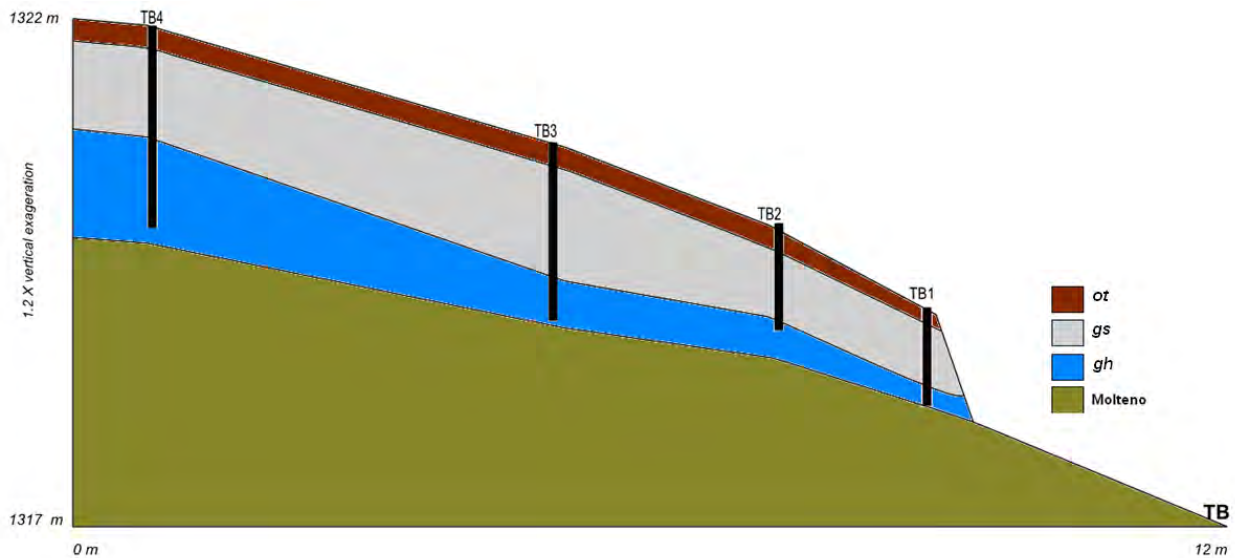


Figure 88 Two dimensional (2-D) representation of transect TB4-TB1 (see Figure 87c for location)

Soil chemical measurements

Soil chemical properties at the sampling points in the TB area (Figure 87c) were measured with a Mid InfraRed (MIR) Spectrometer with wavelengths between 2.5 and 25 μm . Reflectance spectroscopy is an advanced soil analysis technique suited for rapid and simultaneous analysis of biological, chemical and physical attributes of soil (Geet *et al.*, 2007). The resulting chemical properties are presented in Table 8. Selected properties of TB1-TB4 are displayed as a 2-D cross section, with interpolations done using the natural neighbour interpolation technique in ArcMap (ESRI, 2008).

Field determination of vertical and lateral hydraulic conductivities

Indirect methods to calculate lateral flow processes include the continuity equation:

$$\frac{d\theta}{dt} = K_x \cdot \frac{\partial^2 \Delta H}{\partial x^2} + K_y \cdot \frac{\partial^2 \Delta H}{\partial y^2} + K_z \cdot \frac{\partial^2 \Delta H}{\partial z^2} \quad (2.1)$$

To quantify downslope flow in a hillslope, this equation requires measurements of both vertical and lateral hydraulic conductivity, while most studies assume that there is no difference between these two conductivities for particular horizons. We propose a method for measuring the lateral hydraulic conductivity in the field. This method involves taking an undisturbed sample in the horizontal direction with a core 300 mm in diameter and 200 mm in depth, forced into the soil with a hydraulic jack. The core sample in its PVC ring is then carefully removed from the soil profile and placed on a level surface, the pore geometry now directed vertically. A series of hydraulic conductivity measurements (K_s ; and $K(h)$ at $h =$

30, 60 and 150 mm) are then made on the core to provide the important data for the lateral $K(h)$ curve. This procedure was used to determine the lateral hydraulic conductivity of two horizons (*ot* and *ye*) at LC2 (2 Figure 87). Figure 89 shows some steps involved in this method.

K_s was also measured in a vertical direction using the double ring method, where after $K(h)$ at $h = 5, 30, 60$, and 150 mm were measured using a tension infiltrometer. The 5 mm head was not measured at LC2. Hydraulic conductivity measurements were done for two horizons at LC2 (*ot* and *ye*) for four horizons (*ot*, *gs1*, *gs2* and *gh*) at TB4. Undisturbed core samples taken for each of these horizons were used to determine bulk density and porosity.



Figure 89 : Proposed method to determine lateral hydraulic conductivities in the field: a) the PVC ring being forced into a specific horizon by means of a hydraulic jack; b) the setup for double ring K measurements with the core now orientated vertically; c) the setup for lateral $K(h)$ measurements by tension infiltrometer.

Undisturbed cores were taken in both vertical and lateral directions to establish the remainder of the $K(h)$ curve in the laboratory, following the hanging column method of Klute & Dirksen (1986). Parameters for equations describing the relationship between suction and water content as well as water content and hydraulic conductivity (Van Genuchten, 1980), were optimized using RETC version 6.02 (Van Genuchten *et al.*, 2009). These relationships are described by the following equations:

$$S_e = \frac{1}{[1+(\alpha h)^n]^m} \quad (2.2)$$

Where α , n and m are constants affecting the shape of the curve and $m = 1 - 1/n$. S_e is the reduced water content or the effective degree of saturation and is equal to:

$$S_e = \frac{(\theta - \theta_r)}{(\theta_s - \theta_r)} \quad (2.3)$$

Where θ is the volumetric water content θ_r is the residual water content and θ_s is the saturated water content, i.e. the maximum volumetric content of the soil.

$$K_h = K_s (S_e)^{\frac{1}{2}} \left[1 - \left(1 - S_e^{\frac{1}{m}} \right)^m \right]^2 \quad (2.4)$$

Where K_h is the unsaturated hydraulic conductivity and K_s is the saturated hydraulic conductivity. Bulk density and porosity were also determined from the undisturbed samples.

The hydraulic conductivity at the soil/bedrock interface was determined at LC2 and TB with a mobile permeameter. The setup of the permeameter involves a 25 l water reservoir, connected to the permeameter with plastic pipes. The permeameter keeps water at a constant head to reach a final constant value and then converted to K_s . Holes were augured by using a standard bucket auger with a radius of 37.4 mm. A constant head of 250 mm was used in all profiles. The time of a certain amount of water leaving the reservoir was noted and converted to K_s by means of the Glover equation.

DFM probes: installation and calibration

The installation and calibration of DFM probes are discussed in detail in Chapter 7.

Lateral flow measurements

Perforated pipes and slug tests

A total of 10 perforated 55 mm PVC pipes were installed in the TB area (TB1-TB10 in Figure 87c). These pipes are not automated and water table depths were recorded during field visits. Slug tests were also performed in selected pipes, where the piezometers were emptied and the time recorded for the water in the pipe to return to its initial height. From these slug tests, the hydraulic conductivity of the soils was determined with the Hvorslev (1951) method: the elapsed time is plotted against the head ratio (H/H_0) on a one-cycle semi-logarithmic graph, where the head ratio is on the logarithmic and the time on the arithmetic axis. H_0 = the water table height, when the water is removed, i.e. at the beginning of the experiment and H = the water table height after a certain time. A straight line is drawn through the points and T_0 (the basic time lag) is read from the graph when the head ratio equals 0.37. K is then calculated using:

$$K = \frac{r^2 \ln\left(\frac{L}{R}\right)}{2LT_0} \quad (2.5)$$

Where K = hydraulic conductivity; r = radius of pipe; L = length of saturated portion of the perforated area; R = radius of perforated area (the same as r in this experiment and T_0 = basic time lag.

Trench experiment

The problems associated with interception of lateral flow are well known (Andeson & Burt, 1990). Interception of flow usually involves exposing a vertical surface of the soil and collecting water draining out of the vertical face. This artificial free face distorts the flow lines to form a saturated wedge from which water drains at a rate (K_s) greater than the rate under natural conditions. An attempt to intercept flow before this saturated wedge forms, was conducted at LC2 (Figure 90).



Figure 90 Trench experiment at LC2.

The procedure involved 100 × 500 mm channel irons being hammered into the exposed profile face in an upslope direction at different depths. The channels are inserted as follows: Pipe 1 – 300 mm, Pipe 2 – 700 mm, Pipe 3 – 1000 mm, Pipe 4 – 1400 and Pipe 5 – 1900 mm. Water was channelled via the channel irons into 10 ℓ plastic buckets, which are sealed at the top except for a 110 mm PVC pipe connecting the bucket to the surface from where the volume of water in the bucket can be determined, water samples taken and the bucket emptied when necessary. The surface above the part of the conducting channel irons was covered to prevent vertical drainage into the channels. It is believed that by hammering the channel irons into the undisturbed soil, the formation of the saturated wedge can be prevented for the 100 mm width of the channel iron. Although the outflow from the channels into the buckets will probably be faster than the actual rate of lateral flow, the volume of flow should represent the actual volume of lateral flow at the specific depth. Since this experiment was not automated, the rate of flow could not be measured. The volume of inflow at each depth was measured in the different buckets during several field visits.

Slotted pipes

Six slotted pipes were installed on the selected hillslope, four at TB and two at LC1 (nr. 1 in Figure 87c). These slotted pipes differ from the perforated pipes in that they are only slotted at specific depths representing specific horizons (Figure 91). The pipes in the TB area namely *SPTB9-ot* and *SPTB9-gs* were installed next to TB9 in Figure 87c and *SPTB7-ot* and *SPTB7-gs* were installed next to TB7. The two pipes at LC1 are *SPLC1-ot* and *SPLC1-gs*. The *ot* and *gs* in the name refer to the horizon with the open slots and the water measured in these pipes is therefore reflective of the lateral flow in these horizons.

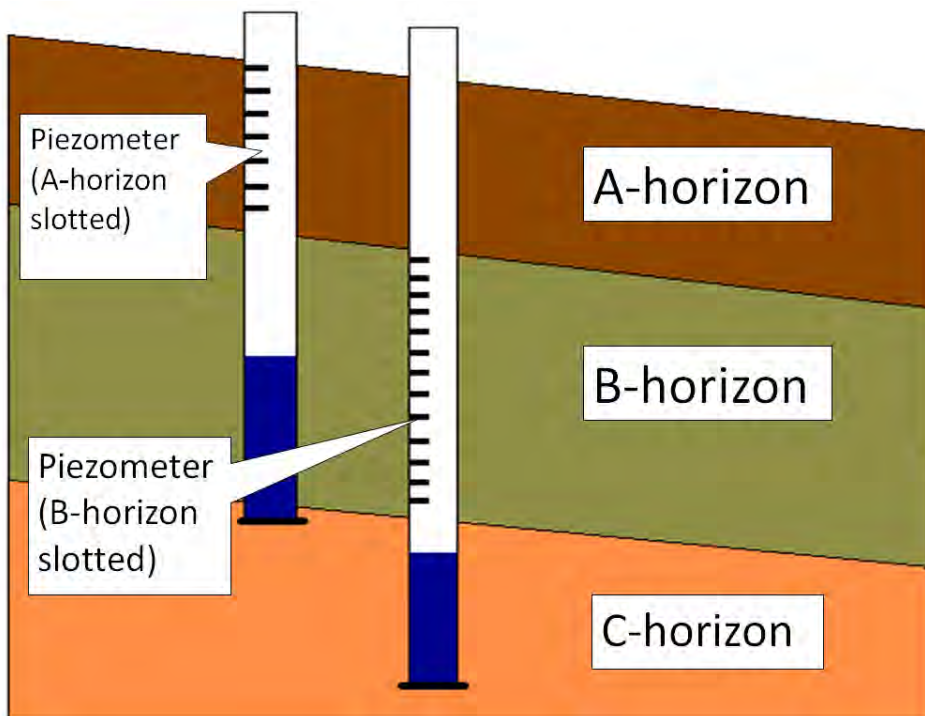


Figure 91 Slotted pipes installed to measure flow from specific horizons

The slotted pipes are sealed at the bottom to ensure that water which flowed laterally into the pipe remained in the pipe for measurements of the volumes during field visits (Figure 91). A plastic surface covering, 400 mm upslope, 100 mm downslope and 100 mm at the sides assured that vertical infiltrating did not enter the pipe. Slug experiments were conducted in selected slotted pipes to calculate the rate of flow in a specific horizon, when the water table level was above the slotted height.

Hillslope outflow experiment

The relative impermeability of the Molteno shelf, protruding at the foot of the hillslope being studied, just below TB1, TB5 and TB8 in Figure 87c, causes a large volume of interflow water to exit from the this hillslope (LC1-LC4, Figure 87b) at the Molteno rock outcrop and flow over the edge of the shelf. A concave area where there is a natural accumulation of water on the outcrop, was identified for measuring outflow from the hillslope. This natural depression (Figure 92) was also used to measure the first and last flows of the rain season over the outcrop. A cement wall was built (approximately 150 mm high) to route the water

into a 110 mm PVC pipe and into a tipping bucket measuring device (Figure 92) installed with an event HOBO logger which, recorded every tip of the bucket. Every two tips equal 5 ℓ of water draining from that portion of the hillslope. Figure 87 presents the experimental setup of the hillslope outflow experiment.



Figure 92 Tipping bucket measuring outflow from a selected portion of hillslope immediately below the investigated sites TB1 to TB4 shown in Figure 87c and in the cross section in Figure 88.

This experiment was used to determine both the volume and the nature (i.e. time lag, flow durations, etc.) of response of this hillslope to rainfall. Unfortunately, the data recorded from this experiment for the 2010/2011 rainfall season is sparse due to equipment failure which frequently occurred soon after we left the catchment.

Hydrus 1-D simulations

The change in water content and potential fluxes at TB4 was simulated from 11/01/2011 at 14:00 till 19/10/19 at 11:00 with Hydrus 1-D (Simunek *et al.*, 2008). This period was selected since it was the longest period of time where all instruments were in working order, i.e. DFM probes, tipping bucket measuring outflow at TB and logger measuring rainfall. Some of the important parameters used in the simulations are presented in Table 7.

Table 7 Hydrus 1-D descriptions used for simulation of water flow at TB4

| Description | Value/unit |
|-----------------------------------|------------------------------------------|
| Length units | mm |
| Number of soil materials | 4 |
| Decline from vertical axis | 0.83 |
| Depth of profile | 2000 |
| Time units | hours |
| Initial time | 0 |
| Final time | 190 |
| Time-Variable boundary conditions | 190 |
| Hydraulic model | Van Genuchten – Mualem |
| Upper boundary condition | Atmospheric boundary with surface runoff |
| Lower boundary condition | Free drainage |

Van Genuchten parameters optimized with the RETC software, were used for the top three soil materials at TB4. A very low K_s value (0.002 mm h^{-1}) was attributed to the fourth material in order to represent the hydrological character of the Molteno bedrock. Measured average hourly rainfall (mm) and an evapotranspiration rate of 0.1 mm h^{-1} was used to represent the upper boundary condition. Initial water contents were obtained from DFM probe measurements expressed as averages for the *ot*, *gs* and *gh* horizon. A total of 7 observation nodes were inserted at 100, 200, 300, 400, 600, 800 and 1200 mm, respectively. The 100-400 mm nodes represent the *ot* horizon, 600 and 800 mm the *gs* horizon and the 1200 mm node represents the *gh* horizon. Simulated water contents were compared with measured water contents.

2.3.3 RESULTS AND DISCUSSION

Soil properties of profiles in the TB area

Selected properties of the profiles at DFM nests in the TB area are presented in Table 8. Profiles TB1-TB4 all classify as Kroonstad soil forms with thick *gs* horizons dominating. These horizons are indicative of removal of colloidal material in a predominantly lateral direction (Soil Classification Working Group, 1991) resulting in gleyed (high value, low chroma Munsell notation) colours. The absence of the *gs* horizon directly underneath the *ot* horizon at TB7 and TB9 is an indication that these profiles are drier than profiles TB1-TB4.

There is a marked change in the colour of the *ot* and the *gs* horizons from TB2 to TB4, where the chroma of the higher lying profiles are higher than that of the lower lying profile (Table 8). Comparisons between colours of TB1 were not made due to differences in the hue, although the surface horizon of TB1 showed gleyed colours, which is not the case for TB3 and TB4. The decrease in chroma is possibly an indication that the profiles closer to the outcrop are saturated for longer periods and/or that removal of colloidal material occurred more intensively at the lower lying positions.

Estimated clay contents of the *ot* and *gs* horizons are low ($<10\%$), whereas a distinct increase in the clay content is observed from *gs2* to *gh* horizons. In general an increase occurs in the clay content of the *gh* with increased distance from the rocky outcrop, i.e. 15, 25, 30 and 35% for TB1-TB4, respectively. This signifies increased weathering, illuviation and neo-formation of clay in the wetter downslope positions. The distribution of selected chemical properties is presented graphically in Figure 93.

Table 8 Selected soil properties at different profiles at TB, chemical properties measured with MIR

| Location | Soil Form | Horizon | Depth mm | Dry | Wet | Gleyed* ¹ | Clay % | Ca | Mg | K | Na | CEC clay | CEC soil | Base sat % | pH H ₂ O | pH KCL | Org C % | N | Fe mg kg ⁻¹ | Mn |
|----------|-----------|---------|-------------|----------|----------|----------------------|-----------|-----|-----|-----|-----|------------------------------------|----------|---------------|------------------------|-----------|------------|-------|---------------------------|------|
| | | | | | | | | | | | | cmol _c kg ⁻¹ | | | | | | | | |
| TB1 | Kroonstad | ot | 200 | 7.5YR5/2 | 10YR4/2 | yes | 7.5 | 1.8 | 1.5 | 0.1 | 0.2 | 89.0 | 12.4 | 23.2 | 5.3 | 4.7 | 0.3 | 228.3 | 9594.9 | 8.8 |
| | | gs1 | 450 | 7.5YR6/3 | 10YR6/3 | yes | 5 | 0.4 | 0.4 | 0.1 | 0.1 | 64.7 | 7.4 | 15.9 | 5.0 | 4.4 | 0.1 | 142.0 | 9265.4 | 15.6 |
| | | gs2 | 700 | 10YR6/3 | 10YR6/6 | yes | 7.5 | 1.0 | 0.9 | 0.1 | 0.1 | 80.0 | 7.5 | 23.5 | 4.9 | 4.2 | 0.3 | 284.2 | 4646.3 | 20.0 |
| | | gh | 850 | 10YR6/4 | 10YR7/8 | yes | 15 | 3.5 | 3.1 | 0.2 | 0.2 | 47.5 | 10.4 | 51.3 | 4.7 | 4.0 | 0.5 | 410.5 | 1331.6 | NC |
| TB2 | Kroonstad | ot | 200 | 10YR5/2 | 10YR3/2 | yes | 7.5 | 2.9 | 2.3 | 0.2 | 0.1 | 71.4 | 9.3 | NC | 4.8 | NC | NC | 577.0 | 5142.0 | 19.0 |
| | | gs1 | 500 | 10YR5/3 | 10YR5/3 | yes | 10 | 1.4 | 1.1 | 0.1 | 0.2 | 58.1 | 7.8 | 31.4 | 5.1 | 4.3 | 0.3 | 280.4 | 3923.6 | 14.4 |
| | | gs2 | 900 | 10YR7/2 | 10YR5/6 | yes | 5 | 1.4 | 1.0 | 0.1 | 0.2 | 92.6 | 8.8 | 23.7 | 4.9 | 4.6 | 0.3 | 287.6 | 6514.8 | 7.8 |
| | | gh | 1200 | 7.5YR7/6 | 7.5YR6/8 | no | 25 | 5.2 | 4.9 | 0.3 | 0.2 | 55.3 | 16.6 | 62.0 | 5.3 | 4.2 | 0.5 | 413.9 | NC | 16.4 |
| TB3 | Kroonstad | ot | 100 | 10YR5/3 | 10YR5/3 | yes | 7.5 | 5.0 | 4.6 | 0.2 | 0.2 | 51.4 | 16.5 | 48.7 | 5.0 | 4.0 | 0.5 | 361.1 | 1947.6 | 18.4 |
| | | gs1 | 600 | 10YR6/4 | 10YR5/4 | yes | 5 | 1.3 | 1.2 | 0.1 | 0.2 | 84.7 | 10.4 | 21.9 | 5.2 | 4.4 | 0.4 | 377.3 | 5535.6 | 13.1 |
| | | gs2 | 1200 | 10YR7/3 | 10YR5/6 | yes | 5 | NC | NC | NC | 0.2 | 18.8 | NC | 62.2 | 5.2 | NC | NC | NC | NC | NC |
| | | gh | 1620 | 10YR8/1 | 10YR7/2 | yes | 30 | NC | NC | NC | NC | NC | NC | NC | NC | NC | NC | NC | NC | NC |
| TB4 | Kroonstad | ot | 450 | 10YR5/6 | 10YR4/6 | no | 7.5 | 1.3 | 1.2 | 0.1 | 0.1 | 74.5 | 8.7 | 25.2 | 5.0 | 4.4 | 0.5 | 392.8 | 4358.5 | 16.4 |
| | | gs1 | 800 | 10YR5/3 | 10YR5/3 | yes | 10 | NC | NC | 0.2 | 0.2 | 37.2 | 7.3 | 52.9 | 5.0 | 4.1 | 0.5 | 381.7 | 3192.7 | 24.0 |
| | | gs2 | 1000 | 10YR7/4 | 10YR6/4 | yes | 7.5 | 1.8 | 1.7 | 0.2 | 0.2 | 72.6 | 10.5 | 27.4 | 5.2 | 4.5 | 0.4 | 383.8 | 4466.4 | 13.5 |
| | | gh | 1650 | 10YR8/1 | 10YR7/2 | yes | 35 | 5.0 | 4.4 | 0.3 | 0.2 | 49.2 | 15.5 | 55.6 | 5.2 | 4.2 | 0.6 | 460.0 | 1763.0 | NC |
| | | so1 | 1750 | 10YR7/6 | 10YR7/8 | no | 30 | 6.7 | NC | 0.5 | 0.3 | 27.8 | NC | 61.6 | 5.0 | 4.6 | NC | NC | 2100.3 | NC |
| | | so2 | 1950 | 2.5YR7/6 | 10YR7/8 | no | 25 | NC | NC | NC | NC | 34.6 | NC | NC | NC | NC | NC | NC | NC | NC |
| TB7 | Pinedene | ot | 480 | 10YR5/4 | 10YR4/4 | no | 5 | 2.0 | 1.8 | 0.2 | 0.2 | 71.3 | 9.9 | 30.3 | 5.1 | 4.4 | 0.5 | 361.5 | 5093.1 | 14.9 |
| | | ye | 620 | 10YR6/6 | 10YR6/6 | no | 5 | 0.9 | 0.7 | 0.1 | 0.1 | 72.8 | 10.1 | 18.2 | 5.3 | 4.6 | 0.2 | 224.5 | 8335.6 | 6.7 |
| | | gs | 860 | 10YR7/4 | 2.5Y7/8 | yes | 5 | 0.0 | 0.0 | 0.0 | 0.1 | 95.2 | 10.4 | 4.8 | 5.4 | 4.8 | 0.3 | 292.6 | 9428.1 | 6.4 |
| | | on | 1260 | 10YR7/3 | 7.5YR7/8 | yes | 25 | 3.1 | 3.1 | 0.3 | 0.2 | 56.7 | 12.9 | 43.4 | 5.3 | 4.5 | 0.4 | 387.7 | 4164.2 | 12.5 |
| | | gh1 | 1600 | 10YR7/4 | 10YR7/3 | yes | 35 | 3.8 | NC | NC | 0.2 | 40.8 | NC | 59.6 | 5.2 | 4.3 | 0.7 | 426.5 | 3483.9 | NC |
| | | gh2 | 1720 | 10YR7/4 | 10YR7/8 | yes | 12 | NC | NC | 0.0 | 0.1 | 84.0 | 7.7 | NC | 5.5 | 4.9 | 0.0 | 58.3 | 16945.0 | NC |
| TB9 | Pinedene | ot | 520 | 7.5YR5/3 | 10YR4/4 | no | 7.5 | 1.1 | 0.9 | 0.1 | 0.1 | 90.6 | 9.1 | 22.2 | 5.2 | 4.5 | 0.5 | 391.0 | 5841.5 | 11.7 |
| | | ye | 800 | 7.5YR5/3 | 10YR5/6 | no | 7.5 | 1.6 | 1.4 | 0.1 | 0.1 | 83.8 | 8.8 | 28.8 | 5.0 | 4.2 | 0.4 | 374.1 | 2471.0 | 17.0 |
| | | gs | 1100 | 10YR6/3 | 10YR6/4 | yes | 7.5 | 0.7 | 0.6 | 0.1 | 0.1 | 97.8 | 9.9 | 16.1 | 5.2 | 4.4 | 0.3 | 304.1 | 5569.7 | 10.0 |
| | | gh1 | 1220 | 10YR6/3 | 10YR7/8 | yes | 15 | 0.7 | 0.6 | 0.1 | 0.1 | 70.7 | 10.3 | 13.7 | 5.4 | 4.7 | 0.0 | 99.1 | 13630.9 | 10.6 |
| | | gh2 | 1500 | 10YR8/1 | 10YR7/2 | yes | 25 | 4.4 | 4.1 | 0.3 | 0.2 | 52.2 | 15.1 | 49.7 | 5.3 | 4.2 | 0.3 | 336.5 | 2409.1 | 21.4 |
| | | gh3 | 1810 | 10YR7/1 | 10YR7/1 | yes | 30 | 6.5 | 6.0 | 0.4 | 0.3 | 40.6 | 18.4 | 68.9 | 5.3 | 4.2 | 0.3 | 426.7 | 22.5 | 18.1 |

*¹Gleyed colours as defined for *gs* horizon in the South African soil classification system (Soil Classification Working Group, 1991)

NC – No correlation: Value not fitting MIR calibration curve and therefore considered incorrect

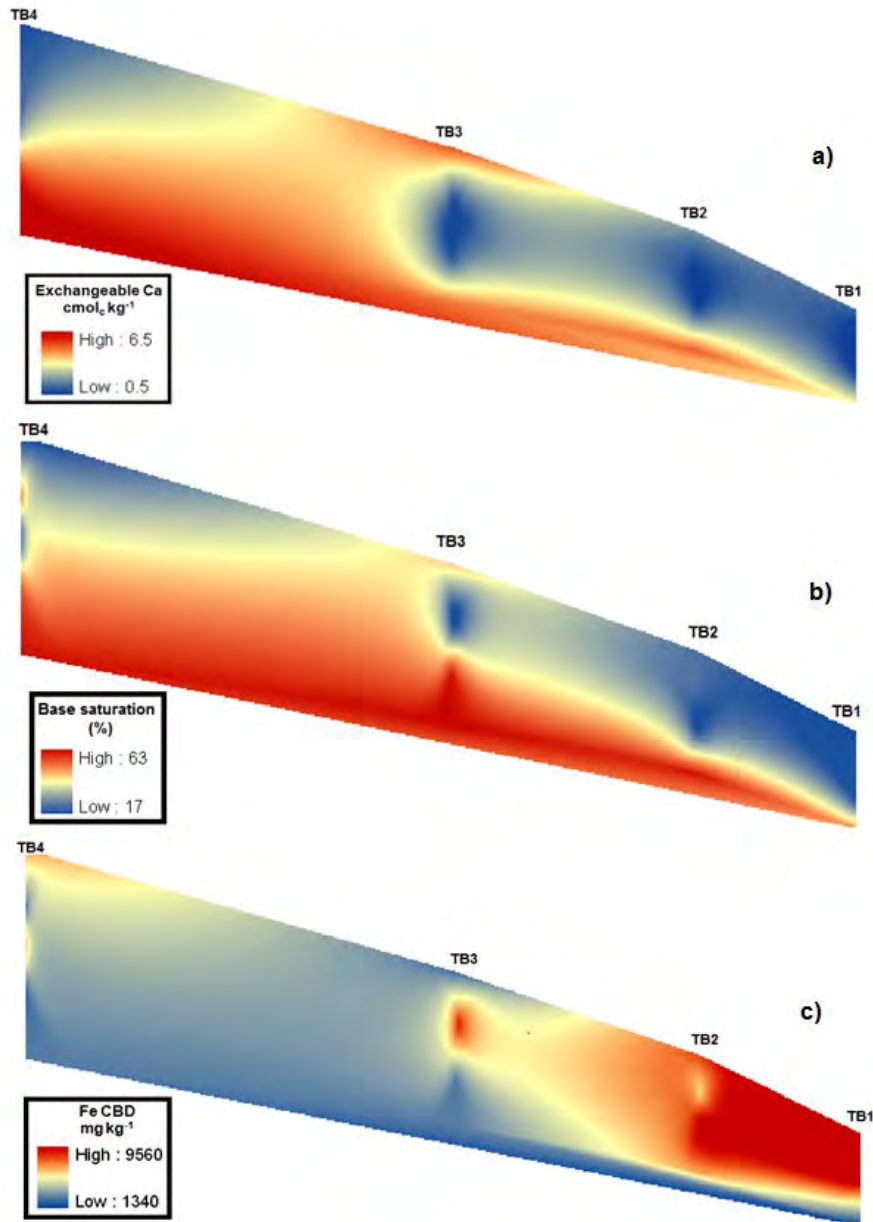


Figure 93 Interpolation of selected soil properties of the cross section TB1-TB4

Note that Figure 93 represents **interpolated** results of selected chemical properties as presented in Table 8 of the four profiles. The distance between the profiles is not uniform leading to possible inaccurate representations of the actual distributions of chemical properties. Sampling at closer horizontal and vertical intervals will improve the accuracy of the interpolations. We do believe however that, if the interpolations in Figure 93 are interpreted attentively, it might reveal interesting correlations between soil chemistry and the physical behaviour of the profiles.

Soil chemistry indicates that the *gh* horizon rather serves as storage mechanism with a small degree of slow lateral flow at the soil/bedrock interface. Both Ca ($\text{cmol}_c \text{ kg}^{-1}$) and base saturation (%) increase with depth (Figure 93a & Figure 93b) indicating limited vertical leaching. Higher clay contents of the deeper horizons (Table 8) with associated higher cation adsorption capacity can be attributed to this tendency. The accumulation of soluble Ca (and

other bases) in the *gh* horizon is also an indication that this horizon is not likely to be a conduit of water.

The increase in Ca and base saturation in the surface and *gs* horizons before TB3 (Figure 93a & Figure 93b) might be due to the relative increase in the thickness of the *gs* horizon between TB4 and TB1 (Figure 88). It was postulated that water will predominantly flow in the lower part of the *gs* horizon, i.e. on top of *gh* horizon. This will result in a possible decrease in the leaching of bases close to the surface and hence the higher Ca and base saturation values in the surface horizons before TB3. The spatial distribution suggests a strong hillslope effect dominating vertical processes.

The combination of a downslope increase in the volume of water and a decrease in the thickness of *gs* horizon from TB3 to TB2 possibly forces water to flow through the entire *gs* horizon and even in the *ot* horizon. This results in the decrease in Ca and base saturation of the *gs* and *ot* horizons at TB2 and TB1. The hillslope effect is not limited to immediately above the less permeable *gh* but extend to the *ot* due to systematic increase in water volume downslope.

The Fe content increase from TB4 to TB1. The deeper layers have a markedly lower Fe content than that of the surface horizons in the vicinity of TB3, TB2 and TB1. Longer periods of saturation and resulting in reduction of Fe, from insoluble ferric to soluble ferrous state, and capillary rise during low water contents in the *gs* might be the reason for low Fe contents in the *gh* horizon. These distributions support the low flow/storage role assigned to *gh* horizons.

A possible explanation of the high Fe contents at TB2 and TB1 is that water accumulates at the bottom of the slope during the rainy season following the well-known *saturated wedge* concept (Weyman, 1973). As the soil water content decrease during the dry season aerobic conditions predominate, dissolved Fe is then oxidized to the insoluble ferric state. Large amounts of dissolved Fe, leached from upslope, accumulate at the bottom of the slope and precipitate during the dry season resulting in relatively higher Fe contents at TB2 and TB1. Lack of morphological support is an indication that these properties are in a storage equilibrium of supply and removal. Water exiting the soil and draining over the Molteno sandstone outcrop remove significant amounts of Fe and Mn. This is visible as black Mn precipitates covering the white sandstone outcrop.

Hydraulic conductivities

Double ring, tension infiltrometer and mobile permeameter measurements

Measured hydraulic conductivities for different sites and horizons are presented in Table 9.

Table 9 Vertical and lateral hydraulic conductivities (mm h^{-1}) for different sites and horizons

| Site | Horizon | Direction | K_s method | K_s | Unsaturated K at tension (mm) | | | |
|------|-----------------|-----------|------------------|-------|-------------------------------|-----|-----|-----|
| | | | | | 5 | 30 | 60 | 150 |
| LC2 | ot | vertical | DR* ² | 92.2 | ND | 2.2 | 1.3 | 0.3 |
| LC2 | ot | lateral | DR | 103.8 | ND | 1.4 | 0.9 | 0.2 |
| LC2 | ye | vertical | DR | 50.0 | ND | 0.8 | 0.6 | 0.2 |
| LC2 | ye | lateral | DR | 321.3 | ND | 2.3 | 1.6 | 0.8 |
| TB4 | ot | vertical | DR | 139.5 | 4.2 | 2.4 | 0.9 | 0.4 |
| TB4 | gs1 | vertical | DR | 41.1 | 12.2 | 6.6 | 2.9 | 2.3 |
| TB4 | gs2 | vertical | DR | 56.7 | 36.0 | ND | 9.6 | 2.8 |
| TB4 | gh | vertical | DR | 2.5 | 0.9 | ND | 0.8 | 0.7 |
| TB4 | R* ¹ | vertical | MP* ³ | <0.02 | ND | ND | ND | ND |

*¹Bedrock interface *²Double ring; *³Mobile permeameter; ND: not determined

The hydraulic measurements in Table 9 show a general decrease in the saturated hydraulic conductivity (K_s) with depth except for the lateral sample of the *ye* horizon at LC2 and the *gs2* horizon at TB. The higher K_s of *ye* horizon at LC2 can be attributed to a layer with coarse fragments between 350 and 550 mm. The vertical K_s of the *ye* is 6 times lower than that of the lateral measurement. This coarse layer in the *ye* horizon of LC2 might therefore be a conduit for water. The slight increase in K_s of *gs2* when compared to *gs1* might be the result of lateral flow dominating in *gs2*, promoted by the relatively impermeable *gh* horizon. Long periods of lateral flow in the *gs2* horizon could have caused more intense illuviation of colloidal material, especially clay, (Table 8) resulting in higher conductivities in this horizon (Table 9).

The difference between vertical and lateral hydraulic conductivities is an area of study neglected in the past. If the anisotropy in terms of the K_s is as principal as expressed in the *ye* horizon of LC2, this is a field definitely worth studying in the future.

A sharp decrease in the hydraulic conductivity was measured in the LC2 as well as the *ot* horizon of TB4 when a small tension was applied. The importance of the contribution of macropores in these horizons is accentuated. This was not the case in *gs* horizons of TB4 indicating that flow through meso- and micropores are probably more dominant in this horizon.

Slug tests

K_s values determined with the slug tests and the Hvorslev (1951) method for different perforated pipes are presented in Table 10. The K_s values represent the conductivity of the total profile beneath the water table and will therefore differ from values obtained with double ring and mobile permeameter methods (Table 9).

Table 10 K_s values determined below the water table with slug tests

| Pipe | TB1 | TB2 | TB5 | TB8 | SPTB7-gs |
|--------------------------------------|------|------|------|------|----------|
| Water table depth below surface (mm) | 200 | 240 | 200 | 240 | 390 |
| K_s (mm h ⁻¹) | 31.1 | 31.7 | 35.6 | 23.4 | 46.2 |

Since the slug tests represents integrated K_s values of the profile, lower rates were expected. This was indeed the case. If we assume that the soils at TB5 and TB8 are similar to that of TB1, the water table did not rise into the *ot* horizon. The relatively high conductivity values of the *ot* horizon did therefore not increase the integrate conductivity of the profile. The low conductivity of the *gh* horizon decreased the integrated conductivity of the profiles.

Slug tests in slotted pipe, i.e. *SPTB7-gs*, provided K_s values very comparable with the double ring infiltration measurements (Table 9). Although the water table rose into the *ot* horizon (Table 8 & Table 10) the relatively high conductivity of the *ot* horizon did not increase the measured conductivity, suggesting that this slotted pipe represent the flow in the *gs* horizon accurately.

Slug tests are an easy, cost effective method that should be exploited more in future to determine the dominant flow path of water in profiles under saturated conditions.

Water retention and hydraulic conductivity curves

The optimized Van Genuchten parameters for the profile at TB4 are presented in Table 11. The parameters were optimized by fitting both measured water release characteristics and measured hydraulic conductivities at and close to saturation. The water retention curves of the different horizons are presented in Figure 94 and the hydraulic conductivity curve in Figure 95.

Table 11 Van Genuchten parameters of different horizons at TB

| Parameter | <i>ot</i> | <i>Gs</i> | <i>gh</i> |
|------------|-----------|-----------|-----------|
| θ_r | 0.055 | 0.019 | 0.078 |
| θ_s | 0.308 | 0.354 | 0.387 |
| α | 0.070 | 0.010 | 0.002 |
| n | 1.155 | 1.288 | 1.264 |
| m | 0.134 | 0.223 | 0.209 |
| λ | 0.500 | 0.500 | 0.500 |
| K_s | 139.500 | 41.000 | 2.500 |

The optimized parameters were used in equation 3 and 5 to estimate the water contents under different suctions (Figure 94) and hydraulic conductivity at different water contents (Figure 95).

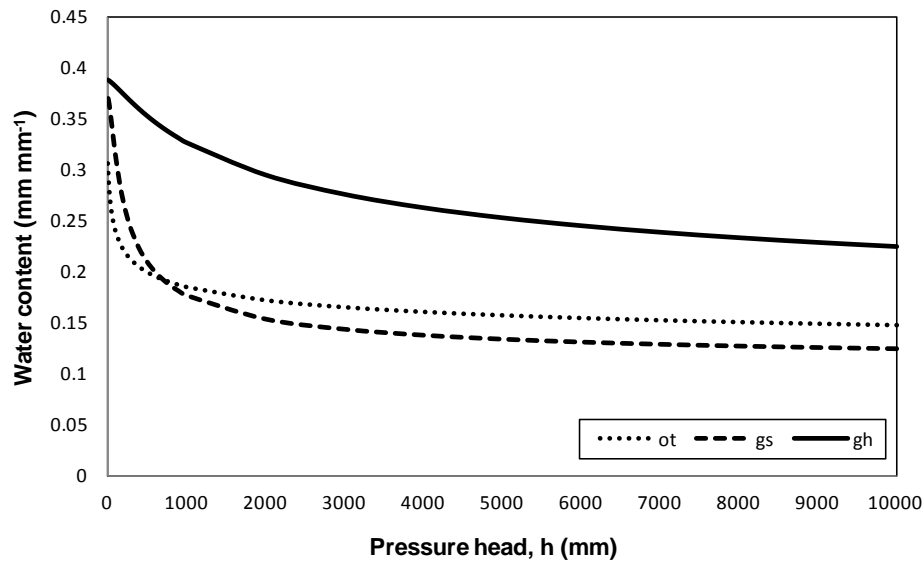


Figure 94 Water retention curves of different horizons at TB

A steep decline in the water content with small differences in the pressure head is evident in the *ot* horizon. The presence and dominance of larger pores can be attributed to this phenomenon. The sharp decline was also observed in the *gs* horizon although it was not as prominent. At approximately 1000 mm suction the *ot* horizon show very little decrease in water content with increased suctions; a similar inflection point is evident at around 2000 mm for the *gs* horizon. The *gh* horizon showed a much steadier decline in the water content than the *ot* and *gs* horizons. The prominence of micropores can be attributed to the high water holding capacity observed in the *gh* horizon.

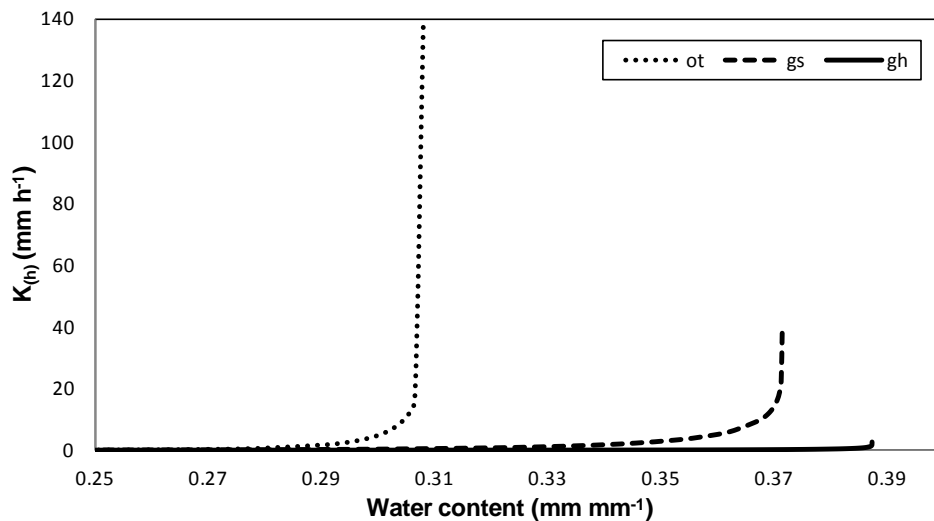


Figure 95 Hydraulic conductivity at different water contents for horizons at TB

The sharp decrease in the hydraulic conductivity at low tensions is evident in the *ot* horizon of TB4 (Figure 95). The *gs* horizon shows a more even decrease close to saturation and the

hydraulic conductivity of the *gh* horizon is shown to be insignificant when compared to the conductivities of the *ot* and *gs* horizons.

Lateral flow measurements

Trench experiment

Lateral flow volumes (ℓ) measured in the different buckets at the profile trench experiment is presented in Table 12. It was unfortunately not possible to isolate an individual rain event. A non-linear relationship between inflow and rainfall volumes is shown in Table 12, highlighting the influence of environmental conditions such as rainfall intensity and antecedent conditions on volumes of lateral flow.

Table 12 Volumes (ℓ) measured at different depths at profile trench experiment

| Date measured | Total rain (mm)* | Pipe 1 (300 mm) | Pipe 2 (700 mm) | Pipe 3 (1000 mm) | Pipe 4 (1400 mm) | Pipe 5 (1900 mm) |
|---------------|------------------|-----------------|-----------------|------------------|------------------|------------------|
| 28/09/2010 | 55 | 2.2 | 0 | 0 | 0 | 0 |
| 13/11/2010 | 168 | 1.9 | 0 | 0 | 0 | 0 |
| 11/01/2011 | 361 | 4.0 | 8.5 | 9.2 | 8.9 | 13.7 |
| 31/01/2011 | 83 | 2.8 | 2.5 | 3.4 | 3.4 | 4.3 |

*Total volume of rain between measurements

Due to the limited measurements the data from Table 12 is only valuable to confirm the presence of lateral flow at LC2 and that lateral contributions are from all the horizons. One may also conclude that lateral flow occurs during most rain storms in the first 300 mm, but only occurs when the profile is wet (i.e. during the middle and end of the rain season) in the lower horizons.

Slotted pipes

Volumes (ℓ) of lateral flow measured in different horizons on various locations with slotted pipes are presented in Table 13.

Table 13 Volumes (ℓ) measured in pipes slotted at various depths

| Date measured | Total rain (mm)* | SPTB9-ot | SPTB9-gs | SPTB7-ot | SPTB7-gs | SPLC1-ot | SPLC1-ot |
|---------------|------------------|----------|----------|----------|----------|----------|----------|
| 11/01/2011 | 361 | 0.13 | 1.27 | 1.39 | 1.63 | 1.55 | 0.8 |
| 31/01/2011 | 83 | 0.11 | 0.96 | 1.32 | 1.00 | 0.13 | 1.38 |
| 05/04/2011 | 371 | 0.16 | 0.96 | 0.22 | 1.00 | ND | ND |

*Total volume of rain between measurements; ND – not determined

As with the trench experiment, the non-linearity between volume of rain and volume of water recorded in the pipes are evident (Table 13). It would therefore be erroneous to interpret the results with the limited amount of information. The need for continuous logging devices in the slotted pipes or more frequent field visits, especially during rain events is evident. It is however encouraging to see that lateral flow can be recorded with the experimental procedure.

Figure 96 Water content measurements

Due to the problems experienced with the calibration of the DFM probes, only measurements of water tables at selected probes will be reported. These measurements are presented in Figure 96.

Interestingly, the water table at TB4 is closer to the surface than the water table at TB3. One would expect that there would be a downslope increase in the height of the water table, i.e. a decrease in the distance from the surface. The lag time of response show the typical behaviour associated with the *saturated wedge* concept (Weyman, 1973). According to this concept, saturation should occur before outflow at the bottom of the slope will take place. As the water content of hillslope increases, during a rain event or rainy season, the saturated wedge will progress upslope, increasing the hydraulic head behind the outflow point and resulting in higher flow volumes.

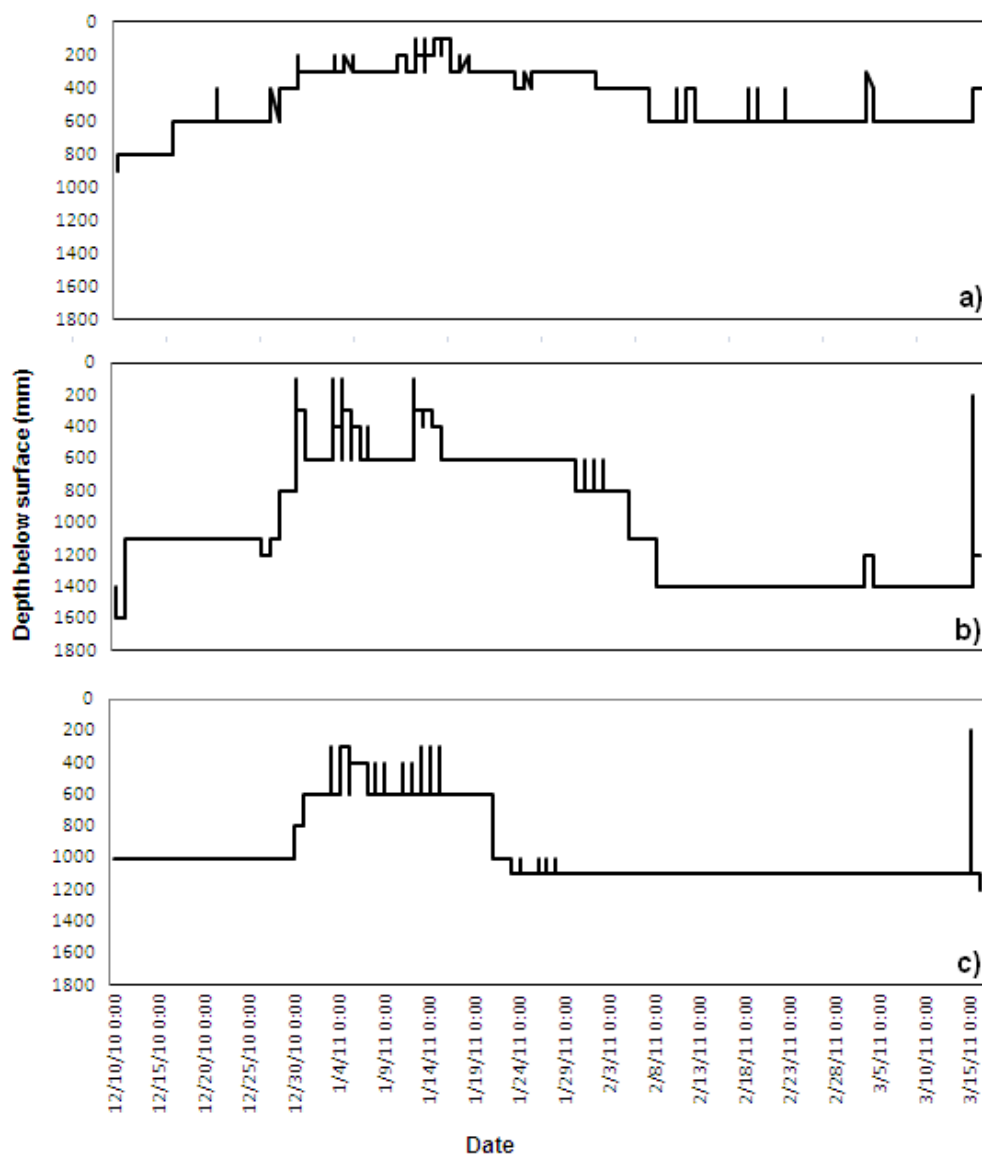


Figure 96 Presence of saturated water at TB2 (a), TB3 (b) and TB4 (c) as measured with DFM probes

The first increase in the water table was recorded on the 16th of December 2010 when the recorded water table rose to around 600 mm below the surface at TB2 with no response at upslope TB3 and 4 (Figure 96). About 12 days (270 hours) after this, on the 28th of December 2010, the depth to the water table at TB3 decreased significantly, from 1100 to 800 mm. Some 54 hours a later water table fluctuation was observed in TB4 when the water table rose to about 800 mm. The expansion of the saturated wedge therefore occurred at roughly 8 mm h⁻¹ between TB2 and TB3 and at a rate of about 80 mm h⁻¹ between TB3 and TB2. There can be a great number of possible explanations for this difference in the expansion rate of the saturated wedge. Without detailed water content data these explanations will however remain only speculations.

Hillslope outflow

Outflow measured with the tipping bucket (Figure 92) is presented for the period 2011/01/11 to 2011/01/19 (Figure 97). The x-axis represents time, expressed as hours after 14:00 on 2011/01/11.

The quick response of the outflow to rainfall is evident in Figure 97. The exposed impermeable bedrock, just above the opening of the pipe leading to the tipping bucket (Figure 92), will facilitate the generation of overland flow, resulting in the quick responses recorded by the tipping bucket. The contribution from subsurface flow is apparent as the decrease in the slope of the outflow curve after the peak measured during individual rain events. When the slope is nearly flat (e.g. between the 2nd and 13th hours, and again between the 79th and 91st hours) we assume that the flow was due to subsurface lateral flow, amounting to approximately 40 mm. h⁻¹. Confirmation for this is provided by the data in Table 9 which shows that the K_s of the *gs* horizon at TB4 (considered to be representative of the *gs* horizons of the TB area) are similar, ranging between 41 and 57 mm h⁻¹. Further, and even more convincing confirmation of the interflow rate is provided by the water table slug test results in Table 10 which gives the K_s values of the *gs* horizon (depths given in Table 8) at TB1 and TB2 at around 31 mm h⁻¹. It is clear that the *gs* horizons are responsible for most of the flow when quickflow stopped. TB2 is located about 2 m above the Molteno shelf (Figure 87c and Figure 88). In Figure 98 the relationship between the outflow measured by the tipping bucket and the water table depth at TB2 over the same period is shown. There is a reasonable correlation between the peaks and level portions of the graphs. The rate of lateral flow corresponds well with the water table depth measured at TB2 (Figure 98). When the water table at TB2 is close to the surface, the lateral contributions from the hillslope are higher (Figure 98). With an increase in the water table depth the lateral contributions are lower and will probably be non-existent once the water table resides to the *gh* horizon during the dry months.

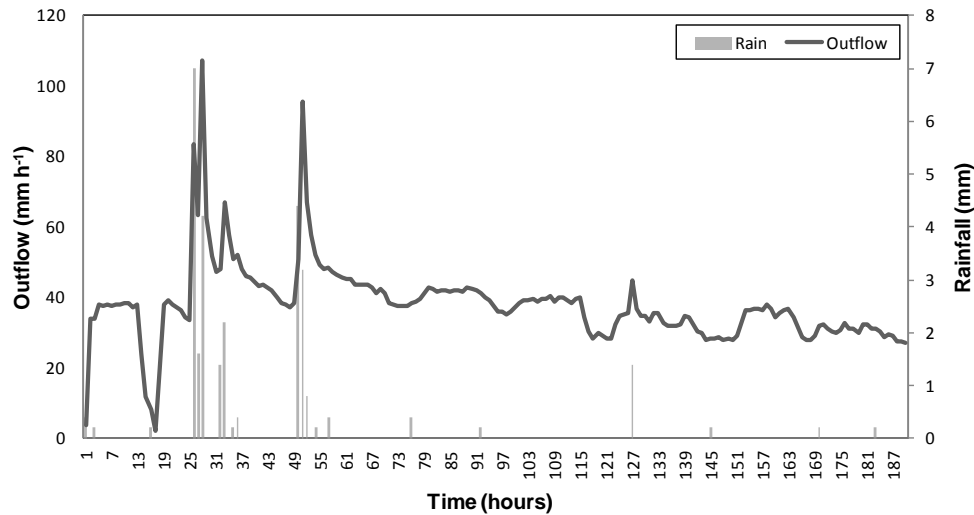


Figure 97 Rainfall (mm) vs. outflow (mm h^{-1}) measured at the hillslope outflow experiment.

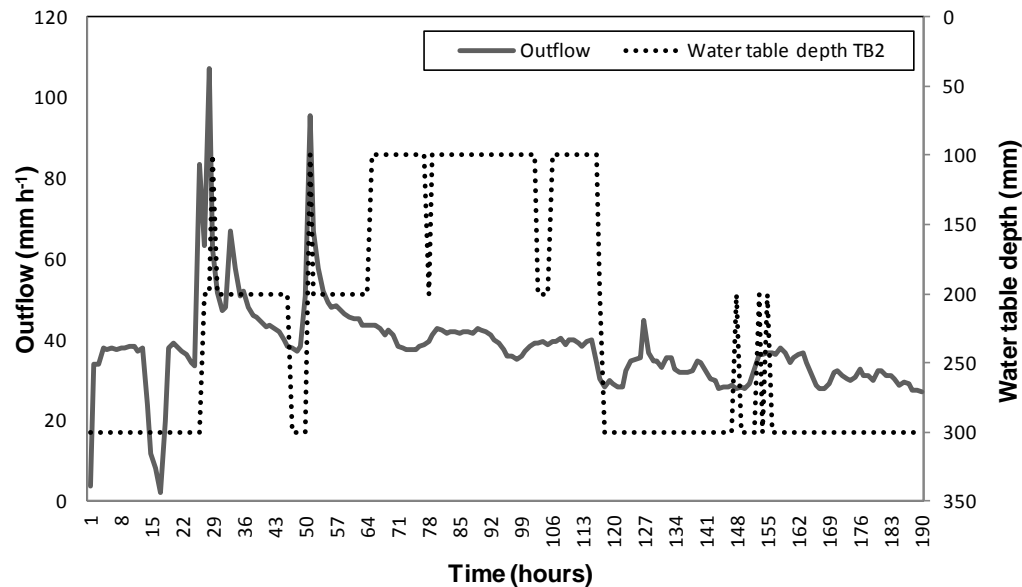


Figure 98 Measured outflow rate (mm h^{-1}) and water table depth from the surface at TB2

3.3.3 Simulation with Hydrus 1-D

Simulated vs. measured water contents of the *ot* horizon at TB4 are presented in Figure 99. Simulations of the *gs* and *gh* horizons are not presented graphically as both simulated and observed showed saturated conditions (water table) for the duration of the simulation period.

Simulations incorrectly predict a decline in the water content of the *ot* horizon before the series of rainfall events starting on 24th hour. Thereafter the simulated water contents increased to the correct value at the 50th hour. From the 50th hour simulated water contents are slightly too high at saturation for approximately 55 hours from where the water content gradually decreased possibly due to evaporation (Figure 99).

Measured water contents showed similar trends as those simulated. The relatively rapid decrease in the beginning of the simulated period was however not imitated, suggesting that evapotranspiration was probably overestimated during this period.

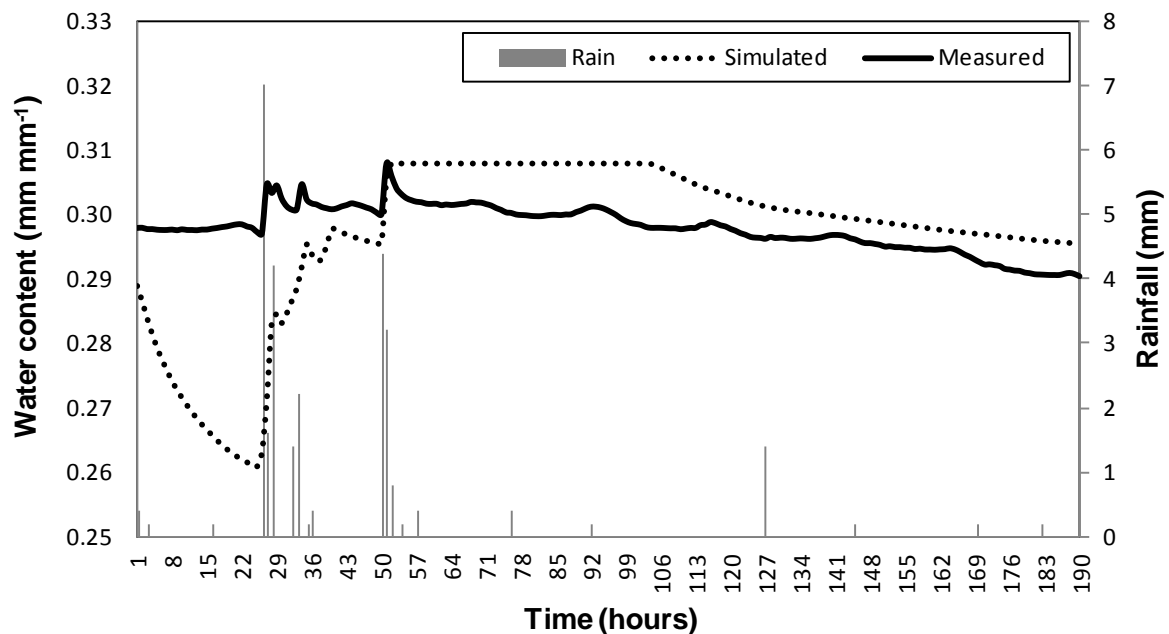


Figure 99 Simulated vs. measured water contents of the *ot* horizon at TB4, together with the daily average rainfall

Simulated and measured water tables were reached on exactly the same time, unlike the simulated results; the measured water table quickly decline out of the *ot* horizon. The constant water content of both the *gs* and the *gh* horizon suggests that vertical drainage from the *ot* to the underlying horizons took place. If outflow from the *gs* horizon occurred at roughly 40 mm h^{-1} as suggested by Figure 97, the vertical feed from the *ot* horizon is too little to keep the *gs* at saturation. Lateral inflow from upslope soils is therefore responsible for maintaining the water table in the *gs* horizon.

2.3.4 Conclusions

This chapter report on the instrumentation and preliminary results of portions of a hillslope in the Weatherley research catchment, South Africa. Weatherley is a well instrumented catchment but we believe that the additional instrumentation will reveal a greater comprehension of the complex hydrological system and of the forces driving it.

Soil morphology serves as a good indicator of the dominant flowpaths in the hillslope. Selected chemical properties confirm the interpretations from the morphology. Soil chemistry, especially the presence (or absence) of easily dissolvable cations, is probably a more recent indicator of hydrology than soil morphology, which can often be indications of historical hydrological behaviour. Future efforts will focus more on the interpretation of the spatial distributions of soil chemical properties on hillslope scale.

The inability to calibrate most of the installed DFM probes is distressing; we are however aiming to rectify this problem in the near future. Preliminary results of the capability of the probes to record the presence of water tables are encouraging.

The hydraulic conductivity of different horizons was measured *in situ* and a method to measure the saturated hydraulic proposed. Preliminary results of the B-horizon at LC2 suggest that significant differences between the vertical and horizontal hydraulic conductivity might occur, an area definitely worth studying in future.

Both the trench experiment and the slotted pipes offer promising results. The inability to measure lateral flow during specific rain storms, i.e. smaller time intervals are however a snag. Continuous logging devices or more regular and longer duration field visits are might overcome this problem.

Outflow measured from the hillslope imply that subsurface lateral flow from the *gs* horizon is the contributing significantly to the outflow from the studied hillslope in between rain events. Simulations with the finite element model, Hydrus 1-D, supported our findings on this regard. Future studies will focus on simulations with 2 and 3-dimensional models.

Although the results are rather limited, we believe that the instrumentation procedure and setup in this hillslope will provide vital information on the hydrological behaviour of the hillslope, catchment and of similar hillslopes.

2.4 IN-SITU MEASUREMENTS OF TWO STREAMS

2.4.1 Introduction

The relationship that exists between soil profile morphology and soil water regimes facilitates the identification of flowpaths in a hillslope (Le Roux *et al.*, 2011), a prerequisite for quantifying streamflow. Soil water regimes play a major role in soil forming processes, which in turn result in the formation of specific soil properties (Soil Survey Staff, 1975). Soil water regimes are controlled by both flowpaths and flow rates (Le Roux *et al.*, 2011). Many soil properties influence the hydrological behaviour of soil profiles, which are also influenced by their position in the hillslope. Therefore, deducing the hydrological behaviour of soil profiles in hillslopes, can lead to better conceptualization of hillslope processes (Van Tol *et al.*, 2011).

Soils in most of the commercially afforested areas in KwaZulu-Natal are generally strongly to slightly acid and are highly leached (Land Type Survey Staff, 2002; Musto, 1994). In the Seven Oaks area of the KwaZulu-Natal midlands, soils with dominantly red and yellow-brown dystrophic, apedal B horizons, under dominantly humic A or orthic A horizons have been identified as one of the major groups of soils with Natal Group sandstone as parent material (Turner, 2000; Land Type Survey Staff, 2002; Le Roux *et al.*, 2013). Humic soils are widespread on cool, moist and elevated tablelands in this region, as a result of exposure to the easterly rain-bearing winds (Turner, 2000). They are generally associated with old land surfaces in the humid, eastern sea-board region of South Africa, especially in KwaZulu-Natal, the Pondoland coast and along the eastern escarpment region of Mpumalanga (Fey, 2013). The orthic A soil zones are located in slightly drier climates or at altitudes a little lower than the corresponding humic zones (Turner, 2000). However, the orthic topsoil group can also form in the moist, humid climate (Turner, 2000).

The dominant flowpath in these soils can be described qualitatively, based on their morphology, as vertical and recharging into the deep groundwater systems (Van Tol *et al.*, 2011; Van Tol *et al.*, 2010 a; Kuenene *et al.*, 2011, Ticehurst *et al.*, 2007). They do not show evidence of redox morphology (an indication of some degree of saturation) in any part of

the profile. However, annual rainfall and potential evapotranspiration need to be considered when classifying a soil as a recharge type, since arid soils might also lack redoximorphic features due to insufficient precipitation. The erroneous result can therefore be that the latter soils are classified as recharge, whereas they are not (Van Tol *et al.*, 2011). Other hydrological soil types classified based on profile morphology are interflow soils and responsive soils (Van Tol *et al.*, 2011). Interflow soils are associated with subsurface lateral flowpaths at either the A/B horizon or soil/bedrock interface. Responsive soils are either shallow on impermeable bedrock, or are close to saturation during rainy periods and therefore limited in storage capacity, resulting in the generation of overland flow after a rain event (Van Tol *et al.*, 2011).

A simple conceptual framework of hillslope hydrologic pathways has been used to evaluate the tropical rainforest soilscape following detailed measurements of saturated hydraulic conductivity (K_s) on different slope units (Elsenbeer, 2001). The study found the dominating vertical flowpath in a Ferralsol soilscape, which is similar to the hillslopes in the Two Streams catchment. The Acrisol soilscape was characterized by predominantly lateral and vertical flowpaths. Ferralsols are red and yellow weathered soils whose colours result from an accumulation of metal oxides, particularly iron and aluminium (Van der Watt & van Rooyen, 1995). Acrisols are soils having a B horizon with illuvial accumulation of clay and low base saturation (Van der Watt & van Rooyen, 1995). The underlying permeable bedrock facilitates infiltration of water in the recharge soils (Van Tol *et al.*, 2011). Because of high leaching status of most of KwaZulu-Natal soils under high rainfall, the degree of weathering of rocks can be high and very deep (Turner, 2000). Criteria for classifying hillslope hydrological responses in South Africa into different classes have been developed based on hydrological soil types (Van Tol *et al.*, 2013). The soil classes are determined by the type and position of the hydrological soil types in a hillslope. The distribution of soils along different hillslopes dictates the type of flowpath direction.

Studies on quantifying flowpaths are not new. For example, the rate of flow into the bedrock out of the soil layer in the Tanakami Mountains, central Japan was estimated as ranging from 0.5 to 3.3 m³ d⁻¹ (Uchida *et al.*, 2003), 50-5% of this water was contributed by bed rock groundwater to streamflow. At the Reedy Creek watershed in the Virginia coastal plain, baseflow was attributed to the drainage of shallow groundwater from the relatively (1-6 m thick) unconfined aquifer with 0.010 cm s⁻¹ saturated hydraulic conductivity (Eshleman *et al.*, 1994). Tracer and isotope techniques have also been used to quantify flowpaths (Rodgers *et al.*, 2005; Wenninger *et al.*, 2008).

Previous studies in this first order research catchment on which this study is focussed (Everson *et al.*, 2006 and Clulow *et al.*, 2011), show clearly the dominating influence of tree growth on the hillslopes and riparian zone on the catchment water balance. These studies provided an excellent opportunity to study soil water flowpaths and storage mechanisms, in conjunction with their detailed hydrological measurements on streamflow, evapotranspiration, rainfall and soil water contents monitored in the catchment since 2000. It is important to identify, define and quantify the pathways, connectivities, thresholds and residence times of components of flow making up stream discharge (Van Tol *et al.*, 2011). If these aspects are efficiently captured in hydrological models, accurate water resource predictions for estimating the hydrologic sensitivity of the land for cultivation, contamination and development, and for quantifying low flow mechanisms can be achieved

(Lorentz *et al.*, 2007; Uhlenbrook *et al.*, 2005; Wenninger *et al.*, 2008). Improving model predictions therefore involves a multidisciplinary approach which can provide solutions to problems of predicting streamflow. Streamflow prediction using the Agrohdrological Catchment Research Unit (ACRU) model in the research catchment showed that accumulated streamflow over time was overestimated despite necessary inputs which included soil information provided by pedologists (Le Roux *et al.*, 2011). Pedologists were of the opinion that their soil information would improve model performance, but this was not the case. A conclusion was that the soil information did not properly define the response coefficients required for model configuration. Defining response coefficients properly is not enough. Flowpaths and storage mechanisms also need to be identified and quantified as well as possible. This has not yet been done for this research catchment, and hence the motivation for the work described here. The hypothesis of the study was that, during the rainy season, infiltrated ET excess water mainly flows vertically and rapidly through deep recharge soils on the hillslopes to become stored in the saprolite, and then flows laterally to exit into the stream via responsive soils in the valley bottom.

2.4.2 Methodology

2.4.2.1 Study site

The investigation was conducted in a first order research catchment located in the Mistley-Canema Estate (Mondi Forests) in the Seven Oaks district (30.67°S, 29.19°E), approximately 70 km from Pietermaritzburg. The catchment lies within the Natal sandstone Group, which are predominantly greyish-white generally flat lying sandstones resting on the basement granite and gneiss. The bioregion is described as the midlands mistbelt grassland, characterized by hilly rolling landscape with a high percentage of arable land (Clulow *et al.*, 2011). Land use within the catchment comprises afforestation with black wattle (*Acacia mearnsii*) and there is also a 7.8 ha field of sugarcane on the east facing slope. The catchment covers an area of approximately 73.3 ha and is drained by one perennial stream (Figure 100). Annual rainfall is approximately 898 mm, concentrated during a rainy season extending from November through March.

A soil survey of the catchment was conducted in 2010. Detailed results are presented in Figure 100.

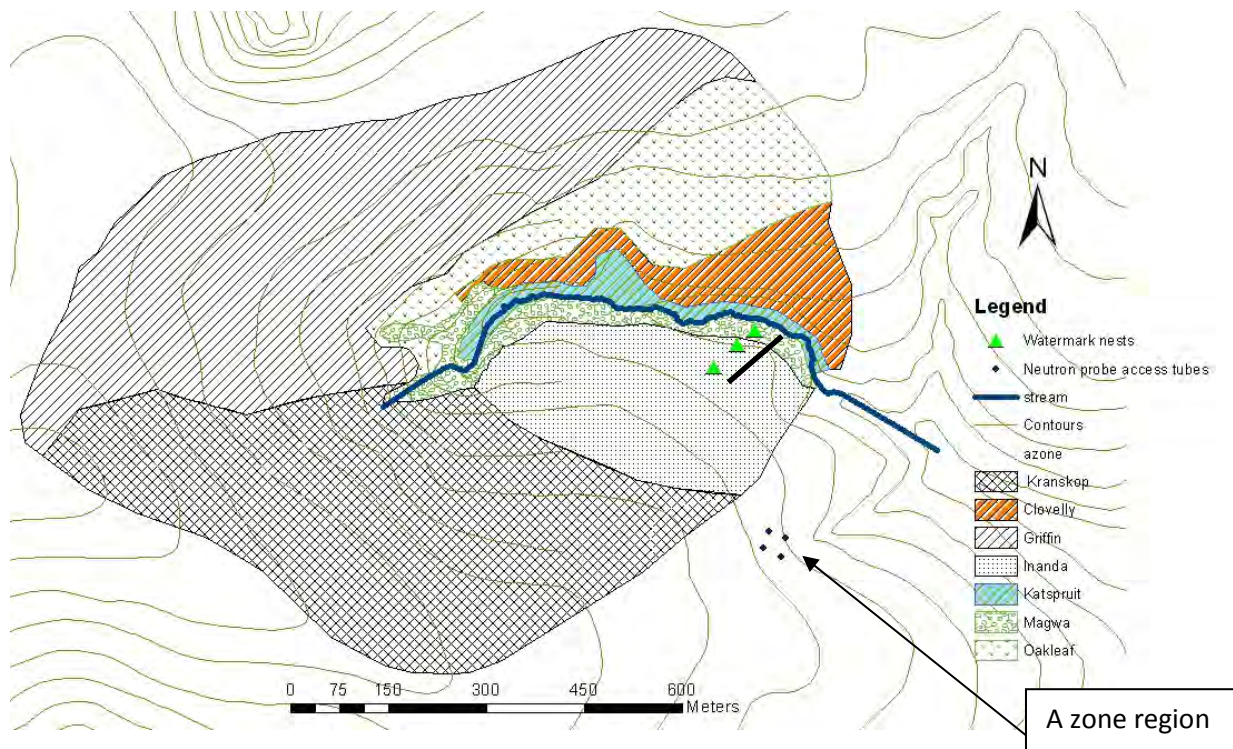


Figure 100 Detailed soil map of the Two streams catchment with location of watermark sensors a) and Neutron water meter access tube in the A zone region

Field measurements and methods

In November 2004 watermark sensors were established along a downslope north-south transect by Everson *et al.* (2006) (Figure 100). They measured soil matric potential, and were arranged in three nests of four watermark sensors each installed at roughly 400 mm, 800 mm, 1200 mm, and 2000 mm depths. All sensors were wired to a datalogger programmed to record soil water potential every 12 minutes. Because, hydrologically the soils on all three hillslopes are of the deep recharge type, for the purposes of this paper they are adequately represented by the results reported here from the three nests on the north facing hillslope (Figure 100).

Neutron water meters were used to measure soil water contents in the A zone region shown Figure 100 (Everson *et al.*, 2006). An A-zone hydrological region is described as a channel associated with ephemeral streams in the upper reaches of a water course that is not associated with a permanent body of saturated soil (Everson *et al.*, 2006). Results from four access tubes (Figure 100), installed to soil depths approaching 5 m, were used in this study. N2 and N3 are in a depression with a gentle north east slope. N4 and N5 are on opposite hillslopes with a slope of approximately 15%. The soils at the measuring sites are similar to those in the hillslopes of the research catchment.

The auger hole pump out method (Van Beers, 1983) was used to determine saturated hydraulic conductivity below the water table level in the saturated riparian zone near the stream bed.

2.4.3 Results and discussion

2.4.3.1 Hillslope characteristics

All the hillslope soils (Figure 100) are deep (2 meters) and of the recharge type with rapid hydraulic conductivity, overlying well weathered sandstone saprolite generally to a depth of around 4 to 5 meters.

A flat riparian zone up to 20 m in width forms a nearly complete border between the stream channel and surrounding hillslopes (Figure 100). The south facing hillslope rises sharply from the riparian zone at a gradient of 15%. The north facing hillslope rises gradually from the riparian zone at a slope of 13% at the Magwa soil profile, to 24% at the Inanda soil profiles. The head water (East facing) hillslope also rises sharply from the riparian zone at a slope of 12%. The relief of the catchment is generally moderately steep with an average 9% interfluve slope, whilst its altitude ranges from 1080 m.a.s.l. at the highest point along the catchment to 1085 m.a.s.l. at the streambed.

The soils are underlain by well weathered sandstone saprolite generally to a depth of 4-5 meters. The Inanda profile is situated in a lower midslope position with a slope of approximately 4% between the two watermark sensor nests (Figure 100). The Magwa profile is situated on a slope of 0.25% at the footslope just above the valley bottom, where the Katspruit soil is located. The Magwa profile is next to the lower nest of watermark sensors (Figure 100). K_s values increase dramatically with depth despite clay increases, and despite a high humus content in the A horizons (Chapter 7, section 7.5). This is attributed to the hydrophobic nature of the A horizons in this catchment. In most cases water repellence in soils can be attributed to coatings on the soil particles of hydrophobic substances of organic origin, especially under wattle plantations (Scott, 2000).

2.4.3.2 Evidence to support the hypothesis

Evidence was obtained from three sources viz. from the shape of the catchment hydrograph after large rain events; by comparing long term neutron water meter (NWM) soil water content measurements in an adjacent A zone area (Figure 100), in the solum (0-2.1 m), with those in the saprolite (2.55-4.65 m); and furthermore by studying daily soil water measurements in the representative hillslope soils of the catchment at four depths during a high rainfall period.

To analyse the hillslope response to precipitation and the influence of soils and saprolite on storage and possible flowpaths, a high rainfall period was selected in the 2004/05 rain season. The sharp peaks of the hydrograph (Figure 1004) are clearly due to storm flow, whereas the absence of any defined recession curve to the hydrograph indicated that the contribution to streamflow from the soil profile component of the hillslope was minimal.

The four access tubes used in the study are N2 and N3, located in the streamless depression, and N4 and N5 on opposite hillslopes sloping gently down to the depression (Figure 100). The soil in this A zone area is similar to those on the hillslopes of the research catchment. Due to the high hydraulic conductivities in the diagnostic A and B horizons, high saprolite recharge was expected. That this actually occurred is shown by comparing the long-term average soil water contents measured in the solum (0-2.1 m) with those in the saprolite (2.55-4.65 m) (

Table 14). These long-term results show that there had been, on average, approximately five times more downslope water movement in the saprolite compared with that in the solum, i.e. 312 mm and 60 mm, respectively.

The results of the daily soil water contents in the A and the B horizons of the representative hillslope soils show very few degree of saturation(S) values > 0.7 (Figure 102). Considering this in relation to the K_h values in Figure 227 (in section 7.5.2.2 of chapter 7) shows that, although there were presumably short periods of high water content in each of the horizons, they drained very rapidly in a vertical direction within a day to a water content at which K_h was very slow. The absence of any significant lateral water movement in the solum is demonstrated by the fact that the upslope and downslope S values in all the horizons are similar. There is no sign of water accumulation in the *on* horizon of the Magwa soil, even at a depth of 2 m.

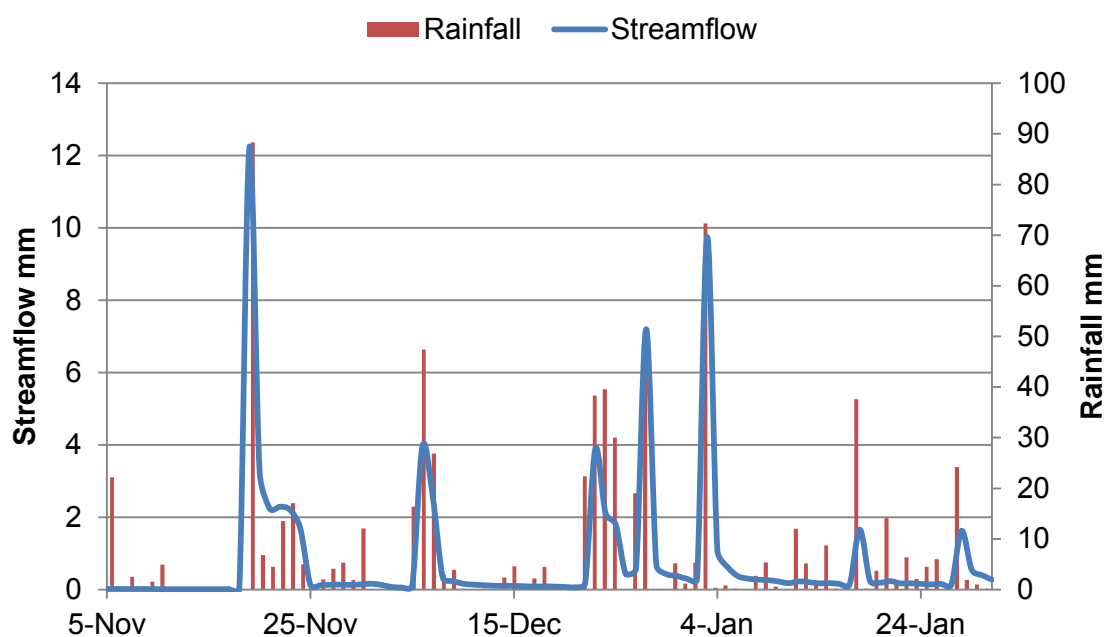


Figure 101 Streamflow vs rainfall during a wet period 5/11/2004-31/1/2005

Table 14 Ten measurements at different times of total soil water contents (mm) in the solum (0-2.1 m; upper vadose zone); and the saprolite (2.55-4.65 m; intermediate vadose zone), at hillslope and valley bottom locations in a terrestrial A zone area (Figure 100) close to the Two Streams catchment

| Reading date | Solum 0-2.1 m | | | Saprolite (2.55-4.65 m) | | |
|--------------|------------------------------------|-----------------------------------|------------|------------------------------------|--------------------------------|------------|
| | Depression (mean of N2 & N3) | Hillslope (mean of N4 & N5) | Difference | Depression (mean of N2 & N3) | Hillslope (mean of N4 & N5) | Difference |
| 3/12/2002 | 345 | 313 | 32 | 490 | 249 | 241 |
| 15/7/2003 | 443 | 399 | 44 | 628 | 299 | 329 |
| 19/8/2003 | 446 | 371 | 75 | 618 | 272 | 346 |
| 11/9/2003 | 433 | 359 | 74 | 614 | 279 | 335 |
| 16/10/2003 | 454 | 373 | 81 | 617 | 290 | 327 |
| 18/12/2003 | 464 | 386 | 78 | 623 | 306 | 317 |
| 9/1/2004 | 469 | 426 | 43 | 618 | 319 | 299 |
| 28/1/2004 | 491 | 459 | 32 | 625 | 350 | 275 |
| 29/6/2004 | 444 | 373 | 71 | 608 | 285 | 323 |
| 29/7/2004 | 453 | 384 | 69 | 625 | 297 | 328 |

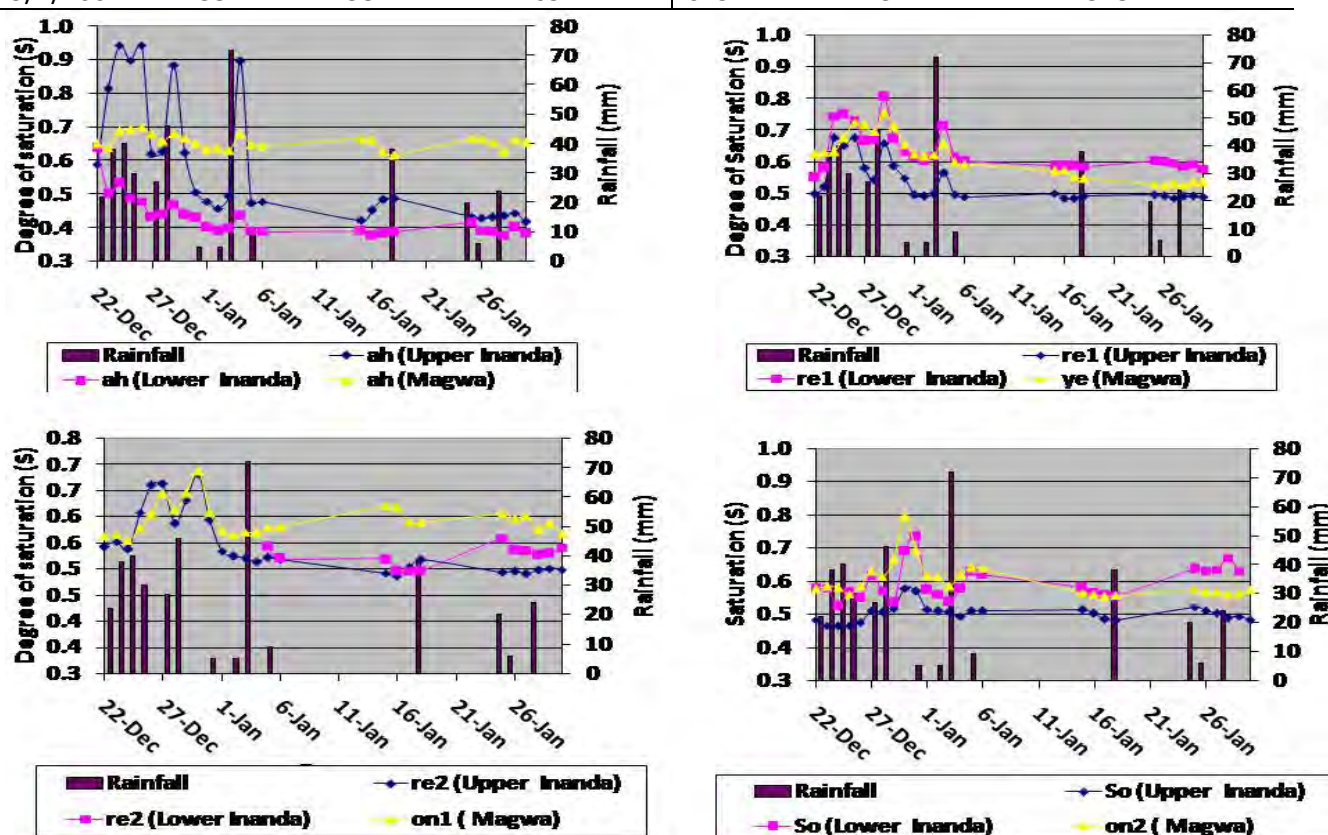


Figure 102 Daily rainfall from 22/12/2004-31/1/2005 and degree of saturation (S) obtained from mean daily measurements by watermark sensors located at depths of 400, 800, 1200 and 2000 mm (a, b, c, and d, respectively), at the three profiles in downslope order, upper Inanda, middle Inanda, Magwa, marked on Figure 100.

Catchment water balance data that supports the hypothesis

A water balance calculation was carried out for a 203 day high rainfall period, 6/9/2004-28/3/2005, for the catchment to obtain an estimate of the total hillslope saprolite storage (ST_{so}) during this period. This was done by means of the hypothesis described by the following equation:

$$\sum P - (\sum ET + \sum SF) = ST_{so} \quad (2.6)$$

Where ΣP , ΣET , ΣSF and ST_{so} represent the total precipitation, total evaporation, streamflow and hillslope saprolite storage respectively for the selected study period. ΣP , and ΣSF were obtained from unpublished data recorded by Everson *et al.* (2006), being 1085 mm and 82.34 mm respectively (Table 15). Outstanding is a value for ΣET for the high rainfall study period 6/9/2004-28/3/2005 using earlier research studies on the catchment made daily estimates of ET for the three vegetation types for the study period, thereby producing a reliable estimate of ΣET for the whole catchment (Table 15).

Table 15 Calculating ΣET (equation 2.6) for the catchment during the 203 period 6/9/2004 to 28/3/2005

| Parameter | Value |
|-------------------------------------------------------------------------------------------------|-----------------------|
| Sugarcane area (ha) | 7.8 |
| Riparian zone area (ha) | 7.5 |
| Treeless hillslope area (ha) | 58.0 |
| Total | 73.3 |
| Mean ET rates during the 203 day measuring period (mm d⁻¹) | |
| Sugarcane | 2.58 |
| Riparian zone | 3.72 |
| Treeless hillslope | 2.99 |
| ET (mm) for the 203 day measuring period | |
| Sugarcane | 523.74 |
| Riparian zone | 755.16 |
| Treeless hillslope | 606.97 |
| ET (m³) for the 203 day measuring period for different parts of the catchment | |
| Sugarcane | 4.0852×10^4 |
| Riparian zone | 5.6637×10^4 |
| Treeless hillslope | 35.2043×10^4 |
| Total (i.e. ΣET for equation 4.1) | 44.9532×10^4 |
| 44.9532 x 10 ⁴ m ³ for the whole catchment of 73.3 ha | |
| converted to mm = $(44.9532/73.3 \times 10^4) \times 1000 = 613 \text{ mm}$ | |

The solution of equation 2.6 is therefore, with all units in mm:

$1085 - (613 + 82.34) = ST_{so}$, giving $ST_{so} = 389.66 \text{ mm}$, which is equivalent to 256620 m^3 for the total hillslope area of $(58.0 + 7.8) = 65.8 \text{ ha}$.

It is this water, stored temporarily in the deep saprolite that, according to our hypothesis, provided the streamflow during the 100 day virtually rain free recession period (29/03/2005-06/07/2005) that followed immediately after the 203 day high rainfall period.

The rate of streamflow during this period starts at $123 \text{ m}^3 \text{ day}^{-1}$ and ends up at $23 \text{ m}^3 \text{ day}^{-1}$ on the 06/07/2005 (Figure 103), and the total volume of water that flowed over the weir during this period was 4793 m^3 (Data from Everson *et al.*, 2006). Since this is far less than ST_{so} (equation 2.6), it provides initial evidence for the validity of the hypothesis.

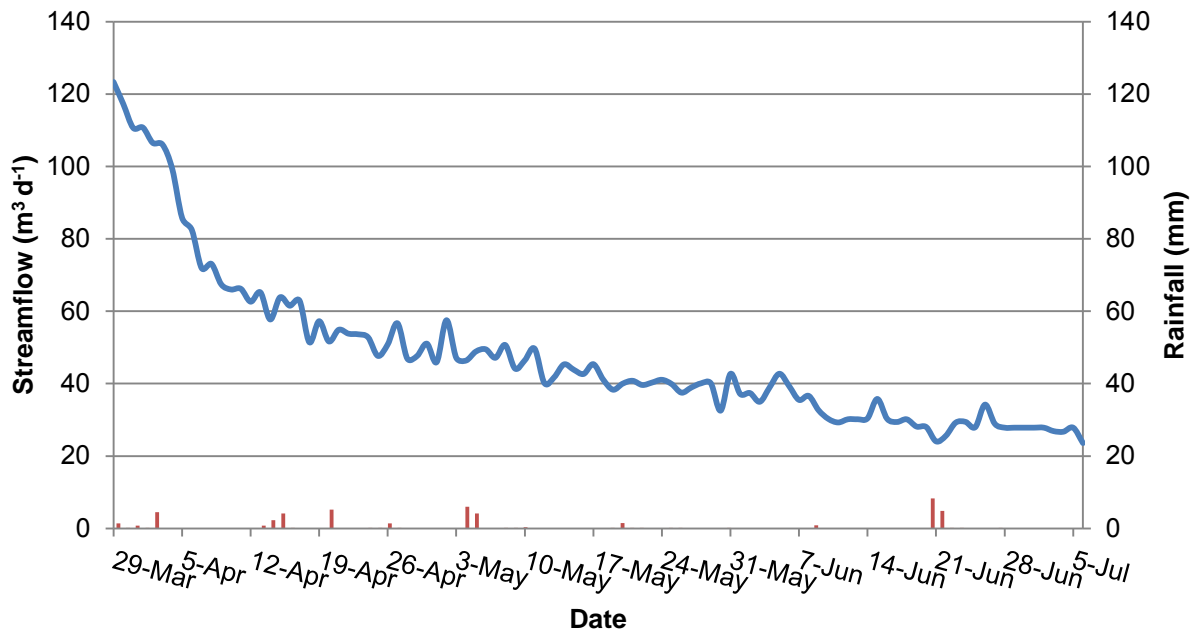


Figure 103 Streamflow and rainfall for the relatively rainfree 100 day hydrograph recession period, 29/03/2005-06/07/2005 immediately following the 203 day high rainfall period (Data from Everson *et al.*, 2006)

Another test calculation needed is concerned with the rate of outflow of ST_{so} during the 100 day hydrograph recession period (Figure 103), through the subsurface layers of the riparian zone. It needs to be kept in mind that, while this flow is taking place, some of this water will be utilized as ET by the vegetation in the riparian zone. Considering the data available the following are reasonable assumptions that need to be made to carry out the test:

The length of the stream from its upper end to the measuring weir is 756 m (Figure 100) giving a total length of 'stream bank' through which the water stored in the hillslopes can flow into the stream of 1512 m;

The depth of the 'feeding stream bank' is 1 m at the start of the study period;

The value of (b) gradually decreases with time as the volume of the water available from the hillslope saprolite decreases and its rate of flow decreases due to a decrease in hydraulic head;

the result of the slug test done in the riparian zone close to the stream to measure the hydraulic conductivity below the water table level provides a reasonably representative value for the whole length of the 'feeding stream bank', i.e. $K = 0.254 \text{ m per 24 hours}$;

The average ET of the vegetation in the riparian zone during the 100 day period is 3.5 mm d^{-1} (Everson *et al.*, 2006), i.e. 350 mm for the period, and considering the area of 7.5 ha this amounts to a volume of 26250 m^3 .

The following equation describes the relationship between the parameters needed for the calculation and enables it to be carried out for the 100 day period. $\Sigma SF < \text{the right hand side}$

of the equation indicates that the estimated volume for the ST_{so} that can flow into the stream during the 100 days is adequate.

$$\sum SF < (\sum ST_{so}F) - (\sum ET_{rz}) \quad (2.7)$$

Where SF, $ST_{so}F$, ET_{rz} are streamflow, water flow from hillslope saprolite, and ET from the riparian zone, respectively. Assuming that the assumptions (a) to (e) are valid, and with units in m^3 the values of the parameters are as follows;

$$4793 < (0.254 \times 1512 \times 1 \times 100) - (26250)$$

$$4793 < 38405 - 26250$$

$$4793 < 12155$$

The conclusion is therefore that the estimated total volume of ST_{so} that could flow into the stream during the 100 days is more than adequate.

Furthermore, the result of equation 2.7 indicates that the estimated volume of ST_{so} that could have flowed out during the 100 day period, i.e. $12155 m^3$, is far less than the estimated volume stored during the preceding 203 day high rainfall period, i.e. 390 mm or $256620 m^3$.

An additional calculation needed to test the validity of the hypothesis is to find out if the estimated flow rate of ST_{so} into the stream ($ST_{so}F$) is adequate at the start of the 100 day period when SF was $123 m^3 d^{-1}$ (Figure 103). $ST_{so}F$ is estimated for one day as $0.254 \times 1512 \times 1 m^3 = 384 m^3 d^{-1}$, i.e. it is estimated to be adequate.

Valuable additional data with regard to our hypothesis, obtained from Clulow *et al* (2011), is presented in Table 16. Also relevant is that Clulow *et al.* (2011) after studying the water balance of the catchment for the period April 2007 to December 2008, focusing specifically on ET rates of young wattle trees, came to the conclusion that, "These data are evidence that wattle trees, whose roots went deeper than 4.8 meters, were able to access deep groundwater reserves". In this regard, it is of particular interest to compare the results of the 2001 and 2008 hydrological years (HY's), in conjunction with the value obtained for ST_{so} from equation 2.6 for the rainfall period of the 2005 HY, i.e. $256620 m^3$. According to our hypothesis, this amount would have been depleted by $4793 m^3$ during the recession stage of the hydrograph (Figure 103), plus total streamflow (SF) during the low flow period ($2443 m^3$) between 7/7/2005 and the end of the 2005 HY on 30/9/2005, which coincided approximately with the start of the new rainfall period of the 2006 HY. The remainder of ST_{so} , i.e. $249384 m^3$ would therefore be available for the 2006 HY, which because of its high rainfall and low ET (minimum wattle) demand would also have resulted in a high ST_{so} value, providing a well water stored deep saprolite for the start of the 2007 HY. Furthermore, because of the similarities of the SF/P ratios for the 2005, 2006, 2007 and 2008 years (Table 16), it is reasonable to assume that ST_{so} for the 2007 HY would also have been high. The comparison between 2001 and 2008 is therefore useful because the rainfall in the two HY's is similar and the vegetation is similar. For 2001, after the whole catchment, including the riparian zone, had been covered by wattle trees extracting water for fourteen years to deeper than 4.8 m depth, it is reasonable to expect ST_{so} would be very low. It is concluded that this is the contributing reason for the low SF/P ratio for 2001 although its rainfall is similar to 2008. The latter value is almost three times as high as the one of 2001, probably due to a much higher ST_{so} value contributing to streamflow.

Table 16 Streamflow – rainfall ratios for the years 2001 – 2008 for the research catchment

| ^a Hydrological year | Rainfall (mm) | Streamflow (mm) | SF/P ratio | ^b Vegetation on N and S facing hillslopes |
|--------------------------------|---------------|-----------------|------------|--------------------------------------------------------------------------------------------------------|
| 2001 | 897 | 26.62 | 0.03 | Mature black wattle(14 year old) |
| 2002 | 1170 | 46.06 | 0.04 | |
| 2003 | 659 | 6.73 | 0.01 | Wattle cleared in different parts during this period with final clearing of whole area in January 2004 |
| 2004 | 727 | 17.79 | 0.02 | |
| 2005 | 1139 | 91.78 | 0.08 | Fallow (no wattle) |
| 2006 | 1106 | 80.49 | 0.07 | Fallow and wattle replanted near the end of this hydrological year |
| 2007 | 689 | 52.17 | 0.08 | Young wattle |
| 2008 | 819 | 65.98 | 0.08 | Rapidly growing wattle with leaf area index already at 2.5 |

a= the period covered, for example for 2001 is from 1/10/2000 to 30/9/2001

b= vegetation on the riparian zone (natural vegetation) and sugarcane areas remained constant throughout this study period.

The attempt to estimate an average effective K value for the whole length of the stream, to describe ST_{soF} , using one slug test in the riparian zone, understandably did not yield satisfactory results. For the whole length of the stream, the slug test indicates a potential flow rate into the stream, i.e. (ST_{soF}) of $384 \text{ m}^3 \text{ day}^{-1}$ at the start of the recession period calculated as follows;

$0.254 \text{ m day}^{-1}(\text{slug test K value}) \times 1 \text{ m (depth of streambank)} \times 1512 \text{ m (length of the streambank)} = 384 \text{ m}^3 \text{ day}^{-1}$.

This rate is far more than the streamflow rate ($123.4 \text{ m}^3 \text{ day}^{-1}$) at the start of the recession during the selected 2005 HY study period. During the 2006 HY, SF at the start of recession period was $251.5 \text{ m}^3 \text{ day}^{-1}$ (Data from Everson *et al.*, 2006). This was the highest initial recession value in the HY's studied by Everson *et al* (2006) and Clulow *et al* (2011). A number of important constraints need to be considered when attempting to estimate an average effective K using slug tests in the riparian zone. These include the number of tests that would be needed along the length of the stream to give a reliable representative value. Slug tests would also be needed at different times during the recession period, i.e. after peak discharge, during recession, and at the beginning of low flow. While slug tests done in the soils of the riparian zone could evaluate the contribution from the surrounding hillslopes, the inflow of water from deep groundwater systems, may also contribute to outflow from the hillslopes.

In the light of the observed physical properties of the soils in this catchment, it is important to consider, using field measurements, what happens in the catchment during a heavy storm event. The study of the stream hydrograph during a heavy downpour is useful in interpreting the run-off and soil infiltrated water on the catchment.

Rainfall events

Five rainfall events with high intensities occurred during observation period December 2004. The events were; (1) 29.2 mm rain event occurring over 2 hours on the 23 December, (2) a 35 mm rain event occurring over 1½ hours on the 24 December, (3) a 25 mm rain event occurring over 2½ hours on the 25 December, (4) an 18 mm rain event occurring 1 hour 20 minutes on the 27 December, (5) a 44 mm event occurring over 3½ hours on 28 December. The general characteristics of the rainfall events are summarized in Table 17. The total rainfall amount recorded during this period was 151 mm. Only one event (event 4) was <20 mm. Event 5 had the highest rainfall, at 44 mm, but with the lowest peak intensity of 1.4 mm min⁻¹. The highest peak intensity of 3.4 mm min⁻¹ was from event 2 which had 35 mm of total rainfall (Table 17).

Table 17 Five selected rainfall events and intensities during the December 2004 rain period

| Event no | Peak period | | | | | |
|-------------|----------------------|------------|----------|----------------|----------------------|------------------------|
| | Date Dec. 2004 | Start time | End time | Total rainfall | Max. intensity | Time of max. intensity |
| | | h:m | | mm | mm min ⁻¹ | h:m |
| 1 | 23 | 18:26 | 18:58 | 25 | 2 | 18:37 |
| 2 | 24 | 13:41 | 14:10 | 29 | 3.4 | 13:44 |
| 3 | 25 | 18:38 | 18:52 | 17 | 1.8 | 18:44 |
| 4 | 27 | 19:23 | 19:30 | 13 | 2 | 19:25 |
| 5 | 28 | 17:36 | 18:49 | 40 | 1.4 | 17:55 |

Hydrologic response of Inanda soil profile and its relations with precipitation and streamflow

Figure 104 show the variations of soil water contents expressed as degree of saturation during the 5 rainfall events. Expressing water content as degree of saturation facilitates pedological interpretation, especially with regard to redox reactions in the soils. The surface horizon responded to the general pattern of precipitation events (Figure 104). Even the subsoil displayed observable response, though in much smaller magnitude compared to the surface horizon (Figure 104). This suggests the rapid movement of water through the soils. This is supported by the soil morphology observed *in situ* (e.g. medium soil texture with red colour, well developed micro-aggregate structure and many root channels). Field tests reveal that in the B horizon of the Inanda soil profile the saturated hydraulic conductivity is 230 mm hr⁻¹; it is this high conductivity which permits the dominance of vertical flow out of the profile into the saprolite of the catchment.

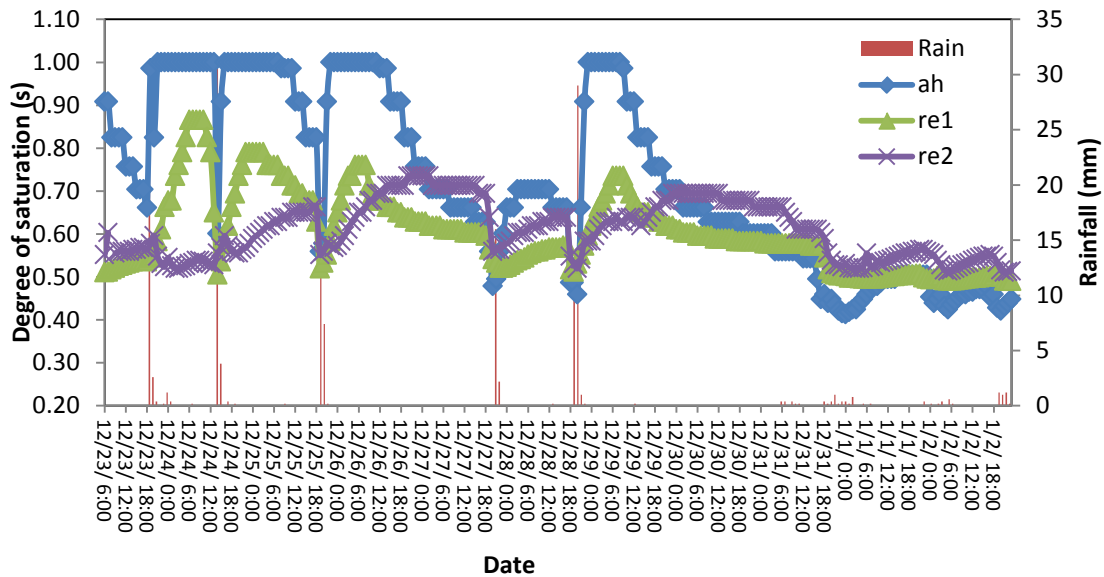


Figure 104 Hourly rainfall from 22/12/2004-31/1/2005 and degree of saturation (S) obtained from mean hourly measurements by watermark sensors located at depths of 400, 800, and 1200 mm in the Inanda soil (Data from Everson *et al.*, 2006)

On the 23rd of December 2004, 29.4 mm of rain fell within the catchment mainly between 6 pm and 8:54 pm with the highest peak 1 min intensity of 2 mm min^{-1} at around 6:37 pm (Table 17). Within an hour of the onset of rainfall, the humic A (*ah*) showed a rapid increase in S values from 0.7 to almost 1 at 9 pm (Figure 104). The horizon stayed saturated till the following day. Thereafter, the S values decreased as water percolated to the deeper horizons of the soil. The S values of the red apedal B1 (*re1*) horizon at 800 mm showed a more gradual response to rainfall as S values increased from approximately 0.55 at the onset of rainfall to a maximum of 0.87 mm just over 10 hrs later. The red apedal B2 (*re2*) at 1200 mm responded more slowly to rainfall and only began to show an increase in S values from midday on the 24th December 2004. However, the S values of the *re2* horizon reached only 0.67 at the end of this 1st rainfall event; this indicates moderately moist but unsaturated conditions. It is only during event 3 that the 1200 mm deep sensor showed a more increase in S values from 0.57 to 0.73, 24 hrs later. However, the S values decreases rapidly as the water percolated to the deeper parts of the soil. Even though the subsoil was never saturated to porosity, the horizons drained rapidly in a vertical direction within days to around 0.5 S. Considering this with the absence of any morphological signs of wetness in the solum, confirms that Inanda soils are hydrologically predominantly of the recharge type. The responses during the other events followed a similar trend discussed above, i.e. humic A gets saturated rapidly, followed by more gradual increase of wetness in the *re1* horizon and a more slowly increase of wetness in the *re2* horizon. A lag time of 11 and 24 hrs was observed for the B1, and B2 horizons to reach peak responses respectively. This lag time was required for drainage before the maximum S value could occur in the subsoil. From the responses of soil water contents in Figure 104, it can be seen that the B2 horizon increased in wetness when the A and the B horizons were draining. This observation was made for nearly all the events. This implies a vertical recharge of the B2 horizon, which is subsequently expected to recharge the saprolite underneath.

There was usually a lag time of 23-46 minutes after the beginning of rainfall prior to streamflow reaction and peak (Figure 105-Figure 107). During each event, the soil water content in the A horizon reacted and peaked prior to streamflow. The event during which the antecedent moisture status in the A horizon was high, the lag time was shorter, suggesting an influence of antecedent soil moisture condition on stormflow. A threshold relationship between soil moisture prior to the event and runoff was found by other authors (Penna *et al.*, 2011). Above 45% volumetric soil moisture content runoff coefficients, streamflow and water table level abruptly increased revealing the strong influence exerted by initial wetness conditions on both surface and subsurface runoff (Penna *et al.*, 2011).

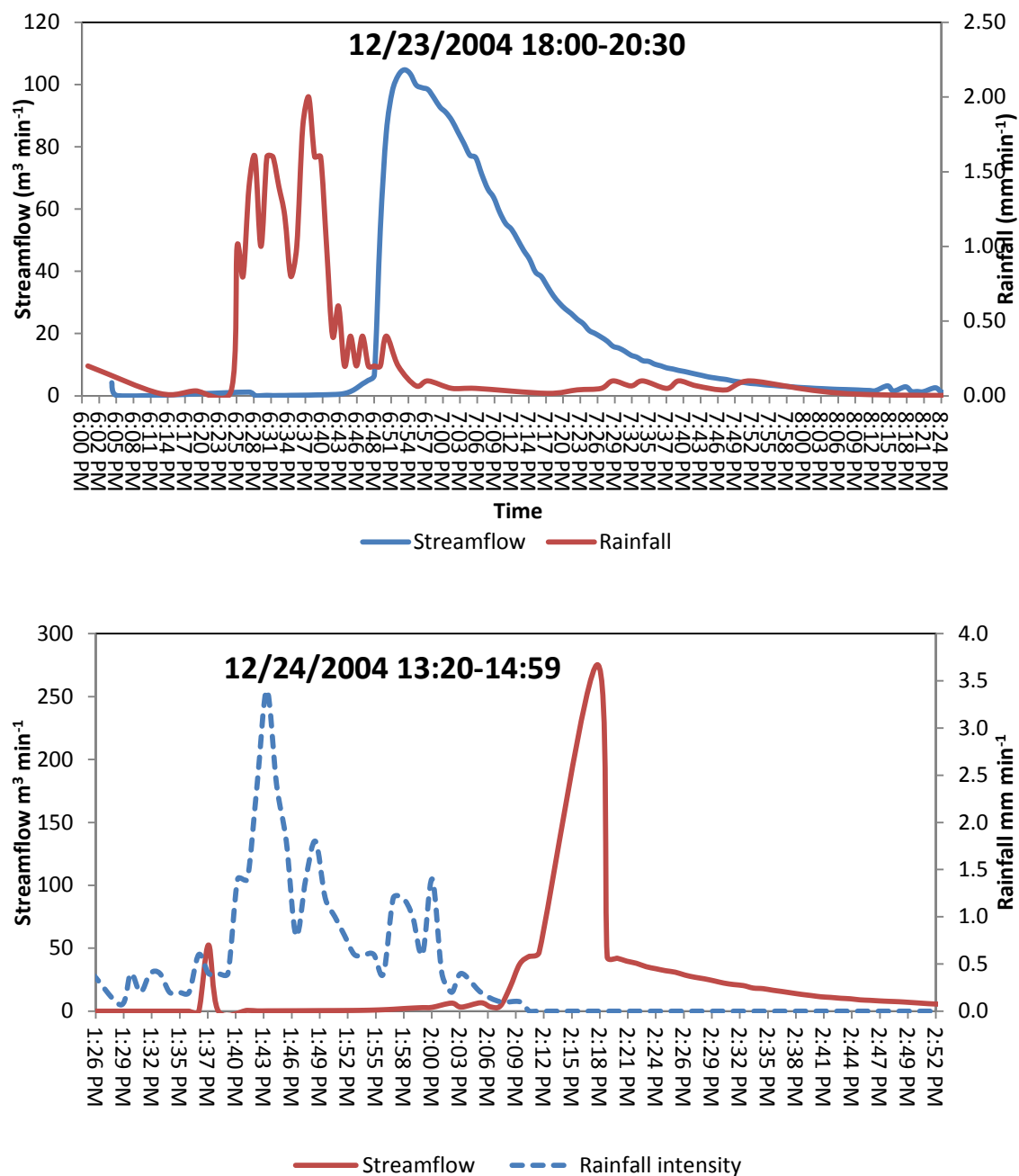


Figure 105 Rainfall and streamflow intensities during rainfall event 1 (a) and 2 (b)

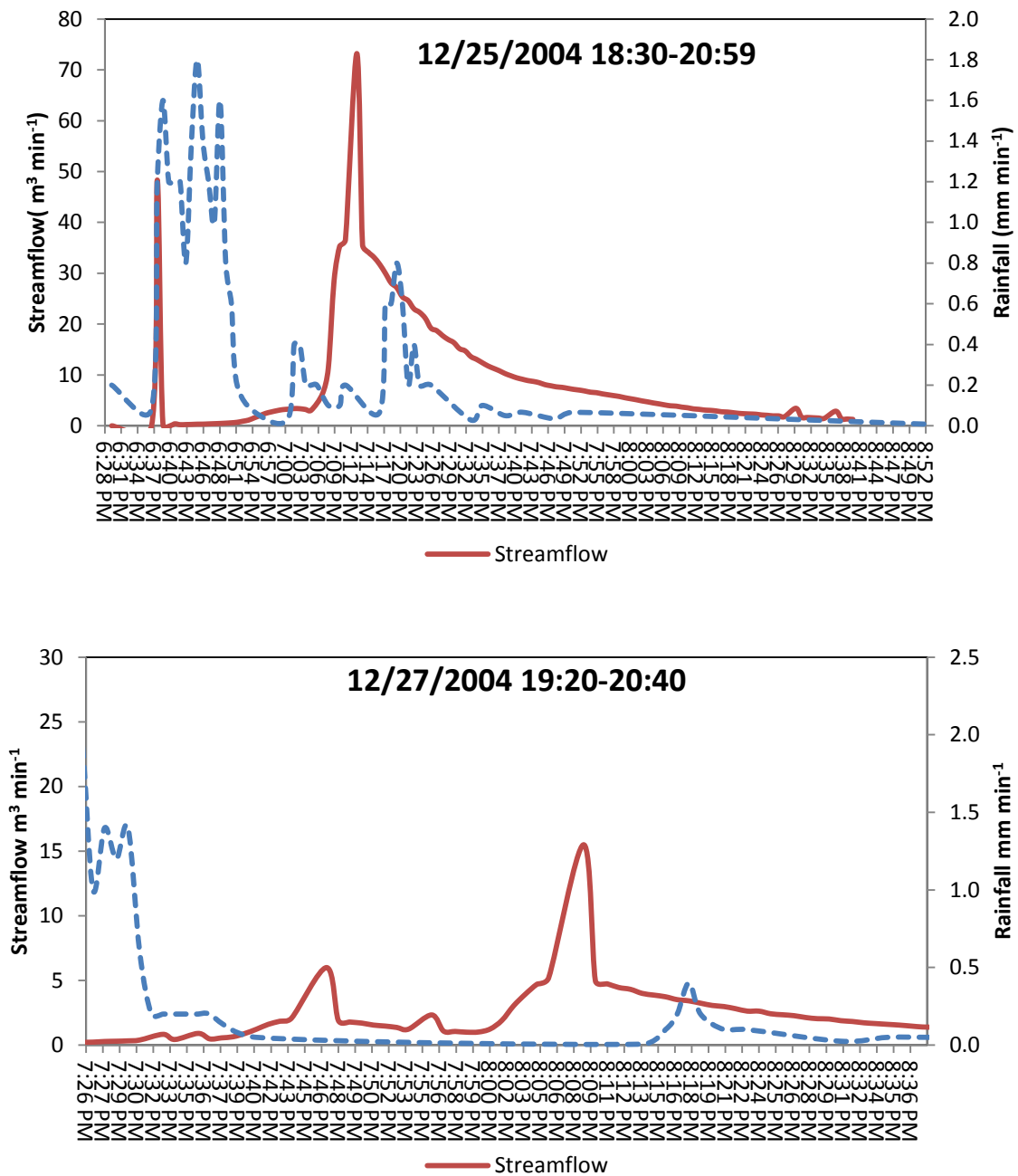


Figure 106 Rainfall and streamflow intensities during rainfall event 1 (a) and 2 (b)

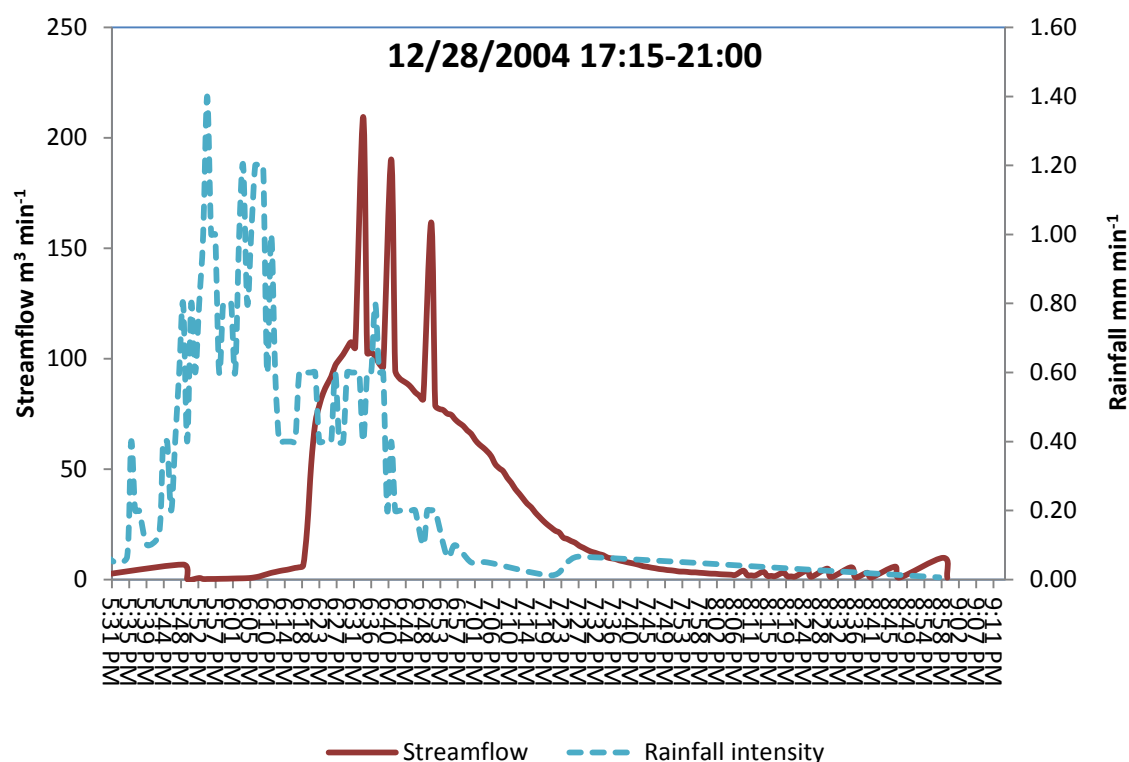


Figure 107 Rainfall and streamflow intensities during rainfall event 1 (a) and 2 (b)

An interesting feature was identified in the one minute interval stream hydrograph presented in Figure 105-Figure 107 during high rainfall events with regard to the influence of antecedent soil water content on runoff generation. The results on this relationship are presented in Table 18. Total runoff was calculated as follows; since the area of the Two Streams catchment is 73.317 ha (Everson *et al.*, 2006), 1 mm of rain on the catchment is equivalent to 733.17 m³ of water. During event 1, two hours before the heavy storm, the estimated hourly streamflow was 21.9 m³. The rainfall event of 6 pm increased this to 1688.15 m³, and the streamflow then receded to 14.72 m³ at 11 pm (Figure 105). Considering the 4 hours (6 pm -11 pm) of the hydrograph as mainly stormflow (totalling 1815.68 m³), and subtracting the estimated low flow of 2 x 21.9 m³ during the two hours, yields an estimated total run-off of 1771.88 m³, which is only 8.3% of the total rainfall (Table 18). The run off for other events is presented in Table 18. It is quite clear that run-off accounts for very small amount of total rainfall. A significant amount of rainfall is therefore expected to infiltrate the soil to increase the soil moisture and recharge the storage of the catchment. A soil with high antecedent soil moisture has the potential to quickly saturate during rainfall events thereby generating quick run-off. A general linear relationship was identified between the percent runoff and the antecedent soil moisture at the surface horizon during the first 4 rainfall events (Figure 108). The anomaly caused by rainfall event 5 could not be explained. When this event was excluded, a good R² was achieved (Figure 108). This linear relationship implies that the higher the antecedent moisture content, the higher the runoff.

Table 18 Antecedent soil water in the A horizon and total rainfall and streamflow during rainfall events in Figure 108

| Event no. | Antecedent soil moisture | Peak streamflow | Total rainfall | Total run off | % runoff |
|-----------|--------------------------|-----------------|----------------|----------------|----------|
| | S | m ³ | m ³ | m ³ | |
| 1 | 0.66 | 1688.15 | 21408.4 | 1771.88 | 8.3 |
| 2 | 0.6 | 1160.77 | 25514.3 | 1213.44 | 4.8 |
| 3 | 0.56 | 900.903 | 18915.7 | 1039.77 | 5.5 |
| 4 | 0.48 | 138.79 | 13343.6 | 117.13 | 0.9 |
| 5 | 0.49 | 3518 | 31086.2 | 4940 | 15.9 |

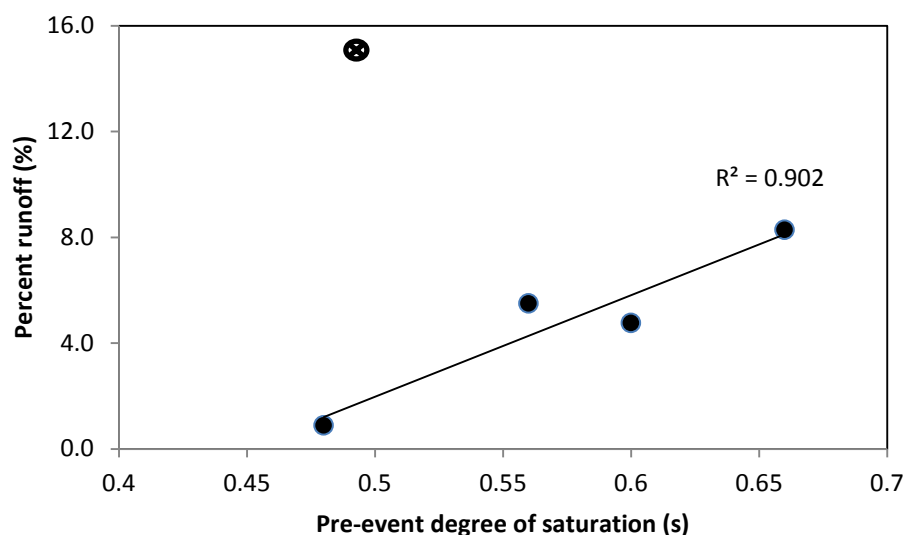


Figure 108 General linear relationship between runoff and the pre-event soil moisture content. The good R^2 is achieved when event 5 (crossed event) is excluded

It was found that rainfall intensities do not correlate well with total amount of runoff. This was particularly noticeable, for instance, during rainfall events 1 and 4, which occurred on 23 Dec. 2004 and 27 Dec. 2004, with similar rainfall intensities (Table 17) but different % percent runoff (Table 18). The % runoff was higher during event 1 as a result of higher pre-event soil moisture content, highlighting a strong control exerted by moisture on runoff in this catchment. While the relative importance of antecedent soil moisture on runoff response is different in various environments, in a semi-humid environment the control exerted by wetness conditions on runoff generation has been shown to be especially important (Penna *et al.*, 2011; Grayson *et al.*, 1997; Sidle *et al.*, 2000; McGlynn, 2005; Zhang *et al.*, 2011). It is therefore imperative in the Two Streams catchment that knowledge of the soil moisture prior to any rainfall event is fundamental to evaluating hydrological response, due to its influence on run-off generation. It is also worth noting that water retention in

these soils is high and could dry slower by ET and replenished quicker by rainfall between short events.

Conceptual hydropedological hillslope model

The conceptual hillslope hydropedological response model based on observed soil profile morphology and measured hydraulic properties are illustrated in Figure 109. Infiltrated water will follow a vertical flowpath (Figure 109, arrow 1) to recharge the deep weathered saprolite. The hillslope soils are considered to be recharge types, since no redoximorphic features indicating periodic saturation, were found in the solum. However, overland flow (arrow 7) can be expected when rainfall intensities exceed the infiltrability of soils. In the valley bottom, the Katspruit soil with a reduction morphology is frequently saturated with water and saturation excess overland flow will be generated during rain events (arrow 4&5). The water in the deep saprolite is expected to flow laterally at the transition to less weathered and less permeable saprolite (arrow 2), and then exit via Katspruit soils (arrow 6) into the stream. It is this water from the saprolite storage that causes prolonged conditions of saturation and the G horizon of Katspruit soils of the valley bottom. Lateral inflow of water from the deep saprolite is expected to raise the water table in the Katspruit soil (arrow 3), resulting in vertical upward flow during rain seasons. Evidence of lateral movement of deep saprolite water also provides for the pedogenetic hypothesis that water from the deep saprolite deposits the chemical constituents (Si, Al, Ca, etc.) needed for the neoformation of clay minerals in the footslope resulting in the unspecified materials with signs of wetness (on) and G horizons of the Magwa and Katspruit soils, respectively. In the Magwa soil the fact that the K_s value of the *on* horizon is considerably lower than that of the *ye* horizon will promote a relatively moist water regime in the *ye* horizon, and presumably be the cause of its yellow colour (relatively high in goethite), compared to the red colour (haematite dominant) of the *re* horizon of the Inanda soil. The latter colour throughout the horizon provides evidence that there is no significant drainage restriction between the Inanda soil and the weathered saprolite below. Vertical return flow from the deep groundwater system into the stream can also be expected in the valley bottom (arrow 7).

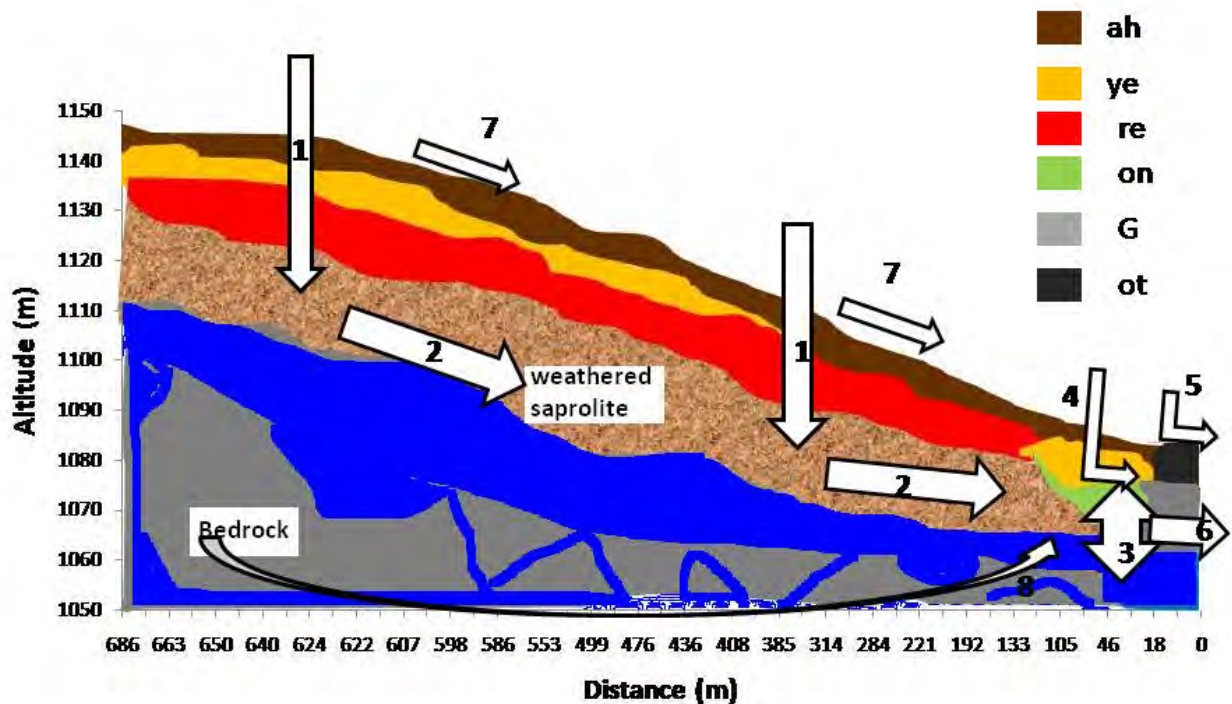


Figure 109 Conceptual flowpaths in the main hillslope of the Two Streams catchment

2.4.4 Conclusion

Quantitative support for the hypothesis was obtained in a number of different ways. Reliable evidence for flowpaths in the research catchment was obtained by studying the hydrological response of soils to rainfall events and the shape of the hydrograph during a selected high rainfall period of the 2005 hydrological year (HY), when the hillslopes were free of wattle trees. Results indicated that the humic A, re and ye horizons of the hillslope soils drained rapidly after rainfall events. In support of our hypothesis, these soils cause the recharge of water into the deep saprolite, which exits via the valley bottom soils into the stream. A procedure used to explain water storage in hillslopes was to study long term, deep neutron water meter measurements. They showed large amounts of water stored in the deep saprolite in an adjacent A zone area with soils similar to those in the research catchment, thereby providing further support for the hypothesis.

Using the catchment water balance for a high rainfall, 203 day period of the 2005 HY, water storage in the deep hillslope saprolite was estimated as 256620 m^3 . This water was therefore available to contribute to streamflow during the following 100 day hydrograph recession period. The streamflow for this period actually amounted to only 4793 m^3 . The large remaining volume would therefore be storage and become available for the 2006 HY, providing further quantitative evidence for the validity of the hypothesis regarding storage. An important observation regarding this storage is made when comparing streamflow to rainfall ratios (SF/P) during the HY's that preceded, and those that followed 2005. The SF/P ratios during the four 2001-2004 HY's was 0.03 on average, with mature wattles on the hillslopes drawing water from below 4.8 m. The SF/P ratio increased to 0.07/0.08 during the

four 2005-2008 HY's, the first two without wattles. A comparison between the 2001 and 2008 HY's with similar rainfall shows SF/P ratios of 0.03 and 0.08 respectively, logically due to large volumes of water stored in saprolite during the three 2005-2007 HY's, compared to depleted saprolite storage by wattles in the catchment for 14 years before 2001, and the four years thereafter. The amount of water stored in the saprolite is therefore clearly shown to be important for streamflow generation during rainfree periods as well as providing water for the fast growing wattle trees.

In the light of the observed physical properties of the soils in this catchment, it was important to consider, using field measurements, what happens in the catchment after a heavy storm event. Five high rainfall events with average intensity of 2.1 mm min^{-1} and streamflow were studied. The response of representative soil to these rainfall events indicates a relative rapid wetting up in the A horizon and steep rapid drainage a couple of hours later. During each rainfall event streamflow responses were delayed by between 23 to 46 minutes, indicating that the infiltration of rainfall into the soil was responsible for the lag time. Once the surface horizon is saturated, runoff is expected to be generated. The percent amount of runoff during the 5 events ranged from 0.9 to 15.9. A linear relationship with $R^2 = 0.902$ was found between percent runoff and the antecedent soil moisture at the surface horizon. No correlation was found between rainfall intensities and the total amount of runoff. This evidence points out clearly the influence of antecedent water content on runoff generation, making soil moisture prior to any rainfall event fundamental to evaluating hydrological processes.

2.5 IN-SITU MEASUREMENTS OF CATHEDRAL PEAK 6

The 67.7 ha CP6 catchment (latitudes $28^{\circ}30'S$ and $30^{\circ}30'S$ and longitudes $28^{\circ}30'E$ and $29^{\circ}30'E$) is located in the foothills of the Drakensburg mountain range in land type Ac265 (Land type survey staff, 2002), characterised by soils of the Clovelly, Mispah, Glenrosa, Magwa, Hutton, Kranskop, Inanda, Nomanci and Champagne forms formed from basalt parent material. A land type, as defined by Van der Watt and Van Rooyen (1995) is "A class of land with specified characteristics used in South Africa as a map unit denoting land, mappable at 1:250 000 scale, over which there is a marked uniformity of climate, terrain form, and soil pattern." The aim of the land type survey in South Africa was to make a systematic inventory of the natural agricultural resources of the country (Land Type Survey Staff, 2002).

The elevation of the catchment ranges from 1 860 m at the weir to 2 070 m at the highest point. The CP6 catchment is characterised by cool temperatures, high rainfall with average aridity index of 1.8 (Table 19). Because of high rainfall, the soils are highly weathered and, promoted by low temperatures, are high in organic matter. They are well drained and acid. The major part of the catchment consists of steeply sloping midslopes with an average slope of 19%, grading to about 8% towards the marsh (Champagne) at the outlet (Figure 110). It is dissected by a number of deep downslope channels which converge midway in the catchment before the outlet (Figure 110). It is considered that these channels play an important role in the hydrology of the catchment. Their depth of approximately 2 m below the surrounding soil surface shows that they have eroded to this depth in this erosion resistant soil over the centuries by conveying large volumes of water. Flowing water was

observed in these channels at the end of a dry season in July and September, indicating considerable lateral water flow in the catchment.

Table 19 Annual climatic data measured for 4 years in the CP6 catchment by Everson *et al.* (1998)

| Year | Mean temperature (°C) | Precipitation (mm) | Actual evaporation (mm) | Aridity index |
|----------------|-----------------------|--------------------|-------------------------|---------------|
| 1990/91 | 15.8 | 1223 | 681 | 1.8 |
| 1991/92 | 14.5 | 1092 | 752 | 1.5 |
| 1992/93 | 14.4 | 1093 | 698 | 1.6 |
| 1993/94 | 13.4 | 1469 | 651 | 2.3 |
| Average | 14.5 | 1219 | 696 | 1.8 |



Figure 110 Soil map of the Cathedral Peak VI catchment (Kuenene, 2008). Three neutron water meter access tube sites for soil water monitoring, and three boreholes, for deep groundwater monitoring are shown. Ch 1200 = Champagne form, R = rock, Ia = Inanda form, Kp = Kranskop form, Ma = Magwa form, No = Nomanci form

Augered soil samples provided the main information needed to classify the soils and facilitate extrapolation of hydraulic properties from comparable soils in other similar areas. Hydraulic properties of the soils were not determined as a result of strict rules regarding digging soil pits in the catchment by KwaZulu-Natal Department of Environmental Affairs. However, previous studies in this area reported that the saturated hydraulic conductivity in the A horizon of an Inanda soil had the high value of 122 mm hr^{-1} (Lorentz *et al.*, 2004). Evidence from measured soil water contents, rainfall and streamflow (Everson *et al.*, 1998) were used to provide evidence for the conceptual hydropedological hillslope models developed initially from soil morphology (Figure 114 & Figure 115). Soil water contents (θ) were measured by neutron water meter (NWM) along a 300 m transect at access tubes placed approximately 20 m apart and to depth of 2 m. However, this transect only covered the middle to lower parts of the slope. Weekly NWM count ratios were routinely taken from these sites and results from three of these sites (see Figure 110) are presented in Figure 112. The θ was expressed as the degree of saturation (S), thereby enabling logical comparisons between different soils, and facilitating pedological interpretation, especially with regard to redox reactions in the soils.

Information regarding the flowpaths and storage mechanisms was sought by studying the streamflow recession curve during the autumn period 24/03/91 through winter to 7/10/91 in spring (Figure 113). The recession curve represents a rain free period following a period with much rain, leaving the hillslopes in the catchment fairly full of water on the starting date. During the 16 days before 24/03/91, 157 mm rain fell and on 24/03/91, 40 mm. This caused a continuous flow over the measuring weir at the outlet of the catchment during the period 24/03/91 to 07/10/91. Measured and estimated responses during the recession periods were analyzed for the catchment. This was done by comparing water draining from the hillslopes in each period with observed streamflow during such a period. Reliable assumptions were made from physical observations made during surveying of the catchment. Segments on the hydrograph were delineated into six different recession phases. The first four exhibit relatively consistent flow rates and therefore produce straight lines on the graph (Figure 113). The fifth line curved slightly while the sixth line is almost straight. It is hypothesised that these different slopes are as a result of different processes contributing to streamflow, generally concurrently, but in different magnitudes during each of the phases.

2.6 RESULTS AND DISCUSSION

2.6.1 Soil distribution on the main hillslope

Soil distribution is presented in Figure 110. The main hillslope, located down the middle and down each of the side slopes of the catchment, between the deep downslope channels varies in length between about 1000 and 500 m long and is represented by the following sequence of soils: Nomanci (summit and upper slopes), Inanda, with some patches of Magwa and Kranskop soils (from midslopes to lowerslopes), Magwa at the footslope near the marsh, and Champagne in the marsh. The Nomanc soil has a thin, dark, loamy humic A underlain by lithocutanic horizon which is soft basalt saprolite that still bears the original rock structure. At some parts the A horizon rests directly on the hard bedrock, resulting in some high level seeps which gave rise to Magwa soil at these seep areas (Figure 110 and arrow no. 3 on Figure 114). Nomanci soil form is well drained with moderately rapid

infiltration rate and rapid permeability through the lithocutanic B or the cracked bedrock. Nomanci are therefore predominantly recharge soils. The Inanda soil form dominates in this hillslope. It is a reddish coloured, well-drained soil that usually occupies upper and midslopes of the catchment (Figure 110). It has a humic A horizon and a diagnostic red apedal B horizon over a deep distinct non-diagnostic yellow brown apedal B horizon (Figure 111).

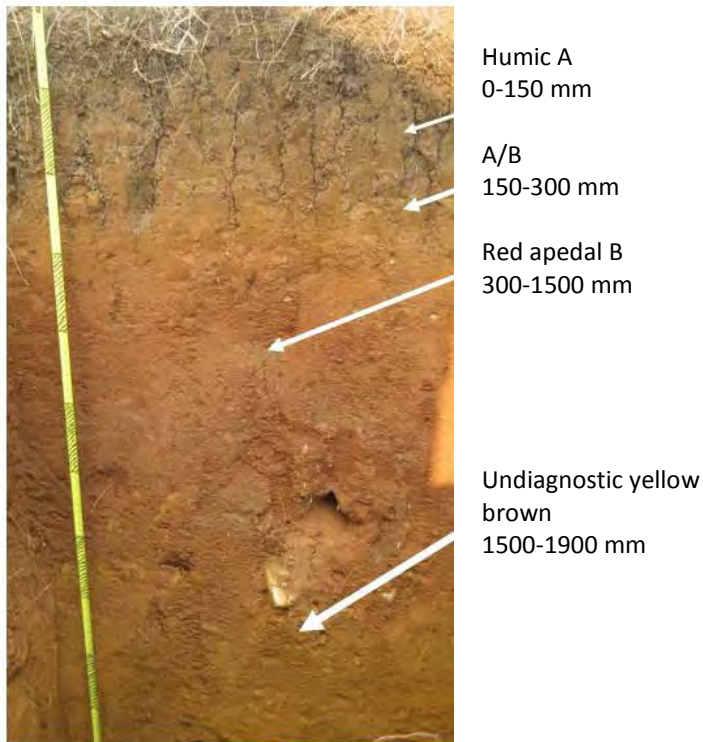


Figure 111 A photo of an Inanda soil profile showing undiagnostic yellow brown apedal B horizon underneath the red apedal B horizon

The red apedal B horizon has lost bases through leaching, and shows gains of clay and minerals through illuviation. Dominant drainage is vertical and it becomes moderate in the lower depths where mottling in the undiagnostic yellow brown apedal B becomes evident. Based on the mottling morphology, and the formation of the yellow brown apedal B horizon under the red apedal B, it is evident that drainage decreases with depth below the yellow brown apedal B horizon. The types of mottles at 2 meter depth were never grey in colour and this shows a non-permanent or shorter duration of saturation in these profiles. This morphology indicates deep interflow (arrow no. 3, Figure 115) which is hypothesised as the major flowpath of soil water, laterally to the adjacent deep downslope channels (arrow no. 4, Figure 115), and downslope to the two wetland areas towards the lower end of the catchment (arrow no. 9, Figure 114).

Magwa soil form has a thin clay loam A horizon over yellow brown apedal B, over unspecified materials with signs of wetness. The mottles in the C horizon indicate periodic saturation as a result of a fluctuating water table. Champagne soil occupies the two wetland areas, which occur, firstly at a topographic convergence midway in the catchment, and secondly where the stream flattens before the catchment outlet (Figure 110). Champagne

has a diagnostic O horizon overlying a Gleyed horizon. This soil shows a marked accumulation of organic material as a result of long-term wetness and cool temperatures. Because of the large amounts of undecomposed organic material the soil is commonly black in colour (10YR 2/2). The fairly continuous wetness has resulted in signs of gleying in the subsoil, typical of wetland soils. Since they remain close to saturation for most of the year, the runoff response (arrow no. 6, Figure 114) from this soil is very rapid after the start of a storm, and also ends relatively abruptly. This soil serves as a buffer by absorbing the lateral drainage water from the upslope parts of the catchment, and retaining it for a considerable time, while releasing it relatively slowly but continuously to the stream.

Soil distribution on the secondary short hillslope, i.e. lateral, towards the deep downslope channels

The soils on this very short hillslope (possibly generally about 40 m in length) are similar to those on the main hillslope, except that Nomanci is absent here. Drainage is into the deep downslope channels via lateral deep interflow (arrows no. 3 & 4, Figure 115). Deep Inanda soil predominates, followed by Magwa with a defined convex slope, adjacent to the deep downslope channels (Figure 115). The Inanda soil has a large soil water storage capacity that releases water continuously during and after the rain season that flows via the Magwa C horizon into the deep downslope channels dissecting the catchment (Figure 110).

2.6.2 Measurements providing evidence for the conceptual hydrological models

Soil water contents

Results obtained from NWM measurements at three sites (Figure 110) and expressed as the degree of saturation (S) are presented in Figure 3. Following the rainfall pattern, the S values in the A (125 mm) and B1 (875 mm) horizons show a strong seasonal trend. This ET influence is far more marked at 125 mm compared to lower depths due to far more roots in the former layer. At site C1 (Figure 110) in the Inanda soil, located at around 100 m from a deep downslope channel, the profile was augered to 1600 mm depth and no distinct morphological signs of wetness were detected within this depth. The absence of any morphological signs of wetness in the Bt horizon at 1600 mm is well supported by the S values of less than 0.78 at 1375 mm depth for most of the time during the measuring period (Figure 112 a). These measurements confirm the morphological evidence that in the solum this profile is hydrologically of the recharge type. Beyond 1500 mm depth, the red apedal B is underlain by a yellow brown apedal B which indicates an increased wetness at the bottom of the profile, confirmed in Figure 112 a by most of the S values at 1875 mm being above 0.78 during the measuring period. This resulted in the formation of yellow hydrated Fe oxide (goethite) formed by reduced compounds under the wet environment. Considering this in relation to mottled morphology at the bottom of the profiles, and the relatively steep slopes on which these profiles are located, indicates a fluctuating water table which when high will promote deep interflow in the more transmissive underlying mineral C horizon.

The θ measurements at NWM sites 2 and 3 in Magwa soil (Figure 112 b and c) provide valuable hydropedological information. Site C2 is located about 60 m from a deep downslope channel (Figure 110). The measurements (Figure 112 b) show that based on weekly readings over a number of rain seasons, θ in the A and B horizons was never > 0.78 S , whereas in the underlying saprolite (deeper than 1375 mm) θ was for most of the time $>$

0.78 S. At Magwa site C3, situated about 20 m from a deep downslope channel, much further downslope than site C2, and adjacent to the midslope marsh (Figure 110), reveal a much wetter soil (Figure 112 c). Only the value at 125 mm depth remains consistently < 0.78 S. It is probable that a reading at the top of the Bt horizon would have given a similar result, and that the 875 mm reading is probably close to the transition to underlying saprolite in which θ is shown to be consistently > 0.78 S. This information together with that in table 20 support the hypothesis that there is much lateral deep interflow to the deep downslope channels.

Hydrograph recession

A long recession curve of the catchment hydrograph for the autumn rain free period of 1991, following a high rainfall period, is presented in Figure 113. The hydrograph represents subsurface flow from both the upper and the lower vadose zones in the catchment, which, it is assumed would have been filled up with water during the preceding rain period and were then starting to drain. Portions of the hydrograph with different slopes are segmented into specific outflow phases (Table 20), and flow rates (Figure 113 b). It was hypothesized that specific factors control drainage during each specific outflow phase. This concept was developed on the assumption that a change in slope of the hydrograph reflects a specific change in soil water regime prevailing in a particular part of the catchment at a specific time. Water that was draining during phases 2 and 3 (Figure 113 b) was hypothesised as being recharge in the upper vadose zone (soil solum) and deep interflow in the intermediate vadose zone (saprolite) draining into the nearby deep downslope channels. The logical information presented in Table 20 provides useful evidence for the conceptual hydrogeological models for the two dominant hillslopes of the catchment.

Table 20 Description of six phases of the hydrograph shown in Figure 113, and hypothesis regarding the main flow processes and sources of water

| Phase | Average flow rate (m ³ /d) | Dates | Days | Quantity per phase (m ³) | Dominant drainage processes and sources of water |
|---------|---------------------------------------|------------------------|------|--------------------------------------|----------------------------------------------------------------------------------------------------------------------------------------------------------------------------------------------------------------------------------------|
| Phase 1 | 4076 | 24/3/1991 | 1 | 4076 | Overland flow and near surface macropore flow in the topsoil flowing rapidly into the deep downslope channels that feed the main stream. |
| Phase 2 | 3100 | 25/3/1991 to 30/3/1991 | 6 | 18597 | Permeable Lithocutanic B horizons of high lying Nomanci soils draining rapidly into nearby deep downslope channels. |
| Phase 3 | 2479 | 31/3/1991 to 16/4/1991 | 17 | 39043 | A and B horizons of soils of Inanda, Magwa and Kranskop draining via saprolite mainly into nearby deep downslope channels. N.B. the lateral short hillslope drainage pattern (secondary hillslope Figure 6) |
| Phase 4 | 1622 | 17/4/1991 to 10/5/1991 | 24 | 38934 | Drainage from deep subsoils of Inanda, Magwa and Kranskop mainly into nearby deep downslope channels and also directly into the marsh. |
| Phase 5 | 857 | 11/5/1991 to 3/8/1991 | 85 | 72866 | Drainage from the catchment's lower vadose zone mainly into the deep downslope channels plus drainage from soils in the two riparian zones. Flowing water was seen in these channels during July and September visits to the catchment |
| Phase 6 | 439 | 4/8/1991 to 7/10/1991 | 65 | 28521 | Baseflow from phreatic zone of the whole catchment plus drainage from Champagne soils |

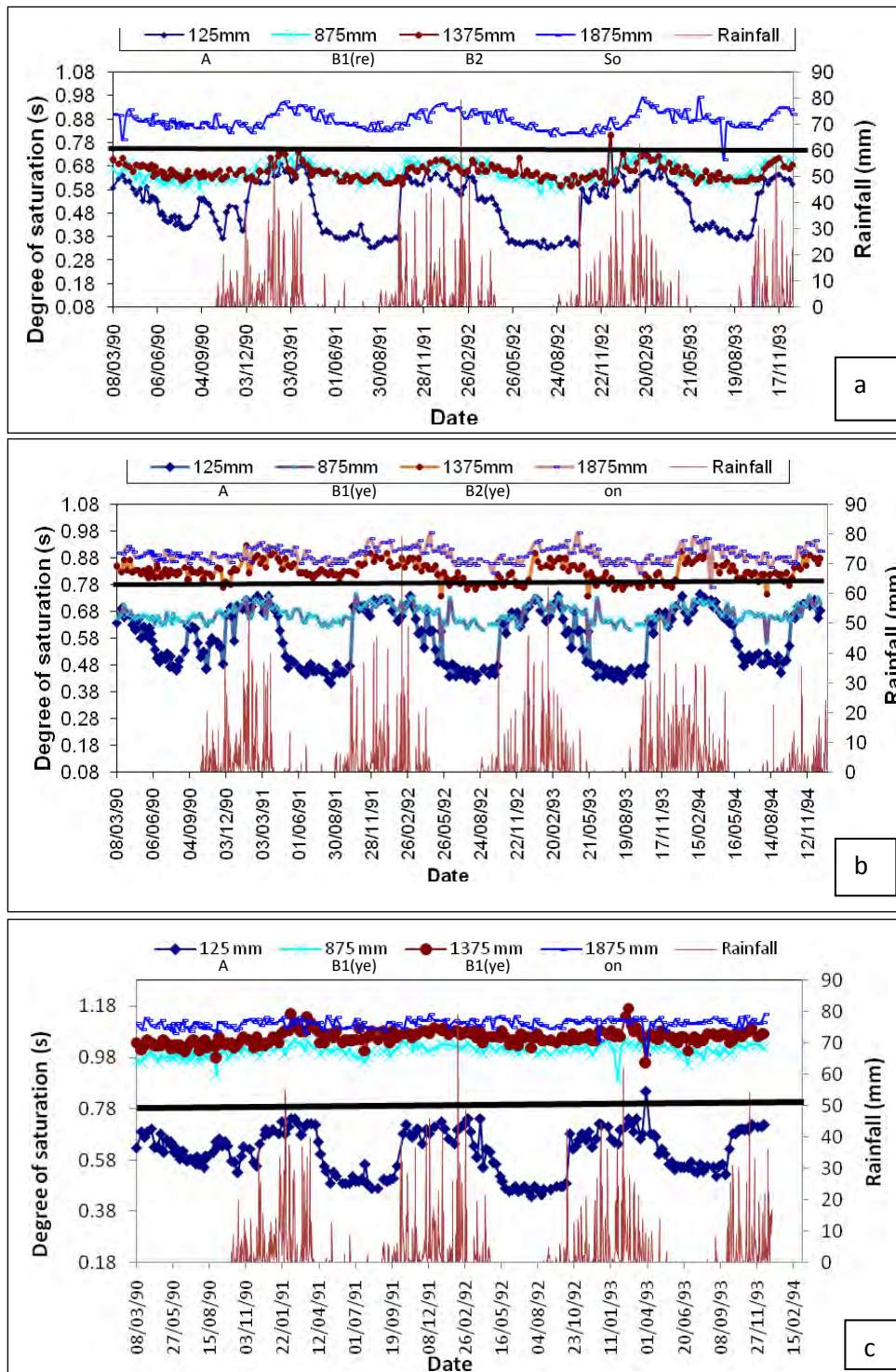


Figure 112 Soil water contents (S) at different depths at the NWM measuring sites marked on Figure 110 (a) Inanda (Site 1); (b) Magwa (Site 2) about 60 m from a deep downslope channel; (c) Magwa (site 3) close to a deep downslope channel; measurement are for the period March 1990 to November 1993 with associated rainfall (basic data from Everson *et al.* 1998)

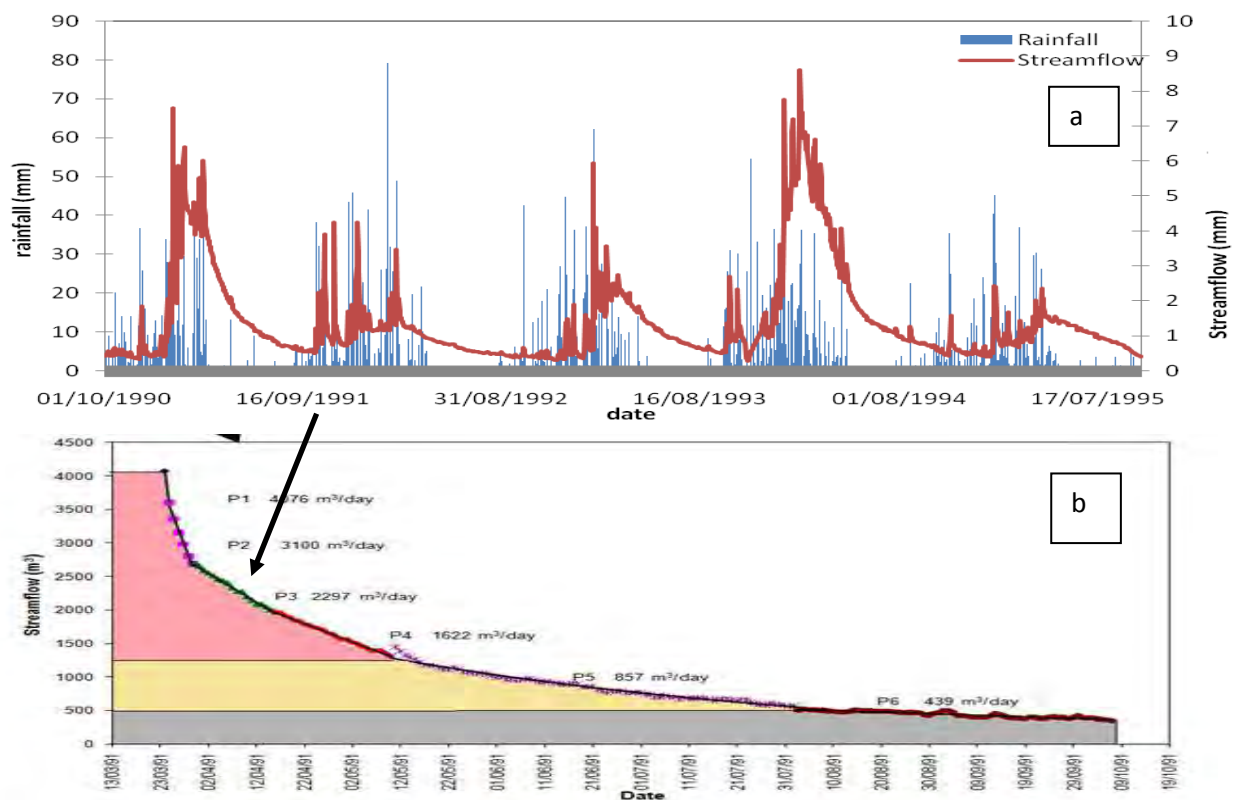


Figure 113 (a) Rainfall and streamflow from 1990/91 to 1994/95 for the Cathedral Peak VI catchment; (b) and the important almost rainfree period of 24/03/91 to 07/10/91 portion of the hydrograph, together with the average flow rates per day during six phases (marked P1 to P6) (Kuenene *et al.*, 2011)

Estimating the contribution of groundwater to low flow

The contribution of groundwater to low flow in the stream was estimated in the flowing way. Measurements were made by Everson *et al.* (1998) of the water table levels at three boreholes DO1, DO2, and DO5 marked in Figure 110, during the 1994-1995 hydrological year (i.e. 1/10/94-30/9/95). Everson *et al.* (1998) make a clear statement that there is not expected to be any leakage out of the base of the catchment. The instrument used for the borehole measurements was a pressure transducer type sensor and Campbell CR 21x logger. The water levels were verified manually each week with a modified leaf wetness sensor. There was good agreement between the two sets of measurements.

The water levels in all three boreholes reached their peak values of approximately 15.94, 5.61 and 1.06 m below the soil surface, respectively, around the end of the rain season early in May 1995. Thereafter they decreased consistently until the end of September. The extent of these decreases and the estimated volumes of water they represent are recorded in Table 21 and related to the total low flow out of the catchment during the period 11/5/1995-30/9/1995.

Table 21 Decreases in water table levels at 3 boreholes, and estimated amount of water supplied to low flow out of the catchment during the period 11/05/95-30/09/95

| Borehole Site | Approx. decrease in water levels (mm) ^A | Estimated area represented (ha) ^B | Estimated volume of storage material (m ³ X 10 ⁴) ^C | Estimated bulk density of the storage material (Mg m ³) | Estimated porosity of storage material | Estimated volume of water that drained out (11/5/95-30/9/95) m ³ X 10 ⁴ |
|---------------|----------------------------------------------------|----------------------------------------------|---------------------------------------------------------------------------------------|---------------------------------------------------------------------|----------------------------------------|-----------------------------------------------------------------------------------------------|
| DO1 | 700 | 22.6* | 15.820 | 2 | 0.245 | 3.876 |
| DO2 | 520 | 22.6 | 11.752 | 2 | 0.245 | 2.879 |
| DO5 | 65 | 22.6 | 1.469 | 2 | 0.245 | 0.360 |
| Total | | | | | | 7.115 |

^AData from Everson *et al* 1998 for the period 11/5/95-30/9/95.

^BThe material in which the groundwater was stored

^CEach borehole represents approx. one third of the catchment

The estimated contribution of groundwater to low flow out of the catchment for the period 11/5/95-30/9/95 is therefore $7.115 \times 10^4 \text{ m}^3$. Unpublished data from Everson *et al.*, 1998 records the low flow for this period as $9.46 \times 10^4 \text{ m}^3$. Although there is considerable difference between these two values, the reason is understandable. This amount is the represented by arrow no. 7 in Figure 114. It is hypothesised that a contribution to the difference between the two estimates is made by the lateral flow from the deep intermediate vadose zone into the deep downslope channels, i.e. arrow no. 4 in Figure 115.

2.6.3 Conceptual hydrogeological hillslope models

Soil morphology in this catchment is the result of long-term persistent flow and transport processes. The conceptual models of what are considered to be the dominant hillslopes are presented in Figure 114 & Figure 115. Flowpaths are shown with numbered arrows. When it rains infiltration dominates on the slopes. On the top part of the long hillslope where Nomanci soil predominates, infiltrated water is expected to flow vertically to recharge regional aquifers (arrows 1 & 2). At some parts where the A horizon rest directly on the hard bedrock, it will flow laterally and come out as return flow (arrow 3) from transient saturation above bedrock, producing Magwa soil below it, i.e. the high lying Magwa areas in Figure 110. Large macropores in saturated soil above the bedrock at some sites become active leading to downslope lateral flow directly into the deep downslope channels. At other sites the lithocutanic horizons of the Nomanci soils evidently connect directly with Inanda. On the mid to lower slopes infiltrated water in the soil matrix of deep Inanda, Magwa and Kranskop soils flows vertically to recharge the deep saprolite to raise θ to above the drained upper limit (Figure 112) in this more transmissive mineral soil, thereby promoting lateral

flow either into nearby deep downslope channels (Figure 115), or into the wetland (arrow no. 4 in Figure 114). In the wetlands upward movement of water is as a result of evapotranspiration of riparian plants and capillary rise (arrow 5 in Figure 115), while on the soil surface precipitation does not infiltrate these soils as they are already saturated. Overland flow can be expected on these wetland soils (arrow 6). On the short hillslope soil water will follow a similar flow path as in the long hillslope, excepting that there the outflow is into the deep downslope channels. Soils and thick vegetation cover on the hillslope favours vertical infiltration (arrow 1 in Figure 115) which will recharge the deep saprolite before exiting into the deep nearby channels (arrow 4 in Figure 115).

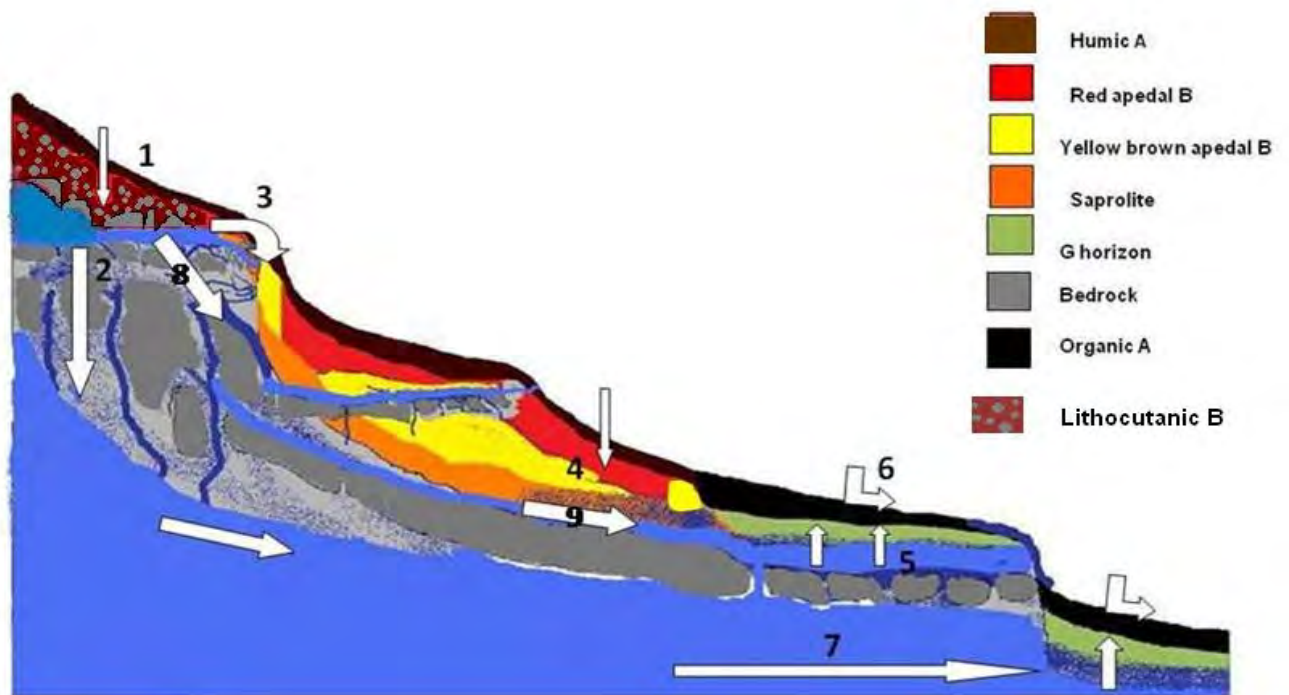


Figure 114 Conceptual flowpaths in the main hillslope of the Cathedral Peak VI catchment

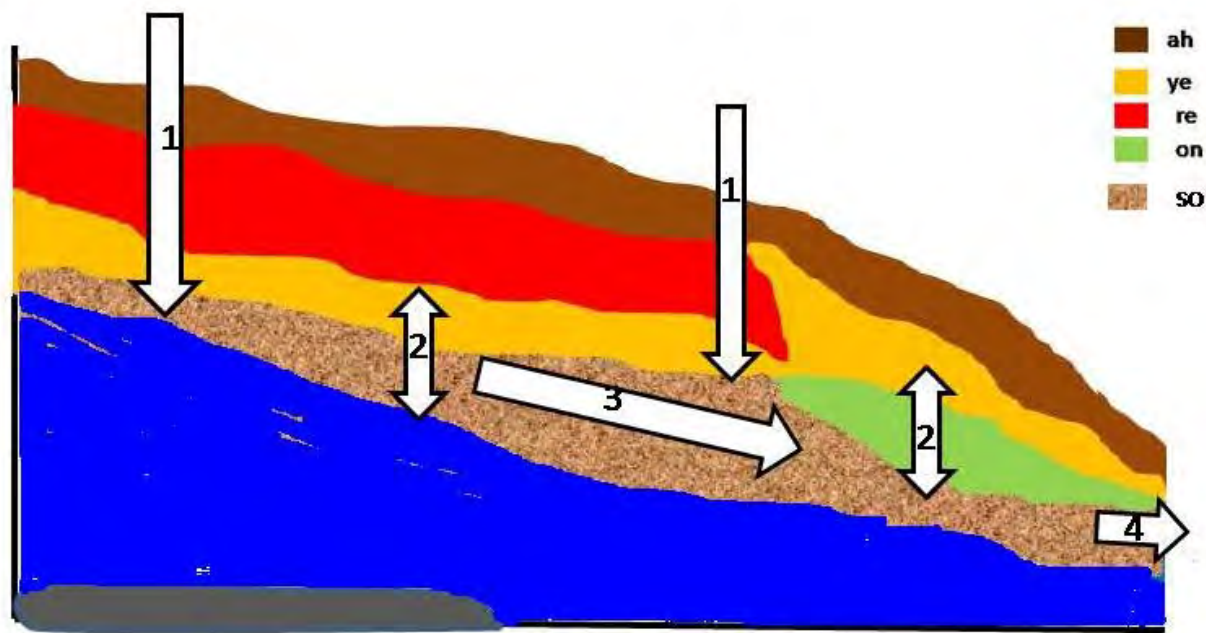


Figure 115 Conceptual flowpaths for the short hillslope of Cathedral Peak VI catchment

2.7 CONCLUSION

Effort to identify the main flowpaths and storage mechanisms in order to construct the conceptual hydrological hillslope models was based primarily on the soil distribution pattern in the hillslopes and the morphology of the soils. Pedologically, soils on the top end of the hillslope are freely drained with no signs of wetness indicating water accumulation. Soils in the mid to lowerslopes are deeply weathered and also freely drained but with decreasing permeability in the deeply weathered saprolite. Evidence supporting this was sought from the formation of the yellow brown B horizon under the red apedal B (Figure 112) as well as the observation of distinct red and yellow mottles in the undiagnostic yellow brown apedal B horizon. This morphology is the result of long-term persistent flow and transport processes. Long term neutron water meter measurements support this by showing θ consistently > 0.78 S at 1875 mm in all monitored profiles.

The long recession hydrograph of the catchment was also used to identify flowpaths and the contribution of soils to streamflow. The hydrograph represents subsurface flow from both the upper and the lower vadose zones in the catchment, which, it is assumed would have been filled up with water during the preceding high rainfall period and were then draining. The hydrograph indicates that for the first 25 days during the hydrograph recession, water that was draining during phases 2 and 3 (Figure 113b) was hypothesised as being deep interflow in the deep vadose zone (saprolite) draining into the nearby deep downslope channels. Using the borehole data of 1/1/95 to 10/5/95, the outflow from the groundwater was estimated at $7.115 \times 10^4 \text{ m}^3$. This amount compares fairly with the low flow for this period as $9.46 \times 10^4 \text{ m}^3$ calculated from streamflow data.

Results of this study showed that, based on the classification of South African hillslopes (Van Tol, *et al.*, 2013), the modal hillslopes in the Cathedral Peak 6 catchment are classified as Class 1-interflow. This class has a full range of recharge, interflow, and responsive soils with

an anticipated hydrograph with peak, long shoulder, and baseflow elements (Van Tol, *et al.*, 2013). The recession hydrograph of autumn 1991 in the Cathedral Peak 6 catchment shows that deep interflow in this catchment can contribute significantly to total streamflow. Since the objective was to elucidate the hydrogeological characteristics of the catchment, attempt is made here to estimate the vadose zone storage, which is responsible for the long recession curve on the hydrograph in Figure 113 b. It is appropriate to relate the vadose zone storage to the outflow volumes of phases 1-5 of the hydrograph in Figure 4 described in Table 20. This storage can be estimated by subtracting the contribution of groundwater (Phase 6) from the contribution of the vadose zone (Phases 1-5). The total outflow from the vadose zone is therefore determined by adding outflow volumes from different phases which is 173516 m³. Considering the baseflow rate of 439 m³ day⁻¹ (Figure 113 & Table 20), the total baseflow amount for the 24/03/91 to 07/10/91 is 58387 m³. Subtracting this amount from 173516 m³ gives an estimated vadose storage of 115129 m³. Because K_s of the B horizon is rapid infiltrating water ends up in a deep vadose zone in few days. Comparing results presented in the Weatherley catchment (Van Huyssteen *et al.*, 2005) with those in the Cathedral Peak 6, the influence of different hillslope hydrogeological behaviour on the vadose zone storage becomes highlighted. The outflow from the vadose zone in the Weatherley and Two Streams catchments for one particular season was only 4362 m³ and 52093 m³, respectively (Van Huyssteen *et al.*, 2005). The hillslopes of Weatherley catchment are dominated by interflow soils feeding the lower lying soils via a bedrock flowpath (Van Tol *et al.*, 2010 a). In the Cathedral Peak 6, most of the water infiltrates into the highly weathered saprolite to recharge the deep high storage vadose zone.

These results provide reliable quantitative evidence for the validity of the Class 1 of the South African classification of hillslopes, and valuable information for the construction of the representative hillslope hydrogeological conceptual model of the catchment. Of considerable significance in this model is the dominant role of the flowpath in the deep saprolite (Arrows No. 9 & 3 in Figure 114 & Figure 115, respectively), which is closely related to the shape of the final, autumnal (rain free) recession period shown in Figure 113b.

2.8 REFERENCE

- CLULOW, A., D. EVERSON, C. S. & GUSH, M.B., 2011. The long-term impact of *Acacia Mearnsii* trees on evaporation, streamflow and groundwater resources. WRC Report no. TT 505/11. Pretoria, South Africa.
- FEY, M. 2010. Soils of South Africa. Cambridge University Press, Cape Town.
- ESHLEMAN, K. N., POLLARD, J. S. & O'BRIEN, A.K., 1994. Interactions between groundwater and surface water in a Virginia coastal plain watershed. 1. Hydrological flowpaths. *Hydrol.Process.* 8, 389-410
- EVERSON, C.S., MOLEFE, G.L. & EVERSON, T.M. 1998. Monitoring and modelling components of the water balance in a grassland catchment in the summer rainfall area of South Africa. WRC Report no. 493/1/98. Water Research Commission, Pretoria.
- ELSENBEER, H., 2001. Hydrologic flowpaths in tropical rainforest soils— a review. *Hydrol.Process.* 15, 1751-1759.
- EVERSON, C.S., MOODLEY, M., GUSH, M., JARMAIN, C., GOVENDER, M. & DYE, P. 2006. Can effective management of riparian zone vegetation significantly reduce the cost of catchment management and enable greater productivity of land resources. WRC Report No, K5/1284, Water Research Commission, Pretoria.

- GRAYSON, R.B., WESTERN, A.W., CHIEW, F.H.S. & BLOSCHL, G. 1997. Preferred states in spatial soil moisture patterns: local and non local controls. *Water Resour. Res.* 33 (12), 2897-2908.
- KUENENE, B.T. 2008. Soil morphology as signature of soil water regime in the Cathedral Peak VI catchment. M.Sc. thesis. University of Free State, Bloemfontein.
- KUENENE, B.T., VAN HUYSSTEEN, C.W., LE ROUX, P.A.L., HENSLEY, M. & EVERSON, C.S., 2011. Facilitating interpretation of Cathedral Peak VI catchment hydrograph using soil drainage curves. *South African Journal of Geology*, 114, 525-534.
- Land Type Survey Staff. 2002. Land Type Soil and Terrain Inventories from Northern Cape, Free State, North West, Gauteng, KwaZulu-Natal and Eastern Cape provinces. Land type survey database of South Africa. Mem. Agric. Nat. Resour. S. Afr. ARC-ISCW, Pretoria.
- LORENTZ, S., THORNTON-DIBB, S., PRETORIUS, C. & GOBA, P., 2004. Hydrological systems modelling research programme: hydrological processes. Report No. 1061 & 1086/1/04. Water Research Commission, Pretoria.
- PENNA, D., TROMP-VAN MEERVELD, H. J., GOBBI, A., BORGA, M. & DALLA FONTANA, G. 2011. The influence of soil moisture on threshold runoff generation processes in an alpine headwater catchment. *Hydrol. Earth Syst. Sci.*, 15, 689-702.
- LE ROUX, P.A.L., VAN TOL, J.J., KUENENE, B.T., HENSLEY, M., LORENTZ, S.A., EVERSON, C.S., VAN HUYSSTEEN, C.W., KAPANGAZIWIRI, E. & RIDELL, E., 2011. Hydropedological interpretation of the soils of selected catchments with the aim of improving efficiency of hydrological models: WRC Project 1748/1/10. Water Research Commission, Pretoria.
- LE ROUX, P.A.L., DU PLESSIS, M.J., TURNER, D.P., VAN DER WAALS, J. & BOOYENS, H.B., 2013. Field book for the classification of South African soils. Reach. Wandsbeck, South Africa.
- LORENTZ, S. A., BURSEY, K. G., IDOWU, O. A., PRETORIUS, J. J. AND NGELEKA, K. J., 2007. Hydrological processes definition and analysis for application in models. WRC Report No K5/1320. Water Research Commission, Pretoria.
- McGLYNN, B.L. 2005. The role of riparian zone in steep mountain catchments. In: *Global Change and Mountain Regions: an Overview of Current Knowledge*. Adv. Global Change Res. Ser., vol. 23, edited by: Huber, U.M., Bugmann, H. K. M. & Reasoner, M. A., 331-342. Springer, New York.
- MUSTO, J. W., 1994. Changes in soil physical properties and related hydraulic characteristics caused by Eucalyptus plantations. MSc thesis. Department of Agronomy, University of Natal, Pietermaritzburg, South Africa.
- RODGERS, P., SOULSBY, C., WALDRON, S. & TETZLAFF, D., 2005. Using stable isotope tracers to assess hydrological flow paths, residence times and landscape influences in a nested mesoscale catchment, *Hydrol. Earth Syst. Sci.* 9, 139-155.
- SIDLE, R. C., TSUBOYAMA, Y., NOGUCHI, S., HOSODA, I., FUJIEDA, M., AND SHIMIZU, T. 2000. Stormflow generation in steep forested headwaters: a linked hydrogeomorphic paradigm, *Hydrol. Process.*, 14, 369-385.
- SCOTT, D. F., 2000. Soil wettability in forested catchments in South Africa; as measured by different methods and as affected by vegetation cover and soil characteristics. *J. Hydrol.* 231-232, 87-104.

- SOIL SURVEY STAFF., 1975. Soil Taxonomy: A Basic System of Soil Classification for Making and Interpreting Soil Surveys. USDA, Soil Conservation Service, Agr. Handbook No. 436. U.S. Govt. Printing Office, Washington, DC.
- TURNER, D.P., 2000. Soils of KwaZulu-Natal and Mpumalanga: Recognition of natural soil bodies. PhD thesis. University of Pretoria.
- TICEHURST, J.L., CRESSWELL, H.P., MCKENZIE, N.J. & CLOVER, M.R., 2007. Interpreting soil and topographic properties to conceptualise hillslope hydrology. *Geoderma* 137, 279-292.
- UCHIDA, T.Y. ASANO, N. OHTE, & T. MIZUYAMA., 2003. Seepage area and rate of bedrock groundwater discharge at a granitic unchanneled hillslope. *Water Resour. Res.* 39, 1018.
- UHLENBROOK, S., WENNINGER, J. & LORENTZ, S., 2005. What happens after the catchment caught storm? Hydrological processes at the small, semi-arid Weatherley catchment, South-Africa. *Advances in Geosciences* 2, 237-241.
- VAN BEERS, W. F. J., 1983. The auger hole method. A field measurement of the hydraulic conductivity of soil below the water table. International Institute for Land Reclamation and Improvement/ILRI, Wageningen, The Netherlands.
- VAN DER WATT, H.V.H. & VAN ROOYEN, T.H., 1995. A glossary of soil science. 2nd ed. *Soil Sci. Soc. S. Afr.*, Pretoria.
- VAN GENUCHTEN, M. Th., 1980. A closed-form equation for predicting the hydraulic conductivity of unsaturated soils. *Soil Sci. Soc. Am. J.* 44, 892-898.
- VAN TOL, J.J., LE ROUX, P.A.L. & HENSLEY, M., 2011. Soil Indicators of Hillslope Hydrology, Principles, Application and Assessment in Soil Science, Dr. Burcu E. Ozkaraova Gungor (Ed.), ISBN: 978-953-307-740-6, InTech, Available from: <http://www.intechopen.com/books/principles-application-and-assessment-in-soilscience/soil-indicators-of-hillslope-hydrology>.
- VAN TOL, J.J. LE ROUX, P.A.L. HENSLEY, M. & LORENTZ, S.A., 2010. Soil as indicator of hillslope hydrological behaviour in the Weatherley Catchment, Eastern Cape, South Africa. *Water SA* 36, 513-520.
- VAN TOL JJ, LE ROUX PAL, LORENTZ SA and HENSLEY M (2013) Hydropedological classification of South African hillslopes. *Vadose Zone J.* **12** (4) DOI:10.2136/vzj2013.01.0007.
- WENNINGER, J., UHLENBROOK, S., LORENTZ, S. & LEIDBUNGUT, C., 2008. Identification of runoff generation processes using combined hydrometric, tracer and geophysical methods in a headwater catchment in South Africa. *Hydrol. Sci.* 53, 65-80.
- ZHANG, Y., WEI, H. & NEARING, M. A. 2011. Effect of antecedent soil moisture on runoff modelling in small semiarid watersheds of southeastern Arizona. *Hydrol. Earth Syst. Sci.* 15, 3171-3179.

Chapter 3 FROM LAND TYPES TO HYDROLOGICAL HILLSLOPES

3.1 INTRODUCTION

All soil measurements (pedological, hydrological, chemical or physical) are based on a specific sample, and as such only pertain to that sample. For the measurement to be of use, one has to be able to extrapolate such a measurement to a defined area. The vehicle used for this extrapolation is soil morphology. The basic building block in soil morphology is the soil horizon, which is a soil layer which has similar soil properties. Thus a measurement taken at a specific point within a soil horizon can be extrapolated to the extent of the soil horizon. To extrapolate data to soil profiles, the succession of soil horizons within a soil profile is used to determine soil profiles with similar characteristics. Within hydropedology, the succession of soil profiles in a hillslope is used to determine similar hillslopes from which for instance conceptual hydrological soil response units (CHSRU's) could be extrapolated. However, this still only allows extrapolation in two dimensions, it being length and depth. To be able to apply the knowledge gained with hydropedological investigations to larger areas such as catchments, one has to know the extent of homogeneous soil bodies in width as well, to facilitate the extrapolation of values in three dimensions. Figure 116 depicts this graphically. A soil map enables this extrapolation to the third dimension.

Unfortunately, conventional methods of soil mapping are cumbersome and expensive (Zhu *et al.*, 2001), limiting the application of soil maps in hydropedological studies. However, the cost of conventional soil surveys can be greatly reduced by digital soil mapping (DSM) (Hensley *et al.*, 2007). DSM harnesses the power of various new and rapidly developing technologies, including information technology, satellite imagery, digital elevation models (DEM's), pedometrics and geostatistics, and combines them in inference systems, incorporating the tacit knowledge gained during field soil surveys. DSM thus aims at utilising various different new technologies to apply expert tacit knowledge to produce the same or better quality soil maps as conventional soil survey at a fraction of the price.

Three different case studies were done wherein DSM methods were used to give spatial soil information to aid hydropedological studies. In the first, a theoretical disaggregation of the land type inventories of two land types near Riversdal was done. In the second case study a soil map was created with a DSM approach near New Castle. The soil map was then used to delineate areas where the same conceptual hydrological soil response models (CHSRM's) would function. In the last case study, the theoretical land type disaggregation method of case study 1 was combined with the DSM approach of case study 2, to provide a hillslope specific conceptual hydrological soil response model map.

The application of DSM methods in hydropedology was tested by using the soil map of case study 3 in an ACRU-int modelling exercise. The aim was to show that pedological information can be utilised in modelling catchment hydrology.

landscape interactions and at a larger scale than at which it is published. This allows us to disaggregate the land types into useable digital soil maps, by applying the tacit knowledge we have today to the land type database. One challenge when using the land type inventory is that it was done using the so-called red book (MacVicar *et al.*, 1977), the previous South African soil classification system. This system does not acknowledge signs of wetness in the subsoil, which limits its use for hydrological purposes.

Due to the complete coverage of the land type database it seems logical that it should be the basis for extracting soil data for surveys. This aim of the case study was to develop a theoretical method on how the land type database could be used to extract useful soil information from it for hydropedological studies.

Material and Methods

Study site

The study site (Figure 117) where this methodology was developed is located near Riversdale in the Western Cape. Its geographical centre point is at 34.027°S and 21.398°E. Two land types occur in this area, Dc32 and Db12. Db12 lies on the TMU5 position and most of it is classified as a peat wetland. Dc32 covers the slopes directly around the wetland. It has steep relief with an average slope of 6.9% and reaching 25%. The average profile curvature is 0.017 and the average planform curvature is 0.007.



Figure 117 The study site, showing the extent of the Dc32 and Db12 land types

Methodology

To get the best possible DEM, the 90 m SRTM DEM was interpolated together with the 20 m contours from the 1: 50 000 topographical map to a DEM with a 62 m resolution. A finer resolution DEM had anomalies on it. From this DEM flow accumulation was determined, by setting the amount of pixels to constitute a river to include the smallest possible streams, without creating double flow lines. The size of the streams determines the scale at which will be worked.

From the flow accumulation layer watersheds were delineated around the streams. Two pour points were placed at each stream junction, as well as one at the end of the stream. The watershed from the stream end pour point determines the headwater hillslope. Watersheds were manually divided into hillslopes by cutting the watershed polygons by following the streams from the flow accumulation layer. Nose hillslopes were determined by using the aspect layer derived from the DEM. The aspect was set to 4 intervals, being North, East, South and West. Where the aspect changed, it was taken as the divide between side hillslopes and nose hillslopes. A visual inspection of the hillslope polygons was done to check whether the hillslope delineation was accurate and minor changes were made to correct anomalies.

Statistical analysis of terrain features of hillslopes were done with the Terrestrial Ecological Unit Inventory (TEUI, USDA Forest Service, 2005). TEUI analyses each polygon based on the raster layers which the user specifies. It takes the value of each individual pixel within the polygon and derives the following statistical parameters for that polygon for each terrain property: Mean, standard deviation, minimum value, maximum value, range, majority, minority, median, variety, total sum and skewness. The terrain attributes which were used as input was altitude above sea level (the DEM), slope, profile curvature and planform curvature. As TEUI only uses whole numbers as input, the curvature data layers were multiplied with a 1000 to obtain meaningful whole numbers.

Thereafter three different major soil catenas were determined from the land type inventories, based on the percentage which each soil occupies on each terrain morphological unit (TMU). The assumption is that these catenas occur on topographically distinct hillslopes. Using expert knowledge, a theoretical expected topography for each catena was determined. It was deduced that the TMU 1 position would be dominantly Mispah (Ms) soil form, irrespective of the topography. The 5 position would be largely determined by the stream, and thus the soils that occur there are also independent of the hillslope. On the 3 and 4 positions though, 4 soil types dominate, i.e. Sterkspruit (Ss), Valsrivier (Va), Shortlands (Sd) and Hutton (Hu). From this it was deduced that the Sterkspruit soils would occur on flat slopes, with the Shortlands and Hutton soils on concave areas, and Valsrivier on convex and steep slopes. Shortlands and Hutton soils are more weathered than Valsrivier soils, and thus would occur in areas where water accumulates. Straight, moderately steep slopes were assigned a Valsrivier-Shortlands-Hutton soil association map unit, as it cannot be determined which soils would be dominant. Thus the 4 major catenas which exist on these hillslopes are Ms-Va-Alluvium, Ms-Sd/Hu-Alluvium, Ms-Ss-Alluvium and Ms-Va/Sd-Alluvium. A computer program written in Microsoft Excel was then used to determine the values of the TEUI derived terrain parameters which fitted with each catena.

By using the Topographical Positioning Tool (TPI, Weiss, 2001), the TMU's of the hillslopes were determined. By applying the conceptual models of the hillslopes to the TPI, a soil map was created, and the spatial extent of the conceptual models could be determined.

Results and discussion

With the hillslope delineation method 196 hillslopes were delineated in the study area. They can be seen in Figure 117 and the position of the hillslopes where the different catenas are expected to be present can be seen in Figure 118. The major catenas of three conceptual hydrological flow models can be deduced. They can be seen in Figure 119, Figure 120 and Figure 121. The conceptual hydrological flow model of the Ms-Va/Sd-Alluvium catena will be either the same as the Ms-Va-Alluvium or the Ms-Sd-Alluvium catena, but it is not possible to tell which conceptual hydrological response model will occur on that specific hillslope. The conceptual hydrological flow paths show a lot of recharge, through the Mispah soils on the TMU 1 positions. Recharge also occurs on the TMU 3 and 4 at the Sd/Hu soil map unit. This recharge probably surfaces again in the TMU 5 position, which will explain the presence of the wetland. On both the Va and Ss soils, surface runoff will be the main flow path, as due to the low infiltration water into the dense B horizon, infiltration excess runoff will occur. The TMU's determined with the TPI tool can be seen in Figure 122. The soil map produced by superimposing the TMU map and the expected soil catena map can be seen in Figure 123.



Figure 118 Hillslopes of the study site

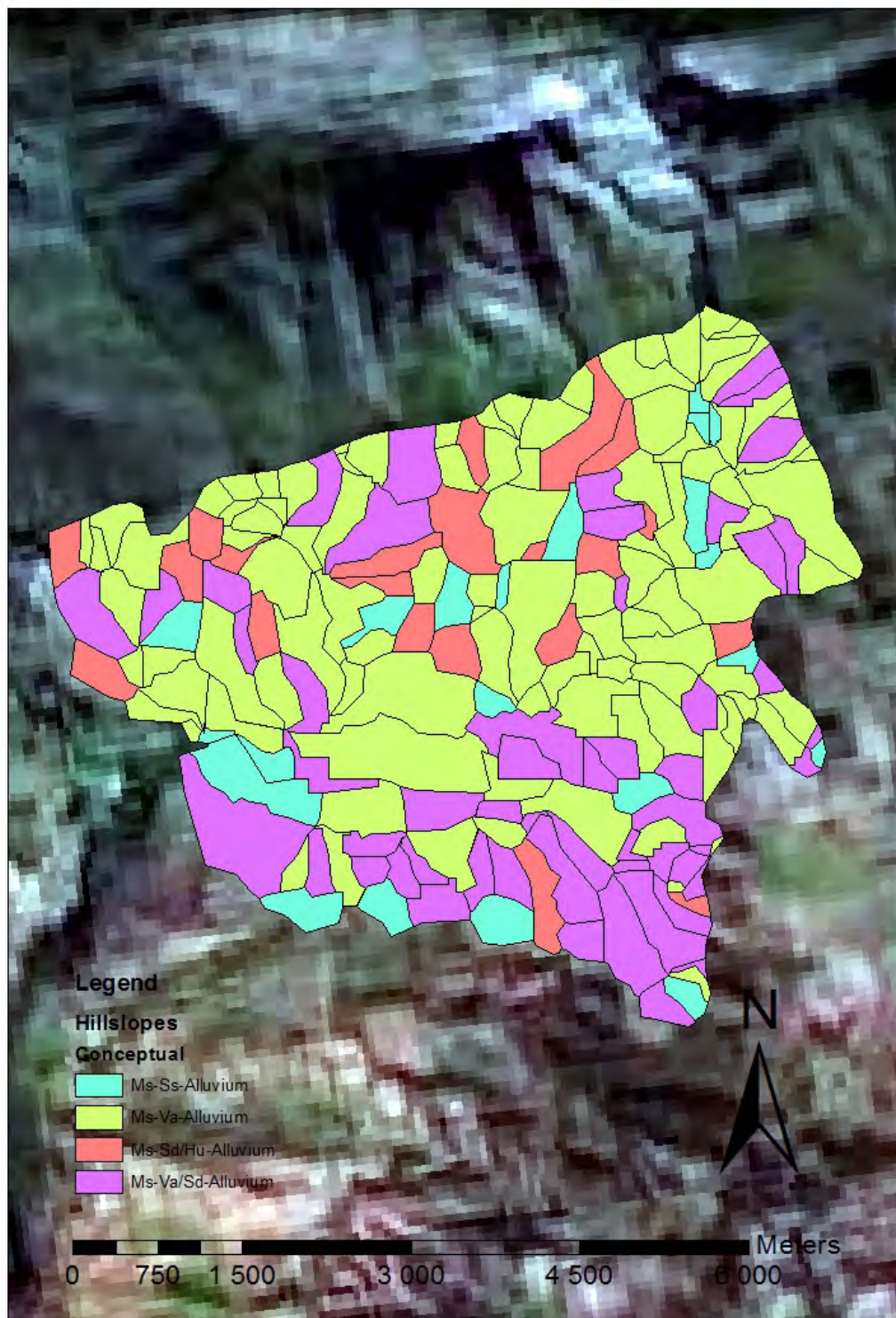


Figure 119 Areas where the different possible catenas are expected to occur

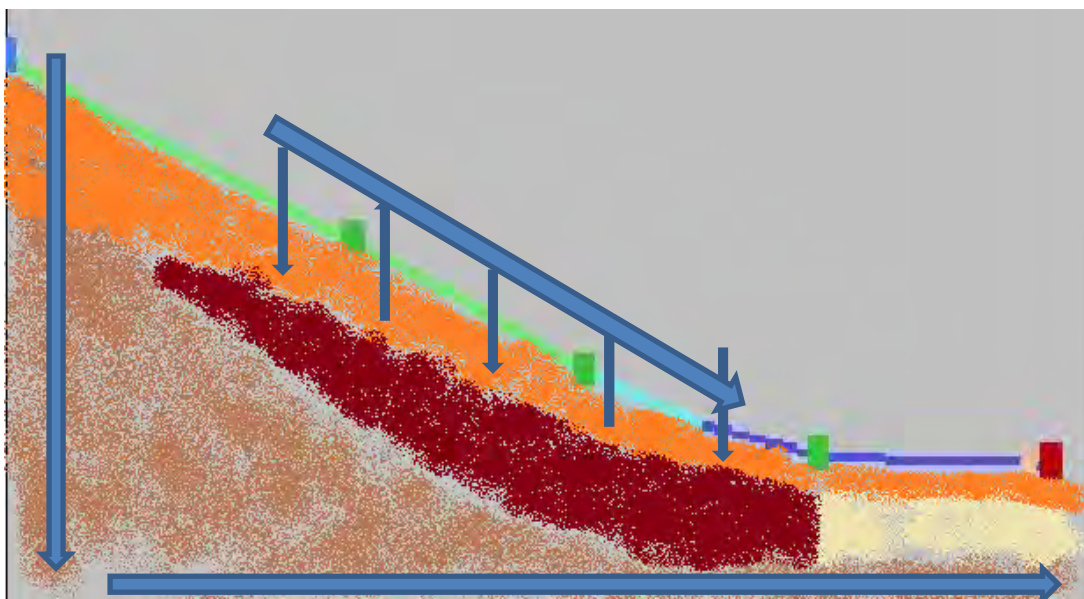


Figure 120 Conceptual hydrological flow model for the Ms – Va – Alluvium catena

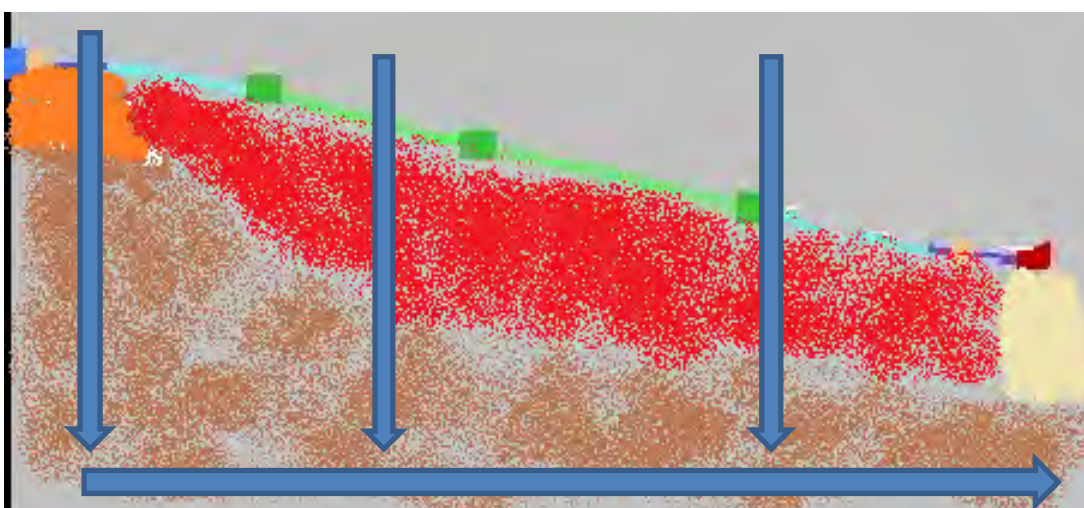


Figure 121 Conceptual hydrological flow model for the Ms – Sd/Hu – Alluvium catena

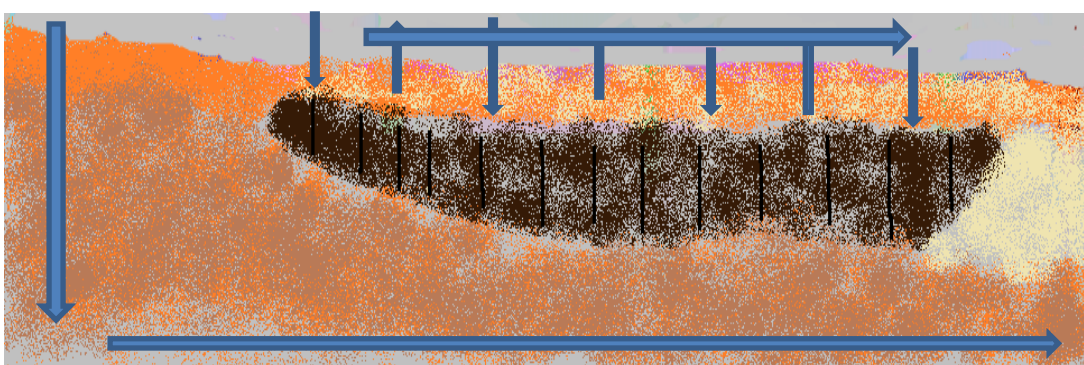


Figure 122 Conceptual hydrological flow model for the Ms – Ss – Alluvium catena



Figure 123 The Terrain morphological units for the study site

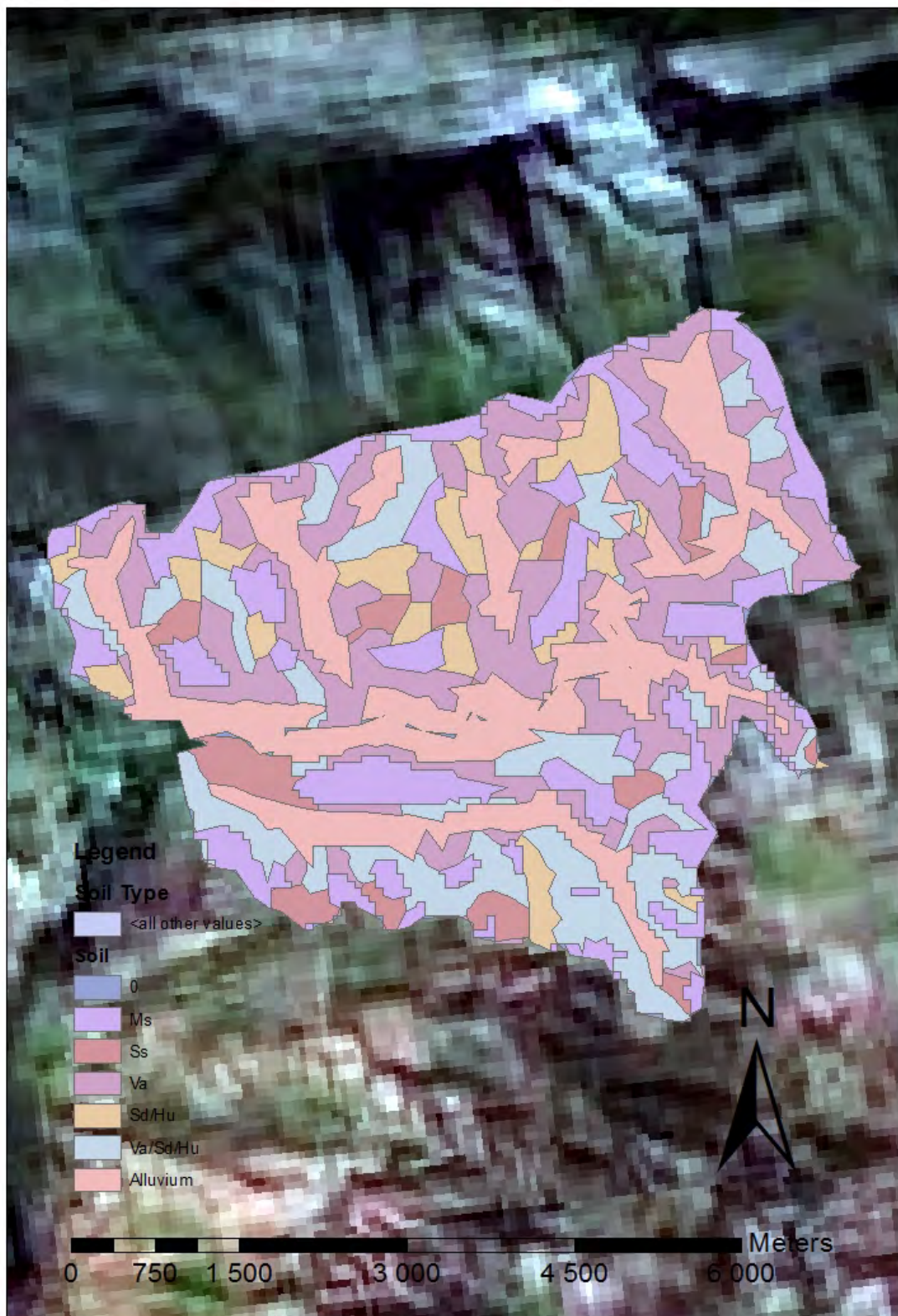


Figure 124 The soil map of the study site

Table 22 shows the area in hectares which was mapped for each soil map unit, as well as the areas calculated from the land type inventories. The total areas vary as the study was done only a part of the land types. The value for the Sd/Hu/Va mapping unit was omitted for from the land type area, as this unit combines information included in the Valsrivier and Shortlands/Hutton map unit. In Figure 124, which shows the percentage of the area mapped against the percentage of the area obtained from the land type inventory, a data point was included which represents the all the soil mapping units of which Shortlands, Hutton and Valsrivier form part.

Table 22 : Areas of mapping units obtained by the methodology as well as from the land type inventory

| Soil Map Unit | Mapped area | | Land type area | |
|-------------------|-------------|-----|----------------|-----|
| | ha | % | ha | % |
| Mispah | 522 | 19 | 4068 | 13 |
| Sterkspruit | 163 | 6 | 7280 | 23 |
| Valsrivier | 685 | 26 | 8873 | 28 |
| Shortlands/Hutton | 191 | 7 | 5212 | 17 |
| Sd/Hu/Va | 450 | 17 | | |
| Alluvium | 672 | 25 | 6030 | 19 |
| Total | 2683 | 100 | 31713 | 100 |

The value for the Sd/Hu/Va mapping unit was omitted for from the land type area, as this unit combines information included in the Valsrivier and Shortlands/Hutton map unit.

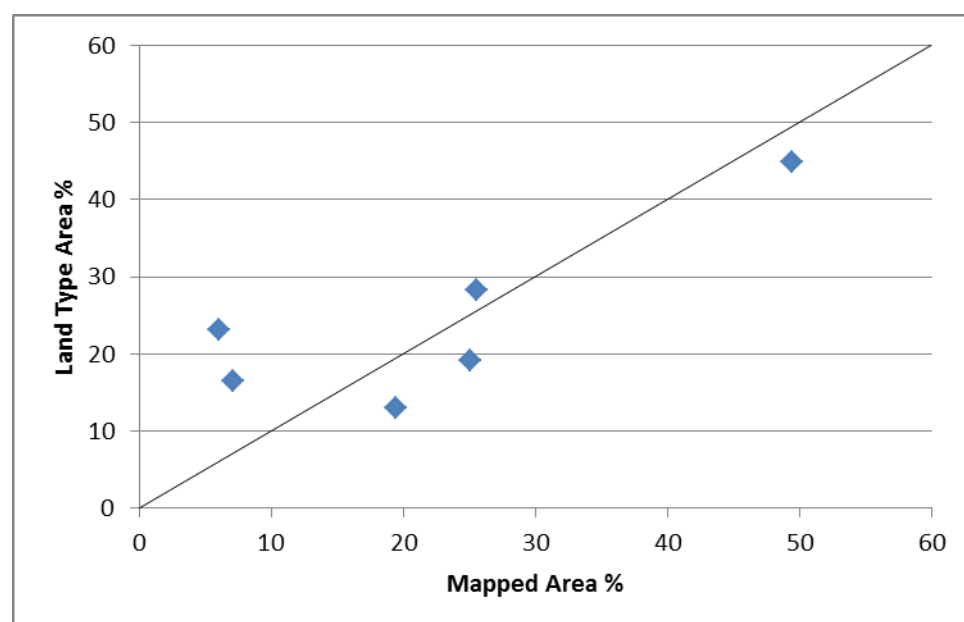


Figure 125 Soil Map unit areas against areas obtained from the land type inventory. A point representing all the mapping units which represents Shortlands, Hutton and Valsrivier soil forms was included. The black line is the 1:1 line

From Table 22 and Figure 125 it can be seen that the soil forms from the soil map and land type inventories cover roughly the same percentage of area. The percentage area mapped of the Valsrivier map unit and the Shortlands, Hutton and Valsriver soil map unit matches very well to the percentage area from the land types, while the areas of the Mispah and Alluvium map units match moderately well. The mapped areas of the Shortlands/Hutton and Sterkspruit mapping units match the land type inventories' areas poorly. The higher percentage of Mispah soils on the map than in the land type inventory is not surprising, as this study only used the upper parts of the land type, where one would expect to find a larger percentage rock than in the whole land type. This could also partially explain the lower map areas of the sterkspruit soil form, as this soil form generally occurs in areas with a low slope. The excellent match between the percentage areas of the Valsrivier and Shortland, Hutton and Valsriver map units and the under prediction of the area of the Shortlands/Hutton map unit suggest that a conceptual error has occurred. When one adds the area mapped for the Sd/Hu/Va map unit to that of the Shortlands/Hutton, the area matches very well to that of the land type inventory. Therefore the data suggests that the conceptual model for the distribution of the Sd/Hu/Va is wrong and that whole mapping unit should be regarded as the Shortlands/Hutton mapping unit. Thus we can use this methodology to refine the expert knowledge of the soil distribution in an area.

Conclusion

It has been shown that terrain analysis can be used to theoretically disaggregate land type inventories into soil maps and conceptual hydrological flow models. This will dramatically enhance hydrological predictions in ungauged basins. Using this methodology a soil map was produced wherein the areas which the mapping units cover acceptably matched the areas of those mapping units in the land type inventory. The theoretical approach still needs field verification.

The proposed methodology is:

Step 1: Determine area to be worked in

Work within land types, as they were created using the soil forming factors. When a land type does not cover the whole of the hillslopes, two or three land types can be joined to include the whole hillslope.

Step 2: Acquire data

The best possible DEM is necessary for this work. The better the resolution of the DEM, the better the results will be. It is however important to note that to acquire a finer resolution, the quality of the DEM should not be compromised.

Step 3: Determine the flow accumulation

Fill the DEM, determine the flow direction and from that determine the flow accumulation. Visually inspect the data to determine what the cut off flow accumulation value will be where it will be counted as a stream.

Step 4: Determine all the watersheds in the area worked on

Determine all the watersheds within the landtype. Place two pour points at places where streams converge and one at the stream end. Convert the watersheds to polygons.

Step 5: Delineate hillslopes

Convert the watershed polygon layer to hillslopes by manually cutting the watershed polygons on the stream lines. Use aspect to decide how nose hillslopes will be delineated. Assign a hillslope number to each hillslope. Inspect hillslopes visually to see whether all

hillslopes extend to a portion of a stream, and whether or not the delineation makes sense. Adjust hillslope delineation if necessary.

Step 6: Determine the major catenas present in the land type

Consult the land type inventory and apply tacit knowledge. Include as much detail as is workably possible.

Step 7: Use TEUI to determine the topographical statistics for each hillslope

The input variables depend on the expected major catenas and on which types of hillslopes they are expected to occur.

Step 8: Assign hillslopes to the major catenas

Using the TEUI statistics, sort the hillslopes according to the types of hillslopes on which it is expected for the major catenas to occur. Create a major catena map from the hillslopes.

Step 9: Determine the TMU's for each hillslope

Use the TPI tool to create a TPI number and with visual inspection reclassify the raster to create polygons for the different TMU's

Step 10: Create final soil map

Superimpose the TMU map on the catena hillslope map. This will allow for TMU's to have soil types to be assigned to them, and thus a soil map will be created.

Step 11: Conceptualize hydrological flow models for each catena

Apply hydopedological knowledge to the major catenas to create conceptual hydrological flow model

3.2.2 Case study 2: Using a soil map to create a hydrological response unit map

Introduction

Initially a different land type disaggregation method that the first case study was used in this case study to disaggregate two land types Ea34 and Ca11 (Land Type Survey Staff, 1986). This method was improved by adding more information to three subsequent soil maps. Thus four soil maps were produced, each with its own accuracy determination. The last two maps were not disaggregation maps, but rather expert knowledge based DSM maps. The final map, which included the most data, had the best accuracy and was therefore used to create a hydrological soil distribution map. The hypothesis expressed in this case study is that there is a sound scientific correlation between the local dominant soil forming factors, topography and parent material. This enables DSM methods to be used to create useful soil maps. These soil maps can then be linked to conceptual hydrological responses, which allows for the extent where certain hydrological responses can be expected to be mapped. This data could be used as input into hydrological models.

Material and methods

Site description

The study site of 6 865 ha is north of Madadeni and Newcastle, in KwaZulu-Natal, close to the border with Mpumalanga and the Free State (Figure 126). Its geographical centre point is 29.95°E and 27.62°S. Two land types occur in this area, namely Ea34 and Ca11 (Land Type

Survey Staff, 1986). The geology of land type Ea34 is dominated by dolerite lithology (Geological Survey, 1988), which weathers to swelling red or black clay soils. Land type Ca11 has sandstone as its main lithology (Geological Survey, 1988), which weathers to sandy soils, often with plinthic character in the deeper subsoil horizons. The mean annual precipitation is 858 mm (SAWS, 2012). The veld types in the area are the KwaZulu-Natal Highland Thornveld and Income Sandy Grassland (Mucina and Rutherford, 2006). Commercial cattle farming is the primary land use. Fields are burnt annually to provide regrowth as fodder for the cattle. This site was chosen as it is one of the sentinel sites for the Africa Soil Information Service (AfSIS) (Vågen *et al.*, 2010).

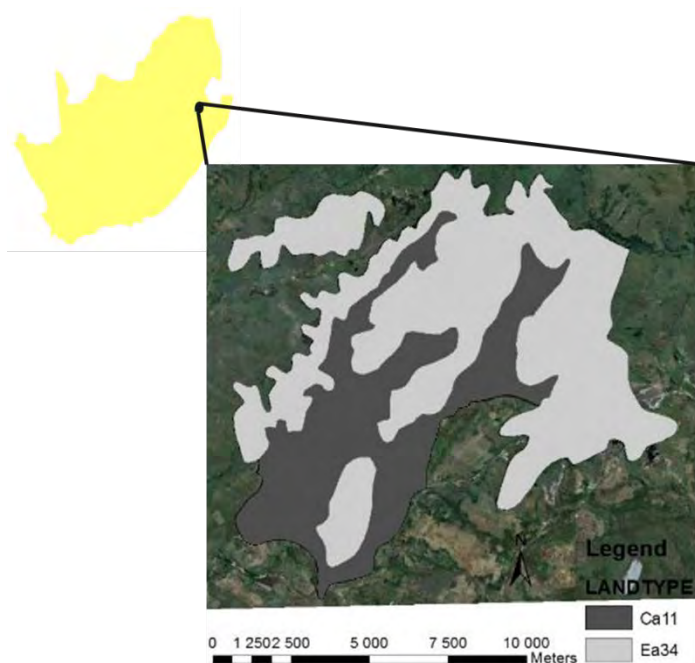


Figure 126 The Madadeni study site, showing the extent of the Ca 11 and Ea 34 land types

The typical topography of the two land types varies (Figure 127). Land type Ea34 has all the topographical positions from crest to valley bottom, largely with short concave slopes. In contrast to this land type Ca11 has long concave slopes and is only comprised of crest, midslope and valley bottom positions.

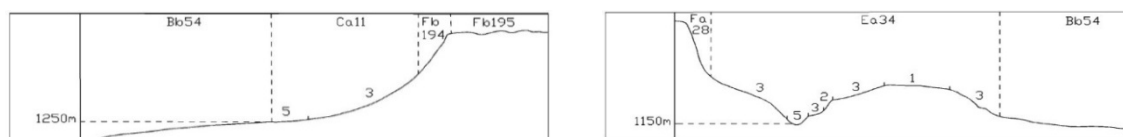


Figure 127 Terrain sketches of Land Types Ca11 (Fig. 127a) and Ea34 (Fig. 127b) (Land Type Survey Staff, 1986)

Software used

The software used in this project is Arc Map 9.3 (Environmental Systems Research Institute Inc., 2010), 3dMapper (Terrain Analytics, L.L.C.; 2003) and the Soil-Land Inference Model (SoLIM, Zhu *et al.*, 1997). 3dMapper and SoLIM have been specifically developed for use in DSM. SoLIM enables the user to capture soil terrain interactions as rules and runs an inference to create maps from these rules. Within 3dMapper terrain attributes and maps created by SoLIM can be viewed in a 3d environment.

Methodology

Four different soil maps were drawn in hierarchical fashion, with each map having increasing levels of input. The first map was drawn in the office, by only using the land type inventory and a 30 m DEM interpolated from the 20 m contours of the 1: 50 000 topographic maps. The land types were divided by hand into their respective terrain morphological units (TMU's), and the soil types listed in the land type inventory on each TMU divided into three groups, i.e. shallow soils, wet soils and intermediate soils. These soil associations were then mapped by hand using 3dMapper and ArcGIS for land type Ca11 and with the SoLIM inference model for land type Ea34.

Thereafter a reconnaissance field visit was undertaken to the study site, along with the land type surveyor of the area, to better grasp the soil genesis of the area. This resulted in incorporating parent material into the equation, by using the 1: 250 000 geological map to differentiate the dolerite from the sandstone. The area was then divided into soilscape or soil landscapes, which are continuous areas with the same soil distribution patterns. From the soilscape the soil associations were mapped by hand in ArcGIS.

A lithology map (Figure 128b) was created for parent material input, as soil formation is influenced by the lithology and not hard geology (Figure 128a). Soil formation on sandstone hillslopes with dolerite colluviums especially underlined this statement. Therefore a Dol_Sand geological map unit was included in the lithology map for areas in the downslope colluvial positions where dolerite influence was noticed in the soil formation.

Field work included one hundred and eighteen auger observations (Figure 129), with the soils being classified according to the Soil Classification Working Group (1991). The observation points were determined in a hierarchical nested sampling plan, which is used by AfSIS (Vågen *et al.*, 2010). The third and fourth soil map was constructed using SoLIM with stratified randomly selected 30% and 60% of the observation points respectively. The map legend was simplified into six soil associations, to improve the maps accuracy, following step 9 of the SCORPAN approach (McBratney *et al.*, 2003). Table 23 shows how the soil forms determined from the field observations were divided into the map units.

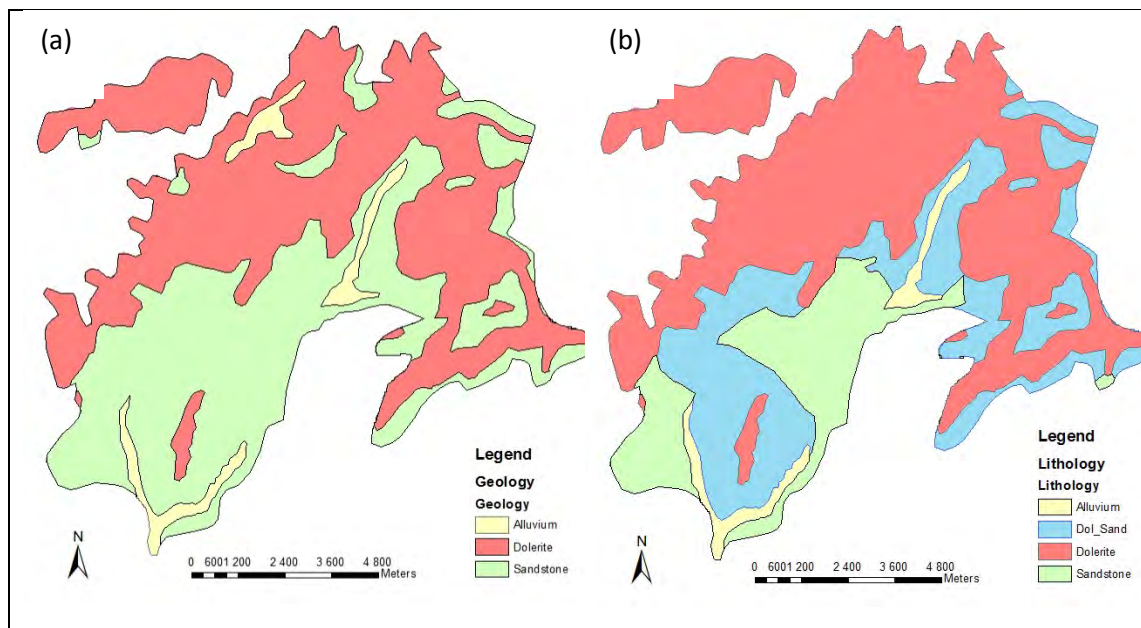


Figure 128 The geology of land types Ca11 and Ea34 (Geological Survey, 1988) (Figure 128a) and the revised lithology map (Figure 128b)

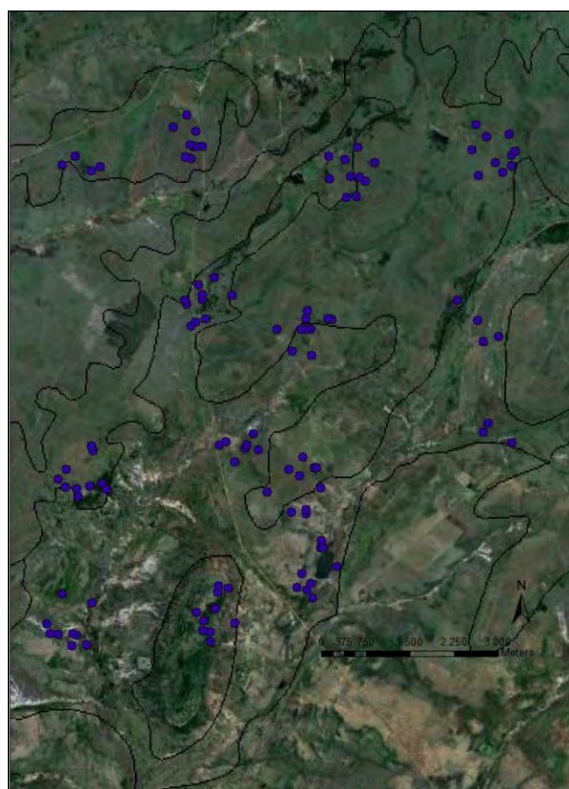


Figure 129 Observation points on a Google Earth image

Shallow soils and wet soils occur throughout the area and their distribution is determined by the topography. Red and dark clays occur on the dolerite parent material, which provides the basic cations needed for clay formation. Plinthic soils occur on the sandstone parent material. On the hillslopes where dolerite overlies sandstone and the dolerite colluvium plays a marked role in soil formation, the intermediate soils occur. These soils are not as clayey as pure dolerite derived soils, but also not as sandy as sandstone derived soils. Some

soil forms fit into more than one soil map unit. This is because they have characteristics of both the soil map units, and is probably a transitional zone between two soil map units.

Table 23 Soil forms comprising each map unit

| <i>Map unit</i> | <i>Soil forms</i> | |
|------------------------|---------------------------------------------------------|----------------------|
| | <i>South Africa</i> | <i>WRB</i> |
| Red Clays (RC) | Shortlands, Hutton | Nitisols, Ferralsols |
| Dark Clays (DC) | Arcadia, Rensburg, Bonheim, Milkwood, Willowbrook | Vertisols, Mollisols |
| Shallow Soils (SS) | Mispah, Milkwood, Glenrosa, Rock | Leptosols |
| Wet Soils(W) | Katspruit, Kroonstad, Dundee, Rensburg, Willowbrook | Gleysols, Stagnosols |
| Plinthic Soils (P) | Avalon, Westleigh, Longlands, Glencoe, Wasbank, Dresden | Plinthosols |
| Intermediate Soils (I) | Bonheim, Valsrivier, Sepane | Luvissols, Lixisols |

Validation was done by using all the observations for the Maps 1 and 2, and the observations which did not form part of the training data for Maps 3 and 4. Thus for maps 1 and 2 ,118 observations were used for validation, for map 3 it was 83 and for map 4 there were 47 validation observations. Map accuracy was calculated by the percentage of observations that was predicted correctly. Observations of soil types which fit into two soil map units were regarded as correct if it fell into either of those soil map units. Borderline observations were regarded as part of both soil map units, if it was unclear into which soil map unit the observation fell at a scale of 1 : 10 000.

The accuracy of the fourth map was 67% which is deemed to be adequate. Each soil association from this map was assigned a hydrological response soil type, which enabled the map to be divided into typical hydrological response soils. The size and position of each hillslope type could be determined from the map, which could then in turn be used for hydrological modelling purposes.

Results and discussion

The four maps created can be seen in Figure 130. The accuracy of the maps improved with higher input into the maps. The first map included some anomalies in the map legend. Avalon soils (Av, plinthosols) and Arcadia soils (Ar, vertisols) were grouped together in the same map unit, since subdivision was only done on the basis of terrain forms. It would be desirable from a soil property and land use perspective to separate these soils.

This was done by including lithology into the second map, which resulted in a better usability of the map, but did not improve the map accuracy. The map legend also became too complex. For the third map the map legend was simplified, and it immediately improved the map accuracy and smoothed out the map units.

The fourth map achieved an accuracy of 67%, slightly better than the average traditional soil map accuracies of 65% as quoted by Marsman and de Gruiter (1986). In addition to being more accurate, it shows a lot more intricacy than the third map. This should closer represent the real situation at a large scale, showing differences in mapping units across short distances. As all the maps were evaluated at a scale of 1: 10 000, the larger measure of

intricacy probably contributed to the higher accuracy of the map. It is clear that using more observations as training data improved the final product.

An error matrix for Map 4 (Table 24) shows the specific accuracy of the different soil map units. The Wet (W) and Shallow soils (SS) map units are very accurate with barely any other observations made in them, although they did not include all the Wet and Shallow soils observations. This shows that the map units might be widened slightly. Seventy seven percent of the dark clay (DC) observations were mapped correctly, but the map unit included a small number of plinthic soils (P), indicating possible small inaccuracies in the lithological map. The presence of shallow soils in the dark clay mapping unit is to be expected and may not be due to mapping errors as rock outcrops will commonly occur in this mapping unit.

The plinthic soil observations were mapped to an acceptable accuracy, but the map unit included quite a few other observations, indicating that the map unit is too broad. The rules governing the delineation between the plinthic and intermediate (I) soil map units could be improved. Sixty six percent of the intermediate observations lie on the plinthic map unit and 50% of the observations on the intermediate map unit are plinthic soils. This might not be a true reflection of the map units' accuracy, as very little observations fell on the intermediate soil map unit.

The combination of soil forming factors giving rise to red structured clay on the one hand and dark swelling clays on the other hand are not well understood in quantitative terms. Although both soils are commonly derived from basic igneous rocks, it is still unknown how soil forming factors determine which type of soil will form at a specific location. Thus, it is no surprise that there are dark clay observations on the red clay (RC) map unit and vice versa.

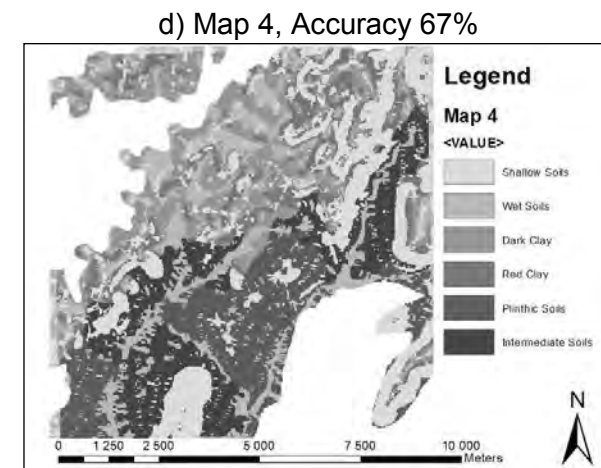
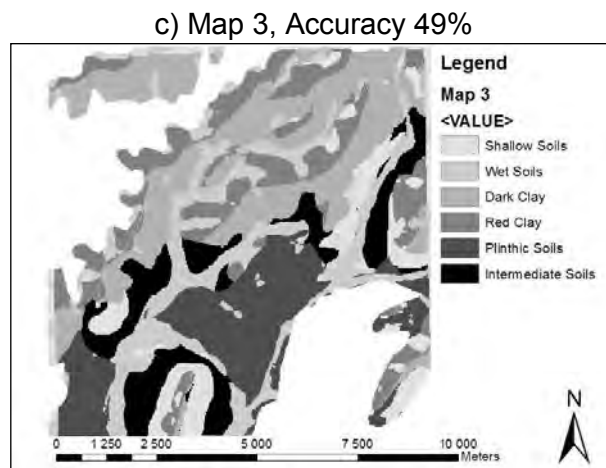
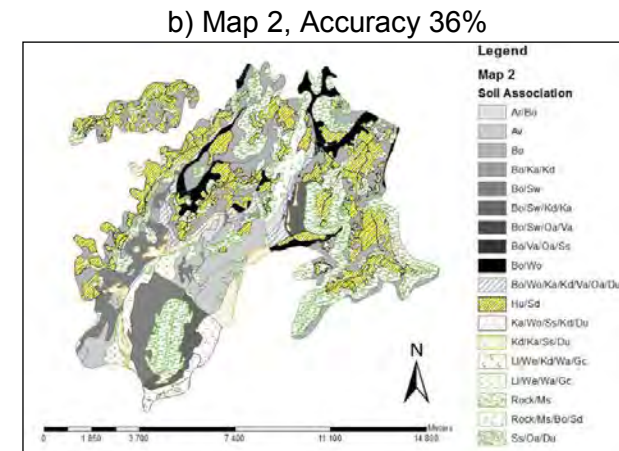
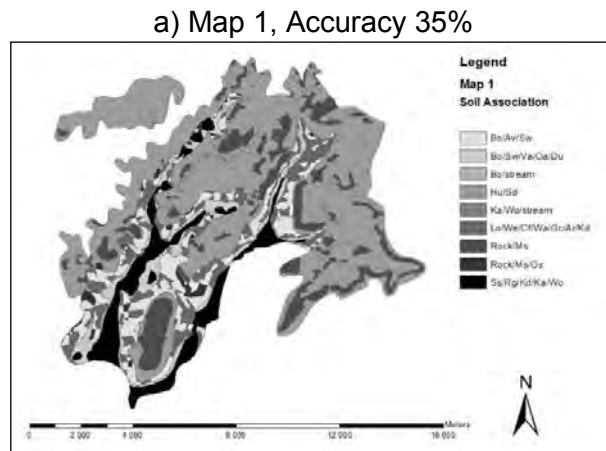


Figure 130 The four maps created in the project, showing their accuracies. The descriptions for the soil map units of Maps 1 and 2 (Figure 130a and Figure 130b) are as follows: Red Clays: Shortlands (Sd), Hutton (Hu); Dark Clays: Arcadia (Ar), Rensburg (Rg), Bonheim (Bo), Milkwood (Mw), Willowbrook (Wo); Shallow Soils: Mispah (Ms), Glenrosa (Gs); Wet Soils: Katspruit (Ka), Kroonstad (Kd), Dundee (Du), Plinthic Soils: Avalon (Av), Westleigh (We), Longlands (Lo), Glencoe (Gc), Wasbank (Wa), Dresden (Dr); Intermediate Soils: Valsrivier (Va), Sepane (Se)

Table 24 An error matrix of Map 4

| <i>Validation</i> | | <i>Observations</i> | | | | | | | | |
|-------------------|--------------------|---------------------|-----------|----------|----------|-----------|----------|--------------------|--------------|--------------------|
| | | <i>RC</i> | <i>DC</i> | <i>I</i> | <i>P</i> | <i>SS</i> | <i>W</i> | <i>Correct (#)</i> | <i>Total</i> | <i>Correct (%)</i> |
| <i>Map</i> | <i>RC</i> | 1 | 2 | 0 | 0 | 0 | 0 | 1 | 3 | 33 |
| | <i>DC</i> | 1 | 10 | 0 | 1 | 3 | 0 | 10 | 15 | 67 |
| | <i>I</i> | 0 | 1 | 1 | 2 | 0 | 0 | 1 | 4 | 25 |
| | <i>P</i> | 1 | 0 | 2 | 6 | 1 | 1 | 6 | 11 | 55 |
| | <i>SS</i> | 1 | 0 | 0 | 0 | 10 | 0 | 10 | 11 | 91 |
| | <i>W</i> | 0 | 0 | 0 | 0 | 0 | 4 | 4 | 4 | 100 |
| | <i>Correct (#)</i> | 1 | 10 | 1 | 6 | 10 | 4 | 32 | | |
| | <i>Total</i> | 4 | 13 | 3 | 9 | 14 | 5 | | 48 | |
| | <i>Correct (%)</i> | 25 | 77 | 33 | 67 | 71 | 80 | | | 67 |
| | | | | | | | | | | |

To convert the soil association map to a hydrological soil map, soil associations were converted to hydrological response units. This was done as in Table 25. This resulted in four distinct hydrological response hillslope types namely: Interflow-Responsive, Recharge-Responsive, Recharge-Interflow-Responsive, Responsive-Recharge-Interflow-Responsive.

Table 25 Conversion of soil associations to soil hydrological response units

| Soil Association | Hydrological Response Unit |
|----------------------------|-----------------------------------|
| Shallow Soils on Dolerite | Recharge |
| Shallow Soils on Sandstone | Responsive |
| Plinthic Soils | Interflow |
| Intermediate Soils | Interflow |
| Red Clays | Recharge |
| Black clays | Responsive |
| Wet soils | Responsive |

Figure 131 graphically shows the individual conceptual response models. For the Interflow-Responsive hydrological response the water will flow within the soil, either at the soil rock interface, the A-B horizon interface or above the plinthic layer, until it reaches the wetland. The Recharge-Responsive hydrological response occurs where either red clays or shallow soils overlies dolerite. Water will move vertically through the soil profile into the bedrock, where it will slowly trickle in cracks and fissures until it reaches the wetland. The Recharge-Interflow-Responsive model fits an area where geologically dolerite overlies sandstone. Recharge will occur on the red clays or shallow soil on the dolerite. Water following this flowpath will return to the soil lower down either in the interflow or responsive hydrological unit. The interflow area is where intermediate soils developed in the dolerite colluvium on the sandstone. Water will flow in the soil until it reaches the wetland. This hydrological response unit thus has two flow paths. The Responsive-Recharge-Interflow-Responsive hydrological response unit will react in the same way as the Recharge-Interflow-Responsive model, except that a responsive area overlies the recharge area. This is due to black clays which form on dolerite at the crest of the soilscares.

Figure 132 shows the extent of the different hydrological response units, while the areas which they cover can be seen in Table 26.

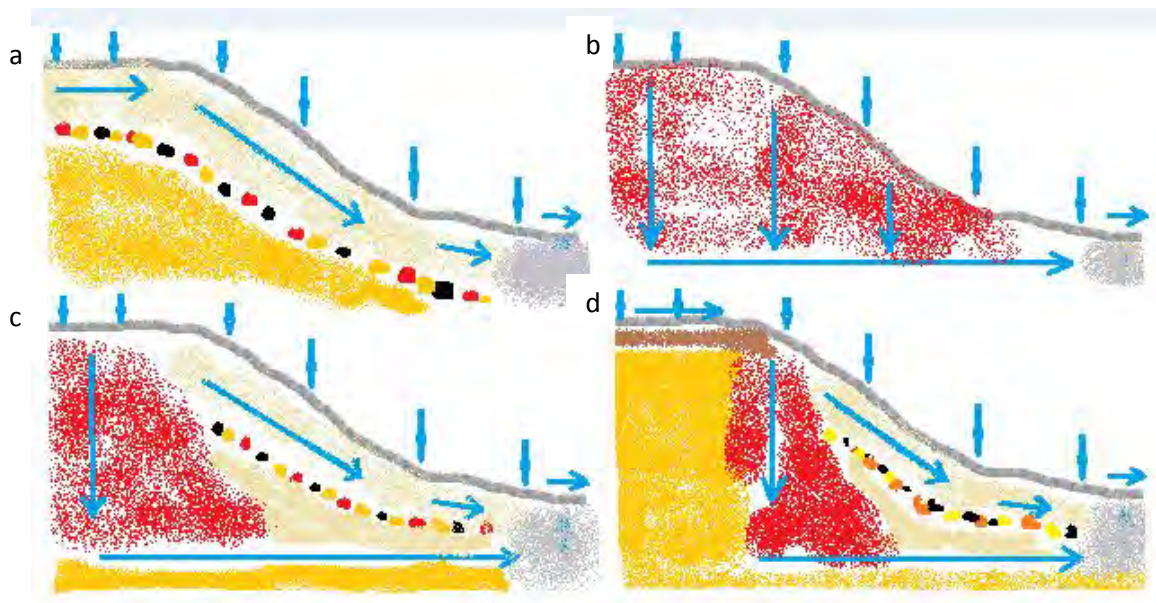


Figure 131 The conceptual hydrological flow models for the four hydrologically different hillslopes. Interflow-Responsive (a), Recharge-Responsive (b), Recharge-Interflow-Responsive (c), Responsive-Recharge-Interflow-Responsive (d)

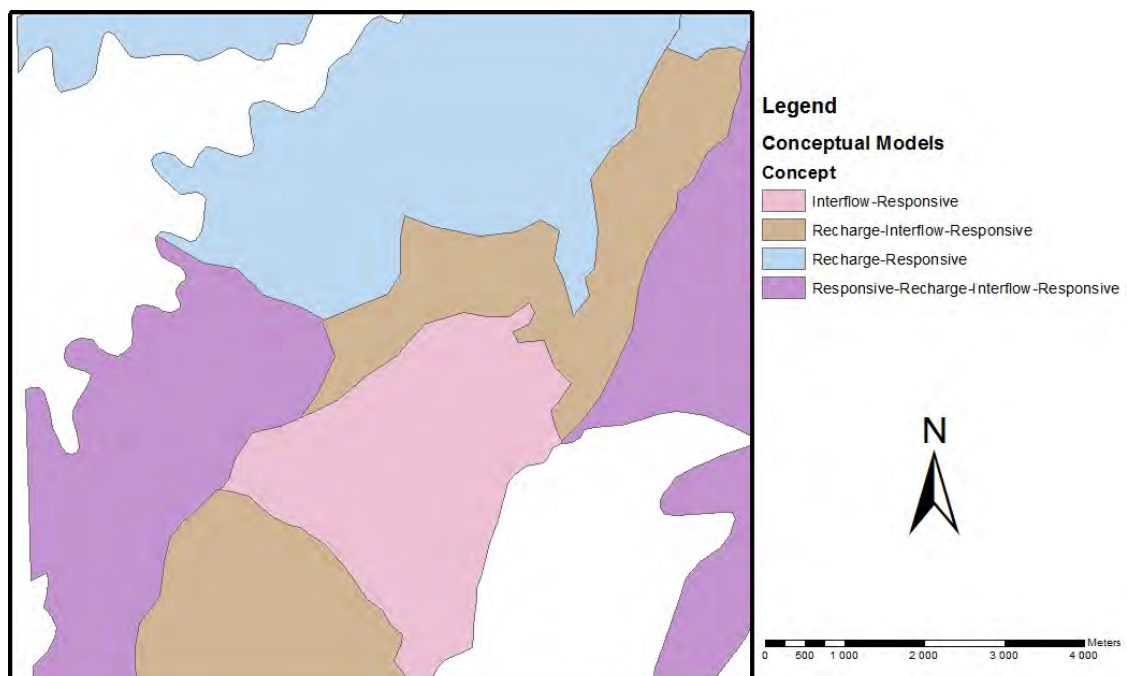


Figure 132 A map showing the extent of each hydrological response model

Table 26 Areas covered by the different conceptual hydrological responses

| Hydrological Response | Area (ha) | Area (%) |
|------------------------------------------|-----------|----------|
| Interflow-Responsive | 1785 | 26 |
| Recharge-Responsive | 2334 | 34 |
| Recharge-Interflow-Responsive | 686.5 | 10 |
| Responsive-Recharge-Interflow-Responsive | 2059.5 | 30 |

The largest part of these two landtypes has a Recharge-Responsive hydrology, closely followed by a Responsive-Recharge-Interflow-Responsive and Interflow-Responsive hydrology. In a small area the hydrological model will follow a Recharge-Interflow-Responsive pathway.

By converting the soil map into hydrological response units, the area, position and conceptual hydrological response of the two land types could be known. This input could further be entered into hydrological models to increase their accuracy.

Conclusions

The land type survey proved to be a good basis to start DSM. Digital soil mapping methods, and specifically the SoLIM software combined with expert knowledge and soil observations can be used to disaggregate land types into accurate soil association maps. The higher the input into these maps, the better the map accuracy will be. Using only terrain analysis, soil form distribution could be predicted from this platform, to a reasonable accuracy. Including parent material as input variable improved the usability of the soil map. A revised lithology map represented the real parent material better than hard geology did, especially in soils where dolerite colluvium influenced soil formation on sandstone geological map units. Simplifying the map legend into soil associations improved the accuracy of the map. Field work is critical to obtain acceptable results. Results improved when more observations were used as training data.

The soil associations maps were then converted to hydrological response units, which allows for the extent of conceptual hydrological response units to be known. Thus from the soil map, the conceptual hydrological response, as well as its extent is known. This information is a valuable asset in hydrological modelling.

3.2.3 Case study 3: Creating a hydrological response unit map from scratch by combining Digital soil mapping and hillslope delineation

Introduction

In the Kruger National Park the so-called “Supersites” project (Smit *et al.*, 2013) have been launched to combine the research done in many disciplines within the Park on specific representative sites. Four sites were chosen to represent the main climatic and ecological regions within the Park. This project is part of a baseline study on the hydrology of the Stevenson Hamilton Research Supersite. This case study combines the expert knowledge DSM approach with a part of the disaggregation methodology wherein the study site is divided into hillslopes to create a soilscape based hydrological map.

Material and methods

Site description

The study site is the 4 001 ha Stevenson Hamilton Research Supersite, approximately 7 km South of Skukuza in the Kruger National Park (Figure 133). The mean annual precipitation is 560 mm/a (Smit *et al.*, 2013), and the geological formation is granite and gneiss of the Nelspruit Suite (Venter, 1990). It lies in the Renosterkoppies land type (Venter, 1990). Furthermore it has a highly dissected landscape, with a high stream density (Smit *et al.*, 2013), with a few prominent inselbergs occurring as rock outcrops. *Combretum apiculatum* and *Combretum zeyher* dominate the woody vegetation on the crests. A distinct seepline commonly occurs between the crest and the midslopes, where *Terminalia sericea* is noticeable. *Acacia nilotica* and other fine leaved woody species are most abundant on the midslopes and footslopes. Sodic sites frequently occur, where of *Eucleadi vinoriumis* occurs commonly (Smit *et al.*, 2013). There is a very good correlation between the vegetation and soil type (Venter, 1990).

Data acquisition

A suite of environmental covariates were assembled including Spot 5 (SPOT image, 2013), Landsat (USGS, 2013) satellite images, remotely sensed biomass and evapotranspiration (ET) for a series of dates (eLeaf, 2013) and the SUDEM (Van Niekerk, 2012) digital elevation model. The SUDEM was re-interpolated to a 10 m and 30 m resolution, as multi-resolution elevation layers are useful to highlight different soil-terrain interactions. Topographic variables were derived from both DEM's with the basic terrain analysis tool in SAGA (SAGA User Group Association, 2011). Several additional co-variate layers, such as normalized difference vegetation index (NDVI), were created by mathematical manipulation of the different bands of the Landsat and SPOT 5 images.

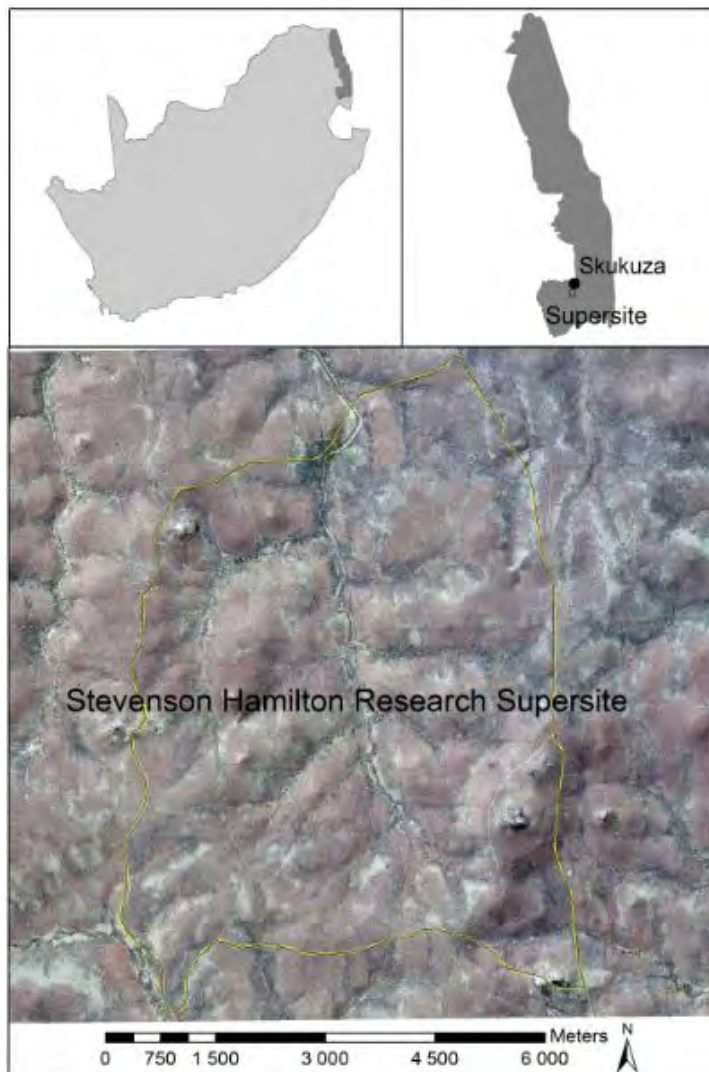


Figure 133 The Stevenson Hamilton Research Supersite

Field sampling

Three different sampling strategies were followed. For the training observations, both “smart sampling” and conditioned Latin hypercube sampling (cLHS) (Minasny and McBratney, 2006) were used. For the smart sampling a colour aerial photograph was subjectively divided into 5 classes, and observation positions were chosen to include all 5 of the classes. Twenty-five smart sampling observations were made. Six co-variate layers were included into the cLHS. These layers were the principal component analysis (PCA) results of the ET, biomass, Landsat images, SPOT 5 images and both the resolutions topographic variable layers. Thirty observation positions were selected, of which one was rejected due to being too close to a road. Thus 29 observations were made by cLHS. Fifty-nine validation observations were at in-field determined positions, with soil surveyors walking transects through the study site, visually selecting representative sites where observations could be made. In this way, the entire study site was covered. The smart sampling and cLHS ensured that the whole attribute space was sampled, whereas the in-field determined sampling ensured full spatial coverage (Figure 134). Soil observations were classified according to the

South African soil classification system (Soil Classification Working Group, 1991). Hand estimated texture, structure, mottles and stoniness were also observed per soil horizon.

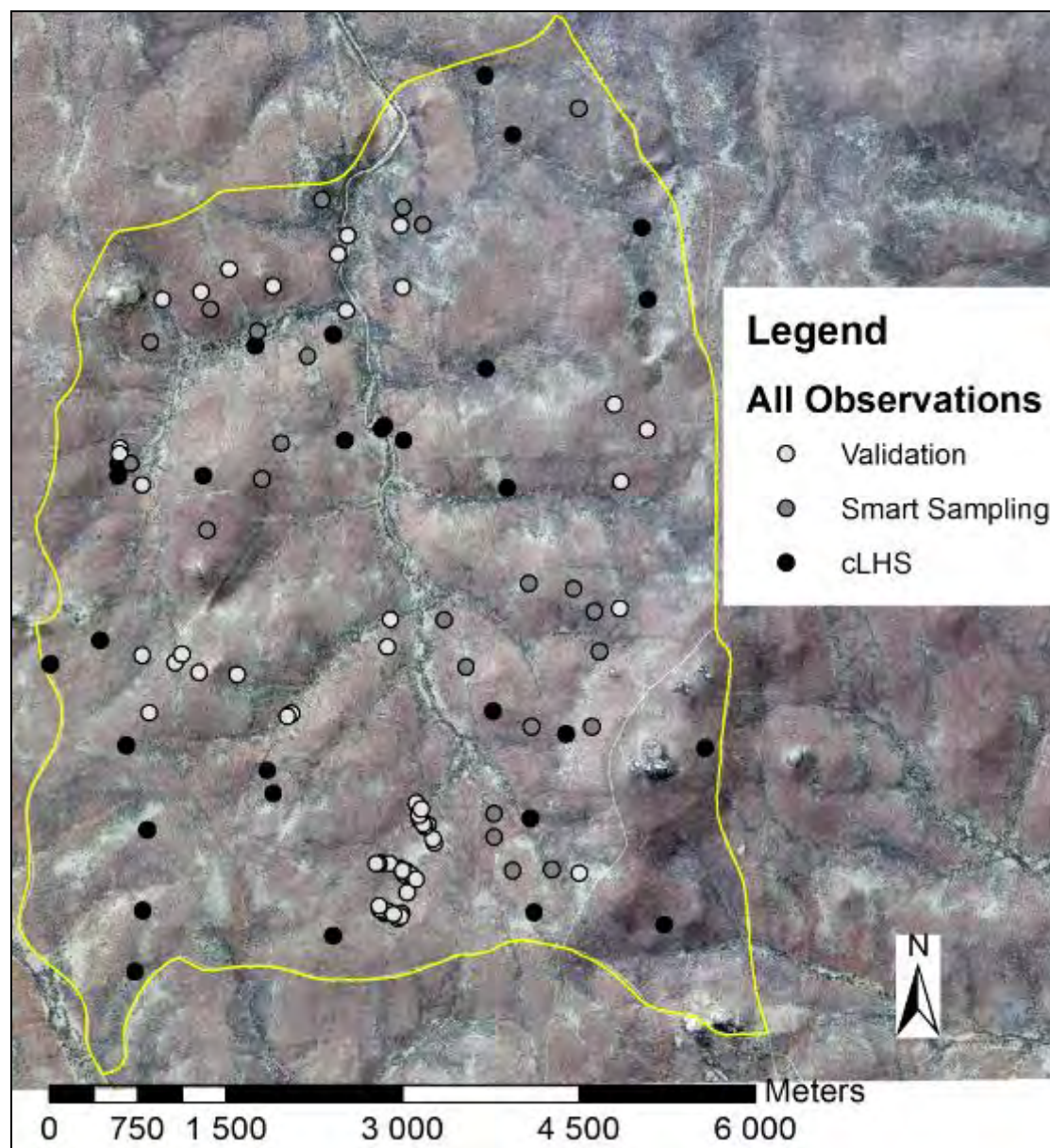


Figure 134 Soil observation positions

Soil map creation

The soil observations were divided into seven soil map units (SMU's) based on texture and the occurrence of a horizon with redox morphology. Descriptions of the SMU's are shown in Table 27. The SMU's were mapped by creating soil-landscape rules for each in SoLIM (Zhu, 1997). Central to these rules is an understanding of the soil distribution, based on the expert knowledge gained during field work for both the training and validation observations. Specific values for the rules are obtained from the values for the different covariates of the training soil observations only. The rules were derived by starting with the easiest, accurately identifiable SMU, the Sodic Soils. Once this SMU was mapped satisfactorily, the

rules which defined its distribution were inverted for the other SMU's. Then the Clayey soils were separated from the Sandy soils. Lastly within both the Clayey and Sandy soils the soils with redox morphology within the profile were distinguished from the soils without redox morphology within the profile.

Table 27 Descriptions of the soil map units

| Soil map unit | Soil forms ¹ | WRB Reference Groups ² | Determining characteristics | CHSRU |
|------------------|------------------------------------------------|-----------------------------------|---------------------------------------------------------------------------------------|------------|
| Sodic Site | Sterkspruit | Solonetz | Abrupt textural transition between the top and subsoil. Redox morphology in C horizon | Responsive |
| Clayey Interflow | Sepane, Bonheim | Luvisols, Phaeozems | High clay percentage in B horizon. Redox morphology in C horizon | Interflow |
| Clayey Recharge | Bonheim, Valsrivier, Swartland, Milkwood, Mayo | Phaeozems, Luvisols, Leptosols | High clay percentage in A and/or B horizon. No redox morphology in C horizon | Recharge |
| Sandy Interflow | Tukulu, Pinedene, Westleigh, Avalon | Arenosols | Coarse textured A and/or E horizon. Redox morphology in C horizon | Interflow |
| Sandy Recharge | Clovelly, Oakleaf, Mispah, Glenrosa | Arenosols, Leptosols | Coarse textured A horizon. No redox morphology in C horizon | Recharge |
| Rock Outcrops | Rock | Rock | Rock outcrop with cracks | Recharge |
| Alluvial Soils | Dundee, Oakleaf, Tukulu | Fluvisols, Arenosols | Coarse textured soils from alluvial deposits | Recharge |

WRB – World Reference Base; HRU – Hydrological Response Unit

¹ Soil Classification Working Group, 1991

² IUSS, 2007

By running an inference of the soil map rules, SoLIM created a soil map for the area. The raster layer soil map was converted to a shapefile, and filtered using a majority filter with a square radius of 2 pixels and a 20 % threshold. Polygons smaller than four pixels were manually included into larger, surrounding polygons. Alluvial soils were mapped by setting buffers around the channel network, which was delineated from the DEM in SAGA. The distance of the buffers were determined by the observations of how far alluvial soils occurred around the different stream orders. Rock outcrops were mapped manually from an aerial photograph, following the effort principal that it is better to map areas than to predict it when it is easier to map it (McBratney *et al.*, 2002).

The map was validated using the independent validation observations. Map accuracy was calculated as a percentage of correctly predicted point observations. A one pixel buffer was included around SMU's, as in Van Zijl *et al.* (2012). An accuracy matrix was created to evaluate the accuracy of each SMU.

Conversion from soil map to hydrological soil map

To create a hydrological soil map, a conceptual hydrological soil response (CHSR) was assigned to each SMU according to Le Roux *et al.* (2011). Thus the hydrological soil map is a spatial representation of the CHSR of the study area, based on the distribution of the SMU's. Recharge soils are defined as soils where the dominant water flow path is one where the free water leaves the evapotranspiration zone, and recharges the lower vadoze zone.

Interflow soils are soils where the dominant flow path is where free water flows laterally within the upper and intermediate vadoze zone, while responsive soils refer to soils where the dominant flow path is overland flow, due to either shallow soils with limited storage capacity or soils saturated with water for long periods (Van Tol *et al.*, 2013).

Results and discussion

The observation positions give a good spatial coverage of the study area. The clusters that formed are due to the in-field determined sampling. The total of 113 observations is very little compared to the 2000 which would have been necessary to draw a soil map with conventional methods of a 150 m grid. Thus a considerable cost and time saving was made.

The SMU's were grouped on the basis of hydrological response (Le Roux *et al.*, 2011). This also meant that observations of the same soil form could be included into different CHSRU's, such as the Bonheim soil form which fits into both the Clayey Interflow and Clayey Recharge classes. The division was made on the basis of whether or not the C-horizon displayed signs of redox morphology. The Oakleaf and Tukulu soil forms also fit into two CHSRU's. Only when it was clear that the soil had formed due to alluvial deposits, was it added to the alluvial SMU, otherwise the observation was added to the Sandy Interflow or Sandy Recharge SMU's respectively. The distinct seep line where *Terminalia sericea* is noticeable commonly occurs above the Sodic site SMU. Here the Glenrosa soil form (Leptosols) is dominant. It was not mapped as it is too thin to be picked up at a 30 m resolution.

The SoLIM rules for the five SMU's mapped with SoLIM are shown in Table 28. The hierarchical fashion of the rule creating and the exclusion from lesser distinct SMU's from ones mapped earlier is evident when considering the values of the rules. Both topographic and vegetation indicating covariates were used, indicating that of the five soil forming factors, not one dominates soil formation in this area. Vegetation is determined by the soil type, rather than playing a big role in the soil formation in this area. However, the parent material plays a dominant role in soil formation. The main geological formation of the area is granite, which weathers to a coarse sandy material, except in extreme cases where Sodic Sites develop. It is however highly unlikely for soils with melanic A horizons (Bonheim, Milkwood, Mayo) to occur. These soils are associated with basic intrusive rocks (Le Roux *et al.*, 2013). Unfortunately the scale of the geological map did not allow for dolerite dykes (which is known to occur in the area) to be mapped. The soil map (Figure 133) shows that there are considerable areas of Clayey Recharge and Clayey Interflow soils, which are largely comprised of soil forms with melanic A horizons. Thus the soil map could be improved if the location and extent of the influence of the dolerite dykes can be mapped.

Table 28 Soil distribution rules for the hydrological soil map units

| | | Co-Variate | | | | | | | |
|------------------|----------|-------------|--------------------|---------------|----------------|----------|-----------|----------|------------------------|
| Soil Map Unit | Instance | Biomass PCA | Biomass 2012-01-11 | ET 2012-03-14 | Landsat band 4 | NDVI | AACN (10) | DEM (30) | Profile Curvature (30) |
| Sodic | 1 | | | x < 23.6 | | | | | |
| | 2 | | | | x > 63 | | | | |
| | 3 | | | | | x < 0.18 | | | |
| Clayey Recharge | 1 | x > -32 | | x > 23.6 | x < 63 | x > 0.18 | x < 7.6 | x < 362 | |
| Clayey Interflow | 1 | x < -32 | | x > 23.6 | x < 63 | x > 0.18 | x < 7.6 | | |
| | 2 | | | x > 23.6 | x < 63 | x > 0.18 | x < 7.6 | x > 362 | |
| Sandy Recharge | 1 | | x < 197 | x > 23.6 | x < 63 | x > 0.18 | x > 7.6 | | |
| | 2 | | | x > 23.6 | x < 63 | x > 0.18 | x > 7.6 | | x > 0.199 |
| Sandy Interflow | 1 | | x > 197 | x > 23.6 | x < 63 | x > 0.18 | x > 7.6 | | x < 0.199 |

PCA – Principal component analysis, ET – Evapotranspiration, NDVI – Normalized difference vegetation index, AACN – Altitude above channel network, DEM – Digital elevation model. Numbers between brackets denote topographical layer's resolutions.

The overall soil map accuracy of 73% (Table 29) is acceptable. This is higher than the 65% commonly accepted as the map accuracy of conventional soil maps (Marsman and De Gruijter, 1986). It also compares well with other studies using comparable methodology, such as MacMillan *et al.* (2010), 69%, Van Zijl *et al.* (2012), 69% and Zhu *et al.* (2008), 76%.

A concern though is the low accuracy values for the Clayey Interflow and Sandy Interflow map units. Seven of the soil observations made on the areas of these map units are actually Clayey Recharge soil observations. Thus the Clayey Interflow and Sandy Interflow SMU's are too large and the Clayey Recharge SMU is too small. To improve the map, the rules predicting the boundaries of these three SMU's need to be improved by observations made along the SMU boundaries. In contrast to this, with conventional methods, a whole new survey would have to be done in order to improve the existing map.

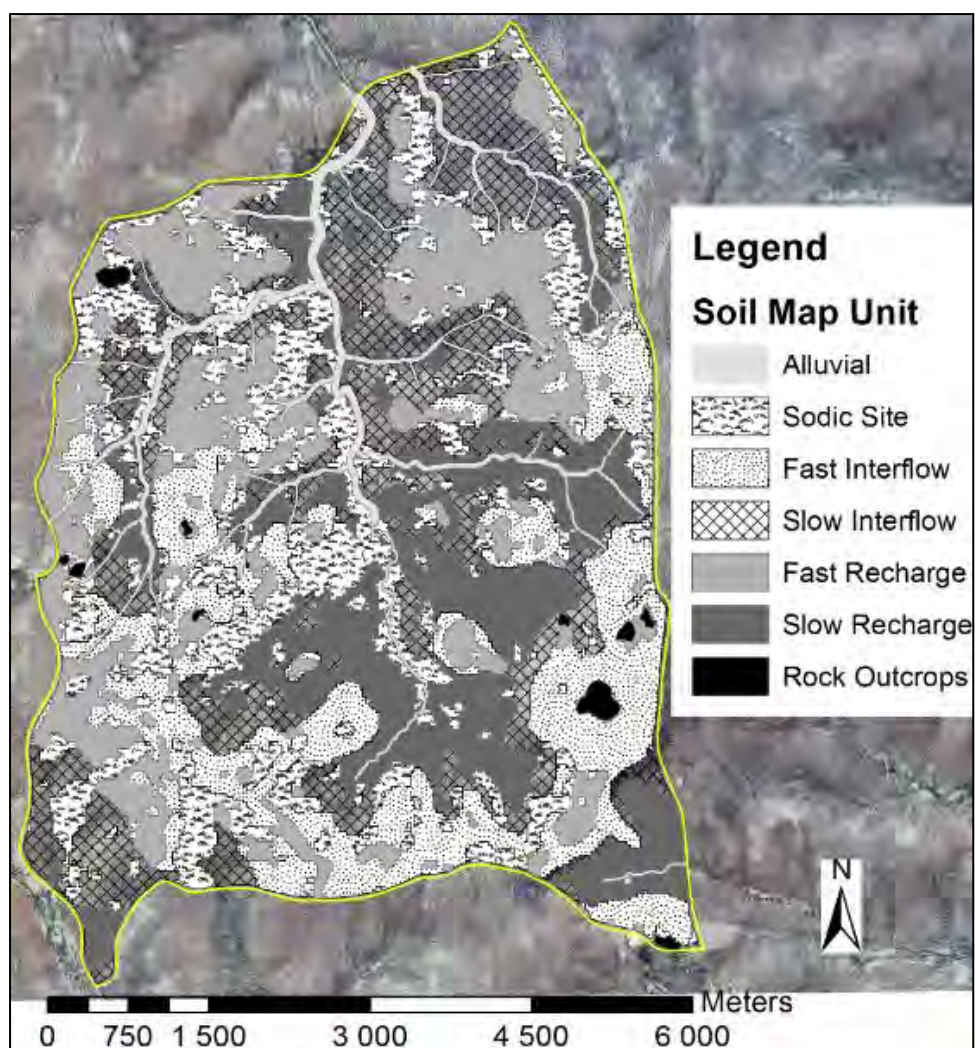


Figure 135 The hydrological soil map

Table 29 An accuracy matrix of the soil map

| | | Map units | | | | | | Total | Correct | % |
|--------------|-----------------|------------|------------------|-----------------|-----------------|----------------|----------|-------|---------|-----|
| | | Sodic Site | Clayey Interflow | Clayey Recharge | Sandy Interflow | Sandy recharge | Alluvial | | | |
| Observations | Sodic | 18 | 1 | 2 | 1 | 0 | 1 | 23 | 18 | 78 |
| | Clayey | 0 | 3 | 0 | 0 | 0 | 0 | 3 | 3 | 100 |
| | Interflow | 0 | 3 | 11 | 4 | 0 | 0 | 18 | 11 | 61 |
| | Clayey Recharge | 0 | 0 | 1 | 5 | 0 | 0 | 6 | 5 | 83 |
| | Sandy Interflow | 0 | 0 | 2 | 0 | 4 | 0 | 6 | 4 | 67 |
| | Sandy Recharge | 1 | 0 | 0 | 0 | 0 | 2 | 3 | 2 | 67 |
| | Alluvial | 19 | 7 | 16 | 10 | 4 | 3 | 59 | 43 | 73 |
| | Total | 18 | 3 | 11 | 5 | 4 | 2 | 43 | | |
| Correct | | 95 | 43 | 69 | 50 | 100 | 67 | 73 | | |
| % | | | | | | | | | | |

The CHSRU map (Figure 136) shows that 41% of the study area is covered by Interflow soils, 40% by Recharge soils and 19% by Responsive soils. However the great advantage of the mapping approach to determining those values is that the position of these soils is also known. This could be invaluable information to hydrological modelers; however, ways to exploit such input should be developed.

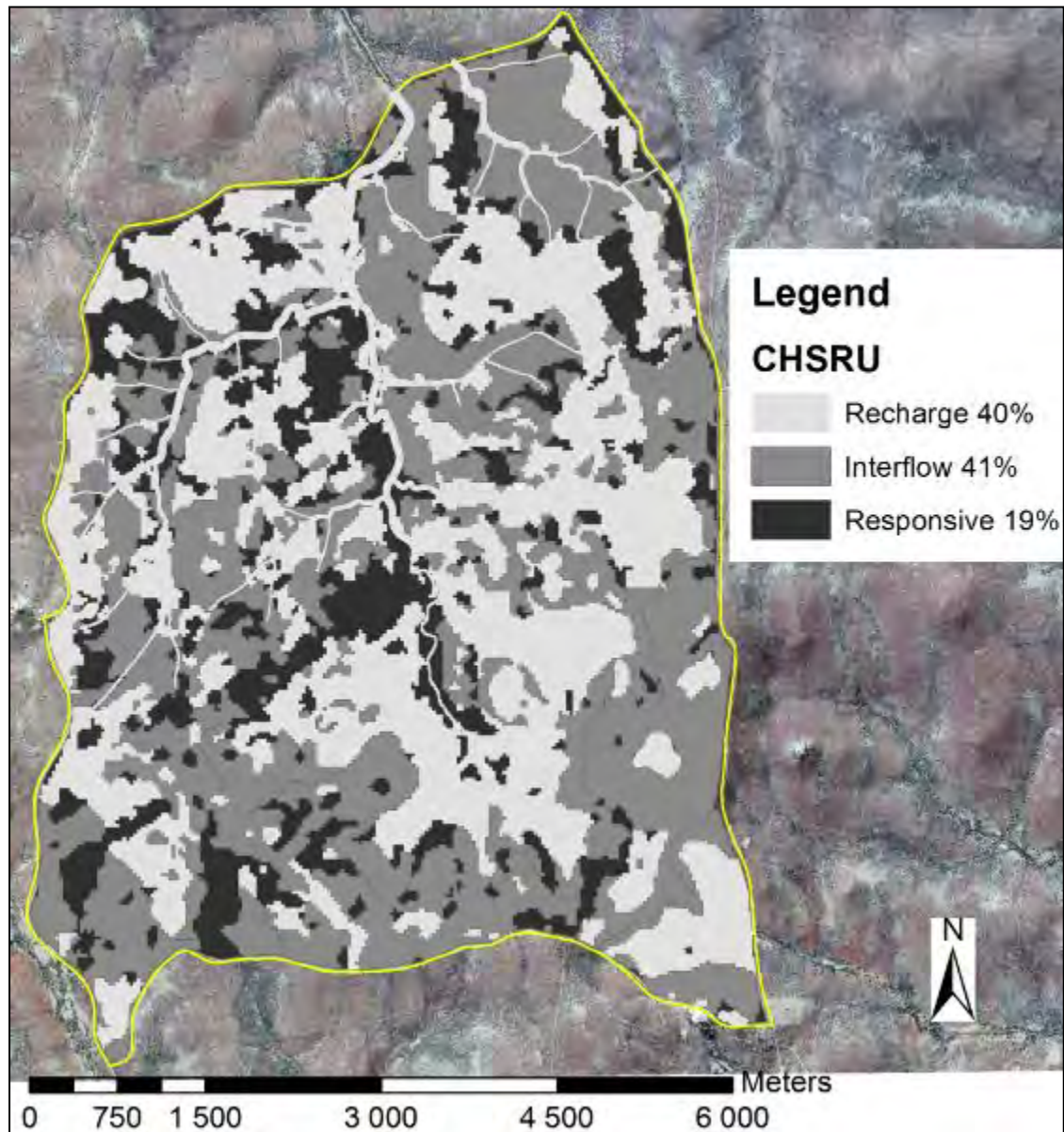


Figure 136 Conceptual hydrological soil response unit map

Conclusions

It was shown that a DSM approach could provide both the size and position of CHSRU's for a large area in a time and cost effective way. One hundred and thirteen soil observations were made to create a soil map which is 73% accurate. In contrast to this, 2000 soil observations would have been necessary in conventional soil mapping. The map could be improved with a geological map showing the dolerite dykes, as well as by making more observations on the boundaries between the Sandy Interflow, Clayey Interflow and Clayey Recharge SMU's, as

pointed out by the error matrix. For this improvement only observations along the SMU boundaries of the three SMU's in question is necessary, in contrast to a new survey needed by conventional methods.

The size and position of the CHSRU's could possibly be useful in improving predictions in ungauged basins, but methodology should be developed to accommodate such input into models. The first step may be to develop conceptual hydrological response models for hillslopes/soilscares.

3.3 APPLICATION OF HYDROPEDOLOGICAL INSIGHTS IN HYDROLOGICAL MODELLING OF THE STEVENSON HAMILTON RESEARCH SUPERSITE, KRUGER NATIONAL PARK, SOUTH AFRICA

3.3.1 Introduction

With a growing awareness of the need to make Predictions in Ungauged Basins (PUB's), the role of soil in hydrology is becoming increasingly recognized. Because soil can transmit, store and react with water (Park *et al.*, 2001) it can be a first order control in water storage, partitioning of hydrological flow paths and residence time distributions (Park *et al.*, 2001; Soulsby and Tetzlaff, 2008). Although hydrologists agree that the spatial variation of soil properties significantly influences hydrological processes, they also recognise that they lack the skill to gather and interpret soil information (Lilly *et al.*, 1998)

There exists an interactive relationship between soil and hydrology. Although soil genesis is a function of climate, vegetation, topography, parent material and time (Jenny, 1941), it is largely these factors' influence on water which determines its influence on soil genesis. Thus, just as soil properties contain unique signatures of the soil forming factors under which the soil formed, it also contains signatures of the water regime under which it formed and which is still operating within the soil. As nearly all hydrological processes important to hydrologists are difficult to observe and measure (Sivapalan, 2003), correct interpretation of the soils' hydrological signatures can provide valuable information as to the dominant hydrological processes (Ticehurst *et al.*, 2007; Van Tol *et al.*, 2010) and improve understanding of hydrological behaviour on the hillslope scale (Lin *et al.*, 2006), which is the smallest scale used for holistically understanding hydrological processes (Tromp van Meerveld & Weiler, 2008).

Catchment hydrological response is dependent on the combination of the hydrological responses of the hillslopes which make up the catchment (Sivapalan, 2003). By understanding the hydrological signatures contained in the soils, conceptual qualitative 2-dimensional descriptions of the hydrological responses of the hillslopes wherein the soils occur can be created. Integration of the 2-D hillslope hydrological models lead to greater understanding of the catchments hydrological response. Thus, interpreting soil hydrological signatures leads to understanding of hillslope hydrology, which in turn leads to understanding the hydrological response at catchment scale, and finally assists in PUB's.

Van Zijl & Le Roux (2014) generated a hillslope based hydrological soil map of the 4001 ha Stevenson Hamilton Research Supersite (SHRS) in the Kruger National Park (KNP), by applying an *expert knowledge* Digital Soil Mapping (DSM) approach to divide the soils of SHRS into different hydrological classes as described by Van Tol *et al.* (2013). In the

paper, Van Zijl and Le Roux (2014) claim that the hillslope based soil information will assist hydrological modelling within the area. In this study we hypothesize that Van Zijl *et al.* (2014) is correct, and that their soil information can be used to improve the efficiency of hydrological models and hydrological modelling. We consequently used three levels of soil detail in a well-known hydrological model (ACRU) for three modelling scales and evaluated the contribution made by the improved soil information. The aim was therefore not to calibrate the model until satisfactory simulations were achieved but rather to parameterise and configure the model with increasing levels of input accuracy.

3.3.2 The ACRU hydrological model

ACRU is an agrohydrological, daily time step, multi-layered soil water budgeting model (Schulze, 1995) which can be run in lumped or distributed mode. The standard version, *ACRU2000*, comprises of two soil layers (A and B- horizon) and a deep groundwater layer (GW). In a revised version of ACRU namely *ACRU-Int*, an intermediate layer (INT) between the B horizon and GW was introduced by Lorentz *et al.* (2007). Soil inputs include; the thickness of soil horizons, water contents at the start of simulation (SMINI and SMBINI), Permanent Wilting Point (PWP), Drained Upper Limit (DUL), saturation (Po), Plant Available Water (PAW), drainage rates (ABRESP, BFRESP and INTRESP) and the erodibility of the soil (K-factor). Except for the latter all inputs are required for both soil horizons (Schulze, 2007). The model allows redistribution of saturated water (RESP), i.e. between DUL and Po, from the A to the B-horizon (ABRESP), from the B-horizon to the intermediate layer (BFRESP) and from the intermediate layer to the groundwater (INTRESP). The distribution is expressed as a fraction of the water above DUL draining vertically downwards from the respective horizons on a daily time step.

The intermediate layer has a mechanism whereby lateral release of water can be induced when certain threshold positive pressures at the saprolite/bedrock interface is achieved using a non-linear partial differential advection-dispersion function (ADF):

$$g(t) = \left(\frac{4\pi D_p t}{\tau}\right)^{-\frac{1}{2}} t^{-1} \exp\left[-\left(1 - \frac{t}{\tau}\right)^2 \left(\frac{\tau}{4D_p t}\right)\right] \quad (3.1)$$

Where $g(t)$ is the lateral response function, D_p a dispersion coefficient and τ the mean response time. In *ACRU-Int* the parameters RESDISP and RESTIME are used to describe D_p and τ respectively. The lateral releases from the intermediate zone can be routed to intermediate layers or groundwater stores of a downslope land segments. This is ideal for imitating flowpaths at hillslope scale. Small RESDISP and RESTIME values will therefore result in water being routed quickly to downslope land segments. High RESDISP and RESTIME values will have the opposite effect; water transported laterally over a long time.

Two other important variables in *ACRU-Int*, not considered a soil input but definitely influenced by the soil, is QFRESP and COFRU. According to definition QFRESP is: *Stormflow response fraction for the catchment/subcatchment, i.e. the fraction of the total stormflow (1.0) that will run off from the catchment/subcatchment on the same day as the rainfall event* (Smithers *et al.*, 2004). QFRESP is inversely correlated with catchment area and will increase with an increase in slope angle, area covered by impervious material, and rainfall intensity. Soils prone to topsoil crusting as well as very shallow or very wet soils should therefore give high QFRESP values. The *Coefficient of baseflow response* (COFRU) is the

fraction of water from the INT/GW zones that becomes streamflow on a particular day (Smithers *et al.*, 2004).

3.3.3 Methodology

3.3.3.1 Study area

The study site forms part of the 4001 ha SHRS, near Skukuza in the Kruger National Park (Figure 137). It lies in the Renosterkoppies land type (Venter, 1990), situated in the wetter part of the KNP with a mean annual precipitation of 560 mm a⁻¹ (Smit *et al.*, 2013). The granite and gneiss of the Nelspruit Suite (Venter, 1990) gives rise to coarse grained sandy soils of the Clovelly, Pinedene and Glenrosa forms, while dolerite dykes provide the parent material for more clayey soils of the Bonheim and Valsrivier form (Van Zijl and Le Roux, 2014). The landscape has a high stream density and is highly dissected (Smit *et al.*, 2013). The dominant vegetation can be linked to the terrain position. On the crests *Combretum apiculatum* and *Combretum zeyher* dominate the woody vegetation. Between the crest and the midslope *Terminalia sericea* indicates a commonly occurring seepage line. The midslopes and footslopes are dominated by fine leaved woody species, especially *Acacia nilotica*. Below seepage lines the so-called Sodic sites are found, where Sterkspruit soils (Van Zijl and Le Roux, 2014) and *Eucleadi vinoriumis* dominates (Smit *et al.*, 2013). This study focused on an area in the South of SHRS (Figure 137b). This area, comprising of three stream orders (Figure 137) has been subjected to hydrometric instrumentation and continuous monitoring since November 2011.

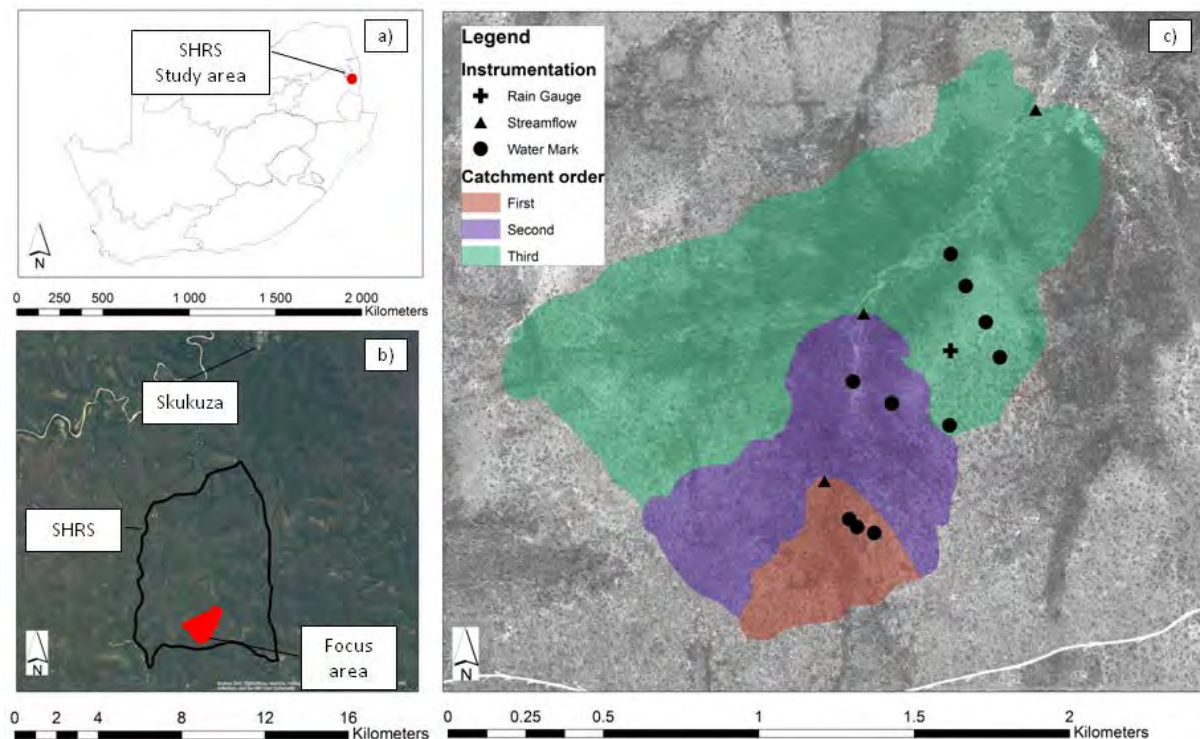


Figure 137 Location of SHRS in South Africa (a), the location of the study area within SHRS (b) and the experimental layout and catchment orders within the study area

The study area was divided into three stream or catchment orders (Figure 137c). The 1st order catchment is approximately 10.8 ha, the 2nd order 42.7 ha and the total area (3rd order) is 148.2 ha. Obviously the 2nd order includes the entire 1st order and the 3rd order catchment includes the 1st and 2nd order.

3.3.3 ACRU simulations and evaluations

Rainfall data was available from 14 November 2011 and this was the starting date for simulations. Simulations were conducted for the three stream orders (Figure 137) with three levels of soil detail. In the first level (*ACRU_lumped* for the remainder of this paper), homogenous soils were assumed, using weighted average soil parameters. The next level (*ACRU2000*) made use of the spatial distribution of the soils and associated properties as presented in Van Zijl *et al.* (2014). In the most detailed level (*ACRU-Int*) the spatial distribution of soils and associated properties were used to construct surface and subsurface routing of water paths. In the *ACRU-Int* simulations efforts were made to include all relevant site information available, for example the absence of groundwater, in the model configuration.

A four month period (15 November 2012 to 15 March 2013) was selected to evaluate the contribution of enhanced soil information to model outputs. This period was selected firstly to allow the model to ‘settle’ using real climatic information and secondly because more detailed climatic information (Figure 138) was available for this period. Simulation outputs were statistically compared to observed streamflow measured for each catchment order (Figure 137) as well as against measured soil water potentials of selected soil profiles measured with Water Mark sensors (Figure 139). Soil water potentials were not yet calibrated against volumetric soil water content and only qualitative comparisons (sensitivity analysis) were possible at this stage. To ensure simplicity in visual comparisons measured tensions had to be log transformed and inversed.

3.3.4 Model parameterisation and configuration

3.3.4.1 Climatic information

Rainfall was recorded with a Texas Instruments TE525 0.1 mm rain gauge since 14 November 2011. In November 2012 the latter was replaced with a compact Davis Vantage Pro 2 Automatic Weather Station logging rainfall (0.2 mm), temperature and relative humidity (RH) at 15 minute intervals. Until November 2012, min and max RH and temperature were obtained as monthly averages from Schulze *et al.* (2007), for the evaluation period daily measured data were used (Figure 138). Vapour Pressure Deficit (VPD), solar radiation (Rad) and evaporation (E) presented in Table 30 were obtained for the site from Schulze *et al.* (2007).

Table 30 Average monthly climatic parameters for the SHRS (Schulze *et al.*, 2007)

| | Jan | Feb | Mar | Apr | May | Jun | Jul | Aug | Sep | Oct | Nov | Dec |
|---------------|------|------|------|------|------|------|------|------|------|------|------|------|
| Min RH | 85.8 | 83.2 | 85.5 | 82.9 | 84.0 | 75.0 | 78.1 | 75.6 | 75.0 | 78.2 | 79.8 | 84.6 |
| Max RH | 44.9 | 43.9 | 43.3 | 37.8 | 30.4 | 23.8 | 25.0 | 26.3 | 30.6 | 36.5 | 40.2 | 43.0 |
| T max | 31.9 | 31.6 | 30.8 | 21.9 | 27.4 | 25.4 | 25.3 | 26.9 | 29.0 | 29.6 | 30.3 | 31.2 |
| T min | 20.0 | 20.0 | 18.7 | 15.4 | 10.2 | 6.2 | 6.3 | 8.9 | 12.9 | 15.8 | 17.7 | 19.0 |
| VPD | 1.3 | 1.3 | 1.2 | 1.2 | 1.1 | 1.0 | 1.0 | 1.1 | 1.3 | 1.3 | 1.3 | 1.3 |
| Rad | 22.5 | 21.2 | 20.0 | 17.3 | 15.9 | 16.2 | 14.6 | 15.6 | 18.0 | 18.6 | 21.0 | 22.6 |
| E | 6.8 | 6.6 | 5.6 | 4.5 | 3.8 | 3.3 | 3.6 | 4.5 | 5.5 | 6.0 | 6.4 | 6.8 |

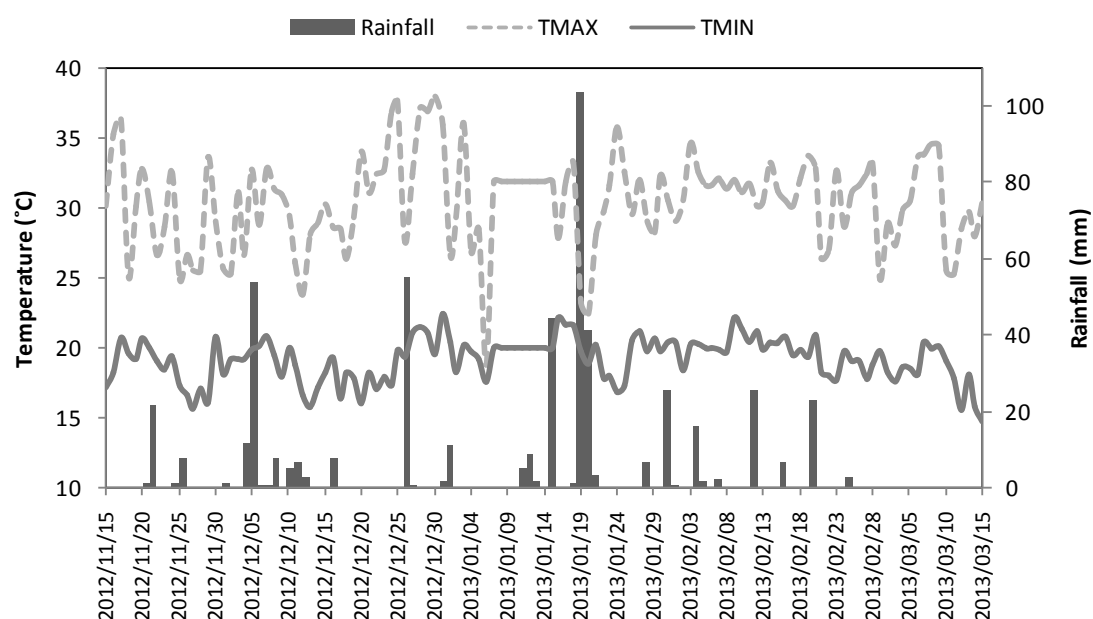


Figure 138 Rainfall (mm) and daily minimum and maximum temperatures recorded during the evaluation period

A total of 524.2 mm of rain was received during the evaluation period of which 194 mm was received between 15 and 22 January 2013 (Figure 138). A total of 103.8 mm was recorded on the 19th of January. Temperature and relative humidity was not recorded between the 7th and 14th of January and the monthly values (Table 30) were surrogated.

Soil information

The hydropedological soil map of the study area is presented in Figure 139 and important parameters of the different soil types are presented in Table 31. Recharge soils are soils that do not show any morphological indications of saturation, i.e. grey matrix or mottle colours. In this study there was distinguished between fast and slow recharge based on the expected rate of infiltration and redistribution through the soil profile as influenced by texture. Clayey soils of the Bonheim, Valsrivier and Milkwood forms will presumably have a lower infiltration rate (QFRESP = 0.4) redistribute water slower (ABRESP = 0.5 and BFRESP = 0.4) than sandy Clovelly, Mispah and Glenrosa soils (QFRESP = 0.05; ABRESP = 0.8 and BFRESP = 0.7). Since morphological indications of saturation are absent from these soils, it would be logical to assume that lateral flow at the soil/bedrock interface is negligible and that most of the water will drain into deeper groundwater aquifers (High INTRESP values of 0.5 and 0.3

for sandy and clayey recharge soils respectively). Lateral distributions from these soils to lower lying land segments were therefore ignored in the model setup.

Similar to the recharge soils there was also distinguished between two types of interflow soil, i.e. sandy and clayey. In the interflow soils soil morphological indicators of saturation were observed at the soil/bedrock interface implying that saturation and lateral flow might occur in these soils. The redistribution rate from the surface to soil/bedrock interface, i.e. ABRESP and BFRESP were the same as for sandy and clayey recharge soils, however low INTRESP values (0.1 and 0.05 for sandy and clayey soils respectively) should allow for the formation of temporal saturation as indicated by the soil morphology. The clayey interflow soils of the Sepane and Bonheim soil form will typically have a slower lateral redistribution rate (RES DISP = 2 and RESTIME = 3) than the sandy Pinedene, Avalon and Tukulu soil forms (RES DISP = 0.5 and RESTIME = 1).

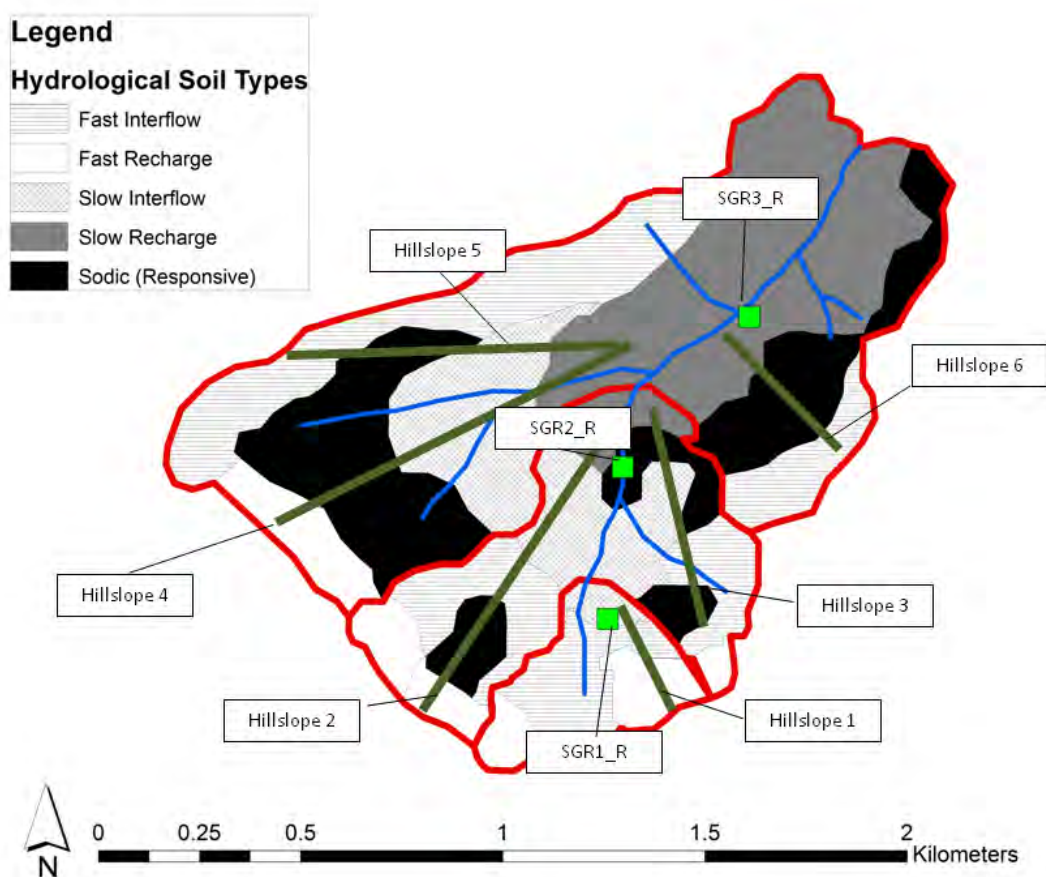


Figure 139 Hydrological soil types, and representative hillslopes of the study area. Main stream channel and catchment orders are demarcated in blue and red respectively. The three profiles used for evaluation purposes are marked SGR1_R, SGR2_R and SGR3_R

Sodic soils are prone to crust formation due to dispersion caused by high Na contents. Low infiltration rates are typically associated with these soils, and it is expected that infiltration excess overland flow will be the hydrological process dominating on these soils (QFRESP = 0.65). Redistribution of water within the sodic soils are limited (ABRESP and BFRESP of 0.2 and 0.1 respectively) with limited drainage towards groundwater aquifers (INTRESP = 0.05).

Lateral drainage in the saprolitic layer of the sodic soils are also expected to be very slow (RESDISP = 5 and RESTIME = 8).

Permanent Wilting Points (PWP) and drained upper limits (DUL) for the soils were derived using a pedotransfer function developed by Hutson (1984). For stable soils (eq. 3.2 & 3.3) and for clayey soils PWP is calculated with eq. 3.4:

$$PWP = 0.0602 + (0.00322 \times Cl) + (0.00308 \times Si) - (0.00260 \times D_b) \quad (3.2)$$

$$DUL = 0.0558 + (0.00365 \times Cl) + (0.00554 \times Si) - (0.0303 \times D_b) \quad (3.3)$$

$$PWP = 0.01616 + (0.00322 \times Cl) + (0.00308 \times Si) \quad (3.4)$$

Table 31 Model parameters of different soil types and catchment orders for model runs

| Distributed mode* ¹ | | | | | | | | | | | | | | |
|--------------------------------|---------|-------|------|------|------|--------------------------|--------|---------------------|---------------------|---------------------|---------|---------|--------|---------------------|
| Hydrological Soil Type | Horizon | Depth | Sand | Silt | Clay | Bd (kg m ⁻³) | Po (%) | PWP | DUL | RESP | RESDISP | RESTIME | QFRESP | COFRU* ³ |
| | | m | % | % | % | kg m ⁻³ | % | mm mm ⁻¹ | mm mm ⁻¹ | mm mm ⁻¹ | | days | | |
| Sandy-Interflow | A | 0.3 | 80.7 | 10.8 | 8.4 | 1.50 | 0.435 | 0.0817 | 0.192 | 0.80 | - | - | 0.05 | 0.009 |
| | B | 0.3 | 77.0 | 14.6 | 8.4 | 1.67 | 0.371 | 0.0889 | 0.218 | 0.70 | - | - | - | - |
| | C | 0.3 | 68.9 | 12.2 | 18.9 | 1.72 | 0.351 | 0.1139 | 0.244 | 0.10 | 0.5 | 1.0 | - | - |
| Sandy-Recharge | A | 0.3 | 80.7 | 10.8 | 8.4 | 1.50 | 0.435 | 0.0817 | 0.192 | 0.80 | - | - | 0.05 | 0.009 |
| | B | 0.4 | 77.0 | 14.6 | 8.4 | 1.67 | 0.371 | 0.0889 | 0.218 | 0.70 | - | - | - | - |
| | C | 0.5 | 72.4 | 14.5 | 13.1 | 1.69 | 0.362 | 0.1029 | 0.235 | 0.50 | - | - | - | - |
| Clay-Interflow | A | 0.3 | 57.3 | 12.2 | 30.6 | 1.45 | 0.451 | 0.2021 | 0.279 | 0.50 | - | - | 0.40 | 0.009 |
| | B | 0.3 | 55.8 | 4.8 | 39.4 | 1.44 | 0.456 | 0.2319 | 0.270 | 0.40 | - | - | - | - |
| | C | 0.4 | 55.1 | 16.9 | 28.0 | 1.49 | 0.436 | 0.1993 | 0.297 | 0.05 | 2.0 | 3.0 | - | - |
| Clay-Recharge | A | 0.3 | 57.3 | 12.2 | 30.6 | 1.45 | 0.451 | 0.2021 | 0.279 | 0.50 | - | - | 0.40 | 0.009 |
| | B | 0.3 | 55.8 | 4.8 | 39.4 | 1.44 | 0.456 | 0.2319 | 0.270 | 0.40 | - | - | - | - |
| | C | 0.5 | 55.1 | 16.9 | 28.0 | 1.49 | 0.436 | 0.1993 | 0.297 | 0.30 | - | - | - | - |
| Sodic (Responsive) | A | 0.2 | 66.3 | 19.0 | 14.8 | 1.67 | 0.369 | 0.1227 | 0.265 | 0.20 | - | - | 0.65 | 0.009 |
| | B | 0.2 | 53.0 | 11.7 | 35.2 | 1.50 | 0.433 | 0.2255 | 0.295 | 0.10 | - | - | - | - |
| | C | 0.2 | 52.0 | 8.9 | 39.1 | 1.72 | 0.351 | 0.2391 | 0.300 | 0.05 | 5.0 | 8.0 | - | - |
| Lumped mode* ² | | | | | | | | | | | | | | |
| Catchment order | | | | | | | | | | | | | | |
| 1 st | A | 0.3 | 77.9 | 11.0 | 11.1 | 1.49 | 0.437 | 0.096 | 0.202 | 0.76 | - | - | 0.10 | 0.009 |
| | B | 0.4 | 74.5 | 13.4 | 12.1 | 1.64 | 0.381 | 0.106 | 0.224 | 0.66 | - | - | - | - |
| 2 nd | A | 0.3 | 71.6 | 12.6 | 16.0 | 1.52 | 0.430 | 0.124 | 0.230 | 0.62 | - | - | 0.25 | 0.009 |
| | B | 0.3 | 67.0 | 11.3 | 21.9 | 1.58 | 0.407 | 0.154 | 0.246 | 0.51 | - | - | - | - |
| 3 rd | A | 0.3 | 67.7 | 13.3 | 19.0 | 1.52 | 0.426 | 0.141 | 0.245 | 0.53 | - | - | 0.34 | 0.009 |
| | B | 0.3 | 62.6 | 9.9 | 24.5 | 1.54 | 0.420 | 0.180 | 0.257 | 0.43 | - | - | - | - |

*¹REDISP & RESTIME and C-horizon parameters are only applicable in *ACRU-Int* simulations

*²Parameter values are weighted average values based on the area covered by different soil types in the specific catchment order

*³Groundwater tables don't intersect stream channels, hence the low COFRU values

14.1.2 Hillslopes and hillslope responses

From the hydrological soil map (Figure 139) six dominant soil distribution patterns were identified (marked hillslope 1-6). These hillslopes represent 3 dimensional areas and were the basis for the configuration for surface routing in *ACRU2000* and *ACRU-Int* as well as subsurface routing in *ACRU-Int* simulations. The dominant hydrological flowpaths in the hillslopes are conceptually presented in Figure 140.

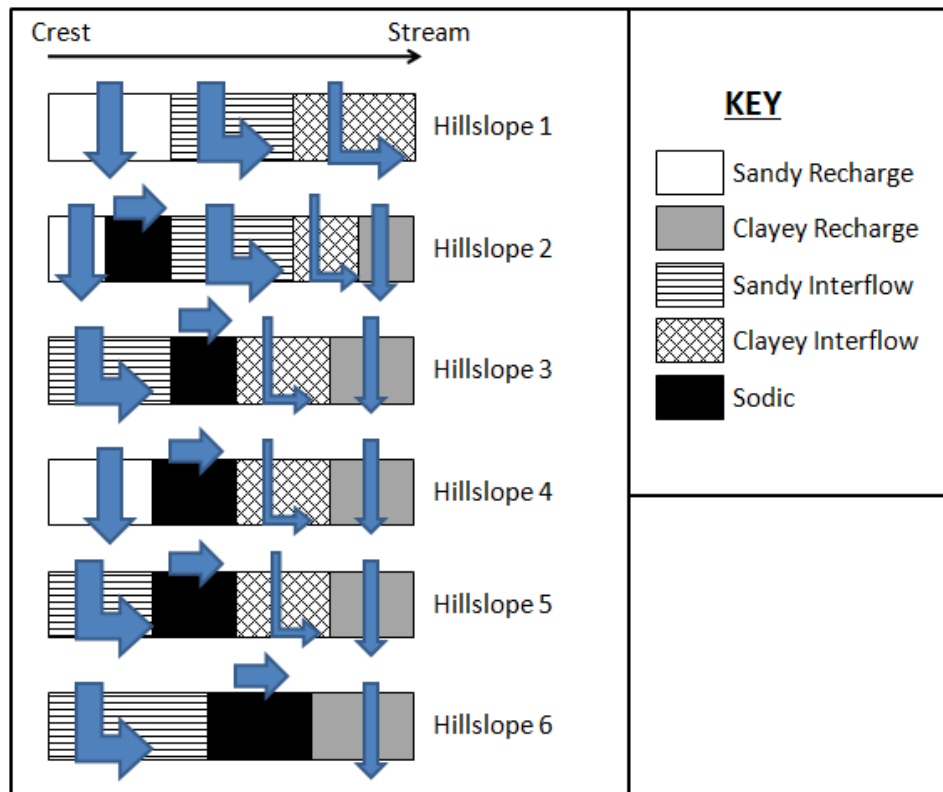


Figure 140 Conceptual hydrological responses of the dominant response of the hillslopes in the study area

The conceptual flowpaths presented in Figure 140 were used to structure the surface and subsurface (*ACRU-Int* only) flow from different land segments (Figure 141). Before the start of the simulations it was known that groundwater tables only intersect stream channels of higher order streams (5th and 6th). The groundwater component in were therefore routed in the detailed configuration (*ACRU-Int*) to a separate land segment which did not contribute to streamflow (GW in Figure 141).

In distributed mode streamflow outputs from land segment 3, 8 and 14 represents streamflow from the 1st, 2nd, and 3rd order catchments respectively. Land segments 3, 10 and 14 represents profiles SGR1_R, SGR2_R and SGR3_R respectively.

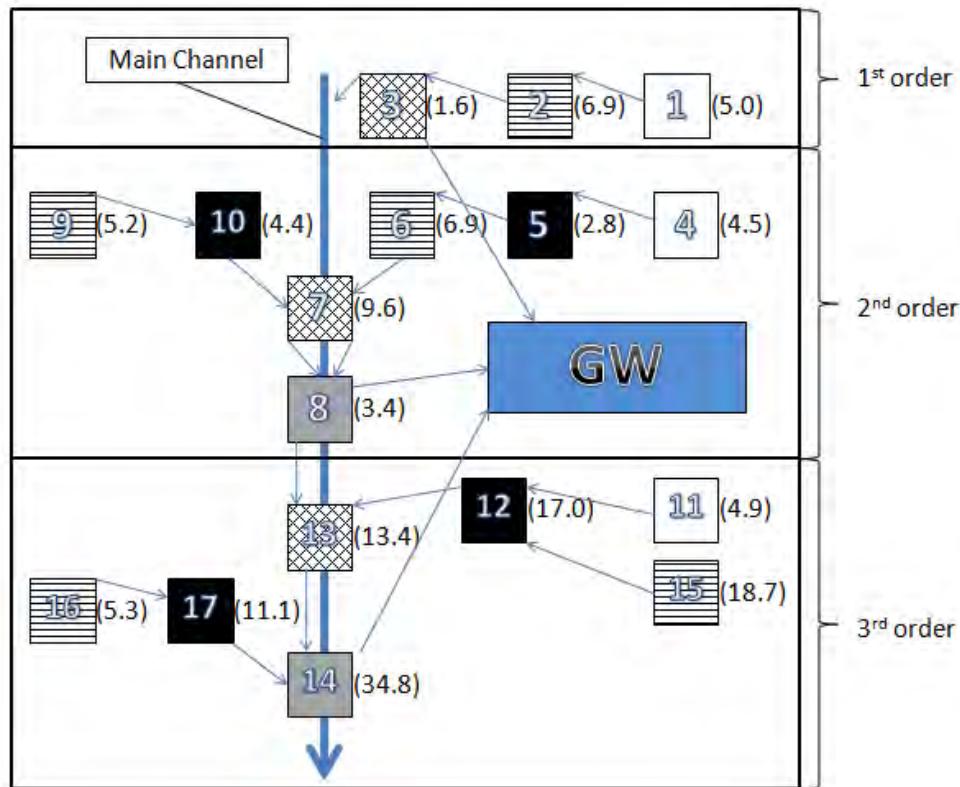


Figure 141 Model configuration (ACRU2000 and ACRU-Int); numbers in shaded blocks refers to land segment number, with numbers in brackets at the right of the land segments as the area (in ha). The key in Figure 140 were used to indicate the hydrological soil type of each land segment

3.3.5 Results and discussion

Simulated streamflow

The efficiency of different simulations is presented in Table 32 and graphically in Figure 142 to Figure 145. With exception of the 1st order catchment, more detailed soil information improved the accuracy of simulations. In the 1st order catchment, all the levels of detail yielded poor results with negative Nash-Sutcliffe efficiency coefficients, implying that the observed mean value will be a better estimation of streamflow than what the model predicted. Figure 142 illustrates the reason behind the poor simulations. The 1st order stream is sustained by a seasonal contribution from a small narrow unchannelled valley bottom wetland, yielding higher streamflows than predicted. Figure 142 indicates that the discharge from this catchment is more than the rainfall received during the evaluation period. This saturated area will also increase the amount of quick flow due to saturation excess overland flow as indicated by the underestimation of peak discharge throughout the evaluation period. In the soil map of Van Zijl *et al.* (2014), this wetland was not recorded. It should however be noted that Van Zijl *et al.* (2014) were tasked to map 4 001 ha and such a small wetland (< 1 ha) can easily be missed. It is clear that these areas can have a huge

impact on the water regime of small catchments, and with large scale (small area) simulations more detail is required to ensure accuracy and efficiency of models.

Table 32 Simulated against observed daily flow efficiency measurements (R²: coefficient of determination; NS: Nash-Sutcliffe; MSE: Mean Square Error)

| Catchment | Model run (level of detail) | R ² | NS | MSE |
|-----------------------|-----------------------------|----------------|-------|-------|
| 1 st order | <i>ACRU_Lumped</i> | 0.49 | -7.62 | 38.58 |
| | <i>ACRU2000</i> | 0.57 | -0.51 | 38.66 |
| | <i>ACRU-Int</i> | 0.51 | -0.71 | 43.59 |
| 2 nd order | <i>ACRU_Lumped</i> | 0.57 | 0.52 | 4.20 |
| | <i>ACRU2000</i> | 0.83 | 0.72 | 2.41 |
| | <i>ACRU-Int</i> | 0.87 | 0.79 | 1.86 |
| 3 rd order | <i>ACRU_Lumped</i> | 0.82 | 0.67 | 8.34 |
| | <i>ACRU2000</i> | 0.90 | 0.72 | 7.15 |
| | <i>ACRU-Int</i> | 0.91 | 0.73 | 6.92 |

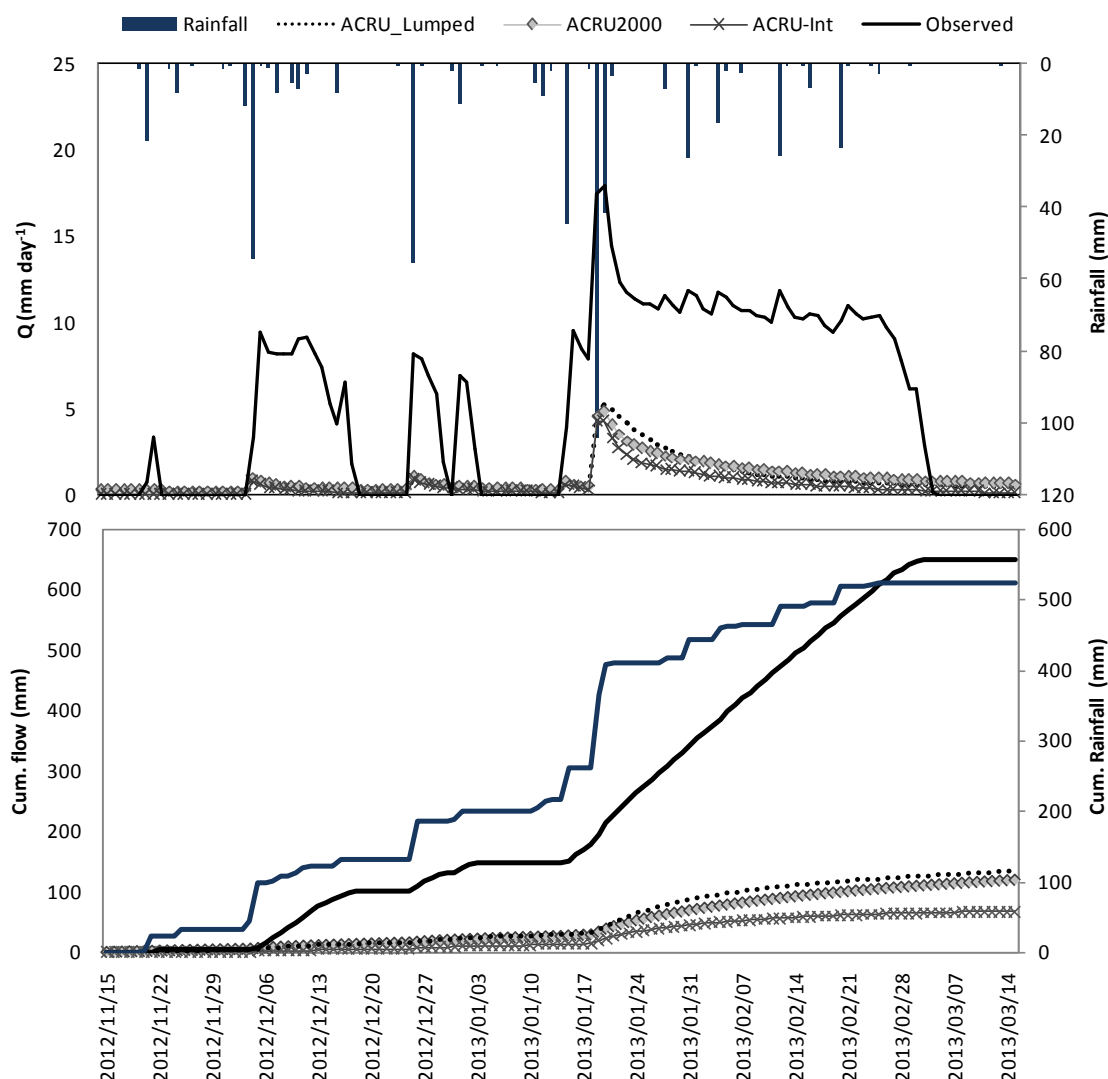


Figure 142 Daily observed and simulated streamflow for the three levels of detail from 1st order catchment as well as cumulative flow during the evaluation period

In the 2nd order catchment streamflow was simulated with reasonable accuracy especially during the first half of the evaluation period (Table 32). Until the 17th of January 2013 peakflows were slightly overestimated and low flows overestimated. Over estimation of low flows were especially made in *ACRU2000* and *ACRU_Lumped* simulations, even with very low COFRU values. The ability of *ACRU-Int* to divert the groundwater contribution from the stream seems to be effective. During the extreme rainfall event of 19 and 20 January 2013, peakflow was underestimated (Figure 145). The overestimation of peak discharge during smaller rain events and underestimation during large rain events is noteworthy. It will imply that the parameter mainly responsible for quickflow (i.e. QFRESP) should be dynamic in nature, a notion also supported by Van Tol *et al.* (2011). Towards the end of the evaluation period observed streamflow responded little to any rain received (Figure 143). This lack of response seems spurious and it is hypothesized that the equipment might have been damaged during the extreme rain event of 19 and 20 January.

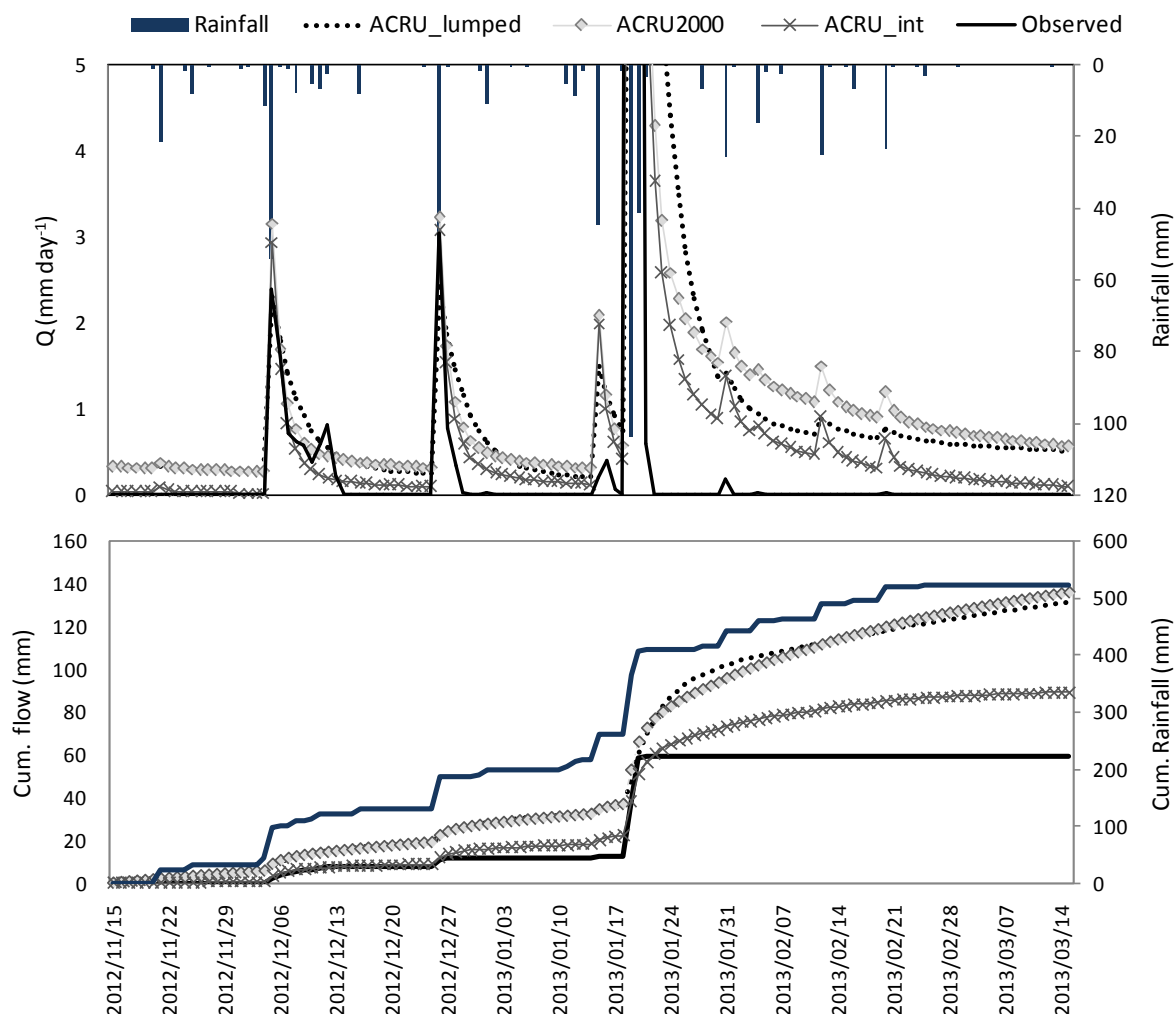


Figure 143 Daily observed and simulated streamflow for the three levels of detail from 2nd order catchment as well as cumulative flow during the evaluation period

In the 3rd order catchment streamflow was overestimated during the first halve of the simulation period (Figure 144). The stream channel consists of coarse sandy alluvial material and although the stream is flowing through the alluvial layer, surface flows are only observed during and after high rainfall events. Peak flow was again underestimated during the extreme rain event of 19 and 20 January 2013 (Figure 145). The *ACRU-Int* model configuration yielded the most accurate streamflow simulations (Table 32) followed by *ACRU2000*. The cumulative observed flow during the evaluation period was 101.9 mm and that simulated *ACRU-Int* was 102.3 mm. Although daily flows were not simulated with the same accuracy it was still better than simulations with less soil information.

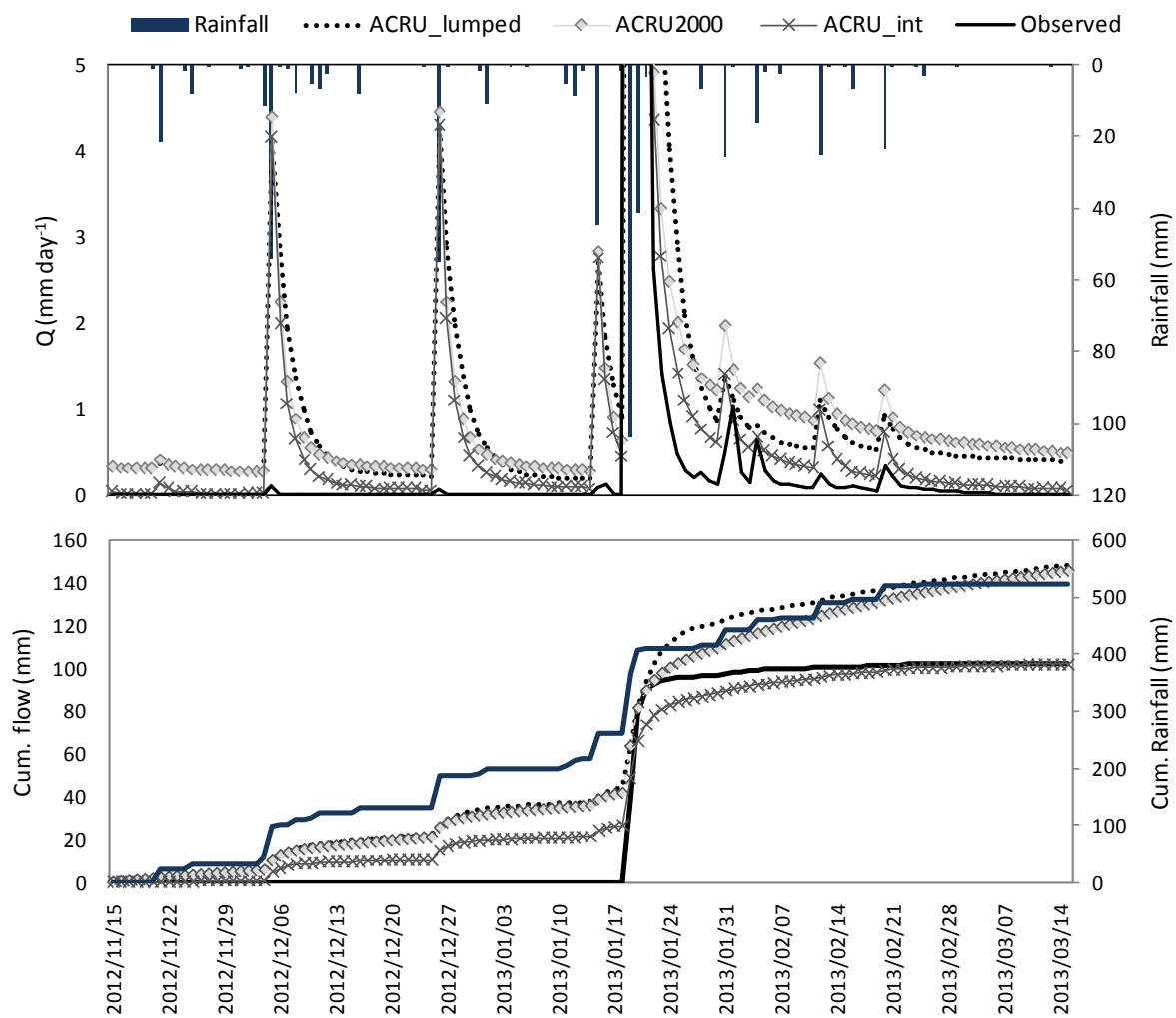


Figure 144 Daily observed and simulated streamflow for the three levels of detail from 3rd order catchment as well as cumulative flow during the evaluation period

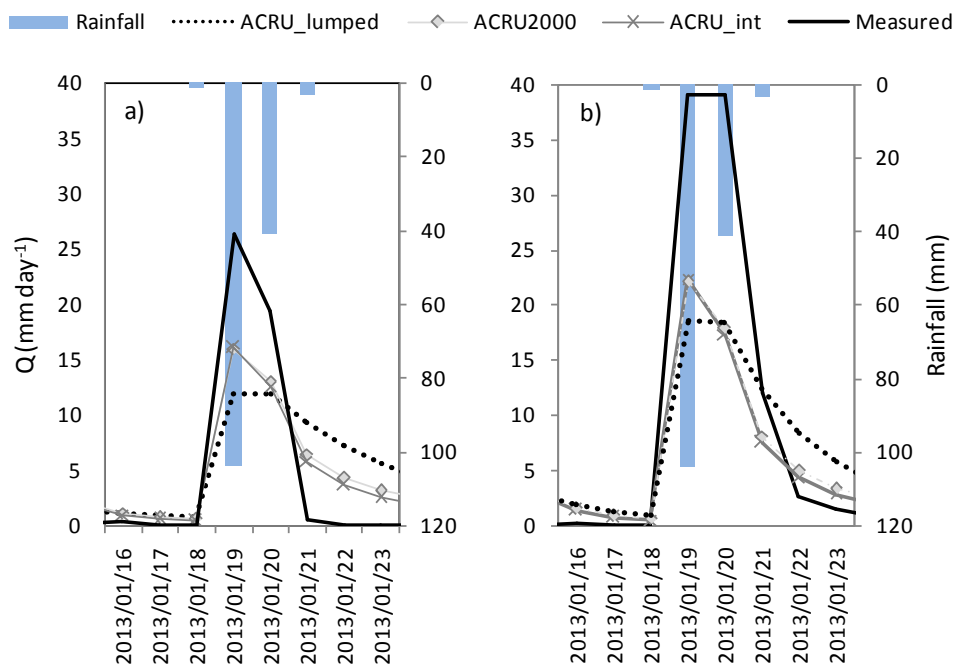


Figure 145 Simulated and observed daily streamflow and rainfall during the large rain event of 19 and 20 January 2013

Simulated soil water contents

Figure 146 shows how the soil water measurements and their simulations reacted to rain events. The simulations achieved variable results. In general the simulations show the same reactions to rainfall events as the measured data. The Pearson correlation values confirm this (Table 33), with correlation values above 0.5 for all soil horizons except the intermediate horizons. The intermediate soil horizons were simulated erratically. On hillslope 1 the simulation achieved the highest overall correlation, while the simulations of the other two intermediate horizons achieved the lowest correlations, even being negative for the hillslope 2 intermediate horizon.

There is little to choose between ACRU int, ACRU 2000 and ACRU lumped. Figure 146 shows that the simulations follow each other closely, and the Pearson correlations (Table 33) are also very close to each other. ACRU lumped simulates the first order catchment better than the other two methods, probably due to the small wetland which is unaccounted for. ACRU int does have the advantage that it simulates the intermediate horizon as well, which leads to a better simulation of the stream flow, as discussed previously.

The indications are that the simulations are more correct when working in a larger area. The Pearson correlation values increased for both the ACRU int and ACRU 2000 simulations from the first order to the second order to the third order. Thus the optimal scale for the detail soil information hydrological modelling is still unknown. The thought is that at small areas unaccounted for effects, such as the small wetland in the first order catchment, would have a big impact on the measured values. This impact decreases as the size of the area increases. But as the size of the area increases other factors such as climate which operates at a larger scale area overwhelms the effect of the soil.

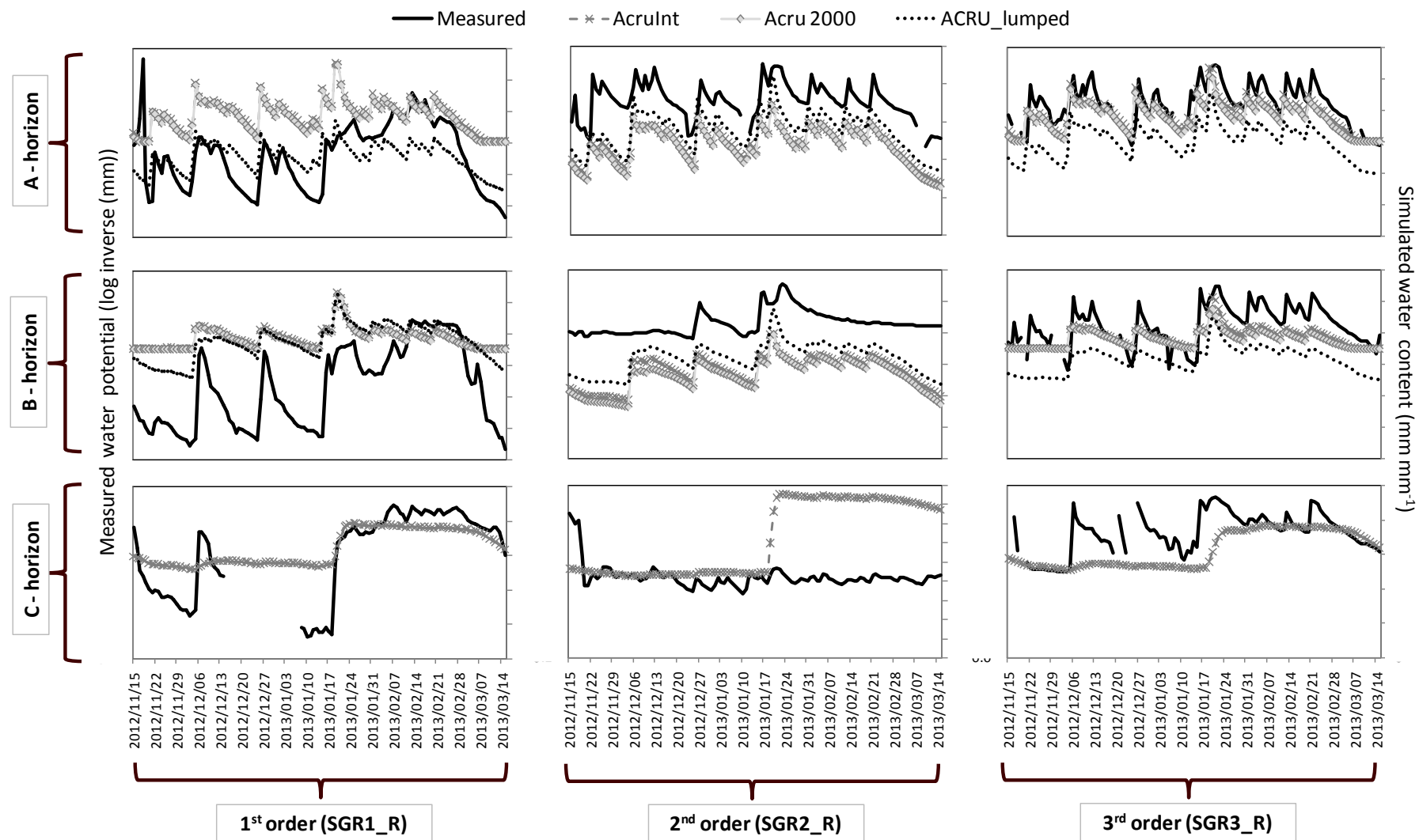


Figure 146 Measured vs. simulated water regimes for different profiles, horizons and soil information levels

Table 33 Pearson's product moment correlation coefficient between measured water tension (inverse log transformed – mm) and simulated water contents (mm mm⁻¹)

| Profile | Horizon | ACRU_lumped | ACRU2000 | ACRU-Int |
|---------|---------|-------------|----------|----------|
| SGR1_R | A | 0.59 | 0.53 | 0.53 |
| SGR1_R | B | 0.81 | 0.57 | 0.61 |
| SGR1_R | C | - | - | 0.87 |
| SGR2_R | A | 0.75 | 0.76 | 0.77 |
| SGR2_R | B | 0.67 | 0.67 | 0.62 |
| SGR2_R | C | - | - | -0.17 |
| SGR3_R | A | 0.81 | 0.80 | 0.80 |
| SGR3_R | B | 0.75 | 0.70 | 0.77 |
| SGR3_R | C | - | - | 0.50 |

3.3.6 Conclusions

Improved soil information does improve the ability of ACRU to simulate real time situations. For the streamflow simulations ACRU *int* and ACRU 2000 outperformed the ACRU lumped simulations. The ability of ACRU *int* to simulate an intermediate horizon between the soil and the groundwater, was also shown to improve the models accuracy. With the water content simulations, there was little to choose between the three model types.

Scale does play a role in the simulated results. At a very large scale, in the first order catchment, the benefit of the improved soil information was overrun by a small unaccounted for wetland. This resulted in better simulation results for ACRU lumped than for ACRU *int* and ACRU2000 for the water content simulations. In general the simulations improved as the scale decreased. There must be a ceiling to these improvements as other factors which operate at smaller scales, such as climate should override the effect of soil as the scale decreases. A future research question is to determine that threshold.

3.3.7 Acknowledgements

We would like to thank Prof Robert Schall from the University of the Free State, who aided us with the statistical analysis.

3.4 CONCLUSIONS

Two different methods of acquiring spatial hydropedological data have been determined. In the first method, the land types of South Africa were disaggregated into soilscares. This was done by dividing the area into hillslopes by spatial analysis, and through expert pedogenesis knowledge assigning soil forms to the different hillslopes to create soilscares. The area of the different soil map units corresponded acceptably with the areas the soils cover in the land type inventories. By allocating a hydrological response to each soil type, a hydropedological map was created. However this method still needs to be tested in the field. The second approach was to create a soil map using an expert knowledge digital soil mapping approach. By allocating conceptual hydrological responses to each soil map unit, a

hydropedological map could be created. This map differed from the map created in the first approach in that it divided the area into large sections, containing various hillslopes. In the third case study the two approaches were combined by first creating an expert knowledge digital soil map of the area, and then dividing the area into hillslopes. The result was a soilscape based hydropedological map. The value of this spatial hydropedological data lies in the fact that it links a conceptual hydrological response to a certain position and area. Knowing the extent of the conceptual hydrological responses allows for intrapolation of hydrological measurements to larger areas, within a scientifically correct setting. Most importantly, it was shown that the soil maps are useful at different scales. Thus pedogenetic information can greatly assist PUB's

3.5 REFERENCES

- eLEAF (2013) Data supplied by the Inkomati Catchment Management Agency on behalf of eLeaf (www.eleaf.com) and the WATPLAN EU project.
- ENVIRONMENTAL SYSTEMS RESEARCH INSTITUTE INC. (2010) ArcGIS version 9.3. www.ESRI.com.
- GEOLOGICAL SURVEY (1988) *1: 250 000 Geological Series 2730 Vryheid*. Geological Survey, Pretoria.
- HENSLEY M, LE ROUX PAL, GUTTER J and ZERIZGHY MG (2007) *Improved soil survey technique for delineating land suitable for rainwater harvesting*. WRC Report K8/685/4, Water Research Commission, Pretoria.
- IUSS WORKING GROUP WRB (2007) World reference base for soil resources 2006, first update 2007. *World Soil Resources Reports No. 103*. FAO, Rome.
- JENNY H (1941) *Factors of soil formation, A system of quantitative pedology*. McGraw-Hill, New York.
- LAND TYPE SURVEY STAFF (1976-2006) Land type Survey Database. ARC-ISCW, Pretoria.
- LAND TYPE SURVEY STAFF (1986) Land types of the map 2730 Vryheid. *Memoirs Agric. Nat. Resour. S. Afr. No. 7*. ARC – Institute for Soil, Climate and Water, Pretoria.
- LE ROUX PAL, VAN TOL JJ, KUENENE BT, HENSLEY M, LORENTZ SA, EVERSON CS, VAN HUYSSTEEN CW, KAPANGAZIWIRI E and RIDDELL ES (2011) *Hydropedological interpretations of the soils of selected catchments with the aim of improving the efficiency of hydrological models*. WRC Report K5/1748, Water Research Commission, Pretoria.
- LE ROUX PAL, DU PLESSIS MJ, TURNER DP, VAN DER WAALS J and BOOYENS HB (2013) *Field Book for the classification of South African soils*. South African Soil Surveyors Organization, Bloemfontein. 173pp.
- LILLY A, BOORMAN DB and HOLLIS JM (1998) The development of a hydrological classification of UK soils and the inherent scale changes. *Nutrient Cycling in Agroecosystems* 50, 299-302.
- LIN HS, KOGELMAN W, WALKER C and Bruns MA (2006) Soil moisture patterns in a forested catchment: A hydropedological perspective. *Geoderma* 131, 345-368.
- LORENTZ SA, BURSEY K, IDOWU O, PRETORIUS C and NGELEKA K (2007) *Definition and upscaling of key hydrological processes for application in models*. Report No. K5/1320. Water Research Commission, Pretoria.

- MACMILLAN RA, MOON DE, COUPÉ RA, and PHILLIPS N (2010) Predictive ecosystem mapping (PEM) for 8.2 million ha of forestland, British Columbia, Canada. In: Boettinger JL, Howell DW, Moore AC, Hartemink AE and Kienast-Brown S (eds.) *Digital soil mapping; bridging research, environmental application and operation*. Springer, Dordrecht.
- MACVICAR CN, DE VILLIERS JM, LOXTON RF, VERSTER E, LAMBRECHTS JJN, MERRYWEATHER FR, LE ROUX J, VAN ROOYEN TH, HARMSE HJ VON M (1977) Soil Classification: A binomial system for South Africa. Department of Agriculture Technical Services, Pretoria.
- MARSMAN BA, and DE GRUIJTER JJ (1986) *Quality of soil maps, a comparison of soil survey methods in a study area*, Soil Survey papers no. 15, Netherlands Soil Survey Institute, Stiboka, Wageningen, The Netherlands.
- McBRATNEY AB, MENDOÇA SANTOS ML and MINASNY B (2003) On digital soil mapping. *Geoderma* **117**, 3-52.
- McBRATNEY AB, MINASNY B, CATTLE SR and VERVOORT RW (2002) From pedotransfer functions to soil inference systems. *Geoderma* **109** 41-73.
- MINASNY B, McBRATNEY AB (2006) A conditioned Latin hypercube method for sampling in the presence of ancillary information. *Computers & Geosciences* **32** 1378-1388.
- MUCINA L, RUTHERFORD MC, (eds.) (2006) *The vegetation of South Africa, Lesotho and Swaziland, Strelitzia 19*. South African National Biodiversity Institute, Pretoria.
- PARK SJ, MCSWEENEY K and LOWERY B (2001) Identification of the spatial distribution of soils using a process-based terrain characterization. *Geoderma*, 103, 249-272.
- SAGA USER GROUP ASSOCIATION (2011) SAGA GUI 2.0.8. <http://www.saga-gis.org>.
- SAWS (2012). Climate data provided by South African Weather Service. Pretoria, South Africa
- SCHULZE RE (1995) Hydrology and agrohydrology: A text to accompany the ACRU 3.00 agrohydrological modelling system. Water Research Commission, Report No 63/2/84. WRC, Pretoria.
- SCHULZE RE (2007) Soils: *Agrohydrological information needs, information sources and decision support*. In Schulze, R.E (Ed). 2007. South African atlas of climatology and agrohydrology. Report No. 1489/1/06. Water Research Commission, Pretoria.
- SIVAPALAN M (2003) Prediction in ungauged basins: a grand challenge for theoretical hydrology. *Hydrol. Process.*, 17, 3163-3170.
- SMIT IPJ, RIDDELL ES, CULLUM C and PETERSEN R (2013) Kruger National Park research supersites: Establishing long-term research sites for cross-disciplinary, multiscaled learning. *Koedoe* **55** (1), Art. #1107, 7 pages. [http:// dx.doi.org/10.4102/koedoe.v55i1.1107](http://dx.doi.org/10.4102/koedoe.v55i1.1107).
- SMITHERS J and SCHULZE RE (2004) *ACRU Agrohydrological modelling system: user manual v4.00*. School of Bioresources Engineering and Environmental Hydrology, University of Natal, Pietermaritzburg.
- SOIL CLASSIFICATION WORKING GROUP (1991) *Soil classification: A taxonomic system for South Africa*. Department of Agricultural Development, Pretoria, South Africa.
- SOULSBY C and TETZLAFF D (2008) Towards simple approaches for mean residence time estimation in ungauged basins using tracers and soil distributions. *Journal of Hydrology* 363, 60-74.
- SPOT IMAGE (2013) SPOT satellite technical data. Available from <http://www.spotimage.com/web/en/229-the-spot-satellites.php> (Accessed 23 June 2013).

- TERRAIN ANALYTICS L.L.C. (2003) 3d Mapper version 4.02. <http://www.terrainanalytics.com>.
- TICEHURST JL, CRESSWELL HP, McKENZIE NJ and Clover MR (2007) Interpreting soil and topographic properties to conceptualise hillslope hydrology. *Geoderma* 137, 279-292.
- USDA FOREST SERVICE, REMOTE SENSING APPLICATION CENTER (2005) Terrestrial Ecological Unit Inventory- Geospatial Toolkit, User guide v4.1. Washington, D. C. U.S. Department of Agriculture, Forest Service, Washington Office, Ecosystem Management Coordination Staff.
- USGS (UNITED STATES GEOLOGICAL SURVEY) (2013) Landsat images. URL: <http://landsat.usgs.gov> (Accessed 23 June 2013).
- VÅGEN TG, WINOWIECKI L, DESTA LT, and TONDOH JE (2010) *Land degradation surveillance framework: Field guide*. AfsIS, Arusha.
- VAN NIEKERK A (2012) Developing a very high resolution DEM of South Africa. *Position IT Nov-Dec* 55-60. http://www.eepublishers.co.za/images/upload/positionit_2012/visualisation_nov-dec12_developing-resolution.pdf.
- VAN TOL JJ, LE ROUX PAL, HENSLEY M and LORENTZ SA (2010) Soil as indicator of hillslope hydrological behaviour in the Weatherley Catchment, Eastern Cape, South Africa. *Water SA*. 36, 513-520
- VAN TOL, J.J., LE ROUX, P.A.L. & HENSLEY, M., 2011. Soil indicators of hillslope hydrology. In: B.O Gungor (eds), *Principles-Application and Assessments in Soil Science*. Intech, Turkey.
- VAN TOL JJ, LE ROUX PAL, LORENTZ SA and HENSLEY M (2013) Hydropedological classification of South African hillslopes. *Vadose Zone J.* **12** (4) DOI:10.2136/vzj2013.01.0007.
- VAN ZIJL GM, LE ROUX PAL and SMITH HJC (2012) Rapid soil mapping under restrictive conditions in Tete, Mozambique. In: Minasny B, Malone BP and McBratney AB (eds.). *Digital soil assessments and beyond*. Balkema: CRC Press. pp 335-339.
- VAN ZIJL GM and LE ROUX PAL (2014) Creating a conceptual hydrological soil response map for the Stevenson Hamilton Research Supersite, Kruger National Park, South Africa. *WaterSA* 40, 331-336.
- VENTER FJ (1990) A classification of land management planning in the Kruger National Park. PhD thesis, Department of Geography, University of South Africa.
- WEISS A (2001) Topographic Position and Landforms Analysis. Poster presentation, ESRI User Conference, San Diego, CA.
- ZHU A-X (1997) A similarity model for representing soil spatial information. *Geoderma* **77**, 217-242.
- ZHU A-X, HUDSON B, BURT J, LUBICH K, SIMONSON D (2001) Soil mapping using GIS, expert knowledge and fuzzy logic. *Soil Science Society of America Journal* 65, 1463-1472.
- ZHU A-X, YANG L, LI B, QIN C, ENGLISH E, BURT JE and ZHOU C (2008) Purposive sampling for digital soil mapping for areas with limited data. In: Hartemink A E, McBratney AB and Mendonça-Santos M De L (eds.). *Digital soil mapping with limited data*. Dordrecht, Springer.

SECTION II: MODELLING

Chapter 4 VIRTUAL EXPERIMENTATION

4.1 INTRODUCTION

Soils integrate the influences of parent material, topography, vegetation/land use, and climate and can therefore act as a first order control on the partitioning of hydrological flow paths, residence time distributions and water storage (Schulze, 1995; Park *et al.*, 2001; Sivapalan, 2003 and Soulsby *et al.* 2006). The relationship between soil and hydrology is interactive. Water is a primary agent in soil genesis, resulting in the formation of soil properties containing unique signatures of the way they formed. The interpretation of soil morphological properties in relation to their hydrological response can be used to describe the hydrological response of hillslopes qualitatively (Ticehurst *et al.*, 2007; Van Tol *et al.*, 2010; Kunene *et al.*, 2011; Van Tol *et al.*, 2013) and to structure distributed models realistically (Van Tol *et al.*, 2011). The next logical step is to quantify the qualitative conceptual descriptions of hydrological processes. Quantification (measurements) should however not be driven by exploring unconventional behaviours of new hillslopes but should rather focus on a systematic examination of first order controls and indicators of first order controls of hillslope hydrological behaviour with the ultimate aim to generalize and extrapolate from one place to another over multiple scales using an interdisciplinary approach (Weiler & McDonnell, 2004; McDonnell *et al.*, 2007).

In a vast range of hillslopes subsurface lateral flow (SLF) is considered to be a dominant streamflow generation process (Retter, Kienzler & Germann, 2006), not only during recession of the hydrograph, but also for peak and low flows (Harr, 1977; Mosley, 1979 and Whipkey & Kirkby, 1979). SLF occurs either through the soil matrix (inter-granular pores or small structure voids) or through larger voids (macropores or pipes) (Atkinson, 1979) and especially when “i) the land is sloping, ii) surface soil is permeable, iii) a water-impeding layer is near the surface, and iv) the soil is saturated” (Whipkey, 1965). In general SLF is generated when infiltrated water flowing (in unsaturated state) vertically, driven by gravity, encounters a layer with lower permeability, such as luvisol horizons or impermeable bedrock (most studies focussed on the latter). Once a condition close to saturation is attained above the impeding layer SLF occurs (Whipkey, 1965; Whipkey *et al.*, 1979; Woods & Rowe, 1996; Kim, Sidle & Moore, 2005; Retter *et al.*, 2006). According to Jackson (2005) SLF only occurs when the vector of the saturated hydraulic conductivity of the conducting layer (K_{sc}) parallel to the slope with angle β is larger than the vertical conductivity of the impeding layer (K_{si}):

$$K_{sc}(\tan\beta) > K_{si} \quad (4.1)$$

Unsaturated SLF can also occur but the direct contribution of this process to streamflow is considered insignificant (Whipkey *et al.*, 1979).

Field measurements of SLF fall into three categories: i) interception of flow, ii) additions of tracers and, iii) indirect methods (Atkinson, 1979). Interception of flow usually involves exposing a vertical surface of the soil and collecting water draining out of the vertical face. This artificial free face distorts the flow lines to form a saturated wedge from which water drains at a rate (K_s) greater than the rate under natural conditions. Additions of tracers are a non-destructive method to determine the actual pathways (e.g. fluorescent dyes) and flow times (e.g. radioactive tracers and breakthrough curves of Br, Cl, etc.). Since hillslope hydrological processes are non-linear (due to differences in antecedent moisture contents and precipitation intensities) the extrapolation value of these experiments over a range of hillslopes and environmental conditions is limited. Indirect methods involve measurements of soil water contents and hydraulic potentials over the slope or experimental plot (Harr, 1977 and Atkinson, 1979). At any point in the matrix the water flux (q) depends on the hydraulic potential gradient ($\Delta H/L$) and the hydraulic conductivity (K) known as *Darcy's law*. Field studies on SLF have however shown that direct application of *Darcy's law* is not realistic for a hillslope (Whipkey, 1965 and Mosley, 1979). This is mainly because the hydraulic conductivity varies with moisture content (θ), there is considerable hysteresis between θ and K , and heterogeneities in K exist along the slope.

Most field measurements of SLF is tedious and expensive and, due to non-linearity's, hysteresis and heterogeneities within a hillslope, have limited extrapolation value. Weiler *et al.* (2004) proposed virtual experiments as an approach to conceptualize hillslope hydrology. They define a virtual experiment as a 'numerical experiment with a model driven by collective field intelligence'. Weiler *et al.* (2004) studied the influence of drainable porosity as a first order control on flow and transport within the virtual experiment framework. From the introduction of the virtual experiment approach in 2004, a great number of studies have used this to investigate *inter alia* nutrient flushing (Weiler & McDonnell, 2005); factors influencing residence times (Dunn & McDonnell, 2007); factors influencing connectivities at hillslope scale (Hopp & McDonnell, 2009); the impact of vegetative canopy on SLF (Keim, Tromp-Van Meerveld & McDonnell, 2006); lateral preferential flow (Weiler & McDonnell, 2007) and evaluation of the desired complexity in hillslope models (Tromp-Van Meerveld & Weiler, 2008), to name a few. These studies focused on examining first order controls on complex hillslope hydrological processes. We recognize the hillslope as a fundamental landscape unit but are also aware of the enormous complexity of hillslope hydrological processes and heterogeneity within a hillslope. Hillslope hydrological response is often not separated in soil and fractured rock SLF but rather the result of complex interactive flow related to a complex soil distribution pattern (Van Tol *et al.*, 2010). In our qualitative descriptions of hillslope responses (e.g. van Tol *et al.*, 2013) we have divided hillslopes into segments of hydrogeological similar soil types based on the interpretations of soil morphology.

$$g(t) = \left(\frac{4\pi D_p t}{\tau}\right)^{-\frac{1}{2}} t^{-1} \exp\left[-\left(1 - \frac{t}{\tau}\right)^2 \left(\frac{\tau}{4D_p t}\right)\right] \quad (4.2)$$

In this study we adopted the virtual experiment approach to examine the first order controls on SLF generation in hillslope soils. Based on literature and our experience the dominant factors influencing SLF is the slope gradient, hydraulic conductivity of the conducting layer, ratio between hydraulic conductivities of the conducting and impeding layers and the depth of the conducting layer, i.e. the distance from the surface to the impeding layer. The study is motivated by recognizing the need for simple descriptions of SLF responses in hydrological

models which still manage to reflect the actual hydrological processes within a section of a hillslope in order to be upscale based on the soil distribution pattern to be applied in ungauged basins. We will therefore not attempt to quantify SLF of whole hillslopes, but only relatively uniform sections of hillslopes. Here we address two important questions 1) can SLF response be described in a range of virtual hillslopes with different soil and slope characteristics by a single equation; 4.2) is there a statistical correlation between soil and slope characteristics and SLF response.

4.2 METHODOLOGY

4.2.1 Virtual hillslope setup

We used the finite element model HYDRUS-2D (Simunek, Sejna & van Genuchten, 1999) for our virtual experiments. The model solves the Richards' equation for variably saturated media. A 25 m slope was used for all simulations (Figure 147), to allow for lateral seepage from upslope sections. In semi-arid areas, dominated by high atmospheric demands, it is unlikely that water will travel great distances (>25 m) downslope before being evapotranspired. The slope gradient (∇) in %, varied (Table 34). The virtual hillslope comprised of two soil horizons with distinct hydrological properties (Figure 147 and Table 34). For the remainder of this discussion the top horizon is termed the *conducting horizon* which overlies the *impeding horizon*. In practice this setup can reflect both an A-horizon overlying a B-horizon with low permeability (A/B – horizon interface SLF) or a soil horizon overlying relatively impermeable bedrock (soil/bedrock interface SLF). A seepage face boundary was assigned to the vertical face of the conducting horizon at the bottom of the virtual slope. An atmospheric boundary condition was assigned to the top of the conducting horizon and a free drainage boundary condition at the bottom of the impeding horizon. The depth of the impeding horizon was kept constant at 500 mm whereas the depth of the conducting horizon was considered to have an influence on the lateral response and therefore varied (Table 34). The finite element (FE) mesh was refined to approximately 50 mm at the seepage face, all other sections of the slope the target FE mesh was 150 mm. The initial water contents were expressed in pressure heads and were -100 mm for the impeding layers and increased linearly with depth, from -1000 to 0 (saturation) in the conducting layer.

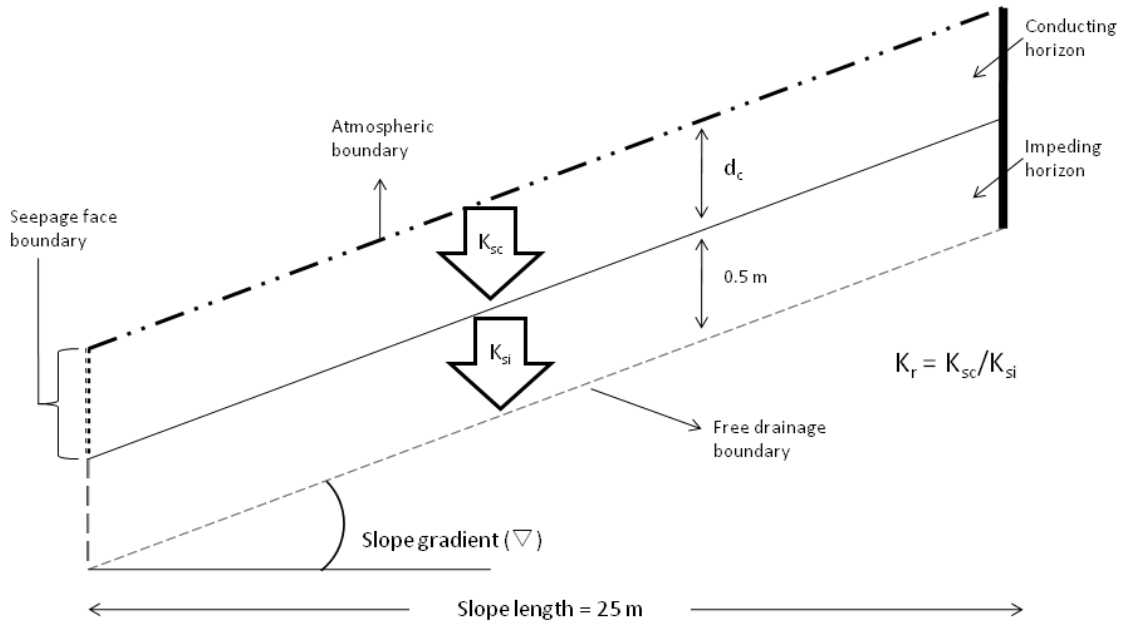


Figure 147 Setup of virtual hillslope in Hydrus-2D

4.2.2 Virtual simulations

A total of 68 simulations with different slope gradients (∇), hydraulic conductivities of the conducting and impeding horizons (K_{sc} and K_{si} , respectively), ratios between K_{sc} and K_{si} (K_r), depth of conducting horizon (d_c), and rainfall volumes were conducted. The ranges of different parameters used for the simulations are presented in Table 34.

Table 34 Ranges of parameter values used in virtual simulations

| 1 st order control | ∇ | K_{sc} | K_{si} | K_r | d_c | Rainfall |
|-------------------------------|----------|--------------------|--------------------|-------|-------|----------|
| Unit | % | mm h ⁻¹ | mm h ⁻¹ | - | mm | mm |
| Minimum | 10 | 30 | 0.5 | 10 | 300 | 30 |
| Maximum | 50 | 300 | 30 | 300 | 900 | 150 |

Each of the 68 simulations was done with a different set of parameters as presented in Table 34. For a specific physical setup (i.e. ∇ , K_{sc} , K_{si} and d_c) at least two different rainfall volumes were applied in order to normalize the impact of rain volume (see discussion in the following section). All the rain was applied in the first hour where after the slope was left to drain for 240 hours, or until seepage ceased. The seepage from the slope (mm) was obtained from the boundary flux output file. Not all simulations produced seepage (3), presumably because K_{si} exceeded the vector of K_{sc} (see eq.4. 1); these were omitted from further analyses.

4.2.3 IUH's and fitting ADF's

Instantaneous Unit Hydrographs (IUH's) were obtained by dividing the cumulative seepage from a simulation by seepage during each hourly time step of that simulation. The influence of rainfall volumes were normalized by averaging the IUH's of simulations with the same physical setup but with different rain volumes. With the exclusion of the simulations which did not produce seepage and normalization of rainfall volumes a total of 23 IUH's were obtained.

Fitting of the Advection-Dispersion Function (ADF) to the IUH's were done by convolution of eq. 4.2 and optimizing D_p and τ values. The influence of the identified 1st order controls on D_p and τ values were then statistically determined by two multiple regression equations.

4.3 RESULTS

The 23 IUH's yielded a well distributed range of D_p and τ values (Table 35). The minimum and maximum D_p values were 0.01 and 1.46 respectively and the minimum and maximum τ values were 1.53 and 54.53 respectively. From Table 35, two multiple regressions using the first order controls (∇ , K_{sc} , K_{si} and d_c) were derived.

4.3.1 Multiple regressions

$$D_p = (0.000921 \times \nabla) + (0.000302 \times K_{sc}) + (0.001882 \times K_r) - (0.00097 \times d_c) + 0.5757$$

$$\tau = -(0.01558 \times \nabla) - (0.11396 \times K_{sc}) + (0.02003 \times K_r) + (0.03769 \times d_c) + 20.3038$$

Table 35 First order controls, and optimized D_p and τ values for the 23 IUH's

| IUH | ∇ | d_c | K_{sc} | K_r | D_p | τ |
|-----|----------|-------|----------|-------|-------|--------|
| 1 | 10 | 600 | 300 | 300 | 0.49 | 15.23 |
| 2 | 10 | 600 | 300 | 60 | 0.14 | 4.85 |
| 3 | 10 | 600 | 300 | 10 | 0.01 | 2.70 |
| 4 | 10 | 600 | 30 | 300 | 0.26 | 37.56 |
| 5 | 10 | 600 | 30 | 60 | 0.02 | 54.53 |
| 6 | 10 | 600 | 30 | 10 | 0.06 | 41.47 |
| 7 | 25 | 600 | 300 | 300 | 0.85 | 16.66 |
| 8 | 50 | 600 | 300 | 300 | 0.68 | 15.86 |
| 9 | 25 | 300 | 300 | 300 | 1.18 | 5.80 |
| 10 | 25 | 900 | 300 | 300 | 0.53 | 22.30 |
| 11 | 50 | 300 | 30 | 30 | 0.22 | 10.59 |
| 12 | 10 | 900 | 300 | 300 | 0.29 | 20.32 |
| 13 | 10 | 600 | 30 | 30 | 0.02 | 52.73 |
| 14 | 10 | 300 | 300 | 300 | 1.46 | 4.42 |
| 15 | 10 | 300 | 300 | 60 | 0.42 | 2.82 |
| 16 | 25 | 300 | 300 | 60 | 0.35 | 2.69 |
| 17 | 25 | 300 | 150 | 10 | 0.69 | 1.53 |
| 18 | 50 | 600 | 300 | 30 | 0.10 | 18.22 |
| 19 | 50 | 600 | 30 | 30 | 0.28 | 43.21 |
| 20 | 50 | 300 | 300 | 300 | 0.62 | 9.17 |
| 21 | 50 | 900 | 300 | 300 | 0.35 | 23.46 |
| 22 | 10 | 600 | 300 | 30 | 0.13 | 2.84 |
| 23 | 50 | 900 | 30 | 30 | 0.07 | 50.37 |

4.4 REFERENCES

- ATKINSON, T. C., 1979. Techniques for measuring subsurface flow on hillslopes. In Kirkby, M. J. (Ed.), *Hillslope Hydrology*. Wiley, New York, 73-120.
- HARR, R. D., 1977. Water flux in soil and subsoil on a steep forested slope. *J. Hydrol.* 33, 37-58.
- HOPP, L. & McDONNELL, J.J., 2009. Connectivity at the hillslope scale: Identifying interactions between storm size, bedrock permeability, slope angle and soil depth. *J. Hydrol.* 376, 378-391.
- JACKSON, C. R., 2005. A conceptual model for characterizing hillslope hydrologic behavior between the bookends of 100% vertical percolation and 100% interflow. Poster. IAHS SLICE workshop, September 25-28, H.J. Andrews Experimental Forest, OR.
- KEIM, R., TROMP-VAN MEERVELD, I. & McDONNELL, J.J., 2006. A virtual experiment on the effects of evaporation and intensity smoothing by canopy interception on subsurface stormflow generation. *J. Hydrol.* 327, 352-364.
- KIM, H. Y., SIDLE, R. C. & MOORE, R. D., 2005. Shallow lateral flow from a forested hillslope: Influence of antecedent wetness. *Geoderma* 60, 293-306.
- KUENENE, B.T., VAN HUYSSTEEN, C.W., LE ROUX, P.A.L., HENSLEY, M. & EVERSON, C.S., 2011. Facilitating interpretation of Cathedral Peak VI catchment hydrograph using soil drainage curves. *South African Journal of Geology*, 114, 525-534.
- McDONNELL, J. J., SIVAPALAN, M., VACHÉ, k., DUNN, S., GRANT, G., HAGGERTY, R., HINZ, C., HOOPER, R., KIRCHNER, J., RODERICK, M. L., SELKER, J. & WEILER, M., 2007. Moving

- beyond heterogeneity and process complexity: A new vision for watershed hydrology. *Water Resour. Res.*, 43, 1-6.
- MOSLEY, M. P., 1979. Streamflow generation in a forested watershed, New Zealand. *J. Hydrol.* 15, 795-806.
- PARK, S.J., MCSWEENEY, K. & LOWERY, B., 2001. Identification of the spatial distribution of soils using a process-based terrain characterization. *Geoderma*, 103, 249-272.
- RETTTER, M., KIENZLER, P. & GERMANN, P. F., 2006. Vectors of subsurface stormflow in a layered hillslope during runoff initiation. *Hydrol. Earth. Syst. Sci.* 10, 309-320.
- SCHULZE, R.E., 1995. Hydrology and Agrohydrology: A Text to Accompany the ACRU 3.00 Agrohydrology Modelling System. Water Research Commission, Pretoria, RSA, Report TT69/95.
- SIMUNEK, J., SEJNA, M. & VAN GENUCHTEN, M. TH., 1999. The HYDRUS-2D software package for simulating two-dimensional movement of water, heat, and multiple solutes in variably saturated media. Version 2.0, IGWMC- TPS-53, Colorado School of Mines, Golden, Colorado, 251 pp.
- SIVAPALAN, M., 2003. Process complexity at hillslope scale, process simplicity at the watershed scale: is there a connection? *Hydrol. Process.*, 17, 1037-1041.
- SOULSBY, C., TETZLFF, D., RODGERS, P., DUNN, S. & WALDRON, S., 2006. Runoff processes, stream water residence times and controlling landscape characteristics in a mesoscale catchment: An initial evaluation. *J. Hydrol.*, 325, 197-221.
- TICEHURST, J.L., CRESSWELL, H.P., MCKENZIE, N.J. & CLOVER, M.R., 2007. Interpreting soil and topographic properties to conceptualise hillslope hydrology. *Geoderma*, 137, 279-292.
- TROMP-VAN MEERVELD, I. & WEILER, M., 2008. Hillslope dynamics modelled with increasing complexity. *J. Hydrol.*, 361, 24-40.
- VAN TOL, J.J., LE ROUX, P.A.L., HENSLEY, M. & LORENTZ, S.A., 2010. Soil as indicator of hillslope hydrological behaviour in the Weatherley Catchment, Eastern Cape, South Africa. *Water SA*. 36, 513-520.
- VAN TOL, J.J., LE ROUX, P.A.L. & HENSLEY, M., 2011. Soil indicators of hillslope hydrology. In: B.O Gungor (eds), *Principles-Application and Assessments in Soil Science*. Intech, Turkey.
- VAN TOL, J.J., LE ROUX, P.A.L., LORENTZ, S.A., HENSLEY, M., 2013. Hydropedological classification of South African hillslopes. *Vadoze Zone Journal*, 12 (4). doi:10.2136/vzj2013.01.0007.
- WEILER, M. & MCDONNELL, J., 2004. Virtual experiments: a new approach for improving process conceptualization in hillslope hydrology. *J. Hydrol.* 285, 3-18.
- WEILER, M. & MCDONNELL, J., 2005. Testing nutrient flushing hypotheses at the hillslope scale: A virtual experiment approach. *J. Hydrol.*, 319, 339-356.
- WEILER, M. & MCDONNELL, J., 2007. Conceptualizing lateral preferential flow and flow networks and simulating the effects on gauged and ungauged hillslopes. *Water Resour. Res.*, 43, W03403, doi:10.1029.
- WHIPKEY, R. Z., 1965. Subsurface stormflow from forested slopes. *Int. Assoc. Sci. Hydrology. Bull.* 10, 74-85.
- WHIPKEY, R. Z. & KIRKBY, M. J., 1979. Flow within the soil. In Kirkby M. J (Ed.), *Hillslope Hydrology*. Wiley, New York, 121-143.
- WOODS, R. & ROWE, L., 1996. The changing spatial variability of subsurface flow across a hillslope. *J. Hydrol.* 31, 49-84.

Chapter 5 **HYDROLOGICAL MODELLING USING HYDROPEDOLOGICAL DATA**

5.1 ABSTRACT

There is a great need for closer collaboration between experimentalist and modellers. This chapter present a modelling exercise in a well-studied catchment in South Africa (Weatherley). The modelling was done by the experimentalist and from an experimentalist's viewpoint. ACRU-Int was used to simulate the hydrological response of the catchment over two rainfall seasons. The ability of ACRU-Int to route the intermediate zone of one land segment to different layers of a land segment downslope is ideal for simulating the hydrology of catchments in terms of the hydrological response of individual hillslopes. The catchment was divided into 7 distinct land segments representing two dominant hillslopes in the catchment. The model predicted low flows very well, but not so for peak flows. Even though the general streamflow predictions were relatively poor, uncertainty in the predictions can't be attributed to calibrations or over parameterization of the model. This is believed to be a step in the right direction for PUB's.

5.2 INTRODUCTION

5.2.1 The hydrological modelling problem

The hydrological response of catchments is dependent on the combined responses of the individual hillslopes within the catchment (Sivapalan, 2003a). The hillslope is generally accepted as a fundamental landscape unit (Weiler and McDonnell, 2004; Lin *et al.*, 2006), and is the smallest scale for holistically understanding and simulating hydrological processes (Tromp van Meerveld & Weiler, 2008). It is therefore not surprising that the hillslope forms the basic building block for a number of hydrological models.

The current dominant paradigm in hydrological modelling involves using an *a priori* set of small scale theories and process descriptions (e.g. Darcy and Richards equations) and splitting the catchment into small enough uniform elements for these theories to work. The models arising from this paradigm emphasize the explicit mapping of landscape heterogeneities and process complexities which, according to McDonnell *et al.* (2007), are an impossible task in even the most intensively studied catchments. Consequently the models based on current theories rely strongly on calibration, mimicking past data, to account and compensate for the lack of understanding of the actual hydrological processes and heterogeneities in the landscape (Sivapalan 2003a and McDonnell *et al.*, 2007). This results in models that 'work' but for the wrong process reasons (Weiler *et al.*, 2004) and models highly overparameterized with many combinations of the parameters resulting in the same final result. This leads to a large degree of modelling uncertainty and models unsuitable for predictions in ungauged basins (Beven, 2001 and McDonnell *et al.*, 2007).

Another hitch in hydrological modelling is the gap between experimentalists and modellers. Experimentalist proposes a conceptual model of hydrological behaviour of a system based on observations, measurements and experience. The appropriateness of the concept can

only be verified when a numerical model is built (Bredehoeft, 2005). Unfortunately modellers usually do not incorporate the experimentalist's knowledge into the model structure (Sivapalan 2003a; Sivapalan 2003b; Weiler *et al.*, 2004; McDonnell *et al.*, 2007 and Tromp-van Meerveld *et al.*, 2008) and when they do; simulations are followed by calibration exercises and our limited understanding of the complex process is further depreciated by "correcting" it with imperfect data (Dunn *et al.*, 2008). On the other hand experimentalists have focussed on the documentation of the unconventional behaviour of new hillslopes instead of the systematic examination of first order controls of hillslope hydrological behaviour, without intercomparisons to obtain common process behaviours (Weiler *et al.*, 2004). The transference or extrapolation value of these hillslope studies is therefore minimal. Some researchers argue that every hillslope is therefore unique (Beven, 2001). This is true to a certain extent, since after hundreds of experiments we appear to be no further towards a common conceptualization of hillslope hydrology and experimentalists have not yet expressed what the minimal set of measurements are to characterize even a single hillslope (Weiler *et al.*, 2004; McDonnell *et al.*, 2007 and Tromp-van Meerveld *et al.*, 2008)! There is a great need for closer collaboration between experimentalist and modellers (Siebert and McDonnell, 2002). Neither the conceptual model of the experimentalist nor the numerical model of the modeller should be considered untouchable, but the common focus should be to, through iteration of concepts and numbers, represent the physical process numerically.

5.2.2 Study objectives

The aim of this study is twofold:

- Firstly to simulate the hydrological response of a well-studied catchment with a hydrological model capable of imitating dominant hydrological processes. Model configuration and parameterization will be based on measured properties and processes, without any end calibrations of the model. Results will be used to evaluate the appropriateness of the model for predictions in ungauged basins as well as the employment of the model for the HOSASH project.
- Secondly to attempt to close the gap between the experimentalist and the modeller, with the 'experimentalist' being the soil scientists from UFS and the 'modeller' being hydrologist from UKZN. Although the 'modeller' probably encompass more field experience than the 'experimentalist' in this exercise, it is believed that the venture into the modelling world will reveal significant insights into the translation of observed and measured 'concepts' into a numerical model. The gained understanding should also aid in more productive and creative cooperation between the two sciences in future and certainly in a more prolific approach when the Hydrology of South African Soils and Hillslopes is studied.

5.3 ACRU HYDROLOGICAL MODEL

5.3.1 Soil parameters in ACRU

ACRU is an agrohydrological, daily time step, multi-layered soil water budgeting model. The standard version, *ACRU2000*, comprises of two soil layers (A and B- horizon) and a deep groundwater layer. Soil inputs include; the thickness of soil horizons, water contents at the

start of simulation (SMAINI and SMBINI) at (Permanent Wilting Point (PWP), Drained Upper Limit (DUL) and saturation (Po), the Plant Available Water (PAW), drainage rates (ABRESP and BFRESP) and the erodibility of the soil (*K*-factor). Except for the latter all inputs are required for both soil horizons (Schulze, 2007).

PWP, DUL and Po are largely determined by the soil texture, organic matter and the bulk density. Typical values for these parameters are proposed in chapter 5 of the *ACRU user manual* (Smithers and Schulze, 2004) for different textural classes and clay distribution models, i.e. change in clay content with depth. The clay distribution models and typical texture classes were assigned to the 501 soil series of the binomial soil classification of South African soils (MacVicar *et al.*, 1977). Relative accurate PWP, DUL and Po values are therefore easily available for all South African soils. The PAW is the difference between DUL and PWP and is used to calculate the initial water content, expressed as a percentage of PAW (Smithers *et al.*, 2004).

The model allows redistribution of saturated water (RESP), i.e. between DUL and Po, from the A to the B horizon (ABRESP) and from the B horizon to the groundwater (BFRESP). The distribution is expressed as a fraction of the saturated water draining vertically downwards from the respective horizons on a daily time step. In Schulze (1995) typical RESP values are presented for different textural classes. Low RESP values will result in the build-up of saturated water in upper soil horizons (A horizon for ABRESP and B horizon for BFRESP) favouring the generation of lateral flow in that layer. Reductions in RESP are therefore suggested based on the “Interflow Potential” (IP) of different soil series, high IP = $RESP \times 0.3$ and moderate IP = $RESP = 0.6$ (Schulze, 1995). The influence of the redistribution fractions on the simulated soil water contents is illustrated in Figure 148.

Water contents in one land segment were simulated with *ACRU-Int* for six years with actual climatic data from the Weatherley catchment in the Eastern Cape (Figure 148). Four different RESP fractions were used *a*) ABRESP = 0.01 & BFRESP = 0.01, *b*) ABRESP = 0.99 & BFRESP = 0.99, *c*) ABRESP = 0.99 & BFRESP = 0.01 and *d*) ABRESP = 0.01 & BFRESP = 0.99. Simulation *a* and *b* show similar trends with a build-up of water in the A horizon, relatively low water contents in the B horizon and a general decrease in the water content of the C-horizon due to very little vertical drainage from the A to lower horizons. In simulation *b*, water is allowed to drain freely to the B horizon and then to the C-horizon, resulting in relatively low water contents in the A and B horizons but accumulation in the C-horizon. Simulation *c* show water freely draining from the A horizon but due to the impeding C-horizon (BFRESP = 0.01) build-up in the B horizon, slowly reducing the water content in the C-horizon.

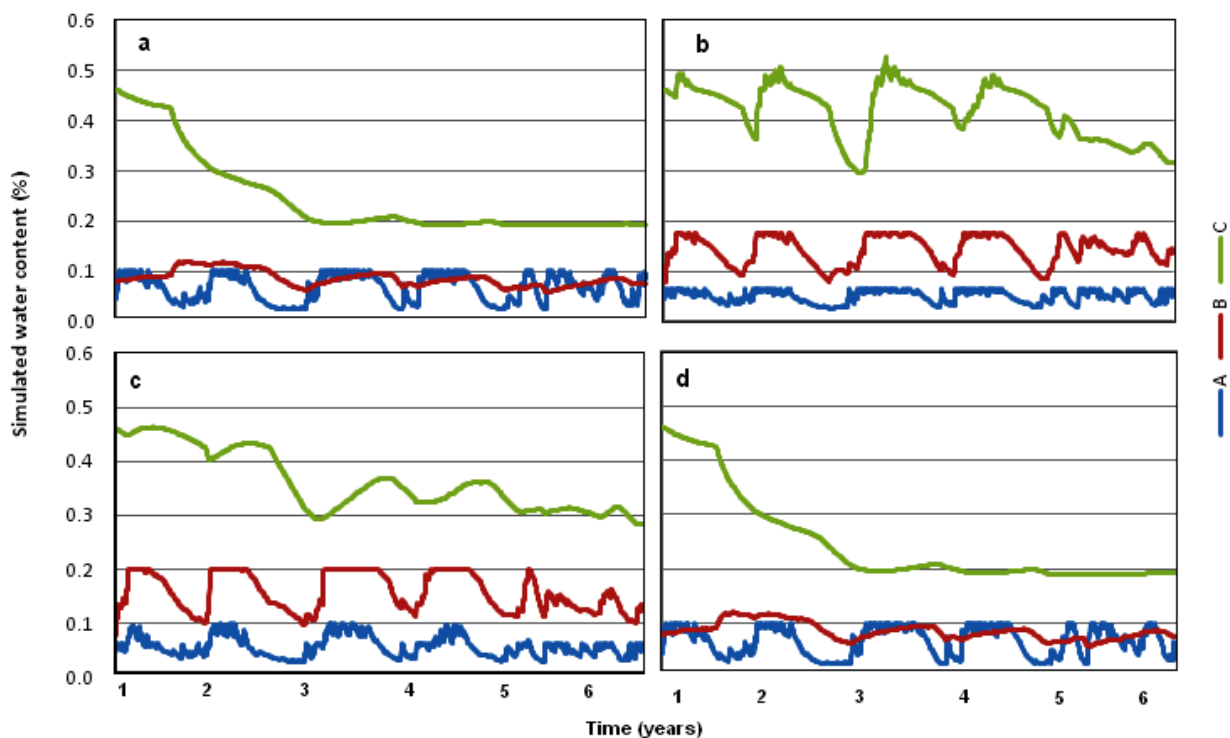


Figure 148 Water contents (%) for three horizons with different RESP values simulated over 6 years with ACUR-Int

It is clear from Figure 148 that the RESP values play an integral part in the simulation of soil water contents and consequently on the outflow of different land segments. Exactly how these values were obtained are however not clear. For example; one would expect a direct relationship between the saturated hydraulic conductivity (K_s) and the distribution fraction, however in Schulze (1995) a SiltyLoam soil with K_s of 6.8 mm.h^{-1} has a RESP of 0.45 whereas a SandyClayLoam with K_s of 4.3 mm.h^{-1} has a RESP of 0.50, similarly, a Loam soil and a SandyClayLoam soil were attributed the same RESP value (0.50) although the K_s of the former is triple that of the latter. The heterogeneous horizonation in terms of the textural distribution is the driving force for lateral flow generation in soils and is the basis for assigning “Interflow Potential” values to different soil series. If texture differences are the main reason for differences in RESP values is it not spurious to reduce the RESP value based on the IP? The volume of water draining vertically in a profile is also related to the slope of the land. Steeper slopes generally favour more lateral flow, and less vertical distribution of saturated water. Also, soils with shallow horizons ought to distribute a greater percentage of water in a particular day compared to soils with deep horizons although the texture and hydraulic conductivities are similar.

Another important parameter, not considered a soil input but definitely influenced by the soil, is QFRESP. According to definition QFRESP is: *Stormflow response fraction for the catchment/subcatchment, i.e. the fraction of the total stormflow (1.0) that will run off from the catchment/subcatchment on the same day as the rainfall event* (Smithers et al., 2004). QFRESP is inversely correlated with catchment area and will increase with an increase in slope angle, area covered by impervious material, and rainfall intensity. Soils prone to topsoil crusting as well as very shallow or very wet soils should give high QFRESP values.

There are however no physical based method to obtain QFRESP values and this appropriateness values used rely on calibration.

ACRU can also account for unsaturated flow of water (IUNSAT) and flow through cracks or fissures in swelling soils (ICRACK). The latter is divided into three classes based on the clay content. Both IUNSAT and ICRACK can be excluded from simulations.

5.3.2 Intermediate zone (*ACRU-Int*)

ACRU-Int is a revised version of the standard *ACRU2000* model; in addition to the 2 soil layers (A & B horizons) an intermediate layer (saprolite) between the soil layers and deep groundwater levels was introduced (Lorentz *et al.*, 2007). The intermediate layer has a mechanism whereby lateral release of water can be induced when certain threshold positive pressures at the saprolite/bedrock interface is achieved. The lateral releases from the intermediate zone can be routed to any layer of a downslope land segments. This is ideal for imitating flowpaths at hillslope scale.

5.4 METHODOLOGY

5.4.1 Study area

The Weatherley research catchment is situated on the footslopes of the Drakensberg mountain range in the north-eastern part of the Eastern Cape, 4 km south-west of Maclear. The catchment covers approximately 160 ha. The catchment is one of many small tributaries of the Mooi River. The highest point in the catchment is in the south western corner at 1352 m above mean sea level. Prominent rock shelves are present at approximately 1320 m above mean sea level. The catchment drains to a north-easterly direction. The geology consists of sandstone and mudstone of the Elliot Formation above 1300 m above mean sea level. Below 1300 m above mean sea level, sandstone and mudstone of the Molteno Formation predominates. Two dolerite dykes with a north-south strike exists in the catchment. The catchment has a relative high rainfall with a Mean Annual Precipitation (MAP) of approximately 1000 mm. year⁻¹ (Van Huyssteen *et al.*, 2005). The Mean Annual Apan Evaporation (MAE) is 1488 mm (BEEH, 2003). The winters are cold, with mean minimum temperatures of 4 °C. Frost and snowfall is common, particularly in the higher lying areas. The summers are hot with a mean maximum temperature of 25 °C (Roberts *et al.*, 1996). The land cover consists of Highland Sourveld grasslands with a basal cover of 50-75% on the hillslopes. *Eucalyptus nitens*, *Pinus elliottii* and *Pinus patula* trees were planted on selected areas during 2002. Wetland conditions exist throughout the catchment along the stream with a width of 100 to 400 m. The widest areas of this wetland are associated with seepage lines from contributing hillslopes (Lorentz *et al.*, 2007).

5.4.2 Model configuration

The catchment was divided into 7 land segments with distinct hydrological responses (Figure 150). The division was made derived from several pedological, soil physical, hydrogeological, geophysical and geochemical studies, as well as in-field observations of visible hydrological processes, in the selected catchment over the past few years (Lorentz. 2001; Lorentz *et al.*, 2004; van Huyssteen *et al.*, 2005; Lorentz *et al.*, 2007 and van Tol *et al.*,

2010). Some soil and landscape attributes, obtained from representative soil profiles, of the land segments are presented in Table 36 and Table 37. Two hillslopes, with diverse hydrological behaviour were identified based on the properties of the land segments, their sequence from the crest to the river, and the area covered by the individual segments. Conceptual 2-dimensional flow models were then developed and applied to construct flow routings for the two hillslopes (Le Roux *et al.*, 2011). Hillslope 1 includes land segments 1-4, and hillslope 2 includes land segments 5-7. Land segments 4 and 7 represent the valley bottom or wetland area; they drain to a separate land segment (9) which represents the stream network. Since the deep groundwater levels are always below the stream channel and does not contribute to low flows, all the drainage out of the intermediate zone into the groundwater layer were routed to another land segment (8). Land segment 8 is therefore not linked to any streamflow generation process. The routing between land segments is presented in Figure 149.

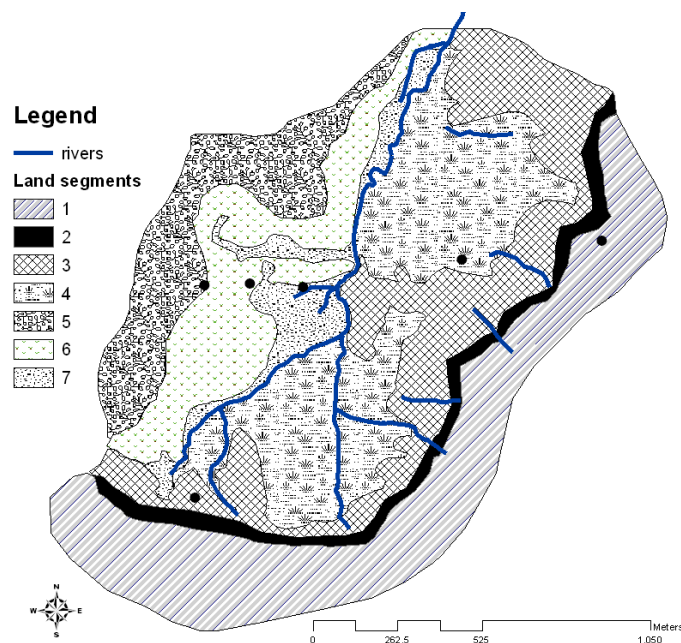


Figure 149 Different land segments with their representing soil profiles in the Weatherley catchment

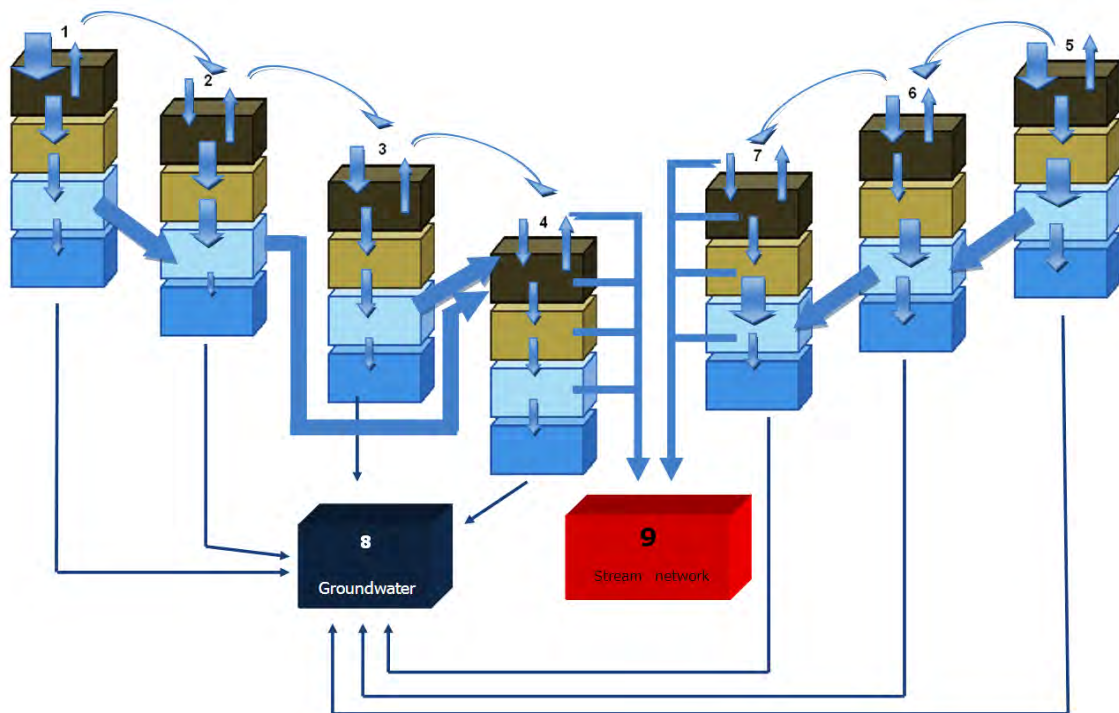


Figure 150 Flow routing for the simulation, magnitude of arrows give indication of dominant flow direction in various land segments

5.4.3 Model parameterization

Imitating the dominant hydrological processes was one of the major aims of this simulation exercise. According to Sivapalan (2003b), parameters without measured values require calibration with gauged data in order to reflect reality. This leads to uncertainty in predictions when moving into ungauged basins. Parameter values, not directly available from the profile description, were therefore physically estimated based on the definition of the parameter and the (limited) understanding of the process influenced by the parameter. These calculations include:

- **ABRESP, BFRESP and INTRESP** The difference between K_s of the top and lower horizon gives an indication of the vertical distribution from the former to the latter. K_s values were calculated using ROSSETA light for all the horizons of profiles representing the different land segments using texture class distributions and bulk densities (D_b). Dividing the K_s of the lower horizon with the K_s of the top horizon is then the particular RESP value. K_s of the R-horizon were measured by Van der Merwe, 2011. Representative texture class, D_b and estimated K_s values are presented in Table 36 and resulting ABRESP, BFRESP and INTRESP values in Table 37.
- **QFRESP** Except for the Molteno outcrop, very few areas in the catchment is marked by impervious top layers. Soil crusting and very shallow soils are also not the norm. The only soil related factor influencing the quick flow response is therefore the water content of the topsoil before and during rain events, where saturated A horizons will impede infiltration, generating overland flow and consequently peak flow. Zere (2007) calculated daily soil water contents over a 6 year period for 28 profiles in the

Weatherley catchment derived from neutron probe measurements. This was used to determine the fraction of the time that A horizons of the representative profiles were close to saturation (>0.7 of P_o) on days with more than 1 mm of rain, 662 days in the 6 year period. The number of days where the A horizon was close to saturation is presented in Table 36 and resulting QFRESP values in Table 37. Approximately half of land segment 2 is covered by the impervious Molteno rock outcrop and was taken into account for calculation of QFRESP.

Table 36 Some attributes of different land segments used in to calculate model parameters

| LandSeg | Representing profiles | Horizon | Sand (%) | Silt (%) | Clay (%) | Texture class | BD | Ks (cm.day ⁻¹) | s $>0.7^*$ |
|---------|-----------------------|---------|----------|----------|----------|-----------------|------|----------------------------|------------|
| 1 | 202 | A | 79.1 | 10.9 | 10.0 | Sandy Loam | 1.68 | 46.00 | 1 |
| | | B | 71.4 | 12.6 | 16.0 | Sandy Loam | 1.61 | 27.00 | |
| | | INT | 57.3 | 16.7 | 26.0 | Sandy Clay Loam | 1.72 | 6.00 | |
| | | R | | | | | | 0.10 | |
| 2 | 204 | A | 78.0 | 10.0 | 12.0 | Sandy Loam | 1.60 | 52.48 | 278 |
| | | B | 78.0 | 12.0 | 10.0 | Sandy Loam | 1.71 | 36.61 | |
| | | INT | 75.0 | 13.4 | 11.6 | Sandy Loam | 1.71 | 26.87 | |
| | | R | | | | | | 0.02 | |
| 3 | 212&205 | A | 74.0 | 16.0 | 10.0 | Sandy Loam | 1.59 | 45.84 | 62 |
| | | B | 70.0 | 15.0 | 15.0 | Sandy Loam | 1.68 | 19.25 | |
| | | INT | 50.0 | 32.0 | 18.0 | Loam | 1.74 | 5.87 | |
| | | R | | | | | | 0.20 | |
| 4 | 206 | A | 50.0 | 40.0 | 10.0 | Loam | 1.52 | 22.37 | 622 |
| | | B | 46.3 | 37.8 | 15.9 | Loam | 1.67 | 7.79 | |
| | | INT | 35.1 | 26.9 | 38.0 | Clay Loam | 1.73 | 2.09 | |
| | | R | | | | | | 0.20 | |
| 5 | 210 | A | 56.0 | 28.4 | 15.7 | Sandy Loam | 1.59 | 15.36 | 99 |
| | | B | 56.4 | 23.9 | 19.7 | Sandy Loam | 1.71 | 7.60 | |
| | | INT | 56.2 | 23.5 | 20.3 | Sandy Clay Loam | 1.66 | 9.18 | |
| | | R | | | | | | 2.00 | |
| 6 | 209 | A | 50.4 | 33.9 | 15.7 | Loam | 1.54 | 14.75 | 437 |
| | | B | 37.7 | 35.0 | 27.3 | Loam | 1.67 | 3.11 | |
| | | INT | 5.0 | 50.8 | 44.2 | Silty Clay | 1.73 | 1.27 | |
| | | R | | | | | | 0.20 | |
| 7 | 208 | A | 45.8 | 39.8 | 14.5 | Loam | 1.47 | 17.04 | 541 |
| | | B | 35.9 | 43.2 | 21.0 | Loam | 1.62 | 5.12 | |
| | | INT | 31.2 | 42.9 | 26.0 | Loam | 1.71 | 2.58 | |
| | | R | | | | | | 0.20 | |

* Number of days with rainfall > 1 mm where A horizon is saturated >0.7 of P_o

The thickness of A and B horizons were obtained from Van Huysteen *et al.*, 2005 for the profiles representing the different land segments. Where the lower depth of the profile was reached the depth of the B2 or C horizon was used as the depth of the intermediate zone, if not, an extra 0.5 m was added to the B2 or C horizon to acquire the intermediate zone depth. PWP, DUL and P_o values were estimated based on typical texture class values proposed in Smithers *et al.*, 2004.

Table 37 Soil parameters used simulating the Weatherley catchment

| LandSeg | Area (km ²) | Horizon | Depth (m) | Po | PWP | DUL | ABresp | BFresp | INTZRESP | QFRESP |
|---------|-------------------------|---------|-----------|------|------|------|--------|--------|----------|--------|
| 1 | 0.315 | A | 0.4 | 0.37 | 0.09 | 0.19 | 0.6 | 0.2 | 0.02 | 0.002 |
| | | B | 0.42 | 0.39 | 0.09 | 0.19 | | | | |
| | | INT | 1.6 | 0.35 | 0.16 | 0.25 | | | | |
| 2 | 0.072 | A | 0.1 | 0.40 | 0.09 | 0.19 | 0.7 | 0.7 | 0.00 | 0.92 |
| | | B | 0.3 | 0.36 | 0.09 | 0.19 | | | | |
| | | INT | 1.2 | 0.35 | 0.09 | 0.19 | | | | |
| 3 | 0.270 | A | 0.3 | 0.40 | 0.09 | 0.19 | 0.4 | 0.3 | 0.03 | 0.1 |
| | | B | 1 | 0.37 | 0.09 | 0.19 | | | | |
| | | INT | 1 | 0.35 | 0.13 | 0.25 | | | | |
| 4 | 0.375 | A | 0.5 | 0.43 | 0.13 | 0.25 | 0.3 | 0.3 | 0.10 | 0.94 |
| | | B | 0.25 | 0.37 | 0.13 | 0.25 | | | | |
| | | INT | 0.25 | 0.35 | 0.20 | 0.31 | | | | |
| 5 | 0.183 | A | 0.16 | 0.40 | 0.09 | 0.19 | 0.5 | 1.0 | 0.22 | 0.15 |
| | | B | 0.9 | 0.36 | 0.09 | 0.19 | | | | |
| | | INT | 0.8 | 0.37 | 0.16 | 0.25 | | | | |
| 6 | 0.225 | A | 0.45 | 0.42 | 0.13 | 0.25 | 0.2 | 1.0 | 0.16 | 0.66 |
| | | B | 0.6 | 0.37 | 0.13 | 0.25 | | | | |
| | | INT | 0.7 | 0.35 | 0.25 | 0.32 | | | | |
| 7 | 0.091 | A | 0.35 | 0.45 | 0.13 | 0.25 | 0.3 | 1.0 | 0.08 | 0.82 |
| | | B | 0.2 | 0.39 | 0.13 | 0.25 | | | | |
| | | INT | 1.1 | 0.36 | 0.13 | 0.25 | | | | |

5.4.4 Simulation period, climatic inputs and comparison data

The simulation period is from 1st Jan 1998 till 31st August 2001. Simulated results are reported for two rainy seasons start from the 1st of September 1999 to allow the model to 'settle' and incorrect data regarding initial water contents to even out. Trees were planted in 2002 and 31st August 2001 was selected as the end of simulation to avoid dissimilarity between vegetative cover.

Rainfall and, when possible, minimum and maximum temperature data were obtained from the BEEH (2003) database. Other climatic data were obtained from the quaternary catchment database.

Streamflow was measured at a crumped weir at the catchment outlet and data regarding the streamflow obtained from BEEH (2003) database. Daily simulated soil water contents were compared to daily water contents calculated from weekly neutron water meter readings (Zere, 2005). Soil water contents are expressed as a percentage of porosity (Po).

5.5 RESULTS

5.5.1 Streamflow

Simulated vs. measured streamflow comparisons are presented in Figure 151 to Figure 157. Discussions of the results follow in section 5.5.

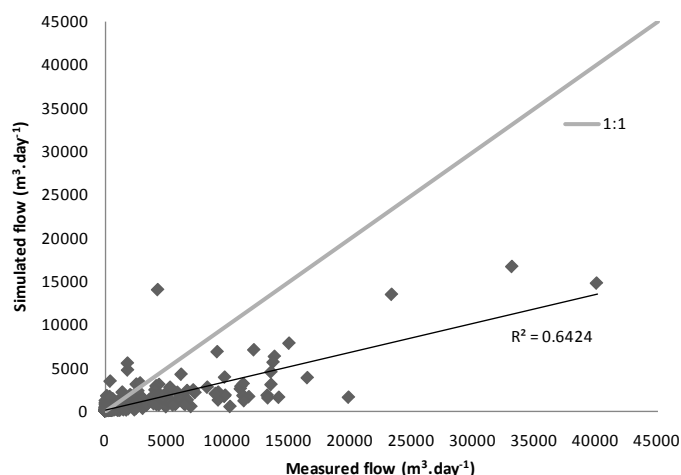


Figure 151 Simulated vs. measured flow during the selected simulation period

Simulated and measured outflow from catchment is presented in Figure 151 for the simulation period. A R^2 value of 0.64 was attained with a linear line deviating of almost 100% from the 1:1 line. The divergence in the direction of measured flow, i.e. a greater volume of flow is measured than simulated. Figure 152 and Figure 153 accentuates the cause of the deviation from the 1:1 line.

Figure 152 illustrates daily measured flow compared to simulated flow and also the influence of rainfall on flow volumes. It is clear from Figure 152 that flows are overestimated during especially towards the end of the rainy seasons. Simulated low flows compared well with measured flows. Rain during the beginning of the season's results in much smaller volumes of stream runoff compared to similar size storms just before the end of the rainy season. This is over estimation of high flows and good representation of low flows is also emphasized in Figure 153 where comparisons are plotted on a log scale.

Figure 153 shows high flows being overestimated with an order of magnitude in under some conditions. Low flows and streamflow recession are however simulated reasonable well in drier periods. The average daily difference between simulated and measured results over the simulation period is $854 \text{ m}^3 \text{ day}^{-1}$. This increase to $1194 \text{ m}^3 \text{ day}^{-1}$ during the rainfall months (October till April) and decrease to $114 \text{ m}^3 \text{ day}^{-1}$ for months normally associated with little or no rainfall. For periods ten days after any recorded rainfall, the difference between simulated and measured streamflows is $16 \text{ m}^3 \text{ day}^{-1}$.

A wet (19th December 1999 till 14th of January 2000) and dry (27th May till 31st August 2001) period was selected to show typical measured and simulated responses from the catchment for distinct environmental conditions (Figure 154 & Figure 155).

During the wet period in Figure 154 every streamflow from every rain event is overestimated. Greater oversimulation occurs when rain persist for a number of days, for example 10 to 16 January 2000. Rainfall and measured streamflow decrease towards the end of the selected period, narrowing the gap between simulated and observed streamflow. The average daily difference between measured and simulated streamflow was $3608 \text{ m}^3 \text{ day}^{-1}$ for the selected period.

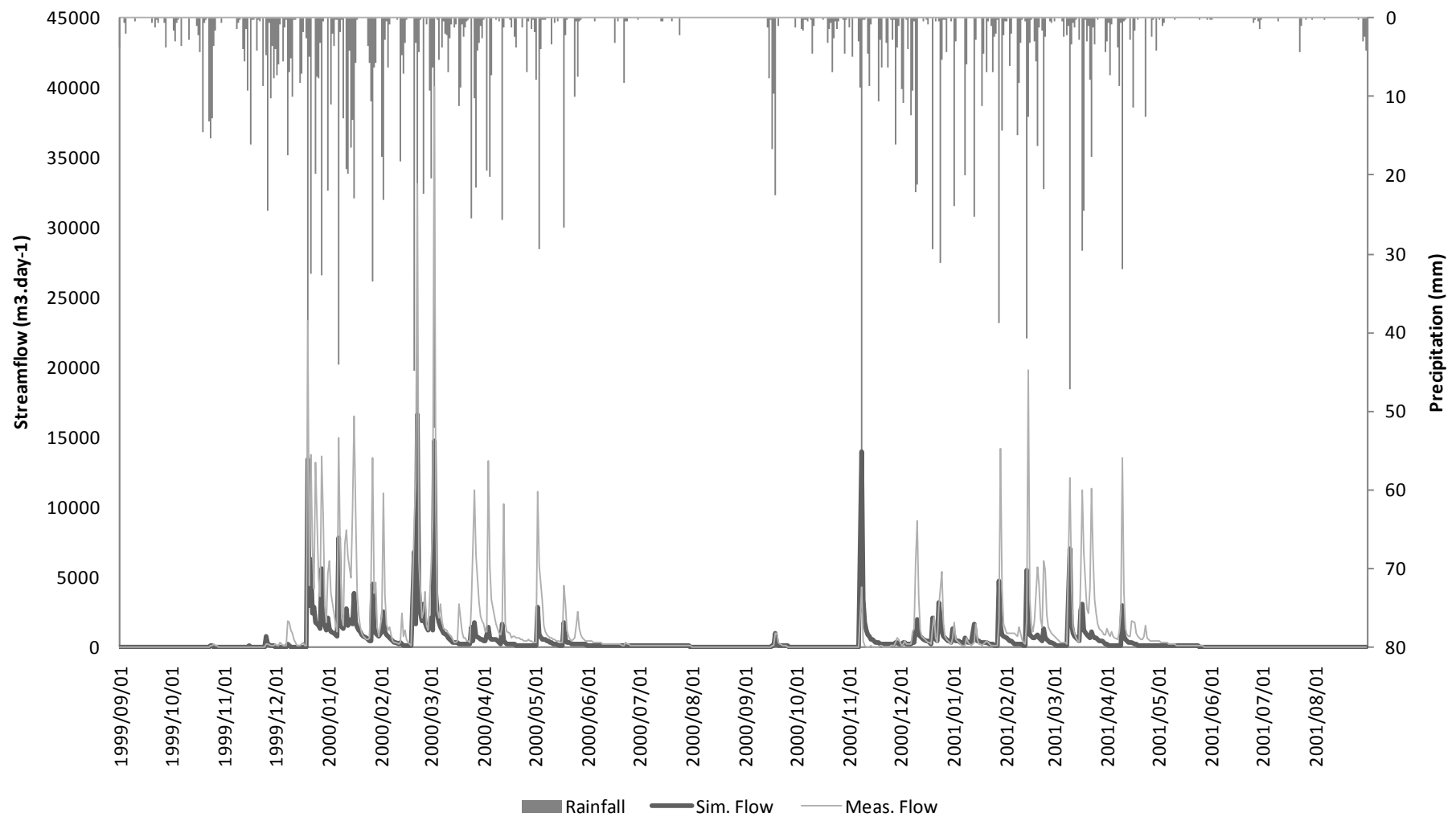


Figure 152 Simulated vs. measured daily streamflow flow plotted against daily rainfall for the simulation period

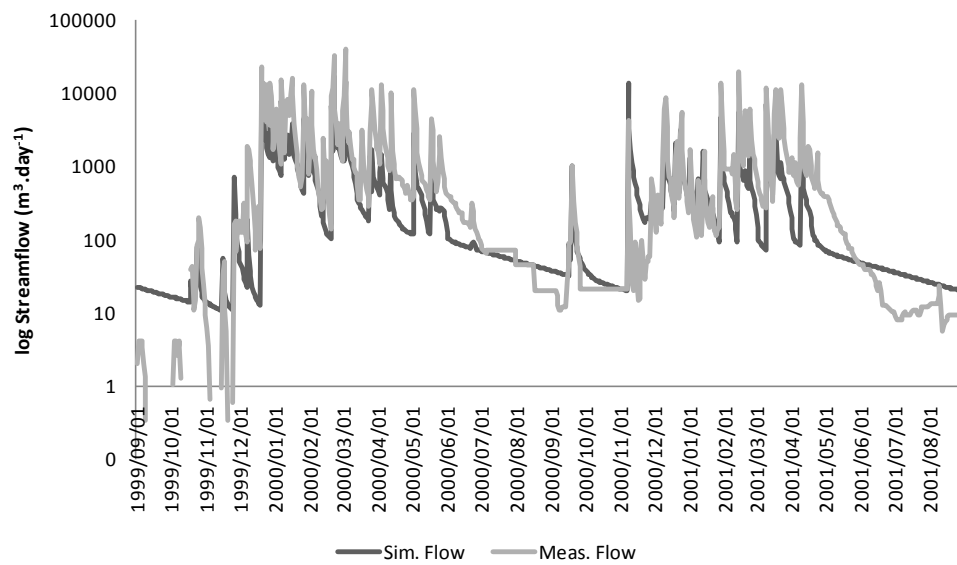


Figure 153 Log of simulated vs. measured flow over selected simulation period

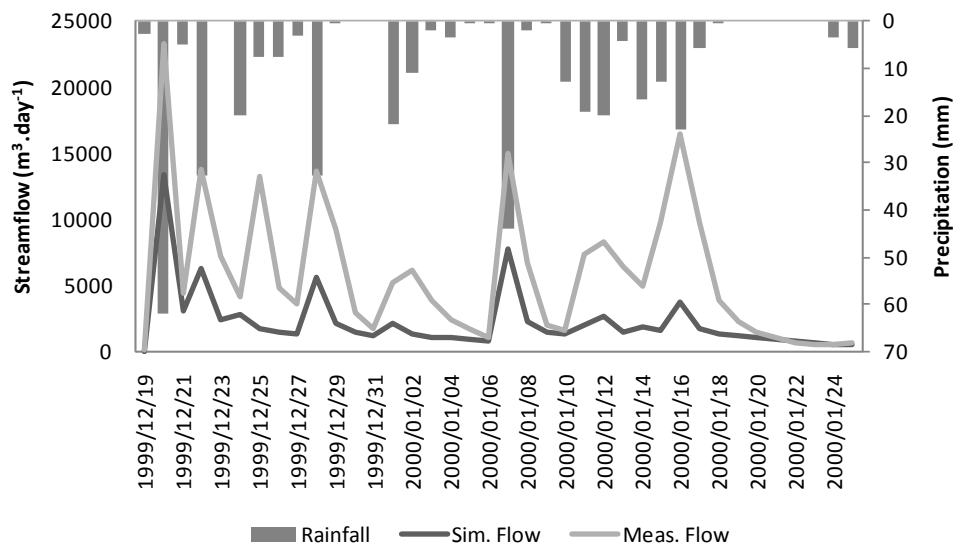


Figure 154 Simulated vs. measured streamflows during a wet period

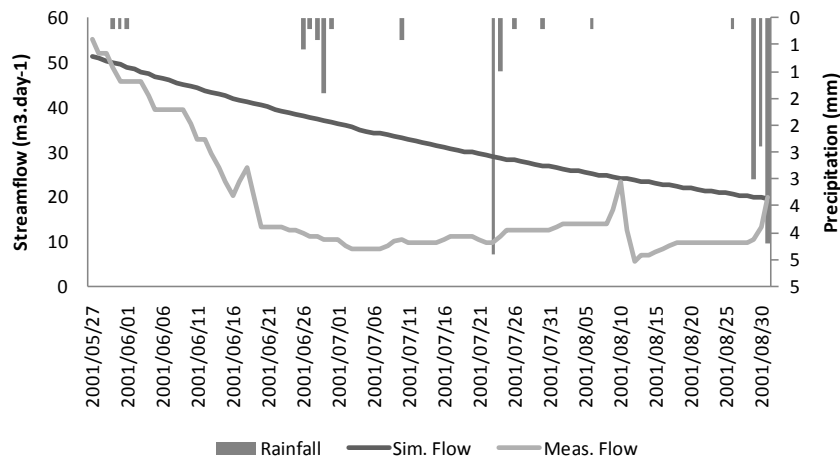


Figure 155 Simulated vs. measured streamflows during a dry period

Figure 155 shows typical flow simulations during dry periods. The differences in the scales of the Y-axis compared to Figure 154 are important to note. During the selected period the average daily difference between simulated and measured streamflow was $15 \text{ m}^3 \text{ day}^{-1}$. Very subtle response to the relatively small rain events can be noted in measured streamflow, these responses were however absent in the simulated streamflows.

Both land segment 4 and 7 drains into the stream network (Figure 149). The relative contribution of the different land segments are presented in Figure 156 & Figure 157. These contributions were weighted against the respective areas of the land segments.

Cumulative flows indicate that land segment 7 contribute more than land segment 4 during high rainfall periods. Contributions from the former stops during dry seasons, whereas land segment 4 contributes throughout the simulation period although less during drier times (Figure 157).

Figure 156 illustrates that the contribution from land segment 7 to streamflow higher than that of land segment 4. Closer inspection show that this greater contribution from land segment 7 only occurs during relatively large flow events. This is stressed when comparing the total cumulative flows from the respective land segments during the simulation period (Figure 157).

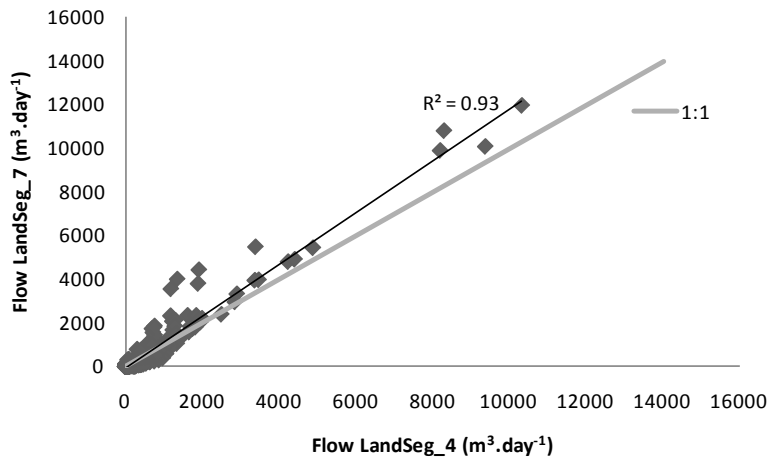


Figure 156 Comparison between the contribution of land segments 4 & 7 to total streamflow

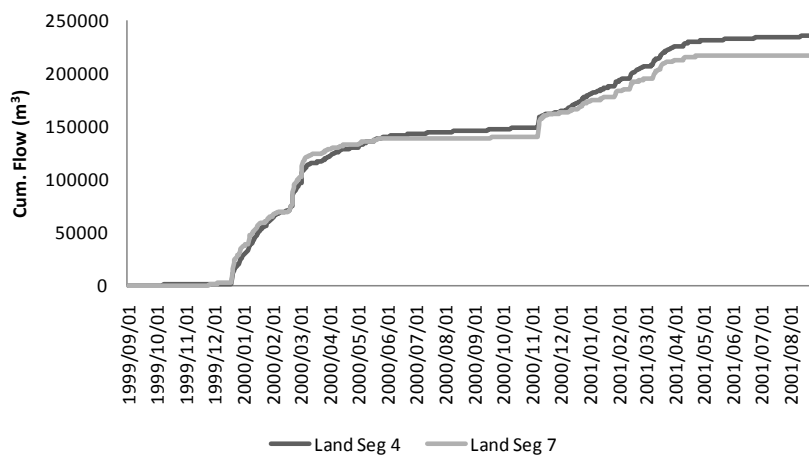


Figure 157 Cumulative flows from land segments 4 & 7 during simulation period

5.5.2 Soil water contents

Comparisons between simulated and measured soil water contents of the different land segments are presented in Figure 158 to Figure 164. Discussions regarding the results follow in section 5.5. The Figures are divided into four segments starting with daily rainfall data at the top then simulated vs. measured water contents of the A and B horizon and then simulated vs. measured water contents of the intermediate zone or C-horizon at the bottom. The water contents are expressed as a fraction of the porosity for the different horizons.

Water contents of the C-horizon are greater than 1, i.e. more than P_o in land segments 2, 3, 4 and 6, which is not physically possible. Therefore, instead of comparing actual differences between simulated and measured water contents of the C-horizon, it was decided to rather focus on the comparison of trends in the wetting and drying of the horizon.

Land segment 1

Figure 158 shows a very good correlation between measured and simulated water contents of the A horizon. Measured water contents for this horizon is slightly higher for most of the simulation period but drains quicker than simulated at the end of the rain season.

Measured water contents are higher than those simulated for the B horizon (Figure 158). Seasonal variation is evident in the simulated water contents but not as profound in the measured values. Sharp increases and decreases are noted in measured values, but not in simulated water contents.

Measured and simulated water contents of the C-horizon compared well, although the measured contents show less seasonal variation than those simulated (Figure 158). The response of this horizon to rainfall at the beginning of the simulation period shows a lag time of about 2 months.

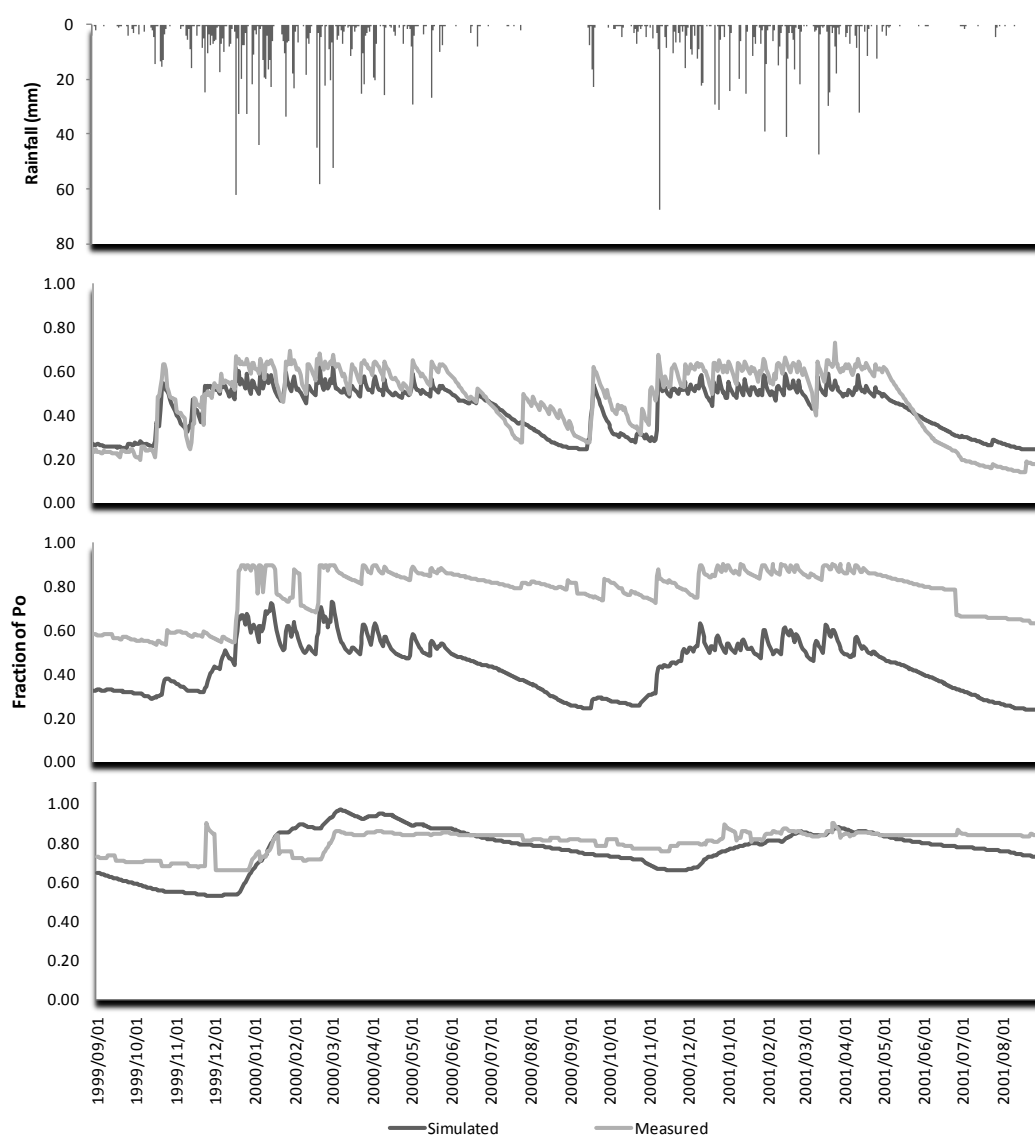


Figure 158 Rainfall and simulated vs. measured water contents of A, B and C-horizons of land segment 1, represented by P202, a Pinedene soil

Land segment 2

Measured water contents are almost always higher than simulated water contents (Figure 159). This is especially true during the middle of the rainfall period where the measured water contents seem to reach field saturation (a value less than P_o which cannot be exceeded under natural conditions).

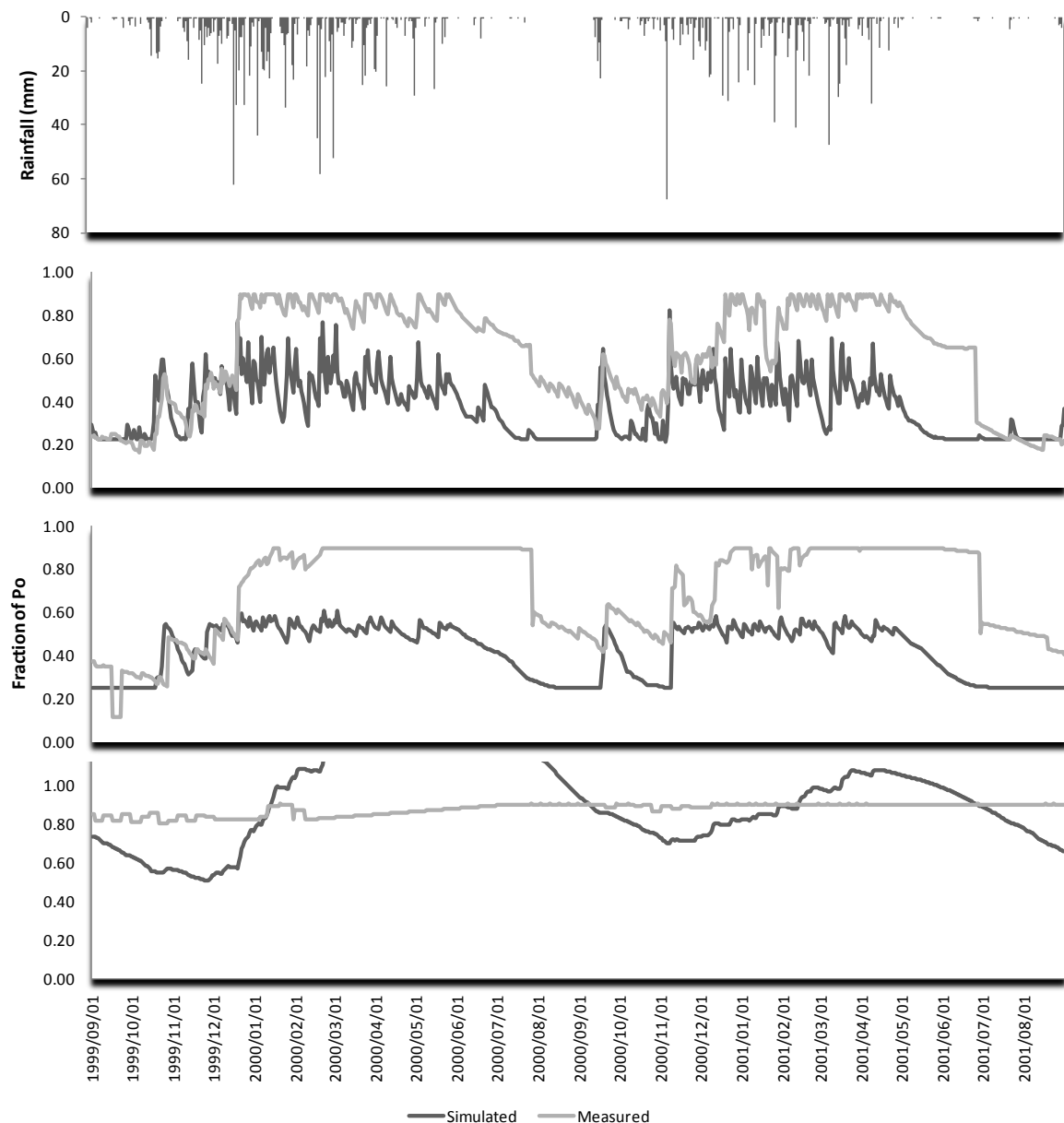


Figure 159 Rainfall and simulated vs. measured water contents of A, B and C-horizons of land segment 2, represented by P204, a Longlands soil

As with the A horizon, measured water contents of the B horizon are continuously higher than simulated water contents (Figure 159). From February till July of both years this horizon seems to be filled up to field saturation. This state is reached approximately 4

months after commence of the rain season. There is a sharp decrease in the water contents at the end of this saturated state in both seasons.

There is no correlation between the simulated and the measured water contents of the C-horizon (Figure 159). Simulated water contents show a definite seasonal fluctuation, whereas the measured results remain fairly constant throughout the simulation period. Interesting to note is the similar trend in measured water contents of the B horizon and those of the C-horizon, especially during the first simulation year, where the C-horizon is above P_o when the B horizon reached a constant water level.

Land segment 3

Simulated results of both the A and the B horizon do not dry out below approximately 0.5 of porosity right through the simulation period (Figure 160). Measured values are comparable with simulated values for the A horizon but slightly less so for the B horizon. A sharper drying gradient was measured for the A horizon, compared to the B horizon.

Simulated water contents for the C-horizon shows similar seasonal trends as the measured water contents, although slightly more exaggerated. Apart from periodic responses in the beginning of the simulation period the measured water contents indicate that this horizon responds approximately 3 months after the start of the rainy season (Figure 160).

The measured water content of this profile is significantly lower than measured water contents of profiles representing the other profiles. Not one of the horizons exceed a fraction of 0.8 of P_o and the average measured water contents are 0.46, 0.44 and 0.51 for the A, B and C-horizon respectively. The second driest profile represents land segment 5 with average water contents of 0.54 for the A, 0.70 for the B and 0.73 for the C-horizon, emphasising the 'dry state' of land segment 3.

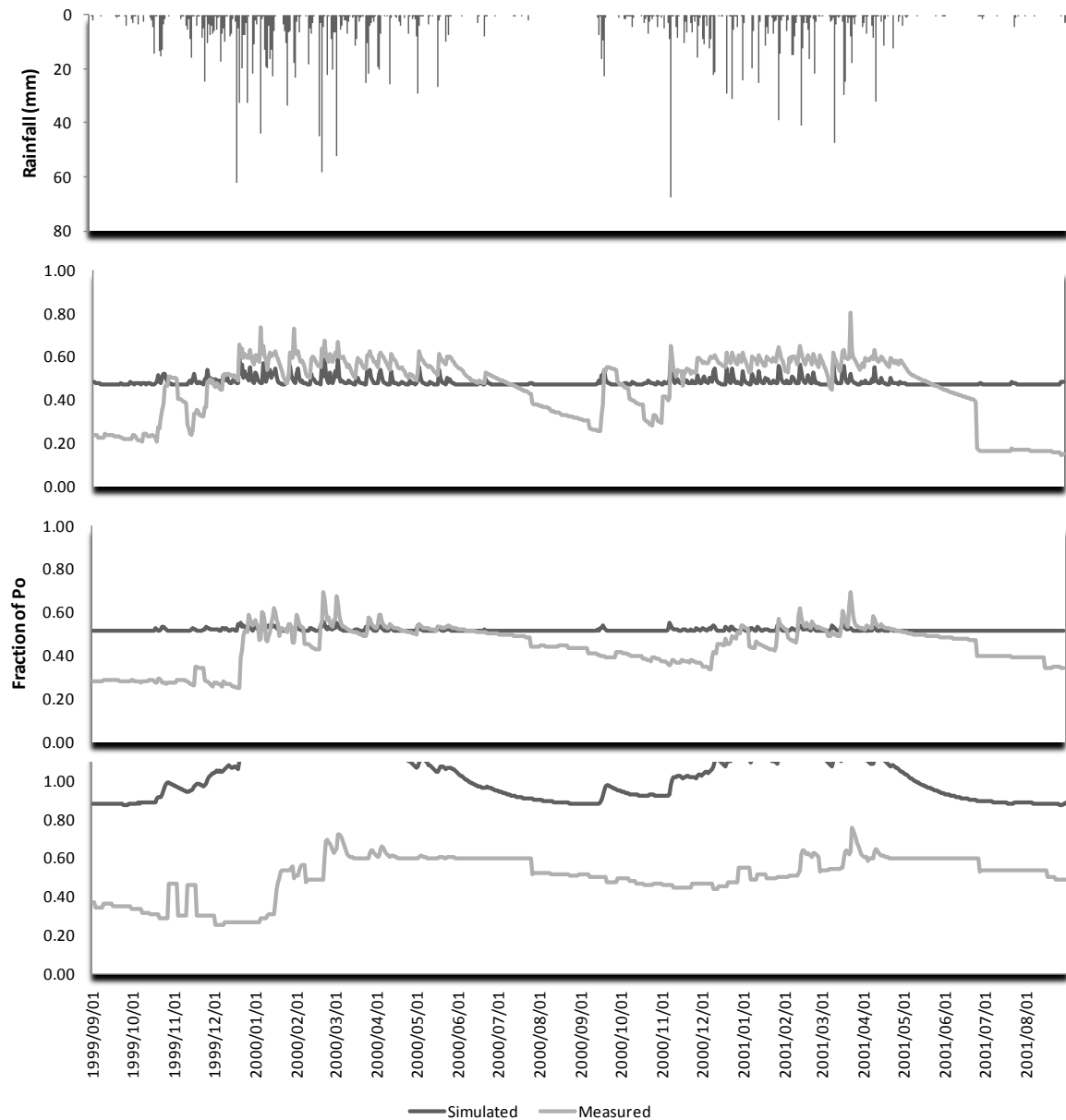


Figure 160 Rainfall and simulated vs. measured water contents of A, B and C-horizons of land segment 3, represented by P212, a Tukulu soil

Land segment 4

As with land segment 2 measured water contents of the A horizon reached field saturation during the rainy season (Figure 161). Simulated results followed the measured trends closely but did not reach the degree of saturation as the measured water contents. The measured water contents remained at a constant, near saturated, level even during the dry winter months raising questions on the accuracy of the measurements of this horizon.

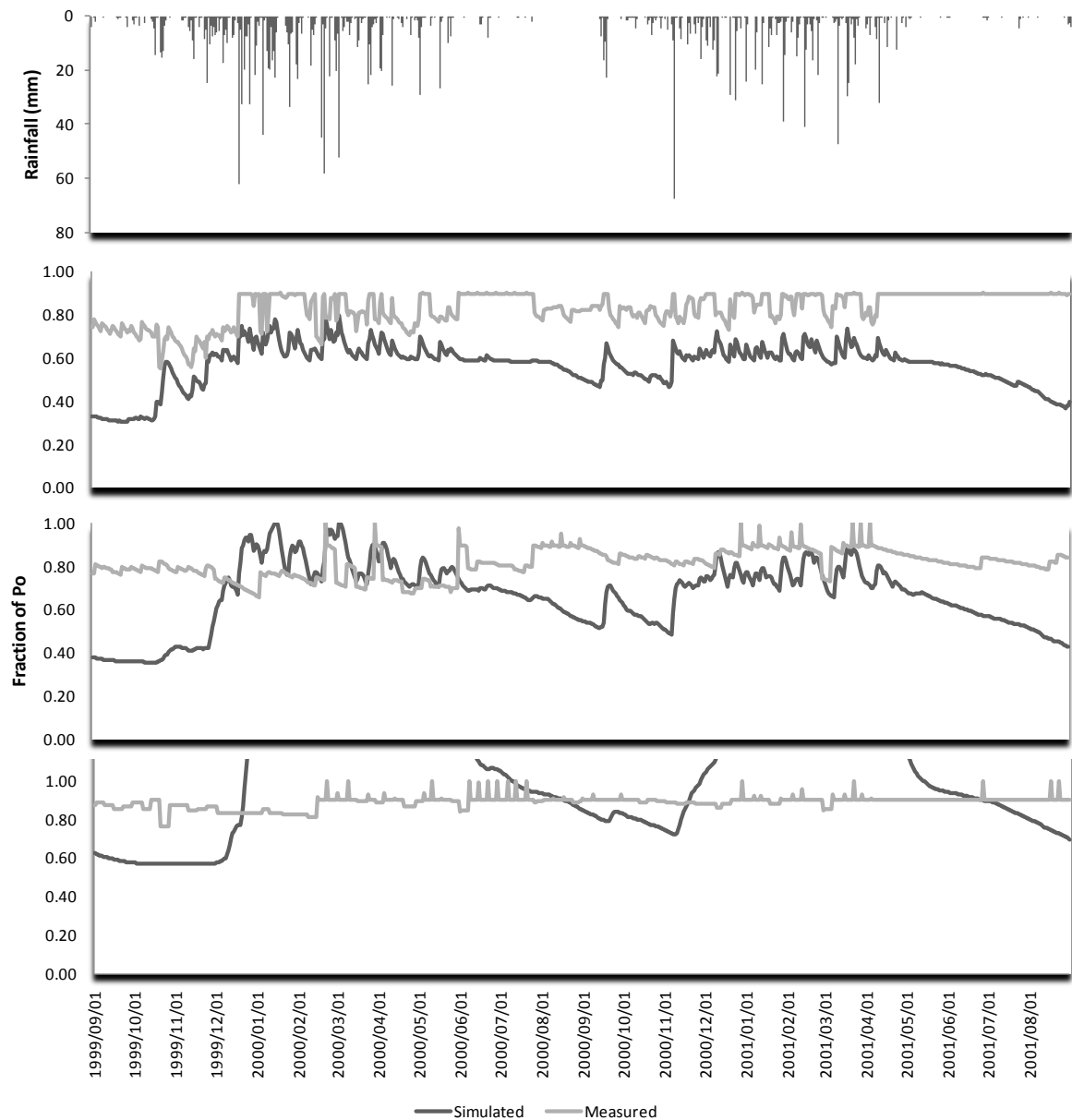


Figure 161 Rainfall and simulated vs. measured water contents of A, B and C-horizons of land segment 4, represented by P206, a Kroonstad soil

The B horizon also followed the wetting and drying trends closely, particularly in year one, this horizon failed however to remain as saturated as what measurements indicate it should be (Figure 161). There is no definite drying out phase in the measured results whereas the simulated results show a wet rainy season and relatively dry winter period. The C-horizon of this profile remains close to saturation all the way through the simulation period as indicated by measured soil water contents (Figure 161). Simulated results show a seasonal fluctuation with the water reaching this horizon approximately two months after the start of the rainy season in year one and 45 days after the start of the rain in year two.

Land segment 5

Simulated water contents of the A horizon mimic the measured water contents to a great extent (Figure 162). A greater extent of drainage at the end of the rainy season is however witnessed in measured compared to simulated results.

Simulated water contents of the B horizon correlates well with measured values in the beginning of the rainy season (Figure 162). Measured water contents are however higher at the end of the rainy season and does not dry out as quick as estimated. There is only slight fluctuation in both the simulated and measured water contents of the C-horizon (Figure 162).

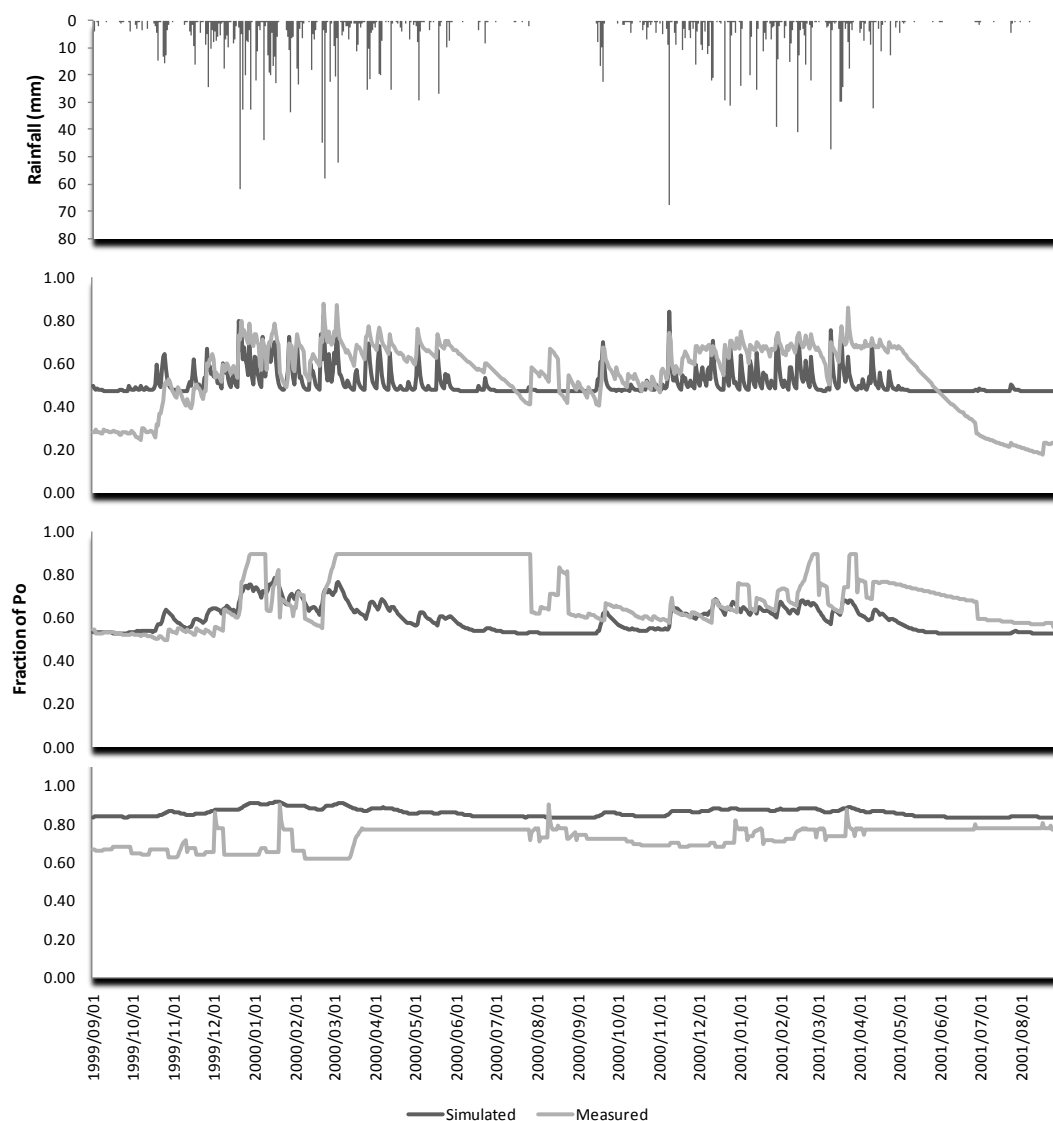


Figure 162 Rainfall and simulated vs. measured water contents of A, B and C-horizons of land segment 5, represented by P210, a Bloemdal soil

Figure 163 Land segment 6

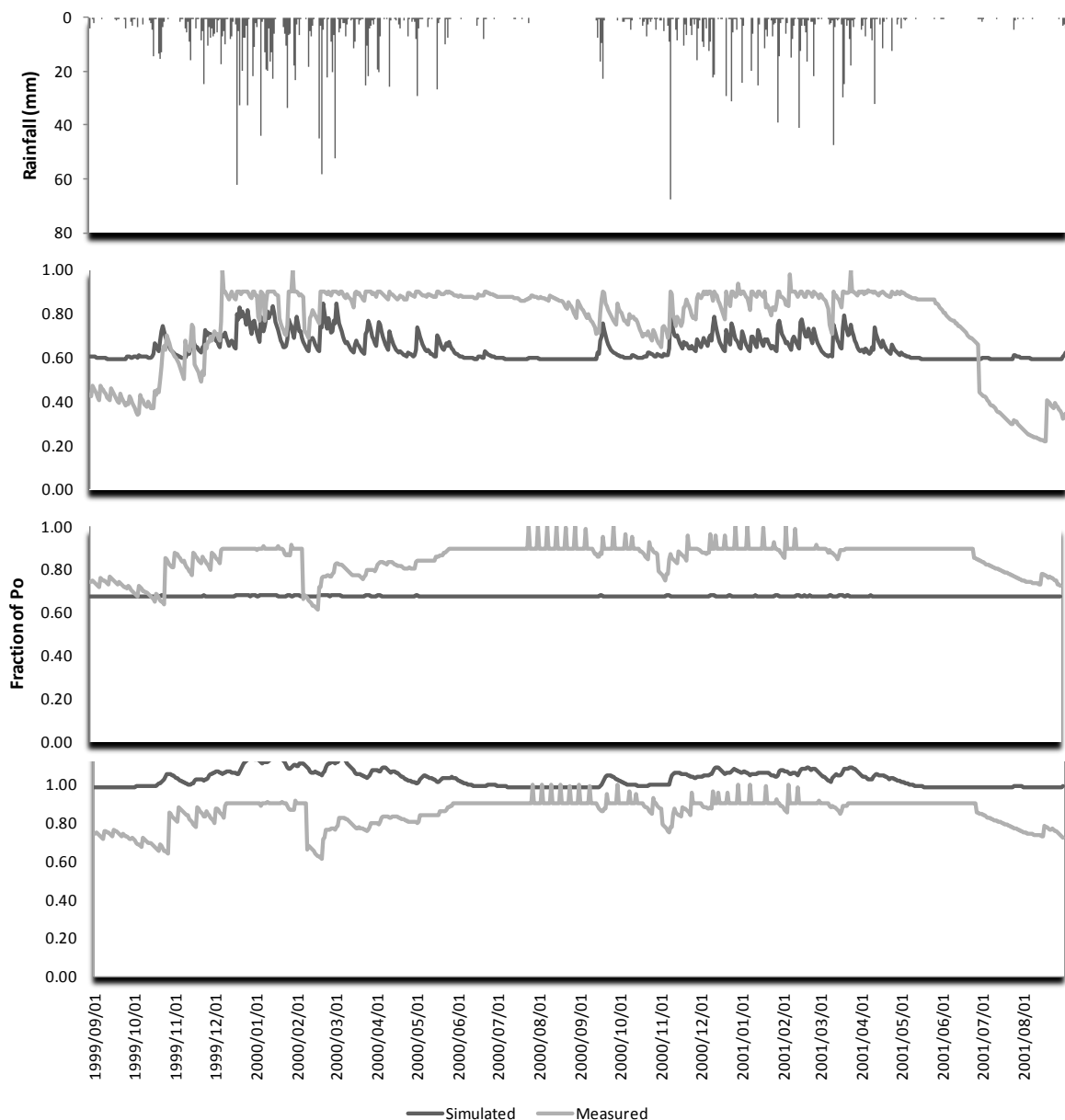


Figure 163 Rainfall and simulated vs. measured water contents of A, B and C-horizons of land segment 6, represented by P209, a Katspruit soil

Measured water contents of the A horizon are only lower than simulated water contents at the start and the end of the simulation period (Figure 163). Fluctuations in the water content due to rainfall are followed by the simulations.

Although measured B horizon water contents are fairly constant, there is almost no variation in the simulated water content of this horizon and it remains constant at 0.68. A number of 'spikes' in the water content were measured from July 2000 to March 2001 (Figure 163). Since there were only two neutron probe measuring depths for P209, the measured values were also used for comparisons with simulated water contents of the C-horizon. The latter show a small degree of seasonal fluctuation, but remains close to saturation throughout the simulation period.

Land segment 7

The simulated water contents follow the same trends in wetting and drying as the measured water contents in the A horizon (Figure 164). There is however a gap of approximately 0.2 of P_o between the measured and simulated values with the measured values being having higher water contents than simulated ones. Simulated values show a more gradual decrease in water content at the end of the rainy season compared to measured water contents.

Measured water contents of the B horizon show similar trends as the A horizon, although this horizon remains closer to saturation for longer periods after the end of the rain season (Figure 164). Again the simulated values follow the wetting and drying trend of the measured values but the water contents simulated are incessantly lower than the measured ones. Based on measured water contents, the C-horizon remain close to saturation for the duration of the simulation (Figure 164). Simulated values show a seasonal fluctuation with a lag time before response of approximately two months.

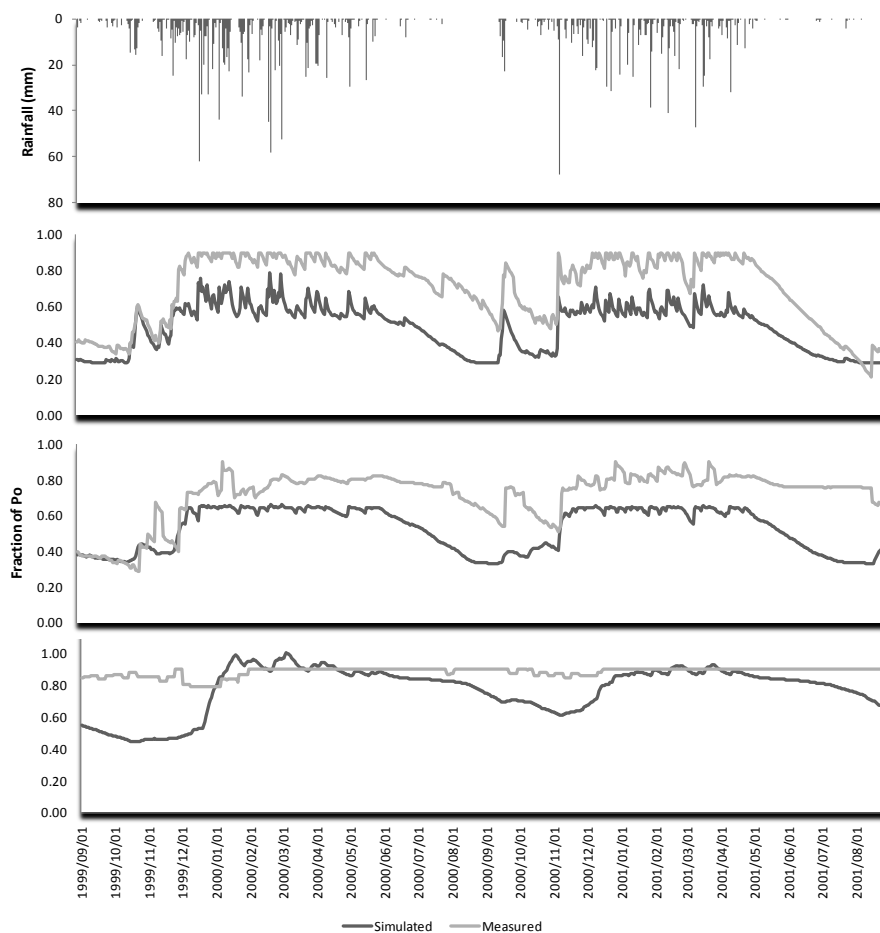


Figure 164 Rainfall and simulated vs. measured water contents of A, B and C-horizons of land segment 7, represented by P208, a Kroonstad soil

5.5.3 Lateral flow from INT zone

Lateral flows simulated with *ACRU-Int* for different land segments during the simulation period are presented in Figure 165. Lateral outflows are presented as mm day^{-1} . Note the difference in the LATFLOW Y-axis between the graphs.

Very little lateral flow is generated in land segment 1 (Figure 165). Lateral flow on this land segment starts in the middle of January in both simulation seasons. Lateral flow from land segment 2 is by far more dominant than later flows generated from any other land segment. In segment 2 lateral flows is generated in the middle of December 1999, correlates with rainfall and gradually decrease in the dry season, before it's prevailing again (middle of November 2000) and continues until the beginning of August 2001.

The volume of lateral flows generated from land segments 3 and 4 are almost similar although more lateral flow is produced by segment 3 (Figure 165). Lateral flows in these land segments are generated concurrent with the start of significant rain.

Lateral flow from land segment 5 commences in the middle of January, and responds only to major rain events throughout the simulation period. Whereas lateral flow from land segment 6 responds in a similar manner as land segment 3 and 4, with almost similar volumes generated as well.

Lateral flow from land segment 7 starts in the beginning of January for first season and middle of December for second simulation season (Figure 165). It follows similar tendencies as land segment 5 although the amplitude is twice that of the latter.

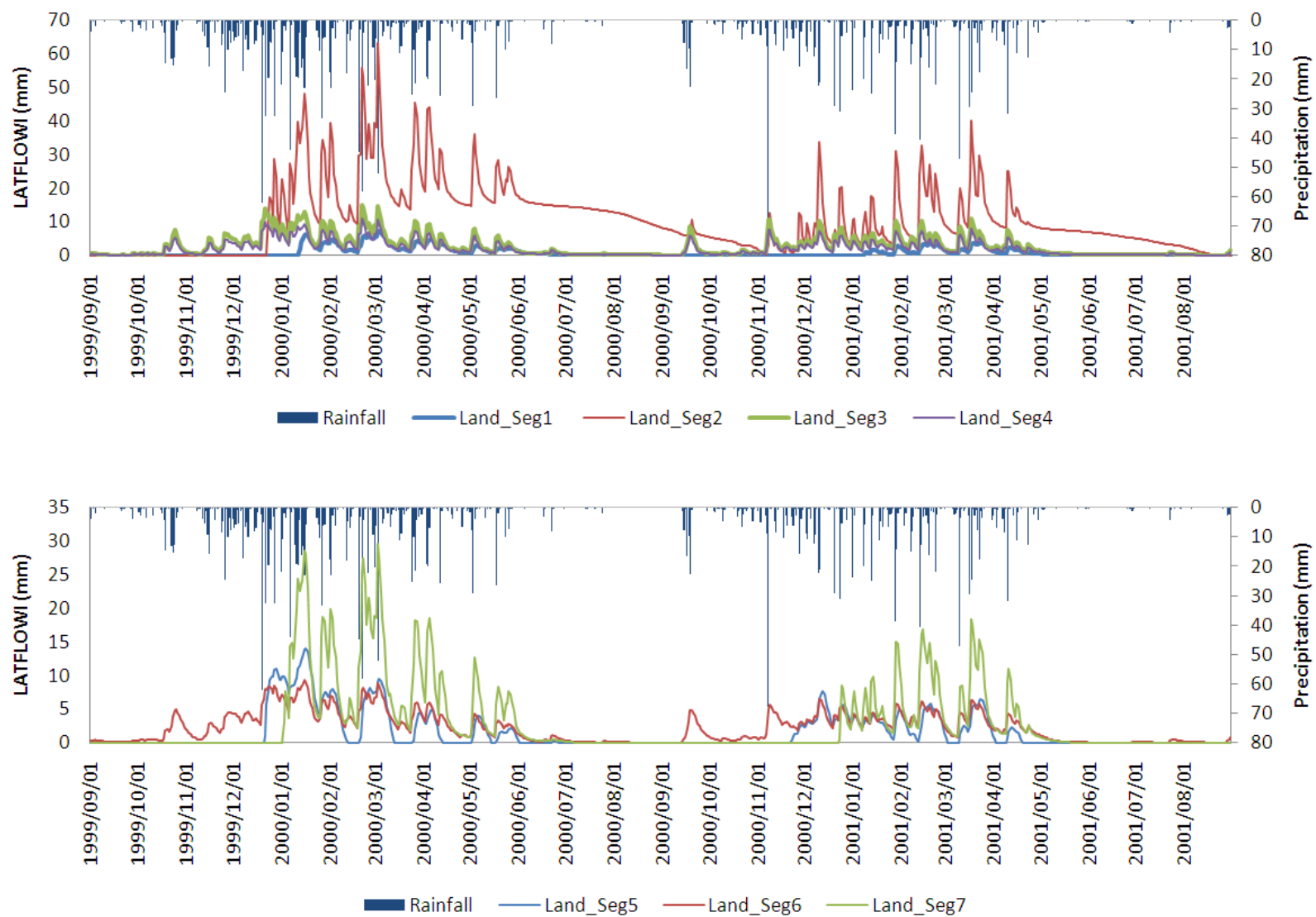


Figure 165 Rainfall and simulated lateral flows ($\text{mm} \cdot \text{day}^{-1}$) for land segment 1-4 (top) and 5-7 (bottom)

5.6 DISCUSSION

In this section simulated results and their accuracy will be discussed. Explanations for deviations from measurements will be offered and adjustments to the parameterization, configuration and possibly model structure will be proposed. However, the inadequate familiarity of the 'experimentalist' with hydrological modelling should be considered whilst reading this section. Since streamflow is strongly related to the soil moisture content as well as the volume of lateral flow, this section will discuss these previously separated sections as one.

The R^2 of 0.64 for the simulated streamflow was disappointingly low (Figure 157) considering a lumped (the catchment is one land segment) simulation by Lorentz and Freese (2009) obtained a R^2 of 0.67. This low R^2 can solely be attributed to the inability of the current model parameterization and configuration to simulate high flows. For the lumped simulation of Lorentz *et al.* (2009) an ABRESP of 0.2 for all the topsoils in the catchment were assigned, resulting in the build-up of water in the A horizon and possibly a greater volume of event water in the stream during rain events. The QFRESP value used is however not clear.

Underestimation of quick flows can be attributed to low QFRESP values. The method proposed to calculate QFRESP award high values for the wetland regions, i.e. land segment 4 and 7. Van Tol (2010) showed that approximately 92% of the precipitation on the wetland will arrive at the catchment outlet on the same day. It was therefore surprising that QFRESP values of 0.92 and 0.82 for land segments 4 and 7 respectively were insufficient to generate comparable peak flows (Table 37). There are two possible explanations for this: some areas of land segment 3 and 5 form part of the wetland and should therefore acquire higher QFRESP values or upslope land segments 1 and 5 make a larger contribution to daily flows than what their QFRESP values suggest.

The latter is supported by findings of Lorentz *et al.* (2007), as well as trench and slotted pipes experiments, showing a significant volume of water flowing lateral in the A horizon of upslope land segments. This near 'surface macropore flow' can contribute approximately 16% of event water (Lorentz *et al.*, 2007) and should be taken into consideration when assigning QFRESP values to land segments.

The accurate simulation of the water contents of the A horizon of land segment 1 is however in disagreement with the previous findings (Figure 158). The most truthful simulations of water contents were achieved for this horizon, indicating that the simulated amount of water infiltrating the profile is more or less in unity with actual infiltration, and that the QFRESP value, i.e. 0.002, for this land segment is correct.

One could argue that increasing QFRESP and lowering ABRESP should present similar water contents in the A horizon, as a smaller quantity water infiltrate but a larger volume build-up in this horizon. This will however deprive water from the already underestimated B horizon and will alter the reasonably well simulated water balance of the intermediate zone (Figure 158). The low volume of lateral flow from the intermediate zone in this land segment (Figure 165), even with a low response threshold (0.02) is a further indication that water a great volume of water is needed to saturate the C-horizon and any removal or re-routing of water will significantly reduce the simulated water content of the deepest horizon.

Similarly one cannot remove surface water from the A horizon of land segment 5 by assigning a higher QFRESP value, as water contents of this horizon is underestimated for the

greatest part of the simulated period (Figure 164). Lowering the ABRESP will decrease the water content of the already underestimated B horizon and changing the BFRESP will adjust the relatively well simulated water contents of the intermediate zone.

In both land segments 1 and 5 the water contents of the C-horizon are simulated fairly well. Assigning higher QFRESP values to compensate for underestimation of peak flows and then lowering ABRESP, BFRESP and also INTRESP should probably result in comparatively water content simulations and might increase the accuracy of streamflow predictions. That would however be the antithesis of the aim of this study and will definitely not contribute to predictions in ungauged basins.

It is clear that a method for attaining accurate QFRESP values is needed. This method should encompass soil and landscape properties and should preferably be dynamic in nature, as one of the major driving forces for quick flow generation is the water content of the topsoil. The latter is in accord with the well-known 'variable source area' concept. The influence of the antecedent water on streamflow is further emphasized in Figure 152. In the 1999/2000 season the first significant increase in streamflow was recorded on the 8th of December after 153 mm of precipitation was recorded from the beginning of September. For the 2000/2001 season the first significant increase in streamflow was recorded on the 7th of November following a 110 mm of precipitation from the beginning of September. Before the 8th December 2000 and the 7th of November, 'peak flows' were overestimated by the model as the storage capacity of the catchment was not filled yet.

Simulated low flows correspond very well with measured flows (Figure 152, Figure 153 & Figure 155). Simulations by Lorentz *et al.* (2009) using *ACRU2000* (in lumped and distributed mode) and *ACRU-Int* (using 1 and 3 soil types), could simulate high flows moderately well but was unsuccessful in simulating low flows. It is believed that the model configuration used in this study represents the actual processes generating base flow, i.e. drainage from the soil and not from groundwater, and it was therefore exhilarating to observe the connection between simulated and measured outflows.

It was surprising that these low flows were not generated through lateral flow in the intermediate zone of land segment 4 and 7, as lateral flow contributions from these land segments cease before the dry season (Figure 165). Interesting is that the lateral flow from land segment 2 does not cease throughout the dry period of 2000 and, although the volumes of lateral flow is significantly smaller than the measured streamflow, there is an exponential relationship with an R^2 of 0.96 between measured low flows and lateral contributions from land segment 2.

The slightly greater weighted contribution during high flows of land segment 7 compared to land segment 4 can be attributed to the larger area (63% compared to 36% of land segment 4) adjacent to the stream with moderately high QFRESP values (Table 37). Contributions from land segment 7 cease during dry periods (Figure 157), probably due to the relatively large volumes of water recharging the groundwater, as a result of high BFRESP and comparatively high INTRESP values of land segment 5 and 6.

Lateral flow contributions from land segments 2 and 5 commenced at a similar time as the stream. It would therefore be fair to assume that the storage capacity of the catchment and the storage capacity of these land segments are closely related. It is relationships such as these, highlighted by modelling, which should be investigated further as they can be first order controls in the hydrological response of catchments.

Water contents of the A horizon are over estimated for the majority of the simulation period of land segments 2, 3, 4, 6 and 7 (Figure 159-Figure 164). The reality that the land

segments represent an area, whereas the profiles, with the measured data, represent a point in that area should be kept in mind. Later flow, such as near surface macropore flow, occurs in a downslope direction, when the representative profile is in the lower regions of the land segment, these lateral contributions might have accumulated in the horizons, resulting in higher measured compared to simulated water contents. The same applies for the underestimation of water contents in the B horizons of all land segments except for 3. Routing of A and B horizons to A, B and C horizons of different land segments might aid in solving this problem and ensure a better imitation of actual hydrological processes.

It has been stated that simulated water contents of the C-horizon is spurious due to the ability of reaching water contents above P_o . This 'over-saturation' of the intermediate zone in land segments 2, 3, 4, 5 and 6 might be amended by decreasing the BFRESP response and thereby rectifying the underestimation in B horizons and the overestimation of water contents in C-horizons. This is again would be in contrast with the aim of this study and it is proposed that new mechanistic methods should be developed, or current methods altered, with the purpose of mimicking actual redistributions of water in the profile.

5.7 CONCLUSIONS

A hydropedological modelling report was compiled for the Weatherley catchment, in the Eastern Cape, South Africa. *ACRU-Int* was used to simulate the hydrological response of the catchment over two rainfall seasons. The catchment was divided into 7 distinct land segments representing two dominant hillslopes in the catchment. Two additional land segments were used to collect contributions from groundwater and streamflow contributions. Configuration and routing between the land segments were done similar to the conceptual hydrological behaviour of the hillslopes as determined from soil morphological properties. Parameters used was obtained and calculated from measured properties and processes when it was possible. On the whole the model were reflecting actual hydrological processes dominating in the catchment.

The model configuration used predicted low flows very well but failed to give good estimations of peak flows. Based on the good representations of low flows but inaccurate peak flow simulations in this study and the reverse in previous studies, it should be concluded that the non-linearity of the hydrological processes in this catchment either calls for time variable parameters for generating peak flows or separate simulations for dry and wet periods.

Even though the general streamflow predictions were relatively poor, uncertainty in the predictions can't be attributed to calibrations or overparameterization of the model. This is believed to be a step in the right direction for PUB's.

Soil water contents were predicted fairly well for certain land segments. Under estimation was however dominant for A- and B horizons for most land segments whereas the water content of the intermediate zone was overestimated in all but one land segments. Incorrect ABRESP, BFRESP and INTRESP functions were probably the main reason for these erroneous predictions. A mechanistic method which consider soil and landscape properties should be developed. Simulated water contents of the intermediate zone were more than P_o in certain land segments. This should be rectified to ensure accurate simulations of the lateral redistribution of water.

The ability of *ACRU-Int* to route the intermediate zone of one land segment to different layers of a land segment downslope is ideal for simulating the hydrology of catchments in

terms of the hydrological response of individual hillslopes and is therefore suitable for hydrological calibrations of identified hillslopes in the HOSASH project. It would however be gratifying if routings can also be made from A and B horizons to all the different layers in downslope land segments to ensure more correct representation of especially near surface lateral processes.

5.8 REFERENCES

- BEEH, 2003. Weatherley Database V1.0. School of Bio-resources Engineering and Environmental Hydrology, University of Natal, Pietermaritzburg.
- BEVEN, K.J., 2001. On fire and rain (or predicting the effects of change). *Hydrol. Process.* 15, 1397-1399.
- BREDEHOEFT, J., 2005. The conceptualization model problem – surprise. *Hydrogeol J.* 13, 37-43.
- DUNN, S.M., FREER, J., WEILER, M., KIRKBY, M.J., SEIBERT, J., QUINN, P.F., LISCHIED, G., TETZLAFF, D. & SOULSBY, C., 2008. Conceptualization in catchment modelling: simply learning? *Hydrol. Process.* 22, 2389-2393.
- LE ROUX, P.A.L., VAN TOL, J.J., KUENENE, B.T., HENSLEY, M., LORENTZ, S.A., EVERSON, C.S., VAN HUYSSTEEN, C.W., KAPANGAZIWIRI, E & RIDDELL, E., 2011. Hydropedological interpretations of the soils of selected catchments with the aim of improving the efficiency of hydrological models. Report No. 1748/1/10. Water Research Commission, Pretoria.
- LIN, H.S., KOGELMAN, W., WALKER, C. & BRUNS, M.A., 2006. Soil moisture patterns in a forested catchment: A hydropedological perspective. *Geoderma* 131, 345-368.
- LORENTZ, S. A., 2001. Hydrological systems modelling research programme: hydrological processes. Report No. 637/1/01. Water Research Commission, Pretoria.
- LORENTZ, S. A., THORNTON-DIBB, S., PRETORIUS, C. & GOBA, P., 2004. Hydrological systems modelling research programme: hydrological processes. Report No. 1061 & 1086/1/04. Water Research Commission, Pretoria.
- LORENTZ, S.A., BURSEY, K., OLUFEMI I., PRETORIUS, C & NGELEKA, K., 2007. Definition and upscaling of key hydrological processes for application in models. Report K3/1320. Water Research Commission, Pretoria.
- LORENTZ, S.A. & FREESE, C.J., 2009. An evaluation and simulation of hydropedological soil properties at the Weatherley catchment. Unpublished report to WRC project No. K5/1748.
- MCDONNELL, J.J., SIVAPALAN, M., VACHÉ, K., DUNN, S., GRANT, G., HAGGERTY, R., HINZ, C., HOOPER, R., KIRCHNER, J., RODERICK, M.L., SELKER, J. & WEILER, M., 2007. Moving beyond heterogeneity and process complexity: A new vision for watershed hydrology. *Water Res. Res.* 43, 1-6.
- ROBERTS, V.G., HENSLEY, M., SMITH-BAILLIE, A.L. & PATTERSON, D.G., 1996. Detailed soil survey of the Weatherley catchment. ARC-ISCW Report No. GW/A/96/33. ARC-ISCW, Pretoria.
- SCHULZE, R.E. 1995. Hydrology and Agrohydrology: A text to accompany the ACRU 3.00 Agrohydrological Modelling System. Water Research Commission, Pretoria TT69/95. pp AT23-1 to AT23-15.

- SCHULZE, R.E., 2007. Soils: Agrohydrological information needs, information sources and decision support. *In* Schulze, R.E (Ed). 2007. South African atlas of climatology and agrohydrology. Report No. 1489/1/06. Water Research Commission, Pretoria.
- SEIBERT, J. & MCDONNELL., On the dialog between experimentalist and modeller in catchment hydrology: Use of soft data for multicriteria model calibration. *Water Resour. Res.* 38, 1241, doi:10.1029/2001WR000978.
- SIVAPALAN, M., 2003a. Process complexity at hillslope scale, process simplicity at the watershed scale: is there a connection? *Hydrol. Process.* 17, 1037-1041.
- SIVAPALAN, M. 2003b. Prediction in ungauged basins: a grand challenge for theoretical hydrology. *Hydrol. Process.* 17, 3163-3170.
- SMITHERS, J. & SCHULZE, R.E., 2004. ACRU Agrohydrological modelling system: user manual v4.00. School of Boiresources Engineering and Enviromental Hydrology, University of Natal, Pietermaritzburg.
- TROMP-VAN MEERVELD, I. & WEILER, M., 2008. Hillslope dynamics modelled with increasing complexity. *J. Hydrol.* 361, 24-40.
- VAN DER MERWE, R.H., VAN TOL, J.J., HENSLEY, M., THERON, L. & LE ROUX, P.A.L., 2011. Deliverable 3: Permeability of selected diagnostic horizons. Project K5/2021, Water Research Commission, Pretoria.
- VAN HUYSSTEEN, C.W., HENSLEY, M., LE ROUX, P.A.L., ZERE, T.B. & DU PREEZ, C.C., 2005. The relationship between soil water regime and soil profile morphology in the Weatherley attachment, an afforestation area in the Eastern Cape. Report no. 1317/1/05. Water Research Commission, Pretoria.
- VAN TOL, J.J., LE ROUX, P.A.L., HENSLEY, M. & LORENTZ, S.A., 2010. Soil as indicator of hillslope hydrological behaviour in the Weatherley Catchment, Eastern Cape, South Africa. *Water SA* 36, 513-520.
- WEILER, M. & MCDONNELL, J., 2004. Virtual experiments: a new approach for improving process conceptualization in hillslope hydrology. *J. Hydrol.* 285, 3-18.
- ZERE, T.B., 2005. The hydropedology of selected soils in the Weatherley catchment on the Eastern Cape province of South Africa. Unpublished Ph.D. thesis, University of the Free State, Bloemfontein.

SECTION III: STUDY TECHNIQUES

Chapter 6 HYDROPEDOLOGICAL STUDY TECHNIQUES (A)

6.1 THE HYDROLOGICAL RESPONSE OF DIAGNOSTIC HORIZONS AND PROFILES

6.1.1 All data plus comparisons of horizons

6.1.1.1 Introduction

The soil surface splits water when transferring water from atmosphere to soil (Park, McSeeney & Lowery, 2001). Splitting begins at the surface and reacts vertically in different soil horizons (Soulsby *et al.*, 2006). This process continues downwards from the soil as upper vadose zone into the transitional saprolite (intermediate vadose zone) and lower vadose zone of fractured rock (Ticehurst *et al.*, 2007; Van Tol *et al.*, 2010a; Le Roux *et al.*, 2010; Kuenene *et al.*, 2011).

Differences in lateral zones, including soil horizons, rock layers and the transitional saprolite participate in two functions, namely storage and discharge (Tromp-van Meerveld, 2004; Tani *et al.*, 1997; Ticehurst *et al.*, 2007). Storage exceeding water holding capacity leads to discharge. Differences in hydraulic conductivity of these horizons, impact on the ratio of lateral-vertical discharge. This coupled with slope and slope length induces subsurface lateral flow (SLF) (Van Tol, *et al.*, 2013).

Soil morphology distinguishes between soil horizons (SCWG, 1991). The morphological features defining soil horizons are closely related to soil forming processes, in which water play the dominant role (Fritsch & Fritzpatrick, 1994, Essington, 2004). By implication: the rate at which water flows through the soil and the duration it remains within the soil, results in conspicuous properties, such as soil color (Schwertmann, 1985). This is supported by a lack of saturation measured in red soils (Van Huyssteen *et al.*, 2005), implying a fast rate of flow. This indicates aerated, oxidized conditions (Schwertmann, 1985; Smith & van Huyssteen, 2011). Long periods of saturation and near saturation in grey soils, indicate permanent reduction under saturated conditions (Van Huyssteen *et al.*, 2005; Smith & Van Huyssteen, 2011; Van Huyssteen, 2013). Van Tol *et al.*, (2010a) discuss both soil morphological indicators of soil response; for example carbonate deposits and redox morphology, and soil morphological indicators controlling response; for example macropore distribution and horizonisation of soils. Soil texture and structure control pore size distribution and therefore soil hydrology (Turner, 1976; Hutson, 1984). Soil horizons differ in morphological properties both indicating and controlling soil water responses in sub-soils (Bouma, 1992). Horizons differ mainly in texture and structure, influencing hydrological

response due to bulk density (Hill & Sumner, 1966). The porosity and hydraulic conductivity potential of a soil changes with depth, as a response due to factors such as bulk density, texture and organic matter content (Hutson, 1984; Weiler *et al.*, 2005). The sequence of horizon hydrological character comprises soil pedon hydrological response (Tani, 1997; Ticehurst *et al.*, 2007; Van Tol *et al.*, 2013).

Limitations to the current applied gathering and classification of soils information is limited to land use and not hydrological functionality (Le Roux *et al.*, 2013). Whole environmental situations have to be considered when gathering pedological information when inferring hydrological response or functionality of soils (Van Tol *et al.*, 2011). Land use evaluation and management is greatly influenced by the hydrology, allowing this to be applied as inferable information (Bouwer, 2013).

Soil hydraulic conductivity measurements are subject to error in replication if the diameter of double rings and hydraulic head height (non-constant head) are applied (Baker & Bouma, 1975). In situ hydraulic property determination of swelling soils, are considered difficult to replicate in order to achieve representative hydrological values. Further issues associated with in situ measurements include antecedent moisture conditions and structure grade. Description of structure can be of assistance for sample size (Bouma, 1980). p(P)ristmatic or a strong structure grade allows/signifies/represents/indicates deep infiltration. Shallow rooted (<1 m, i.e. grass) vegetation increases deep infiltration. Large cracks conduct only along 2% of their volume under moist conditions. Frequency and amount of rainfall influence the depth to which cracks conduct water (Bouma & Decker, 1978).

The use of pedotransfer functions link pedology to modelling (Pachepsky *et al.*, 2006). Although pedotransfer functions aimed at developing quantitative relationships between physical soil properties and hydrology (Bouma, 1989), a preceding step can be to identify flowpaths and characterization of flow direction (Van Tol *et al.*, 2008; Kuenene *et al.*, 2011) and qualification using soil physics and hydrometry (Van Tol *et al.*, 2010b), to create pedo-transferrable information (Van Tol *et al.*, 2012).

The hypothesis is that morphological signatures used to classify soil horizons are associated with soil physical properties, controlling the hydrological response of soils.

METHOD

Hydropedological concepts concerning functionality of diagnostic horizons are developed using tacit knowledge. It includes flow rate, flow direction, storage and source horizons. The following parameters are idealised to represent rainy season antecedent moisture conditions:

1. Hydrological character.
2. Assume that near surface macropore flow in all topsoils is controlled by slope.
3. Application of tacit knowledge.

Hydrological and pedological data were mined from land type data, research reports and own field data (BEEH, 2003; Lorents *et al.*, 2006; Van Huyssteen *et al.*, 2005; Van Tol, Le Roux & Hensley 2012) (Table 38).

Table 38 Origin of published and un-published data used in discussion. Location from where data is obtained, and where in the discussion it is applied, is supplied

| Source | Data used in | Location |
|------------------------------------|----------------------|-----------------------------|
| BEEH, 2003 | Table 39 | 31° 6'17.89"S 28°19'45.73"E |
| Lorents <i>et al.</i> , 2006 | Table 42, 43, 44 | RSA |
| Van Huyssteen <i>et al.</i> , 2005 | Table 39 | 31° 6'17.89"S 28°19'45.73"E |
| Van Tol, Le Roux & Hensley 2012 | Figure 170 | 31° 6'17.89"S 28°19'45.73"E |
| Farms Aucampshope & Riverside, NC | Table 40, Figure 167 | 28°57'51.60"S 24°13'33.60"E |
| UFS agrometeorology grounds | Table 41, Figure 168 | 29° 6'25.97"S 26°11'19.48"E |

Unpublished data: "farms Aucampshope & Riverside, Northern Cape province (NC) and University of the Free State (UFS) agrometeorology grounds". Saturated hydraulic conductivities were measured on these sites, by use of double rings (Haise *et al.*, 1956) with a falling head method.

Replications in Northern Cape: Replication (Rep) 1 and 2 (28°57'51.60"S 24°13'33.60"E) were done next to one another, with replication 3 (28°57'18.60"S 24°14'59.40"E) done \pm 2.79 km away on similar soil. Topsoil was removed and B1 horizons at 300 mm were measured. Both soil forms were classified as Valsrivier forms (SCWG, 1991), with the B horizon being classified as peducutanic B (*pe*) horizon with sub-angular blocky structure. Rep 1 was tested on soil with dry antecedent moisture conditions, whereas Rep 2 & 3 were tested on soils with antecedent moisture conditions.

Replications at University of the Free State: Topsoil was removed to expose an abrupt transition to a prismacutanic B (*pr*) horizon at 250 mm. Three replications were placed equidistant at 15 meters from one another. Replication 3 was placed on a surface crack. This crack was 5 cm in width and 20 cm in length. The crack was filled with water until full. The inner double ring was placed over this crack. The other two replications were placed on soils with no visible surface cracks. Initial consistency included surface cracks up to 20 cm long and 5 cm in width, extending up to 1.2 m into the soil. Ksat of these dry soils are estimated at a randomly chosen crack being filled by a half inch hosepipe running freely at 1bar for 1 hour before being filled. These prismacutanic B horizon were pre-wetted.

Discussion

Tacit knowledge played an important role in the development of the concepts of horizon hydrology. Water flow paths and flow rates formed the basis of the catena concept. However, the understanding has increased with continued research. Quantification of the water contents in different soils turned out to quantify the condition where soil morphology, although ancient, as a signature of chemical processes (Bouwer, 2013), represented a useful hydropedological parameter, namely drainable water (Van Huyssteen *et al.*, 2005; Smith & Van Huyssteen, 2011). The process is well expressed in conspicuous soil morphology. The morphologically different horizons had different $AD_{s<0.7}$ values. Several new concepts developed from this information and were applied to real soilscares.

The rate of flow: Red apedal B horizons, in which water contents does not exceed a value of $s>0.7$, has fast enough flow rates to sustain oxidised conditions. Further, saturated hydraulic conductivity of these soils exceed rainfall intensity and water contents exceeding evapotranspiration demand drain from the horizon, recharging the underlying saprolite. The saturated hydraulic conductivity of the saprolite exceed the rate of water draining from the

above horizon. Horizons with short $AD_{s<0.7}$ values, i.e. yellow-brown apedal B horizons do not necessarily have lower flow rates but have less permeable underlying horizons (Van Tol permeameter measurements P202, BEEH, 2003).

The path of water flow in hillslopes. The concept of water flow was vertical down the pedon into fractured rock. The concept was modified by adding the “return flow” flow-path. Additionally, yellow-brown apedal soils were found lower lying in the landscape than red apedal B horizons. Chemical weathering in saprolite horizons is aided by above lying wetter soil conditions. Increased chemical weathering in saprolite horizons reduces saturated hydraulic conductivities. Initial increase in soil water content can only come from up slope, implying it is drainage from the red soils on a crest or upslope position. This flows in fractured rock or saprolite and returns to the soil, to increase chemical weathering at the end of the slope. There are two sources of water from one soil to another soil within the same pedon, namely vertical drainage and return flow.

Source of water: Soil horizons occur in sequence in soils, which are in sequence distributed in soilcapes. These units (horizons, soils (forms) and soilscapes) having in sequence complementing typical hydrological characteristics, creating a hydrological response of soil as a whole. The $AD_{s<0.7}$ values generally increase from red apedal B horizons to yellow-brown apedal B horizons to soft plinthic B horizons to G-horizons (Van Huyssteen *et al.*, 2005). They are increasingly associated with lower landscape positions and concave profile and planform curvature terrain shapes, implying an either slower flow or addition of water to the flow path. To generate an influx of water in a horizon, there must be a source that supplies the water. The source may come from vertically above or laterally, which at a slope may be a horizon lower in the pedon sequence including saprolite and fractured rock. It may receive water from more than one horizon (Schultze *et al.*, 1995).

Flow direction: The perception was that water flows vertically down the pedon. $AD_{s>0.7}$ greater than substantiated by rainfall-evapotranspiration delivery-demand and interflow gravitational feeding, at lower lying topographical units and hillseep wetlands, indicate water supply other than previously understood. Returnflow from rock and lower vadose zone, allow for riparian moisture conditions greater than explained by climate and vegetation delivery-demand. High clay conditions due to illuviation and greater reduction at lower lying areas in the topography, reduce water lateral penetration and increase water stagnation. This coupled with the higher water holding capacity of clayey soils, substantiates greater $AD_{s>0.7}$ values. Figure 166 as an example of how tacit knowledge has influenced the concept building of horizon hydrology:

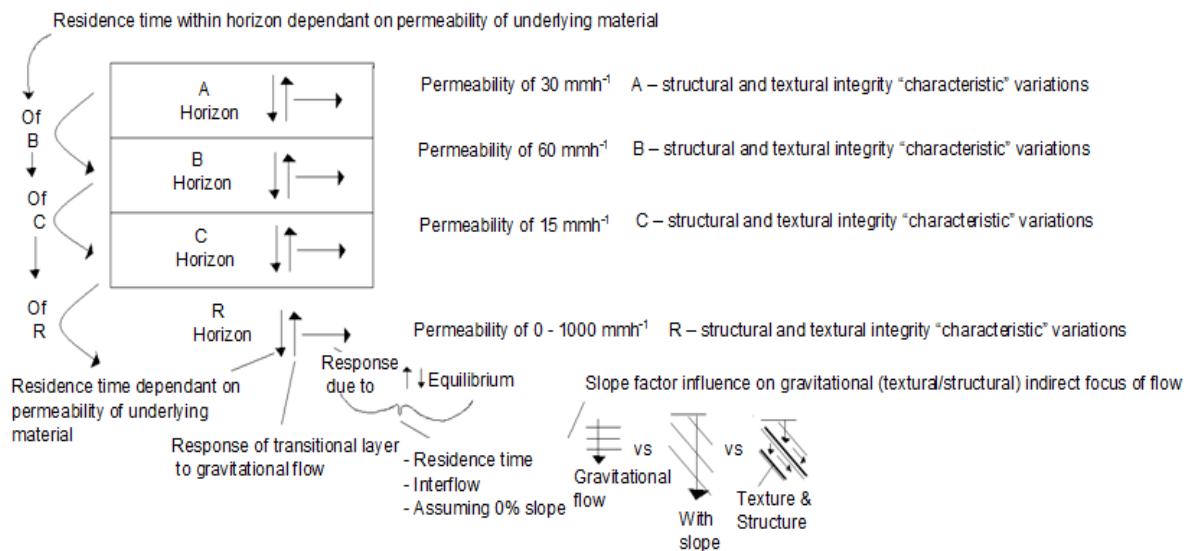


Figure 166 The concept of water flowing through a soil by gravity, with and without slope, with and without textural and structural impeding layers (infiltration rates are idealized) (schematic representation of flow principles derived from Schulze, 1995 and Ticehurst *et al.*, 2007).

Table 39 indicates conceptual hydrological values of horizons: Flow rate as saturated hydraulic conductivity; two storage factors: annual duration of saturation of 70% porosity ($Ad_{s>0.7}$) (redox morphology) and drained upper limit (DUL) to represent water holding capacity; source horizons are within sequence of SCWG (1991), although limitations to this classification system occur (Le Roux *et al.*, 2013, Van Huyssteen *et al.*, 2013)

Table 39 Conceptual hydrological functionality of diagnostic horizons: flow rate, flow direction, storage and source horizons

| | Diagnostic horizon | Flow | Flow | Storage | | Source | Source horizon (s) |
|-----------------------------------------------------------------|-------------------------------|-----------|------------------|--------------------------|-----|-----------------------------------------------------------------|---------------------|
| | | Direction | K _{sat} | AD _{s > 0.7} | DUL | o/so/adj | |
| | | | 0-5 | | | | |
| 1 | Organic O <i>oo</i> | ↔ | 5 | 5 | 5 | so | overland flow, rain |
| 2 | Humic A <i>ah</i> | ↓ | 5 | 1 | 3 | o | rain |
| 3 | Vertic A <i>ve</i> | ↓ | 1 | 4 | 4 | o | rain |
| 4 | Melanic A <i>ml</i> | ↓ | 3 | 3 | 3 | o | rain |
| 5 | Orthic A/G <i>ot</i> | ↑ | 4 | 5 | 3 | o | G |
| 6 | Orthic A/re <i>ot</i> | ↓ | 5 | 1 | 3 | o | rain |
| 7 | E Horizon <i>gs</i> | → | 5 | 5 | 2 | o | ot |
| 8 | G Horizon <i>gc</i> | ↑ | 0 | 5 | 5 | so | on, ot |
| 9 | Red Apedal <i>re</i> | ↓ | 5 | 1 | 1 | o | ot, yb |
| 10 | Y-B Apedal <i>ye</i> | ↓ | 5 | 2 | 2 | o | hu,ot |
| 11 | Red Structured <i>vr</i> | ↓ | 3-4 | 2 | 2 | o | ot |
| 12 | Soft Plinthic <i>sp</i> | ↓ | 4 | 5 | 4 | o | |
| 13 | Hard Plinthic <i>hp</i> | – | 0-2 | 5 | 0 | o | |
| 14 | Prismacutanic <i>pr</i> | ↓ | 1 | 5 | 2 | o | E,ot |
| 15 | Pedocutanic <i>vp</i> | ↓ | 2-3 | 4 | 3 | o | hu,me,E,ot |
| 16 | Lithocutanic <i>li</i> | ↓ | 3-4 | 3 | 3 | o | hu,me,E,ot |
| 17 | Neocutanic <i>ne</i> | ↓ | 3 | 2 | 4 | o | ot,hu |
| 18 | Neocarbonate <i>nc</i> | ↓ | 5 | 2 | 4 | so/adj | ot,E |
| 20 | Regic Sand <i>rs</i> | ↓ | 5 | 4 | 4 | o | ot, un,E,re,yb |
| 21 | Stratified alluvium <i>sa</i> | ↓ | 2-4 | 5 | 5 | o | ot |
| 24 | Saprolite <i>so</i> | ↓ | 5 | 2 | 3 | o | pc,pz |
| 25 | Soft carbonate <i>sc</i> | ↓ | 4 | 5 | 3 | o/so/adj | ot,nb,re,yb,me |
| 26 | Hardpan carbonate <i>hk</i> | – | 0 | 1 | 1 | o/so/adj | ot,nb,nc,re,yb,me |
| 30 | Hard Rock <i>r</i> | – | 0 | 0 | 0 | o | ot |
| First round award hydrological behaviour in wet phase | | | | | | | |
| Near surface macropore flow in ALL topsoils controlled by slope | | | | | | | |
| ↔ | overland flow | | | | | | |
| ↓ | vertical flow | | | | | | |
| → | lateral flow | | | | | | |
| ↑ | responsive flow | | | | | | |
| | | | | | | Where o = overland flow, so = saprolite, adj = adjacent horizon | |

Flow direction In which direction does this horizon channel water. Irrespective of the ideological simplistic horizon itself. This concept is based on the field research of how these horizons function within a natural sphere.

Flow rate (Ksat) This indicates the rate of saturated flow.

Storage AD_{>0.7} Mean annual duration of s > 0.7

Storage DUL This is the ability of the horizon to retain water within the drained upper limit (DUL) and above the drained lower limit (DLL).

Direction of flow

Table 40 shows sequencing of horizons within forms with varying K_{sat} values. These values are influenced by the slowest K_{sat} value within the profile. The diagnostic morphology of these horizons are subject to these rates (Hutson, 1984; Turner, 1976; Van Huyssteen, 1994; Van Tol *et al.*, 2010 a).

Profile 204 has a 1000-fold reduction in K_{sat} of the rock (*r*) to that of the above lying soft plinthic B (*sp*) horizon. This indicates that water will perch above the rock ($AD_{s>0.7}$ 365 days per year). This allows for water to accumulate and be subjected to the influence of slope, promoting SLF in the above lying E-horizon (*gs*). This in turn is subject to the slope length (240 m) and carries a SLF value of 95.16 according to:

$$SLF \text{ index} = \frac{K_{sc}}{K_{si}} \times (\tan\beta \times L) \quad \text{Van Tol, 2013} \quad (6.1)$$

where : K_{sc} is the saturated hydraulic conductivity conducting layer
 K_{si} is the saturated hydraulic conductivity impeding layer
 β is the influence of the hillslope angle ($\tan\beta$)
 L is the slope length.

The occurrence of the *sp* horizon implies a fluctuating water table (SCWG, 1991). Water is added via rainfall and accumulates due to the low permeability of the *r*. This is removed via evapotranspiration and SLF by the *gs* horizon when accumulation extends into the *gs* horizon. Water remaining within the *sp* horizon is lost via evapotranspiration to such an extent that a fluctuation in water content occurs in the upper *sp* horizon ($AD_{s>0.7}$ 264 days per year).

Profile 210 has a 4.5-fold reduction in K_{sat} of the *r* to that of the above lying unspecified (*on*) unspecified with signs of wetness (*uw*). The red-apedal B horizon (*re*) above the *on/uw* is by implication of its morphology freely drained and does not incur reduction. The *re* (7.6 mm h^{-1}) has a lower K_{sat} than the *uw* (9.18 mm h^{-1}). Lateral water inflow from the above lying slope supplies the water for reduction to occur in the *uw* horizon. The comparatively high infiltration rate of the *r*, suggests water is recharged and can feed below lying soils via return-flow.

Profile 209 has a 15-fold reduction in K_{sat} of the *r* to that of the above lying G-horizon (*gc*). The *gc* horizon itself has a slow K_{sat} compared to the other soils overlying the parent material *r*. As profile 210 lies above profile 209 in direct flow line within hillslope topography, the water infiltrating the rock at profile 210, is very likely to feed the *gc* horizon of this profile. This return flow or lower vadose zone water can contribute to the lower infiltration rate of the *r* in this profile. The orthic A horizon (*ot*) has a $AD_{s>0.7}$ value of 203 days per year. This indicates water is added to this horizon by the below lying *gc* horizon via capillarity.

Table 40 Effect of permeability of the underlying rock in Weatherly, contributing on the morphological and hydrological properties of horizons in sequence of a soil form (BEEH, 2003)

| Descriptor Profile no | Depth (m) | Horizon | Texture | Density kg m ⁻³ | Ks mm h ⁻¹ | AD _{s > 0.7} | Slope |
|--------------------------|-----------|---------|---------|-------------------------------|--------------------------|--------------------------|-------|
| 204 | 0.1 | Ot | SaLm | 1600 | 52.48 | 14 | 8 % |
| | 0.3 | Gs | SaLm | 1710 | 36.61 | 14 | |
| | 0.5 | Sp | SaLm | 1710 | 26.87 | 264 | |
| | | Sp | | | | 365 | |
| | | R | | | 0.02 | 365 | |
| 210 | 0.55 | Ot | SaLm | 1590 | 15.36 | 0 | 5 % |
| | 1.2 | Re | SaLm | 1710 | 7.6 | 0 | |
| | 1.6 | On | Lm | 1660 | 9.18 | 300 | |
| | | R | | | 2 | 300 | |
| 209 | 0.45 | Ot | Lm | 1540 | 14.75 | 203 | 8 % |
| | 1.1 | Gc | Lm | 1670 | 3.11 | 340 | |
| | | R | | | 0.2 | 340 | |

Rate of flow through diagnostic horizons

Swelling soils

Pedocutanic B horizons are differentiated in their degree of structure as to their hydrological response (Figure 167 & Figure 168). Angular blocky structure mimic prisms swelling upon wetting (Figure 168), restricting Ksat. Sub angular blocky structure permits higher infiltration rates under saturated conditions (Figure 167).

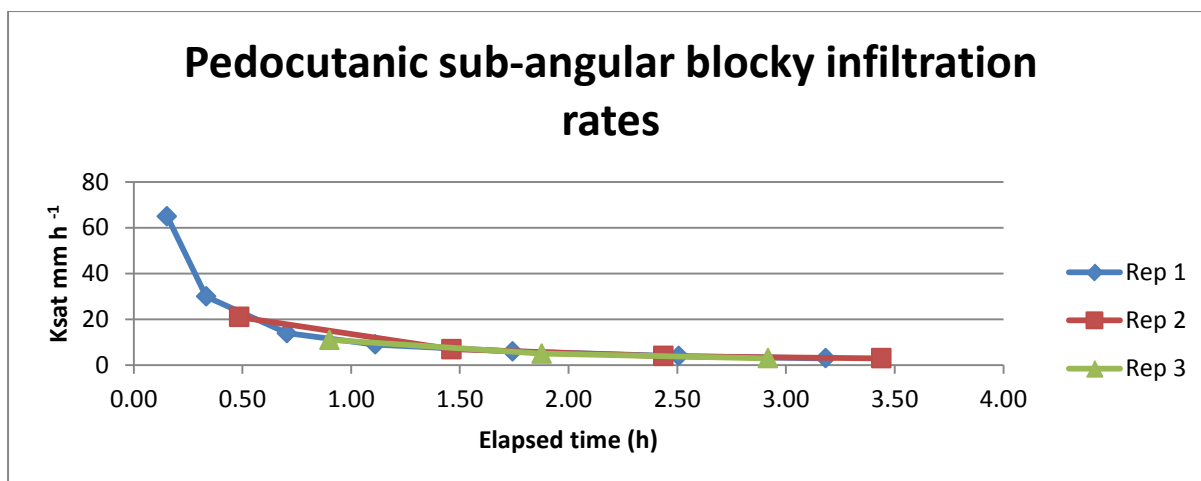


Figure 167 Hydraulic conductivity of pedocutanic B horizon (sub-angular blocky) over time

Figure 167 shows initial infiltration of cutanic (structured) soils in low antecedent moisture conditions as in Rep 1 (Table 41), can be high (65 mm h^{-1}). Reduced infiltration occurs moderately fast (36 min) and is equilibrated slowly (2 h). These replications were done 2.79 km apart. This signifies the homogenous hydrological nature of sub-angular blocky pedocutanic soils of similar origin. Notable is the same equilibrating saturated hydraulic conductivity of all three replications. Median increased with amount of replications done, as well as antecedent moisture content of the horizon. Standard deviation varies according to the initial moisture content of the profile.

Table 41 Saturated hydraulic conductivity of pedocutanic B horizon (sub-angular blocky) with statistical values (Standard deviation (SD)) in mm h^{-1}

| | Number of readings | First reading | Median | SD | Final reading |
|---------------|--------------------|---------------|--------|----------|---------------|
| Replication 1 | 7 | 65 | 9 | 22.40323 | 3 |
| Replication 2 | 4 | 21 | 5.5 | 8.341663 | 3 |
| Replication 3 | 3 | 11 | 5 | 4.163332 | 3 |

Prismacutanic B horizons are characteristic of abrupt transitions to the above lying horizon (SCWG, 1991). Prism bulk density restricts preferential flow to inter-prism spaces, which are closed upon prisms' ped swelling upon wetting. Figure 168 shows a very small change (0.61 mm h^{-1} , average) in K_{sat} versus time to reach equilibrated K_{sat} .

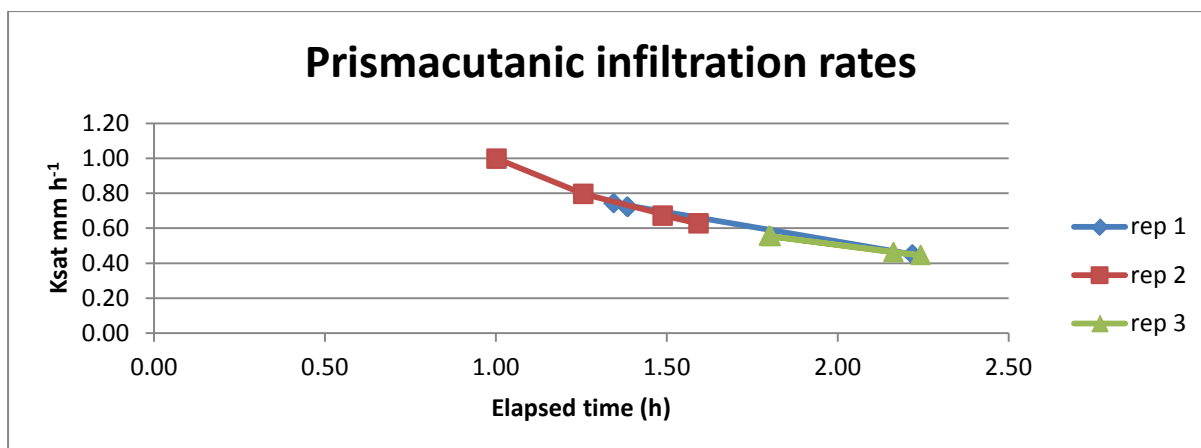


Figure 168 Hydraulic conductivity of prismacutanic B horizon over time

The first readings of Table 42 were $\pm 30\%$ slower at final reading for Rep 1 & 2 and 69% slower for Rep 3. This is as the crack had received more water due to pre-filling with the hosepipe. The lower infiltration (Rep 2) is due to inter-prism spaces being reduced due to the increased water added for a longer period and poor conductivity between the ped surfaces. Rep 1 & 2 have very similar median and standard deviation values, which are expected to have been so for all three replications, had Rep 3 had low antecedent moisture conditions.

Table 42 Saturated hydraulic conductivity of prismacutanic B horizons with statistical analysis. Values (Standard Deviation (SD)) in mm h^{-1}

| | Number of readings | First reading | Median | SD | Final reading |
|---------------|--------------------|---------------|--------|------|---------------|
| Replication 1 | 4 | 0.72 | 0.72 | 0.14 | 0.45 |
| Replication 2 | 4 | 1.00 | 0.73 | 0.17 | 0.67 |
| Replication 3 | 4 | 1.80 | 0.51 | 0.06 | 0.55 |

Non-swelling soils

Horizons which have a high permeability exhibit a trophic or leached character compared to the above or below lying horizon (SCWG, 1991).

Red-apedal B horizons facilitate recharge functions in soil forms (Le Roux *et al.*, 2011). Two types can be generally differentiated: those of extremely high saturated hydraulic conductivity rates of $> 800 \text{ mm h}^{-1}$ and those of high saturated hydraulic conductivity rates of $> 200 \text{ mm h}^{-1}$. The difference is observed morphologically by means of the texture and structure, where dystrophic re's $> 200 \text{ mm h}^{-1}$ with kaolonitic clay and re's with $K_{\text{sat}} > 800 \text{ mm h}^{-1}$ has a texture of mainly windblown coarse aeolian sands (Figure 169).

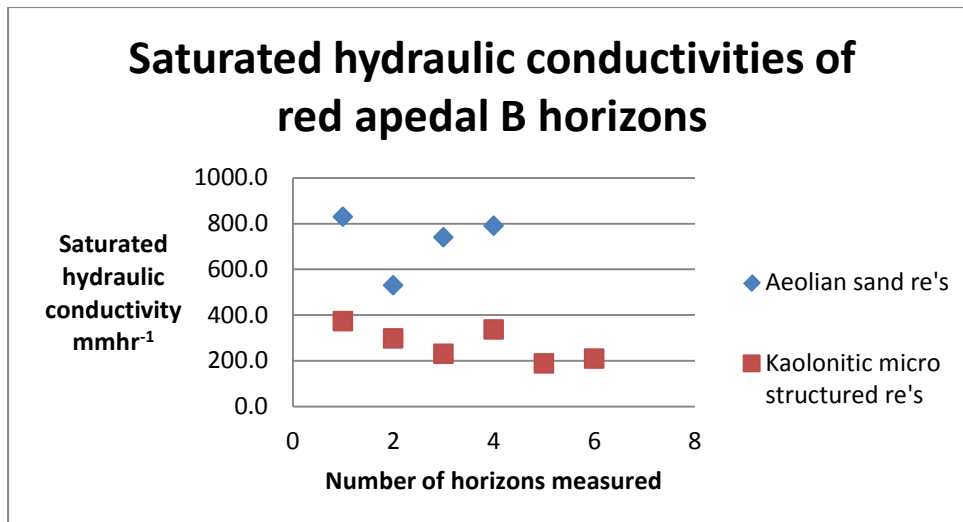


Figure 169 Saturated hydraulic conductivities of two differing parent material red apedal B horizons.

The windblown aeolian sands are found in the eastern and central Free State province, west of the Orange, Riet and Vaal rivers (Hensley *et al.*, 2007). Dystrophic re's are found along the more humid climatic eastern escarpment of the KwaZulu-Natal border (Kuenene, 2013). Table 43 indicates that *re* horizons have a high median value yet vary greatly in their range (lowest: 82.44 mm h⁻¹, highest: 372.43 mm h⁻¹) of saturated hydraulic conductivities. This allows for K_{sat} values > 100 mm h⁻¹ for even lower limit *re* horizons. At rates above 80 mm h⁻¹, soils can accommodate even extreme cloudbursts under natural conditions. This implies that soils with extremely high K_{sat} values are either redundant in their K_{sat} , or create sinks to accommodate overland flow. Storage of water within soil is subject to porosity, clay mineralogy and boundary conditions (Table 40) found at depth above which water can accumulate. The volume available to water perching within soil pore space, the hydrophilic character of the mineralogy and the amount of water below ET and capillary rise, stipulate storage abilities of horizons (Van Huyssteen *et al.*, 2013). Slope induced flow will result in reduced storage time (Le Roux *et al.*, 2011). As with equation 6.1, the greater the slope, the more $\tan\beta$ will contribute to the hydrological effect of the horizon by SLF.

Table 43 Selected red-apedal B horizons subject to statistical analysis to indicate mean and standard deviation of saturated hydraulic conductivities

| Red apedal B horizon measured | In situ K _{sat} (mm h ⁻¹) | | |
|-------------------------------|------------------------------------------------|--------|--------------------|
| 1 | 109.24 | | |
| 2 | 82.44 | | |
| 3 | 372.43 | | |
| 4 | 297.95 | | |
| 5 | 230.05 | | |
| 6 | 335.98 | | |
| 7 | 188.7 | | |
| 8 | 209.4 | Mean | Standard deviation |
| | | 219.70 | 103.23 |

Storage abilities of horizons

Variations of horizons within space occur, subject to formation due to climatic and mineralogical interconnected factors 6.1.1.1. Therefore *ot* horizons can react differently when occurring over horizons with differing permeability (Van Huyssteen, 2012). The use of DUL as a criterion for hydrological classification for storage ability of horizons, signifies the importance of the horizons mineralogy. 'Horizons' here (Table 44), are referred to as the horizon comprising soil of the Bloemdal and Bainvlei soil forms (SCWG, 1991).

The less permeable underlying material, even without slope, contributes to the storage ability of the above lying soils. Shortland soil forms, do not hold water due to their less permeable underlying material, but more so due to their clay mineralogy (SCWG, 1991).

Table 44 Real soils with statistically idealized saturated hydraulic conductivity rates indicating storage capacity due to underlying reduced saturated hydraulic conductivity

| Soil form | A horizon | B Horizon | C Horizon |
|----------------------------------------------|-----------|------------|--------------------------------------------|
| Bainvlei | Orthic | Red apedal | Soft plinthic |
| K _{sat} (median) mm h ⁻¹ | | 219.70 | 18.0 |
| Bloemdal | Orthic | Red apedal | Unspecified material with signs of wetness |
| K _{sat} (median) mm h ⁻¹ | | 219.70 | 10.4 |

Source and source horizons

The horizons water source is influenced to a greater or increasing degree the deeper, or the more sequenced a soil form is (Table 45). Homogenous structure (apedal) and textured (sandy) forms are more homogenous in their subsequent horizon hydrology, whereas the inverse occurs with texture and structural non-homogenous forms. Examples are (Table 39): the orthic A horizon reacting differently due to the source being *gc* (responsive soil) and *re* (recharge soil) (Le Roux *et al.*, 2011). Singularly, the *gs* horizon always reacts hydrologically as SLF due to source water added from above vertically or laterally. Soft plinthic B, *gc* and *uw* horizons are fed at different wetting frequencies, yet are fed by similar sources (Van Huyssteen, 2013).

Table 45 Two soil forms divided into diagnostic horizons with their median/standard deviation hydraulic conductivity values (mm h^{-1}) indicating the effect of underlying horizons on the above lying “source horizon”

| Diagnostic horizon | Ot | gs | Gc |
|--------------------|---------------|-----------|-----------|
| Ot | 57.33/95.75 | 4.11/5.24 | 0.12/0.01 |
| Re | 219.70/103.23 | | |
| Re | 219.70/103.23 | | |
| So | 28.08/15.48 | | |

The vertical sequence in Table 45 of horizons could possibly reflect a Hutton (Hu) soil form, whereas the lateral sequence of horizons a Kroonstad (Kd) soil form (SCWG, 1991). The standard deviation of the Hu is far greater both in deviation as well as in quantity, reflecting greater capacity for water to move through the soil. This is both as a function of receiving water and releasing water rapidly without holding much of it. This makes it a good source for lower lying horizons and forms part of recharge soils in hillslopes (Le Roux *et al.*, 2011). Median as well as standard deviation for the Kd horizons are extremely small in range comparatively. Their low hydraulic conductivity and saturated nature indicate various sources (Van Huyssteen, 2013; Le Roux *et al.*, 2013). The contribution of above lying horizons to be source horizons, is only of value when *gc* horizons are dry and precipitation or overland flow occurs.

The *ot* horizon here reflects a greater standard deviation than median value, indicating its vast range in hydrological functionality and value as source horizon. On recharge soils (Hu), it serves a fast conducting source horizons, whereas on *gc* horizons, it forms a receptacle of upward moving water out of the soil.

The *gs* horizon, similarly as to the *ot* horizon, has a greater standard deviation than median. Although small compared to the *ot*, the difference is of importance as it indicates that it has a greater range of function than its property as a lateral flow conduit. It also contributes water vertically, and SLF only occurs under saturated conditions with sufficient hydraulic head generation.

Storage correlation

Saturation at $>0.7_{\text{porosity}}$ storage induces neoformation of clay due to soil water stagnation, therefore increasing the DUL storage value of soils subjected to longer neoformation periods (Ritchie & Upchurch, 1983). Pedology is more often complex than simple and therefore the values for both types (Table 39) of storage correlate (Figure 170).

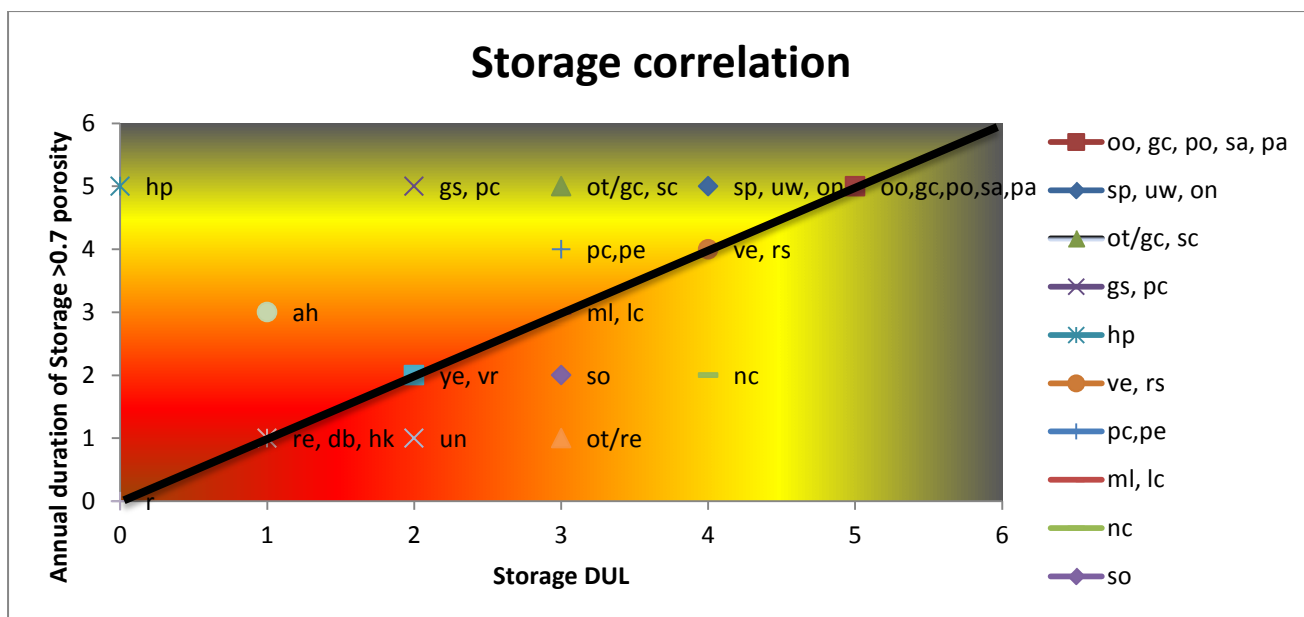


Figure 170 Storage correlation to aid in hydrological grouping of diagnostic horizons according to Table 39.

Surface horizons

Topsoil or surface horizons are the initial acceptor of precipitation. They split this water by virtue of promoting overland flow or permitting this water to percolate into the soil (Table 45). This is followed by water moving through the horizon by virtue of the particle percentage distribution tortuosity, influenced by factors such as bulk density, organic matter content and foreign additives due to climate and pollution (Turner, 1976). Water movement in both saturated and unsaturated conditions of topsoils is controlled by macropore preferential flow (Van Tol *et al.*, 2012). The distribution of macropores within the topsoil and subsoil have special orientation characteristics and tendencies, with more preferential orientation in the topsoil than subsoil (Sidle *et al.*, 2001). Further infiltration of subsoils occurs, affected by factors such as texture, structure and bulk density.

In excess of the horizons classifiable, their hydrological response (Figure 171) has been observed to mimic certain similarities. These allow for some diagnostic horizons to be classed into groups (Van Huyssteen *et al.*, 2013).

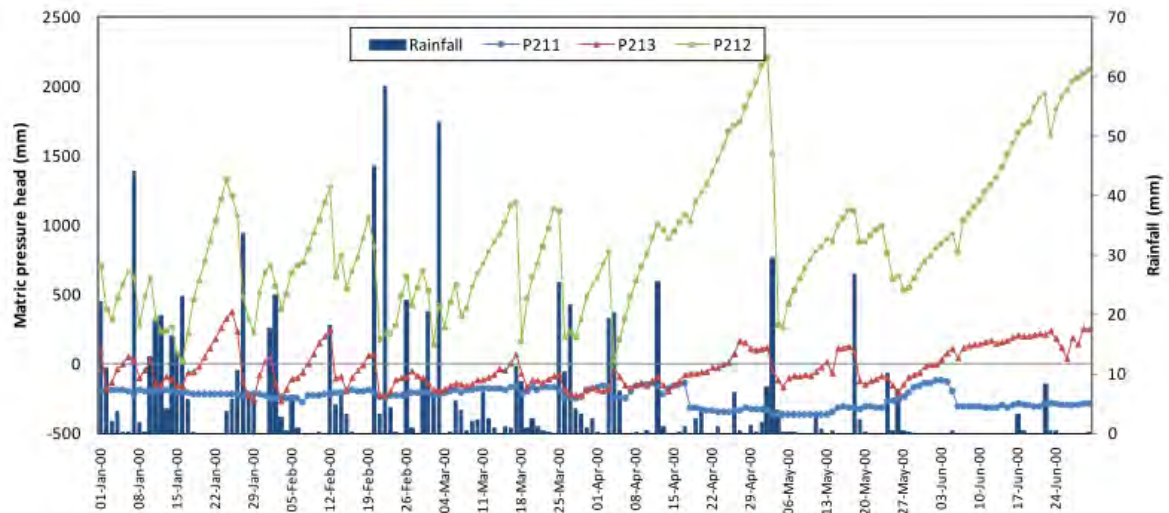


Figure 171 Rainfall and matric pressure head of three orthic A horizons over 6 months in the weatherly catchment (Van Tol *et al.*, 2012, Presented with permission of the authors) (BEEH, 2003)

Hydraulic properties of orthic A horizons are complex and vast in variation, due to their classification criteria allowing them to fall into all kinds of sequence of underlying horizons (Figure 172).

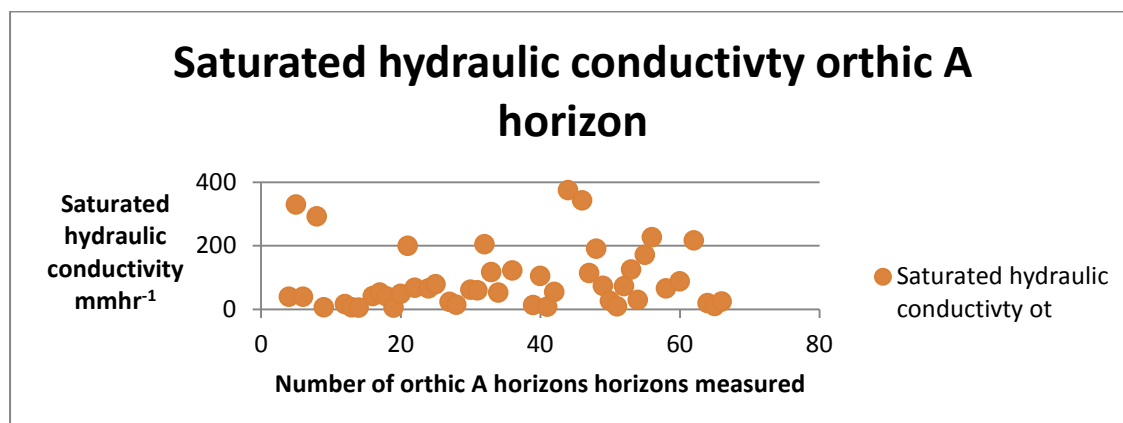


Figure 172 Variation of saturated hydraulic conductivity of orthic A horizons

Conclusion

Horizons can be grouped into hydrological units on hand of their soil physical properties, indicating their different hydrological functionality and assist in understanding hillslope hydrology. Hydrological functionality of each horizon individually allows for rates, direction and storage to be assigned. Unlike HOST, real soils are being dealt with, allowing for numerous scenarios to be conceptually presented.

6.2 REFERENCES

- BAKER, F.G., BOUMA, J. (1975) Variability of hydraulic conductivity in two subsurface horizons of two siltloam soils. *Soil Sci. Soc. Amer. Journal*. Vol. 40: 219-222.
- BEEH. (2003) Weatherly Database V1.0. School of Bioresources Engineering and Environmental Hydrology, University of Natal, Pietermaritzburg.
- BOUMA, J. (1980) Field measurement of soil hydraulic properties characterizing water movement through swelling clay soils. *J. Hydrol.* 45 (1/2): 149-158.
- BOUMA, J. (1989) Using soil survey data for quantitative land evaluation. *Adv. Soil Sci.* 9:177-213.
- BOUWER, D., LE ROUX, P.A.L., VAN TOL, J.J., & HENSLEY, M. (2012) Department of Soil, Crop & Climate Sciences, University of the Free State, Bloemfontein, 9300, South Africa.
- DEKKER, L.W., BOUMA, J. (1978) De invloed van drainage en verbeterde ontwatering op de vertical verzadigde doorlatendheid van komklei- en knipkleigronden. Rapport 1416. Stiboka, Wageningen. 22 pp.
- HENSLEY, M., LE ROUX, P.A.L., DU PREEZ, C., VAN HUYSSTEEN, C.S., KOTZE, E. & VAN RENSBURG, L. (2012) SOILS: THE FREE STATE'S AGRICULTURAL BASE, *South African Geographical Journal*, 88:1, 11-21.
- HUTSON, J.L. (1984) Estimation of hydrological properties of South African soils. University of Natal, Pietermaritzburg, Department of Soil Science and Agrometeorology.
- KUENENE, B.T., VAN HUYSSTEEN, C.W. & LE ROUX, P.A.L. (2011) Selected soil properties of as indicators of soil water regime in the Cathedral Peak VI catchment, KwaZulu-Natal.
- KUENENE, B.T. (2013) HILLSLOPE HYDROPEDOLOGY OF THE TWO STREAMS CATCHMENT IN KWAZULU-NATAL. PhD Dissertation, University of the Free State, Bloemfontein.
- LE ROUX, P.A.L., J.J. VAN TOL, B.T. KUENENE, M. HENSLEY, S.A. LORENTZ, C.S. EVERSON, C.W. VAN HUYSSTEEN, E. KAPANGAZIWIRI, & E. RIDDELL. (2011) Hydropedological interpretations of the soil of selected catchments with the aim of improving the efficiency of hydrological models. WRC Report No.: 1748/1/10. WRC, Pretoria.
- LE ROUX, P.A.L., M.J. DU PLESSIS, D.P. TURNER, J. VAN DER WAALS, & H.B. BOOYENS. (2013) FIELD BOOK For the classification of South African soils. SASSO. Reach Publishers. Wandsbeck.
- PARK, S.J., MCSWEENEY, K., & LOWERY, B. (2001) Identification of the spatial distribution of soils using a process-based terrain characterisation. *Geoderm.* 103 249-272.
- PACHEPSKY, Y.A., RAWLS, W.J., LIN, H.S. (2006) Hydropedology and pedotransfer functions. *Geoderma*, 131: 308-316.
- SCHULZE, R.E. (1995) HYDROLOGY and AGROHYDROLOGY: A TEXT TO ACCOMPANY THE ACRU 3.00 AGROHYDROLOGICAL MODELLING SYSTEM. WRC Report No 63/2/84. WRC, Pretoria.
- SCHWERTMANN, U., (1985) The effect of pedogenic environments on iron oxide minerals. *Advances in Soil Science* 1:171-200.
- SIDLE R.C., NOGUCHI S., TSUBOYAMA Y., LAURSEN K. (2001) A conceptual model of preferential flow systems in forested hillslopes: evidence of self-organization. *Hydrol. Process.* 15, 1675-1692.
- SOIL CLASSIFICATION WORKING GROUP. (1991) Soil Classification – A taxonomic system for South Africa. *Mem. agric. Nat. Resour. S. Afr.* No. 15. Dept. Agric. Dev., Pretoria.

- SOULSBY, C., TETZLFF, D., RODGERS, P., DUNN, S., & WALDRON, S. (2006) Runoff processes, stream water residence times and controlling landscape characteristics in a mesoscale catchment: An initial evaluation. *J. Hydrol.* 325, 197-221
- SOULSBY, C., YOUNGSON, A.F., MOIR, H.J. & MALCOM, I.A. (2001) Fine sediment influence on salmonid spawning habitat in a lowland agricultural stream: a preliminary assessment. *Science of the Total Environment*, 265, 295-307.
- TANI M. (1997) Runoff generation processes estimated from hydrological observations on a steep forested hillslope with a thin soil layer. *Journal of Hydrology*, 200, 84-109.
- TICEHURST, J.L., CRESSWELL, H.P., MCKENZIE, N.J., & CLOVER, M.R. (2007) Interpreting soil and topographic properties to conceptualise hillslope hydrology. *Geoderma* 137, 279-292.
- TROMP-VAN MEERVELD, H.J. (2004) Hillslope Hydrology: from Patterns to Processes, Ph.D. dissertation, Oregon State University, Corvallis, 270 p.
- TURNER, D.P. (1976) A study of water infiltration into soils. M.Sc. University of Natal.
- VAN HUYSSTEEN, C.W. (1995) The relationship between subsoil colour and degree of wetness in a suite of soils in the Grabouw district, Western Cape. M.Sc. Agric. Thesis, University of Stellenbosch.
- VAN HUYSSTEEN, C.W., HENSLEY, M., & LE ROUX, P.A.L. (2005) Refining the interpretation of orthic A horizons in South Africa. *Euras. Soil Sci.*, In Press.
- VAN HUYSSTEEN, C.W., Hensley, M., & Le Roux, P.A.L., Zere, T.B., & Du Preez, C.C., (2005) The relationship between soil water regime and soil profile morphology in the Weatherly catchment, an afforested area in the Eastern Cape. WRC Report No.: 1317/1/05. WRC, Pretoria.
- VAN HUYSSTEEN, C.W., LE ROUX, P.A.L., HENSLEY, M., & ZERE, T.B. (2007) duration of water saturation in selected soils of Weatherly, South Africa, *S. Afr. J. Plant & Soil*, 24:3, 152-160.
- VAN HUYSSTEEN C.W. (2013) Hydrological classification of orthic A horizons in Weatherly, South Africa. *S. Afr. J. Plant & Soil* 29(2) 101-107.
- VAN HUYSSTEEN C.W., P.A.L. LE ROUX, M. HENSLEY, & T.B.ZERE. (2013) Duration of water saturation in selected soils of Weatherly, South Africa. *S. Afr. J. Plant & Soil*, 24:3, 152-160.
- VAN TOL, J.J., LE ROUX P.A.L., & HENSLEY M. (2010 a) Soil indicators of hillslope hydrology in Bedford catchment. *S. Afr. J. Plant & Soil* 27(3) 242-251.
- VAN TOL J.J., LE ROUX, P.A.L., HENSLEY, M., & LORENTZ, S.A. (2010 b) Soil as indicator of hillslope hydrological behaviour in the Weatherly catchment, Eastern Cape, South Africa. *Water SA Vol. 36 No. 5* 513-519.
- VAN TOL J.J., LE ROUX, P.A.L., HENSLEY, M. (2012) Pedotransfer functions to determine water conducting macroporosity in South Africa. *Water Science & Technology*. 65:3, 550-557.
- VAN TOL, J.J., LE ROUX. P.A.L., & LORENTZ S.A. (2012) From genetic soil horizons to hydropedological functional units.
http://www.ru.ac.za/static/institutes/iwr/SANCIAHS/2012/documents/054_Van_Tol.pdf.
- VAN TOL J.J., LE ROUX, P.A.L., & HENSLEY, M. (2013) Pedological criteria for estimating the importance of subsurface lateral flow in E horizons in South African soils.
- WEILER M., MCDONNELL J.J., TROMP-VAN MEERVELD I.L.J.A., & UCHIDA T. (2005) Subsurface Stormflow. *Encyclopedia of Hydrological Sciences*. John Wiley & Sons, Ltd.

6.3 HYDROPEDOLOGICAL CLASSIFICATION OF SOUTH AFRICAN SOIL FORMS

“Theory development will advance if we can develop simple models (which may be caricatures of the basin system but, nevertheless, contain within them the basic properties of the actual basins), provided, importantly, that they can be verified with large-scale patterns extracted from the observed data” (Sivapalan, 2003). In order to develop simple conceptual hydropedological models (and to improve our understanding of the role of hydropedology in both the natural environment and agriculture), it is necessary to understand key hydrological processes, the impact of soil on these processes and the influence of these processes on soil formation.

This relationship between soil and water is however difficult to comprehend at hillslope or catchment scale. For example; water may drain from the soil into the rock and then return to the soil. It may also exit the soil again as return flow. Where a water table occurs in the soil it is often uncertain whether the soil is feeding the rock aquifer or *vice versa*. This interaction between soil and hydrology can be simplified by firstly studying this interaction at a pedon scale. In this section soils are divided into different soil types based on their hydrological behaviour, similar to the Hydrology of Soil Types (HOST) classification system. In HOST the soils of the UK were divided into 29 classes based on their hydrological response (Boorman *et al.*, 1995). In this section we only focus on three main response mechanisms of soils and use six years of soil moisture content measurements to support the classification. Because hydropedology is a rather young and complex subject, with relatively few quantitative measurements worldwide to verify hypotheses, we considered it wise to include only local case studies about which we have sufficient knowledge and as much quantitative information as possible.

6.3.1 Hydrology of soil types

It is hypothesized that soils can be grouped in three main hydropedological types based on their hydrological response: recharge soils, interflow soils and responsive soils. Data from the Weatherley research catchment (31°06'6"S/28°20'13"E) in South Africa (Van Huyssteen *et al.*, 2005) was used to distinguish between these soil types using the degree of water saturation (s), measured over six years. The degree of water saturation is the volume of water relative to the (f) (Hillel, 1980). Porosity can be calculated using equation 7.13 and the degree of water saturation as:

$$s = V_w \div V_f \quad (6.3)$$

Where s is the degree of saturation (as fraction), V_w is the water content ($\text{mm}^3 \text{ mm}^{-3}$) and V_f is the total pore volume ($\text{mm}^3 \text{ mm}^{-3}$). Complete saturation ($s = 1$) is seldom reached since air is usually trapped in pores by water (Hillel, 1980). The drained upper limit (DUL), i.e. the water content below which drainage due to gravity virtually ceases is expected to be around 0.65 in most soils.

The term “annual duration of degree of water saturation above 0.7 of porosity” ($AD_{s>0.7}$) is the first approximated threshold value for the onset of reduction (Van Huyssteen *et al.*, 2005). The degree of saturation before the start of reduction will however differ between areas, soil forms and horizons since numerous factors influence redox conditions in soils. It

is because redox reactions of significant extent in soils leave well defined morphological footprints, e.g. mottling and/or grey colours, that $AD_{s>0.7}$ is considered to be a useful parameter in hydropedological studies. $AD_{s>0.7}$ was measured in days per year. The mean annual duration in days of events with $s>0.7$ ($D_{s>0.7}$) was calculated as follows (Van Huyssteen *et al.*, 2005):

$$D_{s>0.7} = AD_{s>0.7} \div F_{s>0.7} \quad (6.4)$$

Where $F_{s>0.7}$ is the mean annual frequency of events where $s>0.7$ (events year⁻¹).

Soils were classified according to Soil Classification – A taxonomic system for South Africa (Soil Classification Working Group, 1991) although equivalent classification accordance with WRB (IUSS Working Group WRB, 2006).

173.2 Recharge soils

Several soils in the Weatherley catchment qualify as recharge soils. The average annual duration of saturation above 0.7 of porosity ($AD_{s>0.7}$), expressed as a % of 365 days, is not significant in these soils (Figure 173) as conditions near saturation only occur when drainable water accumulates. The short degree of saturation in the subsoil shows that water draining through the soil exits the solum to enter the fractured rock underneath.

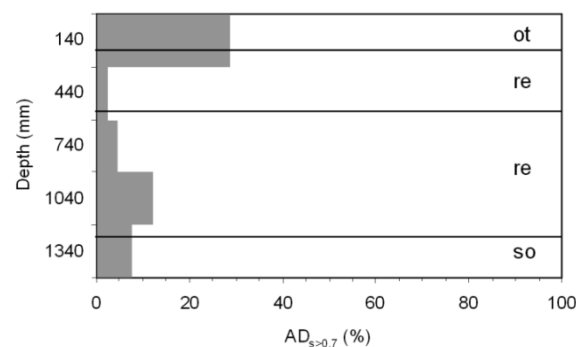


Figure 173 Mean $AD_{s>0.7}$ (%) values in a typical recharge soil: P221, Hutton 2100 (WRB – Orthidistic Cambisol), Weatherley (after Van Huyssteen *et al.*, 2005)

In recharge soils, the hypothesis is that dominant flow direction is vertical. These soils typically occur on the crest or midslope positions on hillslopes with gentle slopes. Precipitation infiltrates the soil and water flows vertically through the pedon under gravitational forces. The underlying permeable bedrock facilitates infiltration of water. From a hydrological perspective the formation and distribution of recharge soils is therefore dependant to a large extent on the permeability of the underlying material. Depending on the nature of the underlying material the infiltrated water can either recharge regional water tables directly, or in the case of aquicludes or aquitards, move laterally after leaving the soil. This lateral moving water can then recharge the stream through transient or perennial groundwater. Its contribution to transient groundwater may be uncertain. Since these flowpaths through the bedrock are usually the longest, recharge soils are important for generating base flow. Recharge soils show no evidence of saturation in any part of the profile. The annual rainfall and potential evapotranspiration should however be considered when classifying a soil as a recharge soil. In arid areas, precipitation is insufficient for

redoximorphic features to form and the soils would be classified as recharge soils based on morphological properties even though they are not *freely drained*.

The contribution of recharge soils to catchment hydrology by implication stops when the soil water balance is negative (i.e. $ET > P$). This limits its activity to the wet part of the rain season (Figure 174). Three phases are clearly visible in the graph namely a wetting up cycle with the start of the rain season, a wet phase during the rainy season and a drying phase in the waning portion of the rain season. The drying phase is only stopped by the start of the wetting up phase of the following rain season or when the water content is lower than the lower limit of plant available water.

The wetting up cycle depends on the precipitation, atmospheric demand (ET) and the size of the reservoir. As the grass vegetation of the Weatherley catchment mainly extracts its water from the upper 900 mm (Zere, 2005) of soil, a relative large volume of soil has to be brought to drained upper limit (DUL) before draining starts. In the majority of years (four out of six) this cycle is two weeks in duration. In the wet cycle the water content of the recharge soils depends mainly on the distribution of rainfall events. Profile water exceeding DUL drains beyond reach of the grass roots.

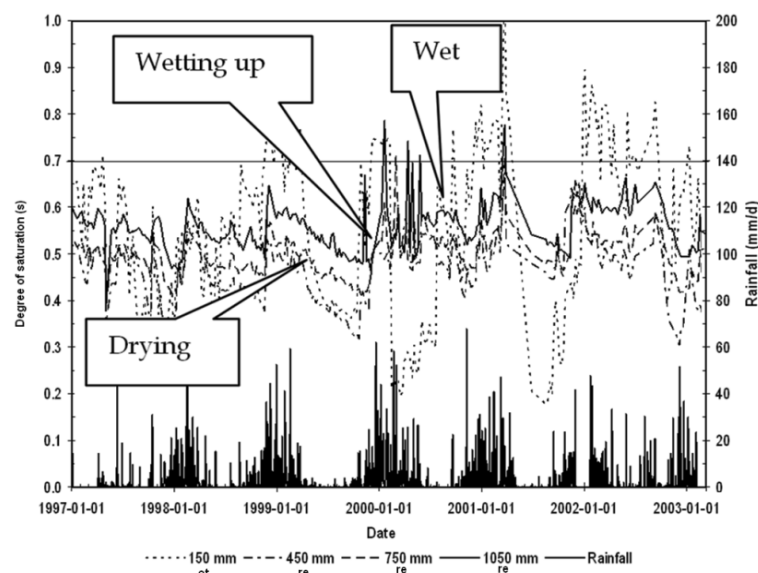


Figure 174 Degree of saturation vs. rainfall over 6 years of a recharge soil: P221, Hutton 2100 (WRB – Orthidistic Cambisol) in the Weatherley catchment (after Van Huyssteen *et al.*, 2005)

2.1.2 Interflow soils

The ($AD_{s>0.7}$) values in the subsoils of interflow soils is distinctive (Figure 175). Conditions of water contents near saturation (drainable water) occur in all horizons but typically increase with depth. Interflow soils are associated with subsurface lateral flowpaths. For interflow to occur a layer with lower hydraulic conductivity must be present (B horizon or bedrock with restricted permeability) as well as a slope favouring lateral movement down the slope. Interflow soils are therefore typically found in midslope positions with fairly steep gradients. Water starts moving laterally when infiltrated water encounters a layer with lower hydraulic

conductivity (A/B horizon interface; soil – bedrock interface or a saturated layer) or when water, fed from upslope recharge soils, encounters such a layer and may return to the soil.

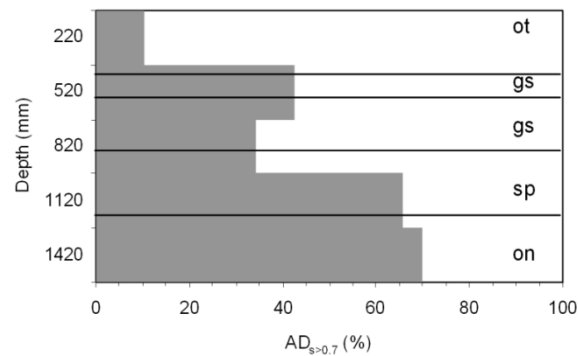


Figure 175 Mean ADs>0.7 (%) values in a typical interflow soil: P225, Longlands 1000 (WRB – Ferric-Endoeutric Albeluvisol) in the Weatherley catchment (Van Huyssteen *et al.*, 2005)

Interflow soils have in contrast with the three phases of recharge soils, a distinctive drainage phase, above DUL (Figure 176). The duration of ADs>0.7 in the soft plinthic (sp) horizon of $\pm 67\%$, i.e. 244 days or 8 months (Figure 175) is an indication that this soil body generally releases water up to the end of August. This implies a 5 month draining phase, i.e. stretching from the end of the rain season (early April) to the end of the dry season in August.

During the wet phase losses of water by drainage and ET are sometimes slower than additions of water by precipitation, and interflow results in a rise of the transient groundwater into the plinthic, E and A horizons. Such a fluctuating water table is typical of subsoils with plinthic and E horizons (Soil Classification Working Group, 1991). These fluctuations are event driven and can be related to rainfall events. The catchment must first fill up before transient groundwater can occur.

Sub soil flowpaths are associated with a residence time shorter than the bedrock flowpaths and longer than overland flow. Interflow soils would therefore contribute mainly to the shoulder of the hydrograph, and to some extent to baseflow. Interflow soils normally have morphological indications of periodic saturation in the profile. If dominant flow exists on the A/B horizon interface, eluvial horizons form. These horizons show marked removal of colloidal material and organic matter. When interflow occurs at the soil/bedrock interface, the transitional horizon usually show indications of periodic saturation.

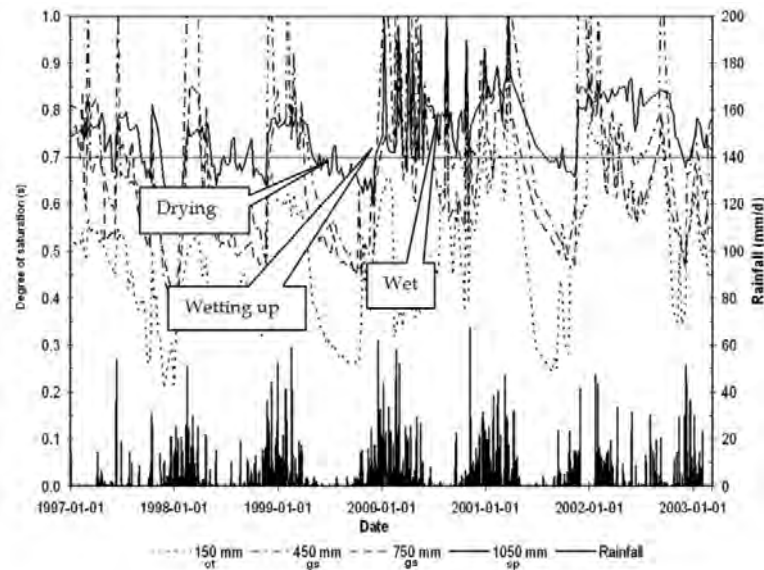


Figure 176 Degree of saturation vs. rainfall over 6 years of an interflow soil: P225, Longlands 1000 (WRB – Ferric-Endoeutric Albeluvisol) in the Weatherley catchment (after Van Huyssteen *et al.*, 2005)

Responsive soils

Responsive soils can either be very shallow soils with low infiltration capacity, saturated soils which prohibit water infiltration or soils prone to form crusts resulting in low infiltration rates and generating *Hortonian* overland flow. In the Weatherley catchment responsive soils generate overland flow due to saturation excess. The overland flow component contributes to peak flow as the first part of the peak of the hydrograph. The influence of the water content of the topsoil on the generation of overland flow is illustrated in Figure 177. The results show that overland flow only becomes significant when the topsoils are close to saturation. Overland flow from responsive soils is therefore expected in the wettest positions in landscapes, i.e. valley bottoms and wetlands. In the Weatherley catchment these soils are at or near saturation for long periods (Figure 178), resulting in conditions called saturation excess overland flow in the rain season.

Due to long periods of saturation the subsoil (*gh* horizon) lacks an obvious wetting and draining phase since it is saturated or close to saturation throughout the year. Only the topsoil horizon loses water to ET during the dry season (Figure 179). In order for these subsoils to remain saturated for such long periods under incessant ET demand there needs to be a constant supply of water. It is hypothesized that the recharge soils of the upper slopes supply water to the responsive soils via the bedrock flowpath and to a lesser extent through interflow.

Relating catchment hydrology to the hydropedology of land types using master recession curves

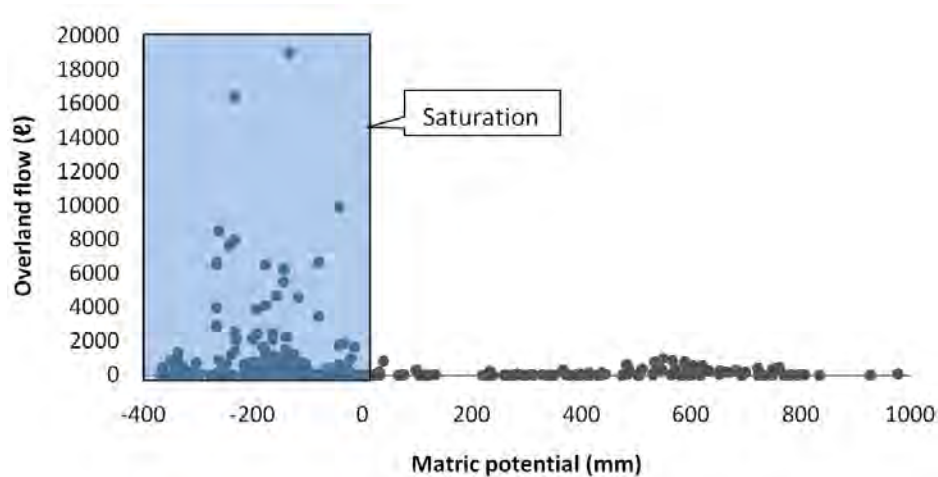


Figure 177 Volume of overland flow measured at five runoff plots vs. topsoil matric potential in the Weatherley catchment

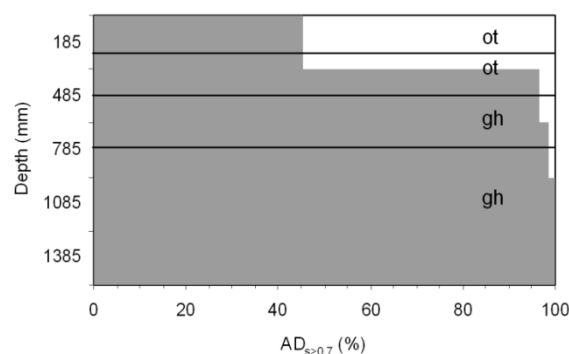


Figure 178 Mean $AD_{S>0.7}$ (%) values in a typical responsive soil: P235, Katspruit 1000, (WRB – Hyperdistic Gleysol) in the Weatherley (Van Huyssteen *et al.*, 2005)

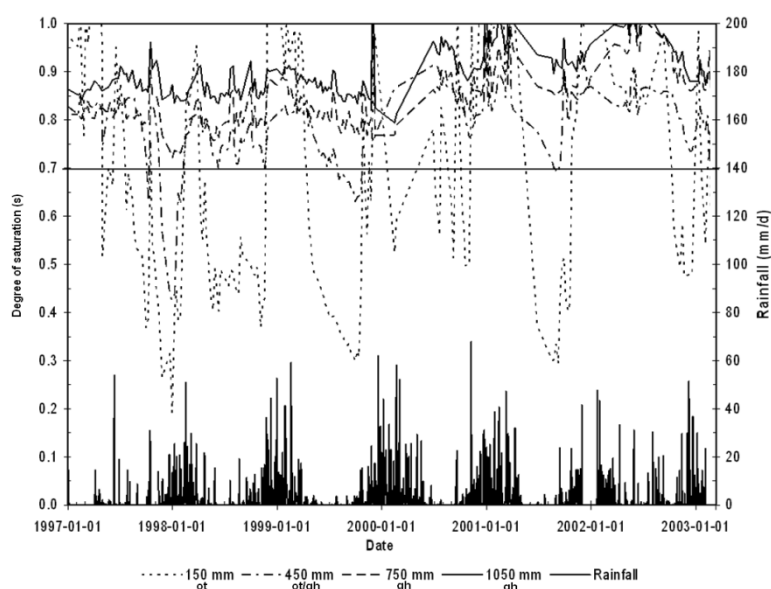


Figure 179 Degree of saturation vs. rainfall over 6 years of a responsive soil: P235, Katspruit 1000, (WRB – Hyperdistic Gleysol) in the Weatherley catchment (after Van Huyssteen *et al.*, 2005)

6.3.2 Introduction

Water is a precious renewable resource that all life depends on. In semi-arid areas, groundwater is an excellent store of water and serves as a natural resource, which needs to be managed. Determining and managing groundwater recharge are challenging as rain water splits several times after making contact with the earth, with every split resulting in a different path of flow with its own direction, rate and volume of flow. The number and nature of flowpaths form a complex network barely measureable in the earth's various layers. Calculating recharge of soil, fractured rock and groundwater is therefore to a large extent dependant on the conceptual understanding of the system.

Groundwater is for several an excellent store of water and serves as a natural resource. Giving all the various flowpaths, the main problem is the rate at which this resource gets renewed. Groundwater is widely used not only for farming but also for industry, residence, mining, etc. All these uses rely on groundwater to be replenished through groundwater recharge, to ensure water for future use.

Researchers have defined groundwater recharge in various ways. Parsons (2004) defined recharge as "the addition of water to the zone of saturation either by the downwards percolation of precipitation or surface water and / or the lateral migration of groundwater from adjacent aquifers." The definition given by Price (1985) for recharge was the precipitation that reaches the water table, as it helps to refill the source of groundwater. Recharge was defined by Harvey (n.d.) as "essentially the amount of water left over after all of the surface and near surface processes impacted the water."

However these definitions are mainly based on groundwater recharge and are therefore vague. Recharge can be subdivided into topsoil/surface recharge, pedo-recharge, vadose zone recharge and groundwater recharge (as defined above). Topsoil/surface recharge occurs in small rain events which result in only wetting of the topsoil. In larger rain events where the whole soil profile becomes wet, it refers to pedo-recharge. The vadose zone recharge refers to the whole vadose zone receiving water from a rain event.

Meulenbeld (2007) stated: "The problem with nature is that it operates in a closed loop system. Everything is connected" To understand the groundwater recharge process one needs to grasp the whole hydrological cycle and all the factors involved. The main factors involved in the hydrological cycle, especially in groundwater recharge includes climate, topography, geology (parent material) and soil. These factors can be further divided and will be discussed in more detail later. The combination of these factors entails that an inter-disciplinary effort is needed to understand the whole process at works. Meulenbeld (2007) stated that it "involves the disciplines of soil scientists, geologists, meteorologists and botanists." Dippenaar and van Rooy (2013) agree with Meulenbeld by emphasising the importance in using a multi-disciplinary approach for acquiring and interpreting data.

In South Africa, groundwater dominantly occurs within secondary aquifers resulting in more than 90% of the surface. These aquifers include groundwater found in fractures, such as faults and joints, within hard rocks and pores in weathered zones along with limestone and dolomite lithology (Meulenbeld, 2007). Potential groundwater recharge zones are defined by van Wyk (2010) as fractured hard rock 'windows' with a lack in soil cover which permits direct infiltration of recharge-producing surplus rainfall into the underlying aquifer.

Vadose zone is defined as the portion above the groundwater table. This includes soil, rock and vegetation, which all influences the groundwater recharge through the vadose zone.

This section will focus on laying the background understanding groundwater recharge, by looking at the factors which influence it.

6.3.3 Factors controlling groundwater recharge

The environment is influenced by various factors which results in different scenarios occurring. These scenarios play a role on the hydrological cycle and therefore on groundwater recharge as well. The main factors include Geology, Climate, Topography and Soil, however each factor affects the other factors and therefore making it a complex system. Each factor can be further subdivided and will be discussed in detail to follow.

Geology

Geology is generally defined as the study of the solid earth, which includes a variety of sub topics. However the focus will be more on the lithology and its role in within the vadose zone. The geology, also known as parent material, is considered a very important variable, due to its ability to determine the soil chemical and physical constituency. It controls the water flow within the lower vadose zone as well as the aquifer space. Water movement and groundwater recharge can be limited by a layer present below the soil that may be considered permeable or impermeable to water. Lithology is defined as the description of the macroscopic features of a specific rock type (Kearey, P. 2001).

Geology is generally divided into 3 rock types namely Sedimentary, Igneous and Metamorphic rocks. Sedimentary rocks mainly forms through the hardening of sediment near or on the surface while Igneous rocks form from magma or lava. Metamorphic rocks is the result of any rocks which has undergone metamorphism due to a change in pressure and/or temperature resulting in an alteration occurring physically or/and chemically.

Water association within rocks are mainly based not only on the rock's porosity, but also its joint and fracture systems. The aperture and spacing of bedrock fractures and also the thickness and hydraulic conductivity of the soil cover needs to be taken into account as vertical flow of groundwater is considered to be dependent on these factors (Gleeson *et al.*, 2009). Fractures in hard rock are most likely to be filled with soil and or vegetation and this may lead to the restriction of infiltration and water flow in these fractures (Stander, 2011). Thus it may lead to increased overland flow and interflow and therefore reduce the groundwater recharge in that area. If we can predict the joint and fracture systems of the underlying rocks, we will be able to deduce where water availability will be the highest and where the associated pathways and storage lies.

Sedimentary rocks originate mainly from weathered material which becomes hardened by a process called lithification. This occurs at low temperatures and pressures near or on the earth's surface. Sedimentary rocks are usually bedded and vary in compositions and texture due to different depositional conditions. There are a great variety of sedimentary rocks however the main four are sandstones, shale, limestone and dolomite. Clastic sedimentary rocks are rocks which are formed by the weathering of pre-existing rocks, transported, deposited and then cemented together. Examples include sandstone, shale, conglomerate, etc. Non-clastic sedimentary rock forms in the same place where it weathers, usually in lakes or pans to form 'chemical' deposits such as dolomite or limestone. The general fracture system for sedimentary rocks tend to be parallel to the bedding planes, however a problem with interpreting the fracture system is encountered with sedimentary rocks

without bedding planes such as sandstone as shown by Figure 180 below. More information is then needed to explain their fracture systems.



Figure 180 Alternating layers of sandstone and mudstone controlling groundwater recharge and its flowpaths

Igneous rocks are formed from silicate melt or magma below the soil surface or from lava above the soil surface. They can therefore be classified into three main groups namely plutonic/intrusive rocks, extrusive rocks and dyke rocks. Most common igneous rocks include granite, basalt (Figure 181), and dolerite (Figure 182). The fracture system of igneous rocks are quite complex however the cooling joint is most common in igneous rocks.



Figure 181 Basalt with pipe amygdales showing its lack in fractures resulting in the hampering of water flow



Figure 182 Dolerite with its complex fracture system which may or may not allow water flow

Metamorphic rocks are the result of alterations to existing rocks (sedimentary, igneous or metamorphic), either physically or chemically, due to a change in temperature and/or pressure. Metamorphism usually takes place in considerable depth which results in minerals becoming unstable leading to the formation of new minerals. The main metamorphic rocks include gneiss, schists, slate, quartzite and breccia.

Climate and Vegetation

Climate mainly includes the processes and properties of precipitation and vegetation. Precipitation is considered as rain, dew, hail, etc. and can vary in time and space. This variation allows it to control various other processes within the other factors, such as leaching in soils for example, and this is why it is so important to take it into consideration in groundwater recharge. Precipitation also acts as the main source of water for groundwater recharge to occur.

Vegetation plays a very important role in water movement and groundwater recharge considerations. However it is controlled by climate (precipitation/evaporation), soil, topography and geology. Climate controls the type of vegetation which will occur where soil and geology will do the same in reference to the nutrient availability and depth available for root development. Topography regulates the amount of vegetation as vegetation struggle to grow on steep slopes and will rather grow on the crest and towards the valley bottom of a hill slope.

When considering water movement, overland flow and evaporation increases with a decrease in vegetation due to more of the surface being exposed and nothing to restrict water flow to allow infiltration. When considering evapotranspiration (ET) the larger vegetation, such as trees, increases ET as their roots penetrate much deeper than grass and small shrubs. The growth stages of the plants in reference to agriculture are considered as an important factor due to the plant's/crop's use different amounts of water depending on their stage of growth. Seasons play a role in the water use of vegetation as the different types of vegetation undergoes diverse reproductive periods. This also influences the water usage of the vegetation and its ET demand, therefore influencing the amount of water left for groundwater recharge.

The aridity index can be explained as a function of precipitation, temperature and/or evapotranspiration. Therefore it is defined as the total precipitation over the atmospheric demands (Figure 183). For instance, when precipitation in an area is high, but the ET is also high, the aridity index will be low and less water will infiltrate into the soil to become groundwater recharge and more water will be released into the atmosphere (Allen *et al.*, 1998).

Topography

Topography refers to the study of surface shape and features. It specifically involves the recording of terrain or relief, the three-dimensional structure of the surface and the identification of specific landforms.

Topography has a direct influence on water movement due to gravity and it determines the general direction of groundwater flow, where other factors may also play a role within the landscape (Figure 184).

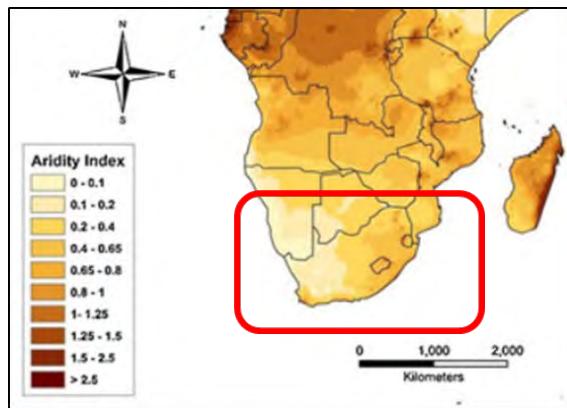


Figure 183 Aridity Index for South Africa (Zomer *et al.*, 2008)

Properties of a slope may include orientation, slope angle and length. The orientation of a slope will influence evaporation due to the sun's inclination and intensity in certain times of the year. For example the in the Southern hemisphere northern facing slopes will generally be warmer than southern facing slopes, and therefore have higher ET.

The higher the angle of a slope the faster water movement will occur, thus overland flow will generally be higher at slopes with higher angles. However this is also dependant on soil and vegetation cover. The slope length can influence the ground water locality and the distance the water, especially interflow water, need to travel before groundwater recharge.

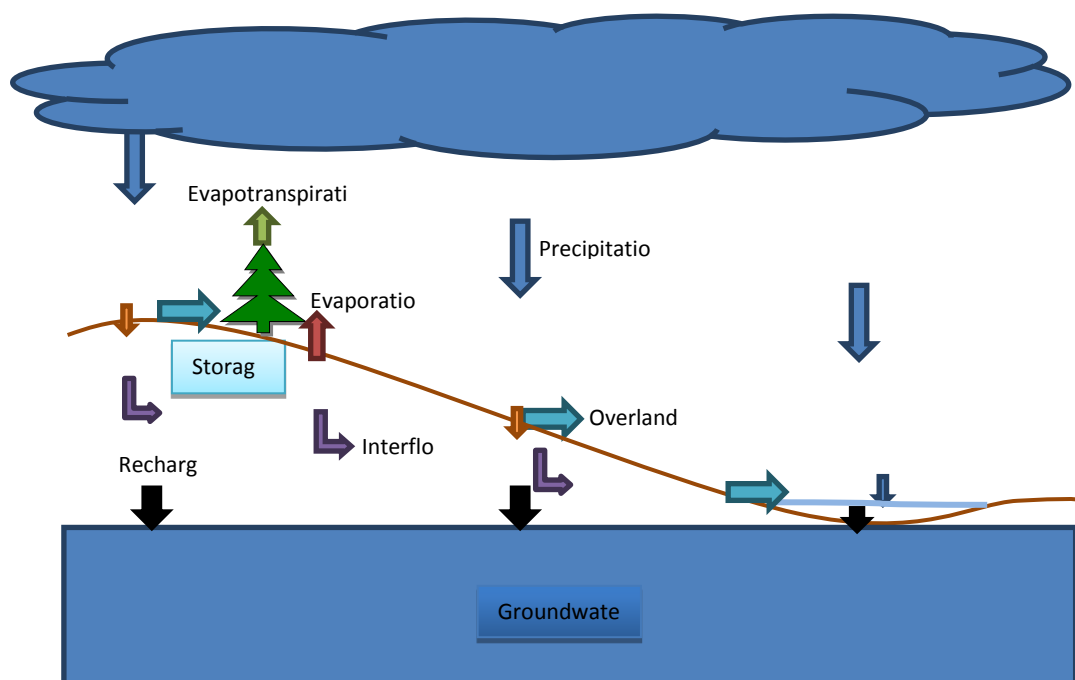


Figure 184 Processes regulating water flow

Soil

“Soil and local topography must inevitably be of dominating importance in all catchments since all the water that reaches the stream must either pass over or through the soil at some stage” (Le Roux *et al.*, 2011).

Soil acts as the transport median between the surface water and the groundwater. Water movement in soils are mainly caused by the force of gravity, capillarity and osmosis. Infiltration of water into the soil is controlled by various factors which include soil texture, agricultural impact (soil crusting), soil structure, soil temperature, the amount of organic matter and water already present in soil, and the depth of the soil to an impermeable layer. Different soil horizons are divided into five topsoil horizons and twenty-five subsoil horizons (Soil Classification Working Group, 1991). Topsoil horizons include Organic O, Humic A, Vertic A, Melanic A and Orthic A. Not all subsoil horizons will be discussed as it will be too much and therefore only a few of the horizons will be conversed in respect to their hydrological properties.

Soils with G horizons are considered to be waterlogged and will typically be found in the valley bottom. It occurs within the Katspruit, Willowbrook, Rensburg and Kroonstad soil forms. They are considered as wetland soils (Van Tol *et al.*, 2010). The long periods of waterlogging is shown in the soil morphology by gleying and mottles. Vertical upward flow commonly dominates in this horizon when wet.

The E horizon is a typical bleached horizon showing high water movement which results in leaching of materials from the horizon. It is characteristically found on the bottom of the slope just before the valley bottom. Lateral flow dominates within this horizon.

Soft plinthic horizons form in the presence of a fluctuating water which is indicative of a fluctuating water table on an impermeable layer underneath. Soft plinthic is a horizon with more than 10% mottles which shows alternating periods of oxidation and reduction known as redox morphology. Therefore vertical water movement mostly dominate in the horizon.

The Red Apedal B horizon is a horizon which is usually freely drained However may be influenced if there is an impermeable layer present below it. This horizon is considered as a groundwater recharge horizon as water percolates vertically through this horizon with considerable ease towards the lower horizons. Dependant on the nature of the lower horizons, this water will recharge the groundwater.

Saprolite as well as lithocutanic horizons usually display a very good porosity (depending on parent material) and acts as a good pathway for water movement down the profile. They consist of a lot of fractures which aids in the water movement.

Hard rock is discussed in detail in the geology section as it describes the different rock types and their affinity for water and their relative porosity or fracture systems.

Soil is classified into different soil forms depending on the sequence of diagnostic horizons that follow each other in the soil profile (Le Roux *et al.*, 2013). For example a Hutton soil form consists of an Orthic A horizon on a Red Apedal B horizon on unspecified material. This soil form has a high infiltration rate and water flow will be unrestricted because of the high flow rates through the Red Apedal B horizon. On the other hand a Katspruit soil form is the opposite of the Hutton soil form with regards to hydrology, as it has a low infiltration rate and the G horizon holds onto the water as storage.

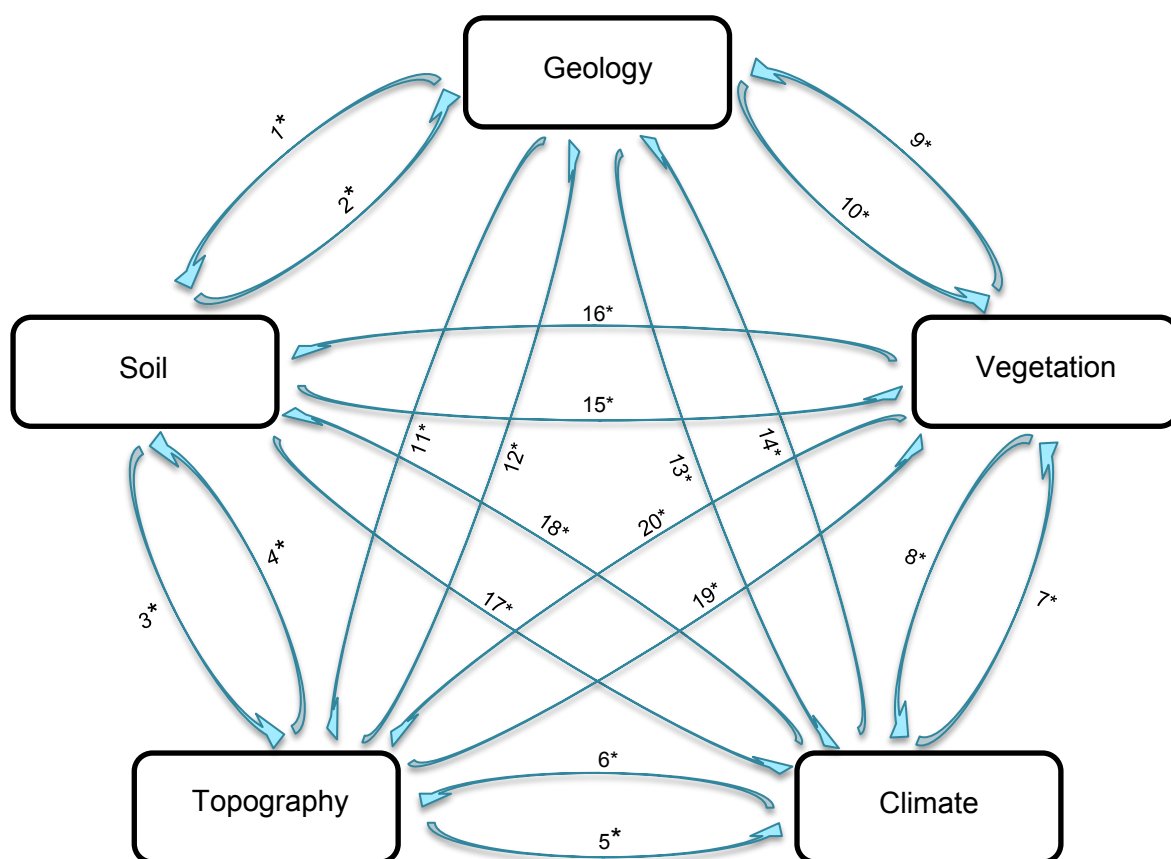
Van Tol *et al.* (2010) classified soil forms into the categories of recharge, interflow and responsive soils. These Classifications where based on the degree of saturation and their hydrology.

6.3.4 Interaction in vadose zone

The environment is a complex system that works through various factors influencing each other. Most of these interactions occur within 'cycles' that repeat over time. The study of these interactions provides valuable information on different processes which may result in the enrichment of our knowledge and everyday life.

Geology plays a large role on topography, soil and therefore on vegetation as well. Climate controls the type of weathering, the soil type and the nature and density of the vegetation. This indicates the complex relationship between the factors and that in reality there exist an interconnected 'network' between the different factors which is represented in Figure 185.

Land type data involves a soil survey done for South Africa providing data on soil profiles their properties and using this data together with geology, climate and topography data, one can determine potential groundwater recharge areas. Using selected catchments one can combine all the factors to determine the effect they cause on each other and formulating a way to predict the optimal combination of factors or groundwater recharge zones. An example may include a recharge soil, e.g. Hutton soil form, upon an extremely physically fractured dolerite with limited shallow rooted vegetation, which may result in a recharge zone.



*Described below

Figure 185 Interactions between the factors of vadozone hydrology

Description of Figure 185 is as follows:

1* – Geology act as parent material for soils which gives rise to properties and distribution of soils which relate to the specific lithology present. Depending on the type of geology and its depth below the soil, it may act as a permeable/impermeable underlying layer which influence water interflow to soils and therefore may contribute to which soil processes will dominate.

2* – Soil also, in return, acts as parent material for sedimentary rocks as discussed in previous section of geology, where predictable properties are found within the rocks. Soil is considered as a cover that store water and increase weathering at the contact with the rock.

3* – Soil influence topography through the process of back weathering and inducing rock/soil/surface interflow.

4* – Topography influence the erosion soil thickness depending on the position on the slope. The Soil type is influenced according to the hydrosequence, where areas of increased interflow cause higher chemical weathering.

5* – The orientation of a slope may influence the climate as discussed in previous section. This is due to different inclination of the sun in different seasons, e.g. in southern hemisphere the southern facing slopes are generally warmer. The height above sea level has an influence especially on temperatures and wind due to different behaviour of hot and cold air.

6* – Climate controls type and intensity of weathering and erosion within topography. Physical weathering dominates in arid regions with steep slopes and concave crests, where chemical weathering will tend to dominate in semi-arid regions and wetter.

7* – Climate, together with soil, controls the type of vegetation as well as the density of the vegetation.

8* – No known influence

9* – No known influence

10* – Geology supplies nutrients and therefore affects the nutrient availability. Depending on the depth at which the rock occurs it may restrict or allow root development.

11* – Geology defines the landscape (topography) depending on the type of rock and the rates at which it weathers, e.g. Table landscapes vs. granite landscapes.

12* – No known influence

13* – No known influence

14* – Climate affects the rate and type of weathering which affects the geology.

15* – Soil affects vegetation type and density as it controls properties such as nutrient content, pH, water content and other chemical properties. Therefore certain soil conditions favour specific vegetation types.

16* – Vegetation can influence soil properties such as increase organic matter, increase structure due to roots and microbial activity, etc. this leads to an increase in nutrient availability. A well-known example is the Podzols soils which form from specific vegetation (fynbos) due to their organic matter and their unique effects.

17* – Soil may influence the climate through the fixation or release of carbon in or from the soil. Carbon release may occur with the oxidation of soils high in organic matter. This may attribute to the global warming affect and therefore act as air pollution.

18* – Climate influences soil in various ways which all cannot be discussed. The main influences may be the driving soil processes in soil which results in different and unique soil properties which allows for soil to be classified.

19* – Topography influence the density of vegetation on slopes, as the vegetation decreases with an increased slope. Topography plays an important role in the hydrology in the landscape which controls the water availability for plants.

20* – No known influence

6.3.5 Soil distribution pattern as a window to soil/rock/soil interaction in hillslopes

Soil and geology makes up the vadoze zone and for this reason these factors will be the main focus. They control and facilitate hydrological controlled flow.

Soil originates from the interaction between water and Parent material (rocks). This leads to soil type being a product of the specific parent material and hydrological conditions. The physical role of soil in hydrology is well known, however the role of soil as indicator of soil/rock/soil interaction is generally neglected.

Rocks acts as parent material, as discussed above, and therefore together with distinct hydrological processes give rise to certain properties within the soil product. This is illustrated by the unique distribution of soil types, known as 'Land types', and geology links up perfectly with this distribution pattern.

Studying the link between the geology and soil distribution will lead to a large understanding in the hydrology active due to the interaction between the two factors within the vadoze zone.

Kuenene & Le Roux, 2011 studied an Ingula soilscape in the Free State and this has been used as an example to describe land types with permission of co-author (see Figure 186, Figure 187 and Figure 188).

Land types are areas that are classified into groups due to their unique characteristics (Figure 186). They are used in various practices such as agriculture, soil science, environmental sciences, etc.

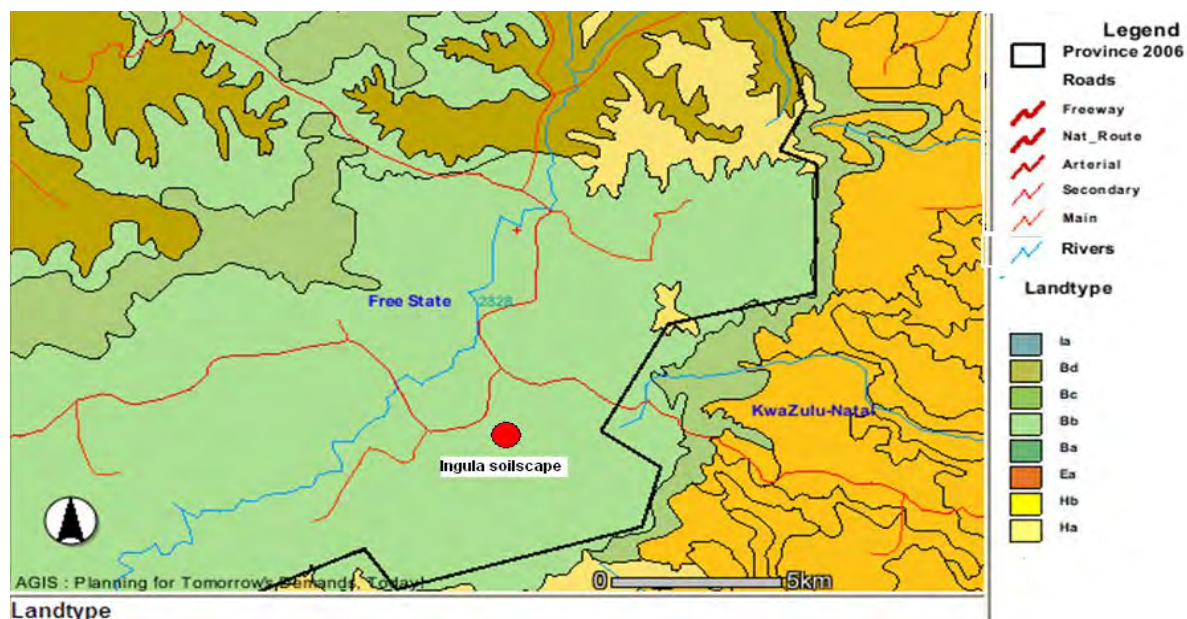


Figure 186 Land type data for Ingula in the Free State (Kuenene & Le Roux, 2011)

| | | | |
|-------------------------------------------------|----------|----------------------------------------------------------------|-----------------------------------|
| LAND TYPE / LANDTIP | Bb122 | Occurrence (maps) and areas Poorkoms (kaarte) en oppervlakte : | Inventory by Inventaris deur : |
| CLIMATE ZONE / KLIMAATSONE | 835 | 3828 Harrismitsh (33012 ha) | R. W. Bruce & J. L. Schoeman |
| Area / Oppervlakte | 33012 ha | | Modal Profiles / Modale profile : |
| Estimated area unavailable for agriculture | | | None / Geen |
| Beraamde oppervlakte onbeskikbaar vir landbou : | 1500 ha | | |

| | | | | | | |
|---------------------------------------------|---------|-------|----------|---------|--------|-------------------------|
| Terrain unit / Terreinseenheid | 1 | 2 | 3 | 4 | 5 | |
| % of land type / % van landtipe | 22 | 3 | 57 | 8 | 10 | |
| Area / Oppervlakte (ha) | 7263 | 990 | 18817 | 2641 | 3301 | |
| Slope / Helling (%) | 0-6 | 0-100 | 4-35 | 1-5 | 0-5 | |
| Slope length / Hellinglengte (m) | 200-500 | 10-50 | 300-1000 | 100-100 | 50-700 | |
| Slope shape / Hellingvorm | Y | Z | Y-X | X | Z-X | |
| MB0, MB1 (ha) | 5727 | 0 | 15618 | 2641 | 3126 | Depth limiting material |
| MB2 - MB4 (ha) | 1525 | 990 | 3199 | 0 | 165 | |

| | | | | | | | | | | | | | | | | | | | |
|-----------------------------------------------------------------|------------------------|-----------|-----------|----------|-----------|----------|-----------|----------|-----------|----------|------------------------|----------------------------------------|----------------------------|------------------------------------|----------------|--------------|-------|----------------|-------|
| Soil series or land classes Grondseries of landklasse | Depth Diepte | MB | ha | % | ha | % | ha | % | ha | % | Total Totaal | Clay content % Klei inhoud % | Texture Tekstuur | Diepte-beperkende materiaal | | | | | |
| Rock / Rots | 4 | | 73 | 1 | 663 | 87 | 376 | 2 | | | 1113 | 3.4 | | | | | | | |
| Outdale Cvl6, Clovelly Cvl7 | 600-1200 | 0 | 3777 | 52 | | | 9408 | 50 | | | 13185 | 39.5 | 15-35 | 20-45 | B | SSeCILm-SaCl | so | | |
| Ruston Avl6, Normandien Avl7, | | | | | | | | | | | | | | | | | | | |
| Ouwert Pul6, Kilbuck Pul7 | 800-1200 | 0 | 1961 | 27 | | | 5645 | 30 | | | 7606 | 23.0 | 15-30 | 20-40 | B | SSeCILm-SaCl | sp-gr | | |
| Williamson Gul6, Mispah Ms10 | 100-450 | 3 | 1207 | 18 | 327 | 33 | 2634 | 14 | | | 4268 | 12.8 | 18-25 | A | SSaCILm | so-R | | | |
| Rosemead Etl5, Dohne Etl3 | 250-500 | 0 | | | | | | | 1637 | 62 | 330 | 10 | 1965 | 6.0 | 12-25 | 35-55 | E | SSaCILm-SaCILm | pr |
| Dundee Du10 | 1000-1200 | 0 | | | | | | | 1650 | 50 | 1651 | 5.0 | 15-30 | A | SSaCILm-SaCILm | so-R | | | |
| Armiston Va31, Chabumna Va32, | | | | | | | | | | | | | | | | | | | |
| Herschell Va30, Swartland Sw31, | | | | | | | | | | | | | | | | | | | |
| Hogsback Sw92 | 200-450 | 0 | | | | | 188 | 1 | 607 | 23 | 165 | 5 | 961 | 2.8 | 18-30 | 33-60 | B | SSaCl-CI | vp |
| Glenagat Bo31, Dumasi Bo30 | 400-000 | 0 | | | | | | | 158 | 6 | 000 | 20 | 119 | 2.3 | 23-43 | 30-55 | A | SSaCILm-SaCl | vp |
| Jozini Oa36 | 800-1200 | 0 | | | | | 188 | 1 | 132 | 5 | 330 | 10 | 650 | 2.0 | 18-30 | 25-35 | D | SSaCILm | so-R |
| Mayo My10, Meintini My11, | | | | | | | | | | | | | | | | | | | |
| Dansland Mw10, Milkwood Mw11 | 200-400 | 3 | 145 | 2 | | | 188 | 1 | | | 333 | 1.0 | 25-40 | A | SSaCILm-SaCl | so-R | | | |
| Waldene Lo12 | 300-1000 | 0 | | | | | 188 | 1 | 100 | 4 | | | 294 | 0.5 | 15-35 | 25-55 | E | SSaCILm-SaCILm | sp-gr |
| Stream beds / Stroombeddings | 4 | | | | | | | | 165 | 5 | 165 | 0.5 | | | | | | | |

| | | |
|------------------------------------------------------|-------|------------------------|
| LAND TYPE / LANDTIP | Bb122 | Continued / Voortgezet |
| Terrain type / Terrein tipe | B4 | |
| Terrain form sketch / Terrein vormskets | | |

| | |
|----------------------|----------------------------------------------------------------------------------------------------|
| Geology | Mudstone and sandstone of the Beaufort Group, occasional dolerite sills and narrow dolerite dykes. |
|----------------------|----------------------------------------------------------------------------------------------------|

| | |
|-----------------------|----------------------------------------------------------------------------------------------|
| Geologie | Moddersteen en sandsteen van die Groep Beaufort, enkele dolerietplate en smal dolerietgange. |
|-----------------------|----------------------------------------------------------------------------------------------|

The Ingula area was studied and resulted in a hillslope model as seen in Figure 188. This figure shows the hydrology and the different flowpaths due to the soil distribution with combination of geology. These flowpaths include general recharge of the soil and fractured rocks, interflow, and return flow from the fractured rock to the soil lower down in the hillslope.

The study of the soil distribution and geology type allowed a vast knowledge of flowpaths within the hillslope which lead to the formation of a wetland. This shows that the soil and geology interaction may lead to improved knowledge of hydrology within different land types and hillslopes which will aid in the identification of high groundwater recharge zones. These zones are essential and of critical importance for the replenishment of groundwater sources.

244

to decipher the vadoze zone which involves the interaction between the soil, geology and, most important, the water.

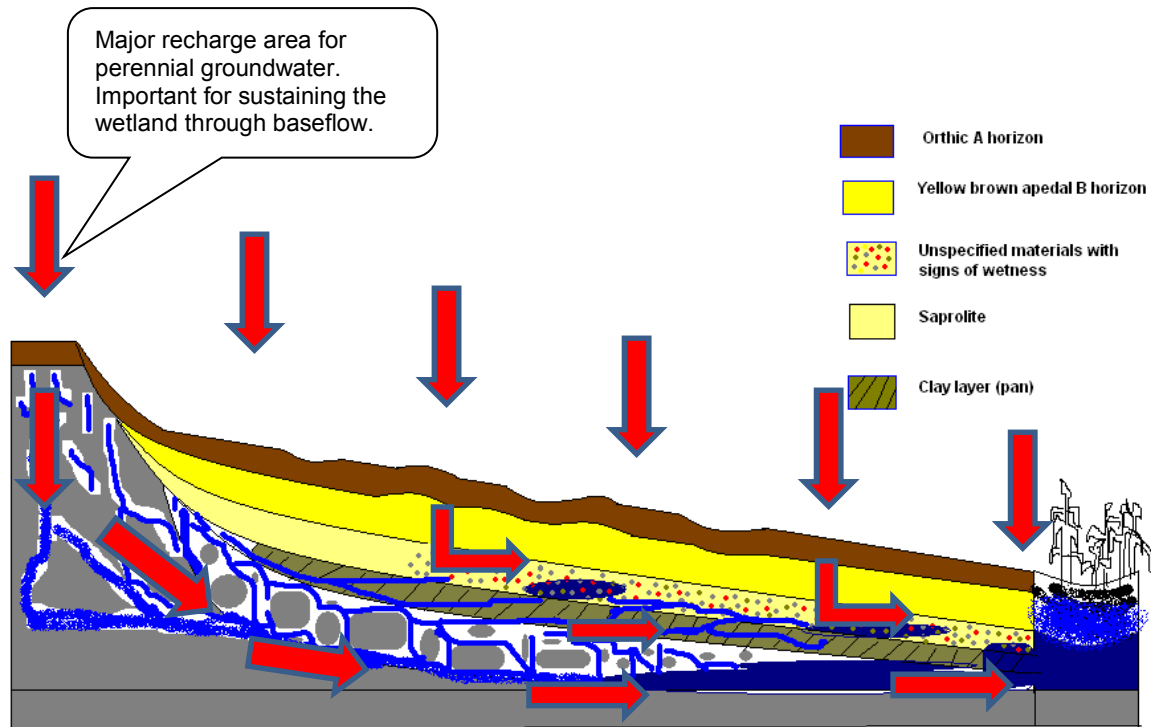


Figure 188 Conceptual hillslope hydrological behavior of Ingula soilscape. (Kuenene & Le Roux, 2011)

6.4 REFERENCES:

- ALLEN, R.G., L.S. PEREIRA, D. RAES, AND M. SMITH. 1998. Crop evapotranspiration: Guidelines for computing crop water requirements. FAO Irrigation and Drainage Paper 56. FAO, Rome.
- DIPPENAAR, M.A., VAN ROOY, J.L., 2013. Review of engineering, hydrogeological and vadose zone hydrological aspects of the Lanseria Gneiss, Goudplaats-Hout River Gneiss and Nelspruit suite Granite (South Africa). *Journal of African Earth Sciences*, 91 (2014): 12-31.
- GLEESON, T., NOVAKOWSKI, K. & KYSER, K., 2009. Extremely rapid and localized recharge to a fractured rock aquifer. *J. Hydrol.*, 378(3-4):496-509.
- HARVEY, F. E., n.d. Groundwater Recharge. <http://watercenter.unl.edu/Downloads/ResearchInBrief/HarveyRecharge.pdf> (Accessed 05/07/2013)
- KEAREY, P., 2001. Dictionary of geology. 2nd Ed. Penguin Reference Books, London
- KUENENE, B.T. & LE ROUX, P.A.L., 2011. Hydropedological interpretations of soils and hydrological conceptual model of Ingula soilscape. University of the Free State, Bloemfontein, South Africa.
- LE ROUX, P.A.L., DU PLESSIS, M.J., TURNER, D.P., VAN DER WAALS, J., BOOYENS, H.B., 2013. Field Book: for the classification of South African soils. Reach Publishers, Wandsbeck, SA.

- LE ROUX, P.A.L., VAN TOL, J.J., KUENENE, B.T., HENSLEY, M., LORENTZ, S.A., EVERSON, C.S., VAN HUYSSTEEN, C.W., KAPANGAZIWIRI, E. & RIDDELL, E., 2011. Hydropedological interpretations of the soils of selected catchments with the aim of improving the efficiency of hydrological models. Water Research Commission (WRC) Report No. 1748/1/10. Bloemfontein: Department of Soil-, Crop and Climate Science, UFS.
- MEULENBELD, P.M.P.B., (2007). Establishing geobotanical-geophysical correlations in the north-eastern parts of South Africa for improving efficient borehole siting in difficult terrain. Ph.D. Thesis, University of the Free State, South Africa.
- PARSONS, R., 2004. Surface Water: Groundwater Interaction in a South African Context – A Geohydrological Perspective-.Water Research Commission (WRC) Report No. TT 218/03. Pretoria.
- PRICE, M., 1985. Introducing groundwater. George Allen & Unwin, London.
- SOIL CLASSIFICATION WORKING GROUP, 1991. Soil classification: A taxonomic system for South Africa. Department of Agricultural Development, Pretoria, South Africa.
- STANDER, M.D.T., 2011. An investigation into the influence of soil pattern on preferential flow and groundwater recharge in fractured bedrock and cover sand aquifers. M.Sc. Thesis, University of Stellenbosch, South Africa. <http://scholar.sun.ac.za> (Accessed 13/07/2013)
- VAN TOL J.J., HENSLEY, M. & LE ROUX, P.A.L., 2010. Literature review on hydrology of soil types (HOST). Water research commission Project k 5/2021. Pretoria.
- VAN WYK, E., (2010). Estimation of episodic groundwater recharge in semi-arid fractured hard rock aquifers. Ph.D. Thesis, University of the Free State, South Africa.
- ZOMER, R.J., TRABUCCO A, BOSSIO, D.A., VERCHOT, L.V., 2008. Climate change migration: A spatial analysis of global land suitability for clean development mechanism afforestation and reforestation. Agric, Eco & Env. Volume 126, Issues 1-2, June 2008, Pages 67-80. <http://www.sciencedirect.com/science/article/pii/S0167880908000169#fig1> (Accessed 29/07/2013)

6.5 ELUCIDATING THE RELATIONSHIP BETWEEN RECENT (SOIL CHEMICAL AND HYDROLOGICAL) SOIL PROPERTIES AND ANCIENT (MORPHOLOGICAL) SOIL PROPERTIES AND HILLSLOPE HYDROPEDOLOGY

6.5.1 INTRODUCTION

The soil distribution pattern controls the hydrological processes such as flowpaths, residence times and storage mechanism (Soulsby *et al.*, 2006) which influence the quantity and chemical composition of the water exiting the soilscape (Jacks and Norrström, 2004). Although soil analytical data usually reported in soil surveys are originally used to design pedotransfer functions (Bouma, 1989), soil morphology, as reported in soil surveys, can also serve as a pedotransfer function to infer the hydrological response of soils (Fritsch & Fitzpatrick, 1994, Soulsby *et al.*, 2006, Ticehurst *et al.*, 2007, Van Tol *et al.*, 2010) and Kuenene *et al.*, 2011). Soil morphology data is more accessible than soil physical and hydrometrically data commonly used to determine hydrological processes within a soilscape. Gathering soil physical and hydrometric data are tedious, time consuming and often unreliable (Park and Burt, 1999). Soil morphology is a visible indicator of the interaction between water and parent material and the resultant variation indicates soil water regimes which correlates with the morphology of soils (Van Huyssteen *et al.*, 2005).

The process of soil formation is relatively long (10^2 - 10^4 years) whereas when compared to the process of pH change which is shorter (10^0 - 10^3 years) at catchment scale (MacEwan, 1997). Properties relating to soil morphology; cutans, drainage which is largely related to structure, soil colour (hue), and the delineation of master horizons is unlikely to change in a lifetime whereas soil chemical properties is likely to change (MacEwan & Fitzpatrick, 1996). Therefore soil chemical properties are an indication of recent hydrological conditions of soil. Chemical weathering can't take place without water and water is the mediator in further chemical reactions in the soil (Essington, 2004). Hydrology therefore plays an important role in resultant soil chemistry. Geochemical indicators are related to hydrological processes (McDaniel *et al.*, 1992 and Park & Burt, 1999) and could transform the procedure of soilscape modelling by reducing time factor of physical measurements and improve the quality as hydrometric and isotope data, which without the support of other data could produce erroneous predictions (McDonnell *et al.*, 2007).

Developing a concept is the first step in scientific research and that is also true of hydromorphology. Soilscape hydrology can be conceptualised using signatures related to the interaction of water with soil and fractured rock. Soil morphology is effectively applied as signatures of this interaction. That emphasises the role of a soil profile description as pedotransfer function. However, the relative slow reaction of soil morphology to changes in soil water regime and the fact that some morphological features are irreversible, question its universal application. Hydrometrics is applied as current (real time) indicators of response but its application is limited by its snapshot nature. Soil chemistry data, as sensitive, equilibrated products of water/soil interaction can fill this gap as it can connect point data in a soilscape and connect soil horizon and soil pedon response at soilscape scale.

Theory

The Fe and Mn concretion contents are highest in horizons with fluctuating water tables rather than in horizons that are more permanently saturated (D'Amore *et al.*, 2004; le Roux, 1996). During periods of saturation Fe^{3+} and Mn are reduced to Fe^{2+} and Mn^{2+} . Smith & Van Huyssteen (2011) found that at 60% saturation not all the samples were reduced, half the samples at 70% saturation were reduced, and most the Fe was reduced at 80% saturation and all the Fe was reduced at 90% saturation. Fe^{2+} is then adsorbed on the exchange sites freeing Ca and Mg and thereby increasing the Fe content and causing a decreasing in pH and base saturation (Phillips and Greenway, 1998). According to Park and Burt (1999) and McDaniel *et al.* (1992), Fe and Mn can be used as pedochemical indicators and is an identification of throughflow in soils.

Aim

The aim is to establish the relationship between ancient (morphological) and recent (chemistry) soil indicators of soilscape hydrology and to verify whether this relationship reflects the current hydrological regime using hydrometric measurements.

Hypothesis

It is hypothesized that soil chemistry, a sensitive, equilibrated product of recent water/soil interactions can be used to: (i) reveal the recent hydrological behaviour of a particular horizon in a soilscape and (ii) due to their relationships with horizon morphology can be extrapolated from point scale hydrometric measurements to soilscape scale.

6.5.2 METHODOLOGY

Site description

A soilscape in the Weatherley catchment was selected (Figure 189). The soilscape on the Molteno sandstone shelf and Elliot formation below the shield. A dolerite dyke intersects the soilscape below the shelf.

Methods and Materials

Four steps were used to design the conceptual soilscape hydrological model: (i) morphology was used to infer hydrological response of the horizons and soil types; (ii) chemical data were interpreted to establish the relationship between morphology and pedological processes; (iii) tensiometer data from a selected period and long term soil water content measurements was used to verify the interpretations; and (iv) a conceptual model was designed using more detailed morphological observations. Profile descriptions and chemical analyses of three profiles (Van Huyssteen *et al.*, 2005) were used to establish the relationship between soil morphology and soil chemistry. These profiles were selected as they had long term hydrometric measurements.

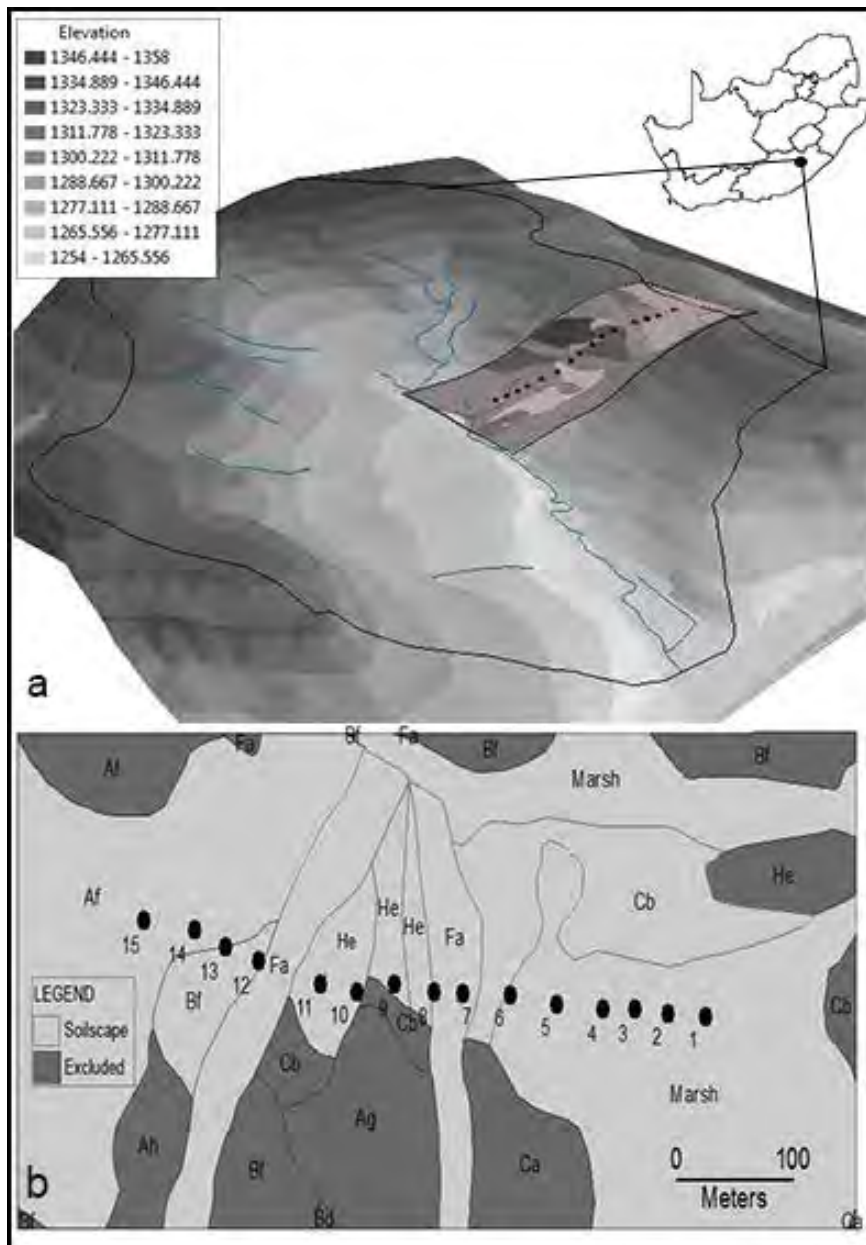


Figure 189 a) Weatherley catchment topography and position of soilscape b) Soil types included in the soilscape and auger observations

Long term water contents were measured using neutron water meters over a period of 6 years on a weekly basis. Water contents are expressed as annual duration of saturation ($AD_{s>0.7}$) which is defined as 70% saturation of porosity and proposed by Van Huyssteen *et al.* (2005) that reduction occurs before 100% saturation. The chemical properties were used as indicators of pedological processes and were used to confirm that the soil morphology was in phase with the recent soil water regime. Tension and soil water content data was used to verify the deductions made from the morphology and soil chemistry. March (31 days) 2001 was selected for the tension evaluation period. The onset of evaluation followed a number of days without any precipitation followed by a few rainy days. This pattern allows a wetting and a drying sequence which gives a good indication regarding fluctuations in the water regimes of the profiles. Soil auger observations were made every 20 m and samples taken at 200 mm intervals and used to identify soil boundaries between profiles and to

construct a base saturations hillslope cross section. At each auger observation the soil morphology was described in detail and classified according to Soil Classification Working Group (1991). Samples were dried, crushed and analysed using the Mid-inferred spectrometer (MIR). Soils were divided into three main soil types found regarding their hydrological response as defined by Van Tol *et al.* (2011) and used to create a conceptual hydrological response model of the soilscape.

6.5.3 RESULTS AND DISCUSSIONS

The morphology of the Bloemdal indicates that it serves as a deep interflow soil (Figure 189). It is situated on the upper midslope below the Molteno sandstone shelf. It has high chroma morphology with reduction morphology restricted to the deep subsoil. The Red apedal B horizon (5YR 4/6) is sandwiched between a bleached Orthic A horizon (10YR 3/2) and grey subsoil horizon with Unspecified with signs of wetness conditions. The Red apedal B horizon serves as a vertical conduit until the water reaches the impeding layer or water table, where water is diverted laterally. Therefore leaching is expected in the Orthic A and Red apedal B horizons. The redox morphology of the Unspecified with signs of wetness is an indication of increased duration of water saturation and drainable water. The increased in water content of the Unspecified with signs of wetness is probably return flow from the higher lying recharge zone. By implication the impeding layer may be a perched water table built up in the fractured rock.

The pH trends in the Bloemdal (Figure 190) indicate a general acidification and leaching in the Orthic A horizon attributed to acid weathering. It is an indication that the soil is seldom water logged (Phillips and Greenway, 1998). The Orthic A horizon is therefore expected to drain vertically and related to the high chroma the Red apedal B horizon is expected to follow suit. The water, by implication, does not arrive enriched or stagnate for long enough to be enriched but flows through the soil. There is an increase in pH at the transition of the Red apedal B and Unspecified with signs of wetness horizon indicating an accumulation of cations and a change from leaching to accumulation in the profile.

Biocycling may play an important role in the decreasing trend in base saturation in the Orthic A horizon (Figure 190). The low base status in the Orthic A and Red apedal B horizons of the Bloemdal is typical of a leaching environment. The accumulation of cations just above the Unspecified with signs of wetness horizon indicates a section in the profile where the leached basic cations accumulate by capillary rise and root extraction of water in the profile. A degree of water stagnation and arrival of enriched water is expected at this transition but it is still considered a faster flowpath than the lower lying G horizons.

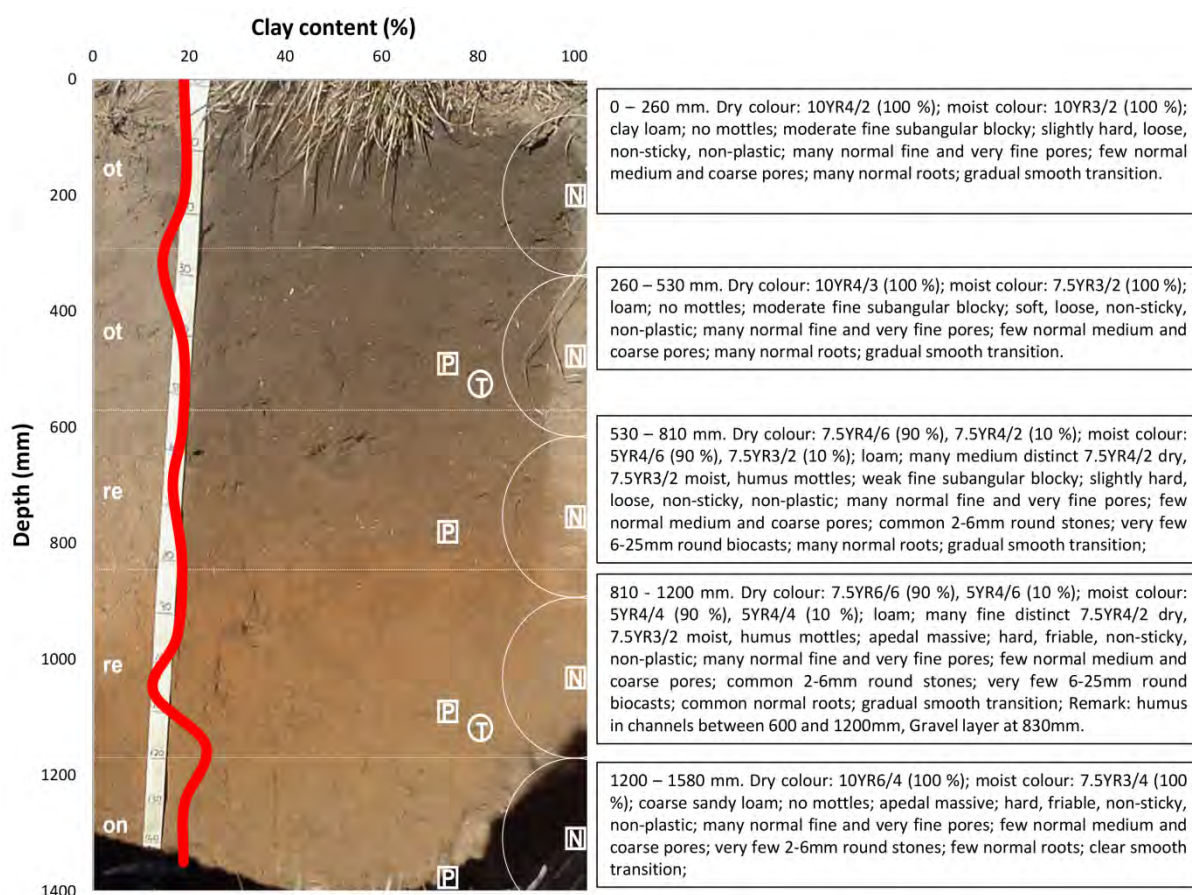


Figure 190 Clay content, photograph and profile description of the Bloemdal soil (Van Huyssteen *et al.*, 2005). P, T and N refer to piezometer, tensiometer and neutron water meter positions, respectively. Redox morphology typical of aquatic conditions was not photographed

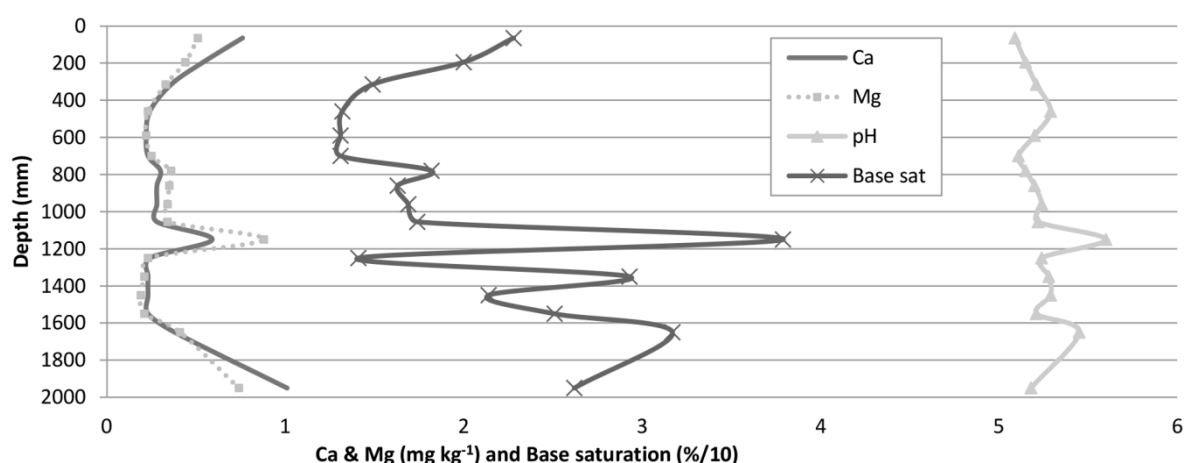


Figure 191 Calcium, Mg, pH and base saturation of the Bloemdal

The Ca and Mg trends support the small accumulation at the surface typical of biocycling and the peak at 1150 mm depth attributed to a water table. The lower Red apedal B horizon

may experience interaction between vertical leaching with relative “young” water and lateral flow with older water.

The results indicate that acid weathering under oxidising conditions is responsible for the Fe accumulation in the Bloemdal (Figure 191). The peaks in Fe concentrations at the transition between a reduced Unspecified with signs of wetness horizon and an oxidised Red apedal B horizon are signatures of redistribution of free Fe under redox conditions.

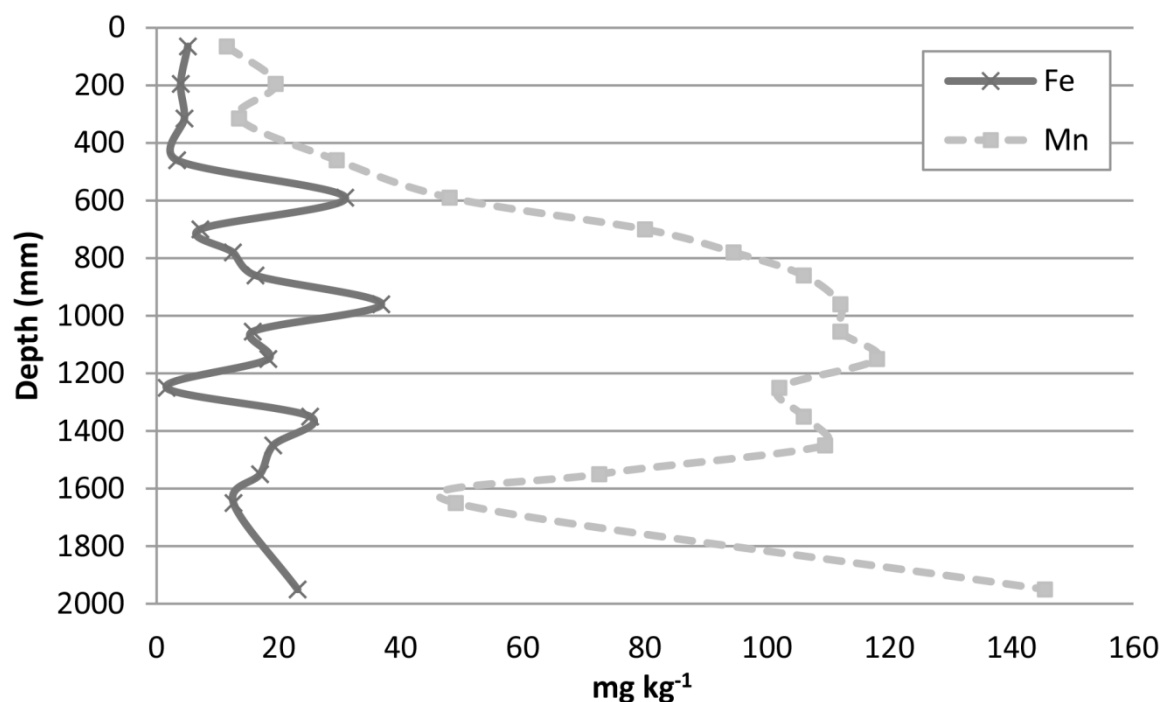


Figure 192 Fe and Mn distribution in the Bloemdal

The Mn is low at the surface (Figure 192) and increases systematically downwards to the horizon with Unspecified with signs of wetness conditions which is an indication of vertical downward movement of water and Mn being released by weathering. Manganese which is reduced during brief periods of saturation can be translocated downwards in the profile and then accumulate below drained upper limit where oxidising conditions are prevailing.

The water tension data enables an interpretation of a soil's response to a rainfall event. In the Bloemdal (Figure 193) the sensor in the Orthic A horizon (400 mm) dried out during the first 10 days of the study period. The small rain events on 8, 9 and 10 March caused a slight decrease in the matric pressure but it was only after the large event of 47 mm that the matric pressure in this horizon dropped significantly. The matric pressure increased in the following 5 days. The pressure dropped following rain events on the 17th and 18th of March and again on the 24th and 25th of March. In between these events there was a steady increase (drying out) in the pressure due to ET and vertical drainage. The sensor at 700 mm in the Red apedal B horizon reacted similar to the sensor in the Orthic A horizon but the gradients in increasing and decreasing pressures are less, probably due to the absence of evaporation from this horizon and less macropores. The sensor also shows a lag time of approximately 3 days in its response to the large event on the 11th of March.

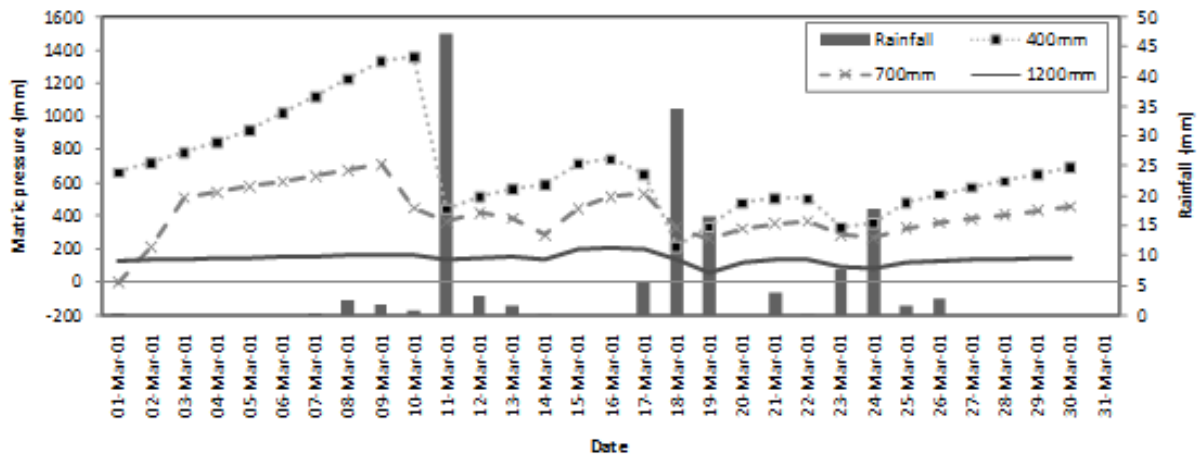


Figure 193 Rainfall and matric pressure measured in the Bloemdal (P210) soil during March 2001

The sensor at 1200 mm is at the transition from the Red apedal B horizon to the Unspecified with signs of wetness. This sensor differs greatly from the two sensors above in that this sensor is relatively constant and has a matric pressure close to 200 mm throughout the study period. There is a slight decrease in pressure after with the event on the 11th and the pressure then increases from the 14th to 16th but decreases with the events on the 17th, 18th and 19th. The pressure then returns to the constant pressure observed in the beginning of the month.

The absence of saturation (matric pressure <0 mm), suggests that this profile is freely drained to a depth of 1200 mm. Even with large rain events (11th of March) the Orthic A and Red apedal B horizons are capable of transmitting this water to deeper horizons without reaching saturation, thereby supporting the morphological and chemical interpretations regarding these horizons.

The $AD_{>0.7}$ values are calculated from 1997 to 2003 and is therefore a long-term indication of water saturation in different horizons (

Table 46). The Bloemdal (Figure 189) shows that the Orthic A horizon is saturated for brief periods and the Red apedal B horizon to 1000 mm is only saturated for 20% of the year. At the bottom of the Red apedal B horizon and at the transition to the Unspecified with signs of wetness horizon there is an increase in $ADs_{>0.7}$ where the horizon is saturated for most of the year. At this depth in Red apedal B horizon there is an increase in pH, base saturation, Ca, Mg, Fe and Mn. This is an indication that the Red apedal B horizon is out of phase with the morphology and in a process of change. The Unspecified with signs of wetness horizon is also saturated for more than 6 months during the year. The pedological processes and hydrological response inferred by the morphology is supported with chemistry. The generally low or slightly increasing parameters in the Orthic A and Red apedal B horizons support a vertical flowpath. The spike in at 1100 mm is expressed in all parameters is associated with the reduction morphology of the underlying horizon and associated with longer water saturation.

The Bloemdal profile is representative of the observations on the crest and upper midslope (Table 47).

Table 46 ADs>0.7 of diagnostic horizons in Bloemdal, Katspruit and Kroonstad

| Profile | Depth (mm) | Diagnostic Horizon | ADs>0.7 | |
|-----------|---------------|-----------------------|-------------------------|-----|
| | | | days year ⁻¹ | % |
| Bloemdal | 160 | ot | 18 | 5 |
| | 460 | ot | 71 | 19 |
| | 760 | re | 73 | 20 |
| | 1060 | re | 340 | 93 |
| | 1360 | on | 195 | 53 |
| Katspruit | 230 | ot | 203 | 56 |
| | 530 | gh | 342 | 94 |
| Kroonstad | 205 | ot | 179 | 49 |
| | 505 | gh | 207 | 57 |
| | 805 | gh | 233 | 64 |
| | 1105 | gh | 365 | 100 |
| | 1405 | gh | 365 | 100 |

Table 47 Observations on the crest and upper midslope represented by Bloemdal profile

| Obs. | Slope shape [†] | Soil Form | Diagnostic horizons | Depth (mm) | Munsell colour | Hydrological response | TMU [‡] |
|------|-----------------------------|-----------|-----------------------------------------|---------------|-------------------|--------------------------|------------------|
| 15 | xl | Hutton | Orthic A | 400 | 7.5YR 4/3 | Recharge | 1 |
| | | | Red apedal B | 2500 | 5YR 5/8 | | |
| | | | Rock | 2500+ | N/A | | |
| 14 | xl | Hutton | Orthic A | 300 | 10YR 4/4 | Recharge | 1 |
| | | | Red apedal B | 1200 | 5YR 7/6 | | |
| | | | Saprolite | 1700 | N/A | | |
| 13 | xl | Griffin | Orthic A | 400 | 10YR 4/4 | Recharge | 1 |
| | | | Yellow-brown apedal B | 900 | 7.5YR 5/8 | | |
| | | | Red apedal B | 1200 | 7.5YR 8/4 | | |
| 12 | ll | Mispah | Orthic A | 300 | 10YR 5/3 | Shallow responsive | 3 |
| | | | Rock | | N/A | | |
| 11 | ll | Hutton | Orthic A | 300 | 10YR 4/3 | Deep interflow | 3 |
| | | | Red apedal B | 1200 | 7.5YR 6/6 | | |
| | | | Saprolite | >1400 | N/A | | |
| 10 | ll | Bloemdal | Orthic A | 200 | 10YR 5/4 | Deep interflow | 3 |
| | | | Red apedal B | 800 | 7.5YR 5/6 | | |
| | | | Unspecified with signs of wetness | 1400 | 10YR 6/3 | | |

[†]Slope shape: l = linear; x = convex, y = concave

[‡]TMU1 (Terrain morphological unit) 1 = crest, TMU3 = midslope, TMU4 = footslope

The high chroma soils above the Molteno shelf (Obs 15, 14, 13) indicate oxidising conditions (Table 47). The colour of the top soil in this zone is consistent with very little change down slope in value and chroma. The surface colour is generally a Hue different from the subsoil but from 200 mm downwards the colours are uniform. The subsoils change slightly in matrix

colour becoming redder in colour. The Red apedal B horizon of the Hutton is uniform in colour with black mottles occurring in the bottom 50 mm just above the hard rock, indicating that water is only stagnant for brief periods and that the underlying Molteno rock is permeable. Down slope the hard rock changes locally to saprolite (Obs 14) and back to hard rock (Obs 13 and 12). The Yellow-brown apedal B horizon, occurring in the horizon in a Griffin (observation 13), is also uniform. The chromas of the Orthic A horizons are similar to that of the subsoils. Total soil depth varies but generally decreases down slope. Before the Molteno sandstone shelf it is shallow and a Mispahon sandstone hard rock occurs. The well expressed shelf probably lies underneath the crest for most of the divide. Lack of redox morphology in the subsoils indicate that it is fractured, probably associated with the intrusion of the nearby dolerite dyke. The soils lack prominent gley and redox morphology reported in nearby soilscares in the catchment (Van Tol *et al.*, 2010).

The oxidic morphology of the Hutton soils indicates that both serve as recharge soils. They serve as conduits of infiltrated water and recharge underlying fractured bedrock. This is indicative of a saturated hydraulic conductivity that is exceeding rainfall intensity in all the horizons as well as that of the fractured rock. The hard rock/saprolite implies variation in degree of weathering in the rock and may be attributed to local variation in composition in the rock or local variation in water regime or both as the water regime is controlled by the fracture pattern of the rock.

The texture of the Hutton show little pedogenetic differences and is therefore probably experiencing a uniform, draining pedogenesis of the sandy material inherited from the quartzitic Molteno sandstone underlying material with low potential to form clay. Contrary to other Red apedal B horizons in the catchment, overlying gleyed horizons, the colour difference in observation 13 can be due to extended saturation and/or increased reduction rate due to the higher OC content of the topsoil. Duration of water contents at near saturation for several days was measured in topsoils in other relevant research. However, quick reduction in the topsoil during prolonged soft rain as described by Fey (1985) could hydrate the Fe-oxides to form the yellow-brown colour. The implication is that the yellow-brown Red apedal B horizons are not a limitation to vertical flow.

Water that infiltrates the soil and water contents exceeding drained upper limit (DUL), will move through the soil, and infiltrate the bedrock. Via bedrock flowpaths this water can either recharge regional groundwater aquifers (vertical) or return to the solum down slope through lateral flow on bedding planes.

The redox morphology in the C horizons indicates an interflow section below the Molteno sandstone shelf and a second sequence of soils represented by Bloemdal profile (Figure 190). This is the highest position in the landscape where subsoil saturation was detected and implies interflow originating from higher lying recharge soils returning from the bedrock to the deep subsoil. It is the transition zone from the recharge soils to the responsive soils. The Red apedal B horizon of the Hutton (Obs 11) is on chemically weathered saprolite that changes to an Bloemdal soil (Obs 10) with redox morphology at 800 mm depth stretching to 1400 mm depth on saprolite. The subsoil disappears to form another Mispahon dolerite. Vertical flow will be dominant in the first subsoil of the deep interflow soils of the interflow zone (Obs 10 and 11). Water will be stagnant in the subsoils as indicated by the redox morphology. The increase in slope (from 3% to 8%) promotes interflow. During the rainy season the vertical source should dominate but a constant lateral contribution is expected for most periods of the year.

The gleyed morphology typical of the Katspruit (P209) is indicative of responsive soils (Figure 194) and associated with drainable water and saturation for long periods. The profile is situated below the dolerite dyke on a lower TMU 3 on mudstone underlying material. The terrain of the Katspruit (slope of 13%) implies a combination of a steadily supply of water from an extremely large aquifer. Water movement is more likely in the saprolite than in the G horizon, the presence of bleached root channels in the saprolite is signs of water movement compared to dark root channels in the G horizon. CEC_{clay} in the G horizon increase downwards from $21.6 \text{ cmol}_c \text{ kg}^{-1}$ to $40.3 \text{ cmol}_c \text{ kg}^{-1}$ indicating a shift in mineralogy from 1:1 towards 2:1 silicate clays. The Orthic A horizon of the Katspruit is thicker than the Orthic A horizon in the Kroonstad (450 mm), as the soil will not receive as much water in this position as the soilscape does not have as big source area when compared to the soils lower down in the landscape. The G horizon has stagnic morphology in contrast to the gleyic morphology of the saprolite. Vertical water movement is expected in the Orthic A horizon and in the saprolite. The G horizon acts as storage mechanisms.

The systematic increase in pH in the Katspruit (Figure 195) is correlated ($R^2 = 0.74$) with an increase in clay. It can be related to water logged conditions and water saturation which is expected to increase with depth.

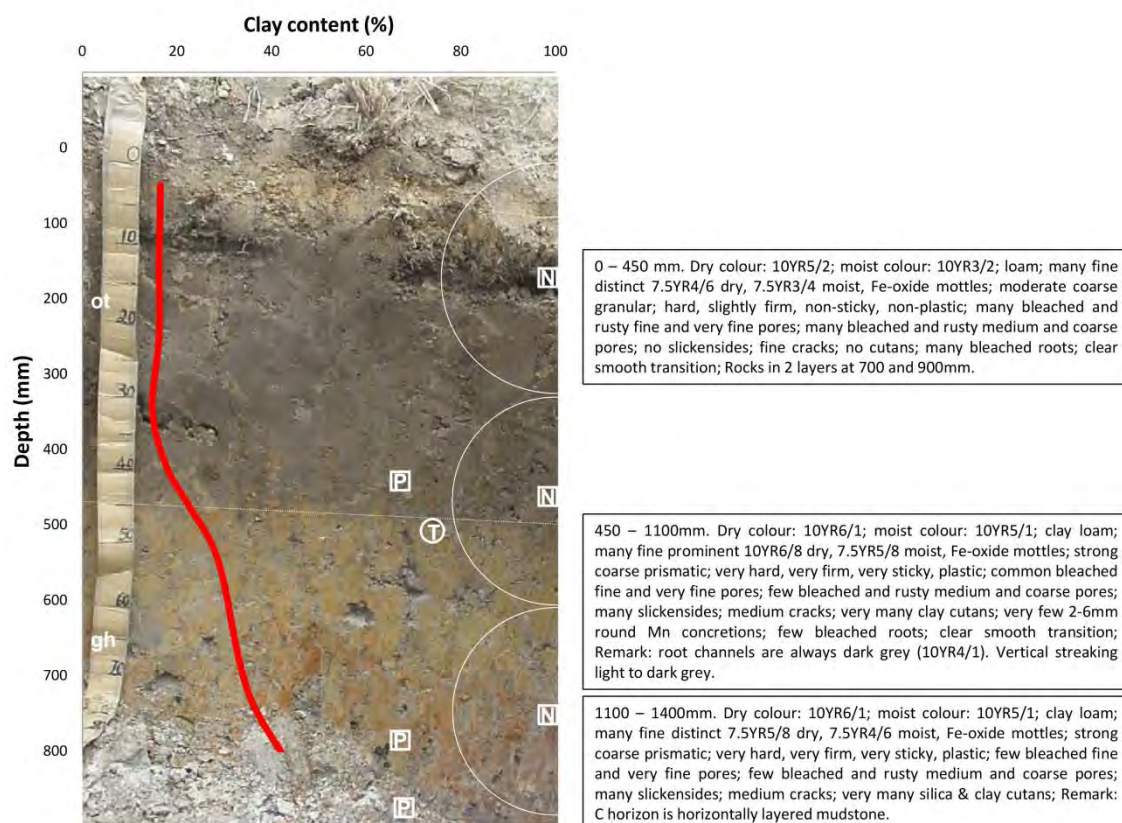


Figure 194 Clay content, photograph and profile description of the Katspruit soil (Van Huyssteen *et al.*, 2005). P, T and N refer to piezometer, tensiometer and neutron water meter positions, respectively

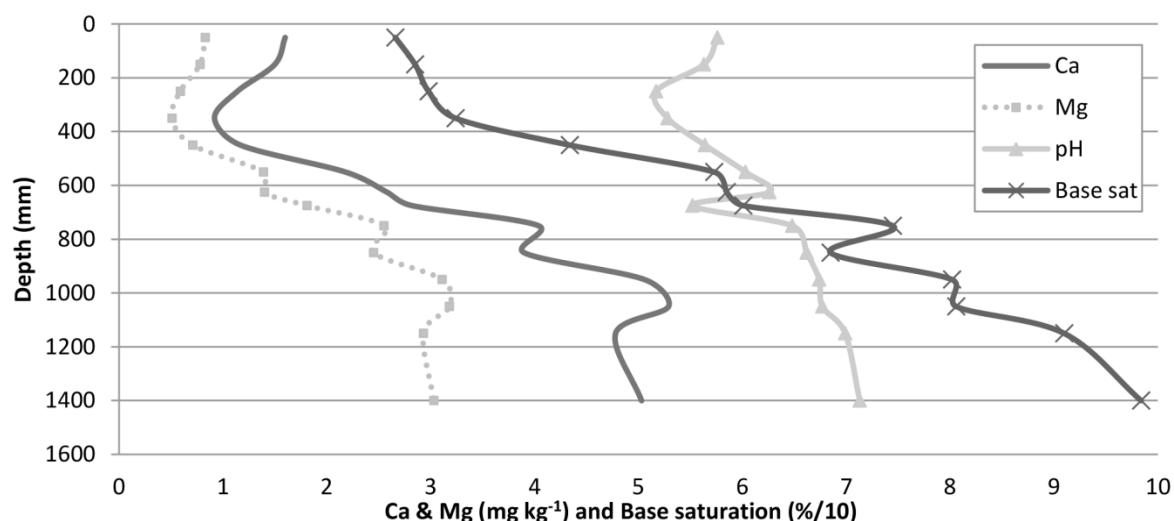


Figure 195 Calcium, Mg, pH and base saturation of the Katspruit

The base saturation profile of the Katspruit supports the interpretations of the pH profile (Figure 195). The variation in the Orthic A horizon may relate to the interaction between acid weathering and ferrollysis driven by rain water and soilscape water entering the soil. The sharp decrease the last 200 mm of the profile can also be due to [contradictory as it has high clay (44.3%), CEC_{soil} (17.8 $cmol_c kg^{-1}$) and CEC_{clay} (40.3 $cmol_c kg^{-1}$)] the parent material which is Molteno mudstone which is low in basic cations.

The Ca and Mg are relatively consistent in the Orthic A horizon but there is a slight decrease at the transition with the G horizon indicating a removal of Mg related to a probable development of a flowpath (Figure 195).

The Fe profile of the Katspruit (Figure 196) indicates that redistribution of Fe occurs and is driven by diffusion and capillary rise. Reducing conditions in the G horizon related to stagnation, interflow of soil water in contact with soil reducing conditions higher up or reduced old water residing in the soilscape, or a combination of them, could be responsible for reducing Fe. Diffusion is predominantly active over short distances and could be responsible for transporting of Fe and precipitation in the bottom of the Orthic A horizon under oxidising conditions. Capillary rise could be responsible for transporting the dissolved Fe to the Orthic A horizon. The high Fe concentration in the deepest sample is an indication of Fe release by mineral weathering of saprolite. It is supported by the drop in the first higher sample indicating a transition of less than 200 mm between mineral weathering in the saprolite and G horizon depletion of Fe processes. The Mn decreases in the Orthic A horizon and is more mobile than Fe due to a lower redox potential and is therefore more erratic in the profile.

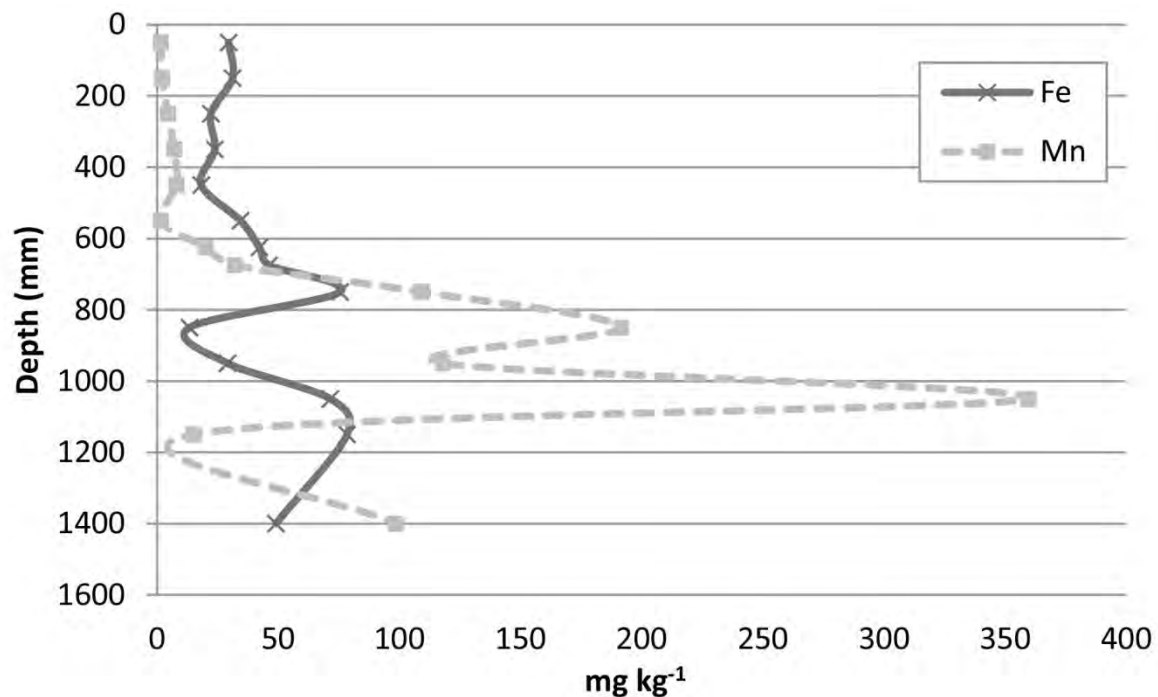


Figure 196 Fe and Mn distribution in the Katspruit

In the Katspruit (Figure 197) the sensor in the Orthic A horizon (300 mm) presents an initial increase in pressure following a rain free period. It decreased after the series of small rain events from 7th to 10th March and reaches saturation after the large event on the 11th of March. This horizon remains close to or at saturation for the remainder of the study period.

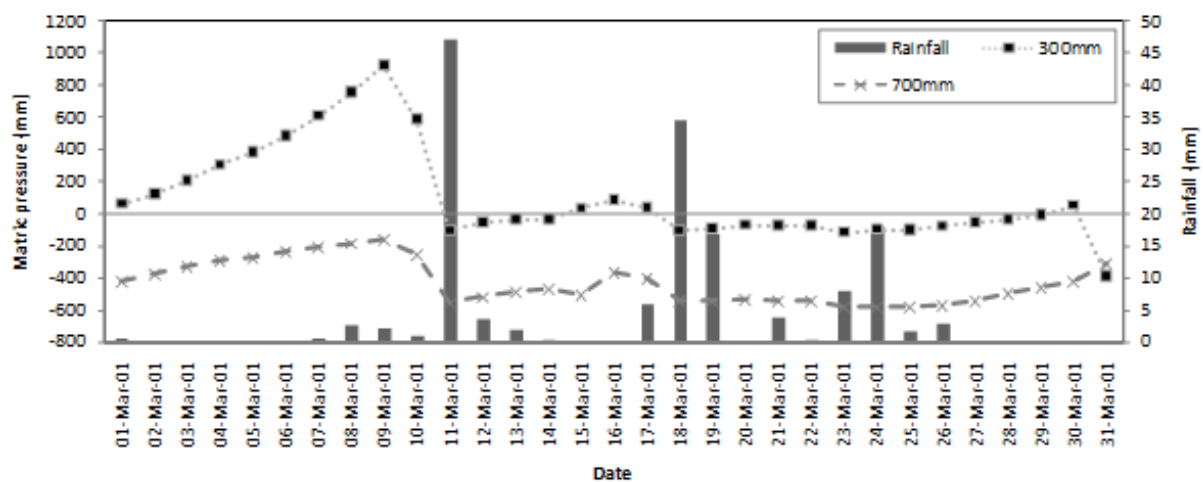


Figure 197 Rainfall and matric pressure measured in the Katspruit (P209) soil during March 2001

The sensor at 700 mm in the G horizon remains negative throughout the study period. Slight variation is noted after the large rainfall event (11th of March), where after this horizon remains at matric pressure of approximately -500 mm. The saturated state of both the Orthic A and the G horizons during the majority of the study period imply that additional rain will not be able to infiltrate, overland flow will therefore be generated due to saturation

excess runoff. Near surface macropore flow can also be generated in the Orthic A horizon as a result of a rising water table.

The Katspruit is saturated for more than 6 months (Table 46) at the surface and saturated for nearly the entire year from the bottom of the Orthic A horizon and the transition to the G horizon. Due to the slope (8%) if the G horizon is saturated water will move laterally on the Orthic A/G interface. This is a response expected in a Kroonstad soil with an E horizon. This response was not distinguished in the morphology but was deduced from the chemical properties and now supported water contents.

The pedological processes and hydrological response inferred by the morphology are supported with chemistry. The basic cation concentration in the G horizon indicates stagnation of water and therefore the accumulation of cations. It confirms the slow movement of water inferred from the gley morphology. The only deviation from morphological deductions is the development of a flowpath at the transition of the of Orthic A and G horizons indicated by the removal of Ca and Mg.

The Katspruit is representative of the footslope observations (Table 48).

Table 48 Observations on the footslope represented by Katspruit profile

| Obs. | Slope shape [†] | Soil Form | Diagnostic horizons | Depth (mm) | Munsell colour | Hydrological response | TMU [‡] |
|------|--------------------------|-----------|---------------------|------------|----------------|-----------------------|------------------|
| 9 | lx | Mispah | Orthic A | 400 | 2.5Y 4/3 | Shallow responsive | |
| | | | Rock | | N/A | | |
| 8 | lx | Katspruit | Orthic A | 300 | 2.5Y 5/3 | Responsive | |
| | | | G Horizon | 1300 | 2.5Y 6/3 | | |
| | | | Saprolite | 1700 | N/A | | |
| 7 | lx | Katspruit | Orthic A | 300 | 2.5Y 6/2 | Responsive | |
| | | | G Horizon | 1200 | 2.5Y 7/4 | | |
| 6 | lx | Katspruit | Orthic A | 300 | 2.5Y 7/2 | Responsive | |
| | | | G Horizon | 1500 | 2.5Y 7/6 | | |
| 5 | lx | Katspruit | Orthic A | 300 | 2.5Y 5/3 | Responsive | |
| | | | G Horizon | 800 | 2.5Y 7/3 | | |
| 4 | lx | Katspruit | Orthic A | 300 | 10YR 5/3 | Responsive | |
| | | | G Horizon | 1800 | 2.5Y 7/3 | | |

[†]Slope shape: l = linear; x = convex, y = concave

[‡]TMU1 (Terrain morphological unit) 1 = crest, TMU3 = midslope, TMU4 = footslope

The dolerite dyke probably acts as an Unspecified with signs of wetnesslode controlling the rate of interflow and increasing lower vadose zone storage. The high storage capacity supplies water to the deep interflow zone and soils of the responsive zone down slope.

The responsive zone (Obs 8, 7, 6, 5, 4) is characterised by gleyed subsoils produced by long periods of water saturation and represented by Katspruit profile (Figure 194). Subsoils are saturated for most of the year indicating a continuous supply of water. These subsoils will also be a continuous water source for subsoils lower in the soilscape.

The Kroonstad (Figure 198) has an E horizon above a G horizon indicating a shallow-interflow responsive soil. Water infiltrating the soil is expected to move largely vertically through the profile until it reaches an impeding layer. There is an increase in the bulk density from 1.62 Mg m⁻³ in the E to 1.76 mg m⁻³ in the G horizon. The restriction of water movement would be caused by the decrease in K_s due to the increase of clay in the

G horizon or water saturation. The impediment can cause water to move laterally above the G horizon in the E horizon resulting in breakdown (ferrolysis) and illuviation of clays in the E horizon. The only prominent morphological feature is Fe mottles found in the Orthic A and E horizon.

The accumulation of water from upslope can result in excessive saturation in the G horizon diverting water into the E horizon and thereby promoting lateral and overland flow. Return flow to the soil implies that the water moves upwards under saturated conditions (besides vertical extraction by capillary rise). Water may exit the G horizon and drain downslope in the sandier E horizon, increasing the redox variation.

The pH in the Kroonstad (Figure 199) is consistent with water table fluctuations predicted by the morphology. The major systematic deviation from the trend in the E and G horizons is due to ferrolysis caused by fluctuating redox conditions mostly in the E horizon but also in the G horizon. The decrease in pH and gradient of decrease in the surface to 300 mm depth cannot be explained by acid weathering but relates to the process of ferrolysis caused by intermittent reduced conditions. A peak minimum at 300 mm is an indication of ferrolysis activity peaking where the water table often meet oxygen supply. Acidification and ferrolysis is less down the profile which could be expected because the lower G horizon will be saturated more constantly. Ferrolysis causes a decrease in clay content.

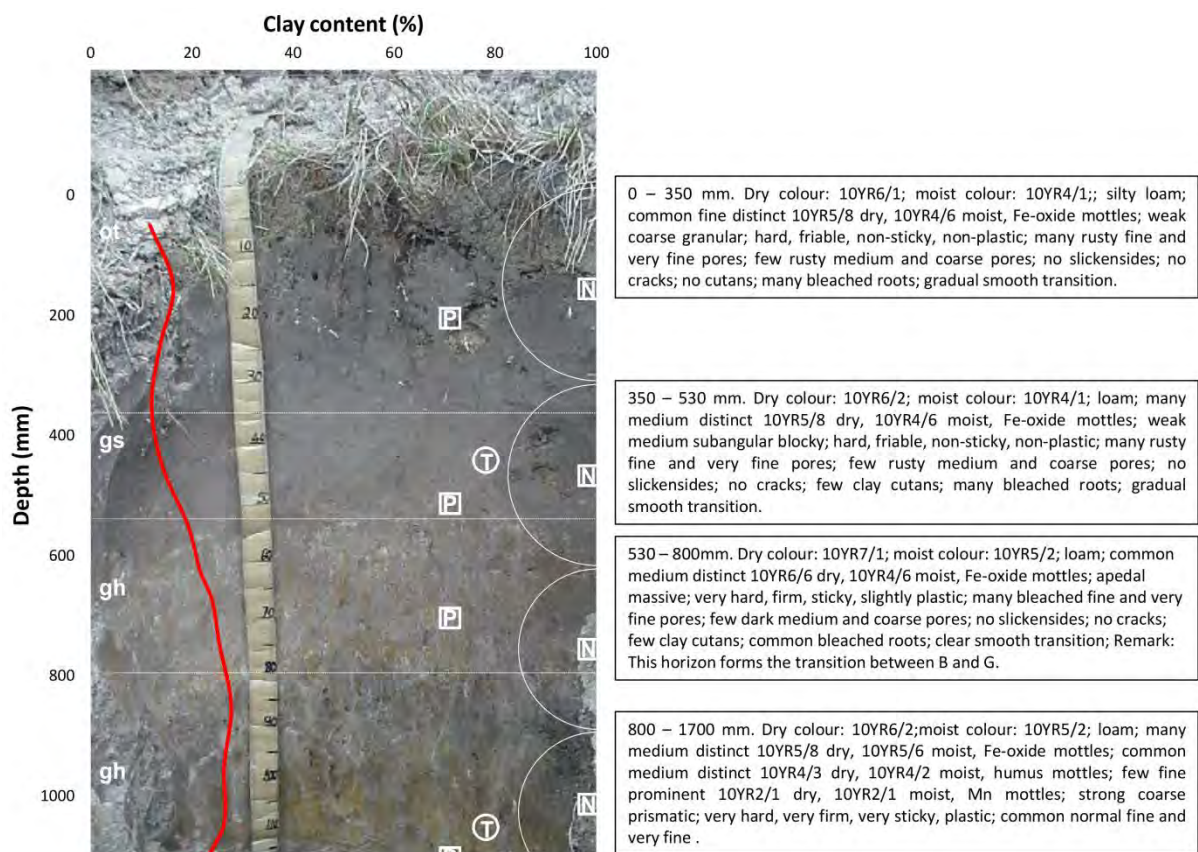


Figure 198 Clay content, photograph and profile description of the Kroonstad soil (Van Huyssteen *et al.*, 2005). P, T and N refer to piezometer, tensiometer and neutron water meter positions, respectively

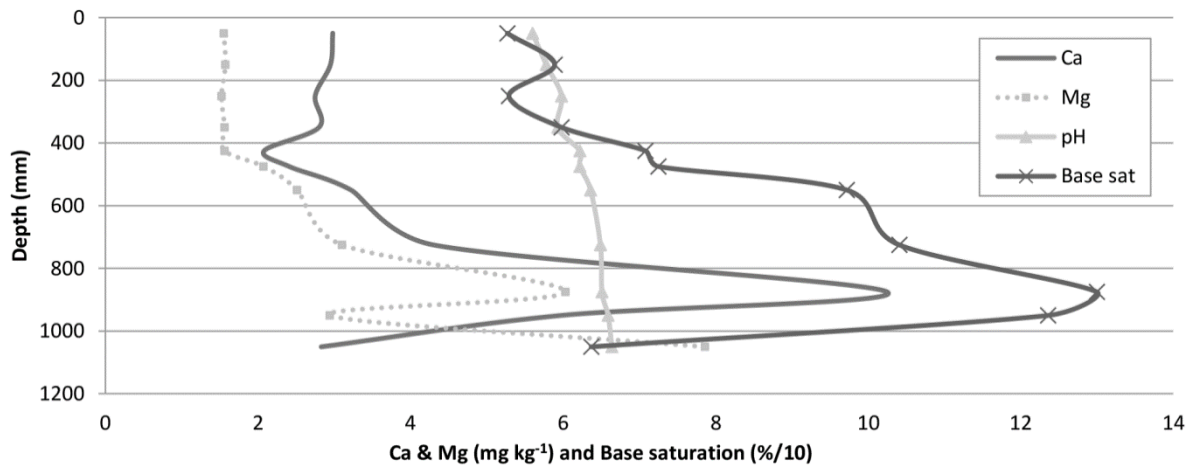


Figure 199 Calcium, Mg, pH and base saturation of the Kroonstad

The base saturation profile of the Kroonstad soil is indicative of leaching (Figure 199). The increase in base saturation with depth is an indication that some rainwater may enter the profile in the wetting up phase at the beginning of the rainy season on the toeslope. Calcium and Mg decrease from the surface to 350 mm in the E horizon (Figure 199). This is the same as the pH and base saturation found at these depths. The Ca is constantly low in the Orthic A and E horizons but there is a sharp increase in transition to the G horizon. The Mg is similar but the concentration is constant in the whole Orthic A horizon. During ferrolysis the Ca and Mg are displaced by Fe and due to the lateral flow in the horizon leached from the horizon. Calcium and Mg profiles support the base saturation distribution. The Fe concentration profiles of the Kroonstad (Figure 200) indicates slight accumulations in the Orthic A horizon compared to the E horizon which indicate capillary rise in Fe during the reduction stage of the G horizon and oxidising state of the Orthic A and E horizons.

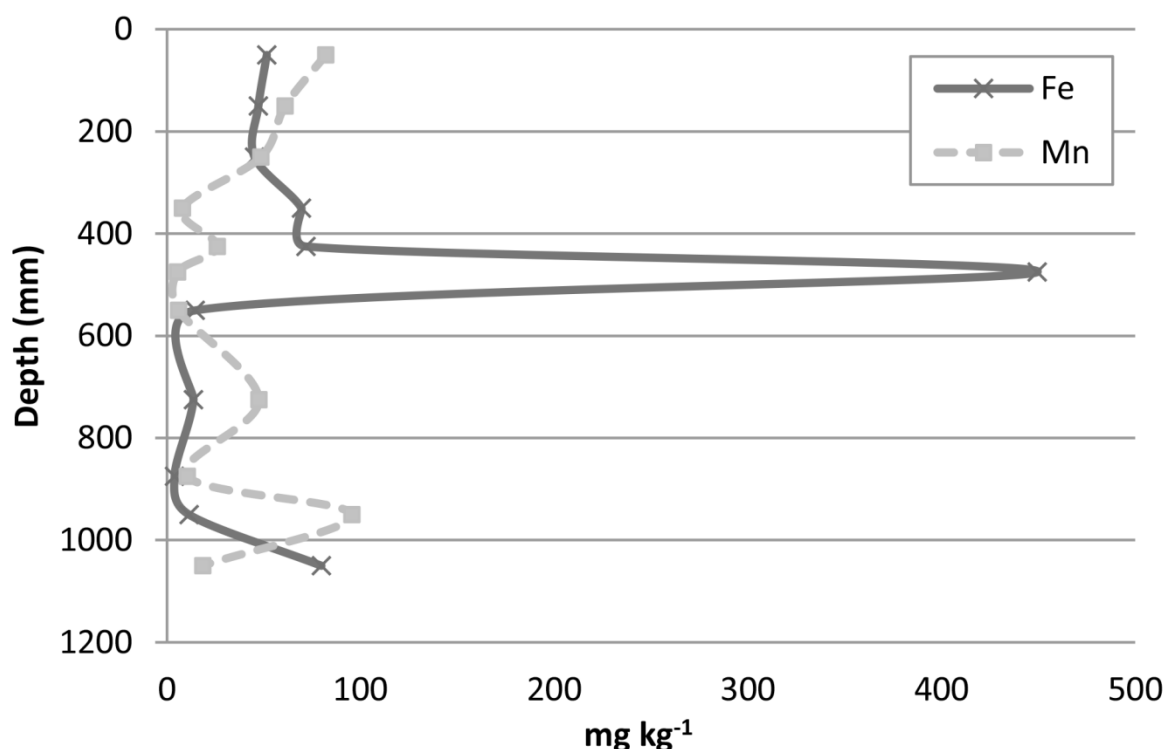


Figure 200 Fe and Mn distribution in the Kroonstad

The Mn on the surface is organically bound and therefore as carbon decreases so does Mn (Figure 200). If reducing conditions are present as expected in an E horizon and water movement is present there will be removal of Mn from that horizon. There is less Mn in the G horizon of the Kroonstad compared to the G horizon of the Katspruit soil which would indicate longer periods of saturation. The Mn concentrations fluctuate indicating water movement in the profile were Mn is translocated and not leached, or if it is leached it is replaced by an upslope source.

In the Kroonstad (Figure 201), the Orthic A horizon (350 mm) was saturated in the beginning of the study period (matric pressure <0 mm) but dried out due to evapotranspiration. It responded to the relatively small rain events on the 9th and 10th of March and reached saturation between the 10th and 11th of March. The Orthic A horizon remained saturated throughout the rest of the study period. The sensor at 700 mm representing the upper part of the G horizon responded very similar to the Orthic A horizon, implying that: 1) there was rapid vertical delivery of water through the Orthic A to the G horizons and/or 2) similar lateral flow processes control the water contents of these two horizons. Towards the end of the study period these horizons did not show the same drying slopes as in the beginning of the event. It is postulated that lateral contributions from upslope kept these horizons wet during this time. The deeper parts of the G horizon remained saturated throughout the study period with very little fluctuation, suggesting that there is a constant feed of water from higher lying terrain positions.

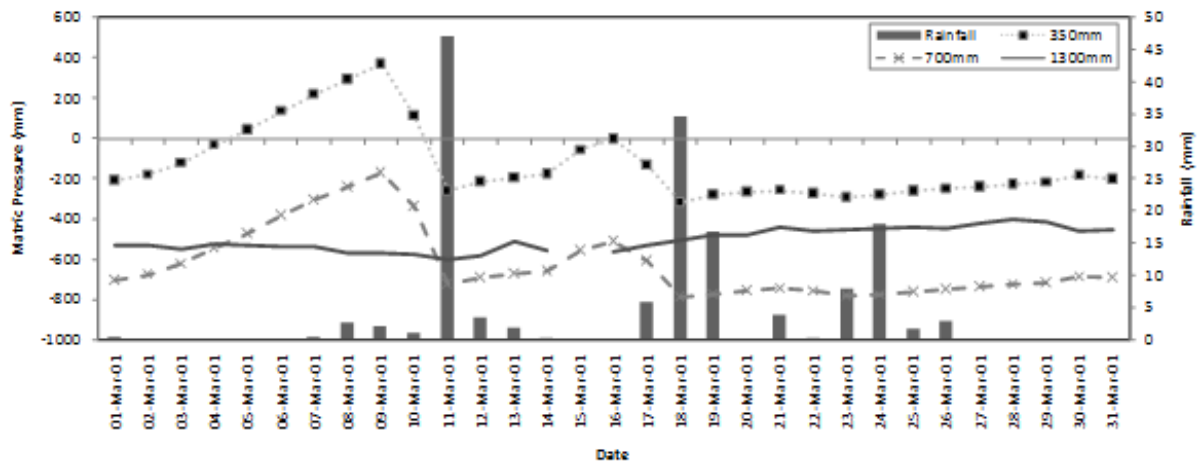


Figure 201 Rainfall and matric pressure measured in the Kroonstad(P208) soil during March 2001

The Kroonstad (Table 46) has very high $AD_{s>0.7}$ values for all horizons. The Orthic A horizon is saturated for almost 6 months a year with increases in the E horizon and the transition to the G horizon. The upper G horizon is saturated considerable less than the lower G horizon which is saturated for the entire year. The high saturation is expected due to the toeslope position of the soil. The interpretations of morphology and chemical properties are supported by water contents.

The pedological processes and hydrological response inferred by the morphology are supported by the chemistry and hydrometrics. There are different pedological and chemical processes in the E and G horizons and well related to the soil water regimes.

The E horizons in the observations at the toeslope (Obs 3, 2, 1; Table 49) indicate that there is an interflow component added to the responsive nature of the soils. Due to the higher bulk density of the G horizon and the pedological processes enhancing flow in the E horizon, lateral flow will occur in the E horizons in this zone. The zone is represented by Kroonstad profile (Figure 198).

The maturity of the soils is visible in the morphology changing downwards featuring as well developed horizons. This is an indication that vertical water movement contributes to soil formation in all the soils of this soilscape. The morphology of soils also changes down slope, especially in the subsoil, with an increase in redox morphology, indicating a strong interflow component (Table 49). Down slope the redox morphology changes to gley morphology indicating saturation due to increased accumulation of interflow water. Gley morphology of near surface horizons of the Katspruit and Kroonstad indicates saturated conditions.

Table 49 Observations on the toeslope represented by the Kroonstad profile

| Obs. | Slope shape [†] | Soil Form | Diagnostic horizons | Depth (mm) | Munsell colour | Hydrological response | TMU [‡] |
|------|--------------------------|-----------|---------------------|------------|----------------|------------------------------|------------------|
| 3 | ll | Kroonstad | Orthic A | 300 | 10YR 6/4 | Shallow interflow responsive | 4 |
| | | | E Horizon | 600 | 7.5YR 7/6 | | |
| | | | G Horizon | 1700 | 2.5Y 7/4 | | |
| 2 | ly | Kroonstad | Orthic A | 300 | 10YR 6/3 | Shallow interflow responsive | |
| | | | E Horizon | 600 | 2.5Y 6/4 | | |
| | | | G Horizon | 1700 | 2.5Y 6/6 | | |
| 1 | yy | Kroonstad | Orthic A | 300 | 5Y 5/2 | Shallow interflow responsive | |
| | | | E Horizon | 400 | 2.5Y 7/4 | | |
| | | | G Horizon | 600 | 2.5Y 5/2 | | |

[†]Slope shape: l = linear; x = convex, y = concave

[‡]TMU1 (Terrain morphological unit) 1 = crest, TMU3 = midslope, TMU4 = footslope

Summary of results

The chemical parameters largely relate to the morphology of the genetic horizons. The pH is low in the leached horizons (Red apedal B and E) and high in G horizons. The interflow soil (Unspecified with signs of wetness Hapludox) has a lower pH than the responsive soils (Katspruit and Kroonstad). The low pH of the Orthic A and E horizons of the Kroonstad is related to acidification by ferrollysis linked to alternating redox conditions. These processes play a role in the Orthic A horizon of the Katspruit explaining the low values of all the parameters and the low clay content. The values for all parameters are higher in the Katspruit than in the Kroonstad. It is an indication that the water impacting on the Katspruit is more enriched. This is because more enrichment is expected in a soil flowpath compared to a fractured rock flowpath.

The general trend of vertical leaching in the topsoils decreases downslope as indicated by all chemical parameters. This is an indication that the whole profile of shallow-interflow responsive and responsive soils is influenced by enriched water. The increase in all parameters with depth is an indication that some rainwater may enter the profile in the wetting up phase at the beginning of the rainy season in Kroonstad on the toeslope. There is generally an increase in base saturation down the profile and an increase in base saturation in the profiles with an increase in distance from the crest with the exception of the E horizon in the Kroonstad.

Implementation

A conceptual hydrological response model of the soilscape was constructed from deductions made from morphological data (Figure 202). In the recharge zone, which consists of Typic Hapludox and Typic Hapludox soils, water is expected to move vertically through the Oxic horizon. The prominent shelf of the Molteno formation plays an important role in the hydrology of the catchment but not in this soilscape. The abrupt transition to an interflow zone is rather related to topography created by the shelf. There is an increase in the slope gradient below the shelf. The deep interflow zone of the soilscape consists of Bloemdal and Typic Hapludox, with redox morphology in the deep subsoils of the Bloemdal and chemically weathered saprolite in the Typic Hapludox. The deep interflow soils cover

the area down to the dolerite dyke which seems to influence the hydrology of the lower sections of hydromorphic soils. This water from the recharge zone moves through the fractures and the subsoil of the deep interflow soils and keep the lower lying hydromorphic soils saturated creating the gleyed horizons found on the lower midslope and the bottom of the soilscape. These horizons will act more as a storage mechanism which is in contrast to the latter which are flowpaths. The shallow-interflow responsive Kroonstad will have interflow in the E horizon. Interflow in the E horizon may be increased from the soils higher up. The environmental setting suggests that return low that keeps the G horizon wet may enter the E horizon and contribute to the interflow. By implication the E horizon controls the water level in the soil as it has a high saturated hydraulic conductivity compared to the G horizon (Van Tol *et al.*, 2012).

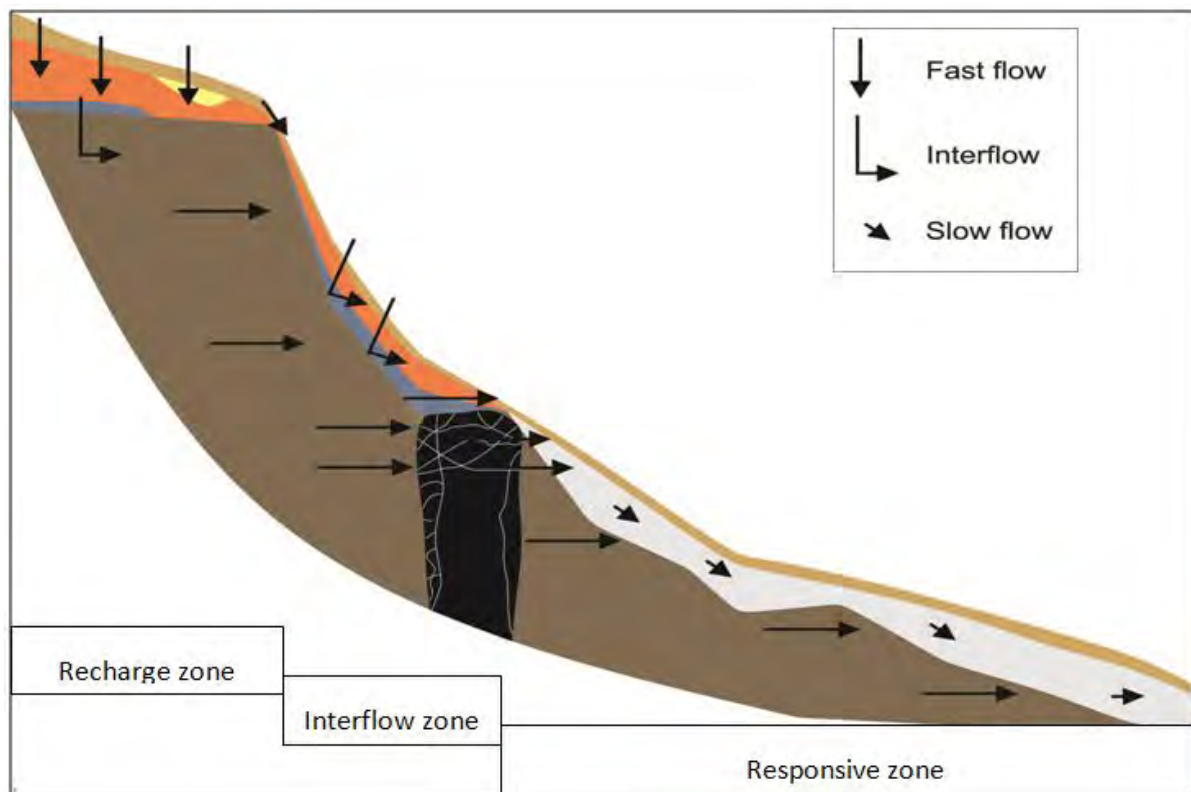


Figure 202 Conceptual hydrological response model of soilscape based on morphology

Due to the relationship established in the soilscape, base saturation was used to support the interpretations of the morphology of the observations. The base saturation profiles and distribution down slope confirms that the recharge zone is a leaching environment and basic cations are leached from the surface horizons and increase concentration with depth, indicating that there is vertical movement of water transporting the cations (Figure 203). In the interflow section there is removal of basic cations in the top horizons or from the entire profile indicating an element of recharge, while an increase of basic cations in the subsoil supports the deduction of horizontal movement and arrival of enriched water. The responsive soils typically have a higher base saturation which implies that enriched water arrives in this zone and that the water is stagnant and enriched further by evapotranspiration. Cations accumulate in these soils. The base saturation support the interpreted hydrological response based on morphology.

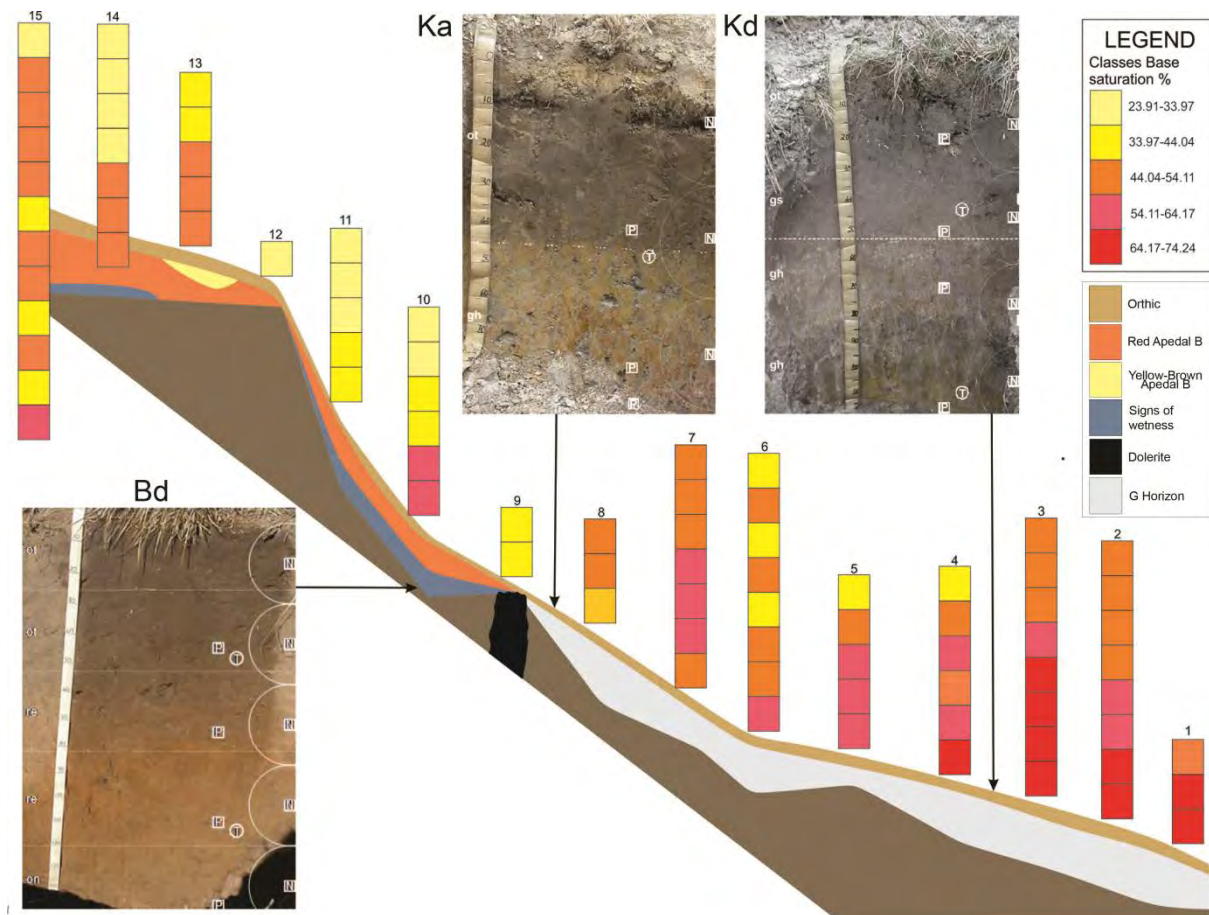


Figure 203 Base saturation distribution and position of representative profiles in the soilscape

6.6 CONCLUSIONS

The recent soil water regime, flowpaths and storage mechanisms indicated by soil chemistry are similar or related to the ancient soil water regime indicated by morphology, and the current soil water regime indicated by hydrometry. Soil chemistry confirmed the hydropedological processes derived from the observed morphology and were validated by hydrometrics. Soil chemical properties are therefore an important tool for hydropedology in the future and can help validate conceptual models based on morphology relatively quickly and inexpensively using conventional soil survey data. This technique can distinguish between diagnostic horizons with different soil water regimes.

Basic cations and pH are important indicators of pedological processes associated with morphology. In the studied soilscape three distinct zones can be identified based on the chemistry namely the recharge zone characterised by profile leaching, the interflow zone characterised preferential leaching, and the responsive zone characterised by accumulation of basic cations. Hydrological processes deduced from chemical properties can therefore be extrapolated at pedon, soilscape and catchment scale.

Selection of representative point locations for hydrometrical instrumentation can be improved by interpretation of soil morphology supported by soil chemistry. Soil morphology and chemistry can act as a transfer vehicle of point-scale data obtained from soil moisture content measurements. This is especially true for the extrapolation of point data, vertically

in the horizons of the soilscape and also horizontally between different soil types. It can also be used to identify representative soils in a larger catchment considering the same soil forming factors thereby improving hydrological predictions in ungauged basins.

6.7 REFERENCES

- BEEH, 2003. Weatherley Database V1.0. School of Bioresources, Engineering and Environmental Hydrology, University of Natal, Pietermaritzburg.
- Bouma, J. 1989. Using soil survey data for quantitative land evaluation. *Advances in Soil Science* 9:177-213.
- D'amore, D.V., S.R. Stewart, and J.H. Huddleston, 2004. Saturation, reduction and the formation of Iron-Manganese concretions in the Jackson-Frazier wetland, Oregon. *Soil Science Society of America Journal* 68:1012-1022.
- Essington, M.E., 2004. *Soil and water chemistry: An Integrative Approach*. CRC Press, New York.
- Fey, M.V., 1983 Hypothesis for the pedogenic yellowing of red soil materials Tech. Commun. S. Afr. Dep. Agric. Fish. 18:130-136.
- Fritsch, E., and R.W. Fitzpatrick, 1994. Interpretation of soil features produced by ancient and modern processes in degraded landscapes: 1. A new Method for Constructing Conceptual Soil-Water-Landscape models. *Australian Journal of Soil Research* 32:889-907.
- Jacks, G., and A-C. Norrström, 2004. Hydrochemistry and hydrology of a forest riparian zone. *Forest Ecology and Management* 196:187-197.
- Kuenene, B.T., C.W. Van Huyssteen, P.A. Le Roux, and M. Hensley, 2011. Facilitating interpretation of the Cathedral Peak VI catchment hydrograph using soil drainage curves. *South African Journal of Geology* 114:525-234.
- Le Roux, P.A. 1996. Die aard, verspreiding en genese van geselekteerde redoksmorfe gronde in Suid-Afrika. Ph.D. Diss. University of the Orange Free State, Bloemfontein.
- MacEwan R.J., 1997. Soil quality indicators: pedological aspects. In: Gregorich EG and Carter MR, editors, *Soil Quality for Crop Production and Ecosystem Health*. Elsevier, New York. p. 143-166.
- McDaniel, P.A., G.R. Bathke, S.W. Boul, D.K. Cassell, and A.L. Falle, 1992. Secondary manganese/iron ratios as pedomorphic indicators of field-scale throughflow water movement. *Soil Science Society of America Journal* 56:1211-1217.
- McDonnell, J. J., Sivapalan, M., Vache', K., Dunn, S., Grant, G., Haggerty, R., Hinz, C., Hooper, R., Kirchner, J., Roderick, M. L., Selker, J. and Weiler, M., 2007. Moving beyond heterogeneity and process complexity: A new vision for watershed hydrology. . *Water Resources Research* 43, W07301, doi:10.1029/2006WR005467.
- Park, S.J., and T.P. Burt, 1999. Identification of throughflow using secondary iron oxides in soils. *Geoderma* 93, 61-84.
- Phillips, I.R. and M. Greenway, 1998. Changes in water soluble and exchangeable ions, cation exchange capacity, and phosphorus_{max} in soils under alternating waterlogged and drying conditions. *Communication in Soil Science and Plant Analysis* 29:51-65.
- SMITH, K. & VAN HUYSSTEEN, 2011. The effect of degree and duration of water saturation on selected redox indicators: pe, Fe²⁺ and Mn²⁺. *South African Journal of Plant and Soil* 28:2, 119-126.

- Soil Classification Working Group, (1991). Soil Classification – A taxonomic system for South Africa. *Mem, agric. Nat. Resour. S. Afr.* No. 15. Dept. Agric. Dev., Pretoria.
- Soulsby, C., Tetzliff, D., Rodgers, P., Dunn, S. & Waldron, S., 2006. Runoff processes, stream water residence times and controlling landscape characteristics in a mesoscale catchment: An initial evaluation. *Journal of Hydrology* 325, 197-221.
- Ticehurst, J.L., H.P. Cresswell, N.J. Mckenzie, and M.R. GLOVER, 2007. Interpreting soil and topographic properties to conceptualize soilscape hydrology. *Geoderma* 137:279-292.
- Van Huyssteen, C.W., M. Hensley, P.A. Le Roux, T.B. Zere, C.C. Du Preez, 2005. The relationship between soil water regime and soil profile morphology in the Weatherley catchment, An afforestation area in the Eastern Cape. WRC Report 1317/1/05, Water Research Commission, Pretoria.
- Van Tol, J.J., P.A. Le Roux, M. Hensley, and S.A. Lorentz, 2010. Soil as an indicator of soilscape hydrological behaviour in the Weatherley catchment, Eastern Cape, South Africa. *Water SA* 36:513-520.

Chapter 7 **HYDROPEDOLOGICAL STUDY TECHNIQUES**

7.1 IN-SITU CONTINUOUS MEASUREMENTS OF THETA IN HILLSLOPE SOILS AND CONCLUSIONS W.R.T. APPROPRIATE INSTRUMENTATION

7.1.1 Introduction

In hydropedological studies reliable understanding and knowledge of the spatial and temporal variations in soil water content (θ) of the diagnostic horizons and pedons of hillslope soils, and of whole hillslopes, is essential for elucidating the relationship between the water regimes of soil profiles and their morphology, and especially for hydropedological modelling. Since hillslope hydrology is influenced by a large number of rainfall events of different intensities and amounts each year, appropriate and reliable continuous in-situ field measurements of θ at different depths are indispensable for effective hydropedological studies, particularly for those aimed at contributing to hydrological modelling of ungauged basins, a specific aim of this project.

The basic reference method for the determination of θ is by the gravimetric procedure, i.e. θ_g . This method is destructive, involving the taking of a disturbed sample in the field that is weighed when moist, and then oven dry at 105°C and weighed again to determine the mass of water lost. θ_g measurements are time-consuming and costly and repeated measurements at exactly the same location are not possible, thereby introducing error due to spatial variation. Many indirect methods for measuring θ have been proposed in the past few decades whereby some variable which is affected by θ is measured, and then related to the relevant θ_g by calibration (Bittelli, 2011). In order for these indirect measurements to be useful they need to have the following characteristics; high accuracy, long term stability and reliability, ability to be easily installed and calibrated, and they should be fairly inexpensive whilst providing continuous measurements (Atkins *et al.*, 1998; Gebregiorgis and Savage, 2006). Modern capacitance based soil water probes are widely used in various sectors (Nhlabatsi, 2011) to measure θ . Their advantage is that the advancement of electronics has enabled them to record continuous measurements of θ (Geesing *et al.*, 2004, Zerizghy *et al.*, 2013), unlike in the past when measurements had to be repeated manually by using devices such as the neutron water meter (NWM) for long term monitoring. Despite the availability of automated continuous measurements of θ by capacitance methods, the NWM method remains the most reliable method for θ determinations in the field (IAEA, 2008). Its disadvantages include the health hazard of exposure to the radioactive source and the lack of continuous logging of θ (Zerizghy *et al.*, 2013).

Advances in technology and basic soil physics have shown that capacitance based soil sensors are capable of meeting the requirements for measuring θ (van Rensburg, 2010). The concept behind capacitance based sensors is that the dielectric constant differs significantly between different soil phases; gas ≈ 1 , solid ≈ 4 and liquid ≈ 80 (Atkins *et al.*, 1998; Bittelli, 2011). Small changes in the soil water content can therefore significantly change the dielectric constant of the soil-water-air mixture and can be related to θ_g by calibration.

According to van der Westhuizen and van Rensburg (2011), there is however a large scope to improve these calibration procedures. It is quite common for manufacturers of capacitance probes to provide general equations to convert dielectric constant measurements to θ (Atkins *et al.*, 1998). This has the disadvantage that the calibrations are instrument dependent (Robison *et al.*, 1998) and therefore not ideal for heterogeneous soil types. For example, Nhlabatsi (2011) reported that all manufacturers' equations had low accuracy levels, the highest level being at 69%. In his experiment the soil water content of the A, B and C soil horizons was over predicted by 45, 39, and 42%, respectively. It is for this reason that manufacturers recommend soil-specific calibration for improved accuracy. The best calibration method is to measure the dielectric constant at known values of soil water content (θ_v) as determined via the θ_g procedure (Atkins *et al.*, 1998). In laboratory calibrations, starting with a totally dry soil and adding known amounts of water a curve of dielectric constant vs volumetric water content (calculated from θ_g) is generated that will serve as a calibration curve for all similar soils (Atkins *et al.*, 1998). Laboratory calibrations always have good correlations with an average precision of more than 95% (Fares *et al.*, 2006; Nhlabatsi, 2010; Polyakov *et al.*, 2005). Laboratory calibrations save time, are easy to reproduce and require less labour compared to field calibration. However, lab methods often use disturbed samples (packed soil columns) from which measurements are determined. With this procedure the whole concept of linking the measurements to morphology of the soil and its physical (especially bulk density), chemical and biological medium is compromised. It is exactly in this context that field calibrations become necessary to represent *in situ* conditions. Field calibrations, on the other hand, have the disadvantages of being time consuming and labour intensive, often resulting in a limited number of data points, as well as the waiting period required to reach desired water contents for calibration (van der Westhuizen and Van Rensburg., 2013). After achieving almost perfect data fits with the evaporative desorption calibration methods (van der Westhuizen and Van Rensburg., 2013), the same authors stated that the balance between highly accurate calibrations for research purposes and more simple, yet scientifically sound, calibrations should be sought (van der Westhuizen and van Rensburg, 2013).

To maximise support for the hydrological modelling of ungauged basins hydrogeological studies need to aim at understanding the soil related aspects of the hydrological functioning of as many hillslopes as possible. This means that θ measurements will always in the future be needed for many different hillslopes where measurements have not previously been made. For hydrogeological studies measurements at a wide variety of depths are also needed, including some >2 m to monitor θ changes in the intermediate vadose zone. Measuring instruments that need specific calibration for each new horizon are therefore undesirable, and hence the important advantage of instruments that measure soil water potential *in-situ*, and provide θ via the water retention curve (also needed for the determination of the K_h curve for each diagnostic horizon). This factor is not important for θ measuring instruments needed for example for some other purposes, e.g. irrigation scheduling (Van Rensburg, 2010) where the instruments remain permanently in one particular soil, or for relatively shallow measurements for evaporation studies in one particular soil (Zerizghy *et al.*, 2013).

7.1.2 DFM Capacitance probes

DFM capacitance probes are multilevel soil water and temperature measuring probes and are extensively used for irrigation scheduling (van Rensburg, 2010) as well as in research projects (Zerizghy *et al.*, 2013). The standard version of these probes consist of six sensors (measuring at 10, 20, 30, 40, 60, and 80 cm) mounted on a vertical probe column which is installed in the soil via a waterproof access tube (Figure 204 a & b). Adjustments to the standard version were made to several probes used in this study for θ readings deeper than 800 mm. The transmitting head was removed and positioned in a separated box called the central point radio located on the surface (Figure 205), with a 5 mm cable connecting the probe with the centre point radio. The length of the cable varied between 4 and 5 meters, which allowed deep installation.



Figure 204 Standard version of 800 mm DFM capacitance probe with 6 sensors

Each sensor consists of an oscillator and a number of electrodes—either two circular rings or an array of parallel metal spikes that form a capacitor. The adjacent soil forms the dielectric of the capacitor, which completes an oscillating circuit. A capacitance field is generated between the two rings of each sensor. This field extends into the soil adjacent to the sensor, and is affected by the soil's dielectric which is affected by θ . Changes in θ cause a change in the frequency of the oscillating circuit which can be related to θ via a calibration curve. The manufacturers (DFM Software Solutions, 2011) guarantee accuracy and reliability of these probes. For these reasons we selected DFM probes to measure θ in two research catchments; Two Streams and Weatherley.

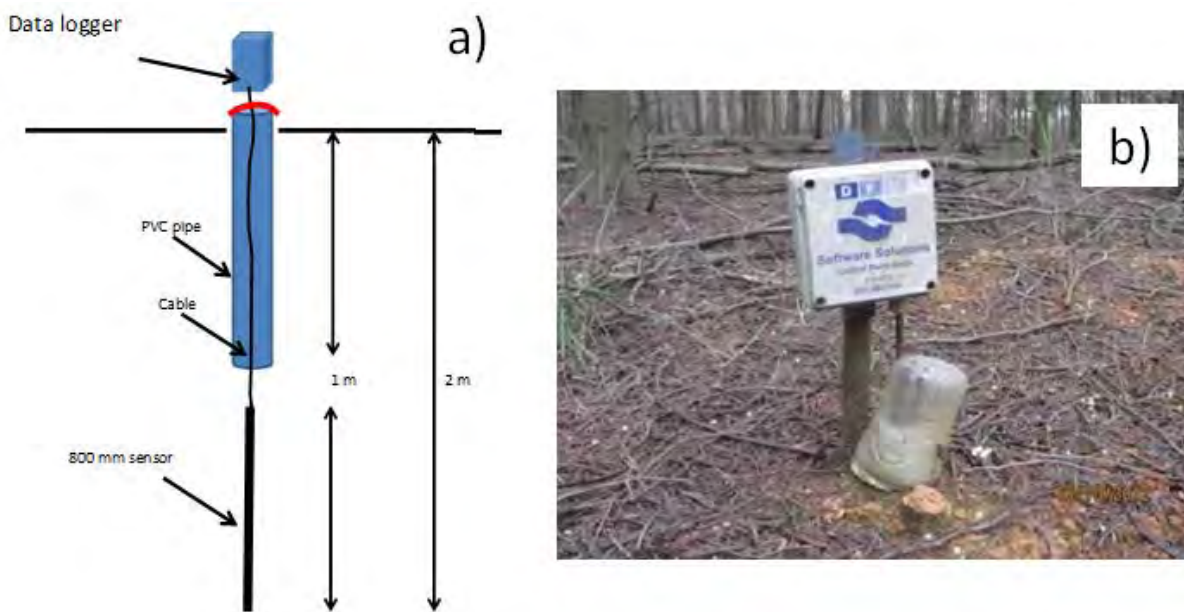


Figure 205 Modified version of DFM probe for deep measurements of soil water contents

Our preliminary results indicated that although changes in θ were recorded by the probes, the DFM values were unrealistic. No calibration equations were provided by the manufacturer, but it was stated that probe readings would plot in a straight line between dry air (0% water) and a free water body (100% water). Field installation of the probes was done prior to calibration. The proposed procedure was to calibrate them *in situ*. We noticed that for all sensors the calibration line against θ_g was not linear and the manufacturer's simple calibration criterion described above was therefore not adhered to. We therefore decided that each sensor in each probe should have its own calibration line/curve. The reasonable hypothesis was that a specific sensor would give a similar field calibration curve in specific kinds of soil horizons with similar characteristics such as bulk density, clay content, clay mineralogy, organic carbon, colour and structure. Assuming this to be true would enable DFM probes to be used repeatedly without recalibration in similar horizons at other locations.

7.1.3 The installation and calibration of DFM probes in the Two Streams catchment

A number of DFM probes were installed in the Two Streams and Weatherley catchments. The calibration procedures followed differed between the catchments and will therefore be discussed separately.

Installation of the probes

Four standard versions (Figure 206) of the DFM probes were installed in Inanda (2), Clovelly and Oakleaf soils on two transects in Two Streams (Figure 206). Adjacent to each 800 mm probe two modified probes (see discussion above) measuring soil water contents at 1100, 1200, 1300, 1400, 1600 and 1800 mm, and at 2600, 2800, 2900, 3000, 3200 and 3400 mm,

respectively were installed following the manufactures guidelines. Sixteen 800 mm probes were installed between representative profiles. The probes were set to read every hour. The data was downloaded using a hand held datalogger onto the computer once a month.

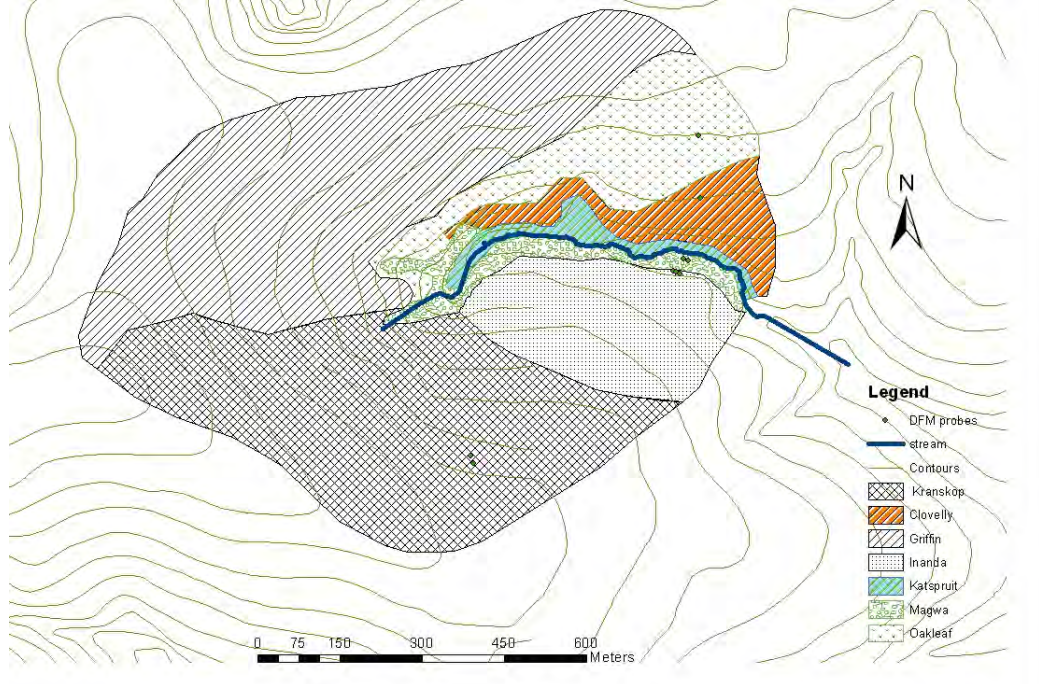


Figure 206 Location of DFM probes in the Two Streams catchment

Calibration procedure

It was decided that the first step to calibrate the DFM probes was to collect samples for θ_g determinations at depths corresponding to the DFM measuring depths, at different times of the year namely; March, 2011, April, 2011, August, 2011, November, 2011, February, 2012 and lastly October, 2012. The guiding hypothesis was that the soils would have a range of different θ values at these different times, and therefore provide the data needed for calibration. Samples were therefore collected with an auger at 50-150 mm, 150-250 mm, 250-350 mm, 350-450 mm, 450-650 mm, and 650-850 mm for the 800 mm surface probes. Samples for DFM probes installed at 1 meter were therefore taken at 1050-1150 mm, 1150-1250 mm, 1250-1350 mm, 1350-1450 mm, 1450-1650 mm and 1650-1850 mm. Those installed at 2600 mm were sampled at 2650-2750 mm, 2750-2850 mm, 2850-2950 mm, 2950-3050 mm, 3050-3250 mm and 3250-3450 mm. Each of these selected sampling depths straddled the depth of the sensor that was being monitored. Soil samples were immediately placed in micro oven plastic bags, weighed in the field, and then taken to the laboratory to be oven dried at 105°C for 24 hrs before reweighing. Volumetric water content θ_v ($\text{cm}^3 \text{cm}^{-3}$) was then calculated for each sample according to the following equation, bulk density (ρ_b) having been determined previously on undisturbed core samples take for water retention curve (Section 7.5):

$$\theta_v = (M_w - M_s) \times \left(\frac{\rho_b}{M_s} \right) \quad (7.1)$$

Where M_w is mass of the wet soil, M_s is mass of the dry soil.

The procedure was repeated 4 to 7 times during the overall monitoring period with the aim of obtaining a broad range of θ_v values for the calibration. This procedure, however, proved unsatisfactory as the all-important readings close to field saturation were generally absent, because of relatively low rainfall and the fact that the soil in the deep levels in many cases never became really wet, and therefore frequently remaining at a constant θ . For hydrogeological studies reliable θ values close to saturation are important because of the influence of the redox reactions occurring at these water contents that influence soil morphology. Ample motivation and evidence in this connection is provided by the results presented in van Huyssteen *et al* (2005). The need to express θ in terms of degree of saturation (S) for these purposes is significant, and therefore for the maximum reading (i.e. field saturation *fsat*) of the measuring instrument to be clearly defined. To solve the problem and obtain wet calibration points, a procedure was developed for selected probes. This was achieved by creating a dam around the probe (Figure 207) and applying water continuously for at least 1 day. This required a large amount of water and was only logistically possible for a few probes selected because of their closeness to the road and their relatively flat topography. With probes close to the road, water was transported from the bakkie with less effort. The water was allowed to infiltrate and redistribute for 24 hours. It is believed that reasonably satisfactory calibration can be achieved by combining the well-established reliable θ measurement capability of the NWM procedure (IAEA, 2008), with the valuable continuous reading capability of the DFM probes. Near to the DFM (probe no. 15291) calibration site (Figure 207), a similar wetting and measuring procedure was conducted around a NWM access tube. The access tube was one of the NWM aluminium access tubes that were installed to a maximum depth of 2 m originally during the previous study by Everson *et al* (2008). Drier calibration points for this access tube had been obtained earlier. Specific advantages of the NWM measuring procedure are, because of the linear relationship between the neutron count ratio (CR) and θ , it is quite clear, at whatever depth the reading is being taken, that when the surrounding soil is at *fsat* (generally around 0.85 S for medium textured soils) the CR will reach a maximum, usually around 2.0 for the CPN neutron probes commonly used in South Africa. As the soil drains from *fsat* to the drained upper limit (DUL), although θ_g determinations cannot be taken because the soil is in a mud condition, NWM readings can continue to be taken until the soil is dry enough to take samples for θ_g determinations. Because of the known linear relationship between CR and θ a reasonably reliable calibration line between *fsat* and DUL can then be drawn and used to provide the θ_v values against which to plot the continuous DFM probe readings taken as the soil drains from *fsat* to DUL. For the fairly wet soil below DUL θ_g determinations were possible for the DFM calibration, and confirmation of these can also be provided by the NWM readings in this range.



Figure 207 The procedure used to saturate the soil around a DFM probe N. 15291 in an Inanda soil at Lat. S. 29°12.47'; Long. E 30°39.125' to obtain calibration readings between f_{sat} and DUL. A similar wetting and measuring procedure was used for a nearby NWM access tube (Calibration results in Table 50)

Results and discussion

The proposed procedure of sampling temporal gravimetric samples to obtain a broad range of θ_v for the calibration proved unsatisfactory as the all-important readings close to field saturation were generally absent, because of relatively little deep infiltration due to dense tree cover and the fact that the soil in the deep levels in many cases never became wet and remained at a constant θ .

Results of the combined DFM-NWM calibration procedure for the wet end of the curve for the A and B horizons of Inanda are presented in Table 50, and calibration equations and scatter diagrams for the relevant detailed NWM and 30 cm DFM sensor calibration data for the A horizon are presented in Figure 208. Calibration equations for the three other DFM sensors of DFM probe 15291 (10 cm, 20 cm and 40 cm) are presented in Table 51. Although the linear relationships give reasonable r^2 values the scatter diagrams all indicate that the relationship may in fact be 'S' shaped, which may however be due to the influence of spatial variation of the θ_g sampling procedure used. Detailed calibration data for all the DFM probes installed at Two Streams is presented in appendix 1. Although somewhat incomplete the data may be of use in the future.

Table 50 Results of combined DFM-NWM calibration procedure in an Inanda soil. The wetting procedure used is shown in Figure 207

| | | Before water application | | | | After water application | | | | | | | |
|--------------------|------------------|--------------------------|------------------------------|------|-------------|-------------------------------------------|------------------------------|------|-------------|---------------------------------------------|------------------------------|------|-------------|
| | | at 8:00 on 3/11/2011 | | | | 3/11/2011 at 19:00 surface soil saturated | | | | 4/11/2011 at 7:45 after drainage for 13 hrs | | | |
| Diagnostic horizon | Reading depth mm | NWM CR | θ_v | | DFM reading | NWM CR | θ_v | | DFM reading | NWM CR | θ_v | | DFM reading |
| | | | $\text{cm}^3 \text{cm}^{-3}$ | S | | | $\text{cm}^3 \text{cm}^{-3}$ | S | | | $\text{cm}^3 \text{cm}^{-3}$ | S | |
| A (ah) | 300 | 1.61 | 0.398 | 0.71 | 51.9 | 2.09 | 0.560 | 1.11 | 65 | 1.93 | 0.506 | 0.9 | 57.4 |
| B (re) | 600 | 1.56 | 0.367 | 0.70 | 15.2 | 2.11 | 0.571 | 1.09 | 19.4 | 1.83 | 0.467 | 0.89 | 17.4 |
| B (re) | 900 | 1.24 | 0.248 | 0.47 | 44.2 | 1.75 | 0.437 | 0.83 | 53.3 | 1.43 | 0.319 | 0.61 | 49.1 |

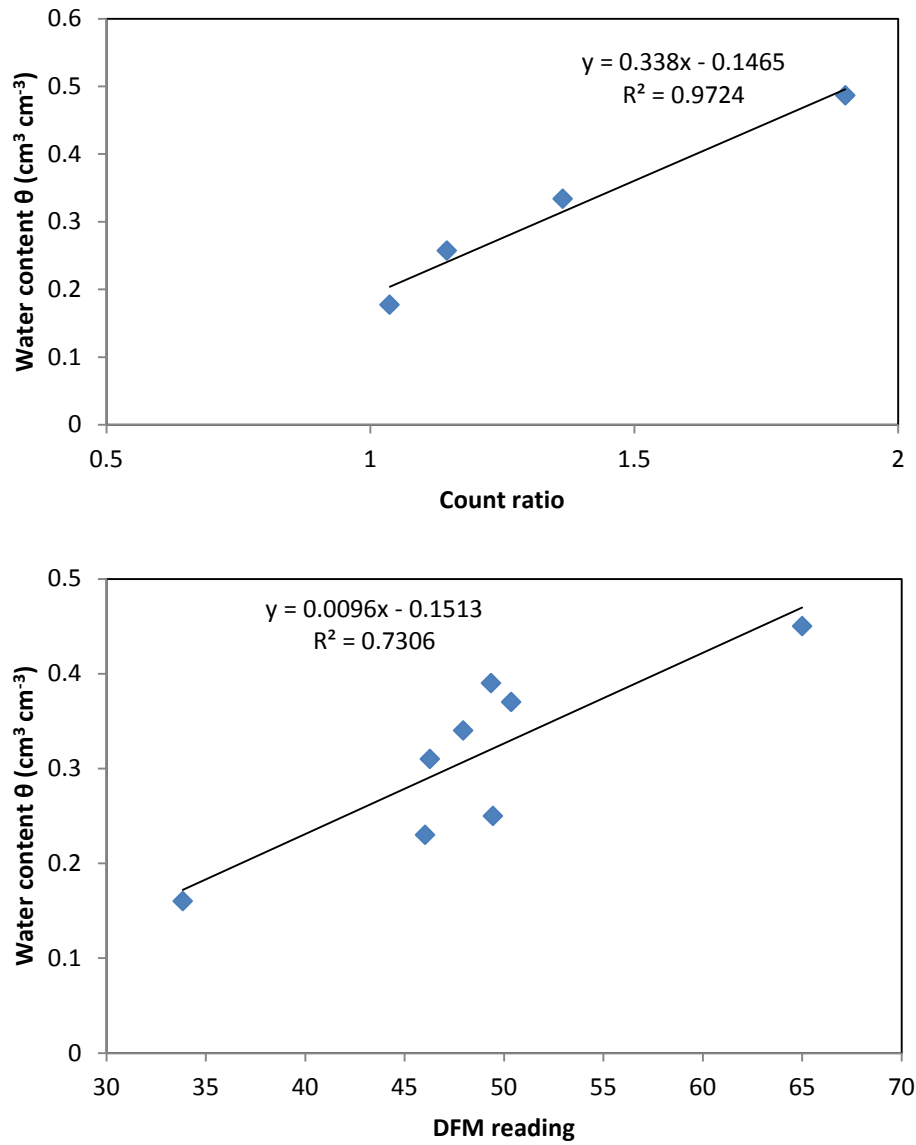


Figure 208 Calibration curve for NWM calibration at 30 cm (a); and DFM probe 15291 calibration curve at 30 cm. The neutron water meter calibration equation for the B horizon is $y=0.009x-0.151$ providing for the results provided in Table 50

Table 51 Calibration curves for DFM 15291 sensors

| Sensor depth | Calibration equations | R ² |
|--------------|-----------------------|----------------|
| 100 mm | $y = 0.008x - 0.162$ | 0.76 |
| 200 mm | $y = 0.010x - 0.220$ | 0.84 |
| 300 mm | $y = 0.009x - 0.151$ | 0.73 |
| 400 mm | $y = 0.008x + 0.002$ | 0.84 |

7.1.4 DFM measurements in the Weatherley catchment

Installation of DFM probes

Fifteen probes were installed at LC2 forming 5 ‘nests’ (Figure 209b) and 2 probes (1 ‘nest’) were installed at TB3 (Figure 209c) in the beginning of March 2010. The probes at ‘nests’ at LC2 include 3 probes each measuring at 100 and 200 mm intervals, depending on the sensor spacing up, to 2400 mm. These nests are approximately 1200 mm apart in a zigzagging in downslope direction.

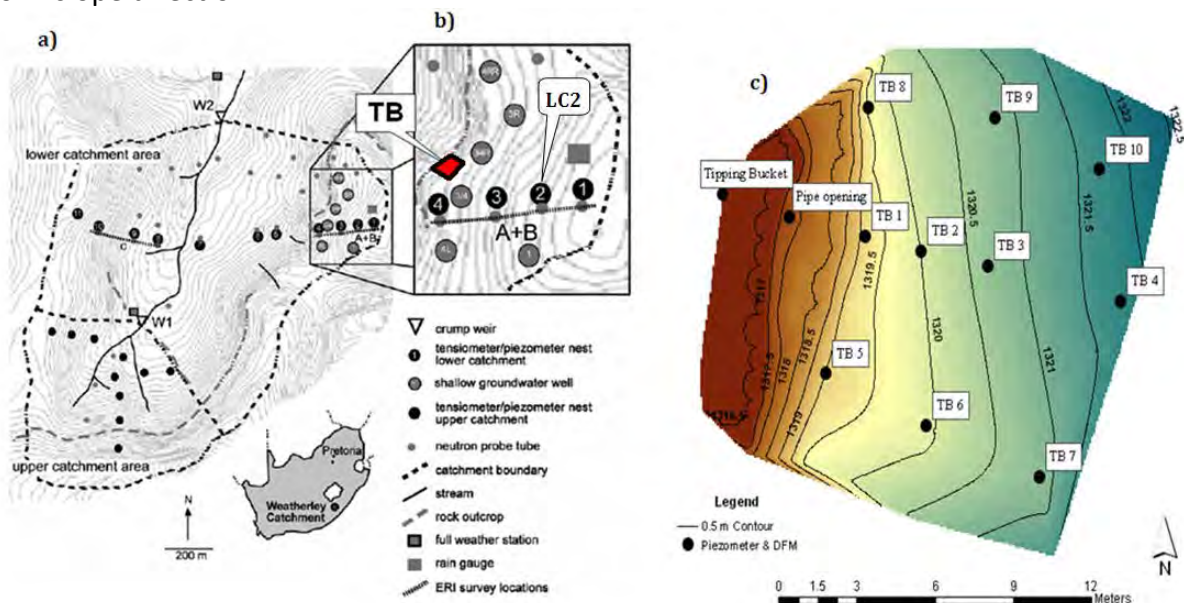


Figure 209 a) Instrumentation of the Weatherley catchment (Lorentz *et al.*, 2004), b) hillslope 1-4 with location of tipping bucket experiment and c) tipping bucket (hillslope outflow) experiment at the footslope of hillslope 1-4. TB1-TB10 in c) are perforated pipe nests. DFM probes were installed at TB1-4, TB7 and TB9

After the first examination of the measurements, it was evident that the close spacing of the nests was unnecessary. Probes from nests 1, 3 and 4 were removed and re-installed at TB1, TB2, TB4, TB7 and TB9 (Figure 209c) in the beginning of September 2010, with one or two

probes per nest depending on the soil depth. All the nests include measurements up to the bedrock. For both the 'old' and 'new' setup measurements were taken at an hourly interval.

Calibration procedure in Weatherley

The manufacturer's calibration of the probes is a straight line between dry air (0%) and a free water body (100%). From first evaluations of the measured data it was clear that the readings don't follow a straight line and the manufacturer's calibration is therefore not suitable. It was also clear that there is not a generic calibration line for all probes and in fact each sensor in each probe should have its own calibration line/curve.

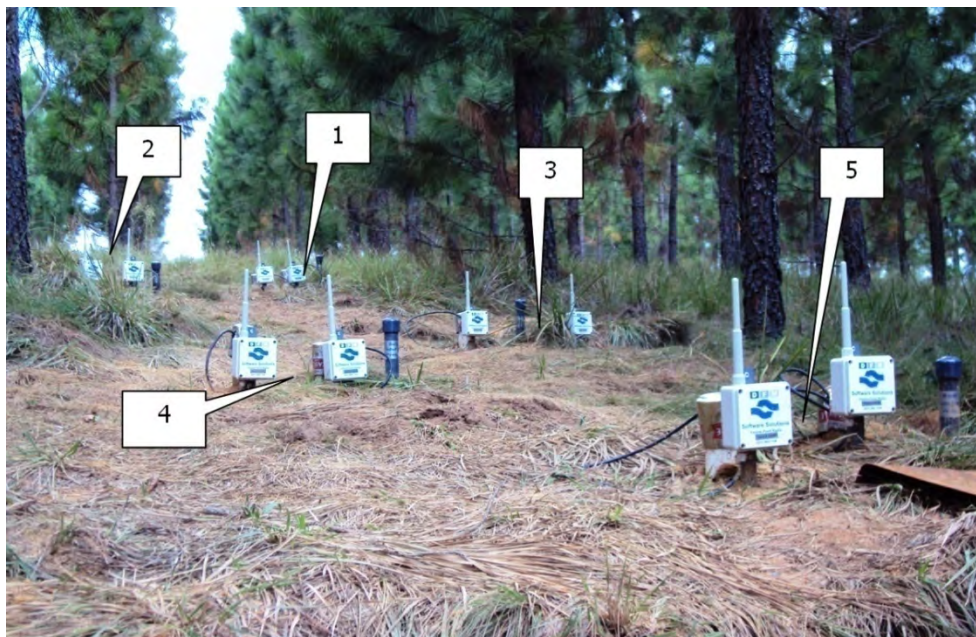


Figure 210 DFM probe setup at LC2 (March-September 2010)

Soil samples were taken at approximately 300 mm intervals during fields visit from 28 September 2010 and utilized to calculate the gravimetric and volumetric water content of the specific layer. The volumetric water contents were used to calibrate the different sensors of each probe. When a water table was observed in piezometers at TB, the water content of the soil below the water table was assumed equal to porosity. Unfortunately the shallowest water table recorded during our field visits was 550 mm below the surface, recorded on the 11th of January 2011. Sensors at 100-400 mm therefore do not have a *saturated point* for calibration.

During the brief field visit on the 11th of January 2011, the surface soils in the vicinity of TB4 was close to saturation; in fact when the *squishy boot* technique described by Dunne, Moore & Taylor (1975) was to be applied, the section of the hillslope (including TB4) would have been mapped as a '*variable source area*', i.e. saturated. On the next day 16.2 mm of rain was recorded between 15:07 and 17:23. We are convinced that the water content of the *ot* horizon was at or extremely close to saturation during and directly after the rain storm on the 12th of January. The highest probe reading of sensors 100-400 during and directly after the event was therefore selected to represent the *saturated point*, i.e. water content equal to porosity. Possible confirmation of this assumption is the that the probe

readings recorded on the 12th of January is close to the maximum probe readings ever recorded; within 2.4%, 2.2%, 1.2% and 0.5% of the maximum for sensors 100, 200, 300 and 400 mm respectively.

Polynomial regression curves with two orders were drawn to obtain the calibration curves for the sensors. The water content of the 100 and 300 mm deep sensors were finally used to represent the water content of the upper and lower part of the *ot* horizon, respectively. The 200 and 400 mm sensors were not used for reasons explained later. The average water content of the 600 and 800 mm deep sensors was used to represent the *gs* horizon.

Due to its position in the landscape the TB area is generally wetter than LC2. Since a range of water contents is essential for good calibrations and water contents were not measured when most of the probes were installed at LC2 it was thought that a back to front approach could be used to gather a greater range of water contents for the probes removed from LC2 and installed in the TB area. The idea was to obtain calibration equations for the remaining probes at LC2, to calculate the water content of different layers and using the average readings of the remaining nests as representative water content for a specific layer at a specific time when all probes were installed. This did not work; for two possible reasons; firstly the bulk density at LC2 differs from that at TB. It would be incorrect to develop a single calibration curve for one sensor to express volumetric water content based on different porosity values. The second reason is that the calibrations of the nests at LC2 only cover relatively dry moisture content readings. Since the calibration curves are not necessarily a straight line, it would be unauthentic to assume that the DFM nests at LC2 are correctly calibrated and small errors in the calibrations of the nests at LC2 could lead to large uncertainty of the water content measurements in the TB area.

Another serious elementary mistake made in the calibration procedure was to assume that the water contents at TB4 represent the water contents of the rest of the DFM nests in the TB area. Although this assumption is partially true for surface horizons during dry periods, it will definitely not work for subsurface horizons as there is an obvious increase in the water content from TB4 in a downslope direction.

The blunder in the calibration of the DFM probes only became evident after a detailed recent analysis of the data. Efforts to improve the calibration are ongoing. At this stage we are only satisfied with the calibration of the sensors at TB4. We are however comfortable to report on the presence and absence of a water table at TB4, TB3 and TB2 based on the DFM measurements. Future work will report on changes in water contents at different positions on the hillslope as measured with DFM probes.

Calibration results of TB4 in Weatherley

Measured water contents for different depths and DFM probe readings at selected dates for profile TB4 are presented in Table 52. The regression equations and accuracy of the calibration curves are presented in Table 53.

Table 52 DFM probe readings and measured water contents at profile TB4

| Date | Sensor depth (mm) | | | | | | | | | | | |
|--------------------------|-------------------|---------------|--------|----------|--------|----------|--------|----------|--------|----------|--------|----------|
| | 100 | | 200 | | 300 | | 400 | | 600 | | 800 | |
| | Sensor* | Θ^{*1} | Sensor | Θ | Sensor | Θ | Sensor | Θ | Sensor | Θ | Sensor | Θ |
| 2010/09/28 | 41.02 | 0.17 | 43.00 | 0.17 | 39.50 | 0.17 | 38.54 | 0.16 | 37.80 | 0.22 | 44.20 | 0.22 |
| 2010/12/11 | 58.06 | 0.24 | 52.63 | 0.24 | 43.05 | 0.18 | 40.24 | 0.18 | 39.81 | 0.23 | 49.13 | 0.27 |
| 2011/02/04 | 49.89 | 0.22 | 55.82 | 0.24 | 54.18 | 0.24 | 57.13 | 0.23 | 42.69 | 0.30 | 53.6 | 0.30 |
| 2011/02/09 | 45.56 | 0.19 | 51.10 | 0.23 | 53.15 | 0.23 | 52.80 | 0.23 | 41.66 | 0.30 | 52.48 | 0.30 |
| 2011/04/05 | 58.58 | 0.25 | 61.51 | 0.27 | 56.65 | 0.27 | 57.13 | 0.24 | 41.91 | 0.30 | 52.33 | 0.30 |
| 2011/01/11 ^{*2} | | | | | | | | | 52.40 | 0.37 | 71.1 | 0.37 |
| 2011/01/12 ^{*3} | 65.07 | 0.31 | 63.22 | 0.31 | 58.41 | 0.31 | 61.57 | 0.31 | | | | |

* DFM sensor reading, all these sensor are mounted on a single probe; ^{*1} water content (mm mm⁻¹); ^{*2} Water table 550 mm below surface; ^{*3} Predicted point of saturation

Table 53 Calibration curves for DFM sensors at TB4

| Sensor depth | Calibration equations | R ² |
|--------------|----------------------------------------|----------------|
| 100 mm | $y = 0.00012x^2 - 0.00739x + 0.27127$ | 0.98 |
| 200 mm | $y = -0.00019x^2 + 0.02479x - 0.55545$ | 0.98 |
| 300 mm | $y = 0.00043x^2 - 0.03528x + 0.892621$ | 0.99 |
| 400 mm | $y = 0.00026x^2 - 0.02091x + 0.58224$ | 0.90 |
| 600 mm | $y = -0.00087x^2 + 0.08940x - 1.92667$ | 0.94 |
| 800 mm | $y = -0.00021x^2 + 0.02921x - 0.66979$ | 0.99 |

The calibration equations are accurate with R² values greater than 0.9 (although polynomial equations with six points seldom yield low regression coefficients). The difference between the calibration lines of the various sensors is however a disadvantage of the DFM measuring probes (Table 53). Every sensor in every new installed probe should be calibrated separately; a laborious and time consuming exercise.

7.1.5 Conclusions

DFM probes

This study showed that DFM capacitance probes can be field calibrated. In an earlier study (Kuenene *et al.*, under review), the value of DFM capacitance probes was demonstrated for determining saturated hydraulic conductivity of an A horizon *in-situ*. Even though some R² values were low, field calibration better reflects real world variability. Variations from a straight line in the current calibration lines could be due to spatial variation of θ_g sampling technique used during the previous calibration procedure. This could be decreased

considerably by the procedure proposed below. The procedure can also improve the precision with which calibration lines can be extrapolated in similar soils.

The following is a proposed procedure for the calibration of DFM probes.

A reconnaissance survey of the hillslopes is necessary for the following purposes:

To identify the important soil pedons (sp) in which continuous measurements of θ will be needed to understand the hydrological functioning of the main hillslopes;

The locations (GPS) of all the important sites at which these sp occur, in order to decide the number of DFM probes that will be needed for each sp.

Select logistically suitable locations for these sp (e.g. easily accessible for water supply and for taking readings) for carrying out the calibration procedure. Fix these locations by GPS.

Describe the modal sp's in detail and take triplicate bulk density (ρ_b) samples to represent each one, together with a reasonably large volume of disturbed soil sample in which the structure has been disturbed as little as possible. The chemical and physical (including water retention curves) analytical results from these samples will be valuable for developing pedotransfer functions (PTF's) that will facilitate future decisions regarding DFM probe calibrations in other catchments for which hydropedological studies are being made. Carry out the calibration procedure in about the middle of the dry season. In each modal sp site, insert the total number of DFM probes that will be needed for the whole hillslopes being studied, arranged according to Figure 211 around a neutron water meter (NWM) access tubes at which a reading can be taken at the same depth as the DFM probe.

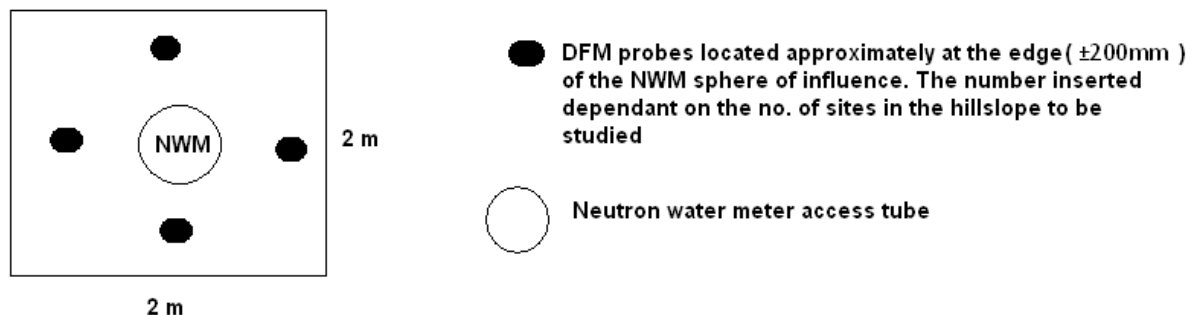


Figure 211 A schematic diagram of a procedure to calibrate DFM probes using a NWM

1. When inserting the NWM access tube, take a soil sample of the 300 mm soil layer a θ_g determination to calibrate the dry end of the NWM calibration curve. Take NWM readings in this dry soil at the appropriate reading depths of the DFM sensors. The dam needs to be $\pm 2 \text{ m} \times 2 \text{ m}$ to avoid a θ gradient towards the edges in this dry soil. Saturate this dam with water while continually reading the NWM and DFM probes, and continue saturating until all the instruments give a maximum reading, indicating field saturation (*fsat*). Record all *fsat* readings. Thereafter take NWM readings hourly for at least 12 hours, and later less frequently. Cover the area efficiently with plastic sheet and leave to drain and record all NWM and DFM probe readings until drained upper limit (DUL) is approximately reached. At DUL take 3 θ_g samples from every diagnostic horizon for θ_g determinations from locations at different points in the "dam".

2. When DUL has been reached remove the DFM's and insert each at its previous selected (see bullet 2) correct location, leaving one set of DFM's *in situ* for its dry end readings to be controlled by the NWM readings as the soil is dried out by the surrounding vegetation.
3. At each subsequent visit to the catchment take θ_g samples to calibrate the dry end of the calibration curves of all the DFM and NWM still at the original site.
4. Process all the data to provide separate calibration curve for each sensor of each DFM.

Watermark sensors

Since these sensors read soil water potential they do not need to be recalibrated for each new soil horizon – a major advantage for hydropedological studies. Also, for hydropedological studies the all-important fsat θ reading for these sensors is well defined, i.e. at zero potential. The good results reported in section 7.3.3.2 using these instruments confirm their value for our field studies. It is recommended that they be used for future hydropedological studies in line with a similar recommendation by an experienced international hydropedologist (J. Bouma, personal communication).

Measurements to monitor θ at depths > 2 m

Measurements to monitor θ continually in the solum are important for a number of reasons. Below the solum, however, where changes in θ are generally less frequent and slower, and a lower degree of precision is required, relatively infrequent measurements for monitoring purposes should generally supply the information required. Clulow *et al* (2011) made detailed studies of continuous changes in θ at depths between 2 and 5 m at one site in a large, deep pit in the Two Streams catchment using sophisticated and expensive measuring equipment (e.g. TDR). They produced valuable results, appropriate for a research catchment, but not generally appropriate for routing hydropedological hillslope studies. For the latter studies infrequent measurements by NWM for depths between 2 and 5 m would provide valuable low cost results for monitoring θ changes in saprolite and, or, the intermediate vadose zone (IVZ). Six meter long, low cost PVC pipes of the correct diameter and suitable for this purpose are readily available. It is likely that around four measurements per year at carefully select hillslope sites would provide valuable information about storage and water movement in the IVZ. In the summer rainfall area measurements in the saprolite/IVZ could be approximately as follows: in September to measure 'empty' or DUL; December/January to measure 'filling up'; March to measure 'full'; April/May to measure 'draining'.

Using NWM measurements made by Everson *et al* (2008), Kuenene (2013) presents valuable relevant results in this connection for a hillslope adjacent to the Two Streams catchment. He also proved that it is possible to auger to a depth of 5 m in the deep saprolite there and use data from this augering to obtain reasonably reliable ρ_b values for the saprolite. Dye *et al* (1997) made successful NWM measurements to a depth of 7 m to monitor changes in θ while studying water use by eucalyptus trees.

7.2 REFERENCES

- ATKINS, RT, PANGBURN, T, BATES, R.E. & BROCKETT, B.E. 1998 Soil moisture determination using capacitance probe methodology. Special report 98-2.US Army Corps of Engineers. CRREL.
- BITTELLI, M. 2011. Measuring soil water content: A review. *HortTechnology*. 21, 293-300.
- CLULOW, A.D., EVERSON, C.S., & GUSH, M.B., 2011. The long-term impact of *Acacia Mearnsii* trees on evaporation, streamflow and groundwater resources. WRC Report no. TT 505/11. Pretoria, South Africa.
- EVERSON, C, MODDLEY, M, GUSH, M, JARMAIN, C, GOVENDER, M. and DYE, P(2008) Can effective management of riparian zone vegetation significantly reduce the cost of catchment management and enable greater productivity of land resources. WRC Report no. 1284/1/07. Pretoria, South Africa.
- DFM SOFTWARE SOLUTIONS C. C., 2011 Continuous logging soil moisture probes. Retrieved March, 2011: <http://www.dfmsoftware.co.za/probes.html>
- DYE, P.J., POULTER, A.G., SOKO, S. & MAPHANGA, D. 1997. The determination of the relationship between transpiration rate and declining available water for *Eucalyptus grandis*. Water Research Commission Report No. 441/1/97.
- DUNNE, T., MOORE, T.R. and TAYLOR, C.H., 1975. Recognition and prediction of runoff producing zones in humid areas. *Hydrol. Sci. bull.* 20:305-327.
- FARES, A and POLYAKOV, VO (2006) Advances in Crop Water Management Using Capacitive Water Sensors. In D. Sparks (ed.), *Advances in Agronomy*. Vol.90, Academic Press.
- INTERNATIONAL ATOMIC ENERGY AGENCY (2008) Field estimation of soil water content. A practical guide to methods, instrumentation and sensor technology. Training course series No. 30. Vienna.
- GEBREGIORGIS, M.F. and SAVAGE, M.J., 2006. Field, laboratory and estimated soil-water content limits. *Water SA*. 32(2):155-162.
- GEESING D, BACHMAIER M and SCHMIDHALTER U (2004) Field calibration of a capacitance soil water probe in heterogeneous fields. *Australian J. Of Soil Res.* 24 289-299.
- KUENENE, B.T. 2013. Hillslope hydrogeology of the Two Streams catchment in KwaZulu-Natal. PhD thesis. University of the Free State, Bloemfontein.
- KUENENE, B.T., LE ROUX, P.A.L., EVERSON, C.S. and HENSLEY, M., 2013. Hydraulic conductivity and macroporosity of diagnostic horizons in the Two Streams first order catchment in KwaZulu-Natal. Under peer review in *WATER SA Journal*.
- LORENTZ, S.A., THORNTON-DIBB, S., PROTORIUS, C. & GOBA, P., 2004. Hydrological systems modelling research programme: hydrological processes. Report No. 1061 & 1086/1/04. Water Research Commission, Pretoria.
- NHLABATSI, NN(2010) Soil water evaporation studies on the Glen/Boheimecotope. PhD Thesis, University of the Free State, Bloemfontein, South Africa.
- POLYAKOV, V., FARES, A., and RYDER, M.H. 2005. Calibration of a capacitance system for measuring water content of tropical soil. *Vadose Zone J.* 2(4): 1004-1010.
- ROBINSON, DA, GARDNER, CMK, EVANS, J, COOPER, JD, HODNETT, MG and BELL, JP (1998) The dielectric calibration of capacitance probes for soil hydrology using an oscillation frequency response model. . *Hydrology and Earth Sys Sci.* 2(1): 110-120.
- ZERIZGHY MG, VAN RENSBURG LD and ANDERSON JJ (2013) Comparison of neutron scattering and DFM capacitance instruments in measuring soil water evaporation. *Water SA* 39 (2) 183-190.

- VAN DER WESTHUIZEN, R.J. & VAN RENSBURG, L.D. 2011. Rapid procedure to calibrate EC-10 and EC-20 capacitance sensors in soil. *Water SA*. 39, 733-737.
- VAN HUYSSTEEN, C.W., HENSLEY, M., LE ROUX, P.A.L., ZERE, T.B. and DU PREEZ, C.C., 2005. The relationship between soil water regime and soil profile morphology in the Weatherley catchment, an afforestation area in the Eastern Cape. WRC report No. 1317/1/05. Water Research Commission, Pretoria
- VAN RENSBURG, L.D. 2010. Advances in soil physics: Application in irrigation and dryland crop production. *S. Afr. J. Plant Soil*. 27, 9-18

7.3 FIELD MEASUREMENTS OF K_s AND K_H LOW TENSIONS – MACROPOROSITY

7.3.1 Introduction

The success and reliability of sophisticated hydrological models are critically dependent on accurate information of hydrogeological system parameters. Double ring and tension infiltrometers on the diagnostic horizons of selected modal profiles can be used to gather information by measuring *in situ* the saturated and near saturation hydraulic conductivity of diagnostic horizons in representative soil types.

For hydrogeological purposes it is useful to focus attention on characterizing hydraulic conductivity (K) for soil wetness values close to saturation, partly because this is important for describing macropore functioning (Jarvis, 2008; Šimunek *et al.*, 1999). It is appropriate to classify macropores as those of diameter >1 mm (Luxmoore, 1981). In the absence of significant matric suctions at near saturation, the saturated hydraulic conductivity (K_s) is representative of the maximum flux rate the soil can assume under steady state conditions. Its dependence to pore size distribution shows that each soil has a different K_s value, and this could also vary under different land use practices.

The importance of macropores was recognised almost 150 years ago when Schumacher (1864) (in Beven and Germann, 1982) noted that the permeability of soils during infiltration is controlled mainly by “big pores” where water is not held by capillary forces. Macropores play an important role in the rapid transport of water, solutes and pollutants through the soil, not only during infiltration but also in subsurface lateral flow and storm (quick) flow generation of streams (Beven and Germann, 1982; Slogar and Moore, 1984; Perroux and White, 1988; McDonnell, 1990; Jarvis and Messing, 1995; Bodhinayaka, *et al.*, 2004; Moret and Arrúe, 2007; Clothier *et al.*, 2008).

Macropore flow, also termed preferential or ‘by-pass flow’, can be defined as ‘*all phenomena where water and solutes move along certain pathways, while bypassing a fraction of the porous matrix*’ (Hendrick and Flury, 2001). This has huge impacts on the environment: agricultural contaminants (fertilizers, pesticides, toxic trace elements); radionuclides from nuclear waste facilities; other pollutants from waste disposal sites; mine tailings, etc. can all be transported to significant depths and over vast distances without being in contact with the soil matrix, where degradation of the potential toxins normally occurs (Šimunek *et al.*, 2003). Transport through macropores moves faster and to greater depths than would be predicted with Richards’s equation, and due to the irregular wetting of the soil it is considered the greatest encumbrance for accurate predictions of

contaminant transport in soils. Besides contaminant transport, preferential flow influences water flow in landscapes to such an extent that it can alter the residence time of water in catchments and cause difficulties in predicting water releases into streams and groundwater bodies. This is especially problematic in ungauged catchments, where data for calibrations of hydrological models are unavailable.

There are four main types of macropores: i) biopores formed by soil fauna, e.g. earthworms and moles, ii) biopores formed by plant roots, iii) structural pores in soils with high 2:1 clay mineral contents and iv) soil pipes formed due to erosive action of subsurface flow. Pores i) and ii) are normally dominant in the A horizon whereas iii) and iv) are found in deeper horizons (Beven *and Germann*, 1982; Nieber *et al.*, 2000 and Lin *et al.*, 2006). Macropores can either be non-continuous (dead-ended) or continuous (interconnected); only the latter contribute to fast flow in soils (Bodhinayake *et al.*, 2004). A high degree of macroporosity does not necessarily mean that the soil has a high hydraulic conductivity, as the pores may be discontinuous. Furthermore, in an interconnected pore system, the section of the pore with the smallest diameter will control the flow rate through the specific pore, i.e. the bottle neck effect. *In situ* measurements of the actual water conducting pores are therefore extremely important as laboratory measurements might not satisfactorily describe the actual *Water Conducting Macroporosity (WCM)*.

Procedures for estimating soil macroporosity, i.e. the fraction of soil volume comprising macropores, includes dye tracing (Bouma *et al.*, 1977; Flury *et al.*, 1994), X-ray computed tomography (Anderson *et al.*, 1990), direct measurements on soil exposures (Edwards *et al.*, 1979), and direct measurement of K at matric potentials close to saturation, using the double ring procedure and tension infiltrometers (Reynolds and Elrick 1991). The latter procedures have proved to be reliable and useful for characterizing hydraulic properties and soil structural conditions at and near the soil surface (Watson and Luxmoore, 1986; Ankeny *et al.*, 1991; Dunn and Philip, 1991; Reynolds and Elrick 1991; Cameira *et al.*, 2003, Van Tol, *et al.*, 2012). The double ring procedure and tension infiltrometer method can be conveniently applied to field conditions because of the simple experimental apparatus and straightforward mathematical models. With the tension infiltrometer one can determine the contribution of different pore size ranges by precisely selecting the water supply potential. From the differences in infiltration rates under different supply potentials, the number and volume fractions of hydraulically effective macropores and mesopores have been derived in agricultural (Dunn and Phillips, 1991; Moret and Arrue, 2007) and forest soils (Watson and Luxmoore, 1986; Wilson and Luxmoore, 1988). Watson and Luxmoore (1986) found that 73% of K_s was due to macropores, which constituted only 0.04% of the soil volume in the forest soils they studied. In the agricultural soils that they studied, Moret and Arrue (2007) found that 75% of K_s was controlled by the macropores and 16% by the mesopores. Development of macropore flow models (PTFs) is a key requirement for enhancing extrapolations of soil properties across similar.

Pedo-transfer functions (PTF's) emphasize the link between soil survey (pedology) and soil hydrology (Bouma, 2004). A vast number of PTF's have been developed, using relatively easily observable and measureable properties such as texture, bulk density (D_b) and organic matter (OM) to estimate hydrological properties and processes which are more difficult and time consuming to determine. Pachepsky and Rawls (2004), with specific reference to Lilly and Lin (2004), present an excellent description of the development, validation and application of PTF's. There is however evidently no current PTF available for estimating

WCM. A study by Griffiths *et al.* (1999), made use of similar approaches as were followed in this study, but focussed only on structural properties without using *WCM* as described here. Soil properties affecting and reflecting macroporosity includes *inter alia*; structure type and size, clay type and percentage, D_b , OM content and the presence of root channels, animal burrows and coarse fragments. In this study these soil properties were used to predict the *WCM* in a range of horizons in South African soils. The *WCM* were measured *in situ* with a combination of double ring and tension infiltrometer procedures. A detailed procedure and results is reported on Two Streams catchment. Using the soil properties in question, three multiple regression equations were formulated; the first two to predict the *WCM* using all available soil information and the last using morphological descriptions of the soils only. The latter was done to support predictions of hydrological processes in ungauged basins (PUB's), i.e. areas with little or no measurements. These pedo-transfer functions (PTF's) will aid in the understanding and prediction of water and contaminant flow in soils and landscapes.

7.3.2 Methodology

K_s and $K(h)$ low tensions *in situ* determination

In the Two Streams catchment (Figure 212), A profile pit was dug at each of the modal profiles and soil properties were described and classified (Soil Classification Working Group, 1991). On each profile, infiltration runs per diagnostic horizon were carried out with a double ring infiltrometer and a tension infiltrometer technique to determine saturated hydraulic conductivity and unsaturated hydraulic conductivity.

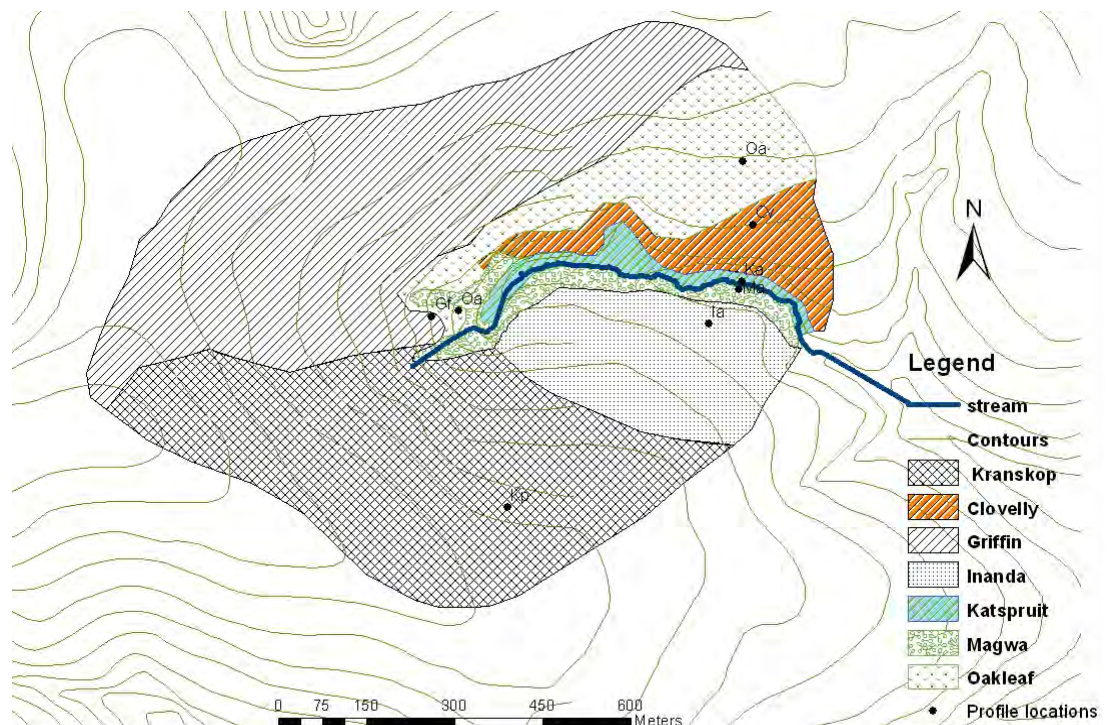


Figure 212 Modal profile locations on the three different soilscares of the Two Streams catchment

Signs of hydrophobicity in the A horizon were noted. The horizon was therefore scraped a bit deeper (2 cm) and pre-wetted to minimize surface water repellency. In order to measure on the B horizon, topsoil was removed across the face of the profile to expose the B-horizon.

Macropores in this study were considered to be pores which will be emptied at a suction head of 3 cm with an equivalent pore radius (r) larger than 0.05 cm, following Luxmoore (1981). Macroporosity was calculated using the Watson & Luxmoore (1986) approach from the difference between ponded (double ring) infiltration rate and the infiltration rate at a tension of 3 cm, together with the assumption that steady state can be assumed at this low tension, i.e. the Darcy equation reduces $q(h) = K(h)$. The theory behind this approach is that the capillary rise equation can be used to calculate the maximum pore size [(r) in cm] which is filled with water at a certain suction head [(h) in cm] (Bear, 1972):

$$r = \frac{2\gamma \cos \beta}{gh\rho_w} = \frac{0.15\text{cm}^2}{h_{cm}} \quad (7.2)$$

Where r is the pore radius (cm), γ is the surface tension of water (g cm^{-2}), β is the contact angle between the water and the pore wall (assumed to be zero), ρ_w is the density of water (g cm^{-3}), g is the acceleration due to gravity (cm s^{-2}) and h is the soil water suction in cm. The constant in equation 7.2 calculates to a value very close to 0.15. Hence with h set at 3 cm the equivalent value of r is 0.05 cm, i.e. a diameter of 1 mm. Using the result (r) from equation 7.2 in conjunction with Poiseuille's equation, the maximum number of hydraulically effective macropores per unit area can be calculated (Watson and Luxmoore, 1986);

In this study macroporosity conductivity (K_m) is considered as the difference between the ponded infiltration rate (K_p) and the infiltration rate [$K(h)$] when $h = 3$ cm. Using the minimum pore radius at a certain tension in conjunction with Poiseuille's law the maximum number of water conducting macropores was determined by (Watson & Luxmoore, 1986):

$$N = \frac{8\mu}{\pi\rho_w g} \times \frac{K_m}{r^4} \quad (7.3)$$

Where μ is the dynamic viscosity of water ($\text{g cm}^{-1} \text{s}^{-1}$), K_m is macropore conductivity described as the difference between the ponded infiltration rate (K_s) and the infiltration rate (K_h) at a selected tension. Other symbols are as in equation 7.2. It is useful to note that the first part of equation 7.5 is a constant with a value of $2.597 \times 10^{-5} \text{ cm s}$. This is correct if one assumes a reasonable average water temperature of 20°C and therefore a μ value of $1.00 \times 10^{-2} \text{ g cm}^{-1} \text{s}^{-1}$. Assuming that the value used for r in equation is 0.05 cm, to ensure appropriate units for N , K_m needs to be expressed in cm s^{-1} , giving the units of N as pores per cm^2 . The total effective water conducting macroporosity ($\text{m}^3 \text{m}^{-3}$) is then given by (Watson and Luxmoore, 1986);

$$\theta_m = N\pi r^2 \quad (7.4)$$

Note that with r taken as 0.05 cm the units of θ_m in equation 7.6 are cm^2 . The contribution of the macropore to K_s is estimated as;

$$\phi(\%) = \frac{K_m}{K_s} * 100 \quad (7.5)$$

Where ϕ (%) is percent of total flux due to the macropores and K_s is the saturated hydraulic conductivity.

The saturated hydraulic conductivity was determined using a modified Bouwer-Rice (1976) falling head method:

$$K_s = \frac{L}{t} \times \frac{(h_0 + L)}{(h_1 + L)} \quad (7.6)$$

Where: L = thickness of horizon (L); t = time till constant infiltration rate was obtained (T) and h_0 and h_1 = head of water above surface before and at the start of test and after t respectively.

Developing water conducting macroporosity (WCM) pedotransfer function (PTF)

The total effective water conducting macroporosity θ_m (determined as above) was calculated for 120 horizons distributed over South Africa following the procedure described above. Soil information used for development of the PTF's was obtained from own field measurements, existing soil profile descriptions and physical measurements from the Land Type database (Land Type Survey Staff, 1972-2006), and from research sites (Lorentz *et al.*, 2004, Van Huyssteen *et al.*, 2005, Le Roux *et al.*, 2011 and Ridell, 2011).

Three multiple regression models were developed; models 1, 2 and 3. The first model made use of all soil properties, both quantitative and qualitative, which might influence *WCM* using a *best model* approach with maximum number of variables. The values obtained were used to determine the appropriateness of different variables for estimating *WCM*. It is important that data and statistics do not surpass common pedological knowledge (Bouma, 2004), and therefore model output values which contradict our understanding of the soil-hydrological system were not used in the development of models 2 and 3. Model 1 is therefore only used for general discussions on soil property influences on *WCM* and purification of the variables used in models 2 and 3. Model 2 was developed using a backward analysis approach where the procedure starts by simultaneously including all variables, the impact of removal of different variables was then evaluated. If the probability of the calculated statistic was greater than the removal threshold value (0.1), the variable was removed from the model. The third model only made use of easily observed soil properties, i.e. no measurements, using the *best model* approach. Two assumptions were made: 1) pedologists are able to estimate the clay content of a soil horizon within 5% of the measured clay percentage; 2) pedologists are able to estimate the organic carbon content within 0.5% of the measured organic carbon percentage. The aim of model 3 is to aid in the prediction of *WCM* in ungauged areas.

Quantitative soil information used in this study is presented in Table 54 and the categories of qualitative information in Table 55. The reason for the inclusion of the different parameters is discussed in the next section. The minimum and maximum values in Table 54 are the range within which the models are tested and can be considered the boundary conditions of the different models.

Table 54 Description of the quantitative soil properties used in the development of the PTF's

| Parameter | Abbreviation | Unit | Maximum | Minimum | Average | Mode |
|--------------------|----------------|-------------------------------|---------|---------|---------|-------|
| Bulk density | D _b | Mg m ⁻³ | 1.86 | 0.70 | 1.50 | 1.68 |
| Organic carbon | OC | % | 6.81 | 0.04 | 1.27 | 0.40 |
| Clay | Cl | % | 68.70 | 3.70 | 28.62 | 24.00 |
| Silt | Si | % | 54.40 | 0.60 | 18.16 | 24.00 |
| Sand | S | % | 86.20 | 8.00 | 52.15 | 41.30 |
| Extractable Sodium | Na | cmol(+) kg ⁻¹ soil | 3.10 | 0.00 | 0.32 | 0.10 |
| Swelling Index | S_Index | | 34.91 | -8.51 | 7.33 | 2.08 |

The swelling index in Table 54 serves as an indication of the physical activeness of the soil, i.e. the extent of shrinking and swelling of the soil during wet and dry periods. The type of clay determines the physical activeness of soils to a large degree, with 2:1 clays being more active than 1:1 clays. The former are usually associated with higher cation exchange capacities (CEC) than the latter; this is the basis for calculation of the swelling index. Organic matter has a CEC of 100-550 cmol_c(-) kg⁻¹ and contains approximately 58% OC. A CEC of 100 cmol_c(-) kg⁻¹ was assumed for organic matter, but since the swelling index is dimensionless an exact value is redundant. The contribution of OC to the total CEC of the soil was subtracted to obtain the contribution of the clay to the CEC of the soil and thereby its influence on the swelling index:

$$\text{Swelling Index} = \text{CEC}_{\text{soil}} - (\text{OC} \times 1.7241) \times 100 \quad (7.7)$$

To compensate for erroneous descriptions of the soils, qualitative variables were divided into broad classes instead of detailed categories, for example; the size of pores are either medium or fine, pore sizes bigger than medium, i.e. coarse and very coarse are all considered medium just as the amount of roots and pores, distinguishes only between few, common and many (Table 55). Distinctions are made between master horizons overlying freely drained horizons and those which overly horizons with indications of saturation. The former are designated by A1 or B1 and the latter by A or B.

The double cross-validation method (Green and Carroll, 1978) was applied to evaluate the stability of regression coefficients and the prediction level of models 2 and 3. The advantage of this approach is that no additional data are required; the data set is randomly split into halves and regression analyses performed on each half using the same variables as in the complete data set. The equation from the first half is then applied on the second and *vice versa*. A correlation between observed and predicted values is then calculated.

Table 55 Description of qualitative soil observations used for development of PTF's

| Variable | Abbreviation | Categories | Frequencies* |
|-----------------|--------------|--------------------|--------------|
| Structure grade | S_Grade | Apedal | 66 |
| | | Moderate | 15 |
| | | Strong | 11 |
| | | Weak | 28 |
| Structure type | S_Type | Angular blocky | 17 |
| | | Massive | 66 |
| | | Prismatic | 7 |
| | | Sub-angular blocky | 30 |
| Amount of roots | Roots | Common | 38 |
| | | Few | 38 |
| | | Many | 44 |
| Amount of pores | P_Amount | Common | 25 |
| | | Few | 46 |
| | | Many | 49 |
| Size of pores | P_Size | Fine | 62 |
| | | Medium | 58 |
| Master horizon | Horizon | A | 18 |
| | | A1 | 44 |
| | | B | 12 |
| | | B1 | 29 |
| | | E | 6 |
| | | G | 11 |

*Number of horizons out of the total of 120

7.3.3 Results and discussions

Pedo-transfer function for water conducting macroporosity

Resultant values of different soil properties in the three different PTF's are presented in Table 56.

Model 1

From model 1 it is clear that an increase in D_b will result in lower WCM , whereas more OC will favour the formation of more water conducting macropores. The swelling index proves that an increase in clays which are physically active will result in the sealing of macropores upon wetting of the soil. An increase in the Si percentage relative to S and Cl percentages will result in slightly less macropores actively conducting water. This is expected as high Si contents are prone to clog pores. The positive correlation between WCM and Na content is however questionable; Na^+ ions have a large hydrated volume compared to their charge, when Na^+ dominates it therefore tends to disperse the soil aggregates causing clogging of the pores and lowering the infiltration rate. This incongruity in the estimated values may be attributed to the relative small amount of extractable Na in the soils used in this study (Table 54). Dispersion by Na occurs normally at Na contents higher than $10 \text{ cmol (+) kg}^{-1}$. Na was not used in models 2 and 3 due to this discrepancy.

Table 56 Description of the model variables and their associated values

| Variable | Categories | Model 1 | Model 2 | Model 3 |
|-------------------------|--------------------|---------|---------|---------|
| Intercept | | -1.159 | -0.126 | -0.325 |
| D_b | | -0.511 | | * |
| OC | | 0.528 | 0.664 | * |
| OC | Estimated | * | | 0.562 |
| S_Index | | -0.035 | -0.027 | * |
| S | | 0.025 | | * |
| Si | | 0.015 | | * |
| Cl | | 0.026 | | * |
| Cl | Estimated | * | | -0.001 |
| Na | | 0.258 | * | * |
| S_Grade | Apedal | 0.369 | 0.310 | 0.405 |
| | Moderate | 0.097 | | -0.184 |
| | Strong | -0.067 | | -0.336 |
| | Weak | 0.000 | | |
| S_Type | Angular blocky | 0.270 | | 0.371 |
| | Massive | 0.000 | | |
| | Prismatic | -0.145 | | -0.510 |
| | Sub-angular blocky | 0.000 | | |
| Roots | Common | -0.314 | * | * |
| | Few | 0.049 | * | * |
| | Many | 0.000 | * | * |
| P_Amount | Common | -0.133 | | -0.209 |
| | Few | -0.228 | | -0.362 |
| | Many | 0.000 | | |
| P_Size | Fine | -0.230 | | -0.340 |
| | Medium | 0.000 | | |
| Horizon | A | -0.357 | | 0.273 |
| | A1 | -0.037 | | 0.637 |
| | B | -0.183 | | 0.356 |
| | B1 | -0.045 | | 0.422 |
| | E | -0.289 | | 0.170 |
| | G | 0.000 | | |
| No. of variables | | 13 | 3 | 7 |
| R² | | 0.782 | 0.737 | 0.689 |

*Variables not used in models

Soil structure has a variable impact on *WCM*. Apedal and moderate grades seem to enhance *WCM*, whereas strong grades lower *WCM*. Neither weak grades nor massive or sub-angular blocky structure types have any significant influence of *WCM*. The inconsequential contribution of massive structure types are a bit in contradiction with the high positive correlation with apedal grades. Angular blocky types are the most porous and will be highly conducting especially when it is moderately developed. Prismatic types hinder *WCM*. The low conductivity of prismatic horizons was observed during the in-field determinations of *WCM*, where water ponded weeks after the last significant rain in and on horizons overlying prismatic structures.

Contrary to expectations *WCM* increases with an increase in the number and size of pores but decreases with an increase in amount of pores. Due to this discrepancy the amount of roots was not used in models 2 and 3.

An increase in soil depth is normally associated with an increase in *D_b* and a decrease in *OC*. It was therefore surprising that the B and B1 horizons have a higher positive correlation than that of the A horizons. Master horizons overlying freely drained horizons, i.e. A1 and B1, have a higher positive correlation compared to their counterparts. Gleyed and prolonged saturated conditions are ordinary in G and E horizons, explaining their slightly lower value.

A total of 13 variables and 22 categories were used in model 1 resulting in a R^2 value of 0.782. Due to the great number of variables the adjusted R^2_{adj} is lowered considerably, 0.73.

Model 2

The majority of the variables used in model 1 are deemed unnecessary when the backward analysis approach was followed. The OC content, calculated S_Index and an apedal structure grade gave relatively good estimations of the WCM with an R^2 of 0.737. Results of the predicted and measured WCM are presented graphically in Figure 213. Interestingly is the discard of particle size distributions, i.e. S , Si and Cl fractions, the composition of soils in terms of these distributions are normally the dominant (and sometimes only) variable in a number of existing PTF's.

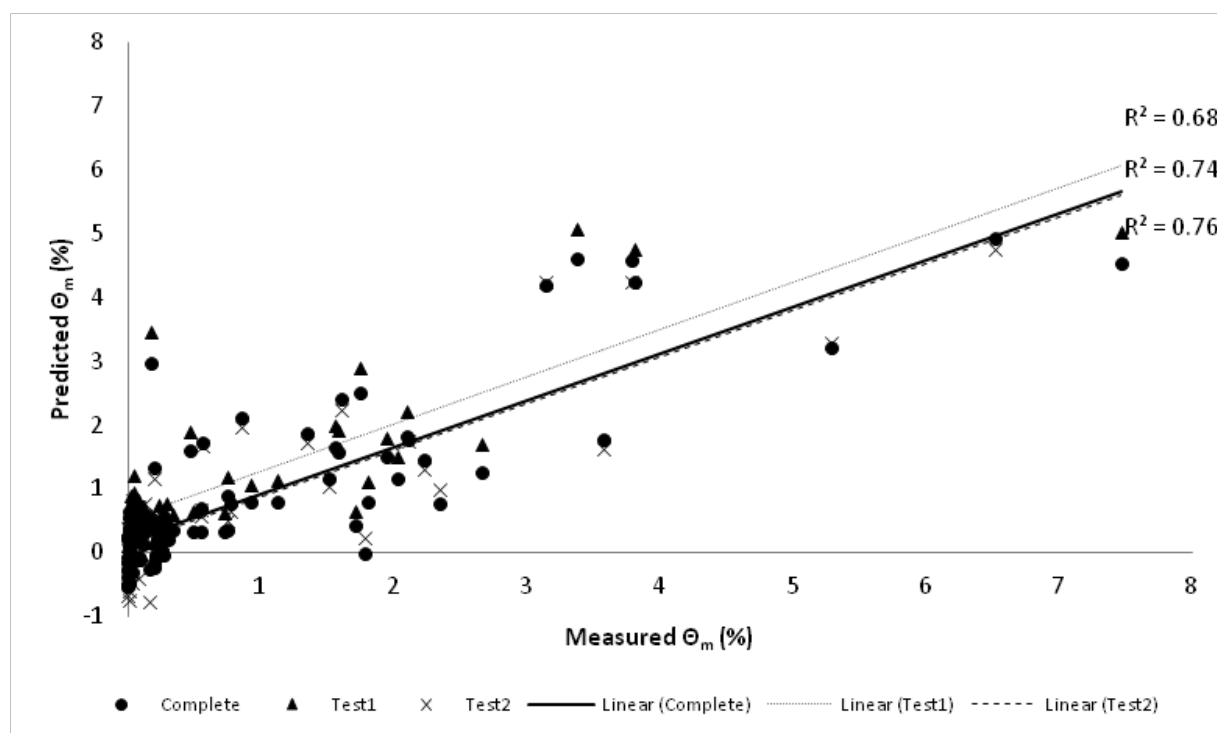


Figure 213 Predicted vs. measured WCM using model 2. Test 1 & 2 represents the double-cross validation prediction results whereas 'complete' represents the original dataset and model equation from Table 56.

The consistency of model 1 to predict the Θ_m is reflected by the similar slopes of the test results compared to that of the original model. The obtained R^2 of the different portions of the dataset indicates that this model is consistent and suitable for estimating the WCM in a range of soil horizons.

Model 3

The last model made use of 7 variables and 15 categories to obtain an R^2 of 0.689. The values assigned to the different variables are in accord with general soil science knowledge. Results of the original model and the validation tests are presented in Figure 214. The low value assigned to estimated clay contents emphasizes that the extent of macroporosity and

consequently the shape of the hydraulic conductivity curve are influenced more by structural and the associated organic matter content than by the particle size distribution. The importance of the OC contents is highlighted by the relatively high positive values in all the models. Although estimations of the OC content can be made with some certainty there is a need for a new method to refine these estimations. This method should include soil, landscape and environmental properties such as the aridity index, the position in the landscape, elevation, aspect, vegetation type and soil colour. Such a method would definitely assist in accurate predictions of *WCM* in ungauged areas.

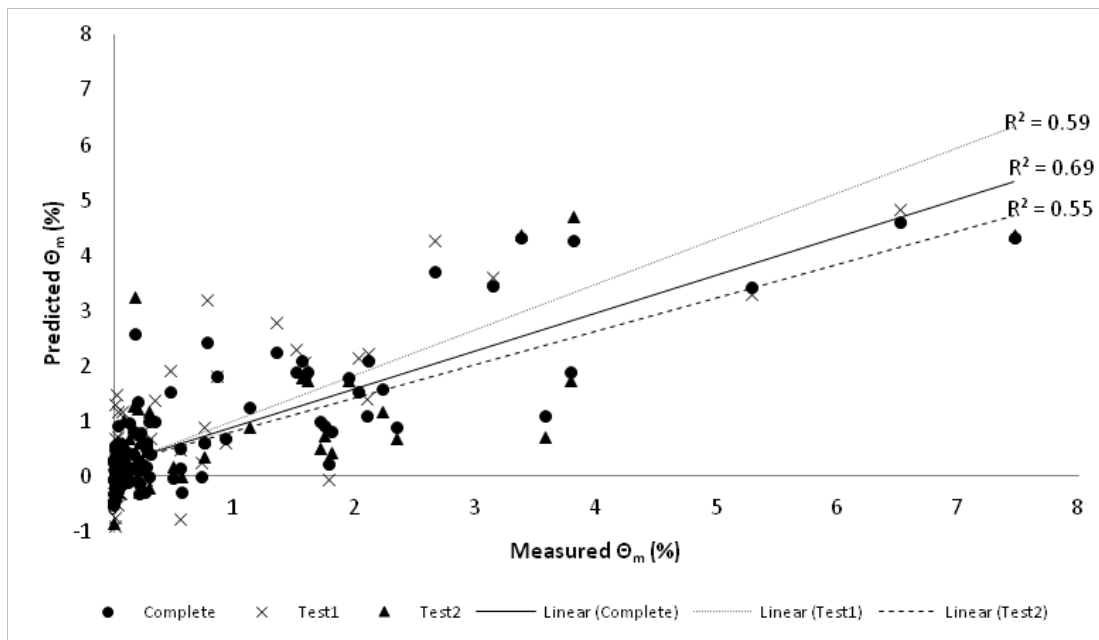


Figure 214 Predicted vs. measured WCM using model 3. Test 1 & 2 represents the double-cross validation prediction results whereas 'complete' represent the original dataset and model equation from Table 56

Differences in the slopes of the validation tests and relatively lower R^2 values are indications that model 3 are not as consistent as model 2. The fact that this model was developed using easily observable and estimated properties should be kept in mind. More accurate morphological descriptions and better estimations of OC contents will increase the accuracy of predictions and also the stability of the model.

In situ determinations at Two Streams

Figure 215 and Figure 216 show the results of the K_s and K_h field measurements of hydraulic conductivity in the eight profiles. Detailed results are presented in Table 57. There is a large decrease in K in all diagnostic horizons as the tension is increased to 30 mm. This large decrease indicates that K was controlled mainly by soil macropore networks that exist in all profiles. K_h values at 30 mm tension in the humic horizons of the Kranskop, Inanda and Magwa soils (Figure 215 and Table 57) averaged 16 mm hr^{-1} , ranging from 12 to 19 mm hr^{-1} . On average, this translates to almost 75% reduction in K (TBLE 57).

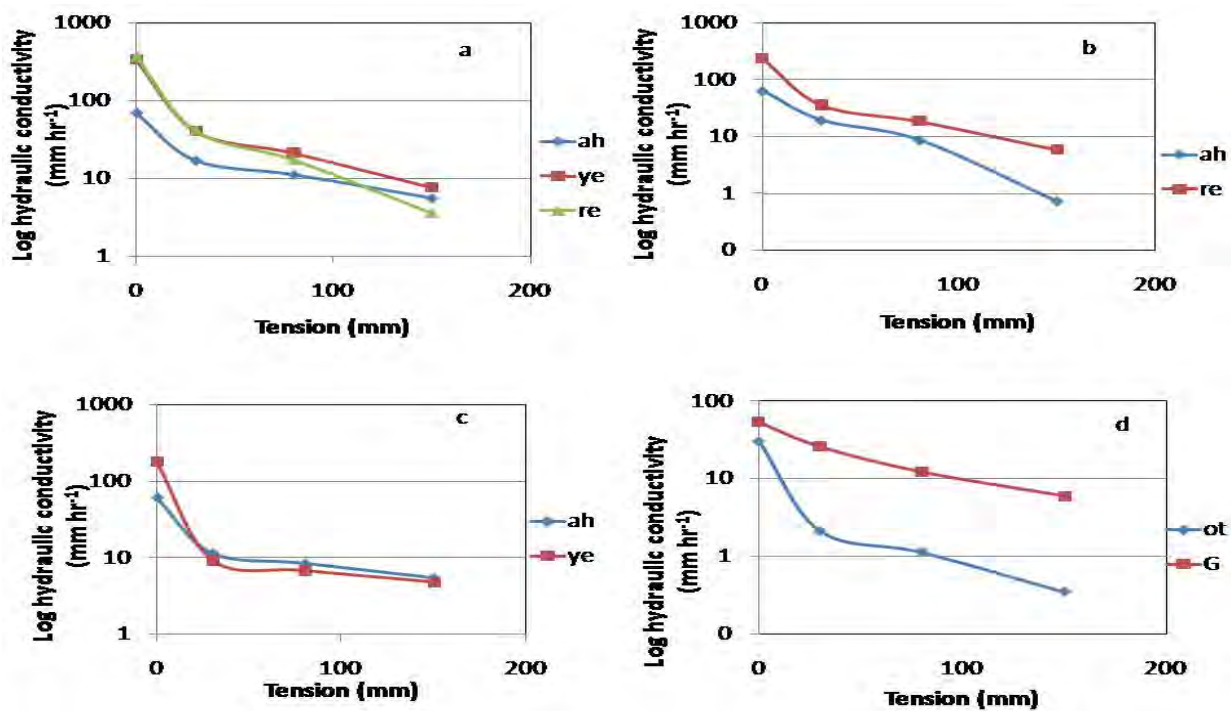


Figure 215 Soil hydraulic conductivity vs tension relationship in diagnostic horizons of (a) Kranskop, (b) Inanda, (c) Magwa profiles located on the north facing hillslope, and (d) Katspruit profile in the valley bottom

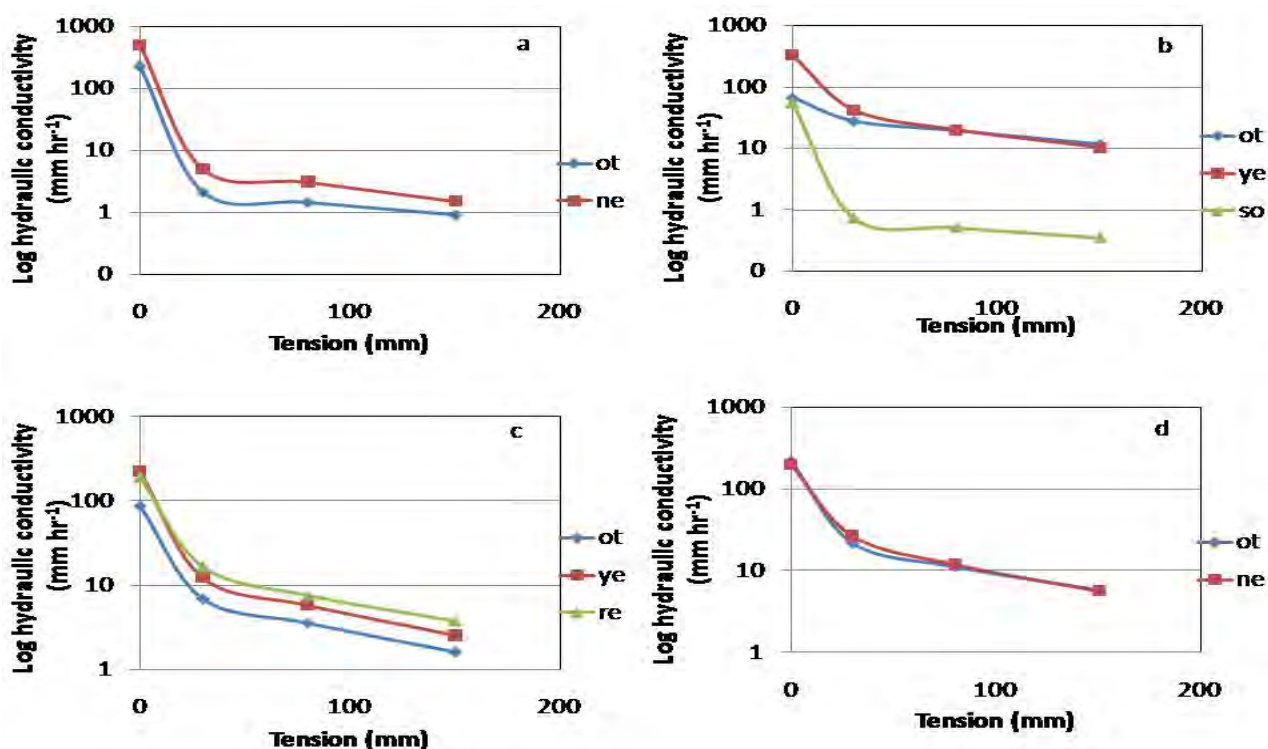


Figure 216 Soil hydraulic conductivity vs. tension relationship in diagnostic horizons of (a) Oakleaf, (b) Clovelly profiles located on the south facing hillslope and (c) Griffin and (d) Oakleaf profile located on the east facing hillslope

The average K_h values at 30 mm tension in the *ot* horizons of the south facing Oakleaf and the Clovelly soils ranged from 2 to 28 mm hr⁻¹, respectively, translating into an almost 99% and 58% reduction in K , respectively in both *ot* horizons. Most of the water infiltrating the *ot* horizon of this Oakleaf soil will therefore flow preferentially in macropores. On the east facing hillslope the *ot* horizons of the Griffin and Oakleaf soils had high macroporosity values with K dropping by 92% at 30 mm tension.

Qualitative observations during profile morphological descriptions and classification showed a substantially greater number of finer cracks and old root channels extending well into the diagnostic B horizons. The root channels were distinct, some lined with persistent root bark, with many extending below the 1 m depth of the profile. High macropore flow was expected to extend below the diagnostic A horizons in these horizons with their well-developed and stable micro-aggregate structure (apedal) (Table 57). The average K value at 30 mm tension on the north facing hillslope was almost 89% reduction of K in *re* and *ye* horizons (Table 57). On the south and east facing hillslopes the reduction was 92% and 91%, respectively for *ne*, *ye* and *re* horizons. In most profiles, the water conducting macropores in the B horizons had higher θ_m (%) values than in the diagnostic A horizons. These high values result from the well-developed micro-aggregate structure of the red/yellow brown apedal B and the neocutanic B horizons. The results indicate that macropores have a major influence on rapid water flow even though they only constitute a small fraction of the total soil volume (i.e. θ_m % in Table 57). The results are in agreement with those of Beven & German (1982) and Wilson & Luxmoore (1988). Similar findings were also reported by Moret & Arrue (2007), Cameira *et al.* (2003), and Van Tol *et al.* (2012) for a wide range of topsoils in South Africa.

High macropore flow is often associated with a high fraction of structural pores, low bulk density, high organic matter and the presence of root channels (Van Tol *et al.*, 2012). Using the procedure for determining θ_m described by Watson & Luxmoore (1986), a pedotransfer function (PTF) for water conducting macroporosity was developed using organic matter content (OC), swelling index and apedal grade of structure as factors affecting macroporosity in South African soils (Equation 7.8. Predicted θ_m values using the WCM PTF were compared with our measured results for the diagnostic A horizons. Results are presented in Figure 217. Lack of correlation in all horizons, excepting for the two Oakleaf's (Oa), can be well explained by the hydrophobic nature observed in these A horizons. Because hydrophobicity in South African soils has evidently been caused by afforestation (Scott, 2000; Scott & Van Wyk, 1990), and because the natural vegetation of this region is grassveld, it is reasonable to conclude that pedogenesis here took place through the centuries without hydrophobic A horizons. It is inconceivable that the kind of highly weathered B horizons that occur here could have developed with that kind of A horizon. It is therefore logical to conclude that the six θ_m values in Figure 151 that are far from the 1:1 line are abnormal because of hydrophobicity. Significant in this regard is the fact that one of the Oa results close to the 1:1 line is located outside of the forest area on a neighbouring farm field. It seems therefore that with more data, preferably subdivided into groups of similar diagnostic horizons, it will be possible to develop a reliable PTF to predict θ_m in South African soils.

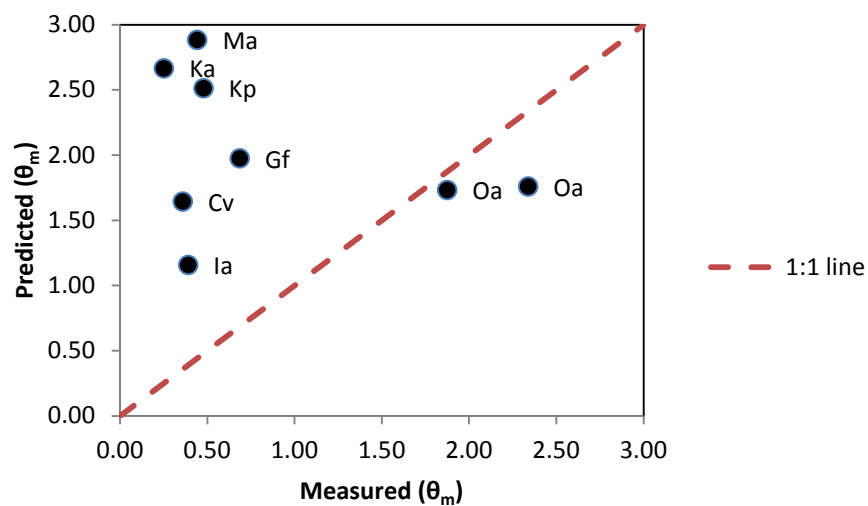


Figure 217 θ_m (cm^2/m^2 of soil surface) with WCM PTF vs. measured θ_m in the A horizons of the soils in the Two Stream's catchment

Table 57 Soil hydraulic conductivity (K), total effective porosity (θ_m), and percentage contribution of macropores to Ks (ϕ)

| Soil form | Horizons | ρ_b g cm ⁻³ | K (mm hr ⁻¹) | | | | Km (cm s ⁻¹ x 10 ⁻³) | ^A Macropores | | | | |
|------------------------|----------|------------------------------------|--------------------------|-------|--------|---------------------------|------------------------------------------------|-------------------------------------------------|-------------------------|-----------------------------|----------------------------|--|
| | | | Ks | K(30) | Km | N (x10 ⁻³) | | ^D Θ_m (x10 ⁻⁵) | ^E Θ_m | ^B θ_m (%) | ^C ϕ (%) | |
| North facing hillslope | | | | | | | | | | | | |
| Kranskop | ah | 1.08 | 71 | 17 | 53.41 | 1.485 | 6.169 | 4.845 | 0.48 | 0.005 | 75.7 | |
| | ye | 1.19 | 336 | 41 | 294.9 | 8.198 | 34.064 | 26.754 | 2.68 | 0.027 | 87.8 | |
| | re | 1.24 | 372 | 42 | 330.8 | 9.196 | 38.210 | 30.010 | 3.00 | 0.03 | 88.8 | |
| Inanda | ah | 1.33 | 63 | 19 | 43.53 | 1.210 | 5.028 | 3.949 | 0.39 | 0.004 | 69.4 | |
| | re | 1.38 | 230 | 35 | 194.8 | 5.415 | 22.501 | 17.672 | 1.77 | 0.018 | 84.7 | |
| Magwa | ah | 1.06 | 61 | 12 | 49.41 | 1.374 | 5.707 | 4.483 | 0.45 | 0.004 | 81.1 | |
| | ye | 1.31 | 178 | 9 | 169.16 | 4.703 | 19.540 | 15.346 | 1.53 | 0.015 | 94.8 | |
| | on | 1.34 | 16 | 0.7 | 15.56 | 0.433 | 1.797 | 1.412 | 0.14 | 0.001 | 95.8 | |
| Valley bottom | | | | | | | | | | | | |
| Katspruit | ot | 0.95 | 30 | 2.1 | 28.27 | 0.786 | 3.265 | 2.565 | 0.26 | 0.003 | 93.1 | |
| | gh | 1.25 | 53 | 26 | 27.48 | 0.764 | 3.174 | 2.493 | 0.25 | 0.002 | 51.7 | |
| South facing hillslope | | | | | | | | | | | | |
| Oakleaf | ot | 1.14 | 211 | 2.1 | 208.52 | 5.797 | 24.086 | 18.917 | 1.89 | 0.019 | 99 | |
| | ne | 1.3 | 374 | 5 | 368.88 | 10.255 | 42.609 | 33.465 | 3.35 | 0.033 | 98.7 | |
| Clovelly | ot | 1.2 | 68 | 28 | 40.01 | 1.112 | 4.622 | 3.630 | 0.36 | 0.004 | 59.2 | |
| | ye | 1.25 | 297 | 42 | 255.23 | 7.095 | 29.481 | 23.155 | 2.32 | 0.023 | 85.8 | |
| | so | 1.45 | 56 | 0.7 | 55.06 | 1.531 | 6.360 | 4.995 | 0.50 | 0.005 | 98.7 | |
| East facing hillslope | | | | | | | | | | | | |
| Griffin | ot | 1.16 | 83 | 6 | 76.44 | 2.125 | 8.830 | 6.935 | 0.69 | 0.007 | 92.5 | |
| | ye | 1.31 | 268 | 17 | 250.81 | 6.973 | 28.971 | 22.754 | 2.28 | 0.023 | 93.7 | |
| | re | 1.33 | 222 | 17 | 205.94 | 5.725 | 23.788 | 18.683 | 1.87 | 0.019 | 92.6 | |
| Oakleaf | ot | 1.22 | 282 | 22 | 260.06 | 7.230 | 30.039 | 23.593 | 2.36 | 0.023 | 92.2 | |
| | ne | 1.36 | 215 | 27 | 187.78 | 5.220 | 21.690 | 17.036 | 1.70 | 0.017 | 87.4 | |

A= pores with diameter >1 mm

B= the total effective macroporosity expressed as a % of the total soil volume. Because the pores are cylindrical, the % area and % volume is the same according to Jury and Horton (2004). Calculation according to equation 7.4 and expressed as %.

C= K_m as a % of K_s ; calculation according to equation 7.5.

D= cm² of pores per cm² of soil area

E= cm² of pores per m² of soil area

Field measurements after a heavy storm

Our data showed that the soil solum enabled rapid movement of water in a vertical direction promoting efficient deep saprolite storage. This was supported by the hydraulic conductivity data which exhibited a significantly faster rate in the B horizons than the A horizons.

In the light of the observed physical properties of the soils in this catchment, it is important to consider, using field measurements, what happens in the catchment after a heavy storm event. The study of the stream hydrograph during a heavy downpour is useful in interpreting the run-off and soil infiltrated water on the catchment. A typical portion of the Two Streams hydrograph during a 72 mm daily rainfall event is shown Figure 218.

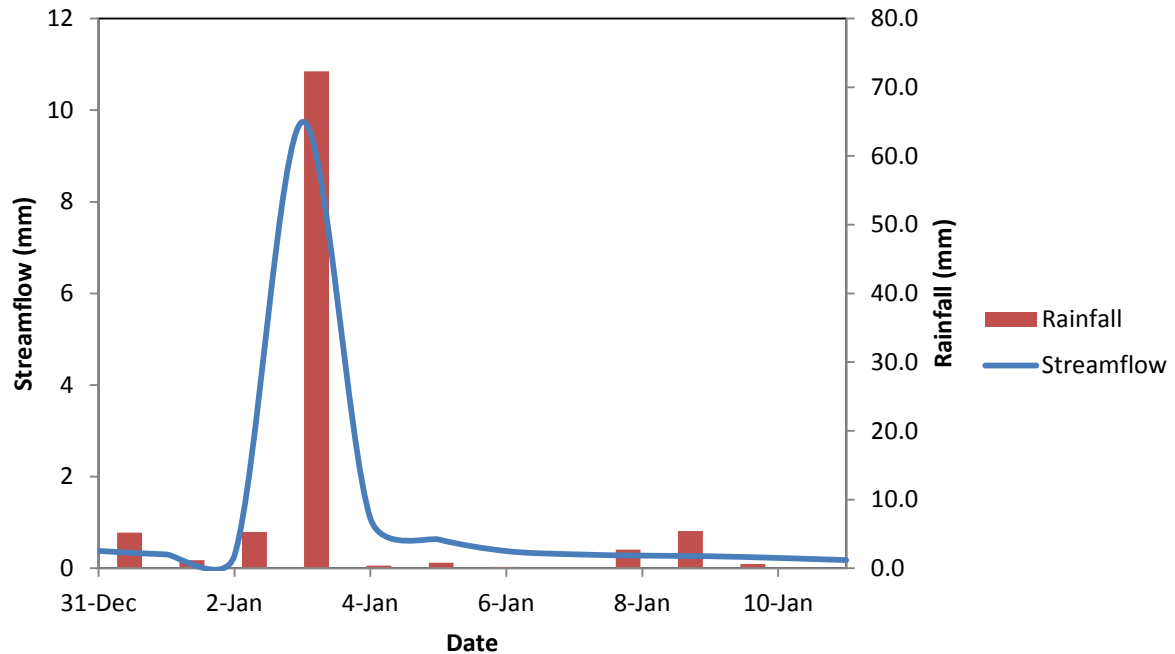


Figure 218 Hydrograph response during the 72 mm event on the 03 January 2005 (Data from Everson *et al.*, 2006)

The sharp peak of the hydrograph (Figure 218) is clearly due mainly to overland flow, whereas the absence of a defined recession curve to the hydrograph also indicates that the contribution to this streamflow was mainly from the surface run-off. To estimate how much must have infiltrated the soils during this storm, we considered the relevant data between 31 December 2004 and 05 January 2005 (Table 58). Since the area of the Two Streams catchment is 73.317 ha (Everson *et al.*, 2006), 1 mm of rain on the catchment is equivalent to 733.17 m³ of water. During the three days before the heavy storm, the estimated daily streamflow was 235 m³. The rainfall event of 3 January increased this to 7143.20 m³, and the streamflow then receded to 274.95 m³ on 6 January (Figure 218 and Table 58). Considering the 3 days (3-5 January) of the hydrograph as mainly stormflow (totalling 8401 m³), and subtracting the estimated low flow of 3 x 235 m³ during the three days, yields an estimated total run-off of 7696 m³. To compare this volume with the amount of the rainfall event of 72.3 mm, it is appropriate to convert this value to m³ by multiplying with the area of the catchment which yields 53008 m³. The estimation of the volume infiltrated is therefore 53008 m³ - 7696 m³ = 45312 m³, equivalent to an estimated average amount of 62 mm of rainfall that would have infiltrated the soils of the catchment.

Table 58 Streamflow and rainfall volumes during the period 31/12/04 and 6/1/05

| Date | Streamflow | | Rainfall (mm) |
|------------|------------|----------------|------------------|
| | mm | m ³ | |
| 12/31/2004 | 0.38 | 277.75 | 5.2 |
| 1/1/2005 | 0.30 | 221.19 | 1.2 |
| 1/2/2005 | 0.28 | 205.02 | 5.3 |
| 1/3/2005 | 9.75 | 7143.20 | 72.3 |
| 1/4/2005 | 1.09 | 796.33 | 0.4 |
| 1/5/2005 | 0.63 | 461.11 | 0.8 |
| 1/6/2005 | 0.38 | 274.95 | 0.2 |

The rate at which the estimated infiltrated amount flowed in the soil profile was sought in two ways 1) the response on the day of the storm flow using the watermark sensors installed in 2004 by Everson *et al.* (2006) to measure soil water contents in the Inanda soil profile described in Table 52; 2) the predicted response that would have occurred had the DFM probes installed in 2011 in the same Inanda soil been in position during the storm on 3/1/2005. The results of the latter K_s profile measuring procedure were obtained during the DFM calibration procedure in the same Inanda soil close to the site at which the watermark sensors were installed in 2004 by Everson *et al.* (2006).

Watermark sensors

The watermark record for the 40 cm sensor during the period 3/1/05 and 6/1/05 is shown in Figure 219 (data from Everson *et al.*, 2006). The sensor records readings at 12 mm intervals with the results in Figure 219 being averages of 12 readings. The soil water content before wetting up started during the 3/1/2005 rainfall at the 40 cm depth was $0.27 \text{ cm}^3 \text{ cm}^{-3}$ (i.e. 27 mm/100 mm = 108 mm/400 mm), indicating relatively dry conditions. With the onset of the rain event, the water content increased rapidly, indicating that the A horizon was wetting up. In fact the soil water content increased over a period of ± 196 minutes until midnight on 1/3/2005 at a rate of $\pm 31 \text{ mm hr}^{-1}$ to porosity ($0.519 \text{ cm}^3 \text{ cm}^{-3}$ which is 51.9 mm/100 mm = 208 mm for the 400 mm of the horizon) and stayed there until midday (12:00) on the 4th when it started to drain (Figure 219). To estimate the K_s value at which the horizon was draining, the main rapid drainage period of 12:36 pm and 15:00 pm on the 04/1/05 was considered. The A horizon (0-400 mm) was saturated, making it appropriate to estimate the K_s value during the period of emptying of the horizon past the 40 cm mark. The water content of the horizon was 207.7 mm at the start of drainage, and 2.4 hours later this amount had drained to $0.4673 \text{ cm}^3 \text{ cm}^{-3}$ (i.e. 46.73 mm/100 mm or 186.88 mm for the horizon). It is reasonable to assume that ET was negligible during these 2.4 hours and that drainage was virtually vertical. The difference from the start to the finish of the drainage period was therefore 20.72 mm. This is the amount that drained out of the A horizon into the B horizon. The K_s value for this period was therefore

$1/2.4 \times 20.72 \text{ mm hr}^{-1} = 8.6 \text{ mm hr}^{-1}$. This K_s value is nine times less than the K_s value determined using a double ring infiltrometer in 2010. It is hypothesised that the difference is probably due to the fact that in the latter case the preparation before measurement requires one to “clean up” the soil surface. This would probably have resulted in scraping off any hydrophobic layer that had impeded K_s during the 2005 determination. The procedure used appears to be reliable and representative of currently prevailing field conditions.

However the traditional method of determining K_s with the use of double rings should provide more reliable information in relation to the overall morphology of the horizon. It also needs to be stated that outflow procedure described above can only be successful if one is certain that K_s of the underlying horizon is faster than that of the one being tested. It would for example not be suitable for this reason for the yellow brown apedal (ye) of the Magwa (Table 57). This aspect also motivates the need for K_s determination of horizons by the double ring procedure.

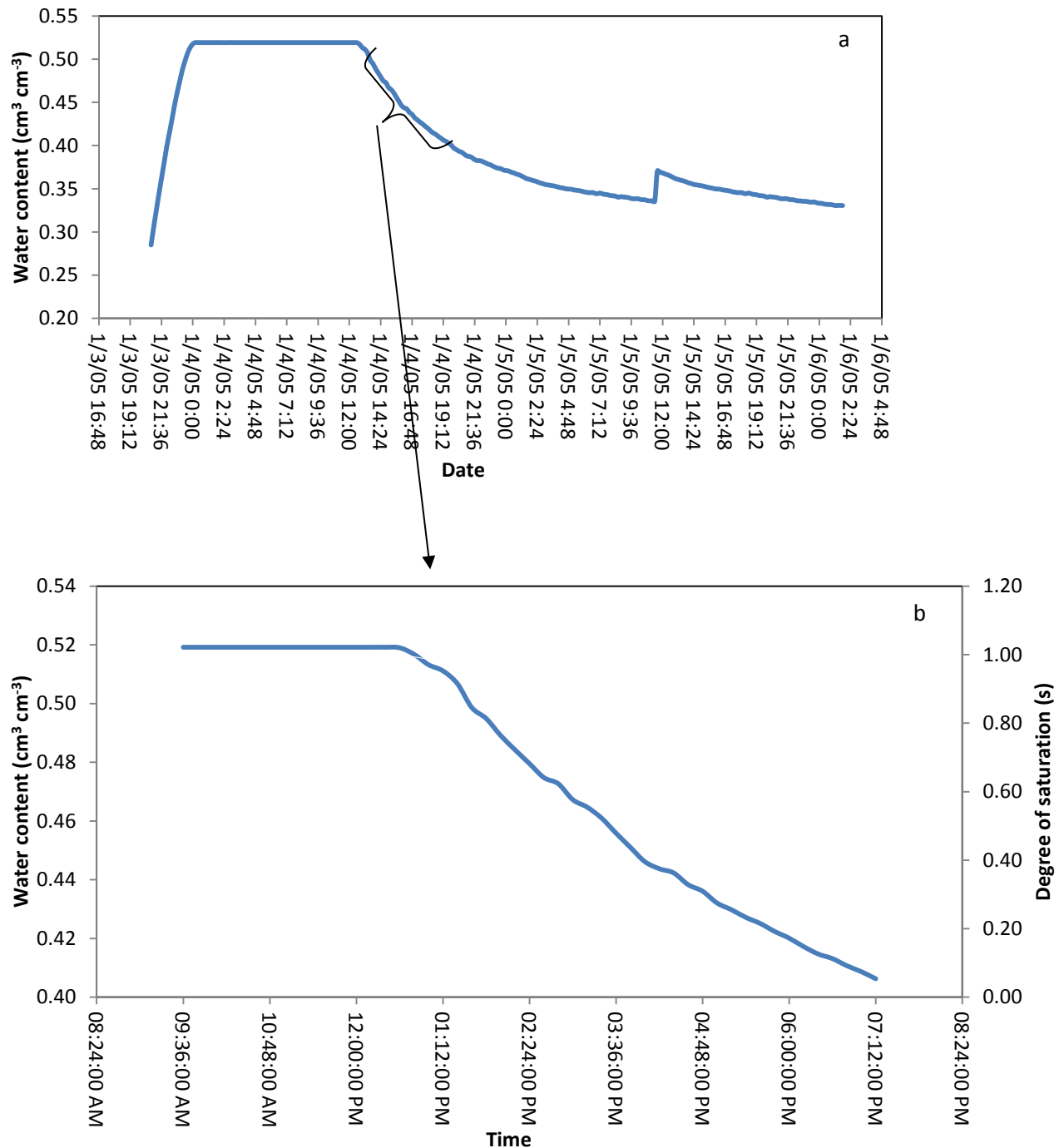


Figure 219 A record of soil water content measured by water sensor, at 40 cm depth in the Inanda soil on the north facing hillslope during the 72 mm rainfall event on 3/1/05 (adapted from Everson *et al.*, 2006) (a); measurements at 2.4 hour intervals (b).

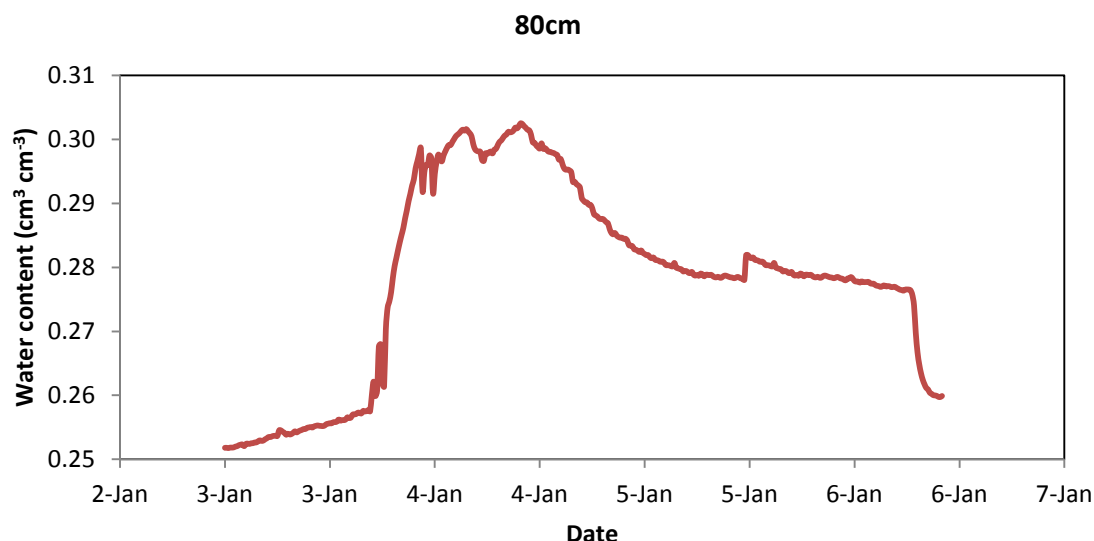


Figure 220 A record of the soil water content at 80 cm depth of the Inanda soil of Figure 219 during the 72 mm rainfall event on 3/1/05 (adapted from Everson *et al.*, 2006)

The response in the 80 cm depth is shown in Figure 220. The increase of water content in the B horizon (80 cm depth) did not reach saturation before it drained.

DFM probe

The installed DFM probe had water content measuring sensors located at 10 cm intervals, starting at 10 cm from the soil surface. The same *in-situ* flow technique for measuring K_s , described above for the watermarks, was used here. The horizon was saturated to porosity for calibration purposes by adding water to a small dam around the probe. The rapid draining period was considered as in the watermark procedure. After calibration, the DFM probes record volumetric water content at 15 minutes intervals. The rapid drainage period (Figure 221) of 19:15:20 to 19:30:20 on 03/11/2011 at the 40 cm sensor (Table 59) will be considered as describing K_s out of the A horizon. The water content of the horizon at the start of the drainage period was 195.2 mm, and at the end of the draining period it was 173.5 mm (Table 59), i.e. 21.7 mm had flowed out through the lower boundary of the horizon in 15 minutes. This translates into a K_s value of 87 mm hr^{-1} .

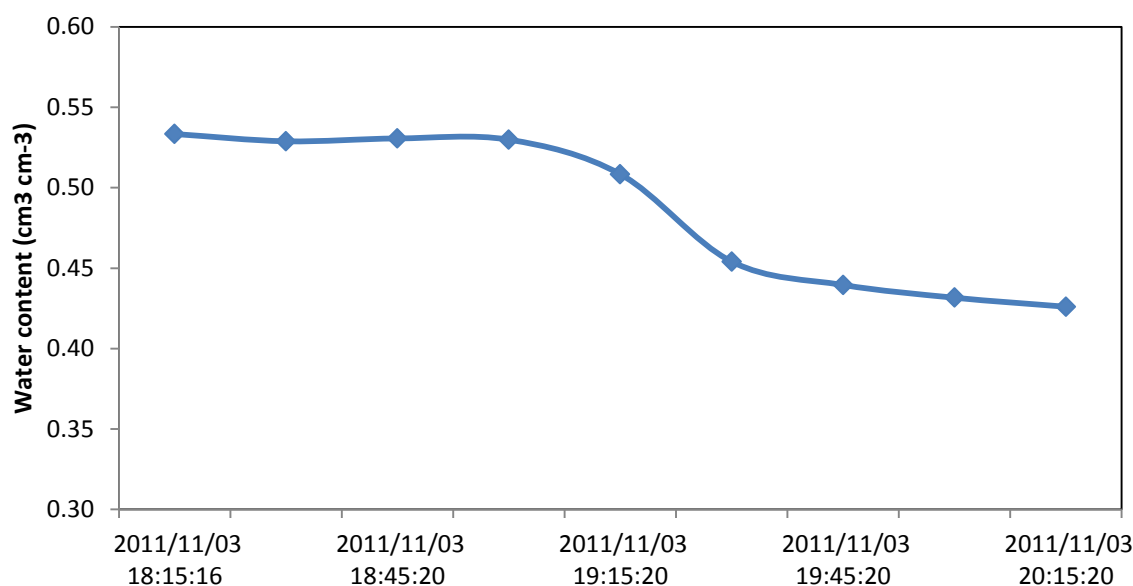


Figure 221 A record of the draining of the saturated A horizon Inanda soil during a DFM probe calibration procedure during 2011

Table 59 Soil water content data during calibration procedure of a DFM probe installed during 2011 in the same Inanda soil profile discussed in the previous section

| Date | 10cm | 20cm | 30 cm | 40cm |
|----------------------------|---------------|---------------|---------------|---------------|
| 2011/11/03 18:15:20 | 0.5167 | - | 0.5257 | 0.5333 |
| 2011/11/03 18:30:20 | 0.5140 | - | 0.5234 | 0.5288 |
| 2011/11/03 18:45:20 | 0.51719 | 0.4689 | 0.5218 | 0.5307 |
| 2011/11/03 19:00:20 | 0.5115 | 0.4676 | 0.5226 | 0.5299 |
| 2011/11/03 19:15:20 | 0.4707 | 0.4596 | 0.5131 | 0.5084 |
| 2011/11/03 19:30:20 | 0.4481 | 0.3958 | 0.4370 | 0.4541 |
| 2011/11/03 19:45:20 | 0.4330 | 0.3789 | 0.4185 | 0.4395 |
| 2011/11/03 20:00:20 | 0.4274 | 0.3731 | 0.4107 | 0.4316 |
| 2011/11/03 20:15:20 | 0.4228 | 0.3692 | 0.4052 | 0.4260 |

The 87 mm hr^{-1} obtained through this procedure compares favourably with K_s determined using the double ring method, i.e. yielding a value of 63 mm hr^{-1} (Table 57). However, it should be noted that using the traditional methods of K_s determination of horizons gives information about them individually in 'separation mode', but does not provide information about the hydrology of the profile as a whole. This is because the movement of water in the lower layers of profiles will be controlled by the rate of the movement in the overlying layers, and vice versa. Ignoring the hydrology at the A horizon, for example, when reporting the hydrology of the B horizon therefore may give unreliable information, because the natural condition under which the B horizon receives water from the A is not taken into account. The use of well calibrated soil water content measuring instruments in all horizons

under field conditions therefore offers a valuable opportunity to understand the hydrology of entire profiles under their natural ecological conditions, as well as their contribution to the functioning of the hillslope as a whole hydrological unit.

7.3.4 Conclusions

Macroporosity influences the rate of transport of water and solutes as well as the breakdown of pollutants. In this study the water conducting macroporosity was determined in 120 soil horizons with diverse properties. Some of these properties were used to estimate the *WCM* using three multiple regression models (Table 56). Model 1 illustrated the influence of various properties on *WCM*, emphasising the important role that *OC* content and structural properties play in the macroporosity of soils. The accurate description of the structure of the soils is therefore of critical importance. An accurate method to estimate the *OC* content of soil horizons in different environments will also improve predictions of *WCM*. Model 2 (equation 7.8), consisting of only three variables, will be used in soils with some chemical analysis. The relative high R^2 value, 0.74, and consistency of the model make it the ideal model to estimate *WCM*.

$$\theta_m = -0.126 + (0.664 \times OC) - (0.027 \times S_index) + 0.31(\text{if } S_Grade = \text{Apedal}) \quad (7.8)$$

The last model (model 3) was developed to facilitate predictions in ungauged basins. Only easily observable properties were used in this model. The model showed some inconsistency but gave relatively accurate estimations ($R^2 = 0.69$) of *WCM*, considering the qualitative nature of model inputs.

As *WCM* is such an important property of soils, more measurements of the saturated and unsaturated hydraulic conductivity, over a range of climates, vegetations and geologies in soils with diverse properties should be conducted. This will reduce the uncertainty and improve the accuracy of predictions of *WCM* in soils.

In the Two Streams catchment, The K_s and Kh of each horizon was successfully determined using double ring and tension infiltrometers. The K_s of the soils is very high, especially in the *re*, *ye*, and *ne* diagnostic B horizons. This is attributed to well-developed micro-aggregate structure and high water conducting macropores. These forest soil profiles show definite evidence of much biological activity, characterized by abundant plant, insect, and animal activity. Roots have penetrated deeply into the profile. The annual decay of some roots has created relatively large continuous openings that serve as hydraulic pathways for the rapid movement of water. The Katspruit is excluded from these comments as it is relatively unimportant. There are mainly two kinds of horizons that dominate the hillslope hydrology. Firstly, A horizons, all with high *OC* (>1.8%). Four of these don't qualify as humic only because of too many cations, a characteristic which probably has negligible influence on horizon hydrology. Apart from the two Oakleaves, the K_s values of all the other A horizons appear to be below normal because of the wattle plantation induced hydrophobicity, or ash (caused by burning of forest trash) probably suppressing K_s because of pore clogging. Results of our study showed that the hydrophobic nature of the topsoil was a significant variable that provides a first-order control of the effective soil macroporosity. Hydrophobicity (Figure 222b) is commonly associated with timber plantations such as eucalypts (*Eucalyptus spp.*) and wattle (*Acacia mearnsii*) in South Africa (Scott, 2000; Musto, 1994). Burning, which is a common management practice in the catchment's afforested zones, also exacerbates

hydrophobicity in the topsoils. Soil heating by fire has been found to intensify water repellence in the soils of mountain catchments in South Africa (Scott & Van Wyk, 1990). Fire destroys, through combustion, organic matter which is an important component of soil structure acting as glue that helps hold mineral soil particles together to form aggregates and thus contributes to soil structure, particularly in the upper part of the A horizons (DeBano *et al.*, 2005). Loss of macropores in the surface soils can therefore reduce infiltration rates and promote overland flow. Pulverized fine soil mixed with ash particles that was observed on the surface (Figure 222a) in the catchment can be translocated to fill structural pores and reduce macroporosity in the soil profile (Figure 222a), probably mainly in the A horizons.

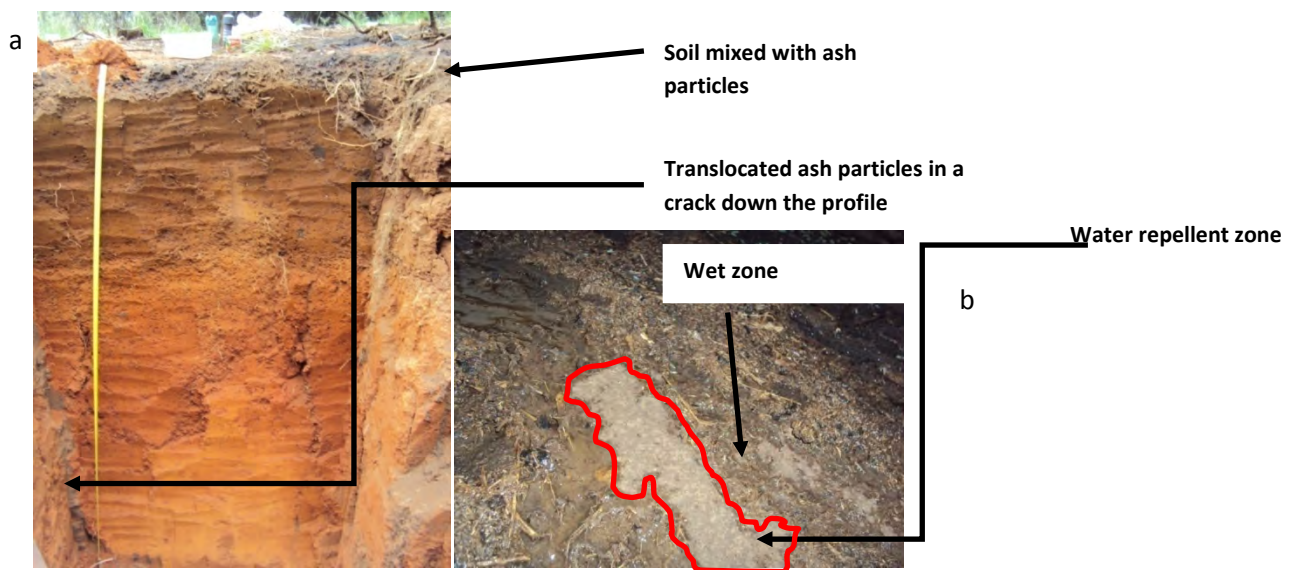


Figure 222 Inanda soil profile (a), with evidence of soil mixed with ash particles on the surface and translocated ash particles down the cracks of the profile and (b) surface evidence of water repellency

Although the effect of hydrophobicity requires further testing, the contribution of macropores to total K_s here remains relatively high, especially in the Magwa, Oakleafs and Griffin soils. Macropores in the Oakleafs, one located in the forest on the south facing slope and one on the non-forested east facing slope, contribute more than 90% to K_s . Particularly in the latter case this can be attributed to no impact of hydrophobicity caused by fires or other forest influences. K_s on this soils' A horizon is 282 mm hr^{-1} (Table 57), compared to the average of the other seven A horizons of only 84 mm hr^{-1} .

The procedure for determining macroporosity is not only important for hydrological studies, but could also be useful for soil conservation studies, for example the benefits of no till, where the impact of cultivation on macropores could easily be quantified. Conventional tillage has a dire consequence of exposing organic matter to oxidation, thereby diminishing organic matter content responsible for soil structure and macropores, and in addition contributing to the greenhouse effect.

7.4 REFERENCES

- ANDERSON, S.H., PEYTON, R.L. and GANTZER, C.J. 1990. Evaluation of constructed and natural soil macropores using X-ray computed tomography. *Geoderma* 46, 13-29.
- ANKENY, M. D., AHMED, M., KASPAR, T. C. & HORTON, R. 1991. Simple field method for determining unsaturated hydraulic conductivity. *Soil Sci. Soc. Am. J.* 55, 467-470.
- BEAR, J. 1972. Dynamics of fluids in porous media, Elsevier Pub. Co., New York.
- BEVEN, K & GERMAN, P. 1982. Macropores and water flow in soils. *Water Resour. Res.* 18, 1311-1325.
- BODHINAYAKA, W., SI, B. C & XIAO, C. 2004. New method for determining water-conducting macro and mesoporosity from tension infiltrometer. *Soil Sci. Soc. Am. J.* 68, 760-769.
- BOUMA, J., JONGERIUS, A., BOERSMA, O. and SCHOONDERBEEK, D. 1977. The function of different types of macropores during saturated flow through four swelling soil horizons. *Soil Sci. Soc. Am. J.* 41, 945-950.
- BOUMA, J. 2004. Foreword. *In: Pachepsky, Y. and Rawls W. J. (Eds), Development of pedotransfer functions in soil hydrology.* Elsevier, Amsterdam.
- BOUWER, H. & RICE, R.C. 1976. A slug test for determining hydraulic conductivity of unconfined aquifers with completely or partially penetrating wells. *Water Resources research.* 12 (3), 423-428
- CAMEIRA, M.R., FERNANDO, R.M. and PEREIRA, L.S. 2003. Soil macropore dynamics affected by tillage and irrigation for a silty loam alluvial soil in southern Portugal. *Soil & Till. Res.* 70, 131-140.
- CLOTHER, B. E., GREEN, S. R. & DEURER, M. 2008. Preferential flow and transport in soil: progress and prognosis. *Eur. J. Soil Sci.* 59, 2-13.
- DEBANO, L.F., NEARY, D.G. and FOLLIOTT, P.F. 2005. Chapter 2. Soil physical properties. *In Wildland Fire in Ecosystems Effects of Fire on Soil and Water.* Eds DeBano, L.F., Neary, D.G. Ryan, K.C Neary, Daniel G.; Ryan, Kevin C.; DeBano, Leonard F., eds. 2005. (revised 2008). *Wildland fire inecosystems: effects of fire on soils and water.* Gen. Tech. Rep. RMRS-GTR-42-vol.4. Ogden, UT: U.S. Department of Agriculture, Forest Service, Rocky Mountain Research Station. 250 p.
- DUNN, G. H., and Phillips, R. E. 1991. Macroporosity of a well-drained soil under no-till and conventional tillage. *Soil Sci. Soc.* 55, 817-823.
- EDWARDS, W. M. VAN DER PLOEG, R. R. and EHLERS, W. 1979. A numerical study of the effects of non-capillary sized pores upon infiltration. *Soil Sci. Soc. Am. J.* 43, 851-856.
- EVERSON, C., MOODLEY, M. GUSH, M. JARMAIN, C. GOVENDER, M. and DYE, P. 2006 Can effective management of riparian zone vegetation significantly reduce the cost of catchment management and enable greater productivity of land
- FLURY, M., FLUHLER, H., JURY, W.A. & LEUENBERGER, J. 1994. Susceptibility of soils to preferential flow of water: A field study. *Water Resources Research.* 30:1945-1954.
- GREEN, P. E. & CARROL, J. D. 1978. Analyzing multivariate data. John Wiley, New York.
- GRIFFITHS, E., WEBB, T. H., WATT, J. P. C. & SINGLETON, P. L. 1999. Development of soil morphological descriptors to improve field estimation of hydraulic conductivity. *Aust. J. Soil Res.* 37, 971-982.
- HENDRICKX, J. M. H. & FLURY, M. 2001. Uniform and preferential flow, mechanisms in the vadose zone. *Conceptual Models of Flow and Transport in the Fractured Vadose Zone*, National Research Council, National Academy Press, Washington, DC, 149-187.

- JARVIS, N. J. & MESSING, I. 1995. Near-saturated hydraulic conductivity in soils of contrasting texture measured by tension infiltrometers. *Soil. Sci. Soc. Am. J.* 59, 27-34.
- JARVIS, N. 2008. Near-saturated hydraulic properties of macroporous soils. *Vadose Zone J.* 7 1302-1310.
- JURY, W., GARDNER W.R & GARDNER, W.H. 1991. Soil Physics (5th Ed.) John Wiley and Sons, New York.
- JURY, W.A. & HORTON, R. 2004. Soil Physics (6th Edition) John Wiley and Sons Inc, New Jersey.
- LAND TYPE SURVEY STAFF, 1972-2006. Land types of South Africa: Digital map (1:250 000 scale) and soil inventory datasets. ARC-Institute for Soil, Climate and Water, Pretoria.
- LE ROUX, P. A. L., VAN TOL, J. J., KUENENE, B. T., HENSLEY, M., LORENTZ, S. A., EVERSON, C. S., VAN HUYSSTEEN, C. W., KAPANGAZIWIRI, E., RIDDEL, E. D and FREESE, C., 2011. Hydropedological interpretations of the soils of selected catchments with the aim of improving the efficiency of hydrological models. Report no. K5/1748. Water Research Commission, Pretoria.
- LILLY, A. & LIN, H. S. 2004. Using soil morphological attributes and soil structure in pedotransfer functions. In: Pachepsky, Y. and Rawls W. J. (Eds), Development of pedotransfer functions in soil hydrology. Elsevier, Amsterdam.
- LIN, H. S., KOGELMAN, W., WALKER, C. & BRUNS, M. A. 2006. Soil moisture patterns in a forested catchment: A hydropedological perspective. *Geoderma* 131, 345-368.
- LORENTZ, S., THORNTON-DIBB, S., PRETORIUS, C. & GOBA, P., 2004. Hydrological systems modelling research programme: hydrological processes. Report No. 1061 & 1086/1/04. Water Research Commission, Pretoria.
- LUXMOORE, R. J. 1981. Micro-, meso-, and macroporosity of soil. *Soil Sci. Soc. Am. J.* 45, 671-672.
- MCDONNELL, J. J. 1990. A rational for old water discharge through macropores in a steep, humid catchment. *Water Resour. Res.* 26, 2821-2832.
- MORET, D. & ARRUE, J. L. 2007. Characterizing soil water-conducting macro- and mesoporosity as influenced by tillage using tension infiltrometry. *Soil Sci. Soc. Am. J.* 71, 500-506.
- MUSTO, J. W., (1994). Changes in soil physical properties and related hydraulic characteristics caused by Eucalyptus plantations. MSc thesis. Department of Agronomy, University of Natal, Pietermaritzburg, South Africa.
- NIEBER, J. L., BAUTERS, T. W. J. STEENHUIS, T. S. & PARLANGE, J. Y. 2000. Numerical simulation of experimental gravity-driven unstable flow in water repellent sand. *J. Hydrol*, 231, 295-307.
- PACHEPSKY, Y. A. & RAWLS, W. J., 2004. Development of pedotransfer functions in soil hydrology. Elsevier, Amsterdam
- PERROUX, K. M. & WHITE, I. 1988. Design for disc permeameters. *Soil Sci. Soc. Am. J.* 52, 1205-1212.
- REYNOLDS, W.D. and ELRICK, D.E. 1991. Determination of hydraulic conductivity using a tension infiltrometer. *Soil Sci. Soc. Am J*, 55: 633-639
- RIDDELL, E. S., 2011. Characterisation of the hydrological processes and responses to rehabilitation of a headwater wetland of the Sand River, South Africa. PhD thesis. University of KwaZulu-Natal, Pietermaritzburg.

- SIMUNEK, J., WENDROTH, O. & VAN GENUCHTEN, M.T. 1999. Estimating unsaturated soil hydraulic properties from laboratory tension disc infiltrometer experiments. *Water resour res.* 35 2965-2979.
- SCOTT, D.F. & VAN WYK D.B. 1990. The effect of wildfire on soil wettability and hydrological behaviour of an afforested catchment. *J. of Hydrol.* 121 239-256.
- SCOTT, D.F. 2000. Soil wettability in forested catchments in South Africa; as measured by different methods and as affected by vegetation cover and soil characteristics. *J. Hydrol.* 231-232 87-104.
- SLOGAN, P. G. & MOORE, I. D. 1984. Modeling subsurface stormflow on steeply sloping forested watersheds. *Water Resour. Res.* 12, 1815-1822.
- ŠIMŮNEK, J., JARVIS, N. J., VAN GENUCHTEN, M. TH. & GÄRDENÄS, A. 2003. Review and comparison of models for describing non-equilibrium and preferential flow and transport in the vadose zone. *J. Hydrol.* 272, 14-35.
- SOIL CLASSIFICATION WORKING GROUP. 1991. Soil classification – A taxonomic system for South Africa. *Mem. agric. nat. resour. S. Afr.* No. 15.
- WATSON, K. W. & LUXMOORE, R. J., 1986. Estimating macroporosity in a forested watershed by use of a tension infiltrometer. *Soil. Sci. Soc. Am. J.* 50, 578-582.
- WILSON, G.V. & LUXMOORE, R.J. 1988. Infiltration, macroporosity, and mesoporosity distributions on two forested watersheds. *Soil Sci. Soc. Am. J.* 52: 329-335
- VAN HUYSSTEEN, C.W., HENSLEY, M., LE ROUX P.A.L., ZERE, T.B. & DU PREEZ, C.C. 2005. The relationship between soil water regime and soil profile morphology in the Weatherley catchment, an afforestation area in the Eastern Cape. WRC Report No. 1317/1/05. Water Research Commission, Pretoria.
- VAN TOL, J.J., LE ROUX, P.A.L. & HENSELY, M. 2012. Pedotransfer functions to determine water conducting macroporosity in South African soils. *Water science and technology* 659 (3) 550-557.
- VAN TOL, J.J., 2011. Characterizing subsurface lateral flow in selected hillslope soils to facilitate hydrological predictions. PhD thesis, University of the Free State.

7.5 WATER RETENTION CURVES TO PROVIDE VAN GENUCHTEN PARAMETERS AND K_h CURVES NEEDED BY HYDROLOGISTS

7.5.1 Methodology

To prepare the undisturbed soil samples for retention measurements, the first step was to cover the base of the cores with filter cloths tightened using elastic bands (Figure 223). This was to enable saturation of the samples from the base upwards, as well as facilitating good contact between core sample and the appropriate extraction material on which they were seated during desorption. Each sample was numbered according to diagnostic horizon and replicate number. The next step was to saturate the soil cores using a two way vacuum saturation chamber setup (Figure 223). There were two of these setups in our soil hydrology laboratory enabling 18 soil cores to be handled simultaneously. One setup consists of four chambers, one of them (the tall one) filled with water with a stirrer placed at the bottom of the vessel to continually stir the water in the vessel during the deairing process. In each of the other three vessels, three core samples were placed on a 3 mm high gauge wire-mesh platform. All the chambers, fitted with air tight lids, were de-aired together using a vacuum pump working at around -70 kPa at room temperature for 24 hours. Thereafter the vacuum pump was turned off. Ensuring that the two way chamber system remained air tight, the de-aired water was allowed to gradually flow into the three smaller chambers containing the de-aired core samples until the water level was just below the top of the core samples. Soil samples were then left for a further 24 hours in the chamber, to ensure that full saturation was achieved.

Thereafter, each sample was carefully weighed on an electronic scale to get the saturation weight measurement. The saturated samples (18) were then immediately mounted on a hanging water column setup (Figure 223) in accordance with the procedure of Dirksen (1999), with the soil core pressed lightly downwards to ensure a good contact between the diatomaceous earth and the sample. Sample tops were covered with aluminum foil, over which were placed and small inverted plastic flower pots fitted inside with moistened sponge to prevent evaporation from the samples. It was found necessary to check continually that all hoses from the extraction cups were filled with water free of air bubbles that would prevent water from being drained. The suction levels (h) were set consecutively at levels of 0, 38, 50, 100, 200, 400, 600, 800 mm read on a measuring tape mounted downwards from the extraction cup (Figure 223).

The gravimetric water content was determined at each level, when equilibrium had been reached, by weighing the samples. Samples were then transferred quickly to a pressure plate apparatus in the soil physics laboratory (Jury *et al.* 1991) to determine volumetric water content at pressures of 10, 30, 80, 100 and 1000 kPa.



Figure 223 Photos illustrating (a) undisturbed core samples, (b) the laboratory vacuum/saturation chamber and hanging water column setup for determining water retention curves

The last step was to oven dry the samples at 105°C to obtain bulk density (ρ_b) and calculate the volumetric water content at each kPa value using the respective ρ_b values. The filter cloth and elastic band were also air dried and weighed. The empty cores had been pre-weighed and numbered prior to field sampling. It is important to weigh everything that is used to hold the sample during the whole process as it contributes significantly to the determined ρ_b and, θ_v from θ_m . Residual water contents (θ_r) for optimizing van Genuchten parameters were determined using the Hutson (1993) pedotransfer function;

$$\theta_{-1500\text{kPa}} = 0.1526 + 0.0028\text{Cl} + 0.0005\text{Si} + 0.0232\text{OC} - 0.106\rho_b \text{ for topsoils} \quad (7.9)$$

$$\theta_{-1500\text{kPa}} = 0.0193 + 0.0031\text{Cl} + 0.0059\text{Si} + 0.029\text{OC} - 0.106\rho_b \text{ for subsoils} \quad (7.10)$$

Where Cl is clay content, Si silt content, OC organic carbon and ρ_b is bulk density. These PTFs were developed with soils of KwaZulu-Natal with almost similar textural range of the soils in Two Streams. Predicting θ at $h = 1500$ kPa will relate, among others particle size distribution (Wotsen *et al.*, 2001).

Soil water retention curves were drawn from the θ_v/h (means of 3 replicates) for each horizon. The θ_v/h data were then fitted to the van Genuchten (1980) equation using the non-linear curve-fitting program RETC (van Genuchten *et al.*, 1991). The parametric θ - h model described by van Genuchten (1980) is written as:

$$S_e = \frac{(\theta - \theta_r)}{(\theta_s - \theta_r)} = \left[\frac{1}{1 + (\alpha h)^n} \right]^m \quad (7.11)$$

Where S_e is effective saturation, θ is the volumetric water content ($\text{cm}^3 \text{ cm}^{-3}$), θ_r and θ_s are the residual and saturated θ_v , respectively ($\text{cm}^3 \text{ cm}^{-3}$), h (cm) is the suction head, α , n , and m are parameters directly dependent on the shape of the θ - h curve. The value of θ_s was fixed as the measured water content at saturation and θ_r was fixed as the water content at 1500 kPa suction, consistent with the suggestion of van Genuchten (1980). The RETC computer programme (van Genuchten *et al.*, 1991) was then used to determine the van Genuchten parameters (α & n) In accordance with the suggestion of van Genuchten (1980), $m = 1 - 1/n$. The hydraulic conductivity curves were predicted from the fitted water retention parameters using van Genuchten-Mualem (VGM) model (Van Genuchten, 1980).

$$K(\theta) = K_s S_e^L \left(1 - \left(1 - S_e^{1/m} \right)^m \right)^2 \quad (7.12)$$

Where K_s is the measured saturated hydraulic conductivity and L is a constant for which the value of 0.5 was used in accordance with van Genuchten (1980). Other parameters are as above. For hydropedological purpose, hydraulic conductivity vs degree of saturation (S) is presented to facilitate pedological interpretation. The degree of saturation (S), is defined as the fraction of the porosity that is occupied by water (Van Huyssteen *et al.*, 2010). It is calculated as follows (Hillel, 1981):

$$S = \theta/f \quad \text{with } f = 1 - \rho_b/\rho_s \quad (7.13)$$

where ρ_s is soil particle density, generally taken as 2.65 Mg m^{-3} for all soils low in organic carbon. The degree of water saturation ranges from 0.0 in an oven dry soil to 1.0 in a completely saturated soil. However, complete saturation is seldom reached in the field conditions, since some air is nearly always trapped by water in a very wet soil (Hillel, 1981). The corresponding relationship between the unsaturated hydraulic conductivity and the pressure head is

$$K(h) = \frac{K_s \left\{ 1 - (\alpha h)^{n-1} \left[1 + (\alpha h)^n \right]^{-m} \right\}}{\left\{ 1 - (\alpha h)^n \right\}^{m/2}} \quad (7.14)$$

Where h is the pressure head. Other parameters are as above. In order to improve the resolution of the Kh curve determined only from the measured θ_v/h water retention data, Kh values close to saturation were determined in the field by means of a tension infiltrometer at h values of 3, 8, and 15 cm. These results were used in combination with the water retention data in the RETC programme (Van Genuchten, 1980) to obtain modified van Genuchten parameters and an improved curve. The results obtained with both procedures have been plotted on the same graph to demonstrate the value of field determinations of Kh near saturation. Selected soil properties are presented in Table 60.

Table 60 Selected morphological description, texture and chemical properties of the diagnostic horizons in the Two Streams catchment

| Profile | Horizon | Depth mm | Moist | Sand % | Silt % | Clay % | Texture | OC % | pH H ₂ O | KCL | CEC cmol _c kg ⁻¹ | Mn mg kg ⁻¹ | Fe mg kg ⁻¹ |
|-----------|---------|-------------|------------|-----------|-----------|-----------|------------------------|---------|------------------------|------|-------------------------------------------|---------------------------|---------------------------|
| Inanda | ah | 400 | 7.5YR2.5/2 | 53 | 18 | 28 | Fine sandy clay loam | 4.13 | 4.35 | 4.01 | 14.31 | 365 | 57100 |
| | ye | 800 | 5YR4/6 | 54 | 17 | 30 | Fine sandy clay loam | 1.14 | 4.35 | 4.07 | 5.89 | 260 | 41200 |
| | re | 2000 | 2.5YR3/6 | 50 | 17.5 | 33 | Fine sandy clay loam | 0.66 | 4.35 | 4.06 | 4.08 | 459 | 32750 |
| Inanda | ah | 400 | 5YR3/3 | 56 | 19 | 25 | Medium sandy clay loam | 2.06 | 4.35 | 4.11 | 9.87 | 970 | 46450 |
| | re | 800 | 2.5YR4/6 | 47 | 22 | 32 | Clay loam | 1.25 | 4.4 | 4.29 | 6.43 | 965 | 38250 |
| | re | 2000 | 2.5YR3/6 | 43 | 24 | 33 | Clay loam | 0.51 | 4.6 | 4.3 | 5.62 | 863 | 48220 |
| Magwa | ah | 400 | 7.5YR2.5/2 | 52 | 24 | 24 | Fine sandy clay loam | 4.77 | 5.1 | 4.6 | 19.75 | 830 | 33800 |
| | ye | 800 | 7.5YR4/6 | 47 | 22 | 32 | Clay loam | 1.34 | 5.6 | 5 | 9.33 | 1335 | 45650 |
| | on | 1200 | 10YR4/6 | 37 | 25 | 38 | Clay loam | 0.71 | 4.8 | 4.2 | 9.33 | 470 | 38300 |
| Katspruit | ot | 800 | 7.5YR3/2 | 44 | 23 | 32 | Clay loam | 4.45 | 5.3 | 4.8 | 19.57 | 340 | 46450 |
| | G | 1200 | 10YR4/1 | 56 | 10 | 33 | Coarse sandy clay loam | 0.75 | 4.7 | 4 | 4.8 | 745 | 28250 |
| Oakleaf | ot | 400 | 7.5YR3/2 | 61 | 13 | 24 | Medium sandy clay loam | 3.02 | 4.7 | 4.2 | 15.22 | 585 | 35000 |
| | ne | 800 | 2.5YR5/6 | 45 | 22 | 33 | Clay loam | 1.59 | 4.9 | 4.4 | 9.07 | 365 | 47650 |
| | ne | 2000 | 2.5YR5/8 | 48 | 19 | 33 | Medium sandy clay loam | 0.78 | 4.8 | 4.2 | 8.43 | 1030 | 47700 |
| Clovelly | ot | 400 | 7.5YR3/2 | 64 | 24 | 22 | Loam | 2.55 | 5.6 | 4.5 | 14.53 | 1260 | 47650 |
| | ye | 800 | 7.5YR4/6 | 57 | 18 | 28 | Medium sandy clay loam | 1.12 | 5.2 | 4.3 | 12.62 | 1030 | 52150 |
| | so | 1200 | 10YR5/6 | 71 | 14 | 15 | Coarse sandy loam | 0.45 | 5.5 | 4.2 | 5.41 | 1745 | 47700 |
| Griffin | ot | 400 | 7.5YR2.5/2 | 57 | 14 | 25 | Coarse sandy clay loam | 3.34 | 4.35 | 4.2 | 14.41 | 365 | 57100 |
| | ye | 700 | 7.5YR4/6 | 56 | 12 | 28 | Fine sandy clay loam | 1.74 | 4.35 | 4.07 | 10.97 | 260 | 43200 |
| | re | 1500 | 2.5YR3/6 | 52 | 9 | 35 | Fine sandy clay loam | 0.42 | 4.4 | 4 | 8.63 | 445 | 22750 |
| Oakleaf | ot | 400 | 7.5YR2.5/2 | 58 | 12 | 27 | Fine sandy clay loam | 2.96 | 4.4 | 4.01 | 16.14 | 530 | 21700 |
| | ne | 800 | 2.5YR3/6 | 55 | 16 | 29 | Clay loam | 1.15 | 4.9 | 4.35 | 8.07 | 977.5 | 42825 |
| | ne | 2000 | 2.5YR5/8 | 55 | 12 | 33 | Fine sandy clay loam | 0.39 | 5.6 | 4.4 | 7.43 | 867.5 | 34250 |

7.5.2 Results and discussion

Water retention curves

Figure 224, Figure 225 and Figure 226 shows the resulting water retention and curve from the hanging column and pressure pots in the laboratory desorption of the eight soil profiles. Most of the retention curves follow a similar sigmodal shape. This implies a similar pore-size distribution due to textural and structural uniformity. Since all core samples were saturated under vacuum for 24 hours, the water content at saturation (θ_s) is equal to porosity. Porosities (θ_s) (Table 61) were therefore not calculated porosities but water filled porosities as determined in the laboratory after saturating the soil. It is generally accepted that at -100 cm suction, important water conducting macropores, which are pores of 0.003 cm in diameter, are all drained. Mass flow of water in soils, occurs in 0 to -100 cm suction range. The high range is relatively unimportant with regard to the processes of downward or lateral flow of water in soils which are so important for hydrological modelling. The amount of water retained at matric suctions less than -100 cm therefore depends primarily on pore size distribution, and thus strongly affected by soil structure. In general, the θ -h relationships of A and B horizon show a gentle slope from 0 up to -10 cm and a relatively steep slope from 10 to -1000 cm suction, indicating the faster rate of flow through the soils. Humic A horizons (*ah*'s) released water from 0.574 to 0.387 cm³ cm⁻³ on average when suction was increased from 0 to -100 cm. The orthic A horizons (*ot*'s) showed a release from 0.589 to 0.307 cm³ cm⁻³ on average when suction was increased from 0 to -100 cm. At this suction value, approximately 32% and 49% of the total pore space is drained for the *ah* and *ot*'s respectively, with *ah*'s showing higher water retention at -100 cm suction. Both diagnostic horizons have similar structure and an average of 26% clay content (Table 55) with *ah*'s having higher average organic carbon content which could explain more water retention at -100 cm suction.

The diagnostic B horizons showed a similar shape to that of the A horizons (Figure 224, Figure 225 and Figure 226) with an almost identical resemblance between neocutanic B and orthic A horizon of the Oakleaf profile on the south facing hillslope (Figure 225b). These horizons showed a release of water from 0.562 to 0.379 cm³ cm⁻³, 0.535 to 0.338 cm³ cm⁻³ and 0.544 to 0.292 cm³ cm⁻³ on average when suction was increased from 0 to -100 cm for yellow brown apedal B (*ye*), red apedal B (*re*) and neocutanic B (*ne*) horizons respectively. At -100 cm suction value, approximately 33%, 37% and 46% of the total pore space is drained for the *ye*, *re* and *ne*'s respectively. The higher water retention for the *ye*'s could be explained by higher OC contents which is important for initially promoting the dissolution of hematite through reduction/complexation, and then favouring the formation of goethite. The hydromorphic unspecified materials with signs of wetness (*on*) and G horizons released water from 0.531 to 0.370 cm³ cm⁻³ and 0.545 to 0.280 cm³ cm⁻³ respectively. This translates into 16 and 49% of the total pore space drained at -100 cm suction for the *on* and G horizons respectively. The *on* horizon with higher clay content (Table 60) will have larger proportion of micropores to hold most of the water.

Values of the hydraulic parameters for estimating or predicting soil water retention relationship are given in Table 61. Estimation of the retention soil water content occurs when all observed $\theta(h)$ and $K(h)$ data were used in parameter estimation. The RETC in this case simultaneously fits the two functions (i.e. VGM model) to observed data. The

estimating curves on Figure 224 and Figure 225 show that estimated values are accurate enough to replace observed values and the simultaneous fitting of the retention and conductivity data improved parameter estimation. Highly significant correlation values, $R^2 > 0.98$, were obtained from fitting of van Genuchten model to laboratory measured $\theta(h)$ relationship (Table 61).

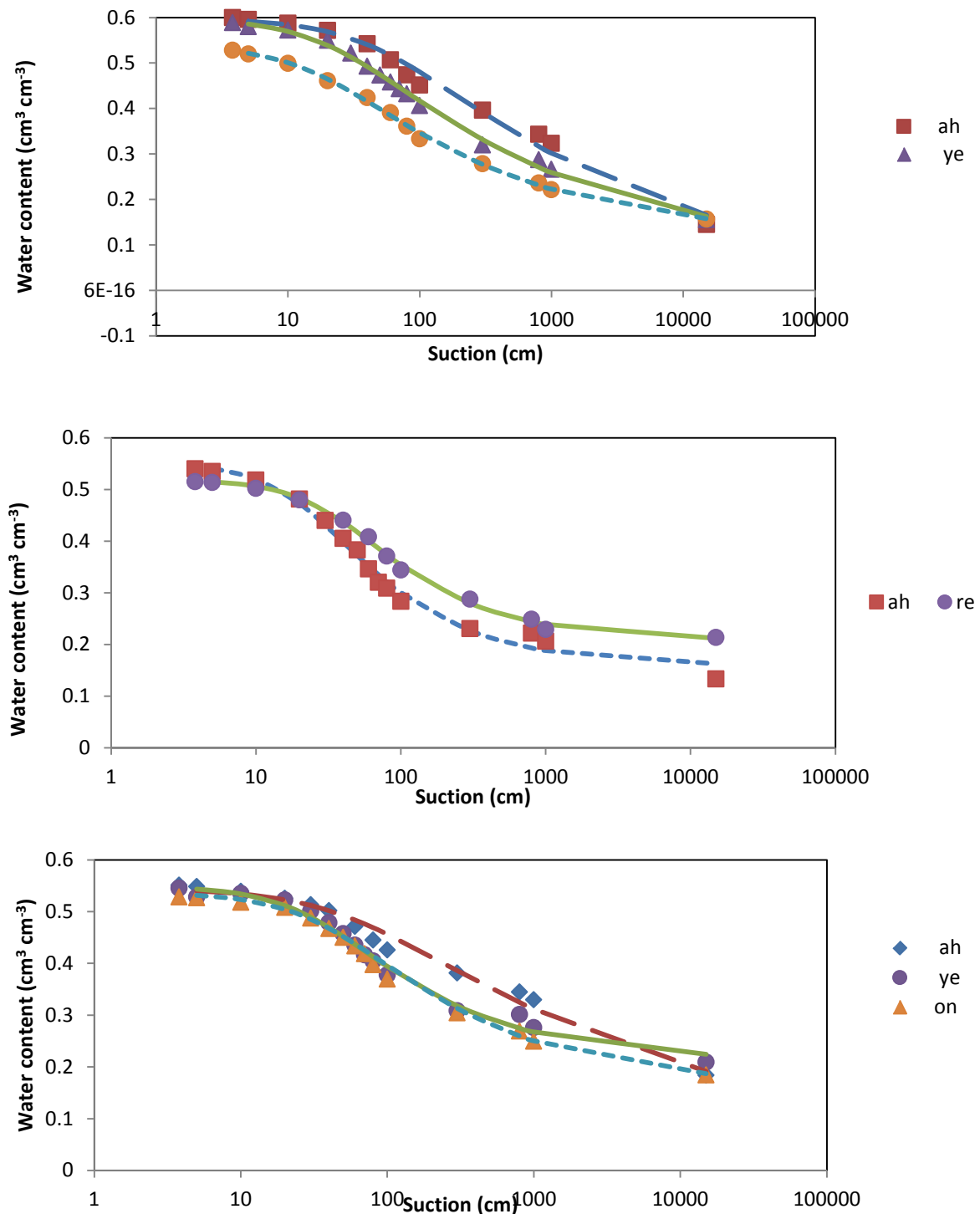


Figure 224 The water retention curves of investigated (a) Kranskop, (b) Inanda, and (c) Magwa soil profiles on the north facing hillslope of the catchment. Mean values measured samples are shown as points. RETC-fitted van Genuchten-Mualem (VGM) curves are

displayed as solid lines. ah = humic A, re = red apedal B, ye = yellow brown apedal B, on = unspecified material with signs of wetness

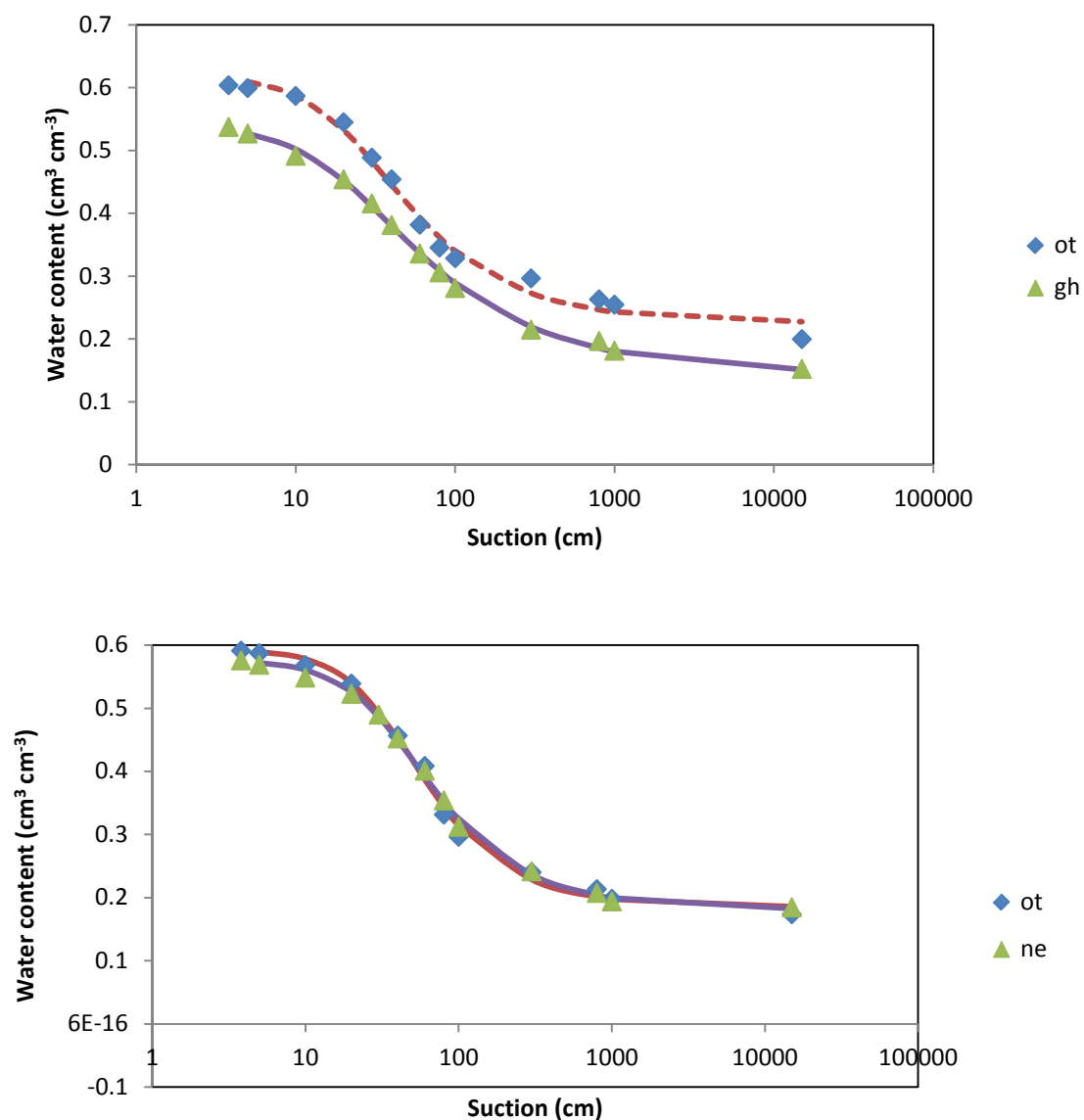


Figure 225 The water retention curves of investigated (a) Katspruit, and (b) Oakleaf soil profiles. Mean values measured samples are shown as points. RETC-fitted van Genuchten-Mualem (VGM) curves are displayed as solid lines. ot = orthic A, gh = G horizon, ne = neocutanic B horizon

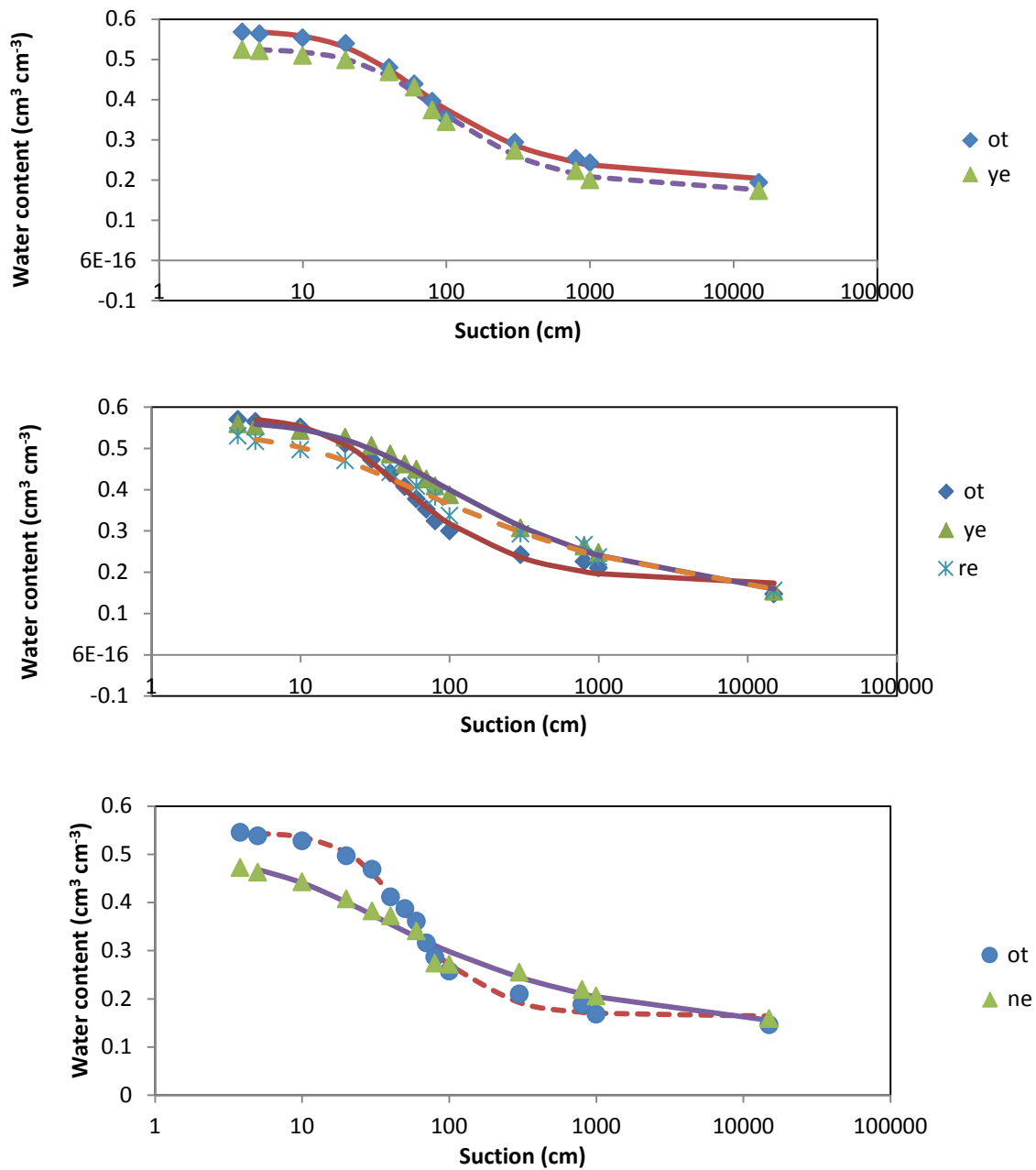


Figure 226 The water retention curves of investigated (a) Clovelly, (b) Griffin and (c) Oakleaf profiles on the south and east facing hillslope. Mean values measured samples are shown as points. RETC-fitted van Genuchten-Mualem (VGM) curves are displayed as solid lines. ot = orthic A, re = red apedal B, ye = yellow brown apedal B, ne = neocutanic B horizon.

Table 61 Van Genuchten parameters and correlation coefficients (R²) obtained from analyzing measured $\theta(h)$ and $K(h)$ data for diagnostic horizons using the RETC program. Measured Ks, Kh (30, 80 , and 150 mm tensions) and bulk density for each horizon are shown

| Soil form | Horizon | Lower depth (mm) | θ_s | θ_r | α | n | R ² | ρ_b | Ks | K(30) | K(80) | K(150) |
|-----------|---------|------------------|----------------------------------|----------------------------------|----------|------|----------------|-----------------------|--------------------|--------------------|--------------------|--------------------|
| | | | cm ³ cm ⁻³ | cm ³ cm ⁻³ | | | | (Mg m ⁻³) | mm h ⁻¹ | mm h ⁻¹ | mm h ⁻¹ | mm h ⁻¹ |
| Kranskop | ah | 400 | 0.60 | 0.01 | 0.02 | 1.24 | 0.986 | 1.08 | 71 | 17 | 11 | 6 |
| | ye | 800 | 0.6 | 0.08 | 0.04 | 1.29 | 0.996 | 1.19 | 343 | 49 | 15 | 1 |
| | re | 2500 | 0.54 | 0.11 | 0.05 | 1.34 | 0.998 | 1.24 | 372 | 42 | 17 | 4 |
| Inanda | ah | 400 | 0.55 | 0.16 | 0.04 | 1.69 | 0.988 | 1.33 | 63 | 19 | 9 | 0.7 |
| | re | 2000 | 0.52 | 0.21 | 0.03 | 1.69 | 0.997 | 1.38 | 230 | 35 | 18 | 6 |
| Magwa | ah | 400 | 0.54 | 0.03 | 0.02 | 1.21 | 0.981 | 1.06 | 61 | 12 | 8 | 5 |
| | ye | 1000 | 0.55 | 0.21 | 0.03 | 1.54 | 0.987 | 1.31 | 178 | 9 | 7 | 5 |
| | on | 2000 | 0.54 | 0.16 | 0.02 | 1.45 | 0.994 | 1.34 | 17 | 0.69 | 0.4 | 0.1 |
| Katspruit | ot | 1000 | 0.62 | 0.23 | 0.04 | 1.83 | 0.989 | 0.95 | 30 | 2 | 1 | 0.3 |
| | G | 1200 | 0.54 | 0.14 | 0.05 | 1.62 | 0.998 | 1.25 | 53 | 26 | 12 | 6 |
| Oakleaf | ot | 400 | 0.6 | 0.17 | 0.03 | 1.49 | 0.995 | 1.14 | 211 | 2 | 1.4 | 0.9 |
| | ne | 2000 | 0.58 | 0.18 | 0.03 | 1.92 | 0.997 | 1.3 | 374 | 5 | 3 | 2 |
| Clovelly | ot | 400 | 0.57 | 0.15 | 0.04 | 1.53 | 0.982 | 1.2 | 66 | 28 | 19 | 12 |
| | ye | 800 | 0.53 | 0.17 | 0.02 | 1.76 | 0.994 | 1.25 | 297 | 42 | 20 | 10 |
| Grffin | ot | 400 | 0.58 | 0.17 | 0.04 | 1.77 | 0.992 | 1.16 | 88 | 7 | 4 | 2 |
| | ye | 800 | 0.57 | 0.11 | 0.03 | 1.37 | 0.997 | 1.31 | 225 | 12 | 6 | 3 |
| | re | 2500 | 0.54 | 0.08 | 0.06 | 1.26 | 0.992 | 1.33 | 209 | 7 | 4 | 2 |
| Oakleaf | ot | 400 | 0.55 | 0.15 | 0.02 | 1.67 | 0.995 | 1.22 | 217 | 22 | 11 | 6 |
| | ne | 1500 | 0.49 | 0.12 | 0.09 | 1.34 | 0.981 | 1.36 | 198 | 27 | 12 | 6 |

ot = orthic A, re = red apedal B, ye = yellow brown apedal B, ne = neocutanic B horizon, G = gleyed horizon, ah = humic

Hydraulic conductivity

Hydraulic conductivity (K) – degree of saturation (s) relationships

The unsaturated hydraulic conductivity ($K\theta$) was estimated using predictive model of van Genuchten-Mualem (VGM) (Van Genuchten and Leij, 1992) using water retention soil parameters in Table 61. The results are presented in Figure 227 & Figure 228. The water contents from retention curves were expressed in terms of the degree of saturation (s) which refers to the fraction of the porosity that occupied by water (Van Huyssteen *et al.*, 2010). The overall K-s relationship showed a sharp decrease in K from saturation (at 1.0 s value) to near saturation values (0.8 and 0.7 s). Considering this in relation to steep slope of water retention curves above show these horizons drain rapidly to a water content at which K is very low. In general, at 0.7 s , K values were already below 1 mm hr⁻¹ for almost all the horizons (Figure 227 & Figure 228). Between this s value and 1.0 s value, most of the large pores will empty first, creating unsaturated soil and soil moisture tensions which, in turn, leads to a strong reduction in the hydraulic conductivity of the soil. The flow in these horizons is therefore largely controlled by macropores, in spite of their very low contribution to the overall porosity (presented in section 7.3.3.2). In the diagnostic B horizons there were a relatively high K_s values as a result of large continuous structural pores which at lower suction was emptied and the K values dropped very strongly between porosity (1.0 s) and 0.80 s where only the relatively small pores inside the matrix are available for flow. The rapid decrease of K values at such high s values is a clear indication that even though the fraction of macropores occupying the total porosity is very low, it is extremely important as far as soil water flow is concerned, especially at near saturation. The fact that s values drops rapidly to almost nothing at 0.7 s in these soils, suggests that conditions favouring reduction reactions are hardly met, hence lack of signs of wetness identified in all profiles located on the slopes. There is a level of saturation at which a sufficient fraction of soil pores are filled with water to inhibit normal oxidative respiration of microbes, causing the onset of reduction. This will be the case if there is impervious layer below porous layer to prevent drainage. Van Huyssteen *et al.* (2005) approximated that reduction will set in when the pores are saturated to 70% of porosity, which is $S_{0.7}$. They based their hypothesis on experience and a set of specific conditions, in the absence of scientific research and data in this regard. Morphology-wise, the Magwa and Katspruit profiles are somewhat poorly drained soils because of the presence of the mottles especially in the B horizons. In other soils, no mottles were observed and therefore they were considered well drained soils. However, considering the K-s relationship and water retention curves of these subsoil horizons, the horizons have a greater capacity to transmit water, although they occur in a poorer natural drainage condition. Even though most of the horizons are apedal, it does not imply that these soils are completely structureless. They have distinct micro-aggregate structure which explains a great capacity of them to transmit water.

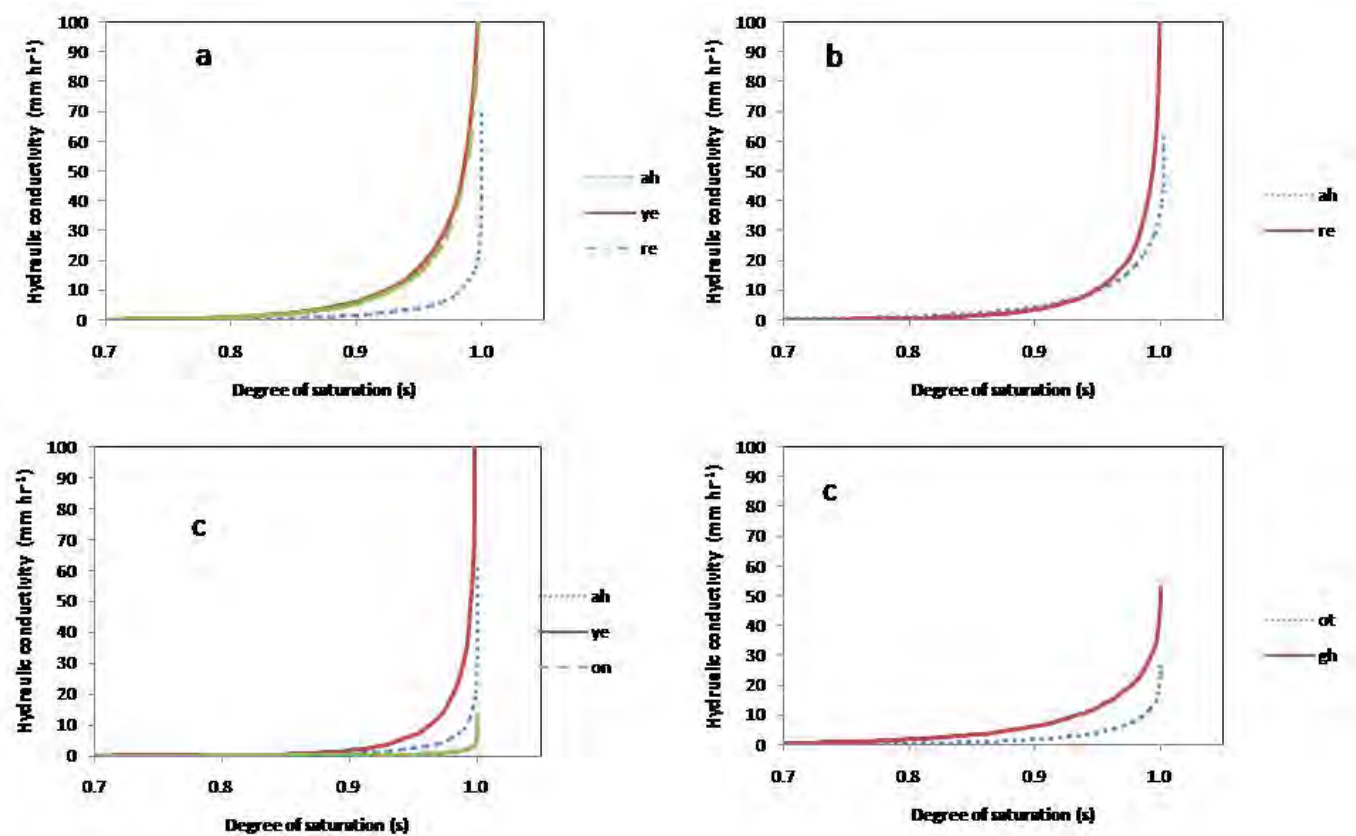


Figure 227 Hydraulic conductivity vs degree of saturation for different soil profile (a), Kranskop (b), Inanda (c), Magwa and (d), Katspruit soil profiles. For convenience regarding scale, the very high Ks values for the B horizons of some profiles are not shown. These K-s relationships are based on K(θ) curves predicted using the VGM hydraulic model.

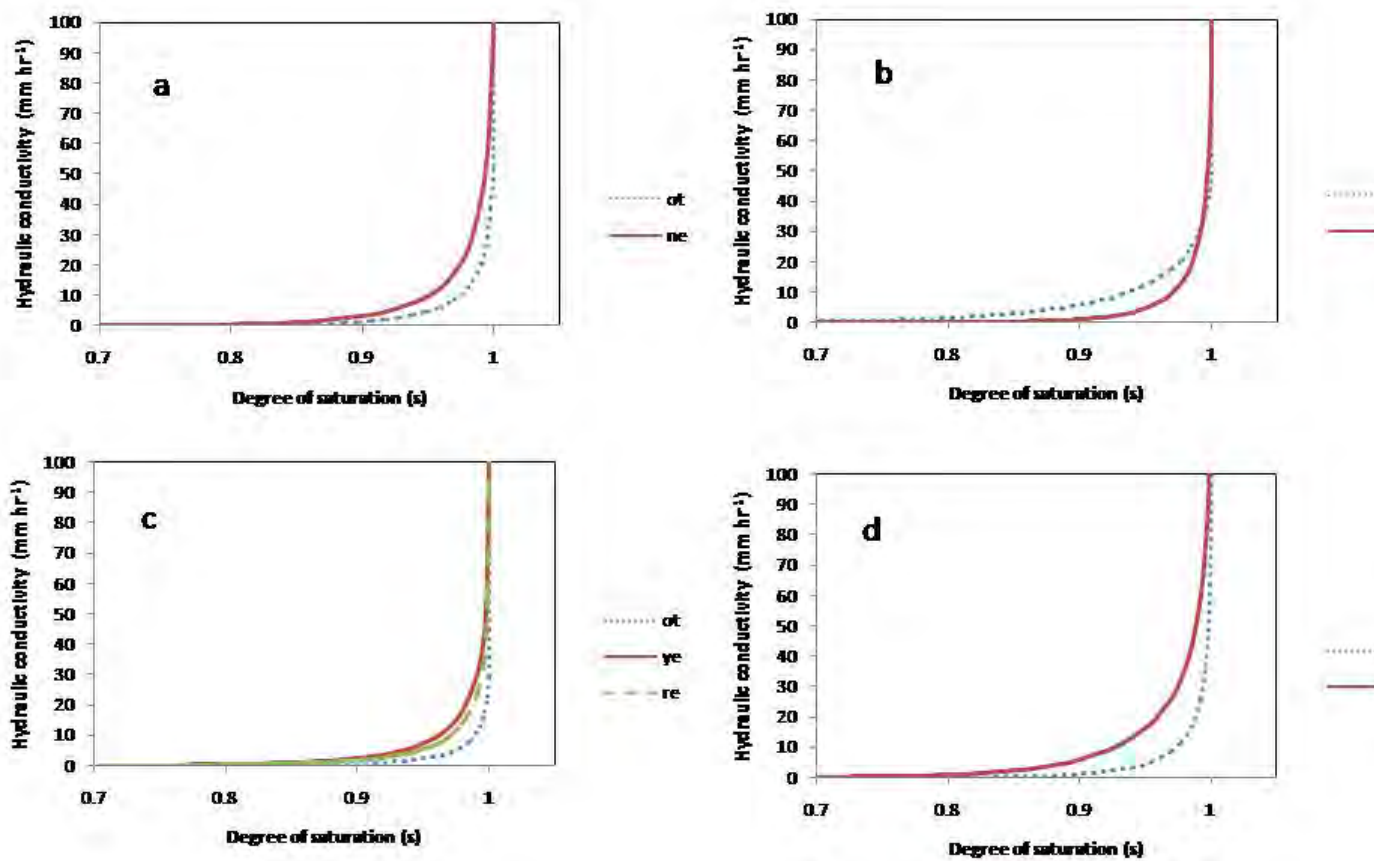


Figure 228 Hydraulic conductivity vs degree of saturation for different soil profile (a), Oakleaf (b), Clovelly (c), Griffin and (d), Oakleaf soil profiles. For convenience regarding scale, the very high Ks values for the B horizons of some profiles are not shown. These K-s relationships are based on K(θ) curves predicted using the VGM hydraulic model.

K-h relationship (Kh curves)

In many hydrogeological studies the predictive model of van Genuchten-Mualem (VGM) (Van Genuchten, 1980,) using water retention soil parameters, is often used to characterise unsaturated hydraulic conductivity (K_h) (Schaap & Leij, 2000). This is necessary given the difficulty and time consuming nature of accurate measurements of unsaturated hydraulic conductivity under field conditions (Schaap & van Genuchten, 2006). It is often presumed enough to run RETC program for retention curve model using the measured retention curve data only. This is because one gets the data-rich output from which the database of hydraulic properties can be constructed. Parameters n , α and θ_s determined from this output are essential in the prediction of water flow through the vadose zone. It is therefore important to improve optimization of such parameters for better prediction of water flow through the vadose zone. While the VGM model proves to be effective in the soil water content (θ) range approximately below drained upper limit (DUL), the effect of macropore flow on conductivity near to saturation is not well represented. It is common that measured K_s is used for the matching point for K at saturation in the VGM model. This often leads to over predicted K_h values at low suction (h) values (Schaap & Leij, 2000). Using K_s derived from texture as in the hierarchical Artificial Neural Network model of the pedo-transfer package (ROSETTA), results in systematically underestimated K_h values between 0 and 10 cm suction (Schaap *et al.*, 2001). The discrepancy between measured K_s and estimated K_s can be explained by the presence of macropores that dominate the flow regime near saturation. Moreover, relatively small laboratory core samples can promote important deviations in hydraulic properties. The deviations are fundamentally associated with soil structure, macropores and specific characteristics of each of the horizons that comprise the pedologic unit. Subsequently the results arising from such studies are compromised to some extent (Lin, 2010). The *in situ* determination of near saturation hydraulic conductivity using the tension infiltrometer can therefore improve the predictions of the VGM model by optimization of VGM parameters using both field measured hydraulic conductivity data and water retention data.

In this study, the RETC code was used to estimate the $K(h)$ curves from field data where all retention and conductivity data were included in the fitting process for parameters estimation. Results are presented in Figure 229 & Figure 230. These figures shows that hydraulic conductivity for the A and the B horizons predicted from the fitted hydraulic parameters were better matching the measured values at near saturation (Figure 229 & Figure 230), even though only near saturated hydraulic conductivity was measured *in situ*. With this field data agreeing well at near saturation with VGM, it is encouraging that predictions of flow through vadose zone will be precise. Using $\theta(h)$ data only to predict $K(h)$ curve do not agree well with field data (Figure 231 & Figure 232). When studying these curves it needs to be kept in mind that the measured K_s value is necessary for the VGM model, that is why all the curves start at the same K_s values. The K_h curves using the two procedures agree reasonably well for the Kranskop, Inanda and Magwa *ah* horizons (Figure 231). K_h curves using retention data only were unsatisfactory in all the A horizons of Oakleaf, Clovelly and Griffin soils (Figure 232). K_h data in the wet range using retention data only are likely to contain large uncertainties. For example, the VGM retention model results show an 8-fold higher simulated K value at 30 mm tension than that measured in the field using tension infiltrometer for the *ot* horizon of the Griffin soil (Figure 232c). The difference between these two curves clearly demonstrates the unreliability of the VGM model at the

very wet end of the curve. Although field measurements of K_h near saturation are rather cumbersome and costly, these results show that this procedure is necessary and worthwhile because of the importance of macropore flow explained by the results in section 7.3.3.2. It is clear that at suction values near zero, K dropped sharply in all horizons from high values to almost 0.01 mm hr^{-1} as the suction head increased to -100 cm . This is because the large pores are emptied in this range leaving only the relatively small pores inside the matrix available for the flow. The water moving at this suction value does not contribute directly to streamflow or deep saprolite storage. It does contribute to transpiration and evaporation. These soils are characterized by high macropore flow as discussed in section 7.3.3.2. These results showed that the soil solum enable rapid movement of water in a vertical direction and promotes efficient deep saprolite storage.

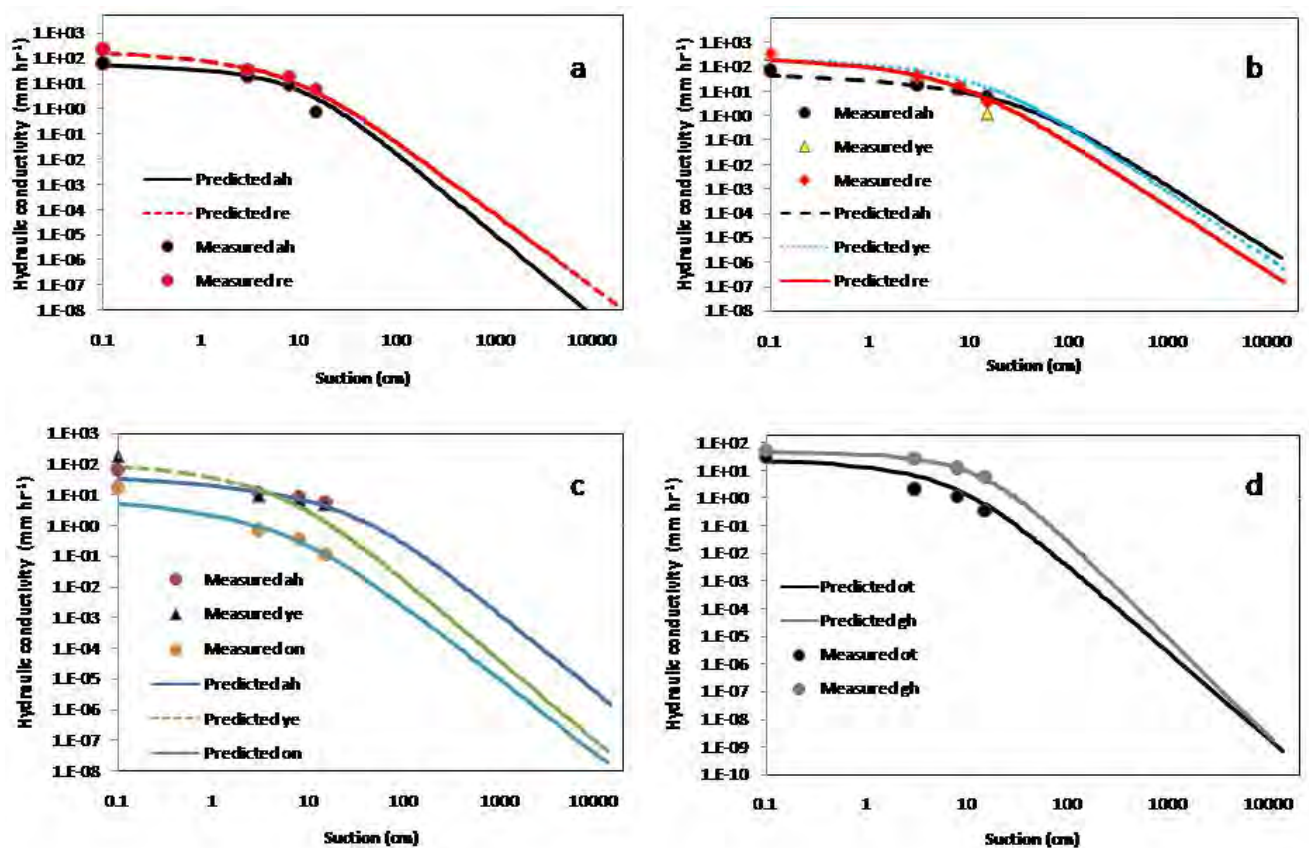


Figure 229 Unsaturated hydraulic conductivity (K_h) curves for the Inanda (a), Kranskop (b), Magwa (c) and Katspruit soil profiles

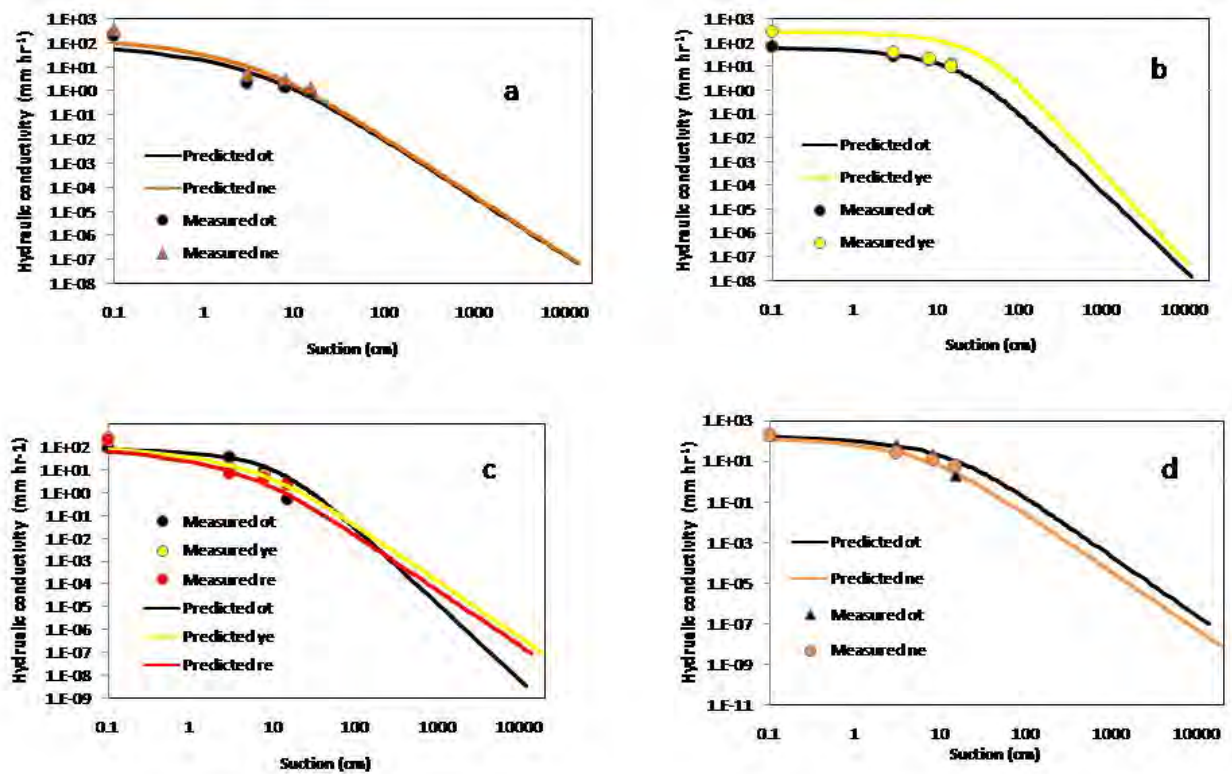


Figure 230 Unsaturated hydraulic conductivity (K_h) curves for the Oakleaf (a), Clovelly (b), Griffin (c) and Oakleaf soil profiles

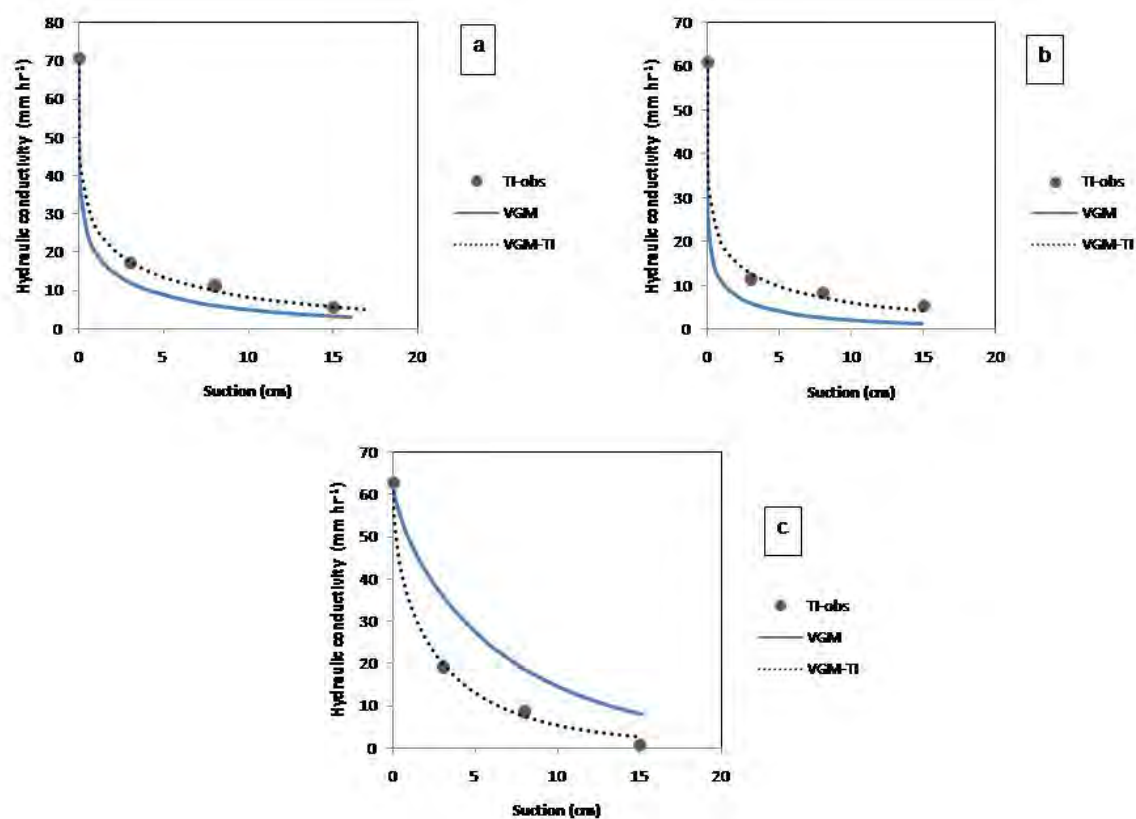


Figure 231 Comparisons between K_h curves obtained in three different ways, i.e. using observed tension infiltrometer (TI-obs) K_h data only; using the VGM hydraulic model with retention data only; and VGM model fitted to tension infiltrometer data (VGM-TI). The results are for the A horizons of the following soils: (a) Kranskop; (b) Inanda, and (c) Magwa.

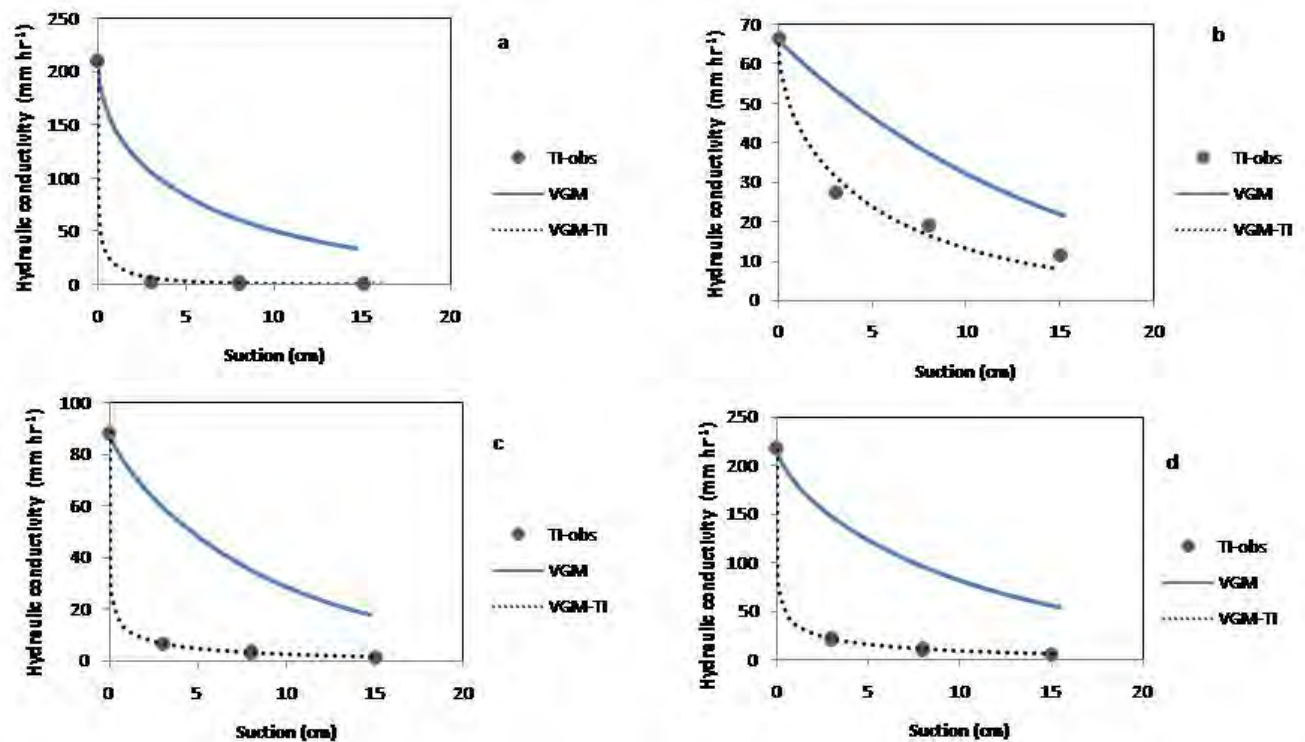


Figure 232 Comparisons between K_h curves obtained in three different ways, i.e. using observed tension infiltrometer (TI-obs) K_h data only; using the VGM hydraulic model with retention data only; and VGM model fitted to tension infiltrometer data (VGM-TI). The results are for the A horizons of the following soils: (a) Oakleaf, (b) Clovelly, both on the southern hillslope; and (c) Griffin and (d) Oakleaf both on the eastern slope

7.5.3 Conclusion

The θ - h relationship of each horizon was successfully determined using standard procedures. The relationships were satisfactorily described by the van Genuchten model. K_h values close to saturation were determined in the field by means of a tension infiltrometer at h values of 30, 80, 150 mm. These results were for simultaneous fit using water retention data and conductivity data in the RETC programme to obtain modified VG parameters and thereby producing a mathematical expression suitable for predicting the hydraulic conductivity $K(h)$ curve for each horizon. The predicted curves agreed well with those determined *in situ*.

7.6 REFERENCES

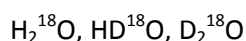
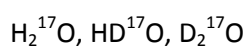
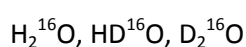
- DIRKSEN, C., 1999. Soil physics measurements. GeoEcology paperback, Catena Verlag GMBH, 35447 Reiskirchen, Germany.
- JURY, W., GARDENER, W.R. & GARDNER, W.H. 1991. Soil Physics (5th Ed.). John Wiley & Sons, New York.
- HILLEL, D., 1981. Fundamentals soil physics. Academic Press, New York.

- HUTSON, J.L. 1983. Estimation of hydrological properties of South African soils. PhD thesis. Department of Soil Science and Agrometereology. University of Natal, Pietermaritzburg, South Africa.
- LIN, H. 2010. Earth's critical zone and hydropedology: concepts, characteristics, and advances. *Hydrology and Earth Sys Sci.* 14: 25-45.
- SCHAAP, G.M. & LEIJ, F.J. 2000. Improved prediction of unsaturated hydraulic conductivity with the Mualem-van Genuchten model. *Soil Sci. Soc. Am. J.* 64 843-851.
- SCHAAP, G.M. & VAN GENUCHTEN, M.T. 2006 A modified Mualem-van Genuchten formulation for improved description of the hydraulic conductivity near saturation. *Vadose Zone J.* 5 27-34.
- SCHAAP, M.G., LEIJ, F.J. & VAN GENUCHTEN, M.T. 2001. ROSETTA: a computer program for estimating soil hydraulic parameters with hierarchical pedotransfer functions. *J of Hydrol.* 251 163-176.
- VAN GENUCHTEN, M.T., LEIJ, F.J., & YATES, S.R. 1991 The RETC code for quantifying the hydraulic functions of unsaturated soils. Rep. EPA/600/2-91/065. R.S. Kerr Environmental Research Laboratory, USEPA, Ada, OK.
- VAN GENUCHTEN, M. Th., 1980. A closed-form equation for predicting the hydraulic conductivity of unsaturated soils. *Soil Sci. Soc. Am. J.* 44, 892-898.
- VAN GENUCHTEN, M. TH., & LEIJ, F.L. 1992. On estimating the hydraulic conductivity properties of unsaturated soils. In M. Th. van Genuchten, F.J. Leij, & L.J. Lund. Eds. Indirect methods for estimating the hydraulic properties of unsaturated soils. Proc. Int. Workshop. Riverside, California. 11-13 October, 1989. University of California.
- VAN HUYSSTEEN, C.W., HENSLEY, M., LE ROUX P.A.L., ZERE, T.B. & DU PREEZ, C.C. 2005. The relationship between soil water regime and soil profile morphology in the Weatherley catchment, an afforestation area in the Eastern Cape. WRC Report No. 1317/1/05. Water Research Commission, Pretoria.
- VAN HUYSSTEEN, C.W., ZERE, T.B. & HENSLEY, M. 2010. Soil-water relationships in the Weatherley catchment, South Africa. *Water SA.* 36: 521-530.
- WOSTEN, J.H.M. AND VAN GENUCHTEN, T.H.M. 1988. Using texture and other soil properties to predict the unsaturated soil hydraulic functions. Division S-6, Soil water management and conservation. *Soil Sci. Soc. Am. J.* 52:1762-1770.

7.7 INTRODUCTION TO THE USE OF ISOTOPES

A number of observation techniques are used in the characterization of hillslope processes. These include remote sensing, soil surveys, tracer and hydrometric methods applied in different combinations. Tracer based studies allow for detailed conclusions with a potentially high level of accuracy at a reasonable cost considering the alternatives. The diverse application of tracer based studies stems from the ability to monitor naturally occurring environmental tracers, as well as artificially injected tracers (Kendall, 2003; Singh and Kumar, 2005; Leibunbgut and Maloszewski, 2009).

Environmental tracers occur naturally in every component of the hydrological cycle, and occur in nine different combinations of the stable isotopes of water, hydrogen and oxygen. The nine combinations are given as:



Contemporary tracer hydrology commonly considers H_2^{16}O , H_2^{18}O , HD^{16}O and H_2^{17}O . These isotopes of water occur in different abundance ratios. This particular ratio of abundance gives insight into the processes that a water molecule has undergone to reach a particular point in the hydrological cycle. The ratio of a depleted isotope, N_i , to an abundant isotope, N , is expressed as:

$$R = N_i / N \quad (7.15)$$

Oxygen and Deuterium isotopes are commonly expressed in terms of Standard Mean Ocean Water (SMOW) or VSMOW as defined by the International Atomic Energy Agency in Vienna. The VSMOW abundance ratios are expressed in the following manner:

$$R^{18\text{O}/16\text{O}} = \left(\frac{^{18}\text{O}}{^{16}\text{O}} \right)_{\text{VSMOW}} = 0.002 \quad (7.16)$$

$$R^{D/H} = \left(\frac{^2\text{H}}{^1\text{H}} \right)_{\text{VSMOW}} = 0.00016 \quad (7.17)$$

The isotopic abundance ratio of a sample R_{sample} is calculated with respect of the VSMOW standard, with an abundance ratio R_{standard} and is expressed as a δ value.

$$\delta = \frac{R_{\text{sample}} - R_{\text{standard}}}{R_{\text{standard}}} \quad (7.18)$$

Oxygen and deuterium isotope δ values are multiplied by a factor of 1000 giving a ‰ difference from the VSMOW standard, for analytical purposes. Positive values indicate the enrichment of oxygen 18 and deuterium, while negative values indicate depletion in respect of the standard (Equation 7.18) (Kendall 2003; Singh and Kumar 2005; Leibunbgut and Maloszewski, 2009).

The practical application of isotopes is based on the occurrence of two processes which influence the abundance ratios of stable isotopes of water. These two processes are functions of evaporation and mixing, which allow for the clear distinction between different bodies of water.

7.7.1 Fractionation

The extent to which an environmental isotope sample is depleted or enriched is as a direct result of the degree of fractionation it has undergone. Fractionation of natural isotopes occurs due to water changing phases through the hydrological cycle. The change in phase from solid to liquid to gas results in changes to the relative abundance ratios of oxygen and deuterium isotopes (Leibunbgut and Maloszewski, 2009). Fractionation processes occur due to both chemical and physical reactions, however it is typically considered the degree of evaporation a water body has experienced (Singh and Kumar 2005).

Attenuation

Attenuation refers to the degree of variation observed in an isotopic time series at a particular point. The resistance to gravity driven infiltration provided by the soil profile causes the mixing of water of different ages. This causes the distinct isotopic signatures of individual events to become dampened over time, caused by the different velocities of a wetting front infiltrating a soil profile. Fine textured soils will show attenuated soil water isotope values at shallower depths than coarse textured soils. This relationship is described by an exponential trend given in Figure 233. Due to the exponential nature of this trend, soil water isotope values will show a higher temporal variance at shallow soil depths. Further down the profile closer to the soil/bed rock interface, values will show relatively little variance over time, as the well mixed nature of these waters has dampened the distinctiveness of any individual event (Kendall 2003; Singh and Kumar 2005; Weiler 2007; Leibunbgut and Maloszewski, 2009). A practical example of attenuation is given in Figure 234, the variability in the soil water isotopic time series becomes increasingly attenuated with increasing soil depth (Leibunbgut and Maloszewski, 2009).

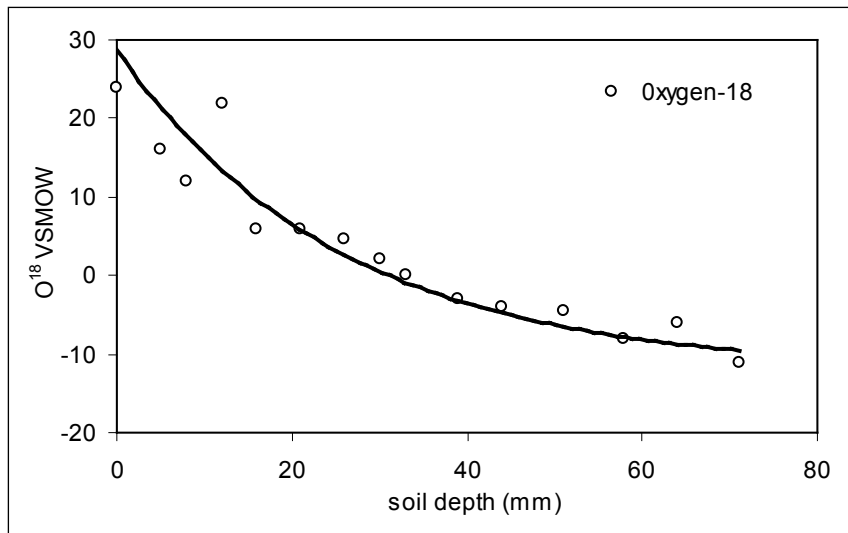


Figure 233 Stable Isotope profile of a saturated soil (after Kendall and McDonnell, 2003)

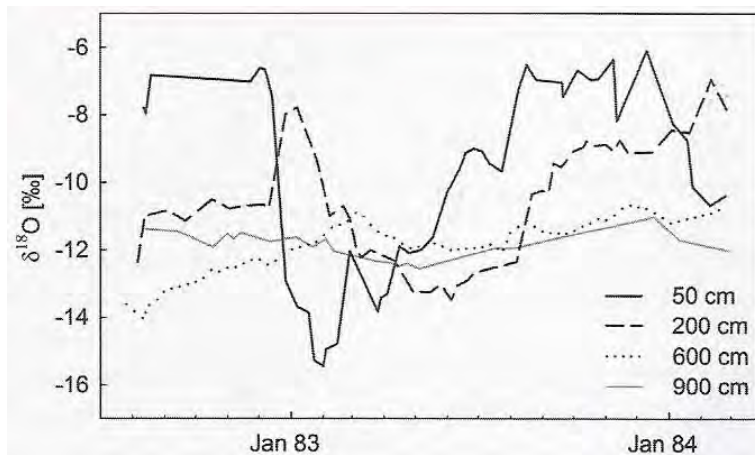


Figure 234 Soil water isotopic composition at varying soil depths, Munich Germany (Leibnizgut and Maloszewski, 2009)

7.7.2 Isotopes of rainfall

Rainfall isotopes form the reference point for any terrestrial based tracer study. The source of all terrestrial water is described by the Global Meteoric Water Line (GMWL), which characterizes the oceanic source feeding global precipitation (Figure 235, a). Local Meteoric Water Lines can be derived for specific study areas and provide insight into the specific sources of rainfall for different climates. Negative values of δO^{18} and δH^2 rainfall values are typical of humid, lower altitude coastal areas where rainfall is mainly ocean derived. In comparison to positive δO^{18} and δH^2 rainfall values of higher lying areas which experience mainly frontal rain which has been carried long distances in the atmosphere, potentially allowing more fractionation to occur.

7.7.3 Isotopes of streamflow/outflow

Isotopes values from the outlet point of a study area are just as crucial as those of rainfall. The isotope values of streamflow/outflow allow conclusions to be drawn on the processes terrestrial water has undergone in its transformation from rainfall to streamflow, thus giving insight into the runoff generation characteristics of an area. The complexity of runoff characteristics implies that a number of various sources could possibly contribute to the isotopic composition of streamflow at a particular point. For the purposes of tracer based application some basic assumptions can be made by simply comparing streamflow isotope data with that of the suspected source.

1. Runoff that is comprised mainly of the current events precipitation will show a linear trend similar to that of the current precipitation (Figure 235, b or c).
2. Runoff originating from previous events precipitation may exhibit evidence of fractionation or attenuation (mixing) shown by (d) in Figure 235. The fractionation processes occurs during either atmospheric or terrestrial residence of water, while attenuation only occurs during terrestrial residence.

The application of these simple assumptions allows for the characterization of different subsurface processes which from the blue print for more analytical methods such as end member mixing analysis and residence time estimations.

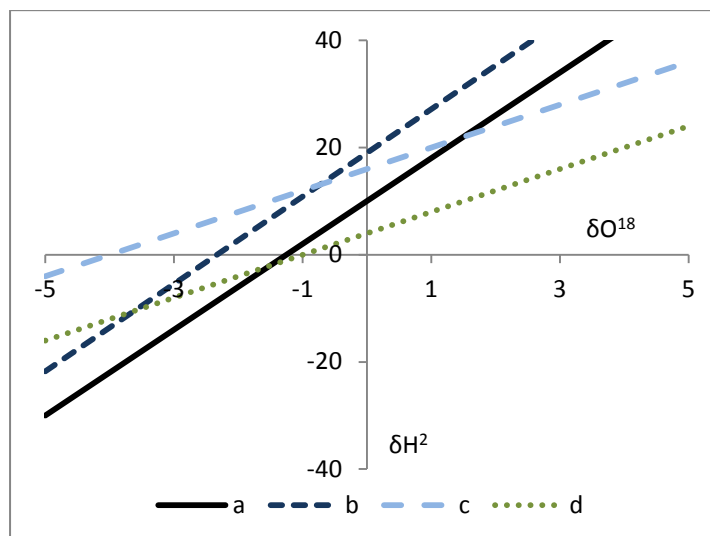


Figure 235 Conceptual isotope compositions of rainfall and runoff

End member mixing analysis

The number of tracers sampled determines the number of source components considered in an end member mixing analysis. Where only a single tracer type is considered, only a two-component end member mixing analysis can be applied. Oxygen 18 and Deuterium cannot be considered independent tracers as their δ values are proportional.

End member mixing analysis using δO^{18} isotopes is based on steady state mass balance equations that have several underlying assumptions:

- significant difference in δO^{18} value between event and pre event contributions,

- variations in pre event and event δO^{18} signal can be accounted for,
- vadose zone contributions are insignificant, or the δO^{18} value of soil water must be similar to that of ground water, as a two component separation cannot distinguish more than one subterranean water source, and
- surface storage contributions to streamflow are insignificant.

The 2-component hydrograph equation is given by:

$$Q_t = Q_p + Q_e \quad (7.19)$$

$$Q_t C_t = Q_p C_p + Q_e C_e \quad (7.20)$$

Re-formed to solve for event and pre event contributions respectively:

$$Q_e = (C_t - C_p)/(C_e - C_p) \quad (7.21)$$

$$Q_p = (C_t - C_e)/(C_p - C_e) \quad (7.22)$$

Where Q = volumetric flow rate

C = δO^{18} value permil

t = total streamflow

p = pre event contribution

e = event derived contribution

The 2-component end member mixing analysis is limited by the number of components it can consider, yet it has versatility as it can be applied at any point with a sampled outflow, without the need for extensive gauging.

Mean residence time

Tracer based observations are commonly applied in the estimation of mean residence time. Mean residence time calculations are carried out by applying an excitation (precipitation) to transfer functions describing subsurface flow characteristics. Temporal fluctuation in the isotope signal is used to replicate observed outputs.

There are a number of models available to estimate mean residence time depending on the intended application. These include the Piston flow model, Exponential model, combined exponential piston flow model and the dispersion model (Asano and Uchida, 2002; Rodgers and Soulsby, 2005; DeWalle *et al.*, 1997; Leibunbgut and Maloszewski, 2009; Maloszewski and Zuber 1982; McGuire *et al.*, 2002; McGuire *et al.*, 2006).

The piston flow and exponential transit time distributions are used for single porosity simulations. For dual porosity simulations, including macropores or porous bedrock, the combined exponential piston flow model or dispersion model is applied so that a distinction can be made between immobile soil water in the micropores and mobile soil water in the macropores ([Leibunbgut and Maloszewski, 2009](#)). The majority of the cases in which these methods have been applied have involved deep ground water bodies with relatively little temporal and spatial variation compared to the shallower subsurface processes considered in the field of hillslope hydrology. This has resulted in a large body of literature biased toward deep ground water studies; while relatively; little literature exists to guide the application of these methods in estimating shallow subsurface processes.

SECTION IV: THE WAY FORWARD

Chapter 8 CONCLUSIONS, NEEDS AND SUGGESTIONS FOR FUTURE STUDIES

8.1 NEEDS

The protection and management of surface and groundwater resources requires the accurate analysis of hydrological processes and their spatial distribution at all scales. In the highly variable hydrological regime of southern Africa the management of water resources is critically dependent on a clear understanding of these hydrological processes (Wenninger *et al.*, 2008). This understanding involves the identification, definition and quantification of the pathways and residence times of components of flow making up stream discharge; it is essential that these aspects be efficiently captured in hydrological models for accurate water resource predictions, estimating the hydrologic sensitivity of the land for cultivation, contamination and development, and for quantifying low flow mechanisms (Lorentz *et al.*, 2007).

Hydrological modelling requires scientifically sound data representative of hydrological units applicable to models. The scientific nature of data is often questioned. Hydrological processes are dynamic in nature with strong temporal variation, making measurements expensive and time consuming (Park & Van de Giesen, 2004; Ticehurst *et al.*, 2007). It also limits temporal extrapolation of data. The need for predictions of hydrological processes, especially in ungauged basins, is becoming increasingly important (Sivapalan, 2003a; Sivapalan *et al.*, 2003). Measurements are commonly made in micro localities with uncertain spatial representation while predictions in ungauged basins are dependent on accurate spatial extrapolation. In order to meet the requirements for predictions the aim of research should be to search for common threads, patterns, concepts and laws in landscape heterogeneity and process complexity or as Weiler *et al.* (2004) pronounced: "To clarify, simplify and classify!"

8.2 THE CLARIFICATION, SIMPLIFICATION AND CLASSIFICATION OF HYDROLOGICAL UNITS

Long-term measurements of the duration of drainable water in South African soil types (Van Huyssteen *et al.*, 2005) showed that the hydrology of South African soil types and their diagnostic horizons differs. This clarified the relationship between soil morphology, an ancient (stable) indicator of hydrological conditions, and hydrometry and micro-scale accurate data indicating current hydrological processes. These data made it possible to group the 73 soil types of South Africa into 5 hydrological classes (Van Tol *et al.* 2011; Le Roux *et al.* 2011). It significantly simplified the numerous possibilities in defining the

hydrology of South African soil types. With the development of conceptual hydrological response models for more than 50 hillslopes in South Africa, applying the rules of hydrological soil types, the predicted response of the hillslopes could be classified into 6 hydrological classes (Van Tol *et al.*, 2013).

In the process of clarifying, simplifying and classifying in hydopedology in South Africa several challenges were met. Although soil properties are in the short term not dynamic in nature (Webster, 2000) their response to environmental change varies, and their relevance may be questioned. Morphological properties by nature respond slower than chemical processes for initiating morphological changes. Therefore soil morphological, and most soil physical, properties are ancient and may not represent current environmental conditions. However, the morphology of Australian and South African soils are, in spite of the fact that they are matured soils, good indicators of hydrological response (Ticehurst *et al.*, 2007; Lorentz *et al.*, 2007; Van Tol *et al.*, 2010a; Van Tol *et al.*, 2010b; Kuenene *et al.*, 2012). Their hydrological response also correlates well with sensitive, natural parameters changing in the short term, e.g. soil chemical properties (Bouwer, 2014), natural isotopes (Freeze, 2014) and snapshot, in-time, current hydrometry (Van Tol *et al.* 2010a; Kuenene *et al.*, 2012, Kuenene, 2013). The soil types, their horizons and distribution in hillslopes of South Africa are therefore suitable spatial units for hydrological response transfer functions.

8.3 SPATIAL APPLICATION: MAPS

Spatial extrapolation of hydrology is dependent on a good relationship with a spatial entity. The interactive relationship between soil and hydrology is expressed in soil horizons, soil types and distribution patterns (hillslopes). The soil properties may be causal or consequential or both, making conceptualisation a prerequisite for the application of data. The relationship is further complicated because prominent soil properties, indicative of hydrological response, may have no control function while other less prominent soil properties may control hillslope hydrology.

As soils integrate the influences of parent material, topography, vegetation/land use, and climate they can therefore act as a first-order control on the partitioning of hydrological flow paths, residence times, distributions and water storage (Schulze, 1995; Park *et al.*, 2001; Sivapalan, 2003; Soulsby *et al.*, 2006). A soil map can therefore serve as a window to subsurface hydrological hillslope and catchment behaviour (Van Zijl *et al.* 2014). This therefore implies, a) that soil types and their distribution patterns are indications of specific soil/hydrology interactions, b) that soil horizons, as diagnostic components of soil types, control hydrological response (Van Tol *et al.* 2013) and are hydrological response units, c) that spatial distribution of hydrological response can be mapped using a hydrological soil classification system (Van Tol *et al.* 2011), d) that soils, their horizons and their topographical distribution has a hydrological relationship with the chemical and physical properties of underlying fractured rock (Van Tol *et al.* 2010a; Kuenene *et al.*, 2012) and the intermediate vadose zone (IVZ) (Van Huyssteen *et al.*, 2005; Lorentz *et al.*, 2007).

Characteristic hydrological responses correlate well with the hillslope related soil distribution pattern used by the Land Type Survey Staff (2004) to define Land Types. The concept was first described as a catena (Milne, 1936), but later modified by Bushnell (1942) to toposequence. This concept of an association of soil properties with topography and hydrological processes is also captured in the terms pedosequence or hydrosequence in relation to hillslopes (Flugel, 1997; Sivapalan *et al.*, 2003; Weiler, *et al.*, 2004). This

motivated research to link the hydrological response of soils to hillslopes and the response of hillslopes to Land Types (Van Zijl *et al.*, 2013; Van Zijl *et al.*, 2014).

8.4 PEDO-LOGIC

Hydrologists agree that the spatial variation of soil properties significantly influences hydrological processes but they lack the skill to gather and interpret soil information (Lilly, Boorman & Hollis, 1998; Chirico, Medina & Romano, 2006). Another challenge was to improve the interpretation value of the national Land Type data base (Land Type Survey Staff, 2004). The spatial variation of soils is not random (Webster, 2000). The catena has a hydrological response relationship because individual soil properties, soil horizons and soil types show signs of increase in duration of drainable water (Van Huyssteen *et al.*, 2005). In the past decade significant progress has been made in the understanding and conceptualisation of hillslope hydrological processes through improved understanding and interpretation of soil morphological properties and their spatial distribution. Some of these advancements include inter alia: the correlation between the soil types of South Africa and duration of drainable water (Van Huyssteen *et al.*, 2005); development and validation of Conceptual Hydrological Response Models (CHRM) of representative hillslopes (Van Tol *et al.*, 2010a & 2010b; Kunene *et al.*, 2011) using soil morphological properties; development of PedoTransfer Functions (PTF's) to estimate macroporosity (Van Tol *et al.*, 2012) and the importance of subsurface lateral flow (Van Tol *et al.*, 2013) from morphological properties; evaluation of the contribution of improved soil data in hydrological modelling (Le Roux *et al.*, 2011); production of hydrological soil maps with advanced soil survey techniques (Van Zijl *et al.*, 2013; Van Zijl *et al.*, 2014); linking soil chemistry as recent indicator of hydrological behaviour with hillslope responses (Bouwer, 2013); applying isotopes to infer hillslope hydrological behaviour (Freese, 2013) and presenting a preliminary hillslope hydrological classification scheme based on the conceptual characterisation of 52 studied hillslopes (Van Tol *et al.*, 2013). Although the conceptual or qualitative description of hillslope hydrological behaviour is a critical component of theory advancement (Sivapalan *et al.*, 2003a), quantification of the hillslope hydrological processes should now receive attention in order to answer international research questions such as: what are the first order controls in hillslope hydrological behaviour?; what is the minimum set of measurements to characterise a hillslope?; what is the extrapolation value of a single researched hillslope and how do hillslopes compare in terms of process behaviour (Weiler *et al.*, 2004; McDonnell *et al.*, 2007 and Tromp-van Meerveld *et al.*, 2008). This accentuates the need for detail, e.g. large scale measurements. The data should be related to soil horizons, soil types and soil distribution patterns of Land Types to make local and small scale vertical and horizontal extrapolation possible.

An important part of simplification is to determine the critical controls of hydrological responses in soil horizons, soil types and hillslopes. In the study dealing with the classification of South African hydrological hillslopes (Van Tol *et al.* 2013), the importance of the fractured rock, as lower vadoze zone (LVZ), in controlling hillslope hydrological behaviour was highlighted. Although recent research has focussed on obtaining a holistic understanding of the complex hydrological system, through surface water, soil water (hydropedological) and groundwater (geohydrological) studies, very little attention has been given to the transitional layer between the upper vadoze zone (UVZ) of surface and soil layers, and LVZ (geological layers). This intermediate vadoze zone (IVZ) often referred to as

saprolite, is traditionally not part of soil, and due its depth (>1.5 m) has seldom been studied in soil related research, and is regarded as part of the geology by most soil scientists (for example in WRC project K5/2021, focussing on hydropedology, no mention is made of the IVZ and measurements are only conducted in/on pedogenetic layers). On the other hand, geologists consider saprolite as an annoying partly weathered obstacle for observing the geology. Consequently the layer between the soil (UVZ) and solid rock (LVZ) is often ignored in surface hydrological, hydropedological and geohydrological studies. A good example of this deficiency is the absence of any IVZ measurements in an interdisciplinary study focussing on surface water – groundwater interactions (WRC project 2054). The IVZ will however control the preferred pathway of water once it exits the soil. It is therefore has a pivotal role in determining the amount and rate of recharge to groundwater, lateral flow to streams and return flow to the soil in downslope positions. The character of the IVZ is determined by the kind of weathering that the parent material has undergone, and it therefore serves as an indicator of pedon hydrology in semi-arid and wetter climates, and of fractured rock/soil return flowpaths. The degree of return flow is expressed as chemical weathering and redoximorphic features.

8.5 FROM EXPERIMENTS TO MODELS

Traditional PedoTransfer Functions (PTF's), often used to derive important hydrological soil properties, are not effective for predicting the hydrological properties of the IVZ. Measurements of hydrological properties in the IVZ are also limited by the depth at which this layer normally occurs. There is consequently very little information available on the hydrological characteristics of the IVZ in South Africa and our understanding of the hydrological behaviour of this layer is limited. Skills to quantify lower vadose zone hydrological response exists (Dippenaar *et al.* 2013) and need to be combined with hillslope hydropedology to improve the conceptualisation, and ultimately quantification, of the hydrological responses of the hydrological hillslopes of South Africa.

In order to convert the conceptual understanding of the soil and IVZ properties (together the Vadose Zone properties) as indicators and controllers of hydrological processes, into quantifications of these processes, a paradigm shift is required. Vadose zone properties must be spatially defined and critical controls on hydrological behaviour within the soil horizons, soil bodies, IVZ, hillslopes and Land Types must be identified, quantified and classified.

With regards to bridging the gap between the large number of soil properties involved, and the application of soil and IVZ/LVZ data to hydrological models, the focus must shift. Vadose zone properties must be spatially defined and reduced to critical controls of the hydrological response of soil horizons, UVZ, IVZ, LVZ, hillslope and Land Type. This implies that two distinct areas of research need to be addressed, namely the complex nature of natural entities controlling hydrology (soil horizons, UVZ, IVZ and LVZ in hillslopes and Land Types) need to be characterised, simplified and classified to fit commonly used hydrological models, thereby challenging them to develop appropriate restructuring strategies.

In the common modelling exercise the focus is on both parameterisation and restructuring of model or models. Catchment modelling has elements that are not related to soil and this aspect is therefore excluded from this research. In order to predict the hydrological response of a UVZ and underlying IVZ and LVZ, hillslope or Land Type, soil data are important as indicators and controls of hydrological responses. An example of an indicator is

the redox E-horizon with a combination of soil colour, texture, chemistry and mineralogy. It may have a similar texture to a red apedal B horizon of a Hutton soil but the vertical saturated hydraulic conductivity is typically $< 5 \text{ mm h}^{-1}$ for the E horizon and $> 50 \text{ mm h}^{-1}$ for the red apedal B horizon. This is because the flow of water in the E horizon is controlled by the underlying slowly permeable horizon. Soil types with these horizons typically occur in different positions in the hillslope and imply a different and very specific interaction with the IVZ/LVZ-lithology and climate. The localised occurrence of particular soil distribution patterns is an indication of uniformity in hydrological response on Land Type scale.

Ultimately the quantification of hydropedological processes should be incorporated into hydrological models for accurate water resource predictions, estimating the hydrologic sensitivity of the land for cultivation, contamination and development, as well as quantifying low flow mechanisms (Uhlenbrook *et al.*, 2005; Lorentz *et al.*, 2007 and Wenninger *et al.*, 2008). Unfortunately Le Roux *et al.* (2011), maintain that most catchment scale hydrological models are not capable of including detailed descriptions and quantifications of hillslope hydrological responses (for example lateral flow at different interfaces, return flow from the fractured rock, and connectivities associated with bedrock topography) into model structures. Finite element mesh models on the other hand are simply too detailed to capture landscape processes. To accurately predict the impact of urbanisation, pollution, wetland degradation and other developments on ecohydrology and hydrology in general, a numerical model driven by field intelligence of first order controls is required.

The characteristic nature of soil horizons, soil types, IVZs and LVZs make it possible to characterise them as hydrological entities and develop hydrological response transfer functions for them. The hydrological response transfer functions are seen as the response of an entity to a storm, vertical and lateral drainage.

Water is supplied to the community as widely distributed rain and therefore the community has an impact on it. The flowpaths and storage mechanisms over the first hundred odd meters of the hillslopes to the river largely control the supply rate (peak flow or base flow) to the river and understanding these flowpaths is important for hydrological predictions. Because the flowpaths and storage mechanisms are close to the land surface they are sensitive to human activity, for example the impacts of developments like urbanisation, mining and crop production. Improved understanding of hillslope redistribution of water and supply to catchments is essential to stabilise water supply to the water course and the community. An improved understanding of flowpaths will improve the treatment of pollutants originating from economic development.

Increased expansion of extreme impacts of land use change, for example urbanisation and mining on hydrology, impacts severely on the distribution of water in hillslopes and ecohydrology. A new focus on urban-ecohydrology and mining-ecohydrology can develop from hillslope hydrology.

Hydropedology research in South Africa is developing as hydrological response units, soils and their related spatial environment of fractured rock and topography. Significant contributions to conceptualisation of the hydrological response of soil horizons, soil types and hillslopes are reported. The contribution of soil morphological indicators of flowpaths and flow rates has become part of developing conceptual hydrological response models in hillslope hydrology. Soil morphology has a good correlation with hydrometrical measurements and is useful for the identification of long-term indicators of hydrological response. It is supported by soil chemical parameters which also do not have any impact on hydrological processes. In contrast to morphological soil properties, chemical soil properties

are sensitive to environmental changes and precede morphological changes. A good relationship between these indicators implies that soil morphology and soil classification systems are useful mechanisms for transferring hydrological concepts. This makes soil maps providers of windows to subsurface hydrological hillslope responses.

The next step, namely to identify and quantify hydrological controls also received attention so that soil horizons, soil types and hillslopes with a distribution pattern of soil types could be classified hydrologically. This cleared the way to distinguish between obvious and important parameters of hydrological response.

8.6 FUTURE NEEDS AND POSSIBILITIES

The current state of knowledge opens up new possibilities that can take the adoption of hillslope mechanisms in hydrological models to a higher level. It will also improve site specific management. Background knowledge makes it possible to refine conceptualisation of hydrological response of the full range of hydrological units participating in hillslope hydrology namely soil horizons, soil types, soil distribution patterns and expanded information about the IVZ and LVZ. This also makes it possible to refine the predicting of hillslope response of Land Types. The current state of knowledge also makes it possible to quantify the hydrological response of these hydrological units, identify the critical controls of each and develop hydrological response transfer functions. New or adjusted hydrological models are not foreseen but rather development of modular information needed for application by catchment management agencies and existing hydrological models.

Surface water and groundwater interacts through the vadose zone and a clear understanding of vadose zone mechanisms and the ability to represent these in hydrological models are paramount to effective prediction of hydrological response. The processes of the vadose zone are controlled by an upper vadose zone or solum/soil (UVZ), intermediate vadose zone (IVZ) or saprolite, and a lower vadose zone (LVZ) or partially saturated fractured bedrock. To improve the understanding of hillslope processes in hydrology in general, and site specific ecohydrology and engineering hydrology, the understanding and quantification of processes needs to be refined and made accessible. It includes:

1. Conceptualisation of flowpaths, storage mechanisms and hydrological response needs to be improved. It is expensive and time consuming to measure indicators of processes of storage and flow of water directly and accurately in the vadose zone and therefore it is often neglected in experimental layouts, in hydrological models and decisions on land-use change in spite of the fact that this process is the conduit between the surface and groundwater aquifers. Correlating slow responding soil morphology and mineralogy with indicators responding at a moderate rate (soil chemistry and geochemistry) and fast responding hydrometry, isotope studies, soil water regimes, etc. can be integrated to refine conceptual responses.
2. Distinguishing between contributions of groundwater and hillslope water as drivers of eco/urban/engineering hydrology of catchments.
3. An improved understanding of LVZ characteristics serving as indicators of hydrological response, more specifically indicating return flow to the IVZ, and UVZ, and controlling downslope hydrology to the extent that a distinguishable IVZ may develop and control hydrology (Le Roux *et al.* 2014). LVZ/IVZ return flow results in increased weathering of the IVZ down slope to form a well expressed clay layer called a clay plug in hydrology and

several clay horizons including “unconsolidated material without/with signs of wetness” by soil scientists.

5. To improve the understanding of how soil distribution patterns, the backbone of Land Type definitions, express the hydrological interactions between vadose zone components and therefore the interaction between surface and groundwater bodies.

6. Relating these interactions to different classes of hydrological hillslopes and hydrological Land Types.

The need is to research the role of soil as a window to subsurface hillslope hydrology, exposing flowpaths and storage mechanisms and as controllers of hydrological response. Two fields of research in soil science needs to be pursued: namely, the science behind indicative and controlling soil properties and secondly the science of extrapolation of soil data linked to hydrological processes. Both hydrological processes and modelling need to be integrated into future research to improve the understanding of surface water/groundwater interactions.

The challenge is to improve and re-address the hydrological response of each component in the hillslope and mould it into a modular system for local, hillslope and catchment model application.

8.7 TRANSFER FUNCTIONS FOR HYDROLOGICAL RESPONSE UNITS

The components of the vadose zone can now be studied and hydrological response transfer functions (TFs) can be developed for each hydrological unit. In a modular form it should make vadose zone data more accessible for hydrological modelling.

Hydrological units include soil horizons (HoTFs), soil types as combinations of horizons (STFs), hillslopes as combinations of soil types (HiTFs) and Land Types as combinations of hillslopes (LTTFs).

8.8 REFERENCES

- ASANO, Y., UCHIDA, T. & OHTE, N., 2002. Residence times and flow paths of water in steep unchannelled catchments, Tanakami, Japan. *Journal of Hydrology* 261, 173-192.
- BEVEN, K. J., 2001. On fire and rain (or predicting the effects of change). *Hydrological processes* 15, 1397 -1399.
- BOORMAN, D. B., HOLLIS, J. M. & LILLY, A., 1995. Hydrology of soil types: a hydrologically? based classification of the soils of the United Kingdom. Report No. 126. Institute of Hydrology. UK. Proposal Number: 1001948 Page 15 of 18
- BOUWER, D. 2013. Developing hydrological response models for selected soils in the Weatherley catchment, Eastern Cape Province. Unpublished M.Sc. thesis, Department of soil, crop and climate sciences, University of the Free State, Bloemfontein.
- BUSHNELL, T.M., 1942. Some aspects of the soil catena concept. *Soil Sci. Soc. Am. Proc.* 7, 466-476.
- CHIRICO, G.B., MEDINA, H. & ROMANO, N., 2007. Uncertainty in predicting soil hydraulic properties at the hillslope scale with indirect methods. *Journal of Hydrology* 334, 405-422.

- CLOTHIER, B. E., GREEN, S. R. & DEURER, M., 2008. Preferential flow and transport in soil: progress and prognosis. *European Journal of Soil Science* 59, 2-13.
- DIPPENAAR, M.A., VAN ROOY, J.L., 2013. Review of engineering, hydrogeological and vadose zone hydrological aspects of the Lanseria Gneiss, Goudplaats-Hout River Gneiss and Nelspruit suite Granite (South Africa). *Journal of African Earth Sciences*, 91 (2014): 12-31. 91:12-31.<http://dx.doi.org/10.1016/j.jafrearsci.2013.11.019>
- DUNN, S. M. & LILLY, A., 2001. Investigating the relationship between a soils classification and the spatial parameters of a conceptual catchment, scale hydrological model. *Journal of Hydrology* 252, 157-173.
- FLUGEL, W. A., 1997. Combining GIS with regional hydrological modelling using hydrological response units (HRU's): An application from Germany. *Mathematics and Computers in Simulation* 43, 297-304.
- FREESE, C.J. 2013. A Description, Quantification and Characterization of Hillslope Hydrological Processes in the Weatherley catchment, Eastern Cape Province, South Africa. Unpublished MSc dissertation. School of Agricultural, Earth and Environmental sciences, University of KwaZulu-Natal, Pietermaritzburg, South Africa.
- KUENENE, B.T., VAN HUYSSTEEN, C.W., LE ROUX, P.A.L., HENSLEY, M. & EVERSON, C.S., 2011. Facilitating interpretation of Cathedral Peak VI catchment hydrograph using soil drainage curves. *South African Journal of Geology*, 114, 525-534.
- LAND TYPE SURVEY STAFF., 2004. Land type Survey Database. ARC-ISCW, Pretoria.
- BT KUENENE A , CW VAN HUYSSTEEN A & PAL LE ROUX, 2013. Selected soil properties as indicators of soil water regime in the Cathedral Peak VI catchment of KwaZulu-Natal, South Africa. *SAJPS* 30: 1, 1-6
- LE ROUX, P.A.L., VAN TOL, J.J., KUNENE, B.T., HENSLEY, M., LORENTZ, S.A., VAN HUYSSTEEN, C.W., HUGHES, D.A., EVISON, E., VAN RENSBURG, L.D. & KAPANGAZIWIRI, E., 2011. Hydropedological interpretation of the soils of selected catchments with the aim of improving efficiency of hydrological models: WRC Project K5/1748. Water Research Commission, Pretoria, South Africa.
- LILLY, A., BOORMAN, D.B. & HOLLIS, J.M., 1998. The development of a hydrological classification of UK soils and the inherent scale changes. *Nutr. Cycl. Agroecosys.*, 50, 299-302.
- LAND TYPE SURVEY STAFF., 2002. Land type Survey Database. ARC-ISCW, Pretoria.
- LILLY, A., BOORMAN, D.B. & HOLLIS, J.M., 1998. The development of a hydrological classification of UK soils and the inherent scale changes. *Nutrient Cycling in Agroecosystems* 50, 299-302.
- LIN, H. S., KOGELMAN, W., WALKER, C. & BRUNS, M. A., 2006. Soil moisture patterns in a forested catchment: A hydropedological perspective. *Geoderma* 131, 345-368.
- LIN, H. S., BOUMA, J., OWENS, P. & VERPRASKAS, M., 2008. Hydropedology: Fundamental issues and practical applications. *Catena* 73, 151-152.
- LORENTZ, S.A, BURSEY, K., IDOWU, O., PRETORIUS, C. & NGELEKA, K., 2007 (a). Definition and upscaling of key hydrological processes for application in models. Report No. K5/1320. Water Research Commission, Pretoria.
- MARCHAL, D. & HOLMAN, I. P., 2005. Development and application of a soil classification based conceptual catchment scale hydrological model. *Journal of Hydrology* 312, 277-293.

- McDONNELL, J. J., SIVAPALAN, M., VACH, K., DUNN, S., GRANT, G., HAGGERTY, R., HINZ, C., HOOPER, R., KIRCHNER, J., RODERICK, M. L., SELKER, J. & WEILER, M., 2007. Moving beyond heterogeneity and process complexity: A new vision for watershed hydrology. *Water Resources Research* 43, 1-6.
- MCGUIRE, K.J., MCDONNELL, J.J., WEILER, M., KENDALL, C., MCGLYNN, B.J., WELKER, J.M. & SEIBERT, J., 2005. The role of topography on catchment-scale water residence time. *Water Resources Research* 41.
- MILNE, G., 1936. A provisional Soil Map of East Africa. East African Agriculture Research Station, Amani Memoirs, Tanganyika Territory.
- PACHEPSKY, Y. A., RAWLS, W. J. & LIN, H. S., 2006. Hydropedology and pedotransfer functions. *Geoderma* 131, 308-316.
- PARK SJ, MCSWEENEY K and LOWERY B (2001) Identification of the spatial distribution of soils using a process-based terrain characterization. *Geoderma*, 103, 249-272.
- PARK, S.J. & VAN DE GIESEN, N., 2004. Soil-landscape delineation to define spatial sampling domains for hillslope hydrology. *Journal of Hydrology*. 295, 28-46.
- QUINN, T., ZHU, A. X. & BURT, J. E., 2005. Effects of detailed soil spatial information on watershed modelling across different model scales. *International Journal of Applied Observation and Geoinformation* 7, 324-388.
- SCHAETZL, R. & ANDERSON, S., 2005. *Soils: Genesis and Geomorphology*. Cambridge University Press, Cambridge, UK.
- SCHULZE, R.E. 1995. Hydrology and agrohydrology: A text to accompany the ACRU 3.00 agrohydrological modelling system. Water Research Commission, Report No 63/2/84. WRC, Pretoria.
- SEVERSON, E. D., LINDBO, D. L. & VERPRASKAS, M. J., 2008. Hydropedology of a coarse loamy catena in the lower Coastal Plain, NC. *Catena* 73, 189-196.
- SIVAPALAN, M. 2003a. Prediction in ungauged basins: a grand challenge for theoretical hydrology. *Hydrol. Process.*, 17:3163-3170.
- SIVAPALAN, M., 2003b. Process complexity at hillslope scale, process simplicity at the watershed scale: is there a connection? *Hydrol. Process.* 17, 1037-1041.
- SIVAPALAN, M., TAKEUCHI, K., FRANKS, S.W., GUPTA, V.K., KARAMBIRI, H., LAKSHMI, V., LIANG, X., MCDONNELL, J.J., MENDIONDO, E. M., O'CONNELL, P.E., OKI, T., POMEROY, J.W., SCHERTZER, D., UHLEBROOK, S., & ZEHE, E., 2003. IAHS decade on prediction in ungauged basins (PUB), 2003-2012: Shaping an exciting future for the hydrological sciences. *Hydrol. Sci. J.* 48 (6) 857-880.
- SOULSBY, C., TETZLAFF, D., RODGERS, P., DUNN, S. & WALDRON, S., 2006. Runoff processes, stream residence times and controlling landscape characteristics in a mesoscale catchment: An initial evaluation. *Journal of Hydrology* 325, 197-221.
- SOULSBY, C. & TETZLAFF, D., 2008. Towards simple approaches for mean residence time estimation in ungauged basins using tracers and soil distributions. *Journal of Hydrology* 363, 60-74.
- TICEHURST, J.L., CRESSWELL, H.P., MCKENZIE, N.J. & CLOVER, M.R., 2007. Interpreting soil and topographic properties to conceptualise hillslope hydrology. *Geoderma* 137, 279-292.
- TROMP-VAN MEERVELD, I. & WEILER, M., 2008. Hillslope dynamics modelled with increasing complexity. *Journal of Hydrology* 361, 24-40.

- UHLENBROOK, S., WENNINGER, J. & LORENTZ, S., 2005. What happens after the catchment caught storm? Hydrological processes at the small, semi-arid Weatherley catchment, South-Africa. *Advances in Geosciences* 2, 237-241.
- VAN TOL, J. J., 2008. Soil indicators of hillslope hydrology in the Bedford and Weatherley catchments. Unpublished M.Sc. Thesis. University of the Free State, Bloemfontein, South Africa.
- VAN TOL, J.J., LE ROUX, P.A.L., HENSLEY, M. & LORENTZ, S.A., 2010a. Soil as indicator of hillslope hydrological behaviour in the Weatherley Catchment, Eastern Cape, South Africa. *Water SA* 36, 513-520.
- VAN TOL, J.J., LE ROUX, P.A.L. & HENSLEY, M., 2010b. Soil properties as indicators of hillslope hydrology in the Bedford catchments. *S. Afr. J. Plant & Soil* 27, 242-251.
- VAN TOL, J.J., LE ROUX, P.A.L. & HENSLEY, M., 2011. Soil indicators of hillslope hydrology. In: B.O Gungor & O. Mayis (eds), *Principles-Application and Assessments in Soil Science*. Intech, Turkey.
- VAN TOL, J.J., LE ROUX, P.A.L. & HENSLEY, M., 2012. Pedological criteria for estimating the importance of subsurface lateral flow in E-horizons of South African soils. *Water SA* 39, 47- 56.
- VAN TOL, J.J., LE ROUX, P.A.L. & HENSLEY, M., 2012. Pedotransfer function to determine the water conducting macroporosity in South African soils. *Water Science and Technology*, 65.3 550-557.
- VAN TOL J.J., P.A.L. LE ROUX, S.A. LORENTZ AND M. HENSLEY, 2013. Hydropedological Classification of South African Hillslopes. *Vadose Zone Journal*. 12 (4).
- VAN TOL, J.J., LE ROUX, P.A.L. & HENSLEY, M., 2011. Soil Indicators of Hillslope Hydrology, Principles, Application and Assessment in Soil Science, Dr. Burcu E. Ozkaraova Gungor (Ed.), ISBN: 978-953-307-740-6, InTech, Available from: <http://www.intechopen.com/books/principles-application-and-assessment-in-soilscience/soil-indicators-of-hillslope-hydrology>.
- VEPRASKAS, M. J. & CALDWELL, P. V., 2008. Interpreting morphological features in wetland soils with a hydrological model. *Catena* 73, 153-165.
- WEBSTER, R. 2000. Is soil variation random? *Geoderma* 97, 149-163. Proposal Number: 1001948 Page 16 of 18.
- WEILER, M. & MCDONNELL, J., 2004. Virtual experiments: a new approach for improving process conceptualization in hillslope hydrology. *Journal of Hydrology* 285, 3-18.
- WENNINGER, J., UHLENBROOK, S., LORENTZ, S. & LEIBUNDGUT, C., 2008. Identification of runoff generation processes using combined hydrometric, tracer and geophysical methods in a headwater catchment in South Africa. *Journal des Sciences Hydrologiques* 53, 65-80.